Wavelet Methods for the Solutions of Partial and Fractional Differential Equations Arising in Physical Problems

Arun Kumar Gupta

Department of Mathematics
National Institute of Technology Rourkela

Wavelet Methods for the Solutions of Partial and Fractional Differential Equations Arising in Physical Problems

Dissertation submitted in partial fulfillment

of the requirements of the degree of

Doctor of Philosophy

in

Mathematics

by

Arun Kumar Gupta

(Roll Number: 512MA604)

based on research carried out

under the supervision of

Prof. Santanu Saha Ray

August, 2016

Department of Mathematics
National Institute of Technology Rourkela

Department of Mathematics
National Institute of Technology Rourkela

Date:

Certificate of Examination

Roll Number: *512MA604*

Name: *Arun Kumar Gupta*

Title of Dissertation: *Wavelet methods for the Solutions of Partial and Fractional Differential Equations arising in Physical Problems*

We the below signed, after checking the dissertation mentioned above and the official record book (s) of the student, hereby state our approval of the dissertation submitted in partial fulfillment of the requirements of the degree of *Doctor of Philosophy* in *Mathematics* at *National Institute of Technology Rourkela*. We are satisfied with the volume, quality, correctness, and originality of the work.

Santanu Saha Ray
Principal Supervisor

Bata Krushna Ojha
Member, DSC

Pradip Sarkar
Member, DSC

Ashok Kumar Turuk
Member, DSC

External Examiner

Snehashis Chakraverty
Chairperson, DSC

Kishore Chandra Pati
Head of the Department

Department of Mathematics
National Institute of Technology Rourkela

Prof. Santanu Saha Ray

Associate Professor

August 19, 2016

Supervisor's Certificate

This is to certify that the work presented in this dissertation entitled *Wavelet methods for the Solutions of Partial and Fractional Differential Equations arising in Physical Problems* by *Arun Kumar Gupta*, Roll Number 512MA604, is a record of original research carried out by him under my supervision and guidance in partial fulfillment of the requirements of the degree of *Doctor of Philosophy* in *Mathematics*. Neither this dissertation nor any part of it has been submitted earlier for any degree or diploma to any institute or university in India or abroad.

Santanu Saha Ray

Associate Professor

Dedication

This work is dedicated to my parents Mrs. Bidusi Gupta and Mr. Rameswar Gupta

Arun Kumar Gupta

Declaration of Originality

I, Arun Kumar Gupta, Roll Number 512MA604 hereby declare that this dissertation entitled *Wavelet methods for the Solutions of Partial and Fractional Differential Equations arising in Physical Problems* presents my original work carried out as a doctoral student of NIT Rourkela and, to the best of my knowledge, contains no material previously published or written by another person, nor any material presented by me for the award of any degree or diploma of NIT Rourkela or any other institution. Any contribution made to this research by others, with whom I have worked at NIT Rourkela or elsewhere, is explicitly acknowledged in the dissertation. Works of other authors cited in this dissertation have been duly acknowledged under the sections "Reference" or "Bibliography". I have also submitted my original research records to the scrutiny committee for evaluation of my dissertation.

I am fully aware that in case of any non-compliance detected in future, the Senate of NIT Rourkela may withdraw the degree awarded to me on the basis of the present dissertation.

August 19, 2016
NIT Rourkela   *Arun Kumar Gupta*

Acknowledgement

This thesis is a result of the research that has been carried out at National Institute of Technology Rourkela. The time that, I have spent at National Institute of Technology, Rourkela given me a source of most precious experience in my life. During this period, I came across with a great number of people whose contributions in various ways helped me throughout my research and they deserve special thanks. It is a pleasure to convey my gratitude to all of them.

Foremost, I would like to express my deepest sense of gratitude to my supervisor Dr. S. Saha Ray for his insightful guidance, lively discussion, expert advice, constant encouragement, constructive and honest criticism. I am greatly indebted to him for his invaluable and sustained supervision during my Ph. D. time. He is an excellent mentor and very supportive throughout the work. I feel extremely fortunate to have had an excellent supervision from him during the past years. I am also thankful to his family for the affection and hospitality I was rendered.

Department of Science and Technology (DST), SERB, Government of India, for the project MA-WFR under Grant No. SR./S4/MS.722/11 and Ministry of Human Resource Development (MHRD), Government of India, are highly acknowledged for financial support of this research work.

I also acknowledge Director, National institute of Technology, Rourkela for providing me a platform to carry out this research. I also would like to express my gratitude to the members of my doctoral scrutiny committee: Prof. B. K. Ojha, Prof. P. Sarkar, Prof. A. K. Turuk, Prof. S. Chakerverty and Prof. K. C. Pati for their invaluable, insightful comments and suggestions that improved the quality of this work. I express my gratitude to all the faculty and staff members of the Department of Mathematics, National Institute of Technology Rourkela for their continuous support and moral encouragement.

I am extremely thankful to all the supporting and technical staff of the Department of Mathematics for their kind help and moral support. I would like to keep in record the incredible moments I spent with some special friends in Prakash, Manas, Subhadarshan Soumyendra and Asim. I am also thankful to my childhood friends Radha Mohan, Anil

Abstract

The subject of fractional calculus has gained considerable popularity and importance during the past three decades or so, mainly due to its demonstrated applications in numerous seemingly diverse and widespread fields of science and engineering. It deals with derivatives and integrals of arbitrary orders. The fractional derivative has been occurring in many physical problems, such as frequency-dependent damping behavior of materials, motion of a large thin plate in a Newtonian fluid, creep and relaxation functions for viscoelastic materials, the $PI^\lambda D^\mu$ controller for the control of dynamical systems etc. Phenomena in electromagnetics, acoustics, viscoelasticity, electrochemistry, control theory, neutron point kinetic model, anomalous diffusion, Brownian motion, signal and image processing, fluid dynamics and material science are well described by differential equations of fractional order.

Generally, nonlinear partial differential equations of fractional order are difficult to solve. So for the last few decades, a great deal of attention has been directed towards the solution (both exact and numerical) of these problems. The aim of this dissertation is to present an extensive study of different wavelet methods for obtaining numerical solutions of mathematical problems occurring in disciplines of science and engineering. This present work also provides a comprehensive foundation of different wavelet methods comprising Haar wavelet method, Legendre wavelet method, Legendre multi-wavelet methods, Chebyshev wavelet method, Hermite wavelet method and Petrov-Galerkin method. The intension is to examine the accuracy of various wavelet methods and their efficiency for solving nonlinear fractional differential equations.

With the widespread applications of wavelet methods for solving difficult problems in diverse fields of science and engineering such as wave propagation, data compression, image processing, pattern recognition, computer graphics and in medical technology, these methods have been implemented to develop accurate and fast algorithms for solving integral, differential and integro-differential equations, especially those whose solutions are highly localized in position and scale. The main feature of wavelets is its ability to convert the given differential and integral equations to a system of linear or nonlinear algebraic equations, which can be solved by numerical methods. Therefore, our main

focus in the present work is to analyze the application of wavelet based transform methods for solving the problem of fractional order partial differential equations.

The introductory concept of wavelet, wavelet transform and multi-resolution analysis (MRA) have been discussed in the preliminary chapter. The basic idea of various analytical and numerical methods viz. Variational Iteration Method (VIM), Homotopy Perturbation Method (HPM), Homotopy Analysis Method (HAM), First Integral Method (FIM), Optimal Homotopy Asymptotic Method (OHAM), Haar Wavelet Method, Legendre Wavelet Method, Chebyshev Wavelet Method and Hermite Wavelet Method have been presented in chapter 1.

In chapter 2, we have considered both analytical and numerical approach for solving some particular nonlinear partial differential equations like Burgers' equation, modified Burgers' equation, Huxley equation, Burgers-Huxley equation and modified KdV equation, which have a wide variety of applications in physical models. Variational Iteration Method and Haar wavelet Method are applied to obtain the analytical and numerical approximate solution of Huxley and Burgers-Huxley equations. Comparisons between analytical solution and numerical solution have been cited in tables and also graphically. The Haar wavelet method has also been applied to solve Burgers', modified Burgers', and modified KdV equations numerically. The results thus obtained are compared with exact solutions as well as solutions available in open literature. Error of collocation method has been presented in this chapter.

Methods like Homotopy Perturbation Method (HPM) and Optimal Homotopy Asymptotic Method (OHAM) are very powerful and efficient techniques for solving nonlinear PDEs. Using these methods, many functional equations such as ordinary, partial differential equations and integral equations have been solved. We have implemented HPM and OHAM in chapter 3, in order to obtain the analytical approximate solutions of system of nonlinear partial differential equation viz. the Boussinesq-Burgers' equations. Also, the Haar wavelet method has been applied to obtain the numerical solution of Boussinesq-Burgers' equations. Also, the convergence of HPM and OHAM has been discussed in this chapter.

The mathematical modeling and simulation of systems and processes, based on the description of their properties in terms of fractional derivatives, naturally leads to differential equations of fractional order and the necessity to solve such equations. The

mathematical preliminaries of fractional calculus, definitions and theorems have been presented in chapter 4. Next, in this chapter, the Haar wavelet method has been analyzed for solving fractional differential equations. The time-fractional Burgers-Fisher, generalized Fisher type equations, nonlinear time- and space-fractional Fokker-Planck equations have been solved by using two-dimensional Haar wavelet method. The obtained results are compared with the Optimal Homotopy Asymptotic Method (OHAM), the exact solutions and the results available in open literature. Comparison of obtained results with OHAM, Adomian Decomposition Method (ADM), VIM and Operational Tau Method (OTM) has been demonstrated in order to justify the accuracy and efficiency of the proposed schemes. The convergence of two-dimensional Haar wavelet technique has been provided at the end of this chapter.

In chapter 5, the fractional differential equations such as KdV-Burger-Kuramoto (KBK) equation, seventh order KdV (sKdV) equation and Kaup-Kupershmidt (KK) equation have been solved by using two-dimensional Legendre wavelet and Legendre multi-wavelet methods. The main focus of this chapter is the application of two-dimensional Legendre wavelet technique for solving nonlinear fractional differential equations like time-fractional KBK equation, time-fractional sKdV equation in order to demonstrate the efficiency and accuracy of the proposed wavelet method. Similarly in chapter 6, two-dimensional Chebyshev wavelet method has been implemented to obtain the numerical solutions of the time-fractional Sawada-Kotera equation, fractional order Camassa-Holm equation and Riesz space-fractional sine-Gordon equations. The convergence analysis has been done for these wavelet methods.

In chapter 7, the solitary wave solution of fractional modified Fornberg-Whitham equation has been attained by using first integral method and also the approximate solutions obtained by optimal homotopy asymptotic method (OHAM) are compared with the exact solutions acquired by first integral method. Also, the Hermite wavelet method has been implemented to obtain approximate solutions of fractional modified Fornberg-Whitham equation. The Hermite wavelet method is implemented to system of nonlinear fractional differential equations viz. the fractional Jaulent-Miodek equations. Convergence of this wavelet methods has been discussed in this chapter. Chapter 8 emphasizes on the application of Petrov-Galerkin method for solving the fractional differential equations such as the fractional KdV-Burgers' (KdVB) equation and the fractional Sharma-Tasso-Olver equation with a view to exhibit the capabilities of this method in handling nonlinear

equation. The main objective of this chapter is to establish the efficiency and accuracy of Petrov-Galerkin method in solving fractional differential equtaions numerically by implementing a linear hat function as the trial function and a quintic B-spline function as the test function.

Various wavelet methods have been successfully employed to numerous partial and fractional differential equations in order to demonstrate the validity and accuracy of these procedures. Analyzing the numerical results, it can be concluded that the wavelet methods provide worthy numerical solutions for both classical and fractional order partial differential equations. Finally, it is worthwhile to mention that the proposed wavelet methods are promising and powerful methods for solving fractional differential equations in mathematical physics. This work also aimed at, to make this subject popular and acceptable to engineering and science community to appreciate the universe of wonderful mathematics, which is in between classical integer order differentiation and integration, which till now is not much acknowledged, and is hidden from scientists and engineers. Therefore, our goal is to encourage the reader to appreciate the beauty as well as the usefulness of these numerical wavelet based techniques in the study of nonlinear physical systems.

Contents

List of Figures

List of Tables

Mathematical Preliminary

1.   Introduction

Partial differential equations (PDEs) are of widespread interest because of their connection with phenomena in the physical world. These are useful tool for describing the natural phenomena of science and engineering models. For instance, in physics, the heat flow and the wave propagation phenomena are well described via PDEs. Many engineering applications are simulated mathematically as partial differential equations with initial and boundary conditions. The diffusion of neutrons in nuclear reactor dynamics, population models, the dispersion of a chemically reactive material and many physical phenomena of fluid dynamics, quantum mechanics, electricity etc. are governed by PDEs.

Partial differential equations are originated from the study of solution of a wide variety of problems in mechanics. Even though the foundation of nonlinear partial differential equations is very ancient, they have undergone remarkable new developments during the last half of the twentieth century. Scientists and methematicians have become actively involved in the study of countless problems offered by PDEs. The primary reason for this research was that it plays a vital role in modern mathematical sciences, mainly in applied physics, mathematical modelling and engineering. With the development of PDEs, several methods such as the characteristics method, spectral methods and perturbation techniques have been employed to evaluate the solution of nonlinear problems. But, there is no general method of finding analytical solutions of nonlinear partial differential equations. Hence new numerical techniques are required for finding solutions of nonlinear equations. Therefore, it becomes increasingly important to be familiar with all traditional and recently developed methods for solving PDEs and the implementations of these methods. In this context, a relatively new and emerging area in mathematical research with a variety of applications in engineering disciplines; viz. wavelets theory have attracted the focus of researchers in the field of science and engineering. Wavelets are very successfully used in signal analysis for wave form demonstration and segmentations, time frequency analysis, medical diagnostics, geophysical signal processing, statistical analysis, pattern

recognition, and fast algorithms for easy execution. This work, particularly, deals with the development of various wavelet methods for the solution of PDEs.

2.   Wavelets

The word "*wavelet*" has been derived from the French word "*ondelette*", which means "small wave". An oscillatory function $\psi(x) \in L^2(\mathfrak{R})$ with zero mean and compact support is a wavelet if it has the following desirable characteristics:

i.   Smoothness: $\psi(x)$ is n times differentiable and their derivatives are continuous.

ii. Localization: $\psi(x)$ is well localized both in time and frequency domains, i.e. $\psi(x)$ and its derivatives must decay rapidly. For frequency localization $\hat{\Psi}(\omega)$ must decay sufficiently fast as $\omega \to \infty$ and that $\hat{\Psi}(\omega)$ becomes flat in the neighborhood of $\omega = 0$. The flatness is associated with number of vanishing moments of $\psi(x)$ i.e.,

$$\int_{-\infty}^{\infty} x^k \psi(x) dx = 0 \text{ or equivalently } \frac{d^k}{d\omega^k} \hat{\Psi}(\omega) = 0 \text{ for } k = 0,1,...,n$$

in the sense that larger the number of vanishing moments more is the flatness when ω is small.

iii. The admissibility condition

$$\int_{-\infty}^{\infty} \frac{\left|\hat{\Psi}(\omega)\right|}{|\omega|} d\omega < \infty$$

suggests that $\left|\hat{\Psi}(\omega)\right|$ decay at least as $|\omega|^{-1}$ or $|x|^{\varepsilon-1}$ for $\varepsilon > 0$.

Although most of the numerical methods have been successfully applied for many linear and nonlinear differential equations, they have also some drawbacks in regions where singularities or sharp transitions occur. In those cases the solutions may be oscillating and for accurate representation of the results adaptive numerical schemes must be used which complicates the solution. To overcome the above difficulty wavelet transform methods are quite useful.

3.   Wavelet Transform [1]

Morlet and Grossmann [2, 3] first introduced the concept of wavelets in early 1980s. Since then, a lot of researchers were involved in development of wavelets. Some notable contributors include Morlet and Grossmann [3] for formulation of continuous wavelet transform (CWT), Stromberg [4] for early works on discrete wavelet transform (DWT), Meyer [5] and Mallat [6] for multi-resolution analysis using wavelet transform, and Daubechies [7] for proposal of orthogonal compactly supported wavelets. Thereafter, a lot of work has been done both on development and application of wavelet analysis on a wide variety of problems like signal and image processing, data condensation and solution of differential equations.

In 1982, Jean Morlet, a French geophysical engineer, first introduced the concept of wavelets as a family of functions constructed from dilation and translation of a single function known as the "mother wavelet" $\psi(t)$. They are defined by

$$\psi_{a,b}(t) = \frac{1}{\sqrt{|a|}}\psi\left(\frac{t-b}{a}\right), \qquad a,b \in \Re, \ a \neq 0 \qquad (1)$$

where a is called a scaling parameter which measures the degree of compression or scale, and b is a translation or shifting parameter that determines the location of the wavelet. If $|a| < 1$, the wavelet (1) is the compressed version of the mother wavelet and corresponds mainly to higher frequencies. On the other hand, when $|a| > 1$, $\psi_{a,b}(t)$ has a larger time width than $\psi(t)$ and corresponds to lower frequencies. Thus, wavelets have time-widths adapted to their frequencies, which is the main reason for the success of the Morlet wavelets in signal processing and time-frequency signal analysis. It can be noted that the resolution of wavelets at different scales varies in the time and frequency domains as governed by the Heisenberg uncertainty principle. At large scale, the solution is coarse in the time domain and fine in the frequency domain. As the scale a decreases, the resolution in the time domain becomes finer while that in the frequency domain becomes coarser.

The success of Morlet's numerical algorithms encouraged Grossmann, a French theoretical physicist, to make an extensive study of the Morlet wavelet transform which led to the recognition that wavelets $\psi_{a,b}(t)$ correspond to a square integrable representation of the affine group. Grossmann was concerned with the wavelet transform of $f \in L^2(\Re)$ defined by

$$\mathscr{W}_\psi[f](a,b) = \left(f, \psi_{a,b}\right) = \frac{1}{\sqrt{|a|}} \int\limits_{-\infty}^{\infty} f(t)\overline{\psi\left(\frac{t-b}{a}\right)}dt, \qquad (2)$$

where $\psi_{a,b}(t)$ plays the same role as the kernel $e^{i\omega t}$ in the Fourier transform. The continuous wavelet transform $\mathscr{W}_\psi$ is linear. The inverse wavelet transform can be defined so that f can be reconstructed by means of the formula

$$f(t) = C_\psi^{-1} \int\limits_{-\infty}^{\infty}\int\limits_{-\infty}^{\infty} \mathscr{W}_\psi[f](a,b)\psi_{a,b}(t)(a^{-2}da)db \qquad (3)$$

provided C_ψ satisfies the so called admissibility condition, that is,

$$C_\psi = 2\pi \int\limits_{-\infty}^{\infty} \frac{\left|\hat{\Psi}(\omega)\right|^2}{|\omega|}d\omega < \infty, \qquad (4)$$

where $\hat{\Psi}(\omega)$ is the Fourier transform of the mother wavelet $\psi(t)$.

Grossmann's ingenious work revealed that certain algorithms that decompose a signal on the whole family of scales, can be utilized as an efficient tool for multiscale analysis. In practical applications, the continuous wavelet can be computed at discrete grid points. For this a general wavelet ψ can be defined by replacing a with $a_0^m (a_0 \neq 0,1)$, b with $nb_0 a_0^m (b_0 \neq 0)$, where m and n are integers and making

$$\psi_{m,n}(t) = a_0^{-m/2}\psi(a_0^{-m}t - nb_0). \qquad (5)$$

The discrete wavelet transform of f is defined as

$$\bar{f}(m,n) = \mathscr{W}[f](m,n) = (f, \psi_{m,n}) = \int\limits_{-\infty}^{\infty} f(t)\overline{\psi}_{m,n}(t)dt \qquad (6)$$

where $\psi_{m,n}(t)$ is given in eq. (5).

The series

$$\sum_{m,n=-\infty}^{\infty} \bar{f}(m,n)\psi_{m,n}(t) \qquad (7)$$

is called the wavelet series of f, and the functions $\{\psi_{m,n}(t)\}$ are called the discrete wavelets or simply wavelets.

In general, the function f belonging to the Hilbert space, $L^2(\mathfrak{R})$ can be completely determined by its discrete wavelet transform if the wavelets form a complete system in $L^2(\mathfrak{R})$. In other words, if the wavelets form an orthonormal basis of $L^2(\mathfrak{R})$, then they are

complete and f can be reconstructed from its discrete wavelet transform $\{\bar{f}(m,n) = (f,\psi_{m,n})\}$ by means of the formula

$$f(t) = \sum_{m,n=-\infty}^{\infty} (f,\psi_{m,n})\psi_{m,n}(t), \qquad (8)$$

provided the wavelets form an orthonormal basis.

Alternatively, the function f can be determined by the formula

$$f(t) = \sum_{m,n=-\infty}^{\infty} (f,\psi_{m,n})\overline{\psi}_{m,n}(t), \qquad (9)$$

provided the wavelets form a basis and $\{\overline{\psi}_{m,n}(t)\}$ is the dual basis.

For some particular choice of ψ and a_0, b_0, the $\psi_{m,n}$ constitute an orthonormal basis for $L^2(\Re)$. If $a_0 = 2$ and $b_0 = 1$, then there exists a function ψ with good time-frequency localization properties such that

$$\psi_{m,n}(t) = 2^{-m/2}\psi(2^{-m}t - n) \qquad (10)$$

form an orthonormal basis for $L^2(\Re)$. These $\{\psi_{m,n}(t)\}$ are known as the Littlewood-Paley wavelets.

Definition of Orthogonal wavelet:

A wavelet $\psi \in L^2(\Re)$ is called an orthogonal wavelet, if the family $\{\psi_{m,n}\}$, is an orthonormal basis of $L^2(\Re)$; that is,

$$\langle \psi_{i,j}, \psi_{m,n} \rangle = \delta_{i,m}\delta_{j,n}, \qquad i,j,m,n \in \mathbb{Z}.$$

Definition of Semi-orthogonal wavelet [8]:

A wavelet $\psi \in L^2(\Re)$ is called an semi-orthogonal wavelet, if the family $\{\psi_{m,n}\}$ satisfy the following condition,

$$\langle \psi_{i,j}, \psi_{m,n} \rangle = 0, \ i \neq m, \ i,j,m,n \in \mathbb{Z}.$$

Obviously, every semi-orthogonal wavelets generates an orthogonal decomposition of $L^2(\Re)$ and every orthonormal wavelet is also an semi-orthogonal wavelet.

Hence the integral wavelet transform (IWT) is defined to be the convolution with respect to the dilation of the reflection of some function, called a "basic wavelet", while the

5

wavelet series (WS) is expressed in terms of a single function, called a "wavelet" by means of two very simple operations: binary dilations and integral translations. In wavelet analysis, WS and IWT are intimately related. The IWT of a function on the real line evaluated at certain points in the time-scale domain gives the coefficients for its wavelet series representation. Wavelet techniques enable us to divide a complicated function into several simpler ones and study them separately. This property, along with fast wavelet algorithm makes these techniques very attractive for analysis and synthesis. Unlike Fourier-based analyses that use global (nonlocal) sine and cosine functions as bases, wavelet analysis uses bases that are localized in time and frequency to more effectively represent nonstationary signals. As a result, a wavelet representation is much more compact and easier for implementation. Using the powerful multiresolution analysis, one can represent a function by a finite sum of components at different resolutions so that each component can be adaptively processed based on the objectives of the application. This capability of representing functions compactly and in several levels of resolutions is the major strength of the wavelet analysis.

4. Multiresolution analysis (MRA) [8]

In 1989, Stephane Mallat and Yves Meyer introduced the idea of multiresolution analysis (MRA). The fundamental idea of MRA is to represent a function as a limit of successive approximations, each of which is a "smoother" version of the original function. The successive approximations corresponds to different resolutions, which leads to the name multiresolution analysis as a formal approach to construct orthogonal wavelet bases utilising a definite set of rules. It also provides the existence of so-called scaling functions and scaling filters which are then used for construction of wavelets and fast numerical algorithms. In applications, it is an effective mathematical framework for hierarchical decomposition of a signal or an image into componenets of different scales represented by a sequence of function spaces on $\Re$.

Any wavelet, orthogonal or semi-orthogonal, generates a direct sum decomposition of $L^2(\Re)$. For each $j \in \mathbb{Z}$, let us consider the closed subspaces

$$V_j = \ldots \oplus W_{j-2} \oplus W_{j-1}, \quad j \in \mathbb{Z},$$

of $L^2(\Re)$. A set of subspaces $\{V_j\}_{j \in \mathbb{Z}}$ is said to be MRA of $L^2(\Re)$ if it possess the following properties:

1. $V_j \subset V_{j+1}$, $\quad \forall j \in \mathbb{Z}$,

2. $\bigcup\limits_{j \in \mathbb{Z}} V_j$ is dense in $L^2(\Re)$,

3. $\bigcap\limits_{j \in \mathbb{Z}} V_j = \{0\}$,

4. $V_{j+1} = V_j \oplus W_j$,

5. $f(t) \in V_j \Leftrightarrow f(2t) \in V_{j+1}$, $\quad \forall j \in \mathbb{Z}$.

Properties (2)-(5) state that $\{V_j\}_{j \in \mathbb{Z}}$ is a nested sequence of subspaces that effectively covers $L^2(\Re)$. That is, every square integrable function can be approximated as closely as desired by a function that belongs to at least one of the subspaces V_j. A function $\varphi \in L^2(\Re)$ is called a scaling function if it generates the nested sequence of subspaces V_j and satisfies the dilation equation, namely

$$\varphi(t) = \sum_k p_k \varphi(at - k), \tag{11}$$

with $p_k \in l^2$ and a being any rational number.

For each scale j, since $V_j \subset V_{j+1}$, there exists a unique orthogonal complementary subspace W_j of V_j in V_{j+1}. This subspace W_j is called wavelet subspace and is generated by $\psi_{j,k} = \psi(2^j t - k)$, where $\psi \in L^2$ is called the wavelet. From the above discussion, these results follow easily

- $V_{j_1} \cap V_{j_2} = V_{j_2}$, $j_1 > j_2$,

- $W_{j_1} \cap W_{j_2} = 0$, $j_1 \neq j_2$,

- $V_{j_1} \cap W_{j_2} = 0$, $j_1 \leq j_2$.

In recent years, there have been many developments and new applications of wavelet analysis for describing complex algebraic functions and analyzing empirical continuous data obtained from many kinds of signals at different scales of resolurions. The wavelet based approximations of ordinary and partial differential equations have been attracting the attention, since the contribution of orthonormal bases of compactly supported wavelet

7

by Daubechies and multiresolution analysis based Fast Wavelet transform algorithm by Beylkin [9] gained momentum to make wavelet approximations attractive.

In order to solve partial differential equations by numerical methods, the unknown solution can be represented by wavelets of different resolutions, resulting in a multigrid representation. The dense matrix resulting from an integral operator can be sparsified using wavelet based thresholding techniques to attain an arbitrary degree of solution accuracy. The main feature of wavelets is its ability to convert the given differential and integral equations to a system of linear or nonlinear algebraic equations that can be solved by numerical methods. The goal of this chapter is to convey a general idea about wavelets.

CHAPTER 1

1 Numerous Analytical and Numerical Methods

1.1 Introduction

The purpose of this chapter is to deliver a brief description of various analytical and numerical methods viz. Variational Iteration Method (VIM), First Integral Method (FIM), Homotopy Perturbation Method (HPM), Homotopy Analysis Method (HAM), Optimal Homotopy Asymptotic Method (OHAM), Haar Wavelet Method, Legendre Wavelet Method (LWM), Chebyshev Wavelet Method (CWM), Hermite Wavelet Method (HWM) and Petrov-Galerkin method etc.

The entire chapter can be divided into two parts. In the first part, the basic ideas of some well-known analytical techniques such as Variational Iteration Method (VIM), First Integral Method (FIM), Homotopy Perturbation Method (HPM), Homotopy Analysis Method (HAM), and Optimal Homotopy Asymptotic Method (OHAM) have been discussed, whereas the second part is devoted to study the elemental concept of various methods based on wavelet functions. The applicability of these proposed methods have been examined for solving nonlinear partial differential equations (PDEs) and fractional partial differential equations (FPDEs). Our goal is to encourage the reader to appreciate the beauty as well as the effectiveness of these analytical and numerical techniques in the study of nonlinear physical phenomena.

Part I

1.2 Variational Iteration Method (VIM)

The concept of variational iteration method (VIM) was first developed by Ji-Huan He in the year 1997 [10]. The method has been favorably applied to various kinds of nonlinear problems by many researchers in a variety of scientific fields. The key advantage of the

method is its flexibility and potential to solve nonlinear equations accurately and conveniently. The method gives the solution in the form of rapidly convergent successive approximations that may give the exact solution if such a solution exists. The method has been proved by many authors to be reliable and efficient for a variety of scientific applications, linear and nonlinear equations as well. To illustrate the elemental concept of variation iteration method [11-13], we consider the general differential equation as follows

$$Lu + Nu = g(x,t) \qquad\qquad (1.1)$$

where L is a linear operator, N is a nonlinear operator and $g(x,t)$ is a known analytical function. According to the variational iteration method, a correction functional can be constructed as follows

$$u_{n+1}(x,t) = u_n(x,t) + \int_0^t \lambda(Lu_n(x,\xi) + N\tilde{u}_n(x,\xi) - g(x,\xi))d\xi, \quad n \geq 0 \qquad (1.2)$$

where λ is a general Lagrange multiplier which can be identified optimally by the variational theory, the subscript n denotes the nth order approximation and $\tilde{u}_n$ is regarded as a restricted variation, i.e., $\delta\tilde{u}_n = 0$. The Lagrange multiplier λ can be determined from the stationary condition of the correction functional $\delta u_{n+1} = 0$.

The main advantages of this method are as follows:

i.   The correction functions can be constructed easily by the general Lagrange multipliers which can be optimally determined by the variational theory. The application of restricted variations in correction functional makes it much easier to determine the multiplier.

ii.   The initial approximation can be freely selected with possible unknown constants which can be identified by various methods.

iii.   The approximations acquired with the aid of this method are valid not only for small parameter, but also for very large parameter.

Being different from the other analytical methods, such as perturbation methods, this method does not depend on small or large parameters, it could possibly in finding wide application in nonlinear problems without linearization, discretization or small perturbations.

1.3   First Integral Method

The first integral method is one of the powerful mathematical techniques for finding exact solutions of partial as well as fractional differential equations. This method is based on the ring theory of commutative algebra. It was first proposed by Feng [14] and was further developed by the same author in [15, 16]. Many authors have used first integral method effectively to establish the exact solutions of various nonlinear partial differential equations (PDEs) and FPDEs arising in mathematical physics [17-19]. In order to apply the first integral method over FPDEs, the fractional differential equations may be transformed into classical ordinary differential equations through fractional complex transform with the help of local fractional derivative. The section below demonstrates the fundamental concept of first integral method via algorithm.

1.3.1   Algorithm of First Integral Method

In this section, the fundamental concept of first integral method has been established. The main steps of this proposed method are described as follows:

Step 1: Consider the following general nonlinear fractional order partial differential equation

$$F(u, u_x, D_t^\alpha u, u_{xx}, D_t^\alpha u_{xx}, u_{xxx}, ...) = 0, \ \ 0 < \alpha \le 1 \tag{1.3}$$

where $u = u(x, t)$ is an unknown function, $D_t^\alpha u$ is local fractional derivative of u, F is a polynomial in u and its numerous partial derivatives in which the highest order derivatives and nonlinear terms are involved.

Step 2: Using the fractional complex transform [20, 21]:

$$u(x, t) = \Psi(\xi), \quad \xi = kx - \frac{\lambda t^\alpha}{\Gamma(\alpha + 1)} \tag{1.4}$$

where k and λ are constants, the FPDE (1.3) is transformed to a nonlinear ordinary differential equation (ODE) for $u(x, t) = \Psi(\xi)$ of the following form

$$F(\Psi, k\Psi_\xi, \lambda\Psi_\xi, k^2\Psi_{\xi\xi}, \lambda k^2\Psi_{\xi\xi\xi}, k^3\Psi_{\xi\xi\xi}, ...) = 0, \tag{1.5}$$

Step 3: Suppose eq. (1.5) has a solution of the form

$$\Psi(\xi) = X(\xi) \tag{1.6}$$

and introducing a new variable $Y(\xi) = \Psi_\xi(\xi)$, leads to a system of ODEs of the form

11

$$\frac{dX(\xi)}{d\xi} = Y(\xi), \quad \frac{dY(\xi)}{d\xi} = H(X(\xi), Y(\xi)) \tag{1.7}$$

In general, it is quite difficult to solve a two-dimensional autonomous planar system of ODEs, such as eq. (1.7).

Step 4: Utilizing the qualitative notion of differential equations [22], if we are able to evaluate the integrals to eq. (1.7) under the same conditions, then the general solutions to eq. (1.7) may also be derived directly. With the aid of the division theorem for two variables in the complex domain $\mathbb{C}$ which is based on the Hilbert-Nullstellensatz theorem [23], one can obtain the first integral to eq. (1.7). This first integral can reduce eq. (1.5) to a first order integrable ordinary differential equation. Then by solving this equation directly, the exact solution to eq. (1.3) is obtained.

Theorem 1.1: (Division theorem)

Let $Q(x, y)$ and $R(x, y)$ are polynomials in $\mathbb{C}[x, y]$ and $Q(x, y)$ is irreducible in $\mathbb{C}[x, y]$. If $R(x, y)$ vanishes at all zero points of $Q(x, y)$, then there exists a polynomial $H(x, y)$ in $\mathbb{C}[x, y]$ such that

$$R(x, y) = Q(x, y)H(x, y) \tag{1.8}$$

The division theorem follows immediately from the Hilbert-Nullstellensatz theorem from the ring theory of commutative algebra [23, 24]. The elementary idea of this procedure is to construct a first integral with polynomial coefficients of an explicit form to an equivalent autonomous planar system by utilizing the division theorem.

1.4 Homotopy Perturbation Method (HPM)

In the last three decades with the rapid development of nonlinear sciences, there has appeared increasing interest of scientists and engineers in the analytical techniques for nonlinear problems. Various perturbation methods have been widely applied to solve nonlinear problems in science and engineering. But, most of the perturbation techniques require the existence of a small parameter in the equation. An unsuitable choice of such parameter would lead to very bad results. The solutions obtained through perturbation methods can be valid only when a small value of the parameter is used. Hence, it is necessary to check validity of the approximations through numerical processes.

In contrast to the traditional perturbation methods, the homotopy perturbation method (HPM) technique is independent of small or large physical parameters, and provides us a simple way to ensure the convergence of solution.

To illustrate the basic ideas of homotopy perturbation method (HPM) [25] we consider the following nonlinear differential equation

$$\mathscr{A}(u) - f(\boldsymbol{r}) = 0, \qquad \boldsymbol{r} \in \Omega \qquad (1.9)$$

with the boundary conditions

$$B\left(u, \frac{\partial u}{\partial n}\right) = 0, \qquad \boldsymbol{r} \in \Gamma \qquad (1.10)$$

where $\mathscr{A}$ is a general differential operator, B is a boundary operator, $f(\boldsymbol{r})$ is a known analytic function, Γ is the boundary of the domain Ω.

The operator $\mathscr{A}$ can be divided into two parts linear $\mathscr{L}$ and nonlinear $\mathscr{N}$. Therefore eq. (1.9) can be rewritten as follows

$$\mathscr{L}(u) + \mathscr{N}(u) - f(\boldsymbol{r}) = 0 \qquad (1.11)$$

We construct a homotopy $v(\boldsymbol{r}, p)$ of eq. (1.9) as follows $v(\boldsymbol{r}, p) : \Omega \times [0,1] \rightarrow \Re$ which satisfies [26]

$$H(v, p) \equiv (1-p)[\mathscr{L}(v) - \mathscr{L}(u_0)] + p[\mathscr{A}(v) - f(\boldsymbol{r})] = 0, \qquad (1.12)$$

or $\qquad H(v, p) \equiv \mathscr{L}(v) - \mathscr{L}(u_0) + p\mathscr{L}(u_0) + p[\mathscr{N}(v) - f(\boldsymbol{r})] = 0.$ (1.13)

where $p \in [0,1]$ is an embedding parameter and u_0 is an initial approximation of eq. (1.9), which satisfies the boundary conditions. It follows from (1.12) and (1.13) that

$$H(v,0) = \mathscr{L}(v) - \mathscr{L}(u_0) = 0 \qquad (1.14)$$

or $\qquad H(v,1) = \mathscr{A}(v) - f(\boldsymbol{r}) = 0 \qquad (1.15)$

The changing process of p from zero to unity is just that of $v(\boldsymbol{r}, p)$ from $u_0(\boldsymbol{r})$ to $u(\boldsymbol{r})$. In topology, this is called deformation, and $\mathscr{L}(v) - \mathscr{L}(u_0)$, $\mathscr{A}(v) - f(\boldsymbol{r})$ are called homotopic.

We assume that the solution of eq. (1.13) can be written as a power series in p

$$v = v_0 + pv_1 + p^2v_2 + \dots \tag{1.16}$$

The approximate solution of eq. (1.9) can be obtained by setting $p = 1$

$$u = \lim_{p \to 1} v = v_0 + v_1 + v_2 + \dots \tag{1.17}$$

The series in eq. (1.17) is convergent for most cases and the convergence rate depends upon the nonlinear operator $\mathscr{A}(v)$.

The nonlinear term $\mathscr{N}(u)$ can be expressed in He polynomials [27] as

$$\mathscr{N}(u) = \sum_{m=0}^{\infty} p^m H_m(v_0, v_1, \dots, v_m) \tag{1.18}$$

where

$$H_m(v_0, v_1 \dots, v_m) = \frac{1}{m!} \frac{\partial^m}{\partial p^m}\left(N\left(\sum_{k=0}^{m} p^k v_k \right) \right)\Bigg|, \; m = 0, 1, 2, \dots \tag{1.19}$$

1.5   Optimal Homotopy Asymptotic Method (OHAM)

Unlike perturbation methods, the Optimal Homotopy Asymptotic Method (OHAM) is independent of small or large physical parameters, and provides us a simple way to ensure the convergence of solution series. The method was first devised by Marinca et al. [28-30]. Recently many researchers have successfully applied this method to various nonlinear problems in science and engineering. This is an effective and powerful method to find the approximate solution of nonlinear problems. The advantage of OHAM is built in convergence criteria, which is controllable. In OHAM, the control and adjustment of the convergence region are provided in a convenient way.

In HPM and OHAM, the concept of homotopy from topology and conventional perturbation technique were merged to propose a general analytic procedure for the solution of nonlinear problems. Thus, these methods are independent of the existence of a small parameter in the problem at hand and thereby overcome the limitations of conventional perturbation technique. OHAM, however, is the most generalized form of HPM as it employs a more general auxiliary function $H(p)$ in place of HPM's p.

To illustrate the basic ideas of optimal homotopy asymptotic method [31, 32], we consider the following nonlinear differential equation

$$A(u(x,t)) + g(x,t) = 0, \ x \in \Omega \tag{1.20}$$

with the boundary conditions

$$B\left(u, \frac{\partial u}{\partial t}\right) = 0, \ x \in \Gamma, \tag{1.21}$$

where A is a differential operator, B is a boundary operator, $u(x,t)$ is an unknown function, Γ is the boundary of the domain Ω and $g(x,t)$ is a known analytic function.

The operator A can be decomposed as

$$A = L + N, \tag{1.22}$$

where L is a linear operator and N is a nonlinear operator.

We construct a homotopy $\varphi(x,t;p) : \Omega \times [0,1] \to \Re$ which satisfies

$$H(\varphi(x,t;p),p) \equiv (1-p)[L(\varphi(x,t;p)) + g(x,t)] - H(p)[A(\varphi(x,t;p)) + g(x,t)] = 0, \tag{1.23}$$

where $p \in [0,1]$ is an embedding parameter, $H(p)$ is a nonzero auxiliary function for $p \neq 0$ and $H(0) = 0$. When $p = 0$ and $p = 1$, we have $\varphi(x,t;0) = u_0(x,t)$ and $\varphi(x,t;1) = u(x,t)$ respectively.

Thus as p varies from 0 to 1, the solution $\varphi(x,t;p)$ approaches from $u_0(x,t)$ to $u(x,t)$.

Here $u_0(x,t)$ is obtained from eq. (1.23) and eq. (1.21) with $p = 0$ yields

$$L(\varphi(x,t;0)) + g(x,t) = 0, \ B\left(u_0, \frac{\partial u_0}{\partial t}\right) = 0. \tag{1.24}$$

The auxiliary function $H(p)$ is chosen in the form

$$H(p) = C_1 p + C_2 p^2 + C_3 p^3 + \ldots \tag{1.25}$$

where $C_1, C_2, C_3, \ldots$ are convergence control parameters to be determined. To get an approximate solution, $\tilde{\varphi}(x,t;C_1,C_2,C_3,\ldots)$ is expanded in a series about p as

$$\tilde{\varphi}(x,t;p,C_1,C_2,C_3,\ldots) = u_0(x,t) + \sum_{i=1}^{\infty} u_i(x,t,C_1,C_2,C_3,\ldots)p^i. \tag{1.26}$$

Substituting eq. (1.26) in eq. (1.23) and equating the coefficients of like powers of p, we will have the following equations

$$L(u_1(x,t) + g(x,t)) = C_1 N_0(u_0(x,t)), \ B\left(u_1, \frac{\partial u_1}{\partial t}\right) = 0. \tag{1.27}$$

$$L(u_2(x,t)) - L(u_1(x,t)) = C_2 N_0(u_0(x,t)) + C_1(L(u_1(x,t)) + N_1(u_0(x,t), u_1(x,t))), \quad (1.28)$$

$$B\left(u_2, \frac{\partial u_2}{\partial t}\right) = 0.$$

and hence the general governing equations for $u_j(x,t)$ is given by

$$L(u_j(x,t)) = L(u_{j-1}(x,t)) + C_j N_0(u_0(x,t)) +$$
$$\sum_{i=1}^{j-1} C_i\left[L(u_{j-i}(x,t)) + N_{j-i}(u_0(x,t),\ldots,u_{j-1}(x,t))\right]; \, j = 2,3,\ldots \quad (1.29)$$

where $N_j(u_0(x,t),\ldots,u_j(x,t))$ is the coefficient of p^j in the expansion of $N(\varphi(x,t;p))$ about the embedding parameter p and

$$N(\varphi(x,t;p,C_1,C_2,C_3,\ldots)) = N_0(u_0(x,t)) + \sum_{j=1}^{\infty} N_j(u_0,u_1,\ldots,u_j)p^j. \quad (1.30)$$

It is observed that the convergence of the series (1.26) depends upon the convergence control parameters $C_1, C_2, C_3,\ldots$

The approximate solution of eq. (1.20) can be written in the following form

$$\tilde{u}(x,t;C_1,C_2,C_3,\ldots) = u_0(x,t) + \sum_{j=1}^{n-1} u_j(x,t,C_1,C_2,C_3,\ldots). \quad (1.31)$$

Substituting eq. (1.31) in eq. (1.20), we get the following expression for the residual

$$R_n(x,t;C_1,C_2,C_3,\ldots) = L(\tilde{u}(x,t;C_1,C_2,C_3,\ldots)) + N(\tilde{u}(x,t;C_1,C_2,C_3,\ldots)) + g(x,t) \quad (1.32)$$

If $R_n(x,t;C_1,C_2,C_3,\ldots) = 0$, then $\tilde{u}(x,t;C_1,C_2,C_3,\ldots)$ is the exact solution. Generally such case does not arise for nonlinear problems. The nth order approximate solution given by eq. (1.31) depends on the convergence control parameters $C_1,C_2,C_3,\ldots$ and these parameters can be optimally determined by various methods such as weighted residual least square method, Galerkin method, collocation method and so on.

Case I

According to the collocation method the optimal values of the parameters $C_1,C_2,C_3,\ldots$ can be obtained by solving the following system of equations.

$$R_n\left(x_i,t_j;C_1,C_2,C_3,\ldots,C_{k^2}\right) = 0 \text{ for } i = 1,2,\ldots,k \text{ and } j = 1,2,\ldots,k \quad (1.33)$$

16

Case II

According to weighted residual least square method, the optimal values of the convergence control parameters $C_1, C_2, C_3,...$ can be obtained by solving the following functional

$$J(C_1, C_2, C_3,...,C_k) = \int_{t_1}^{t_2} \int_a^b R_n^2(x,t;C_1,C_2,C_3,...,C_k) dxdt, \qquad (1.34)$$

where a and b are two values depending on the given problem. The unknown parameters $C_1, C_2, C_3,...$ can be identified from the conditions

$$\frac{\partial J}{\partial C_1} = \frac{\partial J}{\partial C_2} = \ldots = \frac{\partial J}{\partial C_k} = 0. \qquad (1.35)$$

The convergence of the n-th approximate solution depends upon unknown parameters $C_1, C_2, C_3,...$. When the convergence control parameters $C_1, C_2, C_3,...$ are known by the above mentioned method then the approximate solution of (1.20) is well determined.

1.6   Homotopy Analysis Method (HAM)

The homotopy analysis method (HAM) was introduced by Liao [33], is an effective and powerful method to find the approximate solution of nonlinear problems. To illustrate the basic ideas of homotopy analysis method we consider the following nonlinear differential equation [34, 35]

$$\mathcal{N}[u(x,t)] = 0, \qquad (1.36)$$

where $\mathcal{N}$ is a nonlinear operator, x and t denote the independent variables and $u(x,t)$ is an unknown function. For simplicity, we ignore all boundary or initial conditions, which can be treated in the similar way. By means of generalizing homotopy analysis method, we first construct the zeroth-order deformation equation as follows

$$(1-p)\mathcal{L}[\phi(x,t;p) - u_0(x,t)] = p\hbar H(x,t)\mathcal{N}[\phi(x,t;p)], \qquad (1.37)$$

where $p \in [0,1]$ is the embedding parameter, $\hbar \neq 0$ is an auxiliary parameter, $\mathcal{L}$ is an auxiliary linear operator, $\phi(x,t;p)$ is an unknown function, $u_0(x,t)$ is an initial guess of

$u(x,t)$ and $H(x,t)$ is a non-zero auxiliary function. For $p=0$ and $p=1$, the zeroth order deformation equation given by eq. (1.37) leads to

$$\phi(x,t;0) = u_0(x,t) \text{ and } \phi(x,t;1) = u(x,t).$$ (1.38)

Thus as p increases from 0 to 1, the solution $\phi(x,t;p)$ varies from the initial guess $u_0(x,t)$ to the solution $u(x,t)$. Expanding $\phi(x,t;p)$ in Taylor's series with respect to the embedding parameter p, we have

$$\phi(x,t;p) = u_0(x,t) + \sum_{m=1}^{\infty} p^m u_m(x,t),$$ (1.39)

where $u_m(x,t) = \dfrac{1}{m!} \dfrac{\partial^m \phi(x,t;p)}{\partial p^m}\bigg|_{p=0}$. (1.40)

The convergence of the series (1.39) depends upon the auxiliary parameter $\hbar$. If it is convergent at $p=1$, we have

$$u(x,t) = u_0(x,t) + \sum_{m=1}^{\infty} u_m(x,t),$$ (1.41)

which must be one of the solutions of the original nonlinear differential equation. Differentiating the zeroth-order deformation eq. (1.37) for m-times with respect to p then dividing them by $m!$ and finally setting $p=0$, we obtain the following m-th order deformation equation

$$\mathscr{L}\left[u_m(x,t) - \chi_m u_{m-1}(x,t)\right] = \hbar H(x,t)\Re_m(u_0,u_1,...,u_{m-1}),$$ (1.42)

where

$$\Re_m(u_0,u_1,...,u_{m-1}) = \dfrac{1}{(m-1)!} \dfrac{\partial^{m-1} \mathscr{N}[\phi(x,t,p)]}{\partial p^{m-1}}\bigg|_{p=0},$$ (1.43)

and

$$\chi_m = \begin{cases} 1, & m > 1 \\ 0, & m \le 1 \end{cases}$$ (1.44)

Now, the solution for m-th order deformation eq. (1.42) by applying $\mathscr{L}^{-1}$ on both sides, we get

$$u_m(x,t) = \chi_m u_{m-1}(x,t) + \mathscr{L}^{-1}\left[\hbar H(x,t)\Re_m(u_0,u_1,...,u_{m-1})\right].$$ (1.45)

In this way, it is easy to obtain $u_m(x,t)$ for $m > 1$ at M-th order, we have

$$u(x,t) = \sum_{m=0}^{M} u_m(x,t) \qquad (1.46)$$

When $M \rightarrow \infty$, we obtain an accurate approximation of the original eq. (1.36).

Part II

"Wavelets" has been a very popular topic of conversations in many scientific and engineering gatherings these days. The subject of wavelet analysis has recently drawn a great deal of attention from mathematical scientists in various disciplines. The integral wavelet transform (IWT) is defined to be the convolution with respect to the dilation of the reflection of some function, called a "basic wavelet", while the wavelet series is expressed in terms of a single function, called a "wavelet" by means of two very simple operations: binary dilations and integral translations. Analogous to Fourier analysis, there are wavelet series (WS) and integral wavelet transforms (IWT). In wavelet analysis, WS and IWT are intimately related. The IWT of a function on the real line evaluated at certain points in the time-scale domain gives the coefficients for its wavelet series representation. As the polynomial spline functions are the simplest functions for both computational and implementation purposes, they are most attractive for analyzing and constructing wavelets.

Some view wavelets as a new basis for representing functions, some consider it as a technique for time-frequency analysis, and others think of it as a new mathematical subject. Of course, all of them are right, since "wavelets" is a versatile tool with very rich mathematical content and great potential for applications. However, as this subject is still in the midst of rapid development, it is definitely too early to give a unified presentation.

Wavelets are very effectively used in signal analysis for wave form demonstration and segmentations, time frequency analysis, medical diagnostics, geophysical signal processing, statistical analysis, pattern recognition, and fast algorithms for easy execution. The wavelet analysis could be a promising tool for solving various difficulties in physics, engineering and image processing [1]. Wavelet method is an exciting method for solving difficult problems in mathematics, physics and engineering, with modern applications in diverse fields such as wave propagation, data compression, image processing, pattern recognition, computer graphics, the detection of aircraft and submarines and improvement in CAT scans and other medical technology. Also, wavelet methods have been used to develop accurate and fast algorithms for solving integral and differential equations of

fractional order, especially those whose solutions are highly localized in position and scale. While wavelets have gained popularity in these areas, new applications are continually being investigated.

Wavelet techniques enable us to divide a complicated function into several simpler ones and study them separately. This property, along with fast wavelet algorithm makes these techniques very attractive for analysis and synthesis. Unlike Fourier - based analyses that use global (nonlocal) sine and cosine functions as bases, wavelet analysis uses bases that are localized in time and frequency to more effectively represent nonstationary signals. As a result, a wavelet representation is much more compact and easier for implementation. Using the powerful multiresolution analysis, one can represent a function by a finite sum of components at different resolutions so that each component can be adaptively processed based on the objectives of the application. This capability of representing functions compactly and in several levels of resolutions is the major strength of the wavelet analysis. In the case of solving partial differential equations by numerical methods, the unknown solution can be represented by wavelets of different resolutions, resulting in a multigrid representation. The dense matrix resulting from an integral operator can be sparsified using wavelet based thresholding techniques to attain an arbitrary degree of solution accuracy. Wavelets allow accurate depiction of a variety of functions and operators. The main feature of wavelets is its ability to convert the given differential and integral equations to a system of linear or nonlinear algebraic equations that can be solved by numerical methods. The goal of this chapter is to convey a general idea about wavelets and to describe different wavelet methods in details.

Orthogonal functions and polynomial series have received considerable attention in dealing with various problems of dynamic systems. The main characteristic of this technique is that it reduces these problems to those of solving a system of algebraic equations, thus greatly simplifying the problem. Special attention has been given to applications of Haar wavelets, Legendre wavelets, Chebyshev wavelets, and Hermite wavelets.

In the present chapter, we introduce different wavelet based methods viz. the Haar wavelet method, the Legendre wavelet method, the Chebyshev wavelet method and the Hermite wavelet method. These methods are studied in details in subsequent chapters.

1.7　Haar Wavelets and the Operational Matrices

Morlet (1982) [8] first introduced the idea of wavelets as a family of functions constructed from dilation and translation of a single function called the "mother wavelet". Haar wavelet functions have been used from 1910 and were introduced by the Hungarian mathematician Alfred Haar [36]. Haar wavelets (which are Daubechies wavelets of order 1) consist of piecewise constant functions on the real line that can take only three values i.e. 0, 1 and -1 and are therefore the simplest orthonormal wavelets with a compact support. Haar wavelet method to be used due to the following features: simpler and fast, flexible, convenient, small computational costs and computationally attractive. The Haar functions are a family of switched rectangular wave forms where amplitudes can differ from one function to another.

The Haar wavelet family for $x \in [0,1)$ is defined as follows [37]

$$h_i(x) = \begin{cases} 1 & x \in [\xi_1, \xi_2) \\ -1 & x \in [\xi_2, \xi_3) \\ 0 & \text{elsewhere} \end{cases} \tag{1.47}$$

where

$$\xi_1 = \frac{k}{m}, \quad \xi_2 = \frac{k+0.5}{m}, \quad \xi_3 = \frac{k+1}{m}.$$

In these formulae integer $m = 2^j$, $j = 0,1,2,...,J$ indicates the level of the wavelet; $k = 0,1,2,...,m-1$ is the translation parameter. Maximum level of resolution is J. The index i is calculated from the formula $i = m+k+1$; in the case of minimal values $m = 1$, $k = 0$, we have $i = 2$. The maximal value of $i = 2M = 2^{J+1}$. It is assumed that the value $i = 1$ corresponds to the scaling function for which

$$h_i(x) = \begin{cases} 1 & \text{for } x \in [0,1) \\ 0 & \text{elsewhere.} \end{cases} \tag{1.48}$$

In the following analysis, integrals of the wavelets are defined as

$$p_i(x) = \int_0^x h_i(x)dx, \quad q_i(x) = \int_0^x p_i(x)dx, \quad r_i(x) = \int_0^x q_i(x)dx.$$

This can be done with the aid of (1.47)

$$p_i(x) = \begin{cases} x - \xi_1 & \text{for } x \in [\xi_1, \xi_2) \\ \xi_3 - x & \text{for } x \in [\xi_2, \xi_3) \\ 0 & \text{elsewhere} \end{cases} \qquad (1.49)$$

$$q_i(x) = \begin{cases} 0 & \text{for } x \in [0, \xi_1) \\ \dfrac{1}{2}(x - \xi_1)^2 & \text{for } x \in [\xi_1, \xi_2) \\ \dfrac{1}{4m^2} - \dfrac{1}{2}(\xi_3 - x)^2 & \text{for } x \in [\xi_2, \xi_3) \\ \dfrac{1}{4m^2} & \text{for } x \in [\xi_3, 1] \end{cases} \qquad (1.50)$$

$$r_i(x) = \begin{cases} \dfrac{1}{6}(x - \xi_1)^3 & \text{for } x \in [\xi_1, \xi_2) \\ \dfrac{1}{4m^2}(x - \xi_2) + \dfrac{1}{6}(\xi_3 - x)^3 & \text{for } x \in [\xi_2, \xi_3) \\ \dfrac{1}{4m^2}(x - \xi_2) & \text{for } x \in [\xi_3, 1) \\ 0 & \text{elsewhere} \end{cases} \qquad (1.51)$$

The collocation points are defined as

$$x_l = \frac{l - 0.5}{2M}, \qquad l = 1, 2, ..., 2M$$

It is expedient to introduce the $2M \times 2M$ matrices H, P, Q and R with the elements $H(i,l) = h_i(x_l)$, $P(i,l) = p_i(x_l)$, $Q(i,l) = q_i(x_l)$ and $R(i,l) = r_i(x_l)$ respectively.

In 2012, the generalized Haar wavelet operational matrix of integration has been derived by the learned researcher Saha Ray [38]. Usually the Haar wavelets are defined for the interval $t \in [0, 1)$ but in general case $t \in [A, B]$, we divide the interval $[A, B]$ into m equal subintervals; each of width $\Delta t = (B - A)/m$. In this case, the orthogonal set of Haar functions are defined in the interval $[A, B]$ by [38]

$$h_0(t) = \begin{cases} 1 & t \in [A, B], \\ 0 & \text{elsewhere} \end{cases} \qquad (1.52)$$

and
$$h_i(t) = \begin{cases} 1, & \zeta_1(i) \le t < \zeta_2(i) \\ -1, & \zeta_2(i) \le t < \zeta_3(i) \\ 0, & \text{otherwise} \end{cases} \qquad (1.53)$$

where $\qquad \zeta_1(i) = A + \left(\dfrac{k-1}{2^j}\right)(B-A) = A + \left(\dfrac{k-1}{2^j}\right)m\Delta t$,

$$\zeta_2(i) = A + \left(\dfrac{k-(1/2)}{2^j}\right)(B-A) = A + \left(\dfrac{k-(1/2)}{2^j}\right)m\Delta t \ ,$$

$$\zeta_3(i) = A + \left(\dfrac{k}{2^j}\right)(B-A) = A + \left(\dfrac{k}{2^j}\right)m\Delta t \ ,$$

for $i = 1, 2, \cdots, m$, $m = 2^J$ and J is a positive integer which is called the maximum level of resolution. Here j and k represent the integer decomposition of the index i. i.e. $i = k + 2^j - 1$, $0 \le j < i$ and $1 \le k < 2^j + 1$.

1.7.1 Function Approximation

Any function $y(t) \in L^2([0, 1))$ can be expanded into Haar wavelets by [39]

$$y(t) = c_0 h_0(t) + c_1 h_1(t) + c_2 h_2(t) + \cdots, \qquad \text{where } c_j = \int_0^1 y(t) h_j(t) dt \ . \qquad (1.54)$$

If $y(t)$ is approximated as piecewise constant in each subinterval, the sum in eq. (1.54) may be terminated after m terms and consequently we can write discrete version in the matrix form as

$$Y \approx \sum_{i=0}^{m-1} c_i h_i(t_l) = \ \boldsymbol{C}_m^T \, H_m , \qquad (1.55)$$

where Y and $\boldsymbol{C}_m^T$ are the m-dimensional row vectors.

Here H is the Haar wavelet matrix of order m defined by $H = [\boldsymbol{h_0}, \boldsymbol{h_1}, \cdots, \boldsymbol{h_{m-1}}]^T$, i.e.

$$\boldsymbol{H} = \begin{bmatrix} \boldsymbol{h_0} \\ \boldsymbol{h_1} \\ \cdots \\ \boldsymbol{h_{m-1}} \end{bmatrix} = \begin{bmatrix} h_{0,0} & h_{0,1} & \cdots & h_{0,m-1} \\ h_{1,0} & h_{1,1} & \cdots & h_{1,m-1} \\ \vdots & \vdots & & \vdots \\ h_{m-1,0} & h_{m-1,1} & \cdots & h_{m-1,m-1} \end{bmatrix} \qquad (1.56)$$

where $\boldsymbol{h_0}, \boldsymbol{h_1}, \cdots, \boldsymbol{h_{m-1}}$ are the discrete form of the Haar wavelet bases.

The collocation points are given by

$$t_l = A + (l - 0.5)\Delta t \ , \ l = 1, 2, \cdots, m \qquad (1.57)$$

1.7.2 Operational Matrix of the General Order Integration

The integration of the $H_m(t) = [h_0(t), h_1(t),...,h_{m-1}(t)]^T$ can be approximated by [40]

$$\int_0^t H_m(\tau)d\tau \cong QH_m(t) \qquad (1.58)$$

where Q is called the Haar wavelet operational matrix of integration which is a square matrix of m-dimension. To derive the Haar wavelet operational matrix of the general order of integration, we recall the fractional integral of order $\alpha(>0)$ which is defined by Podlubny [41]

$$J^\alpha f(t) = \frac{1}{\Gamma(\alpha)}\int_0^t (t-\tau)^{\alpha-1} f(\tau)d\tau, \ \alpha > 0, \ \alpha \in \Re^+ \qquad (1.59)$$

where $\Re^+$ is the set of positive real numbers.

The operational metrix for general order was first time derived by learned researcher Saha Ray [38]. The Haar wavelet operational matrix Q^α for integration of the general order α is given by [38]

$$Q^\alpha H_m(t) = J^\alpha H_m(t) = \left[J^\alpha h_0(t), J^\alpha h_1(t), \cdots, J^\alpha h_{m-1}(t)\right]^T$$

$$= \left[Qh_0(t), Qh_1(t), \cdots, Qh_{m-1}(t)\right]^T \qquad (1.60)$$

where

$$Qh_0(t) = \begin{cases} \dfrac{t^\alpha}{\Gamma(1+\alpha)}, & t \in [A, B], \\ 0, & \text{elsewhere}. \end{cases} \qquad (1.61)$$

and

$$Qh_i(t) = \begin{cases} 0, & A \le t < \zeta_1(i), \\ \phi_1, & \zeta_1(i) \le t < \zeta_2(i), \\ \phi_2, & \zeta_2(i) \le t < \zeta_3(i), \\ \phi_3, & \zeta_3(i) \le t < B, \end{cases} \qquad (1.62)$$

where

$$\phi_1 = \frac{(t-\zeta_1(i))^\alpha}{\Gamma(\alpha+1)},$$

$$\phi_2 = \frac{(t-\zeta_1(i))^\alpha}{\Gamma(\alpha+1)} - 2\frac{(t-\zeta_2(i))^\alpha}{\Gamma(\alpha+1)},$$

24

$$\phi_3 = \frac{(t-\zeta_1(i))^\alpha}{\Gamma(\alpha+1)} - 2\frac{(t-\zeta_2(i))^\alpha}{\Gamma(\alpha+1)} + \frac{(t-\zeta_3(i))^\alpha}{\Gamma(\alpha+1)}.$$

for $i = 1,2,\cdots,m$, $m = 2^J$ and J is a positive integer, called the maximum level of resolution. Here j and k represent the integer decomposition of the index i. i.e. $i = k + 2^j - 1$, $0 \le j < i$ and $1 \le k < 2^j + 1$.

1.8 Legendre Wavelets

The application of Legendre wavelets for solving differential and integral equations is thoroughly considered by many researchers in [42-44] and references therein. Both initial and boundary value problems can be solved efficiently by using the Legendre wavelet method. Here, the basic idea of Legendre wavelets are introduced, the operational matrix of integration is then derived. The derived operational matrix of fractional order integration is then applied to solve fractional differential equations. The method reduces the fractional initial or boundary value problem to a system of algebraic equations. The large systems of algebraic equations may lead to greater computational complexity and large storage requirements. However the operational matrix for the Legendre wavelets is structurally spare. This reduces the computational complexity of the resulting algebraic system.

Wavelets constitute a family of functions constructed from dilation and translation of single function called the mother wavelet $\psi(t)$. They are defined by

$$\psi_{a,b}(t) = \frac{1}{\sqrt{|a|}} \psi\left(\frac{t-b}{a}\right), \qquad a,b \in \Re \tag{1.63}$$

where a is dilation parameter and b is translation parameter. By restricting a, b to discrete values as: $a = a_0^{-j}$, $b = kb_0 a_0^{-j}$, where $a_0 > 1$, $b_0 > 0$ and $n,k \in N$.

The Legendre polynomials of order m, denoted by $L_m(t)$ are defined on the interval [-1, 1] and can be determined with the help of following recurrence formulae [42]

$$L_0(t) = 1,$$

$$L_1(t) = t,$$

$$L_{m+1}(t) = \frac{2m+1}{m+1} t L_m(t) - \frac{m}{m+1} L_{m-1}(t), \ m = 1,2,3,... \tag{1.64}$$

Legendre wavelets $\psi_{n,m}(t) = \psi(k,\hat{n},m,t)$ have four arguments; defined on interval $[0,1)$ by

$$\psi_{n,m}(t) = \begin{cases} \left(m+\dfrac{1}{2}\right)^{1/2} 2^{k/2} L_m\left(2^k t - \hat{n}\right), & \dfrac{\hat{n}-1}{2^k} \leq t < \dfrac{\hat{n}+1}{2^k}, \\ 0, & \text{elsewhere} \end{cases} \qquad (1.65)$$

where $k = 2,3,... \hat{n} = 2n-1$, $n = 1,2,3,...,2^{k-1}$, $m = 0,1,...,M-1$ is the order of the Legendre polynomials and M is a fixed positive integer. The set of Legendre wavelets form an orthogonal basis of $L^2(\Re)$.

The two-dimensional Legendre wavelets are defined as

$$\psi_{n_1,m_1,n_2,m_2}(x,t) = \begin{cases} A L_{m_1}\left(2^{k_1} x - \hat{n}_1\right) L_{m_2}\left(2^{k_2} t - \hat{n}_2\right), & \dfrac{\hat{n}_1-1}{2^{k_1}} \leq x < \dfrac{\hat{n}_1+1}{2^{k_1}}, \ \dfrac{\hat{n}_2-1}{2^{k_2}} \leq t < \dfrac{\hat{n}_2+1}{2^{k_2}} \\ 0, & \text{elsewhere} \end{cases}$$

$$(1.66)$$

where $A = \sqrt{\left(m_1+\dfrac{1}{2}\right)\left(m_2+\dfrac{1}{2}\right)} \, 2^{\frac{k_1+k_2}{2}}$, $\hat{n}_1$ and $\hat{n}_2$ are defined similarly to $\hat{n}$, k_1 and k_2 are any positive integers, m_1 and m_2 are the orders for Legendre polynomials and $\psi_{n_1,m_1,n_2,m_2}(x,t)$ forms a basis for $L^2([0,1) \times [0,1))$.

1.8.1 Function Approximation

A function $f(x,t)$ defined over $[0,1) \times [0,1)$ can be expanded in terms of Legendre wavelet as [43]

$$f(x,t) = \sum_{n=1}^{\infty} \sum_{i=0}^{\infty} \sum_{l=1}^{\infty} \sum_{j=0}^{\infty} c_{n,i,l,j} \psi_{n,i,l,j}(x,t). \qquad (1.67)$$

If the infinite series in eq. (1.67) is truncated, then it can be written as

$$f(x,t) \cong \sum_{n=1}^{2^{k_1-1}} \sum_{i=0}^{M_1-1} \sum_{l=1}^{2^{k_2-1}} \sum_{j=0}^{M_2-1} c_{n,i,l,j} \psi_{n,i,l,j}(x,t) = \Psi^T(x) C \Psi(t), \qquad (1.68)$$

where $\Psi(x)$ and $\Psi(t)$ are $2^{k_1-1} M_1 \times 1$ and $2^{k_2-1} M_2 \times 1$ matrices respectively, given by

$$\Psi(x) \equiv [\psi_{1,0}(x),...,\psi_{1,M_1-1}(x),\psi_{2,0}(x),...,\psi_{2,M_1-1}(x),...,\psi_{2^{k_1-1},0}(x),...,\psi_{2^{k_1-1},M_1-1}(x)]^T,$$

$$\Psi(t) \equiv [\psi_{1,0}(t),...,\psi_{1,M_2-1}(t),\psi_{2,0}(t),...,\psi_{2,M_2-1}(t),...,\psi_{2^{k_2-1},0}(t),...,\psi_{2^{k_2-1},M_2-1}(t)]^T.$$

Also, C is a $2^{k_1-1}M_1 \times 2^{k_2-1}M_2$ matrix whose elements can be calculated from the formula

$$c_{n,i,l,j} = \int_0^1 \int_0^1 \psi_{n,i}(x)\psi_{l,j}(t)f(x,t)\,dt\,dx, \qquad (1.69)$$

with $n = 1,...,2^{k_1-1}, i = 0,...,M_1-1, l = 1,...,2^{k_2-1}, j = 0,...,M_2-1.$

1.8.2 Operational Matrix of the General Order Integration

The integration of the Legendre wavelet function $\Psi(t)$, $\Psi(t) \equiv [\psi_{1,0}(t),...,\psi_{1,M-1}(t),\psi_{2,0}(t),...,\psi_{2,M-1}(t),...,\psi_{2^{k-1},0}(t),...,\psi_{2^{k-1},M-1}(t)]^T$ can be approximated by

$$\int_0^t \Psi(\tau)\,d\tau \cong Q\Psi(t), \qquad (1.70)$$

where Q is called the Legendre wavelet operational matrix of integration. To derive the Legendre wavelet operational matrix of the general order of integration, we recall the fractional integral of order $\alpha(> 0)$ which is defined by Podlubny [41]

$$J^\alpha f(t) = \frac{1}{\Gamma(\alpha)}\int_0^t (t-\tau)^{\alpha-1} f(\tau)\,d\tau, \; \alpha > 0, \; \alpha \in \Re^+ \qquad (1.71)$$

where $\Re^+$ is the set of positive real numbers.

The Legendre wavelet operational matrix Q^α for integration of the general order α is given by

$$Q^\alpha \Psi(t) = J^\alpha \Psi(t)$$
$$= [J^\alpha \psi_{1,0}(t),..., J^\alpha \psi_{1,M-1}(t), J^\alpha \psi_{2,0}(t),..., J^\alpha \psi_{2,M-1}(t), J^\alpha \psi_{2^{k-1},0}(t),..., J^\alpha \psi_{2^{k-1},M-1}(t)]^T$$

where

$$J^\alpha \psi_{n,m}(x) = \begin{cases} \left(m+\dfrac{1}{2}\right)^{1/2} 2^{k/2} J^\alpha L_m\left(2^k x - \hat{n}\right), & \dfrac{\hat{n}-1}{2^k} \leq x < \dfrac{\hat{n}+1}{2^k}, \\ 0, & \text{elsewhere} \end{cases} \qquad (1.72)$$

for $k = 2,3,...\hat{n} = 2n-1, \; n = 1,2,3,...,2^{k-1}, \; m = 0,1,...,M-1$ is the order of the Legendre polynomials and M is a fixed positive integer.

1.9 Chebyshev Wavelets

The Chebyshev wavelets are competent for solving some fractional and integral equations [45, 46]. Nowadays, Chebyshev polynomials have become more significant in numerical evaluation. Among the four forms of Chebyshev polynomials, the first and second kinds are certain cases of the symmetric Jacobi polynomials, whereas the third and fourth kinds are unique instances of the non-symmetric Jacobi polynomials. Great attention has been focused on first and second kinds of Chebyshev polynomials $T_n(x)$ and $U_n(x)$ and their various uses in numerous applications. Nevertheless, there are very few articles that concentrate on the wavelets shaped through these two types of Chebyshev polynomials for application in fractional partial differential equations. This motivates our curiosity in such wavelets.

There are several advantages of using Chebyshev wavelets approximations based on collocation spectral method. First, unlike most numerical methods, it is now conventional that they are characterized by the use of exponentially decaying errors. Second, various numerical methods do not perform well near singularities, whereas approximations through wavelets effectively handle singularities in the problem. In the end, due to their fast convergence, Chebyshev wavelets method does not undergo from the instability problems related with other numerical methods.

The Chebyshev wavelets $\psi_{n,m}(t) = \psi(k, n, m, t)$ have four arguments; defined on interval [0, 1) by [45]

$$\psi_{n,m}(t) = \begin{cases} 2^{k/2}\, \overline{U}_m\left(2^k t - 2n + 1\right), & \dfrac{n-1}{2^{k-1}} \leq t < \dfrac{n}{2^{k-1}}, \\ 0, & \text{elsewhere} \end{cases} \qquad (1.73)$$

where $n = 1, 2, 3, ..., 2^{k-1}$, k is assumed to be any positive integer, m is the degree of the second kind Chebyshev polynomials and t is the normalized time.

Here $\overline{U}_m(t) = \sqrt{\dfrac{2}{\pi}}\, U_m(t)$, $U_m(t)$, $m = 0, 1, 2, ..., M$ are the second kind Chebyshev polynomials of degree m defined on the interval [-1,1] and satisfy the following recursive formula

$$U_0(t) = 1,$$

$$U_1(t) = 2t,$$

$$U_{m+1}(t) = 2tU_m(t) - U_{m-1}(t), \quad m = 1, 2, 3, \ldots \tag{1.74}$$

The two-dimensional Chebyshev wavelets are defined as

$$\psi_{n_1,m_1,n_2,m_2}(x,t) = \begin{cases} 2^{\frac{k_1+k_2}{2}} \overline{U}_{m_1}\left(2^{k_1}x - 2n_1 + 1\right)\overline{U}_{m_2}\left(2^{k_2}t - 2n_2 + 1\right), & \dfrac{n_1-1}{2^{k_1-1}} \leq x < \dfrac{n_1}{2^{k_1-1}}, \\[2mm] & \dfrac{n_2-1}{2^{k_2-1}} \leq t < \dfrac{n_2}{2^{k_2-1}} \\[4mm] 0, & \text{elsewhere} \end{cases} \tag{1.75}$$

where n_1 and n_2 are defined similarly to n, k_1 and k_2 are any positive integers, m_1 and m_2 are the orders for second kind Chebyshev polynomials.

1.9.1 Function approximation

A function $f(x,t)$ defined over $[0,1) \times [0,1)$ may be expanded in terms of Chebyshev wavelets as [46]

$$f(x,t) = \sum_{n=1}^{\infty}\sum_{i=0}^{\infty}\sum_{l=1}^{\infty}\sum_{j=0}^{\infty} c_{n,i,l,j}\psi_{n,i,l,j}(x,t). \tag{1.76}$$

If the infinite series in eq. (1.76) is truncated, then eq. (1.76) can be written as

$$f(x,t) \cong \sum_{n=1}^{2^{k_1-1}}\sum_{i=0}^{M_1-1}\sum_{l=1}^{2^{k_2-1}}\sum_{j=0}^{M_2-1} c_{n,i,l,j}\psi_{n,i,l,j}(x,t) = \Psi^T(x)\,C\,\Psi(t), \tag{1.77}$$

where $\Psi(x)$ and $\Psi(t)$ are $2^{k_1-1}M_1 \times 1$ and $2^{k_2-1}M_2 \times 1$ matrices respectively, given by

$$\Psi(x) \equiv [\psi_{1,0}(x), \psi_{1,1}(x), \ldots, \psi_{1,M_1-1}(x), \psi_{2,0}(x), \ldots, \psi_{2,M_1-1}(x), \ldots, \psi_{2^{k_1-1},0}(x), \ldots, \psi_{2^{k_1-1},M_1-1}(x)]^T,$$

$$\Psi(t) \equiv [\psi_{1,0}(t), \psi_{1,1}(t), \ldots, \psi_{1,M_2-1}(t), \psi_{2,0}(t), \ldots, \psi_{2,M_2-1}(t), \ldots, \psi_{2^{k_2-1},0}(t), \ldots, \psi_{2^{k_2-1},M_2-1}(t)]^T.$$

Also, C is a $2^{k_1-1}M_1 \times 2^{k_2-1}M_2$ matrix whose elements can be calculated from the formula

$$c_{n,i,l,j} = \int_0^1\int_0^1 \psi_{n,i}(x)\psi_{l,j}(t)f(x,t)\,dt\,dx,$$

with $n = 1, \ldots 2^{k_1-1}, i = 0, \ldots, M_1 - 1, l = 1, \ldots 2^{k_2-1}, j = 0, \ldots, M_2 - 1$.

1.9.2 Operational Matrix of the General Order Integration

The integration of the Chebyshev wavelet function $\Psi(t)$, $\Psi(t) \equiv [\psi_{1,0}(t),...,\psi_{1,M-1}(t),\psi_{2,0}(t),...,\psi_{2,M-1}(t),...,\psi_{2^{k-1},0}(t),...,\psi_{2^{k-1},M-1}(t)]^T$ can be approximated by

$$\int_0^t \Psi(\tau)d\tau \approx P\Psi(t) \tag{1.78}$$

where P is called the Chebyshev wavelet operational matrix of integration. To derive the Chebyshev wavelet operational matrix of the general order of integration, we recall the fractional integral of order $\alpha(>0)$ which is defined by Podlubny [41]

$$J^\alpha f(t) = \frac{1}{\Gamma(\alpha)}\int_0^t (t-\tau)^{\alpha-1}f(\tau)d\tau, \quad \alpha > 0, \ \alpha \in \Re^+ \tag{1.79}$$

where $\Re^+$ is the set of positive real numbers.

The Chebyshev wavelet operational matrix P^α for integration of the general order α is given by

$$P^\alpha\Psi(t) = J^\alpha\Psi(t)$$
$$= [J^\alpha\psi_{1,0}(t),...,J^\alpha\psi_{1,M-1}(t),J^\alpha\psi_{2,0}(t),...,J^\alpha\psi_{2,M-1}(t),J^\alpha\psi_{2^{k-1},0}(t),...,J^\alpha\psi_{2^{k-1},M-1}(t)]^T$$

where

$$J^\alpha\psi_{n,m}(x) = \begin{cases} 2^{k/2}J^\alpha\overline{U}_m(2^k x - 2n + 1), & \frac{n-1}{2^{k-1}} \leq x < \frac{n}{2^{k-1}}, \\ 0, & \text{elsewhere} \end{cases}$$

for $n = 1,2,3,...,2^{k-1}$, $m = 0,1,...,M-1$ is the order of the Chebyshev polynomials and M is a fixed positive integer.

1.10 Hermite Wavelets

The Hermite polynomials $H_m(x)$ of order m are defined on the interval $(-\infty, \infty)$, and can be deduced with the assistance of the following recurrence formulae:

$$H_0(x) = 1,$$
$$H_1(x) = 2x,$$

$$H_{m+1}(x) = 2xH_m(x) - 2mH_{m-1}(x), \quad m = 1, 2, 3, \ldots \tag{1.80}$$

The Hermite polynomials $H_m(x)$ are orthogonal with respect to the weight function e^{-x^2}.

The Hermite wavelets are defined on interval $[0,1)$ by [47]

$$\psi_{n,m}(x) = \begin{cases} 2^{k/2}\sqrt{\dfrac{1}{n!\,2^n\sqrt{\pi}}}\, H_m\!\left(2^k x - \hat{n}\right), & \text{for } \dfrac{\hat{n}-1}{2^k} \le x < \dfrac{\hat{n}+1}{2^k} \\ 0, & \text{otherwise} \end{cases} \tag{1.81}$$

where $k = 1, 2, \ldots$, is the level of resolution, $n = 1, 2, \ldots, 2^{k-1}, \hat{n} = 2n-1$ is the translation parameter, $m = 1, 2, \ldots, M-1$ is the order of Hermite polynomials.

The two-dimensional Hermite wavelets are outlined as

$$\psi_{n_1,m_1,n_2,m_2}(x,t) = \begin{cases} A\, H_{m_1}\!\left(2^{k_1}x - \hat{n}_1\right) H_{m_2}\!\left(2^{k_2}t - \hat{n}_2\right), & \dfrac{\hat{n}_1-1}{2^{k_1}} \le x < \dfrac{\hat{n}_1+1}{2^{k_1}}, \\ & \dfrac{\hat{n}_2-1}{2^{k_2}} \le t < \dfrac{\hat{n}_2+1}{2^{k_2}} \\ 0, & \text{elsewhere} \end{cases} \tag{1.82}$$

where $A = \sqrt{\dfrac{1}{n_1!\,2^{n_1}\sqrt{\pi}}}\sqrt{\dfrac{1}{n_2!\,2^{n_2}\sqrt{\pi}}}\, 2^{\frac{k_1+k_2}{2}}$, n_1 and n_2 defined similarly to n, k_1 and k_2

are any positive integers, m_1 and m_2 are the orders for Hermite polynomials.

1.10.1 Function Approximation

A function $f(x,t)$ defined over $[0,1) \times [0,1)$ can be expanded in terms of Hermite wavelet as [48]

$$f(x,t) = \sum_{n=1}^{\infty}\sum_{i=0}^{\infty}\sum_{l=1}^{\infty}\sum_{j=0}^{\infty} c_{n,i,l,j}\psi_{n,i,l,j}(x,t). \tag{1.83}$$

If the infinite series in eq. (1.83) is truncated, then it can be written as

$$f(x,t) \cong \sum_{n=1}^{2^{k_1-1}}\sum_{i=0}^{M_1-1}\sum_{l=1}^{2^{k_2-1}}\sum_{j=0}^{M_2-1} c_{n,i,l,j}\psi_{n,i,l,j}(x,t) = \Psi^T(x)\,C\,\Psi(t), \tag{1.84}$$

where $\Psi(x)$ and $\Psi(t)$ are $2^{k_1-1}M_1 \times 1$ and $2^{k_2-1}M_2 \times 1$ matrices respectively, given by

$$\Psi(x) \equiv [\psi_{1,0}(x), \psi_{1,1}(x), \ldots, \psi_{1,M_1-1}(x), \psi_{2,0}(x), \ldots, \psi_{2,M_1-1}(x), \ldots, \psi_{2^{k_1-1},0}(x), \ldots, \psi_{2^{k_1-1},M_1-1}(x)]^T,$$

$$\Psi(t) \equiv [\psi_{1,0}(t), \psi_{1,1}(t), \ldots, \psi_{1,M_2-1}(t), \psi_{2,0}(t), \ldots, \psi_{2,M_2-1}(t), \ldots, \psi_{2^{k_2-1},0}(t), \ldots, \psi_{2^{k_2-1},M_2-1}(t)]^T.$$

Also, C is a $2^{k_1-1}M_1 \times 2^{k_2-1}M_2$ matrix whose elements can be calculated from the formula

$$c_{n,i,l,j} = \int_0^1 \int_0^1 \psi_{n,i}(x)\psi_{l,j}(t)f(x,t)dtdx, \qquad (1.85)$$

with $n = 1,...,2^{k_1-1}, i = 0,...,M_1 - 1, l = 1,...,2^{k_2-1}, j = 0,...,M_2 - 1.$

1.10.2 Operational Matrix of the General Order Integration

The integration of the Hermite wavelet function $\Psi(t)$,
$\Psi(t) \equiv [\psi_{1,0}(t),...,\psi_{1,M-1}(t),\psi_{2,0}(t),...,\psi_{2,M-1}(t),...,\psi_{2^{k-1},0}(t),...,\psi_{2^{k-1},M-1}(t)]^T$ can be approximated by

$$\int_0^t \Psi(\tau)d\tau \cong Q\Psi(t), \qquad (1.86)$$

where Q is called the Hermite wavelet operational matrix of integration. To derive the Hermite wavelet operational matrix of the general order of integration, we recall the fractional integral of order $\alpha (> 0)$ which is defined by Podlubny [41]

$$J^\alpha f(t) = \frac{1}{\Gamma(\alpha)}\int_0^t (t-\tau)^{\alpha-1}f(\tau)d\tau, \quad \alpha > 0, \ \alpha \in \Re^+ \qquad (1.87)$$

where $\Re^+$ is the set of positive real numbers.

The Hermite wavelet operational matrix Q^α for integration of the general order α is given by

$Q^\alpha \Psi(t) = J^\alpha \Psi(t)$
$\qquad = [J^\alpha \psi_{1,0}(t),..., J^\alpha \psi_{1,M-1}(t), J^\alpha \psi_{2,0}(t),..., J^\alpha \psi_{2,M-1}(t), J^\alpha \psi_{2^{k-1},0}(t),..., J^\alpha \psi_{2^{k-1},M-1}(t)]^T$

where

$$J^\alpha \psi_{n,m}(t) = \begin{cases} 2^{k/2}\sqrt{\dfrac{1}{n!2^n\sqrt{\pi}}}\, J^\alpha H_m(2^k t - \hat{n}), & \text{for } \dfrac{\hat{n}-1}{2^k} \le t < \dfrac{\hat{n}+1}{2^k} \\ \\ 0, & \text{elsewhere} \end{cases} \qquad (1.88)$$

where $k = 1, 2,...$, is the level of resolution, $n = 1, 2,..., 2^{k-1}, \hat{n} = 2n-1$ is the translation parameter, $m = 1, 2,..., M-1$ is the order of Hermite polynomial.

2 Numerical Solution of Partial Differential Equations by Haar Wavelet Method

2.1 Introduction

Historically, partial differential equations originated from the study of surfaces in geometry and for solving a wide variety of problems in mechanics. Although the origin of nonlinear partial differential equations is very old, they have undergone remarkable new developments during the last half of the twentieth century. A large number of mathematicians became actively involved in the investigation of numerous problems presented by partial differential equations. The primary reason for this research was that partial differential equations both express many fundamental laws of nature and frequently arise in the mathematical analysis of diverse problems in science and engineering. The PDEs arise frequently in the formulation of fundamental laws of nature and in the mathematical analysis of a wide variety of problems in applied mathematics, mathematical physics, and engineering sciences including fluid dynamics, nonlinear optics, solid mechanics, plasma physics, quantum field theory, and condensed-matter physics. This subject plays a central role in modern mathematical sciences, especially in applied physics, mathematical modelling and engineering. In fact, partial differential equations have been found to be essential to develop the theory of surfaces on the one hand and to the solution of physical problems on the other.

The development of linear partial differential equations is characterized by the efforts to develop the general theory and various methods of solutions of linear equations. Several methods such as the characteristics method, spectral methods and perturbation techniques have been utilized to study these problems. But, as most solution methods for linear equations cannot be applied to nonlinear equations, there is no general method of finding analytical solutions of nonlinear partial differential equations. New numerical techniques

are usually required for finding solutions of nonlinear equations. Methods of solution for nonlinear equations represent only one aspect of the theory of nonlinear partial differential equations. Like linear equations, questions of existence, uniqueness, and stability of solutions of nonlinear partial differential equations are of fundamental importance. These and other aspects of nonlinear equations have led the subject into one of the most diverse and active areas of modern mathematics.

Many problems of physical interest are described by partial differential equations with appropriate initial and boundary conditions. These problems are usually formulated as initial-value problems, boundary-value problems, or initial boundary-value problems. Indeed, the theory of nonlinear waves and solitons has experienced a revolution over the past three decades. During this revolution, many remarkable and unexpected phenomena have also been observed in physical, chemical, and biological systems.

2.2   Outline of Present Study

In this chapter, we will focus our study on the nonlinear partial differential equations that have particular applications appearing in applied sciences and engineering. We have considered both analytical and numerical approach for solving some specific nonlinear partial differential equations like Burgers' equation, modified Burgers' equation, Huxley equation, Burgers-Huxley equation, and modified Korteweg–de Vries (mKdV) equation, which have a wide variety of applications in physical models.

2.2.1 Burgers' Equation

The one-dimensional Burgers' equation [49]

$$u_t + uu_x - \nu u_{xx} = 0, \, 0 \leq x \leq 1 \qquad\qquad (2.1)$$

is a nonlinear homogeneous parabolic partial differential equation. Here $\nu \, (> 0)$ can be interpreted as viscosity. The Burgers' equation is considered as a model equation that describes the interaction of convection and diffusion. It arises in many physical problems including one-dimensional turbulence, sound waves in viscous medium, shock waves in a viscous medium, waves in fluid filled viscous elastic tubes and magneto-hydrodynamic waves in a medium with finite electrical conductivity.

Various mathematical methods such as the Galerkin finite element method [50], spectral collocation method [51], quartic B-spline differential quadrature method [52], quartic B-splines collocation method [53], finite element method [54], fourth order finite difference method [55], explicit and exact explicit finite difference method [56] and least-squares quadratic B-splines finite element method [57] have been used in attempting to solve Burgers' equations. Our aim in the present work is to implement the Haar wavelet method to stress its power in handling nonlinear equations, so that one can apply it to various types of nonlinearity.

2.2.2 Modified Burgers' Equation

Modifying the nonlinear term uu_x in eq. (2.1) to $u^p u_x$, the generalized modified Burgers' equation [58] can be obtained in the following form

$$u_t + u^p u_x - \nu u_{xx} = 0, \ 0 \le x \le 1, \tag{2.2}$$

where p is a positive constant and $\nu \ (>0)$ can be interpreted as viscosity.

The modified Burgers' equation [59] has the strong nonlinear aspects of the governing equation in many practical transport problems such as nonlinear waves in medium with low frequency pumping or absorption, ion reflection at quasi perpendicular shocks, turbulence transport, wave processes in thermoelastic medium, transport and dispersion of pollutants in rivers and sediment transport etc. Numerous mathematical methods such as Petrov-Galerkin method [60], Quintic spline method [61], Sextic B-spline collocation method [58], local discontinuous Galerkin method [62], and Lattice Boltzmann model [63] have been used in attempting to solve modified Burgers' equations.

2.2.3 Burgers-Huxley and Huxley Equations

Generalized Burgers-Huxley equation [64-66] is a nonlinear partial differential equation of the form

$$u_t + \alpha u^\delta u_x - u_{xx} = \beta u(1 - u^\delta)(u^\delta - \gamma), \ 0 \le x \le 1, \ t \ge 0, \tag{2.3}$$

where α, β, γ and δ are parameters, $\beta \ge 0, \gamma, \delta > 0$. When $\alpha = 0$, $\delta = 1$, eq. (2.3) reduces to the Huxley equation. The Huxley equation [67, 68] is a nonlinear partial differential equation of second order of the form

$$u_t = u_{xx} + u(k - u)(u - 1), \ k \ne 0. \tag{2.4}$$

This equation is an evolution equation that describes nerve pulse propagation in biology from which molecular CB properties can be calculated. Generalized Burgers-Huxley equation is of high importance for describing the interaction between reaction mechanisms, convection effects, and diffusion transport.

Various powerful mathematical methods such as Adomian decomposition method [64, 69], spectral collocation method [65], the tanh-coth method [66], homotopy perturbation method [67], Exp-Function method [68], variational iteration method [70] and Differential Quadrature method [71] have been used in attempting to solve the Burgers-Huxley and the Huxley equations. The solitary wave solutions of the generalized Burgers-Huxley equation have been studied by the learned researchers Wang et al. [72] and El-Danaf [73].

2.2.4 Modified Korteweg-de Vries (mKdV) Equation

Next, we consider the generalized modified Korteweg-de Vries (KdV) equation, [49] which is a nonlinear partial differential equation of the form

$$u_t + qu^2 u_x + ru_{xxx} = 0, \; 0 \le x \le 1, \; t \ge 0 \qquad (2.5)$$

where q and r are parameters.

The modified Korteweg-de Vries (mKdV) equations are most popular soliton equations and have been extensively investigated. The modified KdV equation is of important significance in many branches of nonlinear science field. The mKdV equation appears in many fields such as acoustic waves in certain anharmonic lattices, Alfvén waves in collisionless plasma, transmission lines in Schottky barrier, models of traffic congestion, ion acoustic soliton, elastic media etc. [74].

2.3 Application of Haar Wavelet Method to Obtain Numerical Solution of Burgers' Equation

Haar wavelet collocation method is used for solving generalized Burgers' equation. This method consists of reducing the problem to a set of algebraic equation by expanding the term, which has maximum derivative, given in the equation as Haar functions with unknown coefficients. The operational matrix of integration is utilized to evaluate the coefficients of Haar functions. This method gives us the implicit form of the approximate solutions of the problems.

Consider the one-dimensional Burgers' equation [49]

$$u_t + uu_x - vu_{xx} = 0, \ 0 \le x \le 1, \tag{2.6}$$

with the following associated initial and boundary conditions

$$u(x,t_0) = f(x), \ \ 0 \le x \le 1$$

$$\text{and} \quad u(0,t) = u(1,t) = 0, \quad t \ge t_0. \tag{2.7}$$

It is assumed that $\ddot{u}''(x,t)$ can be expanded in terms of Haar wavelets as

$$\ddot{u}''(x,t) = \sum_{i=1}^{2M} a_s(i)h_i(x), \quad \text{for } t \in [t_s, t_{s+1}] \tag{2.8}$$

where "." and " ' " stands for differentiation with respect to t and x respectively.

Integrating eq. (2.8) with respect to t from t_s to t and twice with respect to x from 0 to x the following equations are obtained

$$u''(x,t) = (t - t_s)\sum_{i=1}^{2M} a_s(i)h_i(x) + u''(x,t_s), \tag{2.9}$$

$$u'(x,t) = (t - t_s)\sum_{i=1}^{2M} a_s(i)p_i(x) + u'(x,t_s) - u'(0,t_s) + u'(0,t), \tag{2.10}$$

$$u(x,t) = (t - t_s)\sum_{i=1}^{2M} a_s(i)q_i(x) + u(x,t_s) - u(0,t_s) + x[u'(0,t) - u'(0,t_s)] + u(0,t), \tag{2.11}$$

$$\dot{u}(x,t) = \sum_{i=1}^{2M} a_s(i)q_i(x) + x\dot{u}'(0,t) + \dot{u}(0,t). \tag{2.12}$$

By using the boundary conditions at $x = 1$, and from eqs. (2.12) and (2.11) respectively, we have

$$\dot{u}'(0,t) = -\sum_{i=1}^{2M} a_s(i)q_i(1), \tag{2.13}$$

$$\text{and} \quad u'(0,t) - u'(0,t_s) = -(t - t_s)\sum_{i=1}^{2M} a_s(i)q_i(1). \tag{2.14}$$

From eq. (1.50), it is obtained that

$$q_i(1) = \begin{cases} 0.5 & \text{if } i = 1 \\ \dfrac{1}{4m^2} & \text{if } i > 1. \end{cases} \tag{2.15}$$

Substituting eqs. (2.13)- (2.15) in eqs. (2.10)- (2.12) and discretizing the results by assuming $x \to x_l$, $t \to t_{s+1}$, the following equations are obtained

$$u''(x_l, t_{s+1}) = (t_{s+1} - t_s) \sum_{i=1}^{2M} a_s(i) h_i(x_l) + u''(x_l, t_s),$$ (2.16)

$$u'(x_l, t_{s+1}) = (t_{s+1} - t_s) \sum_{i=1}^{2M} a_s(i) [p_i(x_l) - q_i(1)] + u'(x_l, t_s),$$ (2.17)

$$u(x_l, t_{s+1}) = (t_{s+1} - t_s) \sum_{i=1}^{2M} a_s(i) [q_i(x_l) - x_l q_i(1)] + u(x_l, t_s),$$ (2.18)

$$\dot{u}(x_l, t_{s+1}) = \sum_{i=1}^{2M} a_s(i) [q_i(x_l) - x_l q_i(1)].$$ (2.19)

Substituting eqs. (2.16)- (2.19) in eq. (2.6), we have

$$\sum_{i=1}^{2M} a_s(i) [q_i(x_l) - x_l q_i(1)] = v \left[(t_{s+1} - t_s) \sum_{i=1}^{2M} a_s(i) h_i(x_l) + u''(x_l, t_s) \right] -$$

$$\left[(t_{s+1} - t_s) \sum_{i=1}^{2M} a_s(i) [q_i(x_l) - x_l \, q_i(1)] + u(x_l, t_s) \right] \times \quad (2.20)$$

$$\left[(t_{s+1} - t_s) \sum_{i=1}^{2M} a_s(i) [p_i(x_l) - q_i(1)] + u'(x_l, t_s) \right]$$

From eq. (2.20), the wavelet coefficients $a_s(i)$ can be successively calculated using mathematical software. This process starts with

$$u(x_l, t_0) = f(x_l),$$

$$u'(x_l, t_0) = f'(x_l),$$

$$u''(x_l, t_0) = f''(x_l).$$

To show the effectiveness and accuracy of proposed scheme, we consider two test examples. The numerical solutions thus obtained are compared with the analytical solutions as well as available numerical results.

Example 2.1 Consider Burgers' equation with the following initial and boundary conditions [56]

$$u(x,0) = \sin(\pi x), \qquad 0 \le x \le 1$$

$$u(0,t) = u(1,t) = 0, \qquad t > 0.$$ (2.21)

The exact solution of eq. (2.6) is given by [56]

$$u(x,t) = \frac{2\pi v \sum_{n=1}^{\infty} A_n \, n \sin(n\pi x) \exp(-n^2 \pi^2 v \, t)}{A_0 + \sum_{n=1}^{\infty} A_n \cos(n\pi x) \exp(-n^2 \pi^2 v \, t)} \quad , \tag{2.22}$$

where
$$A_0 = \int_0^1 \exp\left(\frac{-1}{2\pi v}\left(1 - \cos(\pi x)\right)\right) dx,$$

$$A_n = 2\int_0^1 \exp\left(\frac{-1}{2\pi v}\left(1 - \cos(\pi x)\right)\right) dx,$$

The numerical solutions of the example 2.1 are presented for $v = 0.01$ with $\Delta t = 0.001$ taking $M = 64$ in Table 2.1 and Figures 2.1 and 2.2. The results are compared with Refs. [56, 57, 75] and consequently it is found that the present method is much better than the results presented in [56, 57, 75]. The Figures 2.1 and 2.2 are in good agreement with the results obtained by learned researcher Jiwari [76].

Example 2.2 In this example, we consider Burgers' equation with initial condition in the following form

$$u(x,0) = \frac{2\pi v \sin(\pi x)}{a + \cos(\pi x)}, \quad a > 1 \tag{2.23}$$

The exact solution of eq. (2.6) is given by [77]

$$u(x,t) = \frac{2\pi v \exp(-\pi^2 v \, t) \sin(\pi x)}{a + \exp(-\pi^2 v \, t) \cos(\pi x)}, a > 1 \tag{2.24}$$

In case of example 2.2, Tables 2.2 and 2.3 show the L_2 and L_∞ errors at different values of a, v and M. Moreover, the results are compared with Refs. [78, 79] and it has been observed that the present method is more accurate and efficient than the other numerical solutions. The physical behaviors of solutions at different time stages are shown in Figures 2.3 and 2.4.

2.3.1 Numerical Results and Discussion for Burgers' Equation

The following Table 2.1 shows the comparison of exact solutions with the approximate solutions of different numerical methods for Burgers' equation. Agreement between present numerical results and exact solutions appears very satisfactory through illustration in Table 2.1. In the following Table 2.1, J has been taken as 6 i.e. $M = 64$ with $v = 0.01$ and different values of t. Similarly Tables 2.2 and 2.3 show the comparison of L_2 and L_∞

errors with other numerical methods for $\nu = 0.01$ and 0.005 with $a = 100$ and $t = 1$. From Tables 2.2 and 2.3, it has been observed that the present method is more accurate and efficient than the other numerical methods presented in References [78, 79].

Table 2.1 Comparison of Haar wavelet solution with other numerical methods for Burgers' equation (example 2.1) at different values of t with $a = 2, \nu = 0.01$ and $\Delta t = 0.001$.

x	t	EFDM [56] $\Delta t = 0.001$	EEFDM [56] $\Delta t = 0.001$	Least-square quadratic B-spline FEM [57] $\Delta t = 0.0001$	Crank-Nicolson method [75] $\Delta t = 0.01$	Present Method $\Delta t = 0.001$	Exact solution
0.25	0.4	0.34244	0.34164	0.34244	0.34229	0.34224	0.34191
	0.6	0.26905	0.26890	0.27536	0.26902	0.26924	0.26896
	0.8	0.22145	0.22150	0.22752	---	0.22170	0.22148
	1.0	0.18813	0.18825	0.19375	0.18817	0.18837	0.18819
	3.0	0.07509	0.07515	0.07754	0.07511	0.07516	0.07511
0.5	0.4	0.67152	0.65606	0.66543	0.66797	0.66106	0.66071
	0.6	0.53406	0.52658	0.53525	0.53211	0.52984	0.52942
	0.8	0.44143	0.43743	0.44526	---	0.43953	0.43914
	1.0	0.37568	0.37336	0.38047	0.37500	0.37476	0.37442
	3.0	0.15020	0.15015	0.15362	0.15018	0.15027	0.15018
0.75	0.4	0.94675	0.90111	0.91201	0.93680	0.90980	0.91026
	0.6	0.78474	0.75862	0.77132	0.77724	0.76745	0.76724
	0.8	0.65659	0.64129	0.65254	---	0.64778	0.64740
	1.0	0.56135	0.55187	0.56157	0.55833	0.55647	0.55605
	3.0	0.22502	0.22454	0.22874	0.22485	0.22497	0.22481

Table 2.2 Comparison of L_2 and L_∞ errors with other numerical methods for Burgers' equation (example 2.2) taking $a = 100, \nu = 0.01$ at $t = 1$.

N	Rahman [78]		Mittal and Jain [79]		M	Present method $\Delta t = 0.01$		Present method $\Delta t = 0.001$	
	L_2	L_∞	L_2	L_∞		L_2	L_∞	L_2	L_∞
10	3.455E-7	4.881E-7	3.284E-7	4.628E-7	4	3.267E-8	4.634E-8	1.498E-8	2.157E-8
20	1.013E-7	1.431E-7	8.192E-8	1.164E-7	8	2.288E-8	3.239E-8	5.235E-9	7.452E-9
40	4.003E-8	5.668E-8	2.047E-8	2.907E-8	16	2.042E-8	2.889E-8	2.779E-9	3.939E-9
80	4.003E-8	3.499E-8	5.119E-9	7.271E-9	32	1.981E-8	2.802E-8	2.165E-9	3.064E-9

Table 2.3 Comparison of L_2 and L_∞ errors with other numerical methods for Burgers' equation (example 2.2) taking $a = 100, \nu = 0.005$ at $t = 1$.

N	Rahman [78]		Mittal and Jain [79]		M	Present method $\Delta t = 0.01$		Present method $\Delta t = 0.001$	
	L_2	L_∞	L_2	L_∞		L_2	L_∞	L_2	L_∞
10	8.819E-8	1.246E-7	8.631E-8	1.215E-7	4	4.266E-9	6.0565E-9	1.9418E-9	2.7999E-9
20	2.403E-8	3.394E-8	2.153E-8	3.062E-8	8	2.9996E-9	4.2463E-9	6.8086E-10	9.7005E-10
40	7.942E-9	1.125E-8	5.378E-9	7.644E-9	16	2.681E-9	3.7933E-9	3.6323E-10	5.1519E-10
80	3.918E-9	5.549E-9	1.345E-9	7.644E-9	32	2.6013E-9	3.6797E-9	2.8393E-10	4.0182E-10

Figures 2.1-2.4 cite the behavior of numerical solutions obtained for Burgers' equation at different time stages taking $v = 0.01$.
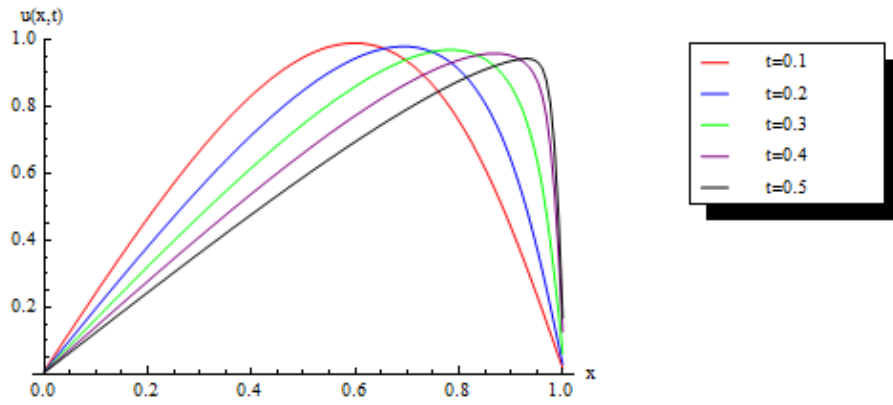
Figure 2.1   Behavior of numerical solutions for Burgers' equation (example 2.1) when $v = 0.01$ and $\Delta t = 0.001$ at times $t = 0.1, 0.2, 0.3, 0.4$ and 0.5.
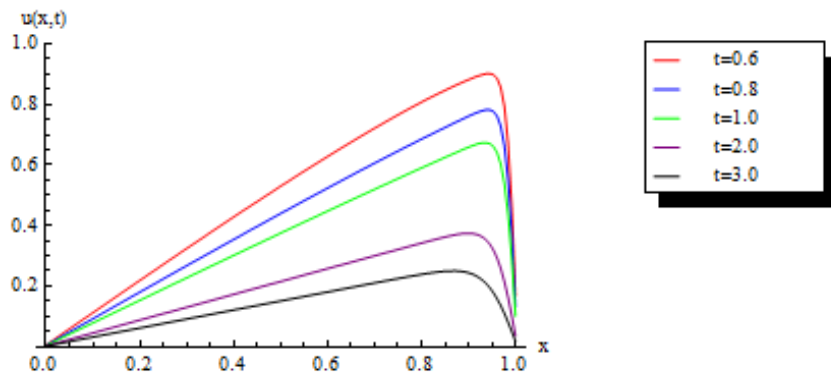
Figure 2.2   Behavior of numerical solutions for Burgers' equation (example 2.1) when $v = 0.01$ and $\Delta t = 0.001$ at times $t = 0.6, 0.8, 1.0, 2.0$ and 3.0.
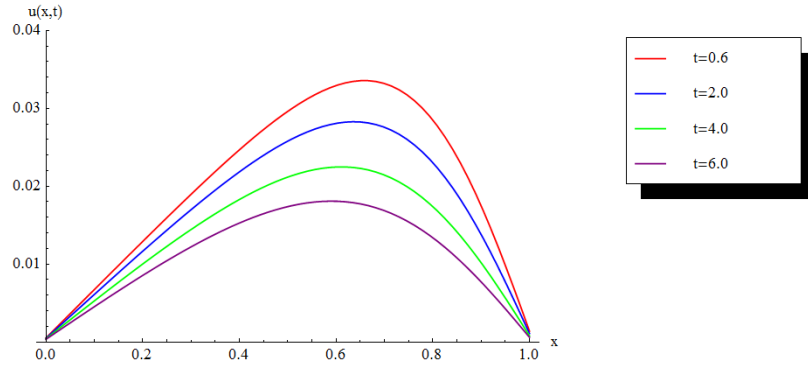
Figure 2.3 Behavior of numerical solutions for Burgers' equation (example 2.2) when $v = 0.01$ and $\Delta t = 0.001$ at times $t = 0.6, 2.0, 4.0$ and $6.0.$
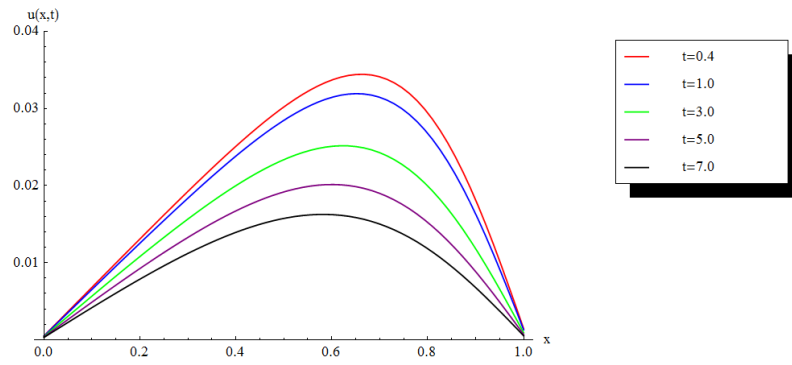
Figure 2.4 Behavior of numerical solutions for Burgers' equation (example 2.2) when $v = 0.01$ and $\Delta t = 0.001$ at times $t = 0.4, 1.0, 3.0, 5.0$ and $7.0.$

2.4 Haar Wavelet Based Scheme for Modified Burgers' Equation

Taking $p = 2$, in eq. (2.2), the generalized modified Burgers' equation [58] can be obtained as follows:

$$u_t + u^2 u_x - v u_{xx} = 0,\ 0 \le x \le 1,\qquad\qquad(2.25)$$

where v is a parameter.

The initial condition associated with eq. (2.25) will be

$$u(x, t_0) = f(x),\ \ 0 \le x \le 1\qquad\qquad(2.26)$$

with boundary conditions

$$u(0, t) = u(1, t) = 0,\quad t \ge t_0$$

Let us suppose that $\ddot{u}''(x,t)$ can be expanded in terms of Haar wavelets as

$$\ddot{u}''(x,t) = \sum_{i=1}^{2M} a_s(i) h_i(x) \text{ for } t \in [t_s, t_{s+1}] \qquad (2.27)$$

where "." and " ' " stands for differentiation with respect to t and x respectively.

Now, integrating eq. (2.27) with respect to t from t_s to t and twice with respect to x from 0 to x the following equations are obtained

$$u''(x,t) = (t-t_s) \sum_{i=1}^{2M} a_s(i) h_i(x) + u''(x,t_s), \qquad (2.28)$$

$$u'(x,t) = (t-t_s) \sum_{i=1}^{2M} a_s(i) p_i(x) + u'(x,t_s) + u'(0,t) - u'(0,t_s), \qquad (2.29)$$

$$u(x,t) = (t-t_s) \sum_{i=1}^{2M} a_s(i) q_i(x) + u(x,t_s) + x[u'(0,t) - u'(0,t_s)] + u(0,t) - u(0,t_s), \quad (2.30)$$

$$\dot{u}(x,t) = \sum_{i=1}^{2M} a_s(i) q_i(x) + x\dot{u}'(0,t) + \dot{u}(0,t). \qquad (2.31)$$

Using the boundary condition at $x=1$, from eq. (2.31) we have

$$\dot{u}'(0,t) = -\sum_{i=1}^{2M} a_s(i) q_i(1), \qquad (2.32)$$

and from eq. (2.30), we obtain

$$u'(0,t) - u'(0,t_s) = -(t-t_s) \sum_{i=1}^{2M} a_s(i) q_i(1). \qquad (2.33)$$

Substituting eq. (2.32) and (2.33) in eqs. (2.29)- (2.31), and discretizing the above results by assuming $x \to x_l$, $t \to t_{s+1}$, we obtain

$$u''(x_l,t_{s+1}) = (t_{s+1} - t_s) \sum_{i=1}^{2M} a_s(i) h_i(x_l) + u''(x_l,t_s), \qquad (2.34)$$

$$u'(x_l,t_{s+1}) = (t_{s+1} - t_s) \sum_{i=1}^{2M} a_s(i)[p_i(x_l) - q_i(1)] + u'(x_l,t_s), \qquad (2.35)$$

$$u(x_l,t_{s+1}) = (t_{s+1} - t_s) \sum_{i=1}^{2M} a_s(i)[q_i(x_l) - x_l q_i(1)] + u(x_l,t_s), \qquad (2.36)$$

$$\dot{u}(x_l, t_{s+1}) = \sum_{i=1}^{2M} a_s(i)[q_i(x_l) - x_l \, q_i(1)]. \tag{2.37}$$

Substituting eqs. (2.34)- (2.37) in eq. (2.25), we have

$$\sum_{i=1}^{2M} a_s(i)[q_i(x_l) - x_l q_i(1)] = v \left[(t_{s+1} - t_s) \sum_{i=1}^{2M} a_s(i) h_i(x_l) + u''(x_l, t_s) \right] -$$
$$\left[(t_{s+1} - t_s) \sum_{i=1}^{2M} a_s(i)[q_i(x_l) - x_l \, q_i(1)] + u(x_l, t_s) \right]^2 \times \tag{2.38}$$
$$\left[(t_{s+1} - t_s) \sum_{i=1}^{2M} a_s(i)[p_i(x_l) - q_i(1)] + u'(x_l, t_s) \right].$$

From eq. (2.38), the wavelet coefficients $a_s(i)$ can be successfully calculated. This process starts with

$$u(x_l, t_0) = f(x_l),$$
$$u'(x_l, t_0) = f'(x_l),$$
$$u''(x_l, t_0) = f''(x_l).$$

To show the efficiency and accuracy of proposed scheme, two test examples have been considered taking $p = 2$. The numerical solutions thus acquired are compared with the analytical solutions as well as available numerical results.

Example 2.3 Consider modified Burgers' equation with the following initial and boundary conditions [60, 61]

$$u(x,1) = \frac{x}{1 + \dfrac{1}{c_0} e^{\frac{x^2}{4v}}} \tag{2.39}$$

$$u(0,t) = u(1,t) = 0, \quad t \geq 1$$

where $c_0 = e^{\frac{1}{8v}}$.

The exact solution of Eq. (2.25) is given by [60, 61]

$$u(x,t) = \frac{\dfrac{x}{t}}{1 + \dfrac{\sqrt{t}}{c_0} e^{\frac{x^2}{4vt}}}, \quad t \geq 1 \tag{2.40}$$

Example 2.4 In this example, we consider modified Burgers' equation with initial and boundary conditions in the following form

$$u(x,0) = \sin(\pi x) \qquad 0 \le x \le 1, \tag{2.41}$$

$$u(0,t) = u(1,t) = 0, \qquad t > 0$$

In case of example 2.3, the Haar wavelet numerical solutions have been compared with the results obtained by Ramadan et al. [61] using the collocation method with quintic splines and in case of example 2.4, the solutions have been compared with the results obtained by Duan et al. [63] using 2-bit lattice Boltzmann method (LBM). Tables 2.5 and 2.6 cite the comparison of Haar wavelet solution with LBM and quintic splines numerical solutions at $t = 0.4$ and $t = 2,$ and hence the numerical solutions at different time stages are shown in Figure 2.5.

2.4.1 Numerical Results for Modified Burgers' Equation

The errors for modified Burgers' equation are measured using two different norms, namely L_2 and $L_\infty,$ defined by

$$L_2 = R.M.S.\ Error = \frac{1}{\sqrt{2M}} \sqrt{\sum_{l=1}^{2M} \left(u_{approx}(x_l, t) - u_{exact}(x_l, t) \right)^2} \tag{2.42}$$

$$L_\infty = \max \left| u_{approx}(x_l, t) - u_{exact}(x_l, t) \right| \tag{2.43}$$

The following Table 2.4 exhibits the L_2 and L_∞ error norms for modified Burgers' equation taking $p = 2,$ $\nu = 0.001$ and different values of t. In Table 2.4, J is taken as 5 i.e. $M = 32$ and Δt is taken as 0.001.

Table 2.4 L_2 and L_∞ error norm for modified Burgers' equation (example 2.3) at different values of t with $\nu = 0.001$ and $\Delta t = 0.001$.

Time (sec)	Present Method		Quintic spline	
	$L_2 \times 10^{-3}$	$L_\infty \times 10^{-3}$	$L_2 \times 10^{-3}$ [61]	$L_\infty \times 10^{-3}$ [61]
2	0.0755325	0.289254	0.0670395601	0.2796704002
3	0.0711446	0.256515	0.0689577701	0.2514379353
4	0.065229	0.214577	0.0666974605	0.2185661439
5	0.0604007	0.182222	0.0636023977	0.1923643818
6	0.0565458	0.157428	0.0604622308	0.1717652452
7	0.0534117	0.138249	0.0575085655	0.1553318123
8	0.0508078	0.123651	0.0548010376	0.1418932282

Table 2.5 Comparison of Haar wavelet solutions with the LBM solutions and 5-Splines solution of modified Burgers' equation (example 2.4) at $t = 0.4$ and $\nu = 0.01$.

x	Approximate solution using Haar wavelet method (u_{approx})	Approximate solution using lattice Boltzmann method [63]	Approximate solution using Quintic spline method [61]
0.10	0.221423	0.22177116	0.22033034
0.20	0.396841	0.39414890	0.39460783
0.30	0.531256	0.53134565	0.53244922
0.40	0.64835	0.64627793	0.64763455
0.50	0.744936	0.74511632	0.74643231
0.60	0.831235	0.83048713	0.83133318
0.70	0.902641	0.90235089	0.90195203
0.80	0.95132	0.95495434	0.95119837
0.90	0.825329	0.83737688	0.82794559
0.99	0.0623064	0.06214261	0.04674614

Table 2.6   Comparison of Haar wavelet solutions with the LBM solutions and 5-Splines solution of modified Burgers' equation (example 2.4) at $t = 2.0$ and $\nu = 0.01$.

x	Approximate solution using Haar wavelet method (u_{approx})	Approximate solution using lattice Boltzmann method [63]	Approximate solution using Quintic spline method [61]
0.10	0.111789	0.11194772	0.11013979
0.20	0.208539	0.20710153	0.20614825
0.30	0.284853	0.28512152	0.28477813
0.40	0.351297	0.35038171	0.35045112
0.50	0.406404	0.40665374	0.40700602
0.60	0.457189	0.45649486	0.45704614
0.70	0.501339	0.50155303	0.50224419
0.80	0.542602	0.54199420	0.54265295
0.90	0.536499	0.53547356	0.53225529
0.99	0.0790367	0.08046491	0.05693884

Figures 2.5-2.8 represent the comparison graphically between the numerical and exact solutions of modified Burgers' equation for different values of t and $\nu = 0.001$. The behavior of numerical solutions of modified Burgers' equation is cited in Figures 2.9 and 2.10.
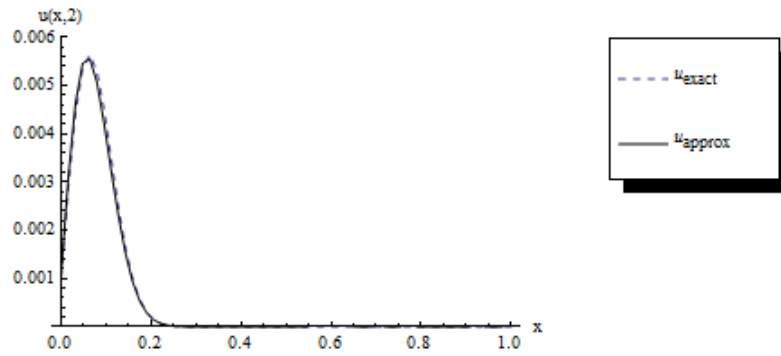
Figure 2.5   Comparison of Numerical solution and exact solution of modified Burgers' equation (example 2.3) when $t = 2.0$ and $\nu = 0.001$.
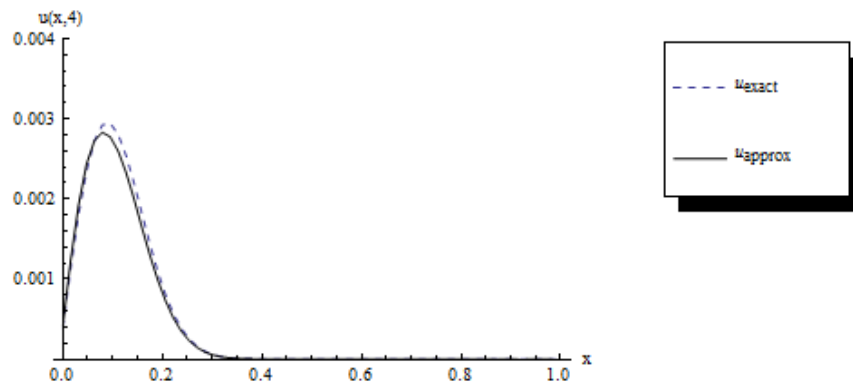
Figure 2.6   Comparison of Numerical solution and exact solution of modified Burgers' equation (example 2.3) when $t = 4$ and $\nu = 0.001$.
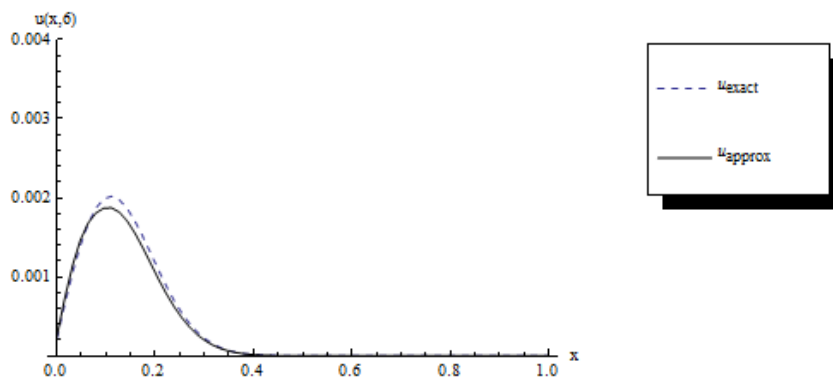
Figure 2.7   Comparison of Numerical solution and exact solution of modified Burgers' equation (example 2.3) when $t = 6$ and $\nu = 0.001$.
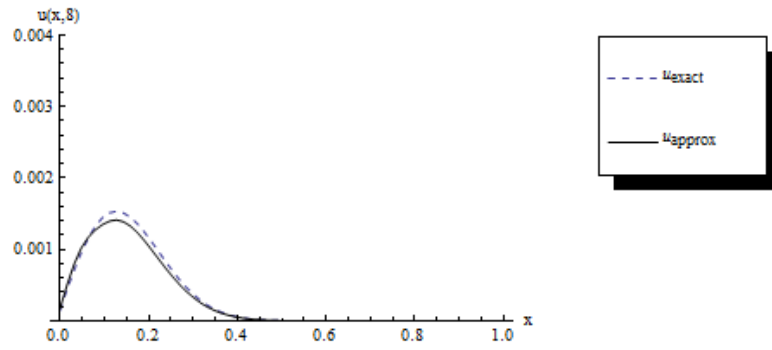
Figure 2.8 Comparison of Numerical solution and exact solution of modified Burgers' equation (example 2.3) when $t = 8$ and $\nu = 0.001$.
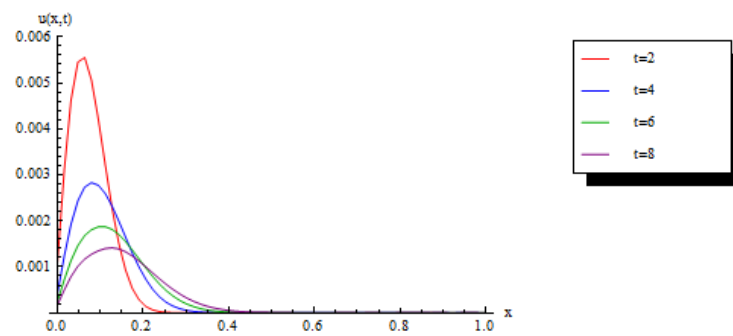
Figure 2.9 Behavior of numerical solutions for modified Burgers' equation (example 2.3) when $\nu = 0.001$ and $\Delta t = 0.001$ at times $t = 2, 4, 6$ and 8.
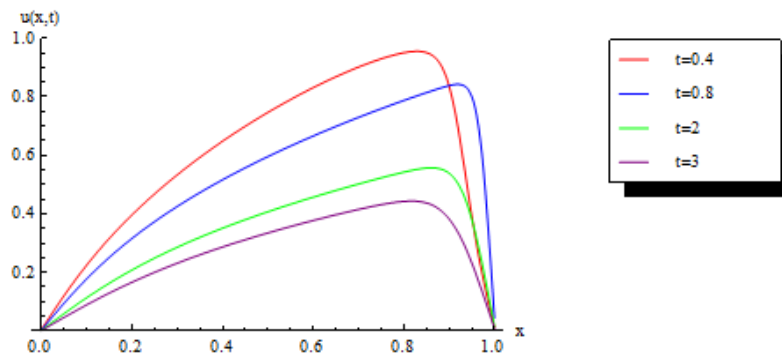
Figure 2.10 Behavior of numerical solutions for modified Burgers' equation (example 2.4) when $\nu = 0.01$ and $\Delta t = 0.001$ at times $t = 0.4, 0.8, 2$ and 3.

2.5 Analytical and Numerical Methods for Solving Burgers-Huxley Equation

The generalized Burgers-Huxley equation [64-66] is a nonlinear partial differential equation of the form

$$u_t + \alpha u^\delta u_x - u_{xx} = \beta u(1 - u^\delta)(u^\delta - \gamma), \ 0 \le x \le 1, \ t \ge 0, \tag{2.44}$$

where α, β, γ and δ are parameters, $\beta \ge 0, \gamma, \delta > 0$.

The initial condition associated with eq. (2.44) is given by

$$u(x,0) = \left(\frac{\gamma}{2} + \frac{\gamma}{2} \tanh[A_1 x]\right)^{1/\delta}. \tag{2.45}$$

The exact solution of eq. (2.44) is given by [65, 72]

$$u(x,t) = \left(\frac{\gamma}{2} + \frac{\gamma}{2} \tanh[A_1(x - A_2 t)]\right)^{1/\delta}, \tag{2.46}$$

where

$$A_1 = \frac{-\alpha\delta + \delta\sqrt{\alpha^2 + 4\beta(1+\delta)}}{4(1+\delta)}\gamma,$$

$$A_2 = \frac{\gamma\alpha}{(1+\delta)} - \frac{(1+\delta-\gamma)\left(-\alpha + \sqrt{\alpha^2 + 4\beta(1+\delta)}\right)}{2(1+\delta)}$$

where α, β, γ and δ are parameters with $\beta \ge 0$ and $\delta \ge 0$.

This exact solution satisfies the following boundary conditions

$$u(0,t) = \left[\frac{\gamma}{2} + \frac{\gamma}{2} \tanh(-A_1 A_2 t)\right]^{1/\delta}, \ t \ge 0$$

$$u(1,t) = \left[\frac{\gamma}{2} + \frac{\gamma}{2} \tanh(A_1(1 - A_2 t))\right]^{1/\delta}, \ t \ge 0 \tag{2.47}$$

In our present study, $\delta = 1$ has been considered.

2.5.1 Application of Variational Iteration Method for Solving Burgers-Huxley Equation

Construct a correctional functional for eq. (2.44) as follows:

$$u_{n+1}(x,t) = u_n(x,t) + \int_0^t \lambda \left[(u_n)_\tau - (u_n^\delta)(\tilde{u}_n)_x - (\tilde{u}_n)_{xx} - u_n(1-u_n)(\tilde{u}_n - 0.001) \right] d\tau, \quad (2.48)$$

where λ is a general Lagrangian multiplier whose optimal value can be found using variational theory and $\tilde{u}_n(x,t)$ is the restricted variation, i.e. $\delta \tilde{u}_n(x,t) = 0$.

$$\delta u_{n+1}(x,t) = \delta u_n(x,t) + \delta \int_0^t \lambda \left[(u_n)_\tau - (u_n^\delta)(\tilde{u}_n)_x - (\tilde{u}_n)_{xx} - u_n(1-u_n)(\tilde{u}_n - 0.001) \right] d\tau. \quad (2.49)$$

From the above eq. (2.49) we have

$$\delta u_{n+1}(x,t) = \delta u_n(x,t) + \delta \int_0^t \lambda \left(\frac{\partial u_n}{\partial \tau} \right) d\tau, \quad (2.50)$$

since $\delta \left((u_n^\delta)(\tilde{u}_n)_x \right) = 0$, $\delta(\tilde{u}_n)_{xx} = 0$ and $\delta(u_n(1-u_n)(\tilde{u}_n - 0.001)) = 0$

Integrating right hand side of eq. (2.50) yields

$$\delta u_{n+1}(x,t) = \delta u_n(x,t)(1+\lambda) - \int_0^t \delta u_n(x,\tau)\lambda' d\tau. \quad (2.51)$$

From stationary condition we know

$$\delta u_{n+1}(x,t) = 0,$$

which yields that

$$\delta u_n(x,t)(1+\lambda) - \int_0^t \delta u_n(x,\tau)\lambda' d\tau = 0.$$

This implies $\quad\quad 1 + \lambda = 0 \quad$ and $\quad \lambda'(t) = 0$

Hence $\quad\quad\quad\quad \lambda = -1.$ $\quad\quad\quad\quad\quad\quad\quad\quad\quad$ (2.52)

Therefore λ can be identified as -1, and the following variational iteration formula can be obtained as

$$u_{n+1}(x,t) = u_n(x,t) - \int_0^t \left[(u_n)_\tau - (u_n)(\tilde{u}_n)_x - (\tilde{u}_n)_{xx} - u_n(1-u_n)(\tilde{u}_n - 0.001) \right] d\tau. \quad (2.53)$$

From the above iteration formula eq. (2.53), we can obtain

$$u_1(x,t) = 0.0005 + 0.0005\tanh(0.00025\,x) - 0.000000249938\,t\,\mathrm{sec}\,h^2(0.00025\,x)$$

with initial condition

$$u_0(x,t) = 0.0005 + 0.0005\tanh(0.00025\,x).$$

2.5.2 Application of Haar Wavelet Method for Solving Burgers-Huxley Equation

Haar wavelet solution of $u(x,t)$ is sought by assuming that $\dot{u}''(x,t)$ can be expanded in terms of Haar wavelets as

$$\dot{u}''(x,t) = \sum_{i=1}^{2M} a_s(i)h_i(x) \text{ for } t \in [t_s, t_{s+1}]. \tag{2.54}$$

Integrating eq. (2.54) with respect to t from t_s to t and twice with respect to x from 0 to x the following equations are obtained

$$u''(x,t) = (t - t_s)\sum_{i=1}^{2M} a_s(i)h_i(x) + u''(x,t_s), \tag{2.55}$$

$$u'(x,t) = (t - t_s)\sum_{i=1}^{2M} a_s(i)p_i(x) + u'(x,t_s) - u'(0,t_s) + u'(0,t), \tag{2.56}$$

$$u(x,t) = (t - t_s)\sum_{i=1}^{2M} a_s(i)q_i(x) + u(x,t_s) - u(0,t_s) + x[u'(0,t) - u'(0,t_s)] + u(0,t), \tag{2.57}$$

$$\dot{u}(x,t) = \sum_{i=1}^{2M} a_s(i)q_i(x) + x\dot{u}'(0,t) + \dot{u}(0,t), \tag{2.58}$$

By using the boundary conditions, at $x = 1$, we have

$$\dot{u}'(0,t) = -\sum_{i=1}^{2M} a_s(i)q_i(1) + \dot{u}(1,t) - \dot{u}(0,t). \tag{2.59}$$

Discretizing the results by assuming $x \to x_l$, $t \to t_{s+1}$ we obtain

$$u''(x_l,t_{s+1}) = (t_{s+1} - t_s)\sum_{i=1}^{2M} a_s(i)h_i(x_l) + u''(x_l,t_s), \tag{2.60}$$

$$u'(x_l,t_{s+1}) = (t_{s+1} - t_s)\sum_{i=1}^{2M} a_s(i)p_i(x_l) + u'(x_l,t_s) - u'(0,t_s) + u'(0,t_{s+1}), \tag{2.61}$$

$$u(x_l,t_{s+1}) = (t_{s+1} - t_s)\sum_{i=1}^{2M} a_s(i)q_i(x_l) + u(x_l,t_s) - u(0,t_s)$$
$$+ x_l[u'(0,t_{s+1}) - u'(0,t_s)] + u(0,t_{s+1}), \tag{2.62}$$

$$\dot{u}(x_l,t_{s+1}) = \sum_{i=1}^{2M} a_s(i)q_i(x_l) + x_l\dot{u}'(0,t_{s+1}) + \dot{u}(0,t_{s+1}). \tag{2.63}$$

Substituting eqs. (2.63) and (2.59) in eq. (2.44), we have

$$\sum_{i=1}^{2M} a_s(i)[q_i(x_l) - x_l q_i(1)] = u''(x_l, t_s) + u(x_l, t_s)[1 - u(x_l, t_s)][u(x_l, t_s) - 0.001]$$

$$- u(x_l, t_s)u'(x_l, t_s) - \dot{u}(0, t_{s+1}) - x_l[\dot{u}(1, t_{s+1}) - \dot{u}(0, t_{s+1})].$$

<div align="right">(2.64)</div>

From the above equation the wavelet coefficients $a_s(i)$ can be successively calculated. This process started with

$$u(x_l, t_0) = 1 + \tanh\left(\frac{x_l}{2}\right),$$

$$u'(x_l, t_0) = \frac{1}{2}\sec h^2\left(\frac{x_l}{2}\right),$$

$$u''(x_l, t_0) = -\frac{1}{2}\sec h^2\left(\frac{x_l}{2}\right)\tanh\left(\frac{x_l}{2}\right).$$

2.5.3 Numerical Results for Burgers-Huxley Equation

The following Tables show the comparisons of the exact solutions with the approximate solutions of Burgers-Huxley equation taking $\alpha = 1$, $\beta = 1$, $\gamma = 0.001$, $\delta = 1$ and different values of t. In Tables 2.7-2.9, J is taken as 3 i.e. $M = 8$ and Δt is taken as 0.0001.

Table 2.7 The absolute errors for the solutions of Burgers-Huxley equation using Haar wavelet method and one iteration of VIM at various collocation points for x with $t = 0.4$ and $\gamma = 0.001$.

x	Approximate solutions using Haar wavelet method (u_{approx})	Approximate solutions using VIM (u_{approx})	Exact solutions (u_{exact})	Absolute Errors using Haar wavelet method	Absolute Errors using VIM
0.03125	0.00050006	0.00049994	0.000500054	6.56610E-9	1.49925E-7
0.09375	0.000500121	0.000499912	0.000500062	5.90949E-8	1.49925E-7
0.15625	0.000500234	0.00049992	0.000500069	1.64153E-7	1.49925E-7
0.21875	0.000500399	0.000499927	0.000500077	3.21739E-7	1.49925E-7
0.28125	0.000500617	0.000499935	0.000500085	5.31854E-7	1.49925E-7
0.34375	0.000500887	0.000499943	0.000500093	7.94498E-7	1.49925E-7
0.40625	0.000501210	0.000499951	0.000500101	1.10967E-6	1.49925E-7
0.46875	0.000501586	0.000499959	0.000500109	1.47737E-6	1.49925E-7
0.53125	0.000502014	0.000499966	0.000500116	1.89760E-6	1.49925E-7
0.59375	0.000502495	0.000499974	0.000500124	2.37036E-6	1.49925E-7
0.65625	0.000503028	0.000499982	0.000500132	2.89565E-6	1.49925E-7
0.71875	0.000503613	0.00049999	0.00050014	3.47347E-6	1.49925E-7

0.78125	0.000504251	0.000499998	0.000500148	4.10381E-6	1.49925E-7
0.84375	0.000504942	0.000500005	0.000500155	4.78669E-6	1.49925E-7
0.90625	0.000505685	0.000500013	0.000500163	5.52210E-6	1.49925E-7
0.96875	0.000506481	0.000500021	0.000500171	6.31009E-6	1.49925E-7

Table 2.8 The absolute errors for the solutions of Burgers-Huxley equation using Haar wavelet method and one iteration of VIM at various collocation points for x with $t = 0.6$ and $\gamma = 0.001$.

x	Approximate solutions using Haar wavelet method $\left(u_{approx}\right)$	Approximate solutions using VIM $\left(u_{approx}\right)$	Exact solutions $\left(u_{exact}\right)$	Absolute Errors using Haar wavelet method	Absolute Errors using VIM
0.03125	0.000500089	0.000499854	0.000500079	9.84903E-9	2.24888E-7
0.09375	0.000500175	0.000499862	0.000500087	8.86412E-8	2.24888E-7
0.15625	0.000500341	0.00049987	0.000500094	2.46226E-7	2.24888E-7
0.21875	0.000500585	0.000499877	0.000500102	4.82602E-7	2.24888E-7
0.28125	0.000500908	0.000499885	0.00050011	7.97771E-7	2.24888E-7
0.34375	0.00050131	0.000499893	0.000500118	1.19173E-6	2.24888E-7
0.40625	0.00050179	0.000499901	0.000500126	1.66400E-6	2.24888E-7
0.46875	0.00050235	0.000499909	0.000500134	2.21600E-6	2.24888E-7
0.53125	0.000502988	0.000499916	0.000500141	2.84700E-6	2.24888E-7
0.59375	0.000503705	0.000499924	0.000500149	3.55600E-6	2.24888E-7
0.65625	0.0005045	0.000499932	0.000500157	4.34300E-6	2.24888E-7
0.71875	0.000505375	0.00049994	0.000500165	5.21000E-6	2.24888E-7
0.78125	0.000506328	0.000499948	0.000500173	6.15500E-6	2.24888E-7
0.84375	0.00050736	0.000499956	0.00050018	7.18000E-6	2.24888E-7
0.90625	0.000508471	0.000499963	0.000500188	8.28300E-6	2.24888E-7
0.96875	0.000509661	0.000499971	0.000500196	9.46500E-6	2.24888E-7

Table 2.9 The absolute errors for the solutions of Burgers-Huxley equation using Haar wavelet method and one iteration of VIM at various collocation points for x with $t = 1$ and $\gamma = 0.001$.

x	Approximate solutions using Haar wavelet method $\left(u_{approx}\right)$	Approximate solutions using VIM $\left(u_{approx}\right)$	Exact solutions $\left(u_{exact}\right)$	Absolute errors using Haar wavelet method	Absolute errors using VIM
0.03125	0.000500145	0.000499754	0.000500129	1.6414E-8	3.74813E-7
0.09375	0.000500284	0.000499762	0.000500137	1.47726E-7	3.74813E-7
0.15625	0.000500555	0.00049977	0.000500144	4.10351E-7	3.74813E-7
0.21875	0.000500957	0.000499777	0.000500152	8.04288E-7	3.74813E-7
0.28125	0.00050149	0.000499785	0.00050016	1.32954E-6	3.74813E-7
0.34375	0.000502154	0.000499793	0.000500168	1.9861E-6	3.74813E-7
0.40625	0.00050295	0.000499801	0.000500176	2.7740E-6	3.74813E-7

0.46875	0.000503877	0.000499809	0.000500183	3.6940E-6	3.74813E-7
0.53125	0.000504935	0.000499816	0.000500191	4.7440E-6	3.74813E-7
0.59375	0.000506125	0.000499824	0.000500199	5.9260E-6	3.74813E-7
0.65625	0.000507445	0.000499832	0.000500207	7.2380E-6	3.74813E-7
0.71875	0.000508898	0.00049984	0.000500215	8.6830E-6	3.74813E-7
0.78125	0.000510481	0.000499848	0.000500223	1.02580E-5	3.74813E-7
0.84375	0.000512196	0.000499856	0.00050023	1.19660E-5	3.74813E-7
0.90625	0.000514042	0.000499863	0.000500238	1.38040E-5	3.74813E-7
0.96875	0.00051602	0.000499871	0.000500246	1.57740E-5	3.74813E-7

In case of $\gamma = 0.001$, the *R.M.S. error* between the Haar wavelet solutions and the exact solutions of Burgers-Huxley equations for $t = 0.4, 0.6$ and 1 are 3.00204E-6, 4.50295E-6 and 7.50449E-6 respectively and that of the VIM solutions and the exact solutions are 1.49925E-7, 2.24888E-7 and 3.74813E-7 respectively. In case of Burgers-Huxley equation, Figures 2.11-2.13 cite the comparison graphically between the numerical solutions obtained by Haar wavelet method, VIM and exact solutions for different values of t and γ.
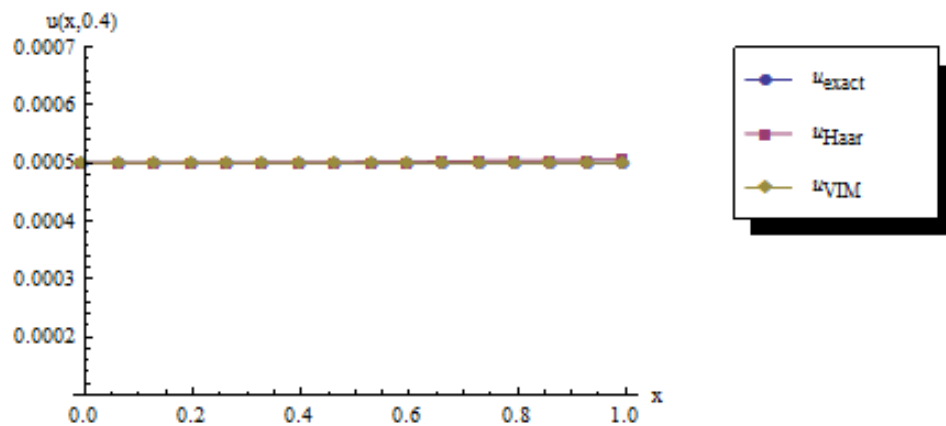
Figure 2.11   Comparison of Haar wavelet solutions and VIM solutions with the exact solution of Burgers-Huxley equation when $t = 0.4$ and $\gamma = 0.001$.
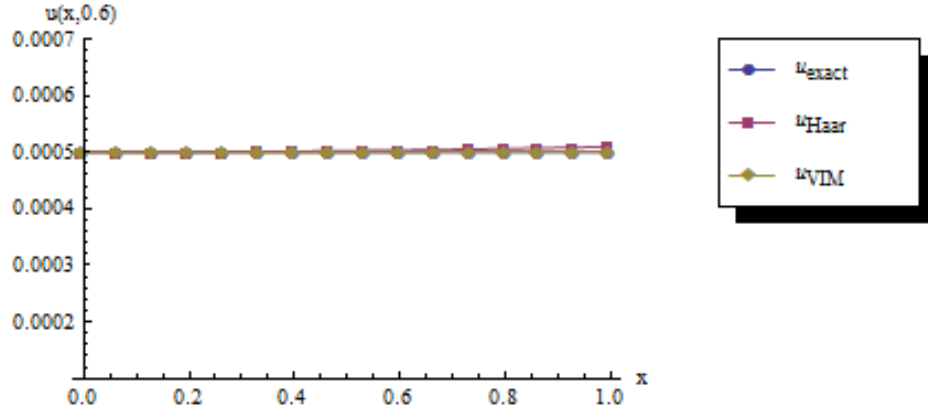
Figure 2.12 Comparison of Haar wavelet solutions and VIM solutions with the exact solution of Burgers-Huxley equation when $t = 0.6$ and $\gamma = 0.001$.
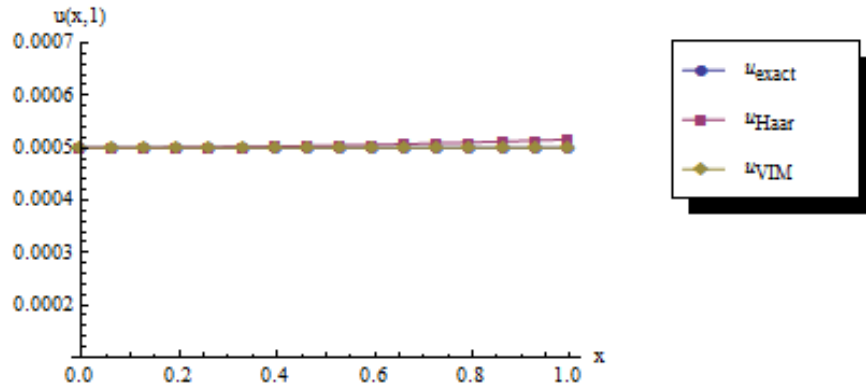
Figure 2.13 Comparison of Haar wavelet solutions and VIM solutions with the exact solution of Burgers-Huxley equation when $t = 1$ and $\gamma = 0.001$.

2.6 Application of Analytical and Numerical Methods for Solving Huxley equation

Huxley equation is a nonlinear partial differential equation of second order of the form

$$u_t = u_{xx} + u(k - u)(u - 1), \quad k \neq 0,$$ (2.65)

with initial condition

$$u(x,0) = \frac{1}{2}\left[1 + \tanh\left(\frac{x}{2\sqrt{2}}\right)\right]$$ (2.66)

The exact solution of eq. (2.65) is given by [68]

$$u(x,t) = \frac{1}{2}\left[1 + \tanh\left\{\frac{1}{2\sqrt{2}}\left(x - \frac{2k-1}{\sqrt{2}}t\right)\right\}\right], \quad k \neq 0$$ (2.67)

55

Taking $k = 1$, the boundary conditions are

$$u(0,t) = \frac{1}{2}\left[1 - \tanh\left(\frac{t}{4}\right)\right],$$

$$u(1,t) = \frac{1}{2}\left[1 + \tanh\left\{\frac{1}{2\sqrt{2}}\left(1 - \frac{t}{\sqrt{2}}\right)\right\}\right].$$ (2.68)

2.6.1 Application of Variational Iteration Method for Solving Huxley Equation

Construct a correctional functional as follows:

$$u_{n+1}(x,t) = u_n(x,t) + \int_0^t \lambda\left[(u_n)_\tau - (\tilde{u}_n)_{xx} - u_n(k - \tilde{u}_n)(u_n - 1)\right]d\tau,$$ (2.69)

where λ is a general Lagrangian multiplier whose optimal value can be found using variational theory and $\tilde{u}_n(x,t)$ is the restricted variation, i.e. $\delta\tilde{u}_n(x,t) = 0$.

$$\delta u_{n+1}(x,t) = \delta u_n(x,t) + \delta\int_0^t \lambda\left[(u_n)_\tau - (\tilde{u}_n)_{xx} - u_n(k - \tilde{u}_n)(u_n - 1)\right]d\tau,$$ (2.70)

From the above eq. (2.70), we have

$$\delta u_{n+1}(x,t) = \delta u_n(x,t) + \delta\int_0^t \lambda\left(\frac{\partial u_n}{\partial \tau}\right)d\tau,$$ (2.71)

since $\delta(\tilde{u}_n)_{xx} = 0$ and $\delta\left(u_n(k - \tilde{u}_n)(u_n - 1)\right) = 0$.

Integrating right hand side of eq. (2.71) yields

$$\delta u_{n+1}(x,t) = \delta u_n(x,t)(1 + \lambda) - \int_0^t \delta u_n(x,t)\lambda' d\tau$$ (2.72)

From stationary condition, we know

$$\delta u_{n+1}(x,t) = 0,$$

which yields that $\delta u_n(x,t)(1 + \lambda) - \int_0^t \delta u_n(x,\tau)\lambda' d\tau = 0$

This implies $1 + \lambda = 0$ and $\lambda'(t) = 0$

Hence $\lambda = -1$ (2.73)

Therefore λ can be identified as -1, and the following variational iteration formula can be obtained as

$$u_{n+1}(x,t) = u_n(x,t) - \int_0^t \left[(u_n)_\tau - (\tilde{u}_n)_{xx} - u_n(k - \tilde{u}_n)(u_n - 1) \right] d\tau .$$

(2.74)

From the above iteration formula eq. (2.74), we can obtained

$$u_1(x,t) = 0.5 + 0.5 \tanh\left(\frac{x}{2\sqrt{2}}\right) - 0.125\, t \sech^2\left(\frac{x}{2\sqrt{2}}\right),$$

(2.75)

with initial condition

$$u_0(x,t) = \frac{1}{2}\left[1 + \tanh\left(\frac{x}{2\sqrt{2}}\right)\right].$$

2.6.2 Application of Haar Wavelet Method for Solving Huxley Equation

It is assumed that $\ddot{u}''(x,t)$ can be expanded in terms of Haar wavelets as

$$\ddot{u}''(x,t) = \sum_{i=1}^{2M} a_s(i) h_i(x) \text{ for } t \in [t_s, t_{s+1}]$$

(2.76)

where "$\cdot$" and "$'$" stands for differentiation with respect to t and x respectively.

Now, integrating eq. (2.76) with respect to t from t_s to t and twice with respect to x from 0 to x the following equations are obtained

$$u''(x,t) = (t - t_s) \sum_{i=1}^{2M} a_s(i) h_i(x) + u''(x,t_s),$$

(2.77)

$$u'(x,t) = (t - t_s) \sum_{i=1}^{2M} a_s(i) p_i(x) + u'(x,t_s) - u'(0,t_s) + u'(0,t),$$

(2.78)

$$u(x,t) = (t - t_s) \sum_{i=1}^{2M} a_s(i) q_i(x) + u(x,t_s) - u(0,t_s) + x[u'(0,t) - u'(0,t_s)] + u(0,t),$$

(2.79)

$$\dot{u}(x,t) = \sum_{i=1}^{2M} a_s(i) q_i(x) + x\dot{u}'(0,t) + \dot{u}(0,t).$$

(2.80)

By using the boundary conditions, at $x = 1$, we have

$$\dot{u}'(0,t) = -\sum_{i=1}^{2M} a_s(i) q_i(1) + \dot{u}(1,t) - \dot{u}(0,t).$$

(2.81)

Discretizing the results by assuming $x \to x_l$, $t \to t_{s+1}$, we obtain

$$u''(x_l, t_{s+1}) = (t_{s+1} - t_s) \sum_{i=1}^{2M} a_s(i) h_i(x_l) + u''(x_l, t_s),$$

(2.82)

$$u'(x_l, t_{s+1}) = (t_{s+1} - t_s) \sum_{i=1}^{2M} a_s(i) p_i(x_l) + u'(x_l, t_s) - u'(0, t_s) + u'(0, t_{s+1}),$$ (2.83)

$$u(x_l, t_{s+1}) = (t_{s+1} - t_s) \sum_{i=1}^{2M} a_s(i) q_i(x_l) + u(x_l, t_s) - u(0, t_s) + x_l[u'(0, t_{s+1}) - u'(0, t_s)] + u(0, t_{s+1}),$$

(2.84)

$$\dot{u}(x_l, t_{s+1}) = \sum_{i=1}^{2M} a_s(i) q_i(x_l) + x_l \dot{u}'(0, t_{s+1}) + \dot{u}(0, t_{s+1}).$$ (2.85)

Substituting eqs. (2.85) and (2.81) in eq. (2.65), we have

$$\sum_{i=1}^{2M} a_s(i)[q_i(x_l) - x_l q_i(1)] = u''(x_l, t_s) - u(x_l, t_s)[1 - u(x_l, t_s)]^2 -$$
$$\dot{u}(0, t_{s+1}) - x_l[\dot{u}(1, t_{s+1}) - \dot{u}(0, t_{s+1})].$$ (2.86)

From eq. (2.86), the wavelet coefficients $a_s(i)$ can be successively calculated. This process started with

$$u(x_l, t_0) = \frac{1}{2}\left[1 + \tanh\left(\frac{x_l}{2\sqrt{2}}\right)\right],$$

$$u'(x_l, t_0) = \frac{1}{4\sqrt{2}} \sec h^2\left(\frac{x_l}{2\sqrt{2}}\right),$$

$$u''(x_l, t_0) = -\frac{1}{8} \sec h^2\left(\frac{x_l}{2\sqrt{2}}\right) \tanh\left(\frac{x_l}{2\sqrt{2}}\right).$$

2.6.3 Numerical Results for Huxley Equation

In the following Tables 2.10-2.12, J has been taken as 3 i.e. $M = 8$ and Δt is taken as 0.0001. Again, the *R.M.S. error* can be calculated for different values of *t*. For $t = 0.4, 0.6$ and 1, the *R.M.S. error* between the Haar wavelet solutions and the exact solutions of Huxley equation are 0.0209303, 0.0354936 and 0.060677 respectively. For $t = 0.4, 0.6$ and 1, the *R.M.S. error* between the VIM solutions and the exact solutions of Huxley equation are 8.10868E-4, 1.696E-3 and 4.03601E-3 respectively.

Table 2.10 The absolute errors for the solutions of Huxley equation using Haar wavelet method and one iteration of VIM at various collocation points for *x* with $k = 1$ and $t = 0.4$.

x	Approximate solutions using Haar wavelet method (u_{approx})	Approximate solutions using VIM (u_{approx})	Exact solutions (u_{exact})	Absolute Errors using Haar wavelet	Absolute Errors using VIM
0.03125	0.455737	0.45553	0.455641	9.55529E-5	1.11054E-4
0.09375	0.467153	0.466622	0.466623	5.30592E-4	8.87183E-7
0.15625	0.478927	0.477746	0.477636	1.29070E-3	1.09283 E-4
0.21875	0.491048	0.488891	0.488672	2.37582E-3	2.19028 E-4
0.28125	0.503505	0.500046	0.499718	3.78609E-3	3.27923E-4
0.34375	0.516287	0.511201	0.510765	5.52185E-3	4.35548E-4
0.40625	0.529385	0.522343	0.521802	7.58360E-3	5.41497E-4
0.46875	0.542789	0.533462	0.532817	9.97205E-3	6.45376E-4
0.53125	0.556488	0.544547	0.5438	1.26880E-2	7.46806E-4
0.59375	0.570474	0.555586	0.554741	1.57326E-2	8.45430E-4
0.65625	0.584736	0.56657	0.565629	1.91070E-2	9.40912E-4
0.71875	0.599266	0.577487	0.576454	2.28126E-2	1.03294E-3
0.78125	0.614057	0.588327	0.587206	2.68510E-2	1.12123 E-3
0.84375	0.629099	0.599081	0.597876	3.12230E-2	1.20552E-3
0.90625	0.645576	0.609739	0.608453	3.71230E-2	1.28559E-3
0.96875	0.668244	0.620291	0.61893	4.93140E-2	1.36124E-3

Table 2.11   The absolute errors for the solutions of Huxley equation using Haar wavelet method and one iteration of VIM at various collocation points for x with $k = 1$ and $t = 0.6$.

x	Approximate solutions using Haar wavelet method (u_{approx})	Approximate solutions using VIM (u_{approx})	Exact solutions (u_{exact})	Absolute Errors using Haar wavelet	Absolute Errors using VIM
0.03125	0.431155	0.430533	0.430968	1.87446E-4	4.34778E-4
0.09375	0.442789	0.441649	0.441837	9.51983E-4	1.88225E-4
0.15625	0.454998	0.452822	0.452763	2.23552E-3	5.90574E-5
0.21875	0.467771	0.46404	0.463734	4.03766E-3	3.06109E-4
0.28125	0.481098	0.475292	0.47474	6.35830E-3	5.51971E-4
0.34375	0.494968	0.486567	0.485771	9.19760E-3	7.95698E-4
0.40625	0.509372	0.497852	0.496816	1.25560E-2	1.03636E-3
0.46875	0.524298	0.509136	0.507863	1.64343E-2	1.27304E-3
0.53125	0.539737	0.520408	0.518904	2.08334E-2	1.50489E-3
0.59375	0.55568	0.531656	0.529925	2.57546E-2	1.73105E-3
0.65625	0.572117	0.542869	0.540918	3.11994E-2	1.95074E-3
0.71875	0.589041	0.554034	0.551871	3.71696E-2	2.16323E-3
0.78125	0.606441	0.565142	0.562774	4.36670E-2	2.36782E-3
0.84375	0.62431	0.57618	0.573616	5.06940E-2	2.56389E-3
0.90625	0.645842	0.58714	0.584389	6.14530E-2	2.75089E-3

| 0.96875 | 0.683829 | 0.598009 | 0.595081 | 8.87480E-2 | 2.92832E-3 |

Table 2.12   The absolute errors for the solutions of Huxley equation using Haar wavelet method and one iteration of VIM at various collocation points for x with $k=1$ and $t=1$.

x	Approximate solutions using Haar wavelet method $\left(u_{approx}\right)$	Approximate solutions using VIM $\left(u_{approx}\right)$	Exact solutions $\left(u_{exact}\right)$	Absolute Errors using Haar wavelet	Absolute Errors using VIM
0.03125	0.383171	0.380539	0.382747	4.23760E-4	2.20814E-3
0.09375	0.395066	0.391704	0.393241	1.82475E-3	1.53709E-3
0.15625	0.407796	0.402974	0.403834	3.96201E-3	8.60175E-4
0.21875	0.421352	0.414338	0.414518	6.83392E-3	1.79977E-4
0.28125	0.435721	0.425783	0.425282	1.04393E-2	5.00891E-4
0.34375	0.450895	0.437298	0.436118	1.47773E-2	1.17981E-3
0.40625	0.466863	0.448869	0.447015	1.98477E-2	1.85419E-3
0.46875	0.483614	0.460485	0.457964	2.56507E-2	2.52146E-3
0.53125	0.501139	0.472132	0.468953	3.21868E-2	3.17912E-3
0.59375	0.519429	0.483797	0.479972	3.94572E-2	3.82474E-3
0.65625	0.538474	0.495467	0.491011	4.74633E-2	4.45598E-3
0.71875	0.558265	0.507129	0.502058	5.62070E-2	5.07062E-3
0.78125	0.578795	0.51877	0.513104	6.56910E-2	5.66659E-3
0.84375	0.600054	0.530378	0.524137	7.59170E-2	6.24192E-3
0.90625	0.632639	0.541941	0.535146	9.74930E-2	6.79482E-3
0.96875	0.718961	0.553445	0.546121	1.72840E-1	7.32368E-3

In case of Huxley equation, the Figure 2.14 present the comparison graphically between the numerical results obtained by Haar wavelet method, VIM and exact solutions for different values of t and $k=1$.
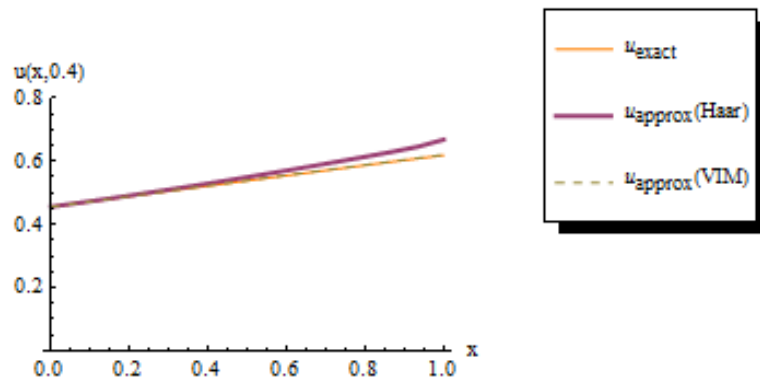
Figure 2.14   Comparison of Haar wavelet solutions and VIM solutions with the exact solution of Huxley equations when $t = 0.4$ and $k = 1$.

2.7 Numerical Solution of Generalized Modified KdV Equation

Consider the generalized modified KdV equation [80-82]

$$u_t + qu^2 u_x + ru_{xxx} = 0, \ 0 \le x \le 1, \ t \ge 0 \tag{2.87}$$

with initial condition

$$u(x,0) = \sqrt{\frac{-6r}{q}} \tanh(x). \tag{2.88}$$

The exact solution of Eq. (2.87) is given by [80]

$$u(x,t) = \sqrt{\frac{-6r}{q}} \tanh(x + 2rt) \tag{2.89}$$

where q and r are parameters.

This exact solution satisfies the following boundary conditions

$$u(0,t) = \sqrt{\frac{-6r}{q}} \tanh(2rt), \ \ t \ge 0$$

$$u(1,t) = \sqrt{\frac{-6r}{q}} \tanh(1 + 2rt), \ t \ge 0 \tag{2.90}$$

Haar wavelet solution of $u(x,t)$ is sought by assuming that $\dot{u}'''(x,t)$ can be expanded in terms of Haar wavelets as

$$\dot{u}'''(x,t) = \sum_{i=1}^{2M} a_s(i) h_i(x) \ \text{ for } t \in [t_s, t_{s+1}] \tag{2.91}$$

Integrating eq. (2.91) with respect to t from t_s to t and thrice with respect to x from 0 to x, the following equations are obtained

$$u'''(x,t) = (t - t_s) \sum_{i=1}^{2M} a_s(i) h_i(x) + u'''(x,t_s), \tag{2.92}$$

$$u''(x,t) = (t - t_s) \sum_{i=1}^{2M} a_s(i) p_i(x) + u''(x,t_s) + u''(0,t) - u''(0,t_s), \tag{2.93}$$

$$u'(x,t) = (t - t_s) \sum_{i=1}^{2M} a_s(i) q_i(x) + u'(x,t_s) + x[u''(0,t) - u''(0,t_s)] + u'(0,t) - u'(0,t_s), \tag{2.94}$$

$$u(x,t)=(t-t_s)\sum_{i=1}^{2M}a_s(i)r_i(x)+u(x,t_s)+\frac{x^2}{2}\left[u''(0,t)-u''(0,t_s)\right]$$
$$+x\left[u'(0,t)-u'(0,t_s)\right]+u(0,t)-u(0,t_s)$$

(2.95)

$$\dot{u}(x,t)=\sum_{i=1}^{2M}a_s(i)r_i(x)+x\dot{u}'(0,t)+\frac{x^2}{2}\dot{u}''(0,t)+\dot{u}(0,t).$$

(2.96)

Using finite difference method

$$\dot{u}(0,t)=\frac{u(0,t)-u(0,t_s)}{(t-t_s)},$$

Equation (2.96) becomes

$$\dot{u}(x,t)=\sum_{i=1}^{2M}a_s(i)r_i(x)+\frac{x^2}{2}\left[\frac{u''(0,t)-u''(0,t_s)}{t-t_s}\right]+x\left[\frac{u'(0,t)-u'(0,t_s)}{t-t_s}\right]$$
$$+\left[\frac{u(0,t)-u(0,t_s)}{t-t_s}\right].$$

(2.97)

By using the boundary condition at $x=1$, eq. (2.94) becomes

$$u'(1,t)=(t-t_s)\sum_{i=1}^{2M}a_s(i)q_i(1)+u'(1,t_s)-u'(0,t_s)+u'(0,t)+\left[u''(0,t)-u''(0,t_s)\right].$$

This implies

$$u''(0,t)-u''(0,t_s)=-(t-t_s)\sum_{i=1}^{2M}a_s(i)q_i(1)+\left[u'(1,t)-u'(1,t_s)\right]-\left[u'(0,t)-u'(0,t_s)\right].$$

(2.98)

Substituting eq. (2.98) in eqs. (2.93) - (2.96), we have

$$u''(x,t)=(t-t_s)\sum_{i=1}^{2M}a_s(i)p_i(x)+u''(x,t_s)+$$
$$\left[-(t-t_s)\sum_{i=1}^{2M}a_s(i)q_i(1)+\left[u'(1,t)-u'(1,t_s)\right]-\left[u'(0,t)-u'(0,t_s)\right]\right],$$

(2.99)

$$u'(x,t)=(t-t_s)\sum_{i=1}^{2M}a_s(i)q_i(x)+u'(x,t_s)-u'(0,t_s)+u'(0,t)$$
$$+x\left[-(t-t_s)\sum_{i=1}^{2M}a_s(i)q_i(1)+u'(1,t)-u'(1,t_s)-u'(0,t)+u'(0,t_s)\right],$$

(2.100)

$$u(x,t)=(t-t_s)\sum_{i=1}^{2M}a_s(i)r_i(x)+\frac{x^2}{2}\left[-(t-t_s)\sum_{i=1}^{2M}a_s(i)q_i(1)+u'(1,t)-u'(1,t_s)-u'(0,t)+u'(0,t_s)\right]$$
$$+u(x,t_s)+x\left[u'(0,t)-u'(0,t_s)\right]+u(0,t)-u(0,t_s),$$

(2.101)

$$\dot{u}(x,t)=\sum_{i=1}^{2M}a_s(i)r_i(x)+\frac{x^2}{2(t-t_s)}\left[-(t-t_s)\sum_{i=1}^{2M}a_s(i)q_i(1)+u'(1,t)-u'(1,t_s)-u'(0,t)+u'(0,t_s)\right]$$

$$+\frac{x}{t-t_s}\left[u'(0,t)-u'(0,t_s)\right]+\frac{1}{t-t_s}\left[u(0,t)-u(0,t_s)\right].$$

<div align="right">(2.102)</div>

Discretizing the above results by assuming $x\to x_l$, $t\to t_{s+1}$, we obtain

$$u'''(x_l,t_{s+1})=(t_{s+1}-t_s)\sum_{i=1}^{2M}a_s(i)h_i(x_l)+u'''(x_l,t_s),$$

$$u''(x_l,t_{s+1})=(t_{s+1}-t_s)\sum_{i=1}^{2M}a_s(i)p_i(x_l)+u''(x_l,t_s)+$$

<div align="right">(2.103)</div>

$$\left[-(t_{s+1}-t_s)\sum_{i=1}^{2M}a_s(i)q_i(1)+\left[u'(1,t_{s+1})-u'(1,t_s)\right]-\left[u'(0,t_{s+1})-u'(0,t_s)\right]\right],$$

$$u'(x_l,t_{s+1})=(t_{s+1}-t_s)\sum_{i=1}^{2M}a_s(i)q_i(x_l)+u'(x_l,t_s)+u'(0,t_{s+1})-u'(0,t_s)+$$

<div align="right">(2.104)</div>

$$x_l\left[-(t_{s+1}-t_s)\sum_{i=1}^{2M}a_s(i)q_i(1)+\left[u'(1,t_{s+1})-u'(1,t_s)\right]-\left[u'(0,t_{s+1})-u'(0,t_s)\right]\right],$$

$$u(x_l,t_{s+1})=(t_{s+1}-t_s)\sum_{i=1}^{2M}a_s(i)r_i(x_l)+u(x_l,t_s)+u(0,t_{s+1})-u(0,t_s)$$

$$+x_l\left[u'(0,t_{s+1})-u'(0,t_s)\right]$$

<div align="right">(2.105)</div>

$$+\frac{x_l^2}{2}\left[-(t_{s+1}-t_s)\sum_{i=1}^{2M}a_s(i)q_i(1)+\left[u'(1,t_{s+1})-u'(1,t_s)\right]-\left[u'(0,t_{s+1})-u'(0,t_s)\right]\right],$$

$$\dot{u}(x_l,t_{s+1})=\sum_{i=1}^{2M}a_s(i)r_i(x_l)+\frac{1}{t_{s+1}-t_s}\left[u(0,t_{s+1})-u(0,t_s)\right]+\frac{x_l}{t_{s+1}-t_s}\left[u'(0,t_{s+1})-u'(0,t_s)\right]$$

<div align="right">(2.106)</div>

$$+\frac{x_l^2}{2(t_{s+1}-t_s)}\left[-(t_{s+1}-t_s)\sum_{i=1}^{2M}a_s(i)q_i(1)+u'(1,t_{s+1})-u'(1,t_s)-u'(0,t_{s+1})+u'(0,t_s)\right].$$

Substituting the above equations in eq. (2.87), we have

$$\sum_{i=1}^{2M}a_s(i)r_i(x_l)+\frac{x_l^2}{2(t_{s+1}-t_s)}\left[-(t_{s+1}-t_s)\sum_{i=1}^{2M}a_s(i)q_i(1)+u'(1,t_{s+1})-u'(1,t_s)-\right.$$

$$\left.u'(0,t_{s+1})+u'(0,t_s)\right]+\frac{x_l}{t_{s+1}-t_s}\left[u'(0,t_{s+1})-u'(0,t_s)\right]+\frac{1}{t_{s+1}-t_s}\left[u(0,t_{s+1})-u(0,t_s)\right]$$

<div align="right">(2.107)</div>

$$=0.001u'''(x_l,t_s)-6\left[u(x_l,t_s)\right]^2\left[u'(x_l,t_s)\right].$$

Therefore,

$$\sum_{i=1}^{2M} a_s(i)\left[r_i(x_l) - \frac{x_l^2}{2} q_i(1)\right] = 0.001 u'''(x_l, t_s) - 6[u(x_l, t_s)]^2[u'(x_l, t_s)]$$

$$- \frac{x_l^2}{2(t_{s+1} - t_s)}[u'(1, t_{s+1}) - u'(1, t_s)] + \frac{x_l^2}{2(t_{s+1} - t_s)}[u'(0, t_{s+1}) - u'(0, t_s)] \qquad (2.108)$$

$$- \frac{x_l}{t_{s+1} - t_s}[u'(0, t_{s+1}) - u'(0, t_s)] - \frac{1}{t_{s+1} - t_s}[u(0, t_{s+1}) - u(0, t_s)] .$$

From the above equation, the wavelet coefficients $a_s(i)$ can be successively calculated. This process starts with

$$u(x_l, t_0) = \sqrt{\frac{-6r}{q}}\ \tanh(x_l),$$

$$u'(x_l, t_0) = \sqrt{\frac{-6r}{q}}\ \sec h^2(x_l).$$

2.7.1 Numerical Results of mKdV Equation

The following Tables show the comparisons of the exact solutions with the approximate solutions of modified KdV equation taking $q = 6, r = -0.001$ and different values of t. In Tables 2.13-2.16, J is taken as 3 i.e. $M = 8$ and Δt is taken as 0.0001.

Table 2.13 The absolute errors for modified KdV equation at various collocation points of x with $t = 0.2$ and $r = -0.001$.

x	Approximate solution (u_{approx})	Exact solution (u_{exact})	Absolute Error
0.03125	0.000975289	0.000975254	3.45313E-8
0.09375	0.00294375	0.00294344	3.10577E-7
0.15625	0.00488976	0.00488889	8.63705E-7
0.21875	0.00679886	0.00679716	1.6977E-6
0.28125	0.00865771	0.00865489	2.8188E-6
0.34375	0.0104545	0.0104502	4.23521E-6
0.40625	0.0121789	0.012173	5.95649E-6
0.46875	0.0138229	0.0138149	7.99297E-6
0.53125	0.01538	0.0153696	1.03551E-5
0.59375	0.0168459	0.0168328	1.30530E-5
0.65625	0.018218	0.0182019	1.60958E-5
0.71875	0.0194955	0.019476	1.94918E-5
0.78125	0.0206791	0.0206558	2.32477E-5
0.84375	0.0217706	0.0217432	2.73688E-5
0.90625	0.0227729	0.022741	3.18592E-5
0.96875	0.0236899	0.0236532	3.67252E-5

Table 2.14 The absolute errors for modified KdV equation at various collocation points of x with $t = 0.5$ and $r = -0.001$.

x	Approximate solution (u_{approx})	Exact solution (u_{exact})	Absolute Error
0.03125	0.000956384	0.000956298	8.64056E-8
0.09375	0.00292541	0.00292463	7.77845E-7
0.15625	0.00487254	0.00487037	2.16512E-6
0.21875	0.00678332	0.00677906	4.25957E-6
0.28125	0.00864442	0.00863734	7.07870E-6
0.34375	0.010444	0.0104333	1.06449E-5
0.40625	0.0121718	0.0121568	1.49840E-5
0.46875	0.0138197	0.0137995	2.01238E-5
0.53125	0.0153812	0.0153552	2.60922E-5
0.59375	0.0168522	0.0168192	3.29164E-5
0.65625	0.0182299	0.0181892	4.06215E-5
0.71875	0.0195135	0.0194643	4.92298E-5
0.78125	0.0207037	0.020645	5.87601E-5
0.84375	0.0218024	0.0217332	6.92277E-5
0.90625	0.0228125	0.0227319	8.06444E-5
0.96875	0.0237378	0.0236448	9.30207E-5

Table 2.15 The absolute errors for modified KdV equation at various collocation points of x with $t = 0.8$ and $r = -0.001$.

x	Approximate solution (u_{approx})	Exact solution (u_{exact})	Absolute Error
0.03125	0.00093748	0.000937341	1.38295E-7
0.09375	0.00290707	0.00290582	1.24525E-6
0.15625	0.00485531	0.00485185	3.46691E-6
0.21875	0.00676778	0.00676095	6.82219E-6
0.28125	0.00863112	0.00861978	1.13399E-5
0.34375	0.0104335	0.0104164	1.70566E-5
0.40625	0.0121647	0.0121406	2.40144E-5
0.46875	0.0138164	0.0137842	3.22585E-5
0.53125	0.0153825	0.0153406	4.18346E-5
0.59375	0.0168584	0.0168056	5.27869E-5
0.65625	0.0182417	0.0181765	6.51565E-5
0.71875	0.0195315	0.0194525	7.89797E-5
0.78125	0.0207283	0.0206341	9.42876E-5
0.84375	0.0218343	0.0217232	1.11105E-4
0.90625	0.0228522	0.0227227	1.29453E-4
0.96875	0.0237858	0.0236364	1.49345E-4

Table 2.16 The absolute errors for modified KdV equation at various collocation points of x with $t = 1$ and $r = -0.001$.

x	Approximate solution (u_{approx})	Exact solution (u_{exact})	Absolute Error
0.03125	0.000924876	0.000924703	1.72895E-7
0.09375	0.00289483	0.00289328	1.55692E-6
0.15625	0.00484383	0.0048395	4.33497E-6
0.21875	0.00675741	0.00674888	8.53102E-6
0.28125	0.00862225	0.00860807	1.41814E-5
0.34375	0.0104265	0.0104051	2.13321E-5
0.40625	0.0121599	0.0121299	3.00363E-5
0.46875	0.0138143	0.0137739	4.03506E-5
0.53125	0.0153833	0.015331	5.23326E-5
0.59375	0.0168626	0.0167965	6.60379E-5
0.65625	0.0182496	0.0181681	8.15183E-5
0.71875	0.0195434	0.0194446	9.88196E-5
0.78125	0.0207448	0.0206268	1.17981E-4
0.84375	0.0218555	0.0217165	1.39034E-4
0.90625	0.0228786	0.0227166	1.62005E-4
0.96875	0.0238178	0.0236309	1.86910E-4

In case of $r = -0.001$, the *R.M.S. error* between the numerical solutions and the exact solutions of modified KdV equations for $t = 0.2, 0.5, 0.8$ and 1 are 1.7137E-5, 4.33416E-5, 6.95581E-5 and 8.70423E-5 respectively and for $r = -0.1$ and $t = 0.2, 0.5, 0.8$ and 1 the *R.M.S. error* is found to be 0.00209359, 0.00624177, 0.011631 and 0.0159099 respectively. In the following Tables 2.17-2.20 also J has been taken as 3 i.e. $M = 8$ and Δt is taken as 0.0001.

Table 2.17 The absolute errors for modified KdV equation at various collocation points of x with $t = 0.2$ and $r = -0.1$.

x	Approximate solution (u_{approx})	Exact solution (u_{exact})	Absolute Error
0.03125	-0.00276621	-0.00276692	7.13784E-7
0.09375	0.0169876	0.0169809	6.65888E-6
0.15625	0.0366175	0.0365968	2.07298E-5
0.21875	0.0559793	0.0559313	4.79820E-5
0.28125	0.0749397	0.0748436	9.60655E-5
0.34375	0.09338	0.0932052	1.74756E-4

0.40625	0.111199	0.110903	2.95389E-4
0.46875	0.128314	0.127843	4.70239E-4
0.53125	0.144661	0.14395	7.11916E-4
0.59375	0.160198	0.159166	1.03281E-3
0.65625	0.174899	0.173455	1.44463E-3
0.71875	0.188756	0.186798	1.95802E-3
0.78125	0.201774	0.199192	2.58235E-3
0.84375	0.213974	0.210648	3.32555E-3
0.90625	0.225384	0.22119	4.19409E-3
0.96875	0.236043	0.23085	5.19293E-3

Table 2.18 The absolute errors for modified KdV equation at various collocation points of x with $t = 0.5$ and $r = -0.1$.

x	Approximate solution (u_{approx})	Exact solution (u_{exact})	Absolute Error
0.03125	-0.0217032	-0.0217065	3.31576E-6
0.09375	-0.00194595	-0.0019764	3.04463E-5
0.15625	0.0178593	0.0177691	9.02230E-5
0.21875	0.0375721	0.0373766	1.95531E-4
0.28125	0.057063	0.0566968	3.66140E-4
0.34375	0.0762172	0.0755894	6.27708E-4
0.40625	0.0949371	0.0939266	1.01047E-3
0.46875	0.113144	0.111596	1.54778E-3
0.53125	0.130779	0.128504	2.27451E-3
0.59375	0.147801	0.144576	3.22569E-3
0.65625	0.16419	0.159755	4.43515E-3
0.71875	0.179941	0.174007	5.93453E-3
0.78125	0.195064	0.187312	7.75255E-3
0.84375	0.209583	0.199668	9.91447E-3
0.90625	0.223529	0.211087	1.24419E-2
0.96875	0.236946	0.221593	1.53524E-2

Table 2.19 The absolute errors for modified KdV equation at various collocation points of x with $t = 0.8$ and $r = -0.1$.

x	Approximate solution (u_{approx})	Exact solution (u_{exact})	Absolute Error
0.03125	-0.0404827	-0.0404909	8.13685E-6
0.09375	-0.0208453	-0.0209195	7.42051E-5
0.15625	-0.000970764	-0.00118585	2.15085E-4
0.21875	0.0190084	0.018557	4.51366E-4
0.28125	0.0389709	0.0381558	8.15061E-4

0.34375	0.05881	0.0574616	1.34835E-3
0.40625	0.0784361	0.0763344	2.10172E-3
0.46875	0.0977786	0.0946469	3.13176E-3
0.53125	0.116786	0.112288	4.49874E-3
0.59375	0.135428	0.129163	6.26422E-3
0.65625	0.153689	0.1452	8.48888E-3
0.71875	0.171574	0.160343	1.12307E-2
0.78125	0.189101	0.174557	1.45436E-2
0.84375	0.206301	0.187824	1.84763E-2
0.90625	0.223215	0.200143	2.30719E-2
0.96875	0.239891	0.211525	2.83664E-2

Table 2.20 The absolute errors for modified KdV equation at various collocation points of x with $t = 1$ and $r = -0.1$.

x	Approximate solution (u_{approx})	Exact solution (u_{exact})	Absolute Error
0.03125	-0.0528499	-0.0528626	1.27575E-5
0.09375	-0.0333573	-0.0334734	1.16031E-4
0.15625	-0.0134928	-0.0138262	3.33334E-4
0.21875	0.00661869	0.00592858	6.90107E-4
0.28125	0.0268634	0.0256371	1.22625E-3
0.34375	0.0471421	0.0451472	1.99484E-3
0.40625	0.0673727	0.0643127	3.06007E-3
0.46875	0.0874922	0.0829976	4.49462E-3
0.53125	0.107457	0.10108	6.37673E-3
0.59375	0.127243	0.118455	8.78725E-3
0.65625	0.146843	0.135037	1.18068E-2
0.71875	0.16627	0.150757	1.55134E-2
0.78125	0.185549	0.165569	1.99805E-2
0.84375	0.204718	0.179443	2.52756E-2
0.90625	0.223827	0.192368	3.14593E-2
0.96875	0.24293	0.204347	3.85831E-2

Similarly, in case of modified KdV equation, the Figures 2.15-2.19 demonstrate the comparison graphically between the numerical and exact solutions for different values of t and r.
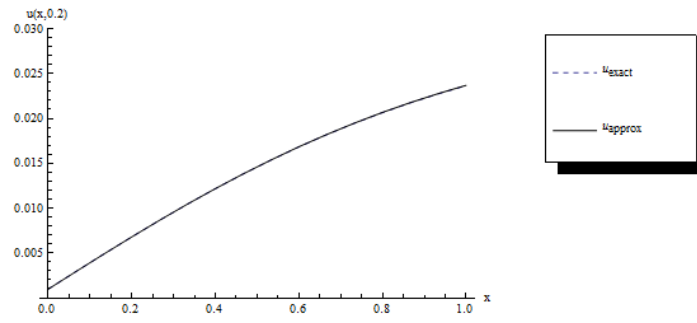
Figure 2.15 Comparison of Numerical solution and exact solution of modified KdV equation when $t = 0.2$ and $r = -0.001$.
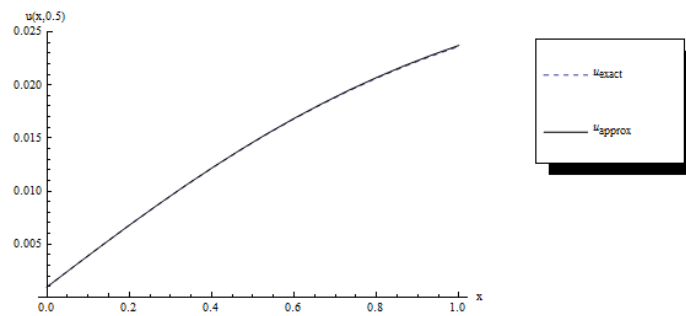
Figure 2.16 Comparison of Numerical solution and exact solution of modified KdV equation when $t = 0.5$ and $r = -0.001$.
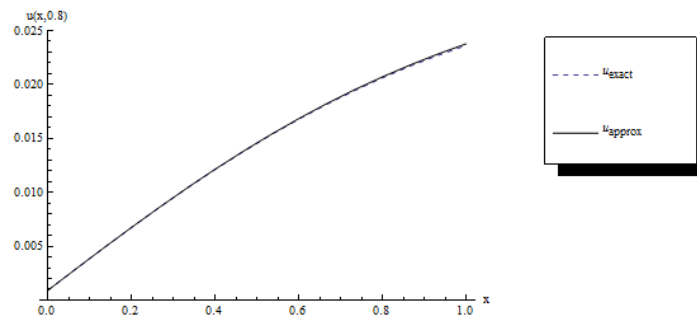
Figure 2.17 Comparison of Numerical solution and exact solution of modified KdV equation when $t = 0.8$ and $r = -0.001$.
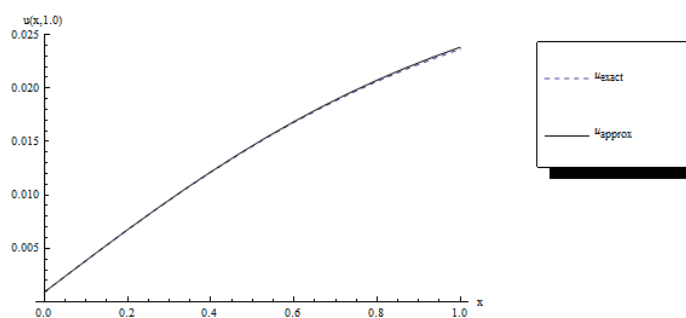
Figure 2.18   Comparison of Numerical solution and exact solution of modified KdV equation when $t = 1.0$ and $r = -0.001$.
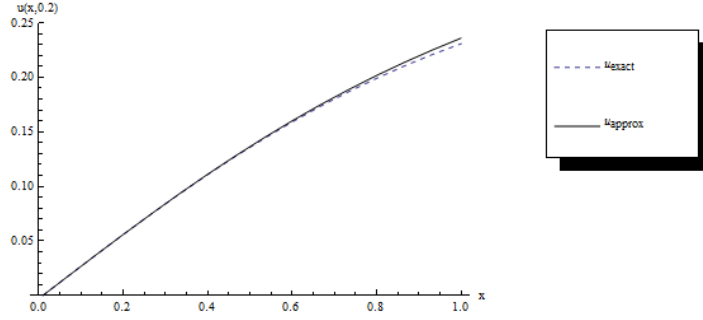
Figure 2.19   Comparison of Numerical solution and exact solution of modified KdV equation when $t = 0.2$ and $r = -0.1$.

2.8   Error of Collocation Method

The Haar wavelet family for $x \in [0, 1)$ is defined as follows

$$h_i(x) = \begin{cases} 1 & x \in [\xi_1, \xi_2) \\ -1 & x \in [\xi_2, \xi_3) \\ 0 & \text{elsewhere} \end{cases} \qquad (2.109)$$

where

$$\xi_1 = \frac{k}{m}, \; \xi_2 = \frac{k + 0.5}{m}, \quad \xi_3 = \frac{k + 1}{m}.$$

Consider $u(x, \tilde{t}) = (\tilde{t} - t_s) \sum_{i=1}^{2M} u(i) Q_i(x) + \psi(x, \tilde{t}), \qquad \tilde{t} \in [t_s, t_{s+1}]$ (2.110)

Define a projection map

$$P_m : L^2(\Omega) \to V_J$$

by the rule

$$P_m u(x, t_{s+1}) = u_m(x, t_{s+1}) = h \sum_{i=1}^{2M} u(i) Q_i(x) \qquad (2.111)$$

where $\Omega = [0, 1)$

and V_J is a subspace of $L^2(\Omega)$.

Now we have to estimate $\|u - P_m u\|$ for arbitrary $u \in L^2(\Omega)$.

70

Lemma 2.1   Let $u(x,t)$ be defined on $L^2(\Omega)$ and P_m be the projection map defined as above then

$$\|u - P_m u\| \leq \frac{\max|u|}{4M^2}$$

Proof: The integral $\int_0^1 u_m(x,t)dx$ is a ramp $\frac{u_i}{4M^2}\left[\frac{1}{2M} + (x - \xi_3)\right]$ on the interval $[0,1)$

with average value $\frac{u_i}{8M^2}\left[\frac{1}{2M} + (1 - \xi_3)\right]$.

The error in approximating the ramp by this constant value over the interval $[0,1)$ is

$$r(x) = \frac{u_i}{8M^2}\left[\frac{1}{2M} + (1 - \xi_3)\right] - \frac{u_i}{4M^2}\left[\frac{1}{2M} + (x - \xi_3)\right]$$

Hence, using $E(x)$ as least square of the error on Ω, we have

$$E^2(x) = \int_0^1 [r(x)]^2\, dx$$

$$= \int_0^1 \left(\frac{u_i}{8M^2}\left[\frac{1}{2M} + (1 - \xi_3)\right] - \frac{u_i}{4M^2}\left[\frac{1}{2M} + (x - \xi_3)\right]\right)^2 dx$$

$$= \int_0^1 \left(\frac{-u_i}{16M^3} + \frac{u_i}{8M^2} - \frac{u_i\xi_3}{8M^2} - \frac{u_i x}{4M^2} + \frac{u_i\xi_3}{4M^2}\right)^2 dx$$

$$= \int_0^1 \left(\frac{u_i\xi_3}{8M^2} + \frac{u_i}{8M^2} - \frac{u_i}{16M^3} - \frac{u_i x}{4M^2}\right)^2 dx$$

$$= \left(\frac{u_i}{4M^2}\right)^2 \int_0^1 \left(\frac{\xi_3}{2} + \frac{1}{2} - \frac{1}{4M} - x\right)^2 dx$$

$$\leq \left(\frac{u_i}{4M^2}\right)^2$$

This implies that

$$|E(x)| \leq \frac{|u_i|}{4M^2}. \tag{2.112}$$

On the interval Ω, we have

$$\|u - P_m u\| = \max_{x \in \Omega} E(x) \leq \frac{\max |u|}{4M^2} \tag{2.113}$$

2.9 Error Analysis

Let $P_m : L^2(\Omega) \rightarrow V_J$ be a projection map and is defined by

$$P_m u(x, t_{s+1}) = u_m(x, t_{s+1}) = h \sum_{i=1}^{2M} u(i) Q_i(x). \tag{2.114}$$

Let us consider the generalized modified Burgers' equation

$$\frac{\partial u}{\partial t} + u^2 \frac{\partial u}{\partial x} = v \frac{\partial^2 u}{\partial x^2}. \tag{2.115}$$

Suppose that $u_m = P_m u$ be the approximate solution of eq. (2.115) obtained by wavelet collocation method

$$\frac{\partial u_m}{\partial t} + u_m^2 \frac{\partial u_m}{\partial x} = v \frac{\partial^2 u_m}{\partial x^2} + e \tag{2.116}$$

then $\|e\| \leq \dfrac{A}{4M^2}$,

where $A = \max \left| \dfrac{\partial u}{\partial t} \right| + v \max \left| \dfrac{\partial^2 u}{\partial x^2} \right| + \max \left| u^2 \dfrac{\partial u}{\partial x} \right| + P_m u^2 \max \left| \dfrac{\partial u}{\partial x} \right|.$

Proof: Subtracting eq. (2.115) from eq. (2.116), we have

$$e = \frac{\partial u_m}{\partial t} + u_m^2 \frac{\partial u_m}{\partial x} - v \frac{\partial^2 u_m}{\partial x^2} - \frac{\partial u}{\partial t} - u^2 \frac{\partial u}{\partial x} + v \frac{\partial^2 u}{\partial x^2}$$

$$= \frac{\partial u_m}{\partial t} - \frac{\partial u}{\partial t} - v \left(\frac{\partial^2 u_m}{\partial x^2} - \frac{\partial^2 u}{\partial x^2} \right) + u_m^2 \frac{\partial u_m}{\partial x} - u^2 \frac{\partial u}{\partial x}$$

$$= \frac{\partial (u_m - u)}{\partial t} - v \frac{\partial^2 (u_m - u)}{\partial x^2} + (u_m)^2 \frac{\partial (u_m - u)}{\partial x} - \left(u^2 - u_m^2 \right) \frac{\partial u}{\partial x}$$

$$= \frac{\partial (P_m - I) u}{\partial t} - v \frac{\partial^2 (P_m - I) u}{\partial x^2} + (P_m u)^2 \frac{\partial (P_m - I) u}{\partial x} - (I - P_m) u^2 \frac{\partial u}{\partial x}$$

This implies

$$\|e\| \leq \|P_m - I\| \max \left| \frac{\partial u}{\partial t} \right| + v \|P_m - I\| \max \left| \frac{\partial^2 u}{\partial x^2} \right| + \|P_m - I\| (P_m u)^2 \max \left| \frac{\partial u}{\partial x} \right| + \|P_m - I\| \max \left| u^2 \frac{\partial u}{\partial x} \right|$$

$$\leq \|P_m - I\| \left[\max \left| \frac{\partial u}{\partial t} \right| + \nu \max \left| \frac{\partial^2 u}{\partial x^2} \right| + (P_m u)^2 \max \left| \frac{\partial u}{\partial x} \right| + \max \left| u^2 \frac{\partial u}{\partial x} \right| \right]$$

$$\leq \frac{A}{4M^2}$$

where $A = \max \left| \frac{\partial u}{\partial t} \right| + \nu \max \left| \frac{\partial^2 u}{\partial x^2} \right| + (P_m u)^2 \max \left| \frac{\partial u}{\partial x} \right| + \max \left| u^2 \frac{\partial u}{\partial x} \right|$.

2.10 Conclusion

In this chapter, variational iteration method and Haar wavelet method have been successfully implemented to compute approximate analytical as well as numerical solutions of nonlinear partial differential equations viz. the generalized Burgers-Huxley and Huxley equations. The obtained results are then compared with the exact solutions. The results thus obtained have been cited in Tables and also graphically to demonstrate the comparison of variational iteration method and Haar wavelet method. Also, the Burgers' equation, modified Burgers' equation and modified KdV equation have been solved by Haar wavelet method. The acquired results are then compared with the exact solutions as well as solutions available in open literature. These have been reported in Tables and also have been shown in the graphs in order to demonstrate the accuracy and efficiency of the proposed scheme based on Haar wavelet method. The present numerical scheme is reliable and convenient for solving nonlinear partial differential equations. The main advantages of the proposed scheme are its simplicity, applicability and less computational errors. Moreover, the error may be reduced significantly if we increase level of resolution which prompts more number of collocation points.

CHAPTER 3

3 Numerical Solution of System of Partial Differential Equations

3.1 Introduction

Numerical solutions of nonlinear differential equations are of great importance in physical problems since so far there exists no general technique for finding analytical and numerical solutions of system of nonlinear partial differential equations. It is well known that many physical, chemical and biological problems are characterized by the interaction of diffusion and reaction processes. With the development of science and engineering, nonlinear evolution equations have been used as the models to describe physical phenomena in fluid mechanics, plasma waves, solid state physics, chemical physics etc. System of nonlinear partial differential equations has also been noticed to arise in many chemical and biological applications. So, for the last few decades, a great deal of attention has been directed towards the solution (both exact and numerical) of these problems. Various methods are available in the literature for the exact and numerical solution of these problems. But, nonlinear partial differential equations are not in general easy to handle.

In this chapter, we apply Homotopy Perturbation Method (HPM), Optimal Homotopy Asymptotic Method (OHAM) and Haar wavelet method in order to compute the numerical solutions of nonlinear system of partial differential equations like Boussinesq-Burgers' equations. Our aim in the present work is to implement homotopy perturbation method (HPM) and optimal homotopy asymptotic method (OHAM) in order to demonstrate the capability of these methods in handling system of nonlinear equations, so that one can apply it to various types of nonlinearity.

In HPM and OHAM, the concept of homotopy from topology and conventional perturbation technique were merged to propose a general analytic procedure for the solution of nonlinear problems. Thus, these methods are independent of the existence of a small parameter in the problem at hand and thereby overcome the limitations of

conventional perturbation technique. OHAM, however, is the most generalized form of HPM as it employs a more general auxiliary function $H(p)$ in place of HPM's p.

OHAM provides a simple and easy way to control and adjust the convergence region for strong nonlinearity and is applicable to highly nonlinear fluid problem like Boussinesq-Burgers' equations. In the proposed OHAM procedure, the construction of the homotopy is quite different. The way to ensure the convergence in OHAM is quite different and more rigorous. Unlike other homotopy procedures, OHAM ensure a very rapid convergence since it needs only two or three terms for achieving an accurate solution instead of an infinite series. This is in fact the true power of the method. The convergence control parameters $C_1, C_2, C_3, ...$ provide us a convenient way to guarantee the convergence of OHAM series solution. Moreover, the optimal values of convergence control constants guarantee the certain convergence of OHAM series solution.

3.2 Overview of the Problem

Generalized Boussinesq-Burgers' equation [83-85] is a nonlinear partial differential equation of the form

$$u_t - \frac{1}{2}v_x + 2uu_x = 0, \tag{3.1}$$

$$v_t - \frac{1}{2}u_{xxx} + 2(uv)_x = 0, \ \ 0 \le x \le 1. \tag{3.2}$$

with initial conditions

$$u(x,0) = \frac{ck}{2} + \frac{ck}{2}\tanh\left(\frac{-kx - \ln b}{2}\right), \tag{3.3}$$

$$v(x,0) = \frac{-k^2}{8}\sec h^2\left(\frac{kx + \ln b}{2}\right). \tag{3.4}$$

The exact solutions of eq. (3.1) and (3.2) is given by [86]

$$u(x,t) = \frac{ck}{2} + \frac{ck}{2}\tanh\left(\frac{ck^2t - kx - \ln b}{2}\right), \tag{3.5}$$

$$v(x,t) = \frac{-k^2}{8}\sec h^2\left(\frac{kx - ck^2t + \ln b}{2}\right). \tag{3.6}$$

The Boussinesq-Burgers' equations arise in the study of fluid flow and describe the propagation of shallow water waves. Here x and t respectively represent the normalized space and time, $u(x,t)$ is the horizontal velocity field and $v(x,t)$ denotes the height of the water surface above a horizontal level at the bottom.

Various analytical methods such as Darboux transformation method [87], Lax pair, Bäcklund transformation method [86] have been used in attempting to solve Boussinesq-Burgers' equations.

These exact solutions given in eqs. (3.5) and (3.6) satisfies the following boundary conditions

$$u(0,t) = \frac{ck}{2} + \frac{ck}{2}\tanh\left(\frac{ck^2 t - \ln b}{2}\right),$$

$$u(1,t) = \frac{ck}{2} + \frac{ck}{2}\tanh\left(\frac{ck^2 t - k - \ln b}{2}\right),$$

$$v(0,t) = \frac{-k^2}{8}\sec h^2\left(\frac{-ck^2 t + \ln b}{2}\right),$$

$$v(1,t) = \frac{-k^2}{8}\sec h^2\left(\frac{k - ck^2 t + \ln b}{2}\right).$$

3.3 Analytical Solution of System of Nonlinear PDEs

3.3.1 Application of HPM to Boussinesq-Burgers' equation

Using homotopy perturbation method [25, 26], the homotopy for eqs. (3.1) and (3.2) can be written as

$$(1-p)\left(\frac{\partial u}{\partial t} - 0\right) + p\left(\frac{\partial u}{\partial t} - \frac{1}{2}\frac{\partial v}{\partial x} + 2u\frac{\partial u}{\partial x}\right) = 0, \tag{3.7}$$

$$(1-p)\left(\frac{\partial v}{\partial t} - 0\right) + p\left(\frac{\partial v}{\partial t} - \frac{1}{2}\frac{\partial^3 u}{\partial x^3} + 2\frac{\partial(uv)}{\partial x}\right) = 0. \tag{3.8}$$

This implies

$$\frac{\partial u}{\partial t} = p\left(\frac{1}{2}\frac{\partial v}{\partial x} - 2u\frac{\partial u}{\partial x}\right), \tag{3.9}$$

$$\frac{\partial v}{\partial t} = p\left(\frac{1}{2}\frac{\partial^3 u}{\partial x^3} - 2\frac{\partial(uv)}{\partial x}\right) . \tag{3.10}$$

By substituting $u(x,t) = \sum\limits_{n=0}^{\infty} p^n u_n(x,t)$ and $v(x,t) = \sum\limits_{n=0}^{\infty} p^n v_n(x,t)$, in eqs. (3.9) and (3.10), we get

$$\frac{\partial}{\partial t}\left(\sum_{n=0}^{\infty} p^n u_n(x,t)\right) = p\left(\frac{1}{2}\frac{\partial}{\partial x}\left(\sum_{n=0}^{\infty} p^n v_n(x,t)\right)\right.$$
$$\left. -2\left(\sum_{n=0}^{\infty} p^n u_n(x,t)\right)\left(\frac{\partial}{\partial x}\left(\sum_{n=0}^{\infty} p^n u_n(x,t)\right)\right)\right), \tag{3.11}$$

$$\frac{\partial}{\partial t}\left(\sum_{n=0}^{\infty} p^n v_n(x,t)\right) = p\left(\frac{1}{2}\frac{\partial^3}{\partial x^3}\left(\sum_{n=0}^{\infty} p^n u_n(x,t)\right)\right.$$
$$\left. -2\frac{\partial}{\partial x}\left(\left(\sum_{n=0}^{\infty} p^n u_n(x,t)\right)\left(\sum_{n=0}^{\infty} p^n v_n(x,t)\right)\right)\right). \tag{3.12}$$

Comparing the coefficients of different powers in p for eqs. (3.11) and (3.12), we have the following system of partial differential equations.

Coefficients of p^0 : $\dfrac{\partial u_0}{\partial t} = 0$, $\qquad\qquad$ (3.13)

$$\frac{\partial v_0}{\partial t} = 0. \tag{3.14}$$

Coefficients of p^1 : $\dfrac{\partial u_1}{\partial t} = \dfrac{1}{2}\dfrac{\partial v_0}{\partial x} - 2u_0\dfrac{\partial u_0}{\partial x}$, $\qquad$ (3.15)

$$\frac{\partial v_1}{\partial t} = \frac{1}{2}\frac{\partial^3 u_0}{\partial x^3} - 2\frac{\partial}{\partial x}(u_0 v_0). \tag{3.16}$$

Coefficients of p^2 : $\dfrac{\partial u_2}{\partial t} = \dfrac{1}{2}\dfrac{\partial v_1}{\partial x} - 2\left(u_0\dfrac{\partial u_1}{\partial x} + u_1\dfrac{\partial u_0}{\partial x}\right)$, $\qquad$ (3.17)

$$\frac{\partial v_2}{\partial t} = \frac{1}{2}\frac{\partial^3 u_1}{\partial x^3} - 2\frac{\partial}{\partial x}(u_0 v_1 + u_1 v_0). \tag{3.18}$$

Coefficients of p^3 : $\dfrac{\partial u_3}{\partial t} = \dfrac{1}{2}\dfrac{\partial v_2}{\partial x} - 2\left(u_0\dfrac{\partial u_2}{\partial x} + u_1\dfrac{\partial u_1}{\partial x} + u_2\dfrac{\partial u_0}{\partial x}\right)$, $\qquad$ (3.19)

$$\frac{\partial v_3}{\partial t} = \frac{1}{2}\frac{\partial^3 u_2}{\partial x^3} - 2\frac{\partial}{\partial x}(u_0 v_2 + u_1 v_1 + u_2 v_0). \tag{3.20}$$

Coefficients of p^4: $\dfrac{\partial u_4}{\partial t} = \dfrac{1}{2}\dfrac{\partial v_3}{\partial x} - 2\left(u_0 \dfrac{\partial u_3}{\partial x} + u_1 \dfrac{\partial u_2}{\partial x} + u_2 \dfrac{\partial u_1}{\partial x} + u_3 \dfrac{\partial u_0}{\partial x} \right)$,   (3.21)

$$\dfrac{\partial v_4}{\partial t} = \dfrac{1}{2}\dfrac{\partial^3 u_3}{\partial x^3} - 2\dfrac{\partial}{\partial x}\left(u_0 v_3 + u_1 v_2 + u_2 v_1 + u_3 v_0 \right).$$ (3.22)

and so on.

By putting $u(x,0) = \tilde{u}_0$ and $v(x,0) = \tilde{v}_0$ in eqs. (3.13)- (3.22) and solving them, we obtain

$$u_1 = \dfrac{t}{2}\dfrac{\partial \tilde{v}_0}{\partial x} - 2t\tilde{u}_0 \dfrac{\partial \tilde{u}_0}{\partial x},$$

$$v_1 = \dfrac{t}{2}\dfrac{\partial^3 \tilde{u}_0}{\partial x^3} - 2t\dfrac{\partial}{\partial x}\left(\tilde{u}_0 \tilde{v}_0 \right).$$

$$u_2 = \dfrac{t^2}{2}\left(\dfrac{1}{2}\dfrac{\partial v_1}{\partial x} - 2\left(\tilde{u}_0 \dfrac{\partial u_1}{\partial x} + u_1 \dfrac{\partial \tilde{u}_0}{\partial x} \right) \right),$$

$$v_2 = \dfrac{t^2}{2}\left(\dfrac{1}{2}\dfrac{\partial^3 u_1}{\partial x^3} - 2\dfrac{\partial}{\partial x}\left(\tilde{u}_0 v_1 + u_1 \tilde{v}_0 \right) \right).$$

$$u_3 = \dfrac{t^3}{6}\left(\dfrac{1}{2}\dfrac{\partial v_2}{\partial x} - 2\left(\tilde{u}_0 \dfrac{\partial u_2}{\partial x} + u_1 \dfrac{\partial u_1}{\partial x} + u_2 \dfrac{\partial \tilde{u}_0}{\partial x} \right) \right),$$

$$v_3 = \dfrac{t^3}{6}\left(\dfrac{1}{2}\dfrac{\partial^3 u_2}{\partial x^3} - 2\dfrac{\partial}{\partial x}\left(\tilde{u}_0 v_2 + u_1 v_1 + u_2 \tilde{v}_0 \right) \right).$$

$$u_4 = \dfrac{t^4}{24}\left(\dfrac{1}{2}\dfrac{\partial v_3}{\partial x} - 2\left(\tilde{u}_0 \dfrac{\partial u_3}{\partial x} + u_1 \dfrac{\partial u_2}{\partial x} + u_2 \dfrac{\partial u_1}{\partial x} + u_3 \dfrac{\partial \tilde{u}_0}{\partial x} \right) \right),$$

$$v_4 = \dfrac{t^4}{24}\left(\dfrac{1}{2}\dfrac{\partial^3 u_3}{\partial x^3} - 2\dfrac{\partial}{\partial x}\left(\tilde{u}_0 v_3 + u_1 v_2 + u_2 v_1 + u_3 \tilde{v}_0 \right) \right).$$

In general,

$$u_n = \dfrac{t^n}{n!}\left(\dfrac{1}{2}\dfrac{\partial v_{n-1}}{\partial x} - 2\left(\sum_{i=0}^{n-1} u_i \dfrac{\partial u_{n-i}}{\partial x} \right) \right),$$ (3.23)

$$v_n = \dfrac{t^n}{n!}\left(\dfrac{1}{2}\dfrac{\partial^3 u_{n-1}}{\partial x^3} - 2\dfrac{\partial}{\partial x}\left(\sum_{i=0}^{n} u_i v_{n-i} \right) \right).$$ (3.24)

Finally, the approximate solutions for Boussinesq-Burgers' equations are given by

$$u = \tilde{u}_0(x,t) + u_1(x,t) + u_2(x,t) + \dots ,$$ (3.25)

$$v = \tilde{v}_0(x,t) + v_1(x,t) + v_2(x,t) + \dots .$$ (3.26)

3.3.2 Application of OHAM to Boussinesq-Burgers' equation

Using optimal homotopy asymptotic method [88], the homotopy for eqs. (3.1) and (3.2) can be written as

$$(1-p)\frac{\partial \varphi(x,t;p)}{\partial t} = H(p)\left[\frac{\partial \varphi(x,t;p)}{\partial t} - \frac{1}{2}\frac{\partial \psi(x,t;p)}{\partial x} + 2\varphi(x,t;p)\frac{\partial \varphi(x,t;p)}{\partial x}\right], \qquad (3.27)$$

$$(1-p)\frac{\partial \psi(x,t;p)}{\partial t} = H'(p)\left[\frac{\partial \psi(x,t;p)}{\partial t} - \frac{1}{2}\frac{\partial^3 \varphi(x,t;p)}{\partial x^3} + 2\frac{\partial}{\partial x}[\varphi(x,t;p)\psi(x,t;p)]\right]. \quad (3.28)$$

Here
$$\varphi(x,t;p) = u_0(x,t) + \sum_{i=1}^{\infty} u_i(x,t)p^i, \qquad (3.29)$$

$$\psi(x,t;p) = v_0(x,t) + \sum_{j=1}^{\infty} v_j(x,t)p^j, \qquad (3.30)$$

$$H(p) = C_1 p + C_2 p^2 + C_3 p^3 + \dots, \qquad (3.31)$$

$$H'(p) = D_1 p + D_2 p^2 + D_3 p^3 + \dots, \qquad (3.32)$$

$$N(\varphi(x,t;p)) = N_0(u_0(x,t)) + \sum_{k=1}^{\infty} N_k(u_0,u_1,\dots,u_k)p^k, \qquad (3.33)$$

$$N(\psi(x,t;p)) = N_0(v_0(x,t)) + \sum_{k=1}^{\infty} N_k(v_0,v_1,\dots,v_k)p^k. \qquad (3.34)$$

Substituting eqs. (3.29)- (3.34) in eqs. (3.27) and (3.28) and equating the coefficients of different powers in p, we have the following system of partial differential equations.

Coefficients of p^0 : $\dfrac{\partial u_0(x,t)}{\partial t} = 0$, $\qquad (3.35)$

$$\frac{\partial v_0(x,t)}{\partial t} = 0. \qquad (3.36)$$

Coefficients of p^1 :

$$\frac{\partial u_1(x,t)}{\partial t} - \frac{\partial u_0(x,t)}{\partial t} = C_1\left[\frac{\partial u_0(x,t)}{\partial t} - \frac{1}{2}\frac{\partial v_0(x,t)}{\partial x} + 2u_0(x,t)\frac{\partial u_0(x,t)}{\partial x}\right], \qquad (3.37)$$

$$\frac{\partial v_1(x,t)}{\partial t} - \frac{\partial v_0(x,t)}{\partial t} = D_1\left[\frac{\partial v_0(x,t)}{\partial t} - \frac{1}{2}\frac{\partial^3 u_0(x,t)}{\partial x^3} + \frac{\partial}{\partial x}(2u_0(x,t)v_0(x,t))\right]. \qquad (3.38)$$

Coefficients of p^2 :

$$\frac{\partial u_2(x,t)}{\partial t} - \frac{\partial u_1(x,t)}{\partial t} = C_1\left[\frac{\partial u_1(x,t)}{\partial t} - \frac{1}{2}\frac{\partial v_1(x,t)}{\partial x} + 2u_0(x,t)\frac{\partial u_1(x,t)}{\partial x}\right.$$
$$\left. + 2u_1(x,t)\frac{\partial u_0(x,t)}{\partial x}\right] + C_2\left[\frac{\partial u_0(x,t)}{\partial t} - \frac{1}{2}\frac{\partial v_0(x,t)}{\partial x} + 2u_0(x,t)\frac{\partial u_0(x,t)}{\partial x}\right],$$

(3.39)

$$\frac{\partial v_2(x,t)}{\partial t} - \frac{\partial v_1(x,t)}{\partial t} = D_1\left[\frac{\partial v_1(x,t)}{\partial t} - \frac{1}{2}\frac{\partial^3 u_1(x,t)}{\partial x^3} + \frac{\partial}{\partial x}\big(2u_0(x,t)v_1(x,t) + 2u_1(x,t)v_0(x,t)\big)\right]$$
$$+ D_2\left[\frac{\partial v_0(x,t)}{\partial t} - \frac{1}{2}\frac{\partial^3 u_0(x,t)}{\partial x^3} + \frac{\partial}{\partial x}\big(2u_0(x,t)v_0(x,t)\big)\right].$$

(3.40)

and so on.

For solving Boussinesq-Burgers' equation using OHAM we consider the following initial conditions for Boussinesq-Burgers' equations (3.1) and (3.2).

$$u(x,0) = \frac{-1}{4} - \frac{1}{4}\tanh\left(\frac{x - \log 2}{2}\right),$$

(3.41)

$$v(x,0) = \frac{-1}{8}\sec h^2\left(\frac{-x + \log 2}{2}\right).$$

(3.42)

Using the initial conditions and solving eqs. (3.35)- (3.40), we obtain

$$u_0(x,t) = \frac{-1}{4} - \frac{1}{4}\tanh\left(\frac{x - \log 2}{2}\right),$$

(3.43)

$$v_0(x,t) = \frac{-1}{8}\sec h^2\left(\frac{-x + \log 2}{2}\right).$$

(3.44)

$$u_1(x,t) = \frac{1}{16}t\, C_1\text{sech}^2\left(\frac{x - \log 2}{2}\right),$$

(3.45)

$$v_1(x,t) = \frac{-1}{2}t\, D_1\text{cosech}^3\,(x - \log 2)\sinh^4\left(\frac{x - \log 2}{2}\right).$$

(3.46)

$$u_2(x,t) = \frac{1}{128}t\,\text{sech}^4\left(\frac{x - \log 2}{2}\right)\left[4C_1 + 4C_1^2 - 2tC_1^2 + 4C_2 + 2tC_1 D_1\right.$$
$$\left. + \cosh(x - \log 2)\big[(4 + t)C_1^2 + 4C_2 + C_1(4 - tD_1)\big] + tC_1^2\sinh(x - \log 2)\right]$$

(3.47)

$$v_2(x,t) = \frac{-1}{256} t \operatorname{sech}^5\left(\frac{x-\log 2}{2}\right)\left[-3t\cosh\left(\frac{x-\log 2}{2}\right)D_1{}^2 + t\cosh\left(\frac{3(x-\log 2)}{2}\right)D_1{}^2\right.$$

$$-2t(-3+\cosh(x-\log 2))(C_1 - D_1)D_1\sinh\left(\frac{x-\log 2}{2}\right) \tag{3.48}$$

$$\left.+4\operatorname{cosech}\left(\frac{x-\log 2}{2}\right)(D_1 + D_1{}^2 + D_2)\sinh^2(x-\log 2)\right].$$

Using eqs. (3.43)-(3.48), the second order approximate solution is obtained as follows

$$u(x,t) = \frac{-1}{4} - \frac{1}{4}\tanh\left(\frac{x-\log 2}{2}\right) + \frac{1}{16}t\, C_1 \sec h^2\left(\frac{x-\log 2}{2}\right)$$

$$+\frac{1}{128}t \sec h^4\left(\frac{x-\log 2}{2}\right)\left[4C_1 + 4C_1{}^2 - 2tC_1{}^2 + 4C_2 + 2tC_1D_1 + \right. \tag{3.49}$$

$$\left. \cosh(x-\log 2)\left[(4+t)C_1{}^2 + 4C_2 + C_1(4-tD_1)\right] + tC_1{}^2\sinh(x-\log 2)\right],$$

$$v(x,t) = \frac{-1}{8}\sec h^2\left(\frac{-x+\log 2}{2}\right) + \left(\frac{-1}{2}\right)t\, D_1\operatorname{cosech}^3(x-\log 2)\sinh^4\left(\frac{x-\log 2}{2}\right)$$

$$+\left(\frac{-1}{256}\right)t \operatorname{sech}^5\left(\frac{x-\log 2}{2}\right)\left[-3t\cosh\left(\frac{x-\log 2}{2}\right)D_1{}^2 + t\cosh\left(\frac{3(x-\log 2)}{2}\right)D_1{}^2\right.$$

$$\tag{3.50}$$

$$-2t(-3+\cosh(x-\log 2))(C_1 - D_1)D_1\sinh\left(\frac{x-\log 2}{2}\right)$$

$$\left.+4\operatorname{cosech}\left(\frac{x-\log 2}{2}\right)(D_1 + D_1{}^2 + D_2)\sinh^2(x-\log 2)\right].$$

The optimal values of the convergence control constants C_1, C_2, D_1 and D_2 can be obtained using collocation method.

3.4 Convergence of HPM

The series $u = \lim_{p\to 1} v = v_0 + v_1 + v_2 + ...$, given in eq. (1.17) of chapter 1 is convergent for most cases. The following suggestions has been made by He [26] to find the convergence rate on nonlinear operator $A(v)$.

(i)   The second derivative of $N(u)$ with respect to u must be small because the parameter may be relatively large, i.e. $p \to 1$.

(ii)   The norm of $L^{-1}\dfrac{\partial N}{\partial u}$ must be smaller than one so that the series converges.

Let us write eq. (1.13) of chapter 1 in the following form

$$L(v) = L(u_0) + p[f(r) - N(v) - L(u_0)]$$ (3.51)

Applying the inverse operator, L^{-1} to both sides of eq. (3.51), we obtain

$$v = u_0 + p[L^{-1}f(r) - L^{-1}N(v) - u_0]$$ (3.52)

Suppose that

$$v = \sum_{i=0}^{\infty} p^i v_i$$ (3.53)

Substituting (3.53) into the right-hand side of eq. (3.52), we have

$$v = u_0 + p\left[L^{-1}f(r) - (L^{-1}N)\left[\sum_{i=0}^{\infty} p^i v_i\right] - u_0\right]$$ (3.54)

If $p \to 1$, the exact solution may be obtained by using

$$u = \lim_{p \to 1} v = L^{-1}f(r) - (L^{-1}N)\left[\sum_{i=0}^{\infty} v_i\right]$$

$$= L^{-1}f(r) - \sum_{i=0}^{\infty} (L^{-1}N)v_i$$ (3.55)

To study the convergence of the method let us state the following Theorem.

Theorem 3.1 [87]   Suppose that V and W be Banach spaces and $N : V \to W$ be a contraction mapping such that for all $v, v^* \in V$;

$$\left\|N(v) - N(v^*)\right\| \leq \varepsilon \left\|v - v^*\right\|, \qquad \varepsilon \in (0,1)$$ (3.56)

Then according to Banach's fixed point theorem N has a unique fixed point u (say) such that $N(u) = u.$

The sequence generated by the homotopy perturbation method will be assumed in the following form as

$$V_n = N(V_{n-1}), \qquad V_{n-1} = \sum_{i=0}^{n-1} v_i, \quad n = 1,2,3,...$$

and suppose that $V_0 = v_0 \in B_r(v)$ where $B_r(v) = \left\{v^* \in V \middle| \left\|v^* - v\right\| < r\right\}$, then we have

(i) $\left\|V_n - v\right\| \leq \varepsilon^n \left\|v_0 - v\right\|$

(ii) $V_n \in B_r(v)$

(iii) $\lim_{n \to \infty} V_n = v.$

Proof. Part (i) of the above theorem is proved by using method of induction.

For $n=1$, $\|V_1 - v\| = \|N(V_0) - N(v)\| \le \varepsilon\|v_0 - v\|$ (from eq. (3.56))

Assume that $\|V_{n-1} - v\| \le \varepsilon^{n-1}\|v_0 - v\|$ as induction hypothesis, then

$$\|V_n - v\| \le \|N(V_{n-1}) - N(v)\|$$

$$\le \varepsilon\|V_{n-1} - v\|$$

$$\le \varepsilon\,\varepsilon^{n-1}\|v_0 - v\| \qquad \text{(from induction hypothesis)}$$

$$\le \varepsilon^n\|v_0 - v\|.$$

Hence $\|V_n - v\| \le \varepsilon^n\|v_0 - v\|$.   □

(ii) Using (i), we have

$$\|V_n - v\| \le \varepsilon^n\|v_0 - v\| \le \varepsilon^n r < r$$

This implies $V_n \in B_r(v)$.

(iii) From (i) we know $\|V_n - v\| \le \varepsilon^n\|v_0 - v\|$.

Again since $0 < \varepsilon < 1$, $\lim\limits_{n\to\infty} \varepsilon^n = 0$.

So $\lim\limits_{n\to\infty}\|V_n - v\| = 0$,

which yields $\lim\limits_{n\to\infty} V_n = v$.   □

3.5 Convergence of OHAM

Theorem 3.2 Let the solution components $u_0, u_1, u_2, \ldots$ be defined as given in eqs. (1.27)-(1.29). The series solution $\sum\limits_{k=0}^{m-1} u_k(x,t)$ defined in eq. (1.31) converges if there exists δ, $0 < \delta < 1$ such that $\|u_{k+1}\| \le \delta\|u_k\|$, for all $k \ge k_0$ for some $k_0 \in N$.

Proof: Define the sequence $\{S_n\}_{n=0}^{\infty}$ as follows

$$S_0 = u_0,$$

$$S_1 = u_0 + u_1,$$

$$S_2 = u_0 + u_1 + u_2,$$

$$\ldots$$

$$S_n = u_0 + u_1 + u_2 + \ldots + u_n,$$

We have to show $\{S_n\}_{n=0}^{\infty}$ is a Cauchy sequence in the Hilbert space $\mathfrak{R}$.

Consider
$$\|S_{n+1} - S_n\| = \|u_{n+1}\|$$

$$\leq \delta \|u_n\|$$

$$\leq \delta^2 \|u_{n-1}\|$$

$$\ldots$$

$$\leq \delta^{n-k_0+1} \|u_{k_0}\|.$$

Now for every $n, m \in N$, $n \geq m > k_0$

$$\|S_n - S_m\| = \|(S_n - S_{n-1}) + (S_{n-1} - S_{n-2}) + \ldots + (S_{m+1} - S_m)\|$$

$$\leq \|S_n - S_{n-1}\| + \|S_{n-1} - S_{n-2}\| + \ldots + \|S_{m+1} - S_m\| \qquad \text{(Triangle inequality)}$$

$$\leq \delta^{n-k_0} \|u_{k_0}\| + \delta^{n-k_0-1} \|u_{k_0}\| + \ldots + \delta^{m-k_0+1} \|u_{k_0}\|$$

$$= \left(\frac{1-\delta^{n-m}}{1-\delta}\right) \delta^{m-k_0+1} \|u_{k_0}\|$$

This implies $\lim\limits_{n,m\to\infty} \|S_n - S_m\| = 0$. \qquad (since $0 < \delta < 1$)

Therefore, $\{S_n\}_{n=0}^{\infty}$ is a Cauchy sequence in the Hilbert space $\mathfrak{R}$ and hence the series solution $\sum\limits_{k=1}^{\infty} u_k(x,t)$ converges. \hfill $\square$

3.6 Numerical Results and Discussions

The following Tables 3.1 and 3.2 show the comparisons of the absolute errors of Boussinesq-Burgers' equations obtained by using two terms and three terms approximations of HPM and OHAM at different values of c, k, b, x and t. To show the effectiveness and accuracy of proposed schemes, L_2 and L_∞ error norms have been presented in Tables 3.3 and 3.4 respectively.

Table 3.1   The absolute errors in the solutions of Boussinesq-Burgers' equations using two terms approximation for HPM and OHAM at various points with $c = \frac{1}{2}$, $k = -1$, $b = 2$ and $C_1 = -1.01653$, $D_1 = 0.934599$ obtained by eq. (1.33).

(x, t)	$\lvert u_{Exact} - u_{HPM} \rvert$	$\lvert v_{Exact} - v_{HPM} \rvert$	$\lvert u_{Exact} - u_{OHAM} \rvert$	$\lvert v_{Exact} - v_{OHAM} \rvert$
(0.1, 0.1)	4.03765E-5	5.49815E-5	5.43565E-5	5.30293 E-5
(0.1, 0.2)	1.57743E-4	2.24577E-4	3.17229E-5	8.55529E-6
(0.1, 0.3)	3.46200E-4	5.15476E-4	6.20012E-5	1.91443E-4
(0.1, 0.4)	5.99524E-4	9.33935E-4	2.20592E-4	5.01892E-4
(0.1, 0.5)	9.11191E-4	1.48572E-3	4.37526E-4	9.45668E-4
(0.2, 0.1)	3.45343E-5	6.17326E-5	6.27431E-5	3.12906E-5
(0.2, 0.2)	1.33936E-4	2.51026E-4	6.06192E-5	6.49797E-5
(0.2, 0.3)	2.91679E-4	5.73647E-4	1.52649E-7	2.94577E-4
(0.2, 0.4)	5.00967E-4	1.03482E-3	1.11857E-4	6.62723E-4
(0.2, 0.5)	7.54752E-4	1.63915E-3	2.68365E-5	1.17404E-3
(0.3, 0.1)	2.80601E-5	6.75811E-5	7.13609E-5	8.76219E-6
(0.3, 0.2)	1.07664E-4	2.73710E-4	9.11785E-5	1.21023E-4
(0.3, 0.3)	2.31765E-4	6.23007E-4	6.64983E-5	3.93977E-4
(0.3, 0.4)	3.93103E-4	1.11945E-3	4.58083E-6	8.14078E-4
(0.3, 0.5)	5.84236E-4	1.76633E-3	8.71313E-5	1.38462E-3
(0.4, 0.1)	2.10557E-5	7.23025E-5	8.00687E-5	1.40750E-5
(0.4, 0.2)	7.93485E-5	2.91751E-4	1.22900E-5	1.75296E-4
(0.4, 0.3)	1.67436E-4	6.61637E-4	1.35937E-4	4.86954E-4
(0.4, 0.4)	2.77729E-4	1.18453E-3	1.26768E-4	9.51621E-4
(0.4, 0.5)	4.02528E-4	1.86226E-3	1.03094E-4	1.57112E-3
(0.5, 0.1)	1.36435E-5	7.57082E-5	8.87114E-5	3.67202E-5
(0.5, 0.2)	4.94924E-5	3.04426E-4	1.55217E-4	2.26450E-4
(0.5, 0.3)	9.98476E-5	6.87978E-4	2.07217E-4	5.71013E-4
(0.5, 0.4)	1.56938E-4	1.22742E-3	2.52482E-4	1.07147E-3
(0.5, 0.5)	2.12957E-4	1.92305E-3	2.98817E-4	1.72811E-3

Table 3.2   The absolute errors in the solutions of Boussinesq-Burgers' equations using three terms approximation for HPM and OHAM at various points with $c = \frac{1}{2}, k = -1, b = 2$ and $C_1 = 0.9786175, C_2 = -3.9162929$, $D_1 = 1.0514603$, $D_2 = -4.209964$ obtained by eq. (1.33).

(x, t)	$\lvert u_{Exact} - u_{HPM} \rvert$	$\lvert v_{Exact} - v_{HPM} \rvert$	$\lvert u_{Exact} - u_{OHAM} \rvert$	$\lvert v_{Exact} - v_{OHAM} \rvert$
(0.1, 0.1)	9.11428E-7	1.19150E-6	3.15534E-6	5.85344E-7
(0.1, 0.2)	7.40859E-6	9.41690E-6	7.33961E-7	2.12165E-6
(0.1, 0.3)	2.53911E-5	3.13655E-5	1.36454E-6	1.12982E-5
(0.1, 0.4)	6.10825E-5	7.32950E-5	3.08338E-6	3.43727E-5
(0.1, 0.5)	1.21007E-4	1.40972E-4	2.06021E-5	7.71116E-5
(0.2, 0.1)	1.02449E-6	1.06292E-6	3.23055E-6	8.39207E-7
(0.2, 0.2)	8.29954E-6	8.34741E-6	1.05314E-6	3.45590E-6
(0.2, 0.3)	2.83495E-5	2.76201E-5	7.84907E-9	2.08340E-6
(0.2, 0.4)	6.79737E-5	6.41010E-5	6.84685E-6	8.49823E-6
(0.2, 0.5)	1.34218E-4	1.22412E-4	2.86627E-5	3.29106E-5
(0.3, 0.1)	1.12268E-6	8.94544E-7	3.34664E-6	2.35740E-6
(0.3, 0.2)	9.06757E-6	6.96343E-6	1.53865E-6	9.48698E-6

(0.3, 0.3)	3.08802E-5	2.28283E-5	1.62153E-6	1.67671E-5
(0.3, 0.4)	7.38211E-5	5.24659E-5	1.08559E-5	2.02210E-5
(0.3, 0.5)	1.45333E-4	9.91676E-5	3.66844E-5	1.65572E-5
(0.4, 0.1)	1.20223E-6	6.91094E-7	3.50880E-6	3.92344E-6
(0.4, 0.2)	9.68307E-6	5.30519E-6	2.20317E-6	1.57786E-5
(0.4, 0.3)	3.28850E-5	1.71337E-5	3.52562E-6	3.22743E-5
(0.4, 0.4)	7.83973E-5	3.87483E-5	1.50654E-5	5.08384E-5
(0.4, 0.5)	1.53919E-4	7.19747E-5	4.45217E-5	6.96457E-5
(0.5, 0.1)	1.25997E-6	4.59601E-7	3.72005E-6	5.48493E-6
(0.5, 0.2)	1.01214E-5	3.43102E-6	3.05227E-6	2.21052E-5
(0.5, 0.3)	3.42835E-5	1.07397E-5	5.69591E-6	4.80354E-5
(0.5, 0.4)	8.15178E-5	2.34456E-5	1.94224E-5	8.22156E-5
(0.5, 0.5)	1.59629E-4	4.18318E-5	5.20368E-5	1.24363E-4

Table 3.3 L_2 and L_∞ error norm for Boussinesq-Burgers' equations using two terms approximation for HPM and OHAM at various points of x.

x	Homotopy Perturbation Method (HPM)				Optimal Homotopy Asymptotic Method (OHAM)			
	Error in case of two terms approximation for $u(x,t)$		Error in case of two terms approximation for $v(x,t)$		Error in case of two terms approximation for $u(x,t)$		Error in case of two terms approximation for $v(x,t)$	
	L_2	L_∞	L_2	L_∞	L_2	L_∞	L_2	L_∞
0.1	5.16927E-4	9.11191E-4	1.48572E-3	1.48572E-3	2.22663E-4	4.37526E-4	4.86974E-4	9.45668E-4
0.2	4.30076E-4	7.54752E-4	9.11434E-4	1.63915E-3	1.35752E-4	1.11857E-4	6.17988E-4	1.17404E-3
0.3	3.35248E-4	5.84236E-4	9.83942E-4	1.76633E-3	7.13313E-5	9.11785E-5	7.41598E-4	1.38462E-3
0.4	2.34067E-4	4.02528E-4	1.03916E-3	1.86226E-3	1.15493E-4	1.35937E-4	8.53470E-4	1.57112E-3
0.5	1.28519E-4	2.12957E-4	1.07484E-3	1.92305E-3	2.13513E-4	2.98817E-4	9.50063E-4	1.72811E-3

Table 3.4 L_2 and L_∞ error norm for Boussinesq-Burgers' equations using three terms approximation for HPM and OHAM at various points of x.

x	Homotopy Perturbation Method (HPM)				Optimal Homotopy Asymptotic Method (OHAM)			
	Error in case of three terms approximation for $u(x,t)$		Error in case of three terms approximation for $v(x,t)$		Error in case of three terms approximation for $u(x,t)$		Error in case of three terms approximation for $v(x,t)$	
	L_2	L_∞	L_2	L_∞	L_2	L_∞	L_2	L_∞
0.1	6.17644E-5	1.21007E-4	7.25523E-5	1.40972E-4	9.44786E-6	2.06021E-5	3.81056E-5	7.71116E-5
0.2	6.85690E-5	1.34218E-4	6.31305E-5	1.22412E-4	1.32663E-5	2.86627E-5	1.53122E-5	3.29106E-5
0.3	7.43079E-5	1.45333E-4	5.12978E-5	9.91676E-5	1.72034E-5	3.66844E-5	1.45583E-5	2.02210E-5
0.4	7.87576E-5	1.53919E-4	3.74272E-5	4.18318E-5	2.11601E-5	4.45217E-5	4.18116E-5	6.96457E-5
0.5	8.17386E-5	1.59629E-4	2.20314E-5	7.19747E-5	2.50625E-5	5.20368E-5	7.07837E-5	1.24363E-4

Graphical representation of results is very useful to demonstrate the efficiency and accuracy of the proposed methods for the discussed problem. The following Figures 3.1 and 3.2 cite the comparison graphically between the approximate solutions obtained by five terms HPM, three terms OHAM and exact solutions for different values of x and

$t = 0.5$. Figures 3.3 and 3.4 respectively show one soliton approximate solutions of $u(x,t)$ and $v(x,t)$, obtained by OHAM for Boussinesq-Burgers' equations.
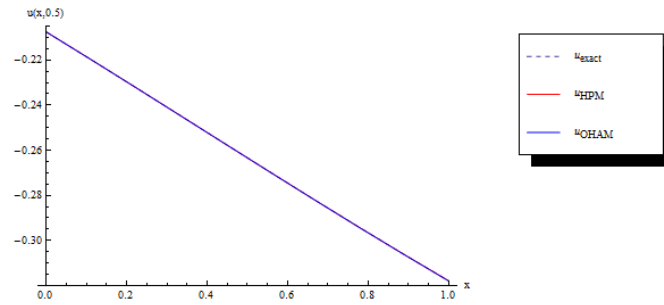
Figure 3.1   Comparison of five terms HPM solution and three terms OHAM solution with the exact solution of $u(x,t)$ for Boussinesq-Burgers' equations when $c = 0.5, k = -1, b = 2$ and $t = 0.5$.
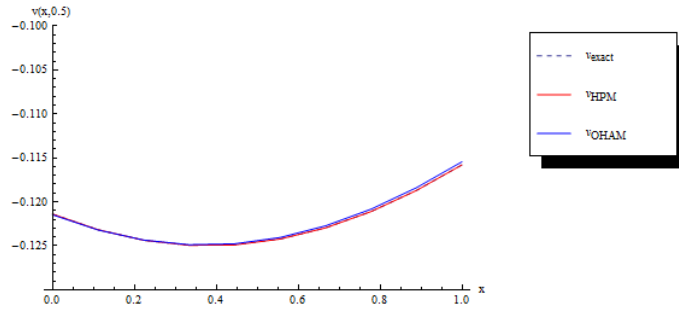
Figure 3.2   Comparison of five terms HPM solution and three terms OHAM solution with the exact solution of $v(x,t)$ for Boussinesq-Burgers' equations when $c = 0.5, k = -1, b = 2$ and $t = 0.5$.
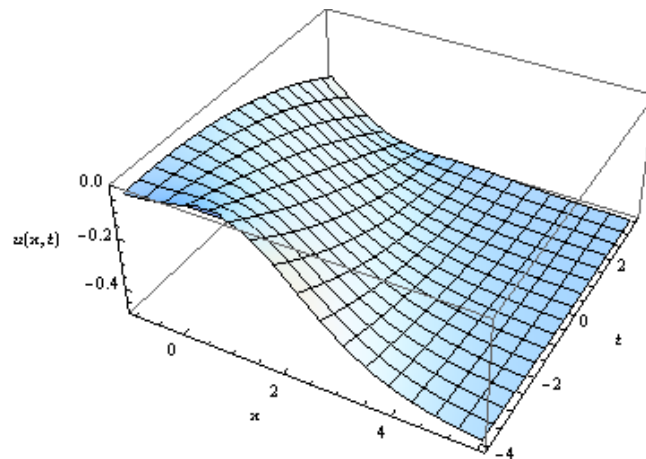
Figure 3.3   One soliton approximate solution of $u(x,t)$, obtained by OHAM for Boussinesq-Burgers' equations with parameters $c = 0.5, k = -1$ and $b = 2$.
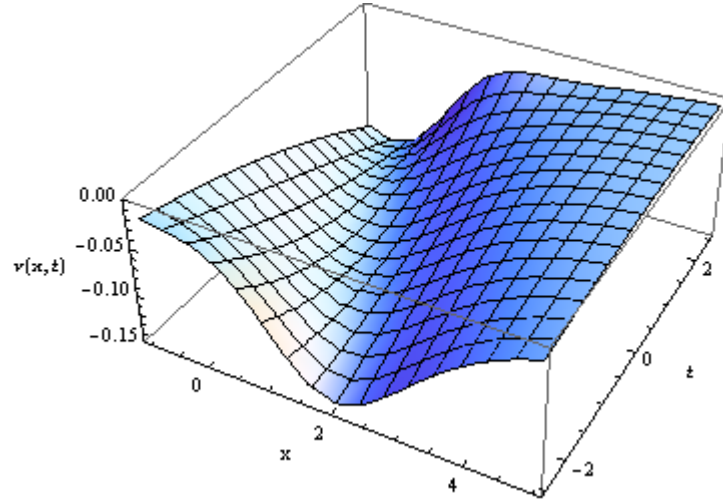
Figure 3.4 One soliton approximate solution of $v(x,t)$, obtained by OHAM for Boussinesq-Burgers' equations with parameters $c = \dfrac{1}{2}, \; k = -1$ and $b = 2$.

From the above Figures, one can see a very good agreement between the exact solutions and the solutions obtained by HPM and OHAM. Tables 3.1-3.4 depict the performance of OHAM in comparison with HPM and clearly witness the reliability and efficiency of OHAM for the solutions of Boussinesq-Burgers' equations.

3.7 A Numerical Approach to Boussinesq-Burgers' Equations

The Haar wavelet solutions of $u(x,t)$ and $v(x,t)$ are sought by assuming that $\dot{u}'''(x,t)$ and $\dot{v}'(x,t)$ can be expanded in terms of Haar wavelets as

$$\dot{u}'''(x,t) = \sum_{i=1}^{2M} a_s(i)h_i(x),\tag{3.57}$$

$$\dot{v}'(x,t) = \sum_{i=1}^{2M} b_s(i)h_i(x), \quad \text{for } t \in [t_s, t_{s+1}]\tag{3.58}$$

where "$\cdot$" and "$'$" stands for differentiation with respect to t and x respectively.

Integrating eq. (3.57) with respect to t from t_s to t and thrice with respect to x from 0 to x, the following equations are obtained

$$u'''(x,t) = (t - t_s)\sum_{i=1}^{2M} a_s(i)h_i(x) + u'''(x,t_s),\tag{3.59}$$

89

$$u''(x,t) = (t-t_s)\sum_{i=1}^{2M} a_s(i)p_i(x) + u''(x,t_s) - u''(0,t_s) + u''(0,t), \qquad (3.60)$$

$$u'(x,t) = (t-t_s)\sum_{i=1}^{2M} a_s(i)q_i(x) + u'(x,t_s) - u'(0,t_s) + x[u''(0,t) - u''(0,t_s)] + u'(0,t), \quad (3.61)$$

$$u(x,t) = (t-t_s)\sum_{i=1}^{2M} a_s(i)r_i(x) + u(x,t_s) - u(0,t_s) + \frac{x^2}{2}[u''(0,t) - u''(0,t_s)] + \\ x[u'(0,t) - u'(0,t_s)] + u(0,t), \qquad (3.62)$$

$$\dot{u}(x,t) = \sum_{i=1}^{2M} a_s(i)r_i(x) + \frac{x^2}{2}\dot{u}''(0,t) + x\dot{u}'(0,t) + \dot{u}(0,t). \qquad (3.63)$$

Integrating eq. (3.58) with respect to t from t_s to t and once with respect to x from 0 to x, the following equations are obtained

$$v'(x,t) = (t-t_s)\sum_{i=1}^{2M} b_s(i)h_i(x) + v'(x,t_s), \qquad (3.64)$$

$$v(x,t) = (t-t_s)\sum_{i=1}^{2M} b_s(i)p_i(x) + v(x,t_s) - v(0,t_s) + v(0,t), \qquad (3.65)$$

$$\dot{v}(x,t) = \sum_{i=1}^{2M} b_s(i)p_i(x) + \dot{v}(0,t). \qquad (3.66)$$

Discretizing the above results by assuming $x \to x_l$, $t \to t_{s+1}$, from eqs. (3.64), (3.65) and (3.66), we obtain

$$v'(x_l,t_{s+1}) = (t_{s+1} - t_s)\sum_{i=1}^{2M} b_s(i)h_i(x_l) + v'(x_l,t_s), \qquad (3.67)$$

$$v(x_l,t_{s+1}) = (t_{s+1} - t_s)\sum_{i=1}^{2M} b_s(i)p_i(x_l) + v(x_l,t_s) - v(0,t_s) + v(0,t_{s+1}), \quad (3.68)$$

$$\dot{v}(x_l,t_{s+1}) = \sum_{i=1}^{2M} b_s(i)p_i(x_l) + \dot{v}(0,t_{s+1}). \qquad (3.69)$$

Using finite difference method

$$\dot{u}(0,t) = \frac{u(0,t) - u(0,t_s)}{(t-t_s)}.$$

Equation (3.63) becomes

$$\dot{u}(x,t) = \sum_{i=1}^{2M} a_s(i) r_i(x) + \frac{x^2}{2}\left(\frac{u''(0,t) - u''(0,t_s)}{t - t_s}\right) + x\left(\frac{u'(0,t) - u'(0,t_s)}{t - t_s}\right)$$
$$+ \left(\frac{u(0,t) - u(0,t_s)}{t - t_s}\right). \tag{3.70}$$

By using the boundary condition at $x = 1$, eq. (3.61) becomes

$$u'(1,t) = (t - t_s)\sum_{i=1}^{2M} a_s(i) q_i(1) + u'(1,t_s) - u'(0,t_s) + [u''(0,t) - u''(0,t_s)] + u'(0,t).$$

This implies

$$u''(0,t) - u''(0,t_s) = -(t - t_s)\sum_{i=1}^{2M} a_s(i) q_i(1) + u'(1,t) - u'(1,t_s) - u'(0,t) + u'(0,t_s). \tag{3.71}$$

Substituting eq. (3.71) in eqs. (3.60), (3.61), (3.62) and (3.70) and discretizing the resultant equations by assuming $x \rightarrow x_l$, $t \rightarrow t_{s+1}$, we obtain

$$u'''(x_l, t_{s+1}) = (t_{s+1} - t_s)\sum_{i=1}^{2M} a_s(i) h_i(x_l) + u'''(x_l, t_s), \tag{3.72}$$

$$u''(x_l, t_{s+1}) = (t_{s+1} - t_s)\sum_{i=1}^{2M} a_s(i) p_i(x_l) + u''(x_l, t_s) - (t_{s+1} - t_s)\sum_{i=1}^{2M} a_s(i) q_i(1) +$$
$$[u'(1, t_{s+1}) - u'(1, t_s)] - [u'(0, t_{s+1}) - u'(0, t_s)], \tag{3.73}$$

$$u'(x_l, t_{s+1}) = (t_{s+1} - t_s)\sum_{i=1}^{2M} a_s(i) q_i(x_l) + u'(x_l, t_s) - u'(0, t_s) + u'(0, t_{s+1}) +$$
$$x_l\left[-(t_{s+1} - t_s)\sum_{i=1}^{2M} a_s(i) q_i(1) + [u'(1, t_{s+1}) - u'(1, t_s)] - [u'(0, t_{s+1}) - u'(0, t_s)]\right], \tag{3.74}$$

$$u(x_l, t_{s+1}) = (t_{s+1} - t_s)\sum_{i=1}^{2M} a_s(i) r_i(x_l) + u(x_l, t_s) - u(0, t_s) + u(0, t_{s+1}) + x_l[u'(0, t_{s+1}) - u'(0, t_s)]$$
$$+ \frac{x_l^2}{2}\left[-(t_{s+1} - t_s)\sum_{i=1}^{2M} a_s(i) q_i(1) + [u'(1, t_{s+1}) - u'(1, t_s)] - [u'(0, t_{s+1}) - u'(0, t_s)]\right], \tag{3.75}$$

$$\dot{u}(x_l, t_{s+1}) = \sum_{i=1}^{2M} a_s(i) r_i(x_l) + \frac{x_l}{t_{s+1} - t_s}[u'(0, t_{s+1}) - u'(0, t_s)] + \frac{1}{t_{s+1} - t_s}[u(0, t_{s+1}) - u(0, t_s)]$$
$$+ \frac{x_l^2}{2(t_{s+1} - t_s)}\left[-(t_{s+1} - t_s)\sum_{i=1}^{2M} a_s(i) q_i(1) + [u'(1, t_{s+1}) - u'(1, t_s)] - [u'(0, t_{s+1}) - u'(0, t_s)]\right]. \tag{3.76}$$

Substituting the above equations in eq. (3.1) and eq. (3.2), we have

$$\sum_{i=1}^{2M} a_s(i)\left[r_i(x_l) - \frac{x_l^2}{2}q_i(1)\right] + \frac{x_l^2}{2(t_{s+1}-t_s)}\left[u'(1,t_{s+1}) - u'(1,t_s) - u'(0,t_{s+1}) + u'(0,t_s)\right]$$

$$+ \frac{x_l}{t_{s+1}-t_s}\left[u'(0,t_{s+1}) - u'(0,t_s)\right] + \frac{1}{t_{s+1}-t_s}\left[u(0,t_{s+1}) - u(0,t_s)\right]$$

$$= \frac{1}{2}\left((t_{s+1}-t_s)\sum_{i=1}^{2M} b_s(i)h_i(x_l) + v'(x_l,t_s)\right) - 2\left[(t_{s+1}-t_s)\sum_{i=1}^{2M} a_s(i)\left[r_i(x_l) - \frac{x_l^2}{2}q_i(1)\right] + u(x_l,t_s)\right.$$

$$- u(0,t_s) + u(0,t_{s+1}) + x_l\left[u'(0,t_{s+1}) - u'(0,t_s)\right] + \frac{x_l^2}{2}\left[u'(1,t_{s+1}) - u'(1,t_s) - u'(0,t_{s+1}) + u'(0,t_s)\right]\right]$$

$$\times \left[(t_{s+1}-t_s)\sum_{i=1}^{2M} a_s(i)\left[q_i(x_l) - x_l q_i(1)\right] + u'(x_l,t_s) - u'(0,t_s) + u'(0,t_{s+1}) + \right.$$

$$x_l\left[u'(1,t_{s+1}) - u'(1,t_s) - u'(0,t_{s+1}) + u'(0,t_s)\right]\Big].$$

(3.77)

$$\sum_{i=1}^{2M} b_s(i)p_i(x_l) + \dot{v}(0,t_{s+1}) = \frac{1}{2}\left((t_{s+1}-t_s)\sum_{i=1}^{2M} a_s(i)h_i(x_l) + u'''(x_l,t_s)\right) -$$

$$2\left[(t_{s+1}-t_s)\sum_{i=1}^{2M} a_s(i)\left[r_i(x_l) - \frac{x_l^2}{2}q_i(1)\right] + u(x_l,t_s) - u(0,t_s) + u(0,t_{s+1}) + x_l\left[u'(0,t_{s+1}) - u'(0,t_s)\right]\right.$$

$$+ \frac{x_l^2}{2}\left[\left[u'(1,t_{s+1}) - u'(1,t_s)\right] - \left[u'(0,t_{s+1}) - u'(0,t_s)\right]\right]\right] \times \left((t_{s+1}-t_s)\sum_{i=1}^{2M} b_s(i)h_i(x_l) + v'(x_l,t_s)\right)$$

$$- 2\left((t_{s+1}-t_s)\sum_{i=1}^{2M} b_s(i)p_i(x_l) + v(x_l,t_s) - v(0,t_s) + v(0,t_{s+1})\right) \times \left[(t_{s+1}-t_s)\sum_{i=1}^{2M} a_s(i)\left[q_i(x_l) - x_l q_i(1)\right]\right.$$

$$+ u'(x_l,t_s) - u'(0,t_s) + u'(0,t_{s+1}) + x_l\left[u'(1,t_{s+1}) - u'(1,t_s) - u'(0,t_{s+1}) + u'(0,t_s)\right]\Big].$$

(3.78)

From the above two eqs. (3.77) and (3.78), the wavelet coefficients $a_s(i)$ and $b_s(i)$ can be successively calculated using mathematical software. This process starts with

$$u(x_l,t_0) = \frac{-1}{4} - \frac{1}{4}\tanh\left(\frac{x_l - \log 2}{2}\right),$$

$$u'(x_l,t_0) = \frac{-1}{8}\sec h^2\left(\frac{x_l - \log 2}{2}\right),$$

$$u''(x_l,t_0) = \frac{1}{8}\sec h^2\left(\frac{x_l - \log 2}{2}\right)\tanh\left(\frac{x_l - \log 2}{2}\right),$$

$$v(x_l,t_0) = \frac{-1}{8}\sec h^2\left(\frac{-x_l + \log 2}{2}\right),$$

$$v'(x_l, t_0) = \frac{-1}{8} \sec h^2 \left(\frac{-x_l + \log 2}{2} \right) \tanh \left(\frac{-x_l + \log 2}{2} \right).$$

3.8 Convergence of Haar Wavelet Approximation

The convergence of the method may be discussed on the same lines as given by learned researcher Saha Ray, 2012 [38].

Theorem 3.3 Let $f(x) \in L^2(R)$ be a continuous function defined on $[0,1)$. Then the error

at J th level may be defined as $E_J(x) = |f(x) - f_J(x)| = \left| f(x) - \sum_{i=1}^{2M} a_i h_i(x) \right| = \left| \sum_{i=2M}^{\infty} a_i h_i(x) \right|$.

The error norm for $E_J(x)$ is obtained as

$$\|E_J(x)\|_2 \le \frac{K^2}{12} 2^{-2J} \tag{3.79}$$

where $|f'(x)| \le K$, for all $x \in [0,1)$ and $K > 0$ and M is a positive number related to the J

th level of resolution of the wavelet given by $M = 2^J$.

Proof: The error at J th level resolution is defined as

$$E_J(x) = |f(x) - f_J(x)| = \left| f(x) - \sum_{i=1}^{2M} a_i h_i(x) \right| = \left| \sum_{i=2M}^{\infty} a_i h_i(x) \right|.$$

$$\|E_J(x)\|^2 = \int_{-\infty}^{\infty} \left(\sum_{i=2M}^{\infty} a_i h_i(x), \sum_{s=2M}^{\infty} a_s h_s(x) \right) dx = \sum_{i=2M}^{\infty} \sum_{s=2M}^{\infty} a_i a_s \int_{-\infty}^{\infty} h_i(x) h_s(x) dx \le \sum_{i=2M}^{\infty} |a_i|^2.$$

Now, $a_i = \int_0^1 2^{j/2} f(x) h(2^j x - k) dx$,

where $h_i(x) = 2^{j/2} h(2^j x - k)$, $k = 0, 1, 2..., 2^j - 1$, $\qquad j = 0, 1, 2..., J$

and $h(2^j x - k) = \begin{cases} 1, & \dfrac{k}{2^j} \le x < \dfrac{k+0.5}{2^j} \\ -1, & \dfrac{k+0.5}{2^j} \le x < \dfrac{k+1}{2^j} \\ 0, & \text{elsewhere} \end{cases}$.

Hence $a_i = 2^{\frac{j}{2}} \left[\int\limits_{\frac{k}{2^j}}^{\frac{k+0.5}{2^j}} f(x)dx - \int\limits_{\frac{k+0.5}{2^j}}^{\frac{k+1}{2^j}} f(x)dx \right]$

$= 2^{\frac{j}{2}} \left[\left(\frac{k+0.5}{2^j} - \frac{k}{2^j} \right) f(\xi_1) - \left(\frac{k+1}{2^j} - \frac{k+0.5}{2^j} \right) f(\xi_2) \right]$ (applying mean value theorem)

where $\xi_1 \in \left(\dfrac{k}{2^j}, \dfrac{k+0.5}{2^j} \right)$ and $\xi_2 \in \left(\dfrac{k+0.5}{2^j}, \dfrac{k+1}{2^j} \right)$

Consequently,

$a_i = 2^{\frac{j}{2}} \left[\left(\frac{0.5}{2^j} \right) f(\xi_1) - \left(\frac{0.5}{2^j} \right) f(\xi_2) \right]$

$= 2^{\frac{j}{2}-j-1} \left[f(\xi_1) - f(\xi_2) \right]$

$= 2^{-\frac{j}{2}-1} (\xi_1 - \xi_2) f'(\xi), \quad \text{where } \xi \in (\xi_1, \xi_2).$ (applying mean value theorem)

This implies $a_i^2 = 2^{-j-2} (\xi_2 - \xi_1)^2 f'(\xi)^2 \leq 2^{-j-2} 2^{-2j} K^2 = 2^{-3j-2} K^2$.

Therefore,

$\|E_J(x)\|^2 \leq \sum\limits_{i=2M}^{\infty} a_i^2 \leq \sum\limits_{i=2M}^{\infty} 2^{-3j-2} K^2 = K^2 \sum\limits_{j=J+1}^{\infty} \sum\limits_{i=2^j}^{2^{j+1}-1} 2^{-3j-2}$

$= K^2 \sum\limits_{j=J+1}^{\infty} 2^{-3j-2} \left(2^{j+1} - 1 - 2^j + 1 \right)$

$= K^2 \sum\limits_{j=J+1}^{\infty} \left(2^{-2j-1} - 2^{-2j-2} \right)$

$= K^2 \sum\limits_{j=J+1}^{\infty} 2^{-2j} \left(2^{-1} - 2^{-2} \right)$

$= \frac{K^2}{4} \sum\limits_{j=J+1}^{\infty} 2^{-2j} = \frac{K^2}{4} \frac{2^{-2(j+1)}}{\left(1 - \dfrac{1}{4} \right)} = \frac{K^2}{12} 2^{-2j}.$

From eq. (3.79), it can be observed that the error bound is inversely proportional to the level of resolution J. So, more accurate result can be obtained by increasing the level of resolution in the Haar wavelet method.

3.9 Numerical Results

The following Tables show the comparisons of the exact solutions with the approximate solutions of Boussinesq-Burgers' equations at different collocation points. In the following Tables 3.5-3.7, J has been taken as 4 i.e. $M = 16$ and Δt is taken as 0.0001.

The *R.M.S. error* between the numerical solutions and the exact solutions of $u(x,t)$ for Boussinesq-Burgers' equations at $t = 0.5, 1.0$ and 1.5 are 0.000142255, 0.000216937 and 0.000935793 respectively and for $v(x,t)$ the *R.M.S. error* is found to be 0.0118472, 0.0236667 and 0.0346156 respectively.

The figures 3.5-3.8 cite the comparison graphically between the numerical and exact solutions for different values of t.

Table 3.5   The absolute errors in the solutions of Boussinesq-Burgers' equations at various collocation points of x with $t = 0.5$.

x	Approximate solution (u_{approx})	Approximate solution (v_{approx})	Exact solution (u_{exact})	Exact solution (v_{exact})	Absolute Error $\lvert u_{Exact} - u_{Approx} \rvert$	Absolute Error $\lvert v_{Exact} - v_{Approx} \rvert$
0.015625	-0.197367	-0.118653	-0.197359	-0.119458	8.35980E-6	8.05119E-4
0.046875	-0.201157	-0.119271	-0.201104	-0.120218	5.29589E-5	9.47342E-4
0.078125	-0.204944	-0.122098	-0.204872	-0.120927	7.19897E-5	1.17066E-3
0.109375	-0.20869	-0.12456	-0.208662	-0.121582	2.82735E-5	2.97813E-3
0.140625	-0.212446	-0.124475	-0.212471	-0.122183	2.42459E-5	2.29235E-3
0.171875	-0.216279	-0.123392	-0.216297	-0.122728	1.87152E-5	6.63754E-4
0.203125	-0.220164	-0.124375	-0.22014	-0.123217	2.37371E-5	1.15814E-3
0.234375	-0.224021	-0.127389	-0.223998	-0.123648	2.32677E-5	3.74124E-3
0.265625	-0.227829	-0.129227	-0.227868	-0.12402	3.87521E-5	5.2064E-3
0.296875	-0.23166	-0.128271	-0.231749	-0.124334	8.83945E-5	3.93697E-3
0.328125	-0.23557	-0.127024	-0.235638	-0.124587	6.77895E-5	2.4362E-3
0.359375	-0.239511	-0.128457	-0.239535	-0.124781	2.37165E-5	3.67564E-3
0.390625	-0.243396	-0.131492	-0.243436	-0.124914	4.01933E-5	6.57804E-3
0.421875	-0.24723	-0.132477	-0.247341	-0.124986	1.11453E-4	7.49073E-3
0.453125	-0.251101	-0.130649	-0.251247	-0.124997	1.46677E-4	5.65231E-3

95

x	-0.255048	-0.129425	-0.255153	-0.124947	1.04846E-4	4.47776E-3
0.484375	-0.255048	-0.129425	-0.255153	-0.124947	1.04846E-4	4.47776E-3
0.515625	-0.258996	-0.131357	-0.259056	-0.124836	5.93702E-5	6.52131E-3
0.546875	-0.262864	-0.134199	-0.262954	-0.124664	9.07736E-5	9.53507E-3
0.578125	-0.266683	-0.134123	-0.266847	-0.124432	1.63839E-4	9.69100E-3
0.609375	-0.270555	-0.1315	-0.270731	-0.12414	1.76238E-4	7.35999E-3
0.640625	-0.274493	-0.130521	-0.274605	-0.123789	1.11967E-4	6.73224E-3
0.671875	-0.278397	-0.132961	-0.278467	-0.123379	6.97724E-5	9.58204E-3
0.703125	-0.282198	-0.135353	-0.282315	-0.122911	1.17448E-4	1.2442E-2
0.734375	-0.285962	-0.13405	-0.286148	-0.122387	1.86803E-4	1.16634E-2
0.765625	-0.289792	-0.130795	-0.289964	-0.121806	1.71833E-4	8.98884E-3
0.796875	-0.293671	-0.130309	-0.293761	-0.12117	8.93953E-5	9.13864E-3
0.828125	-0.297477	-0.133207	-0.297537	-0.120481	5.94947E-5	1.2726E-2
0.859375	-0.301163	-0.13486	-0.30129	-0.119739	1.26730E-4	1.51218E-2
0.890625	-0.304831	-0.132242	-0.30502	-0.118946	1.88492E-4	1.32964E-2
0.921875	-0.308579	-0.128677	-0.308724	-0.118103	1.44573E-4	1.05737E-2
0.953125	-0.312353	-0.129219	-0.312401	-0.117212	4.80031E-5	1.20066E-2
0.984375	-0.316031	-0.13366	-0.316049	-0.116275	1.80034E-5	1.73849E-2

Table 3.6 The absolute errors in the solutions of Boussinesq-Burgers' equations at various collocation points of x with $t = 1.0$.

x	Approximate solution (u_{approx})	Approximate solution (v_{approx})	Exact solution (u_{exact})	Exact solution (v_{exact})	Absolute Error $\lvert u_{Exact} - u_{Approx} \rvert$	Absolute Error $\lvert v_{Exact} - v_{Approx} \rvert$
0.015625	-0.227876	-0.123436	-0.227868	-0.12402	8.38233E-6	5.84734E-4
0.046875	-0.231802	-0.124054	-0.231749	-0.124334	5.32620E-5	2.79865E-4
0.078125	-0.235711	-0.12688	-0.235638	-0.124587	7.30976E-5	2.29300E-3
0.109375	-0.239566	-0.129343	-0.239535	-0.124781	3.09406E-5	4.56229E-3
0.140625	-0.243417	-0.129258	-0.243436	-0.124914	1.90610E-5	4.34445E-3
0.171875	-0.247331	-0.128175	-0.247341	-0.124986	9.87667E-6	3.18901E-3
0.203125	-0.251285	-0.129158	-0.251247	-0.124997	3.75151E-5	4.16092E-3
0.234375	-0.255196	-0.132172	-0.255153	-0.124947	4.33927E-5	7.22497E-3
0.265625	-0.259045	-0.13401	-0.259056	-0.124836	1.07795E-5	9.1736E-3
0.296875	-0.262903	-0.133054	-0.262954	-0.124664	5.10099E-5	8.38921E-3
0.328125	-0.266827	-0.131807	-0.266847	-0.124432	1.93935E-5	7.37414E-3

0.359375	-0.270768	-0.133239	-0.270731	-0.12414	3.72955E-5	9.09897E-3
0.390625	-0.27464	-0.136275	-0.274605	-0.123789	3.50153E-5	1.24855E-2
0.421875	-0.278446	-0.137259	-0.278467	-0.123379	2.05208E-5	1.38802E-2
0.453125	-0.282277	-0.135432	-0.282315	-0.122911	3.85771E-5	1.25206E-2
0.484375	-0.28617	-0.134208	-0.286148	-0.122387	2.17555E-5	1.18209E-2
0.515625	-0.290051	-0.13614	-0.289964	-0.121806	8.69255E-5	1.43344E-2
0.546875	-0.293837	-0.138982	-0.293761	-0.12117	7.62424E-5	1.78123E-2
0.578125	-0.297561	-0.138906	-0.297537	-0.120481	2.47286E-5	1.84257E-2
0.609375	-0.301325	-0.136283	-0.30129	-0.119739	3.44909E-5	1.65447E-2
0.640625	-0.305141	-0.135304	-0.30502	-0.118946	1.21288E-4	1.63586E-2
0.671875	-0.30891	-0.137744	-0.308724	-0.118103	1.86102E-4	1.96411E-2
0.703125	-0.312561	-0.140136	-0.312401	-0.117212	1.60845E-4	2.2924E-2
0.734375	-0.316162	-0.138833	-0.316049	-0.116275	1.1339E-4	2.25577E-2
0.765625	-0.319817	-0.135577	-0.319667	-0.115293	149407E-4	2.02845E-2
0.796875	-0.323506	-0.135092	-0.323254	-0.114268	2.51678E-4	2.08239E-2
0.828125	-0.327108	-0.137989	-0.326809	-0.113201	2.99826E-4	2.47885E-2
0.859375	-0.330578	-0.139643	-0.330329	-0.112095	2.48857E-4	2.75487E-2
0.890625	-0.334015	-0.137025	-0.333814	-0.11095	2.00973E-4	2.60745E-2
0.921875	-0.337519	-0.13346	-0.337263	-0.10977	2.55958E-4	2.36893E-2
0.953125	-0.341035	-0.134002	-0.340674	-0.108556	3.6035E-4	2.54455E-2
0.984375	-0.344442	-0.138443	-0.344047	-0.10731	394479E-4	3.11327E-2

Table 3.7 The absolute errors in the solutions of Boussinesq-Burgers' equations at various collocation points of x with $t = 1.5$.

x	Approximate solution (u_{approx})	Approximate solution (v_{approx})	Exact solution (u_{exact})	Exact solution (v_{exact})	Absolute Error $\lvert u_{Exact} - u_{Approx}\rvert$	Absolute Error $\lvert v_{Exact} - v_{Approx}\rvert$
0.015625	-0.259065	-0.124493	-0.259056	-0.124836	8.80296E-6	3.42744E-4
0.046875	-0.263011	-0.125112	-0.262954	-0.124664	5.70662E-5	4.47176E-4
0.078125	-0.26693	-0.127938	-0.266847	-0.124432	8.3701E-5	3.50573E-3
0.109375	-0.270783	-0.130401	-0.270731	-0.12414	5.17642E-5	6.26042E-3
0.140625	-0.27462	-0.130316	-0.274605	-0.123789	1.53796E-5	6.52672E-3
0.171875	-0.278509	-0.129233	-0.278467	-0.123379	4.15244E-5	5.85325E-3
0.203125	-0.282425	-0.130215	-0.282315	-0.122911	1.09137E-4	7.30402E-3
0.234375	-0.286287	-0.13323	-0.286148	-0.122387	1.38385E-4	1.08429E-2

0.265625	-0.290075	-0.135067	-0.289964	-0.121806	1.10593E-4	1.32615E-2
0.296875	-0.29386	-0.134111	-0.293761	-0.12117	9.95855E-5	1.29412E-2
0.328125	-0.2977	-0.132864	-0.297537	-0.120481	1.63072E-4	1.23836E-2
0.359375	-0.301544	-0.134297	-0.30129	-0.119739	2.54057E-4	1.45584E-2
0.390625	-0.305308	-0.137332	-0.30502	-0.118946	2.88254E-4	1.83867E-2
0.421875	-0.308995	-0.138317	-0.308724	-0.118103	2.71105E-4	2.0214E-2
0.453125	-0.312694	-0.13649	-0.312401	-0.117212	2.9305E-4	1.92774E-2
0.484375	-0.316444	-0.135265	-0.316049	-0.116275	3.94684E-4	1.89901E-2
0.515625	-0.320169	-0.137198	-0.319667	-0.115293	5.02116E-4	2.19049E-2
0.546875	-0.323789	-0.14004	-0.323254	-0.114268	5.34300E-4	2.57723E-2
0.578125	-0.327335	-0.139964	-0.326809	-0.113201	5.25882E-4	2.67630E-2
0.609375	-0.330908	-0.137341	-0.330329	-0.112095	5.78576E-4	2.52464E-2
0.640625	-0.334522	-0.136362	-0.333814	-0.11095	7.07734E-4	2.54116E-2
0.671875	-0.338077	-0.138802	-0.337263	-0.10977	8.13912E-4	2.90315E-2
0.703125	-0.341503	-0.141194	-0.340674	-0.108556	8.28591E-4	3.26377E-2
0.734375	-0.344867	-0.13989	-0.344047	-0.10731	8.19196E-4	3.25803E-2
0.765625	-0.348272	-0.136635	-0.347381	-0.106034	8.9094E-4	3.06012E-2
0.796875	-0.3517	-0.136149	-0.350674	-0.104729	1.02614E-3	3.14198E-2
0.828125	-0.35503	-0.139047	-0.353926	-0.103399	1.10396E-3	3.56484E-2
0.859375	-0.358215	-0.140701	-0.357136	-0.102044	1.07891E-3	3.86573E-2
0.890625	-0.361357	-0.138083	-0.360304	-0.100666	1.05272E-3	3.74164E-2
0.921875	-0.364553	-0.134517	-0.363428	-0.0992682	1.12470E-3	3.52490E-2
0.953125	-0.367749	-0.135059	-0.366508	-0.0978518	1.24090E-3	3.72076E-2
0.984375	-0.370825	-0.1395	-0.369543	-0.0964187	1.28116E-3	4.30817E-2
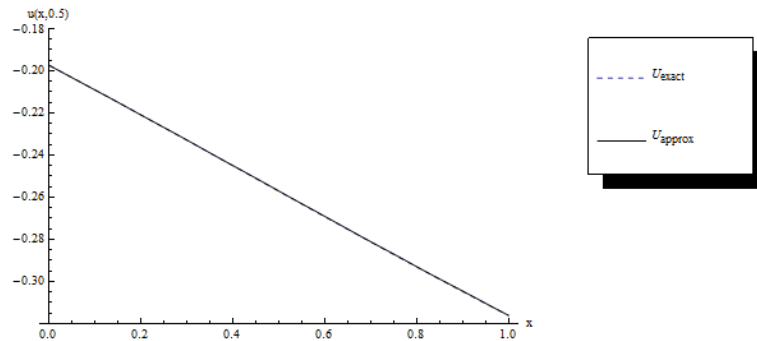
Figure 3.5   Comparison of numerical solution and exact solution of Boussinesq-Burgers' equations when $t = 0.5$.
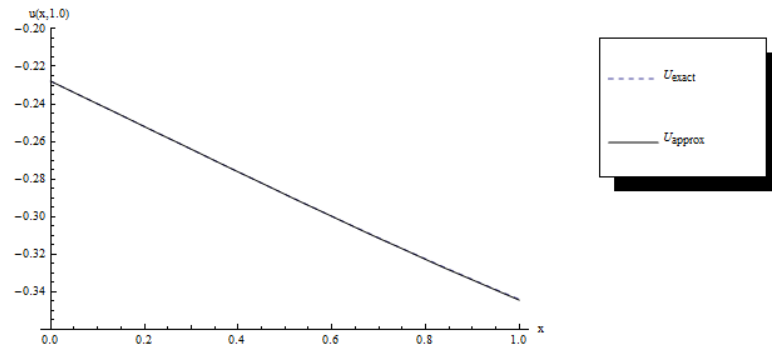
Figure 3.6 Comparison of numerical solution and exact solution of Boussinesq-Burgers' equations when $t = 1.0$.
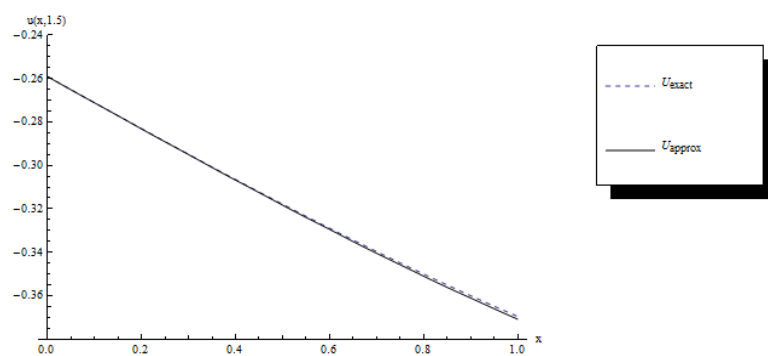
Figure 3.7 Comparison of numerical solution and exact solution of Boussinesq-Burgers' equations when $t = 1.5$.
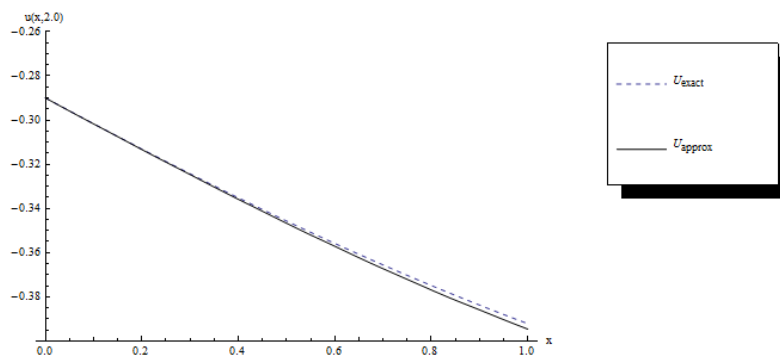
Figure 3.8 Comparison of numerical solution and exact solution of Boussinesq-Burgers' equations when $t = 2.0$.

3.10 Conclusion

In this chapter, the Boussinesq-Burgers' equations have been solved by using optimal homotopy asymptotic method (OHAM). The obtained results are then compared with exact solutions as well as homotopy perturbation method (HPM). Also, the Haar wavelet

method has been implemented to find numerical solution of Boussinesq-Burgers' equations. These results have been cited in the Tables and also graphically demonstrated in order to justify the accuracy and efficiency of the proposed schemes.

This present chapter explores the reliability and powerfulness of OHAM over other perturbation method for system of nonlinear partial differential equations like Boussinesq-Burgers' equations. An advantage of OHAM over perturbation methods is that it does not depend on small parameters. Unlike other analytical method viz. HPM, OHAM allows fine tuning of convergence region and rate of convergence by suitably identifying convergence control parameters $C_1, C_2, C_3, \ldots$. Additionally, we conclude that OHAM provides a simple and easy way to control and adjust the convergence region for strong nonlinearity and is applicable to highly nonlinear fluid problem like Boussinesq-Burgers' equations. Consequently, the present success of these methods for the highly nonlinear problem verifies that these methods are useful tool for nonlinear problems in science and engineering.

4 Numerical Solution of Fractional Differential Equations by Haar Wavelet Method

4.1 Introduction to Fractional Calculus

Fractional calculus is 300 years old topic, but not very popular amongst science and engineering community. The history of fractional calculus used to be started on the end of the 17th century and the birth of fractional calculus was because of a letter exchange. At the moment scientific journals didnot exist and scientist were exchange their information by means of letters. The fractional calculus was first anticipated by Leibnitz, was one of the founders of standard calculus, in a letter written in 1695. The primary effort to give logical definition is because of Liouville. Subsequently, many mathematicians such as Abel, Caputo, Euler, Fourier, Grünwald, Hadamard, Hardy, Heaviside, Holmgren, Laplace, Leibniz, Letnikov, Riemann, Riesz and Weyl made predominant contributions to the theory of fractional calculus.

Fractional calculus is a branch of calculus that generalizes the derivative of a function to arbitrary order. It is often referred to as generalized integral and differential calculus of arbitrary order [41]. In contemporary years, fractional calculus has become the focus of curiosity for many researchers in exclusive disciplines of applied science and engineering because of the fact that a realistic modelling of a physical phenomenon can be efficiently executed by way of utilizing fractional calculus. Indeed fractional derivatives [90, 91] provide an excellent instrument for the description of memory and hereditary properties of various materials and processes. This is the key advantage of fractional derivatives as compared to classical integer order derivatives in which such effects are abandoned. Many authors pointed out that the FDEs are inherently multi-disciplinary with its application across diverse disciplines of applied science and engineering for the description of

properties of various real physical phenomena. However, a reliable and effective general technique for solving them cannot be found even in the most useful works on fractional derivatives and integrals. So, in this chapter, our aim is to implement a reliable, appropriate and efficient wavelet based technique for the numerical solution of fractional differential equations.

In this chapter, the brief description for fractional calculus and the numerical solutions for nonlinear fractional differential equations are discussed. This present work is intended to make this subject available as popular subject to science and engineering community.

4.2 Fractional Derivative and Integration

Fractional calculus is a field of applied mathematics which deals with derivatives and integrals of arbitrary orders. Several approaches were used to define the derivatives of fractional order. The primary effort to give logical definition is because of Liouville. Since then several definitions of fractional integrals and derivatives have been proposed. This fractional calculus involves different definitions of the fractional operators such as the Riemann–Liouville, the Caputo, the Weyl, the Hadamard, the Marchaud, the Riesz, the Grünwald-Letnikov and the Erdelyi–Kober etc [90-92]. Riemann-Liouville fractional derivative is mostly used by mathematician but this is not suitable for real world physical problems as it requires the definition of fractional order initial conditions, which have no physically significant explanation yet. An alternative definition introduced by Caputo has the advantage of defining integer order initial conditions for fractional order differential equations. As a result, on this work we will use the Caputo fractional derivative by means of Caputo in his work on the theory of viscoelasticity [93].

4.2.1 Riemann-Liouville Integral and Derivative Operator

The definition of first fractional integral was initially given by Liouville, after a rigorous investigation in a series of papers from 1832-1837. Later on research and further improvements have been made by many others directed to the development of the integral-based Riemann-Liouville fractional integral operator, which has been an essential foundation in fractional calculus ever since. The primal effort of Liouville was later purified in 1865 by the Swedish mathematician Holmgren [94], who made substantial contributions to the growing study of fractional calculus. But it was Riemann [95] who

reconstructed it to fit Abel's integral equation, and hence made it enormously more useful. Even now there exist numerous forms of fractional integral operators, starting from divided-difference types to infinite-sum types, however the Riemann-Liouville operator remains to be probably the most frequently used when fractional integration is carried out. Probably the most conventionally encountered definition of an integral of fractional order is the Riemann-Liouville integral [41], in which the fractional integral operator J^{α} $(\alpha > 0)$, of a function $f(t)$, is defined as [41, 90]

$$J^{\alpha} f(t) = \frac{1}{\Gamma(\alpha)} \int_0^t (t - \tau)^{\alpha - 1} f(\tau) d\tau, \qquad \alpha > 0, \alpha \in \mathfrak{R}^+ \tag{4.1}$$

where $\Gamma(.)$ is the well-known gamma function, $\mathfrak{R}^+$ is the set of positive real numbers .

The gamma function Γ is outlined by

$$\Gamma(n) = \int_0^{\infty} e^{-t} t^{n-1} dt \quad \text{and for real number } n, \ \Gamma(n) = (n-1)!$$

Some properties of the operator J^{α} are as follows

$$J^{\alpha} J^{\beta} f(t) = J^{\alpha + \beta} f(t), \qquad \qquad (\alpha > 0, \beta > 0)$$

$$J^{\alpha} t^{\gamma} = \frac{\Gamma(1 + \gamma)}{\Gamma(1 + \gamma + \alpha)} t^{\alpha + \gamma}. \qquad \qquad (\gamma > -1)$$

The Riemann-Liouville fractional derivative is defined by

$$D^{\alpha} f(t) = D^m J^{m-\alpha} f(t)$$

$$= \frac{d^m}{dt^m} \left[\frac{1}{\Gamma(m - \alpha)} \int_0^t \frac{f(\tau)}{(t - \tau)^{\alpha - m + 1}} d\tau \right], \ m - 1 < \alpha < m, \ m \in \mathbb{N}. \tag{4.2}$$

The left Riemann-Liouville fractional derivative can be defined by

$$_a D_t^{\alpha} f(t) = \frac{1}{\Gamma(n - \alpha)} \left(\frac{d}{dt} \right)^n \int_a^t (t - \tau)^{n - \alpha - 1} f(\tau) d\tau . \tag{4.3}$$

The right Riemann-Liouville fractional derivative can be defined by

$$_t D_b^{\alpha} f(t) = \frac{1}{\Gamma(n - \alpha)} \left(-\frac{d}{dt} \right)^n \int_t^b (\tau - t)^{n - \alpha - 1} f(\tau) d\tau . \tag{4.4}$$

Fractional Riemann-Louville derivatives have various interesting properties. For example the fractional derivative of a constant is not zero, i.e.

$$_aD_t^\alpha C = \frac{C(t-\alpha)^{-\alpha}}{\Gamma(1-\alpha)}. \tag{4.5}$$

Lemma 4.1: The integral formula of Riemann-Liouville fractional derivative

$$\int_\Gamma \left(_0D_t^\alpha f(t)\right) g(t)dt = \int_\Gamma f(t)\left(_tD_T^\alpha g(t)\right)dt$$

is valid under the assumption that $f, g \in C(\Gamma)$ and $_0D_t^\alpha f(t)$, $_tD_T^\alpha g(t)$ exist for all $t \in \Gamma$ and are continuous in t.

4.2.2 Caputo Fractional Derivative

An alternative definition of fractional derivative introduced by M. Caputo in 1967 [93], is called Caputo fractional derivative. The Caputo fractional derivative $_0D_t^\alpha$ of a function $f(t)$ is defined as [41, 93]

$$D_t^\alpha f(t) = J^{m-\alpha}D^m f(t)$$

$$= \begin{cases} \dfrac{1}{\Gamma(m-\alpha)}\displaystyle\int_0^t (t-\tau)^{(m-\alpha-1)}\dfrac{d^m f(\tau)}{d\tau^m}d\tau, \text{ if } m-1 < \alpha < m, \ m \in \mathbb{N} \\[4mm] \dfrac{d^m f(t)}{dt^m}, \qquad\qquad\qquad\qquad\quad \text{if } \alpha = m, m \in \mathbb{N} \end{cases} \tag{4.6}$$

where the parameter α is the order of the derivative and is allowed to be real or even complex. For the Caputo's derivative, we have

$$D^\alpha C = 0, \qquad (C \text{ is a constant}). \tag{4.7}$$

Similar to integer order differentiation Caputo derivative is linear.

$$D^\alpha(\gamma f(t) + \delta g(t)) = \gamma D^\alpha f(t) + \delta D^\alpha g(t). \tag{4.8}$$

where γ and δ are constants, and satisfies the so called Leibnitz rule

$$D^\alpha(g(t)f(t)) = \sum_{k=0}^\infty \binom{\alpha}{k} g^{(k)}(t) D^{\alpha-k} f(t), \tag{4.9}$$

if $f(\tau)$ is continuous in [0, t] and $g(\tau)$ has continuous derivatives sufficient number of times in [0, t].

The following are two basic properties of the Caputo fractional derivative

$$_0D_t^\alpha t^\beta = \frac{\Gamma(1+\beta)}{\Gamma(1+\beta-\alpha)}t^{\beta-\alpha}, \quad 0 < \alpha < \beta+1, \beta > -1 \tag{4.10}$$

$$J^\alpha D^\alpha f(t) = f(t) - \sum_{k=0}^{n-1} f^k(0^+)\frac{t^k}{k!}, \quad n-1 < \alpha \le n \text{ and } n \in \mathbb{N}. \tag{4.11}$$

4.2.3 Grünwald-Letnikov Fractional Derivative

The Grünwald-Letnikov fractional derivative was first introduced by Anton Karl Grünwald (1838–1920) from Prague, in 1867, and by Aleksey Vasilievich Letnikov (1837-1888) from Moscow in 1868. The Grünwald-Letnikov fractional derivative of order p (>0) is defined as [41]

$$_aD_t^\alpha f(t) = \lim_{\substack{h \to 0 \\ nh=t-a}} h^{-p} \sum_{r=0}^{n} \omega_r^p f(t-rh) \tag{4.12}$$

where $\omega_r^p = (-1)^r \binom{p}{r}$.

$$\omega_0^p = 1 \text{ and } \omega_r^p = \left(1 - \frac{p+1}{r}\right)\omega_{r-1}^p, \quad r = 1,2,...$$

4.2.4 Riesz Fractional Derivative

Here, we present some significant definitions viz. the Right Riemann–Liouville derivative, Left Riemann–Liouville derivative, Riesz fractional derivative and Riesz fractional integral which are to be used subsequently in consequent chapters.

The left and right Riemann-Liouville fractional derivative of a function $f(x)$ of order α $(n-1 < \alpha < n)$, are defined as [41, 90]

$$_{-\infty}D_x^\alpha f(x) = \frac{1}{\Gamma(n-\alpha)}\frac{\partial^n}{\partial x^n}\int_{-\infty}^{x}(x-\zeta)^{n-1-\alpha}f(\zeta)d\zeta, \tag{4.13}$$

$$_xD_\infty^\alpha f(x) = \frac{(-1)^n}{\Gamma(n-\alpha)}\frac{\partial^n}{\partial x^n}\int_{x}^{\infty}(\zeta-x)^{n-1-\alpha}f(\zeta)d\zeta. \tag{4.14}$$

The Riesz fractional derivative of a function $f(x)$ is defined as [41, 90]

$$\frac{\partial^\alpha}{\partial|x|^\alpha}f(x) = \frac{-1}{2\cos\left(\frac{\alpha\pi}{2}\right)}\left[_{-\infty}D_x^\alpha f(x) + _xD_{+\infty}^\alpha f(x)\right]. \tag{4.15}$$

105

The fractional Riesz integral of a function $f(x)$ is defined as [41, 90]

$$_{RZ}I^\alpha f(x) = \frac{1}{2\cos\left(\frac{\alpha\pi}{2}\right)}\left[I_+^\alpha + I_-^\alpha\right]f(x)$$

$$= \frac{1}{2\Gamma(\alpha)\cos\left(\frac{\alpha\pi}{2}\right)}\int_{-\infty}^{+\infty}|x-\zeta|^{\alpha-1}f(\zeta)d\zeta, \qquad \alpha > 0, \alpha \neq 1,3,5,... \qquad (4.16)$$

where $I_+^\alpha f(x) = \frac{1}{\Gamma(n-\alpha)}\int_x^\infty (\zeta-x)^{n-\alpha-1}f(\zeta)d\zeta,$

and $I_-^\alpha f(x) = \frac{1}{\Gamma(n-\alpha)}\int_{-\infty}^x (x-\zeta)^{n-\alpha-1}f(\zeta)d\zeta.$

4.3 Outline of Present Study

In this chapter we have considered both analytical and numerical approach for solving some particular nonlinear fractional differential equations like fractional Burgers-Fisher equation, fractional Fisher's type equation, and time- and space-fractional Fokker-Plank equation, which have a wide variety of applications in various physical phenomena. These fractional differential equations have proved particularly beneficial in the context of anomalous diffusion model, fluid dynamics model, heat conduction, elasticity and capillary-gravity waves.

Consider the generalized one dimensional Burgers-Fisher equation of fractional order

$$\frac{\partial^\alpha u}{\partial t^\alpha} + \xi u^\eta \frac{\partial u}{\partial x} = \mu \frac{\partial^2 u}{\partial x^2} + \beta u(1-u^\eta), \qquad (4.17)$$

where ξ, μ and β are parameters and $0 < \alpha \leq 1$. This equation has a wide range of applications in fluid dynamics model, heat conduction, elasticity and capillary-gravity waves. When $\xi = 0$ and $\eta = 1$, eq. (4.17) reduces to Fisher type equation.

The generalized time-fractional Fisher's biological population diffusion equation is given by

$$\frac{\partial^\alpha u}{\partial t^\alpha} = \frac{\partial^2 u}{\partial x^2} + F(u), \qquad u(x,0) = \varphi(x), \qquad (4.18)$$

where $u(x,t)$ denotes the population density and $t > 0$, $x \in \Re$, $F(u)$ is a continuous nonlinear function satisfying the following conditions $F(0) = F(1) = 0$, $F'(0) > 0 > F'(1)$. The derivatives in eqs. (4.17) and (4.18) are the Caputo derivative of order α.

Next, we consider the time- and space-fractional Fokker-Planck equation (FPE). The classical Fokker-Planck equation was introduced by Adriaan Fokker and Max Planck, commonly used to describe the Brownian motion of particles [96]. A FPE describes the change of probability of a random function in space and time; hence it is naturally used to describe solute transport. The general FPE for the motion of a concentration field $u(x,t)$ of one space variable x at time t has the form [97-99]

$$\frac{\partial u}{\partial t} = \left[-\frac{\partial}{\partial x} A(x) + \frac{\partial^2}{\partial x^2} B(x) \right] u(x,t), \tag{4.19}$$

with the initial condition

$$u(x,0) = f(x), \qquad x \in \Re \tag{4.20}$$

where $A(x)$ and $B(x) > 0$ are referred as the drift and diffusion coefficients. The drift and diffusion coefficients may also depend on time.

There is a more general form of FPE called nonlinear Fokker-Planck equation which is of the form [97-99]

$$\frac{\partial u}{\partial t} = \left[-\frac{\partial}{\partial x} A(x,t,u) + \frac{\partial^2}{\partial x^2} B(x,t,u) \right] u(x,t). \tag{4.21}$$

The nonlinear Fokker-Planck equation (FPE) has important applications in various fields such as plasma physics, surface physics, population dynamics, biophysics, engineering, neuroscience, nonlinear hydrodynamics, polymer physics, laser physics, pattern formation, psychology and marketing etc. [100].

In recent years there has been a great deal of interest in fractional diffusion equations. These equations arise in continuous time random walks, modelling of anomalous diffusive and subdiffusive systems, unification of diffusion and wave propagation phenomenon etc. [101].

Consider the generalized nonlinear time- and space-fractional Fokker-Planck equation [102]

$$\frac{\partial^{\alpha}u}{\partial t^{\alpha}} = \left[-\frac{\partial^{\beta}}{\partial x^{\beta}} A(x,t,u) + \frac{\partial^{2\beta}}{\partial x^{2\beta}} B(x,t,u) \right] u(x,t), t > 0, \ x > 0 \qquad (4.22)$$

where α and β are parameters describing the order of the fractional time and space derivatives respectively. The function $u(x,t)$ is assumed to be a casual function of time and space, i.e. vanishing for $t < 0$ and $x < 0$. The fractional derivatives are considered in the Caputo sense.

Various mathematical methods such as the Adomian decomposition method (ADM) [103], Variational iteration method (VIM) [103], Operational Tau method (OTM) [104] and homotopy perturbation method (HPM) [105] have been used in attempting to solve fractional Fokker-Planck equations.

4.4 Application of Analytical and Numerical Techniques to Fractional Burgers-Fisher Equation

4.4.1 Haar Wavelet Based Scheme for Fractional Burgers-Fisher Equation

Consider the generalized fractional order Burgers-Fisher equation given in eq. (4.17) with following initial and boundary conditions

$$u(x,0) = \left[\frac{1}{2} + \frac{1}{2}\tanh\left(\frac{-\xi\eta}{2(\eta+1)} x \right) \right]^{\frac{1}{\eta}}, \qquad (4.23)$$

$$u(0,t) = \left(\frac{1}{2} + \frac{1}{2}\tanh\left[\frac{-\xi\eta}{2(\eta+1)}\left(-\left(\frac{\xi}{\eta+1} + \frac{\beta(\eta+1)}{\xi} \right)t \right) \right] \right)^{\frac{1}{\eta}}, \ t \geq 0 \qquad (4.24)$$

$$u(1,t) = \left(\frac{1}{2} + \frac{1}{2}\tanh\left[\frac{-\xi\eta}{2(\eta+1)}\left(1 - \left(\frac{\xi}{\eta+1} + \frac{\beta(\eta+1)}{\xi} \right)t \right) \right] \right)^{\frac{1}{\eta}}, \ t \geq 0 \qquad (4.25)$$

When $\alpha = 1$, the exact solution of eq. (4.17) is given by [106]

$$u(x,t) = \left(\frac{1}{2} + \frac{1}{2}\tanh\left[\frac{-\xi\eta}{2(\eta+1)}\left(x - \left(\frac{\xi}{\eta+1} + \frac{\beta(\eta+1)}{\xi} \right)t \right) \right] \right)^{\frac{1}{\eta}}. \qquad (4.26)$$

Let us divide both space and time interval $[0,1]$ into m equal subintervals; each of width $\Delta = \dfrac{1}{m}$. Here we have taken $\eta = 1, \mu = 1$ and $\xi = \beta = 0.01$. Therefore, eq. (4.17) reduces to

$$\frac{\partial^\alpha u}{\partial t^\alpha} - \frac{\partial^2 u}{\partial x^2} + 0.01\left(u\frac{\partial u}{\partial x} + u(u-1)\right) = 0. \tag{4.27}$$

Haar wavelet solution of $u(x,t)$ is sought by assuming that $\dfrac{\partial^2 u(x,t)}{\partial x^2}$ can be expanded in terms of Haar wavelets as

$$\frac{\partial^2 u(x,t)}{\partial x^2} = \sum_{i=1}^{m}\sum_{j=1}^{m} c_{ij} h_i(x)h_j(t). \tag{4.28}$$

Integrating eq. (4.28) with respect to x from 0 to x we get

$$\frac{\partial u(x,t)}{\partial x} - p(t) = \sum_{i=1}^{m}\sum_{j=1}^{m} c_{ij} Q h_i(x)h_j(t). \tag{4.29}$$

Again, integrating eq. (4.29) with respect to x from 0 to x we get

$$u(x,t) = \sum_{i=1}^{m}\sum_{j=1}^{m} c_{ij} Q^2 h_i(x)h_j(t) + q(t) + xp(t). \tag{4.30}$$

Putting $x = 0$, in eq. (4.30) we get

$$q(t) = u(0,t). \tag{4.31}$$

Putting $x = 1$, in eq. (4.30) we get

$$p(t) = u(1,t) - u(0,t) - \sum_{i=1}^{m}\sum_{j=1}^{m} c_{ij} \left[Q^2 h_i(x)\right]_{x=1} h_j(t). \tag{4.32}$$

Again $q(t) + xp(t)$ can be approximated using Haar wavelet function as

$$q(t) + xp(t) = \sum_{i=1}^{m}\sum_{j=1}^{m} r_{ij} h_i(x)h_j(t). \tag{4.33}$$

This implies

$$u(0,t) + x\left[u(1,t) - u(0,t) - \sum_{i=1}^{m}\sum_{j=1}^{m} c_{ij}\left[Q^2 h_i(x)\right]_{x=1} h_j(t)\right] = \sum_{i=1}^{m}\sum_{j=1}^{m} r_{ij} h_i(x)h_j(t). \tag{4.34}$$

Substituting eq. (4.33) in eq. (4.30) we get

$$u(x,t) = \sum_{i=1}^{m}\sum_{j=1}^{m} c_{ij} Q^2 h_i(x)h_j(t) + \sum_{i=1}^{m}\sum_{j=1}^{m} r_{ij} h_i(x)h_j(t). \tag{4.35}$$

The nonlinear term presented in eq. (4.27) can be approximated using Haar wavelet function as

$$u\frac{\partial u}{\partial x}+u(u-1)=\sum_{i=1}^{m}\sum_{j=1}^{m}d_{ij}h_i(x)h_j(t).$$ (4.36)

Therefore from eq. (4.29), (4.32) and (4.35) we have

$$\left(\sum_{i=1}^{m}\sum_{j=1}^{m}c_{ij}Q^2h_i(x)h_j(t)+\sum_{i=1}^{m}\sum_{j=1}^{m}r_{ij}h_i(x)h_j(t)\right)\times\left[\sum_{i=1}^{m}\sum_{j=1}^{m}c_{ij}Qh_i(x)h_j(t)+u(1,t)-u(0,t)\right]$$

$$-\sum_{i=1}^{m}\sum_{j=1}^{m}c_{ij}\left[Q^2h_i(x)\right]_{x=1}h_j(t)\right]+\left(\sum_{i=1}^{m}\sum_{j=1}^{m}c_{ij}Q^2h_i(x)h_j(t)+\sum_{i=1}^{m}\sum_{j=1}^{m}r_{ij}h_i(x)h_j(t)\right)\times \qquad (4.37)$$

$$\left(\sum_{i=1}^{m}\sum_{j=1}^{m}c_{ij}Q^2h_i(x)h_j(t)+\sum_{i=1}^{m}\sum_{j=1}^{m}r_{ij}h_i(x)h_j(t)-1\right)=\sum_{i=1}^{m}\sum_{j=1}^{m}d_{ij}h_i(x)h_j(t)$$

Substituting eq. (4.28) and eq. (4.36) in eq. (4.27) we will have

$$\frac{\partial^{\alpha}u}{\partial t^{\alpha}}=\sum_{i=1}^{m}\sum_{j=1}^{m}c_{ij}h_i(x)h_j(t)-0.01\sum_{i=1}^{m}\sum_{j=1}^{m}d_{ij}h_i(x)h_j(t).$$ (4.38)

Now applying J^{α} to both sides of eq. (4.38) yields

$$u(x,t)-u(x,0)=J^{\alpha}\left(\sum_{i=1}^{m}\sum_{j=1}^{m}c_{ij}h_i(x)h_j(t)\right)-0.01J^{\alpha}\left(\sum_{i=1}^{m}\sum_{j=1}^{m}d_{ij}h_i(x)h_j(t)\right).$$ (4.39)

Substituting eq. (4.23) and eq. (4.35) in eq. (4.39) we get

$$\sum_{i=1}^{m}\sum_{j=1}^{m}c_{ij}Q^2h_i(x)h_j(t)+\sum_{i=1}^{m}\sum_{j=1}^{m}r_{ij}h_i(x)h_j(t)-\left[\frac{1}{2}+\frac{1}{2}\tanh\left(\frac{-\xi\eta}{2(\eta+1)}x\right)\right]=$$

$$\sum_{i=1}^{m}\sum_{j=1}^{m}c_{ij}h_i(x)Q_t^{\alpha}h_j(t)-0.01\left(\sum_{i=1}^{m}\sum_{j=1}^{m}d_{ij}h_i(x)Q_t^{\alpha}h_j(t)\right)$$ (4.40)

Now substituting the collocation points $x_l=\dfrac{l-0.5}{m}$ and $t_k=\dfrac{k-0.5}{m}$ for $l,k=1,2,...,m$

in eqs. (4.34), (4.37) and (4.40), we have $3m^2$ equations in $3m^2$ unknowns in c_{ij}, r_{ij} and

d_{ij}. By solving these system of equations using mathematical software, the Haar wavelet

coefficients c_{ij}, r_{ij} and d_{ij} can be obtained.

4.4.2 Application of OHAM to time-fractional Burgers-Fisher Equation

Using optimal homotopy asymptotic method, the homotopy for eq. (4.27) can be written as

$$(1-p)\frac{\partial^\alpha \varphi(x,t;p)}{\partial t^\alpha} = H(p)\left[\frac{\partial^\alpha \varphi(x,t;p)}{\partial t^\alpha} - \frac{\partial^2 \varphi(x,t;p)}{\partial x^2}\right.$$
$$\left. + \varphi(x,t;p)\frac{\partial \varphi(x,t;p)}{\partial x} - \varphi(x,t;p)(1-\varphi(x,t;p))\right].$$

(4.41)

Here

$$\varphi(x,t;p) = u_0(x,t) + \sum_{i=1}^\infty u_i(x,t)p^i ,$$

(4.42)

$$H(p) = C_1 p + C_2 p^2 + C_3 p^3 + \ldots,$$

(4.43)

$$N(\varphi(x,t;p)) = N_0(u_0(x,t)) + \sum_{k=1}^\infty N_k(u_0,u_1,\ldots,u_k)p^k .$$

(4.44)

Substituting eqs. (4.42)- (4.44) in eq. (4.41) and equating the coefficients of like powers of p, we have the following system of partial differential equations.

Coefficients of p^0 : $\dfrac{\partial^\alpha u_0(x,t)}{\partial t^\alpha} = 0$,

(4.45)

Coefficients of p^1 : $\dfrac{\partial^\alpha u_1(x,t)}{\partial t^\alpha} - \dfrac{\partial^\alpha u_0(x,t)}{\partial t^\alpha} = C_1\left[\dfrac{\partial^\alpha u_0(x,t)}{\partial t^\alpha} - \dfrac{\partial^2 u_0(x,t)}{\partial x^2}\right.$

$$\left. + 0.01\left[u_0(x,t)\frac{\partial u_0(x,t)}{\partial x} + (u_0(x,t))^2 - u_0(x,t)\right]\right],$$

(4.46)

Coefficients of p^2 :

$$\frac{\partial^\alpha u_2(x,t)}{\partial t^\alpha} - \frac{\partial^\alpha u_1(x,t)}{\partial t^\alpha} = C_1\left[\frac{\partial^\alpha u_1(x,t)}{\partial t^\alpha} - \frac{\partial^2 u_1(x,t)}{\partial x^2} + 0.01\left[u_0(x,t)\frac{\partial u_1(x,t)}{\partial x}\right.\right.$$
$$\left.\left. + 2u_0(x,t)u_1(x,t) + u_1(x,t)\frac{\partial u_0(x,t)}{\partial x} - u_1(x,t)\right]\right] +$$

(4.47)

$$C_2\left[\frac{\partial^\alpha u_0(x,t)}{\partial t^\alpha} - \frac{\partial^2 u_0(x,t)}{\partial x^2} + 0.01\left[u_0(x,t)\frac{\partial u_0(x,t)}{\partial x} + (u_0(x,t))^2 - u_0(x,t)\right]\right],$$

and so on.

For solving fractional order Burgers-Fisher equation using OHAM, we consider the initial condition eq. (4.23) and solving eq. (4.45) to eq. (4.47), we obtain

$$u_0(x,t) = \left[\frac{1}{2} + \frac{1}{2}\tanh\left(\frac{-0.01}{4}x\right)\right], \tag{4.48}$$

$$u_1(x,t) = \frac{-0.00250625 C_1 \sec h^2(0.0025x)t^\alpha}{\Gamma(1+\alpha)}, \tag{4.49}$$

$$u_2(x,t) = u_1(x,t) + C_1\left[u_1(x,t) - \frac{C_1\left(\sec h^4(0.0025x) - 2\sec h^2(0.0025x)\tanh^2(0.0025x)\right)t^{2\alpha}}{\Gamma(1+2\alpha)}\right.$$

$$+ 0.01\left[\frac{C_1 \sec h^2(0.0025x)(-1+\tanh(0.0025x))\tanh(0.0025x)t^{2\alpha}}{\Gamma(1+2\alpha)} + \right.$$

$$\frac{C_1 \sec h^4(0.0025x)t^{2\alpha}}{\Gamma(1+2\alpha)} + \frac{0.00250625 C_1 \sec h^2(0.0025x)(-1+\tanh(0.0025x))t^{2\alpha}}{\Gamma(1+2\alpha)}$$

$$\left.\left.- \frac{0.00250625 C_1 \sec h^2(0.0025x)t^{2\alpha}}{\Gamma(1+2\alpha)}\right]\right] +$$

$$C_2\left[-\frac{\partial^2 u_0(x,t)}{\partial x^2} + 0.01\left[u_0(x,t)\frac{\partial u_0(x,t)}{\partial x} + (u_0(x,t))^2 - u_0(x,t)\right]\right]\frac{t^\alpha}{\Gamma(1+\alpha)}, \tag{4.50}$$

and so on.

Using eq. (4.48), (4.49) and (4.50), the second order approximate solution is obtained as follows

$$u(x,t) = u_0(x,t) + u_1(x,t) + u_2(x,t)$$

$$= \frac{1}{2} + \frac{1}{2}\tanh\left(\frac{-0.01}{4}x\right) - \frac{0.00250625 C_1 \sec h^2(0.0025x)t^\alpha}{\Gamma(1+\alpha)} + u_1(x,t)$$

$$+ C_1\left[u_1(x,t) - \frac{C_1\left(\sec h^4(0.0025x) - 2\sec h^2(0.0025x)\tanh^2(0.0025x)\right)t^{2\alpha}}{\Gamma(1+2\alpha)}\right.$$

$$+ 0.01\left[\frac{C_1 \sec h^2(0.0025x)(-1+\tanh(0.0025x))\tanh(0.0025x)t^{2\alpha}}{\Gamma(1+2\alpha)} + \right.$$

$$\frac{C_1 \sec h^4(0.0025x)t^{2\alpha}}{\Gamma(1+2\alpha)} + \frac{0.00250625 C_1 \sec h^2(0.0025x)(-1+\tanh(0.0025x))t^{2\alpha}}{\Gamma(1+2\alpha)}$$

$$-\frac{0.00250625 C_1 \sec h^2(0.0025x)t^{2\alpha}}{\Gamma(1+2\alpha)}\Bigg]\Bigg]+$$

$$C_2\left[-\frac{\partial^2 u_0(x,t)}{\partial x^2}+0.01\left\{u_0(x,t)\frac{\partial u_0(x,t)}{\partial x}+(u_0(x,t))^2-u_0(x,t)\right\}\right]\frac{t^{\alpha}}{\Gamma(1+\alpha)}$$

<div align="right">(4.51)</div>

The optimal values of the convergence control constants C_1 and C_2 can be obtained by using collocation method from eq. (1.33) of chapter 1.

4.5 Numerical Results for Fractional Burgers-Fisher Equation

The following Table 4.1 shows the comparison of the absolute errors of Burgers-Fisher equation obtained by using Haar wavelet method and OHAM at different values of x and t taking $\alpha=1$. Similarly, Tables 4.2-4.4 exhibit the comparison of approximate solutions obtained by Haar wavelet method and OHAM for fractional order Burgers-Fisher equation taking $\alpha=0.75, 0.5$ and 0.25 respectively. In the following Tables 4.1 -4.4, m has been taken as 16. The obtained results in Tables 4.1-4.4 demonstrate that these methods are well suited for solving fractional Burgers-Fisher equation. Both the methods are quite efficient and effective.

Table 4.1 The absolute errors in the solution of fractional order Burgers-Fisher equation given in eq. (4.27) using Haar wavelet method and three terms for second order OHAM with convergence control parameters $C_1=0, C_2=-0.99999$ at various points of x and t for $\alpha=1$.

x	$|u_{Exact}-u_{Haar}|$				$|u_{Exact}-u_{OHAM}|$			
	$t=0.2$	$t=0.4$	$t=0.6$	$t=0.8$	$t=0.2$	$t=0.4$	$t=0.6$	$t=0.8$
0.1	5.4804E-5	2.3476E-5	7.85260E-6	3.9181E-5	4.229E-11	8.408E-10	3.403E-9	8.7368E-9
0.2	2.3553E-5	7.7785E-6	3.91080E-5	7.0440E-5	8.333E-11	3.384E-10	2.273E-9	6.7268E-9
0.3	7.0426E-5	3.9091E-5	7.75940E-6	2.3578E-5	2.089E-10	1.642E-10	1.142E-9	4.7168E-9
0.4	3.9169E-5	7.8222E-6	2.35157E-5	5.4870E-5	3.346E-10	6.667E-10	1.13E-11	2.7068E-9
0.5	7.9054E-6	2.3463E-5	5.48121E-5	8.6199E-6	4.602E-10	1.1692E-9	1.119E-9	6.968E-10
0.6	5.4768E-5	2.3384E-5	7.97308E-6	3.9384E-5	5.858E-10	1.6717E-9	2.249E-9	1.3132E-9
0.7	2.3489E-5	7.9370E-6	3.93167E-5	7.0791E-5	7.115E-10	2.1742E-9	3.381E-9	3.3232E-9
0.8	7.0337E-5	3.8884E-5	7.48940E-6	2.4026E-5	8.371E-10	2.6767E-9	4.511E-9	5.3332E-9
0.9	3.9031E-5	7.5074E-6	2.39232E-5	5.5543E-5	9.627E-10	3.1792E-9	5.642E-9	7.3432E-9
1.0	8.5852E-5	5.4286E-5	2.28326E-5	8.8514E-6	1.0883E-9	3.6817E-9	6.772E-9	9.3532E-9

Table 4.2 Comparison between the approximate solutions of fractional order Burgers-Fisher equation given in eq. (4.27) using Haar wavelet method and three terms for second order OHAM with convergence control parameters $C_1=-0.000104528, C_2=-0.99979$ at various points of x and t for $\alpha=0.75$.

x	$t=0.2$		$t=0.4$		$t=0.6$		$t=0.8$	
	u_{Haar}	u_{OHAM}	u_{Haar}	u_{OHAM}	u_{Haar}	u_{OHAM}	u_{Haar}	u_{OHAM}
0.1	0.50043	0.500691	0.5009	0.501247	0.501369	0.501734	0.501839	0.502182
0.2	0.500271	0.500566	0.50074	0.501122	0.501207	0.501609	0.501674	0.502057
0.3	0.500187	0.500441	0.500656	0.500997	0.501119	0.501484	0.501584	0.501932
0.4	0.500028	0.500316	0.500495	0.500872	0.500944	0.501359	0.5014	0.501807
0.5	0.499873	0.500191	0.500335	0.500747	0.500758	0.501234	0.501197	0.501682
0.6	0.499789	0.500066	0.500248	0.500622	0.500653	0.501109	0.50108	0.501557
0.7	0.499641	0.499941	0.500092	0.500497	0.500446	0.500984	0.500839	0.501432
0.8	0.499559	0.499816	0.500005	0.500372	0.500326	0.500859	0.500697	0.501307
0.9	0.499423	0.499691	0.499855	0.500247	0.500092	0.500734	0.500409	0.501182
1.0	0.499345	0.499566	0.499767	0.500122	0.499953	0.500609	0.500236	0.501057

Table 4.3   Comparison between the approximate solutions of fractional order Burgers-Fisher equation given in eq. (4.27) using Haar wavelet method and three terms for second order OHAM with convergence control parameters $C_1 = 0.000163239, C_2 = -1.00032796$ at various points of x and t for $\alpha = 0.5$.

x	$t=0.2$		$t=0.4$		$t=0.6$		$t=0.8$	
	u_{Haar}	u_{OHAM}	u_{Haar}	u_{OHAM}	u_{Haar}	u_{OHAM}	u_{Haar}	u_{OHAM}
0.1	0.500429	0.50114	0.500898	0.501664	0.501368	0.502066	0.501837	0.502404
0.2	0.500273	0.501015	0.500736	0.501539	0.501201	0.501941	0.501666	0.502279
0.3	0.50019	0.50089	0.500646	0.501414	0.501105	0.501816	0.501566	0.502154
0.4	0.500056	0.500765	0.500484	0.501289	0.500921	0.501691	0.501363	0.502029
0.5	0.499953	0.50064	0.500329	0.501164	0.500725	0.501566	0.501132	0.501904
0.6	0.499898	0.500515	0.500238	0.501039	0.500605	0.501441	0.500986	0.501779
0.7	0.49986	0.50039	0.500098	0.500914	0.500386	0.501316	0.500698	0.501654
0.8	0.499838	0.500265	0.50001	0.500789	0.500246	0.501191	0.500513	0.501529
0.9	0.499889	0.50014	0.499894	0.500664	0.499999	0.501066	0.500153	0.501404
1.0	0.499912	0.500015	0.499814	0.500539	0.499838	0.500941	0.499922	0.501279

Table 4.4   Comparison between the approximate solutions of fractional order Burgers-Fisher equation given in eq. (4.27) using Haar wavelet method and three terms for second order OHAM with convergence control parameters $C_1 = -0.00019986, C_2 = -0.999602$ at various points of x and t for $\alpha = 0.25$.

x	$t=0.2$		$t=0.4$		$t=0.6$		$t=0.8$	
	u_{Haar}	u_{OHAM}	u_{Haar}	u_{OHAM}	u_{Haar}	u_{OHAM}	u_{Haar}	u_{OHAM}
0.1	0.500427	0.501724	0.500897	0.502074	0.501366	0.502309	0.501836	0.50249
0.2	0.50027	0.501599	0.500733	0.501949	0.501196	0.502184	0.50166	0.502365
0.3	0.500184	0.501474	0.500639	0.501824	0.501095	0.502059	0.501552	0.50224
0.4	0.500056	0.501349	0.50048	0.501699	0.500909	0.501934	0.50134	0.502115
0.5	0.49997	0.501224	0.500339	0.501574	0.500717	0.501809	0.501099	0.50199
0.6	0.49992	0.501099	0.500248	0.501449	0.500591	0.501684	0.500937	0.501865
0.7	0.499923	0.500974	0.500142	0.501324	0.500385	0.501559	0.500637	0.50174
0.8	0.499916	0.500849	0.500064	0.501199	0.500243	0.501434	0.500432	0.501615

| 0.9 | 0.500043 | 0.500724 | 0.500011 | 0.501074 | 0.500027 | 0.501309 | 0.500059 | 0.50149 |
| 1.0 | 0.500097 | 0.500599 | 0.499954 | 0.500949 | 0.499869 | 0.501184 | 0.499805 | 0.501365 |

The following Figures 4.1 and 4.2 cite the comparison graphically between the numerical solutions obtained by Haar wavelet method, optimal homotopy asymptotic method (OHAM) and exact solutions for different values of t and x.
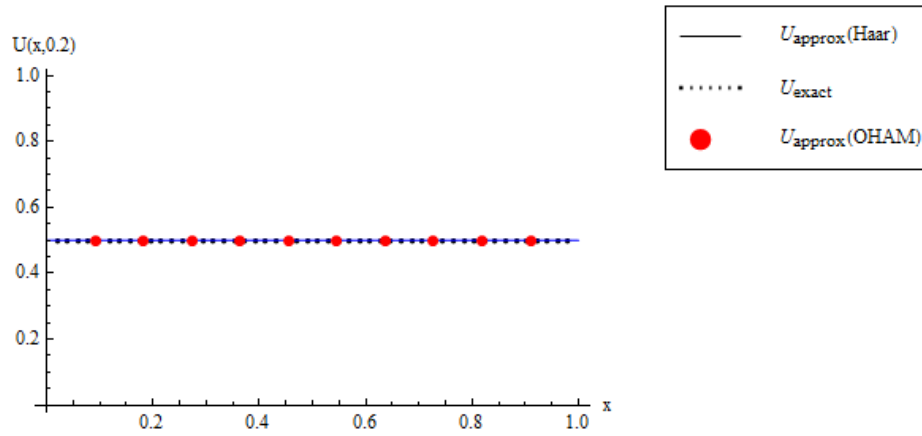
Figure 4.1   Comparison of Haar wavelet solution and OHAM solution with the exact solution of Burgers-Fisher equation when $t = 0.2$.
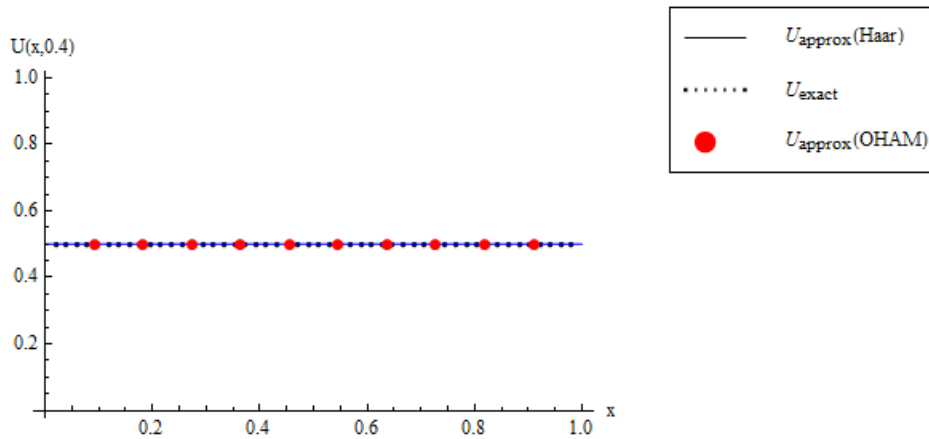
Figure 4.2   Comparison of Haar wavelet solution and OHAM solution with the exact solution of Burgers-Fisher equation when $t = 0.4$.

4.6 Application of Analytical and Numerical Methods to Fractional Fisher's type Equation

4.6.1 Haar Wavelet Based Scheme for Generalized Fisher's Equation

Consider the generalized Fisher's equation [107] of fractional order

$$\frac{\partial^\alpha u}{\partial t^\alpha} = \frac{\partial^2 u}{\partial x^2} + u\left(1 - u^6\right), \quad 0 < \alpha \le 1, 0 \le x \le 1, \tag{4.52}$$

with the initial condition

$$u(x,0) = \frac{1}{\left(1 + e^{\frac{3}{2}x}\right)^{\frac{1}{3}}}. \tag{4.53}$$

When $\alpha = 1$, the exact solution of eq. (4.52) is given by [108]

$$u(x,t) = \left(\frac{1}{2} + \frac{1}{2}\tanh\left[\frac{-3}{4}\left(x - \frac{5}{2}t\right)\right]\right)^{\frac{1}{3}} \tag{4.54}$$

Let us divide both space and time interval [0, 1] into m equal subintervals; each of width $\Delta = \frac{1}{m}$.

The Haar wavelet solution of $u(x,t)$ is sought by assuming that $\dfrac{\partial^2 u(x,t)}{\partial x^2}$ can be expanded in terms of Haar wavelets as

$$\frac{\partial^2 u(x,t)}{\partial x^2} = \sum_{i=1}^{m}\sum_{j=1}^{m} c_{ij} h_i(x) h_j(t). \tag{4.55}$$

Integrating eq. (4.55) twice with respect to x from 0 to x, we get

$$u(x,t) = \sum_{i=1}^{m}\sum_{j=1}^{m} c_{ij} Q^2 h_i(x) h_j(t) + q(t) + x p(t). \tag{4.56}$$

Putting $x = 0$, in eq. (4.56), we get

$$q(t) = u(0,t). \tag{4.57}$$

Putting $x = 1$, in eq. (4.56), we get

$$p(t) = u(1,t) - u(0,t) - \sum_{i=1}^{m}\sum_{j=1}^{m} c_{ij}\left[Q^2 h_i(x)\right]_{x=1} h_j(t). \tag{4.58}$$

116

Substituting eq. (4.57) and (4.58) in eq. (4.56), we have

$$u(x,t) = \sum_{i=1}^{m}\sum_{j=1}^{m} c_{ij} Q^2 h_i(x) h_j(t) + u(0,t) +$$

$$x\left[u(1,t) - u(0,t) - \sum_{i=1}^{m}\sum_{j=1}^{m} c_{ij}\left[Q^2 h_i(x)\right]_{x=1} h_j(t)\right]. \tag{4.59}$$

The nonlinear term presented in eq. (4.52) can be approximated using Haar wavelet function as

$$u(1 - u^6) = \sum_{i=1}^{m}\sum_{j=1}^{m} d_{ij} h_i(x) h_j(t), \tag{4.60}$$

which implies

$$\left(\sum_{i=1}^{m}\sum_{j=1}^{m} c_{ij} Q^2 h_i(x) h_j(t) + u(0,t) + x\left[u(1,t) - u(0,t) - \sum_{i=1}^{m}\sum_{j=1}^{m} c_{ij}\left[Q^2 h_i(x)\right]_{x=1} h_j(t)\right]\right)$$

$$\left[1 - \left(\sum_{i=1}^{m}\sum_{j=1}^{m} c_{ij} Q^2 h_i(x) h_j(t) + u(0,t) + x\left[u(1,t) - u(0,t) - \sum_{i=1}^{m}\sum_{j=1}^{m} c_{ij}\left[Q^2 h_i(x)\right]_{x=1} h_j(t)\right]\right)^6\right] \tag{4.61}$$

$$= \sum_{i=1}^{m}\sum_{j=1}^{m} d_{ij} h_i(x) h_j(t).$$

Substituting eq. (4.55) and eq. (4.60) in eq. (4.52), we have

$$\frac{\partial^\alpha u}{\partial t^\alpha} = \sum_{i=1}^{m}\sum_{j=1}^{m} c_{ij} h_i(x) h_j(t) + \sum_{i=1}^{m}\sum_{j=1}^{m} d_{ij} h_i(x) h_j(t). \tag{4.62}$$

Now applying J^α to both sides of eq. (4.62) yields

$$u(x,t) - u(x,0) = J^\alpha\left(\sum_{i=1}^{m}\sum_{j=1}^{m} c_{ij} h_i(x) h_j(t)\right) + J^\alpha\left(\sum_{i=1}^{m}\sum_{j=1}^{m} d_{ij} h_i(x) h_j(t)\right). \tag{4.63}$$

Substituting eq. (4.53) and eq. (4.59) in eq. (4.63) we get

$$\sum_{i=1}^{m}\sum_{j=1}^{m} c_{ij} Q^2 h_i(x) h_j(t) + u(0,t) + x\left[u(1,t) - u(0,t) - \sum_{i=1}^{m}\sum_{j=1}^{m} c_{ij}\left[Q^2 h_i(x)\right]_{x=1} h_j(t)\right]$$

$$-\frac{1}{\left(1 + e^{\frac{3}{2}x}\right)^{\frac{1}{3}}} = \sum_{i=1}^{m}\sum_{j=1}^{m} c_{ij} h_i(x) Q_t^\alpha h_j(t) + \sum_{i=1}^{m}\sum_{j=1}^{m} d_{ij} h_i(x) Q_t^\alpha h_j(t) \tag{4.64}$$

Now substituting the collocation points $x_l = \dfrac{l-0.5}{m}$ and $t_k = \dfrac{k-0.5}{m}$ for $l,k = 1,2,\ldots,m$ in eqs. (4.64) and (4.61), we have $2m^2$ equations in $2m^2$ unknowns in c_{ij} and d_{ij}. By solving these system of equations using mathematical software, the Haar wavelet coefficients c_{ij} and d_{ij} can be obtained.

4.6.2 Application of OHAM to Generalized Fisher's Equation

Using optimal homotopy asymptotic method, the homotopy for eq. (4.52) can be written as

$$(1-p)\frac{\partial^\alpha \varphi(x,t\,;\,p)}{\partial t^\alpha} = H(p)\left[\frac{\partial^\alpha \varphi(x,t\,;\,p)}{\partial t^\alpha} - \frac{\partial^2 \varphi(x,t\,;\,p)}{\partial x^2} - \varphi(x,t\,;\,p)\left[1-(\varphi(x,t\,;\,p))^6\right]\right].\text{(4.65)}$$

Here $\varphi(x,t\,;\,p) = u_0(x,t) + \sum_{i=1}^{\infty} u_i(x,t)p^i$, $\qquad$ (4.66)

$$H(p) = C_1 p + C_2 p^2 + C_3 p^3 + \ldots, \qquad (4.67)$$

$$N(\varphi(x,t\,;\,p)) = N_0(u_0(x,t)) + \sum_{k=1}^{\infty} N_k(u_0,u_1,\ldots,u_k)p^k . \qquad (4.68)$$

Substituting eqs. (4.66), (4.67) and (4.68) in eq. (4.65) and equating the coefficients of like powers of p, we have the following system of partial differential equations.

Coefficients of p^0 : $\dfrac{\partial^\alpha u_0(x,t)}{\partial t^\alpha} = 0$ $\qquad$ (4.69)

Coefficients of p^1 :

$$\frac{\partial^\alpha u_1(x,t)}{\partial t^\alpha} - \frac{\partial^\alpha u_0(x,t)}{\partial t^\alpha} = C_1\left[\frac{\partial^\alpha u_0(x,t)}{\partial t^\alpha} - \frac{\partial^2 u_0(x,t)}{\partial x^2} + (u_0(x,t))^7 - u_0(x,t)\right]. \quad (4.70)$$

Coefficients of p^2 :

$$\frac{\partial^\alpha u_2(x,t)}{\partial t^\alpha} - \frac{\partial^\alpha u_1(x,t)}{\partial t^\alpha} = C_1\left[\frac{\partial^\alpha u_1(x,t)}{\partial t^\alpha} - \frac{\partial^2 u_1(x,t)}{\partial x^2} + 7(u_0(x,t))^6 u_1(x,t) - u_1(x,t)\right]$$
$$+ C_1\left[\frac{\partial^\alpha u_0(x,t)}{\partial t^\alpha} - \frac{\partial^2 u_0(x,t)}{\partial x^2} + (u_0(x,t))^7 - u_0(x,t)\right] \quad (4.71)$$

and so on.

We consider the initial condition given in eq. (4.53) and solving above equations, we obtain

$$u_0(x,t) = \cfrac{1}{\left(1 + e^{\frac{3}{2}x}\right)^{\frac{1}{3}}}, \qquad (4.72)$$

$$u_1(x,t) = \cfrac{-5C_1 e^{\frac{3x}{2}} t^\alpha}{4\left(1 + e^{\frac{3x}{2}}\right)^{4/3} \Gamma(1+\alpha)}, \qquad (4.73)$$

and so on.

The fourth order approximate solution can be obtained by using the formula

$$u(x,t) = u_0(x,t) + u_1(x,t) + u_2(x,t) + u_3(x,t) + u_4(x,t).$$

The optimal values of the convergence control constants C_1, C_2, C_3 and C_4 can be obtained using collocation method from eq. (1.33) of chapter 1.

4.7 Numerical Results for Fractional Fisher's Equation

Tables 4.5-4.8 present the comparison of approximate solutions obtained by Haar wavelet method and OHAM for fractional order generalized Fisher's equation given in eq. (4.52). The obtained results in Tables demonstrate that these methods are well suited for solving fractional order generalized Fisher's equation. Both the methods are quite efficient and effective.

Table 4.5 The absolute errors in the solution of generalized Fisher's equation (4.52) using Haar wavelet method and five terms for fourth order OHAM with convergence control parameters $C_1 = -0.637012, C_2 = -0.151156, C_3 = 0.023432, C_4 = -0.0012788$ at various points of x and t for $\alpha = 1$.

x	$|u_{Exact} - u_{Haar}|$				$|u_{Exact} - u_{OHAM}|$			
	$t = 0.2$	$t = 0.4$	$t = 0.6$	$t = 0.8$	$t = 0.2$	$t = 0.4$	$t = 0.6$	$t = 0.8$
0.1	0.0051104	0.0054849	0.0042629	0.0027556	6.67439E-5	0.0040747	0.023752	0.0740709
0.2	0.0096957	0.0106181	0.0085377	0.0058225	1.99503E-4	0.0023417	0.019345	0.0678136
0.3	0.013553	0.0151142	0.0125286	0.0089272	4.65337E-4	4.3112E-4	0.013810	0.0581267
0.4	0.0163976	0.018593	0.0158324	0.0116856	7.18406E-4	0.0015578	0.007399	0.0453319
0.5	0.0179265	0.0206477	0.0180051	0.0136684	9.47663E-4	0.0035178	4.521E-4	0.030035
0.6	0.017924	0.0209528	0.0186691	0.0145062	0.0011444	0.0053436	0.006645	0.013062
0.7	0.0163414	0.01935	0.0175984	0.013973	0.0013029	0.0069445	0.013494	0.0046328
0.8	0.0133823	0.015939	0.0148102	0.0120755	0.0014207	0.0082540	0.019736	0.0220718

| 0.9 | 0.0095361 | 0.0111158 | 0.0106057 | 0.0090918 | 0.0014982 | 0.009231 | 0.025078 | 0.0383517 |
| 1.0 | 0.0055837 | 0.0055837 | 0.0055837 | 0.0055837 | 0.0015382 | 0.0098632 | 0.029315 | 0.0527218 |

Table 4.6   The approximate solutions of generalized Fisher equation (4.52) using Haar wavelet method and five terms for fourth order OHAM with convergence control parameters $C_1 = -0.649458, C_2 = 0.053658, C_3 = -0.1822726, C_4 = 0.0894301$ at various points of x and t for $\alpha = 0.75$.

x	$t = 0.2$		$t = 0.4$		$t = 0.6$		$t = 0.8$	
	u_{Haar}	u_{OHAM}	u_{Haar}	u_{OHAM}	u_{Haar}	u_{OHAM}	u_{Haar}	u_{OHAM}
0.1	0.859185	0.899389	0.920547	0.931947	0.957952	0.927394	0.978665	0.902524
0.2	0.838644	0.888856	0.905313	0.930017	0.948042	0.930519	0.972681	0.905646
0.3	0.817612	0.877253	0.889588	0.927859	0.93764	0.934718	0.966206	0.91116
0.4	0.796431	0.864492	0.873714	0.92523	0.927088	0.939825	0.959581	0.919341
0.5	0.775484	0.850503	0.858074	0.921857	0.916772	0.945568	0.953191	0.930278
0.6	0.755093	0.835244	0.84299	0.917456	0.90701	0.951569	0.947357	0.943809
0.7	0.735424	0.818704	0.828628	0.911753	0.897971	0.957356	0.942244	0.959482
0.8	0.716399	0.800908	0.81491	0.904497	0.889575	0.962388	0.937776	0.976567
0.9	0.697656	0.781918	0.801474	0.895481	0.881463	0.966095	0.933591	0.994112
1.0	0.678526	0.761827	0.787651	0.884559	0.872963	0.967927	0.929017	1.01104

Table 4.7   The approximate solutions of generalized Fisher equation (4.52) using Haar wavelet method and five terms for fourth order OHAM with convergence control parameters $C_1 = -0.5059152, C_2 = -0.0211535, C_3 = -0.05081612$ and $C_4 = 0.0574318$ at various points of x and t for $\alpha = 0.5$.

x	$t = 0.2$		$t = 0.4$		$t = 0.6$		$t = 0.8$	
	u_{Haar}	u_{OHAM}	u_{Haar}	u_{OHAM}	u_{Haar}	u_{OHAM}	u_{Haar}	u_{OHAM}
0.1	0.859121	0.927731	0.920482	0.943924	0.957888	0.943779	0.9786	0.939948
0.2	0.838402	0.921616	0.905071	0.943123	0.947799	0.94491	0.972438	0.940694
0.3	0.817123	0.914826	0.889099	0.942438	0.937151	0.946615	0.965717	0.941956
0.4	0.795694	0.907206	0.872977	0.941713	0.926351	0.948908	0.958844	0.944068
0.5	0.774576	0.898605	0.857166	0.940787	0.915864	0.951841	0.952284	0.947508
0.6	0.754149	0.888882	0.842046	0.93948	0.906066	0.955446	0.946413	0.952761
0.7	0.734584	0.877915	0.827789	0.937586	0.897131	0.959662	0.941405	0.96016
0.8	0.715744	0.865607	0.814255	0.934862	0.888921	0.964283	0.937121	0.969739
0.9	0.697156	0.851889	0.800975	0.931031	0.880963	0.968937	0.933091	0.98117
1.0	0.678052	0.83673	0.787178	0.925803	0.872489	0.973109	0.928543	0.993777

Table 4.8   The approximate solutions of generalized Fisher equation (4.52) using Haar wavelet method and five terms for fourth order OHAM with convergence control parameters

$C_1 = -0.33833012, C_2 = -0.04303056, C_3 = 0.1230816$ and $C_4 = -0.0545852$ at various points of x and t for $\alpha = 0.25$.

x	$t = 0.2$		$t = 0.4$		$t = 0.6$		$t = 0.8$	
	u_{Haar}	u_{OHAM}	u_{Haar}	u_{OHAM}	u_{Haar}	u_{OHAM}	u_{Haar}	u_{OHAM}
0.1	0.859016	0.949105	0.920377	0.959635	0.957783	0.964066	0.978495	0.966453
0.2	0.837987	0.943681	0.904655	0.955839	0.947384	0.960802	0.972023	0.963262
0.3	0.816234	0.937961	0.88821	0.9522	0.936261	0.957955	0.964827	0.960634
0.4	0.79426	0.93184	0.871543	0.948657	0.924917	0.95553	0.95741	0.958645
0.5	0.772676	0.925203	0.855266	0.945143	0.913963	0.953545	0.950383	0.957415
0.6	0.752001	0.917922	0.839899	0.941569	0.903919	0.951996	0.944265	0.957051
0.7	0.732474	0.909857	0.825678	0.937799	0.895021	0.950809	0.939295	0.957571
0.8	0.713871	0.900851	0.812383	0.933634	0.887048	0.949804	0.935249	0.958845
0.9	0.695534	0.890742	0.799352	0.928815	0.87934	0.948678	0.931468	0.96056
1.0	0.676507	0.87937	0.785633	0.923035	0.870944	0.947027	0.926998	0.96224

In case of generalized Fisher's equation, the Figures 4.3 and 4.4 present the comparison graphically between the numerical results obtained by Haar wavelet method, OHAM and exact solutions for different values of t and x.
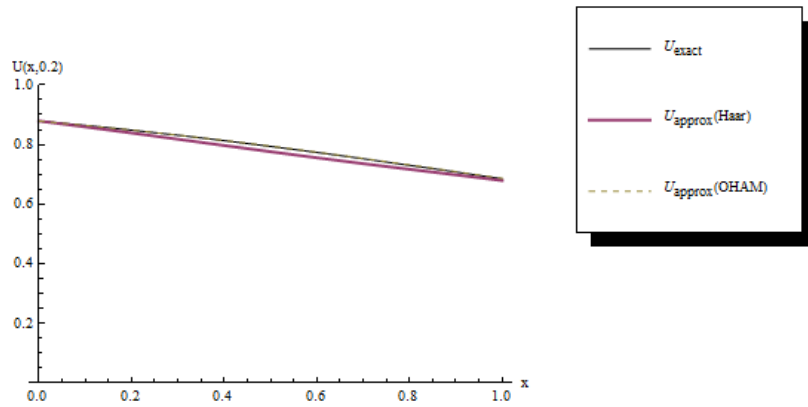
Figure 4.3   Comparison of Haar wavelet solution and OHAM solution with the exact solution of generalized Fisher's equation when $t = 0.2$.
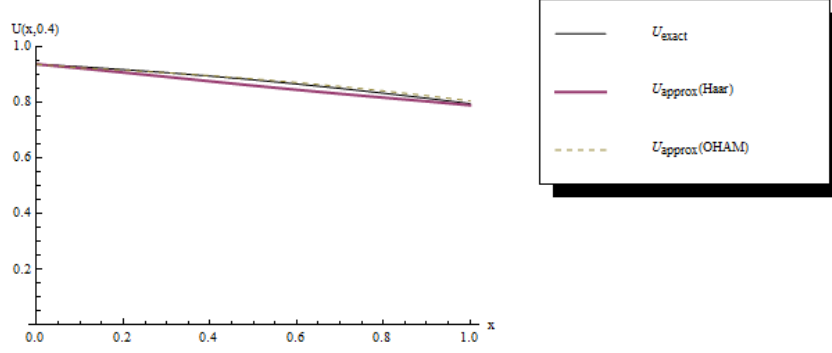
Figure 4.4   Comparison of Haar wavelet solution and OHAM solution with the exact solution of generalized Fisher's equation when $t = 0.4$.

4.8   Solution of Fractional Fokker-Planck Equation

4.8.1 Application of Haar Wavelets to Time-Fractional Fokker-Planck Equation

Consider the nonlinear time-fractional Fokker-Planck equation [103, 105]

$$\frac{\partial^\alpha u}{\partial t^\alpha} = \left[-\frac{\partial}{\partial x}\left(\frac{4u}{x} - \frac{x}{3} \right) + \frac{\partial^2 u}{\partial x^2} \right] u(x,t),\ t > 0,\ x > 0,\ 0 < \alpha \le 1, \tag{4.74}$$

subject to the initial condition

$$u(x,0) = x^2. \tag{4.75}$$

When $\alpha = 1$, the exact solution of eq. (4.74) is given by [103, 105]

$$u(x,t) = x^2 e^t. \tag{4.76}$$

Let us divide both space and time interval [0, 1] into m equal subintervals; each of width $\Delta = \frac{1}{m}$. Haar wavelet solution of $u(x,t)$ is sought by assuming that $\dfrac{\partial^2 u(x,t)}{\partial x^2}$ can be expanded in terms of Haar wavelets as

$$\frac{\partial^2 u(x,t)}{\partial x^2} = \sum_{i=1}^{m}\sum_{j=1}^{m} c_{ij} h_i(x) h_j(t). \tag{4.77}$$

Integrating eq. (4.77) with respect to x from 0 to x, we get

$$\frac{\partial u(x,t)}{\partial x} - p(t) = \sum_{i=1}^{m}\sum_{j=1}^{m} c_{ij} Q h_i(x) h_j(t). \tag{4.78}$$

Again, integrating eq. (4.78) with respect to x from 0 to x, we get

$$u(x,t) = \sum_{i=1}^{m} \sum_{j=1}^{m} c_{ij} Q^2 h_i(x) h_j(t) + q(t) + xp(t). \tag{4.79}$$

Putting $x = 0,$ in eq. (4.79), we get

$$q(t) = u(0,t) = 0. \tag{4.80}$$

Putting $x = 1,$ in eq. (4.79), we get

$$p(t) = u(1,t) - u(0,t) - \sum_{i=1}^{m} \sum_{j=1}^{m} c_{ij} \left[Q^2 h_i(x) \right]_{x=1} h_j(t)$$

$$= u(1,t) - \sum_{i=1}^{m} \sum_{j=1}^{m} c_{ij} \left[Q^2 h_i(x) \right]_{x=1} h_j(t). \tag{4.81}$$

Putting eq. (4.81) in eqs. (4.78) and (4.79), we have

$$\frac{\partial u(x,t)}{\partial x} = \sum_{i=1}^{m} \sum_{j=1}^{m} c_{ij} Q h_i(x) h_j(t) + u(1,t) - \sum_{i=1}^{m} \sum_{j=1}^{m} c_{ij} \left[Q^2 h_i(x) \right]_{x=1} h_j(t), \tag{4.82}$$

$$u(x,t) = \sum_{i=1}^{m} \sum_{j=1}^{m} c_{ij} Q^2 h_i(x) h_j(t) + x \left[u(1,t) - \sum_{i=1}^{m} \sum_{j=1}^{m} c_{ij} \left[Q^2 h_i(x) \right]_{x=1} h_j(t) \right]. \tag{4.83}$$

The nonlinear term presented in eq. (4.74) can be approximated using Haar wavelet function as

$$\frac{\partial^2 u^2}{\partial x^2} - \frac{\partial}{\partial x} \left(\frac{4u^2}{x} \right) = \sum_{i=1}^{m} \sum_{j=1}^{m} d_{ij} h_i(x) h_j(t).$$

This implies

$$2u \left(\frac{\partial^2 u}{\partial x^2} + \frac{2u}{x^2} \right) + 2 \left(\frac{\partial u}{\partial x} \right) \left(\frac{\partial u}{\partial x} - \frac{4u}{x} \right) = \sum_{i=1}^{m} \sum_{j=1}^{m} d_{ij} h_i(x) h_j(t). \tag{4.84}$$

Therefore substituting eqs. (4.77), (4.82) and (4.83) in eq. (4.84), we have

$$2\left(\sum_{i=1}^{m}\sum_{j=1}^{m}c_{ij}Q^2h_i(x)h_j(t)+x\left[u(1,t)-\sum_{i=1}^{m}\sum_{j=1}^{m}c_{ij}\left[Q^2h_i(x)\right]_{x=1}h_j(t)\right]\right)\times$$

$$\left[\sum_{i=1}^{m}\sum_{j=1}^{m}c_{ij}h_i(x)h_j(t)+\frac{2}{x^2}\left(\sum_{i=1}^{m}\sum_{j=1}^{m}c_{ij}Q^2h_i(x)h_j(t)+x\left[u(1,t)-\sum_{i=1}^{m}\sum_{j=1}^{m}c_{ij}\left[Q^2h_i(x)\right]_{x=1}h_j(t)\right]\right)\right]$$

$$+2\left(\sum_{i=1}^{m}\sum_{j=1}^{m}c_{ij}Qh_i(x)h_j(t)+u(1,t)-\sum_{i=1}^{m}\sum_{j=1}^{m}c_{ij}\left[Q^2h_i(x)\right]_{x=1}h_j(t)\right)\times$$

$$\left[\left(\sum_{i=1}^{m}\sum_{j=1}^{m}c_{ij}Qh_i(x)h_j(t)+u(1,t)-\sum_{i=1}^{m}\sum_{j=1}^{m}c_{ij}\left[Q^2h_i(x)\right]_{x=1}h_j(t)\right)\right.$$

$$\left.-\frac{4}{x}\left(\sum_{i=1}^{m}\sum_{j=1}^{m}c_{ij}Q^2h_i(x)h_j(t)+x\left[u(1,t)-\sum_{i=1}^{m}\sum_{j=1}^{m}c_{ij}\left[Q^2h_i(x)\right]_{x=1}h_j(t)\right]\right)\right]$$

$$=\sum_{i=1}^{m}\sum_{j=1}^{m}d_{ij}h_i(x)h_j(t)$$

(4.85)

Substituting eq. (4.84) in eq. (4.74), we have

$$\frac{\partial^{\alpha}u}{\partial t^{\alpha}}=\sum_{i=1}^{m}\sum_{j=1}^{m}d_{ij}h_i(x)h_j(t)+\frac{x}{3}\frac{\partial u}{\partial x}+\frac{u}{3}.$$

(4.86)

Now applying J^{α} to both sides of eq. (4.86) yields

$$u(x,t)-u(x,0)=J^{\alpha}\left(\sum_{i=1}^{m}\sum_{j=1}^{m}d_{ij}h_i(x)h_j(t)+\frac{x}{3}\frac{\partial u}{\partial x}+\frac{u}{3}\right).$$

(4.87)

Substituting eqs. (4.75), (4.82) and (4.83) in eq. (4.87), we get

$$\sum_{i=1}^{m}\sum_{j=1}^{m}c_{ij}Q^2h_i(x)h_j(t)+x\left[u(1,t)-\sum_{i=1}^{m}\sum_{j=1}^{m}c_{ij}\left[Q^2h_i(x)\right]_{x=1}h_j(t)\right]-x^2=$$

$$\sum_{i=1}^{m}\sum_{j=1}^{m}d_{ij}h_i(x)Q_t^{\alpha}h_j(t)+$$

$$\frac{x}{3}\left(\sum_{i=1}^{m}\sum_{j=1}^{m}c_{ij}Qh_i(x)Q_t^{\alpha}h_j(t)+J^{\alpha}u(1,t)-\sum_{i=1}^{m}\sum_{j=1}^{m}c_{ij}\left[Q^2h_i(x)\right]_{x=1}Q_t^{\alpha}h_j(t)\right)+$$

$$\frac{1}{3}\left(\sum_{i=1}^{m}\sum_{j=1}^{m}c_{ij}Q^2h_i(x)Q_t^{\alpha}h_j(t)+x\left[J^{\alpha}u(1,t)-\sum_{i=1}^{m}\sum_{j=1}^{m}c_{ij}\left[Q^2h_i(x)\right]_{x=1}Q_t^{\alpha}h_j(t)\right]\right)$$

(4.88)

Now substituting the collocation points $x_l = \dfrac{l-0.5}{m}$ and $t_k = \dfrac{k-0.5}{m}$ for $l, k = 1, 2, ..., m$

in eqs. (4.85) and (4.88), we have $2m^2$ equations in $2m^2$ unknowns in c_{ij} and d_{ij}. By solving these system of equations using mathematical software, the Haar wavelet coefficients c_{ij} and d_{ij} can be obtained.

4.8.2 Application of two Dimensional Haar Wavelet for Solving Time- and Space-Fractional Fokker-Planck Equation

Consider the time- and space-fractional Fokker-Planck equation [103, 105]

$$\frac{\partial^\alpha u}{\partial t^\alpha} = \left[-\frac{\partial^\beta}{\partial x^\beta}\left(\frac{x}{6}\right) + \frac{\partial^{2\beta}}{\partial x^{2\beta}}\left(\frac{x^2}{12}\right) \right] u(x,t), \, t > 0, x > 0, \tag{4.89}$$

where $0 < \alpha, \beta \le 1$, subject to the initial condition

$$u(x,0) = x^2. \tag{4.90}$$

When $\alpha = 1$ and $\beta = 1$, the exact solution of eq. (4.89) is given by [103, 105]

$$u(x,t) = x^2 e^{\frac{t}{2}}. \tag{4.91}$$

Let us divide space interval [0, 1] into m equal subintervals; each of width $\Delta = \dfrac{1}{m}$.

Haar wavelet solution of $u(x,t)$ is sought by assuming that $\dfrac{\partial^\alpha u(x,t)}{\partial t^\alpha}$ can be expanded in terms of Haar wavelets as

$$\frac{\partial^\alpha u(x,t)}{\partial t^\alpha} = \sum_{i=1}^{m}\sum_{j=1}^{m} a_{ij} h_i(x) h_j(t). \tag{4.92}$$

Applying J^α both sides of eq. (4.92), we get

$$u(x,t) = x^2 + \sum_{i=1}^{m}\sum_{j=1}^{m} a_{ij} h_i(x) Q^\alpha h_j(t). \tag{4.93}$$

Now $\quad \dfrac{\partial^\beta}{\partial x^\beta}(xu(x,t)) = \dfrac{\partial^\beta}{\partial x^\beta}(x^3) + \sum_{i=1}^{m}\sum_{j=1}^{m} a_{ij} \dfrac{\partial^\beta}{\partial x^\beta}(xh_i(x)) Q^\alpha h_j(t),$ \hfill (4.94)

and $\quad \dfrac{\partial^{2\beta}}{\partial x^{2\beta}}(x^2 u(x,t)) = \dfrac{\partial^{2\beta}}{\partial x^{2\beta}}(x^4) + \sum_{i=1}^{m}\sum_{j=1}^{m} a_{ij} \dfrac{\partial^{2\beta}}{\partial x^{2\beta}}(x^2 h_i(x)) Q^\alpha h_j(t).$ \hfill (4.95)

Substituting eqs. (4.92), (4.94) and (4.95) in eq. (4.89), we get

$$\sum_{i=1}^{m}\sum_{j=1}^{m}a_{ij}h_i(x)h_j(t) = \frac{-1}{6}\left(\frac{\partial^{\beta}}{\partial x^{\beta}}(x^3) + \sum_{i=1}^{m}\sum_{j=1}^{m}a_{ij}\frac{\partial^{\beta}}{\partial x^{\beta}}(xh_i(x))Q^{\alpha}h_j(t)\right) +$$
$$\frac{1}{12}\left(\frac{\partial^{2\beta}}{\partial x^{2\beta}}(x^4) + \sum_{i=1}^{m}\sum_{j=1}^{m}a_{ij}\frac{\partial^{2\beta}}{\partial x^{2\beta}}(x^2h_i(x))Q^{\alpha}h_j(t)\right). \tag{4.96}$$

Now substituting the collocation points $x_l = \dfrac{l-0.5}{m}$ for $l=1,2,...,m$ in eq. (4.96), we have m^2 equations in m^2 unknowns a_{ij}. By solving this system of equations using mathematical software, the Haar wavelet coefficients a_{ij} can be obtained.

4.9 Numerical Results for Fractional Fokker-Planck Equation

The following Table 4.9 shows the comparison of exact solutions with the approximate solutions of different numerical methods for time-fractional Fokker-Planck equation. Agreement between present numerical results with other approximate solutions and exact solutions appear very satisfactory through illustrations in Tables 4.9 and 4.10. Table 4.10 shows the comparison of approximate solutions of fractional order time-fractional Fokker-Planck equation obtained by using two dimensional Haar wavelet method with the solutions of Adomian decomposition method (ADM) and Variational iteration method (VIM) presented in Ref. [103]. Similarly Tables 4.11 and 4.12 show the comparison of approximate solutions obtained by different numerical methods for time- and space-fractional Fokker-Planck equation. It is found that the solutions obtain by using present method are in good agreement with the results presented by Odibat et al. [103] and even better than the results obtained by Operational Tau method (OTM) presented by Vanani et al. [104]. However, the errors may be reduced significantly if we increase level of resolution which prompts more number of collocation points.

Table 4.9   Comparison of present method solution with other numerical methods for classical order time fractional Fokker-Planck equation (4.74) at various points of x and t for $\alpha = 1$.

t	x	u_{ADM} [103]	u_{VIM} [103]	u_{Exact}	u_{Haar}
0.2	0.25	0.076333	0.076333	0.076338	0.0756165
	0.5	0.305333	0.305333	0.305351	0.304392
	0.75	0.687000	0.687000	0.687039	0.686321

	1.0	1.221333	1.221333	1.221403	1.2214
0.4	0.25	0.093167	0.093167	0.093239	0.0958469
	0.5	0.372667	0.372667	0.372956	0.376435
	0.75	0.838500	0.838500	0.839151	0.841761
	1.0	1.490667	1.490667	1.491825	1.49182
0.6	0.25	0.113500	0.113500	0.113882	0.110663
	0.5	0.454000	0.454000	0.455530	0.451238
	0.75	1.021500	1.021500	1.024942	1.02172
	1.0	1.816000	1.816000	1.822119	1.82212

Table 4.10   Comparison of present method solution with other numerical methods for time fractional Fokker-Planck equation (4.74) at various points of x and t taking $\alpha = 0.5$ and $\alpha = 0.75$.

t	x	$\alpha = 0.5$			$\alpha = 0.75$		
		u_{ADM} [103]	u_{VIM} [103]	u_{Haar}	u_{ADM} [103]	u_{VIM} [103]	u_{Haar}
0.2	0.25	0.110744	0.091795	0.0900792	0.087699	0.084593	0.0714745
	0.5	0.442978	0.367179	0.421013	0.350796	0.338372	0.329117
	0.75	0.996699	0.826154	0.990531	0.789291	0.761337	0.773339
	1.0	1.771910	1.468717	1.79902	1.403180	1.353488	1.40468
0.4	0.25	0.143997	0.118678	0.13581	0.111718	0.106178	0.0973803
	0.5	0.575909	0.474712	0.587481	0.446872	0.424712	0.431178
	0.75	1.295980	1.068102	1.35217	1.005460	0.955602	0.998822
	1.0	2.303960	1.898849	2.43004	1.787490	1.698849	1.80046
0.6	0.25	0.176478	0.146209	0.167654	0.138479	0.129926	0.116878
	0.5	0.705914	0.584835	0.749162	0.553918	0.519702	0.534521
	0.75	1.588310	1.315878	1.742	1.246320	1.169330	1.24986
	1.0	2.823650	2.339338	3.14621	2.215670	2.078809	2.26291

Table 4.11   Comparison of approximate solutions obtained by using VIM, ADM and Haar wavelet method for time- and space-fractional Fokker-Planck equation (4.89) at various points of x and t taking $\alpha = 1$ and $\beta = 1$.

t	x	u_{ADM} [103]	u_{VIM} [103]	u_{Exact}	u_{Haar}
0.2	0.25	0.069062	0.069062	0.069073	0.0689468
	0.5	0.276259	0.276250	0.276293	0.274611
	0.75	0.621563	0.621563	0.621659	0.619337
0.4	0.25	0.076250	0.076250	0.076338	0.0753937
	0.5	0.305000	0.305000	0.305351	0.299222
	0.75	0.686250	0.686250	0.687039	0.676175
0.6	0.25	0.084062	0.084063	0.084366	0.0818405
	0.5	0.336250	0.336250	0.337465	0.323833
	0.75	0.756562	0.756562	0.759296	0.733012

Table 4.12 Comparison of approximate solutions of fractional order time- and space-fractional Fokker-Planck equation (4.89) obtained by using VIM, ADM, OTM and Haar wavelet method at various points of x and t taking $\alpha = \beta = 0.5$ and $\alpha = \beta = 0.75$.

t	x	$\alpha = 0.5$ and $\beta = 0.5$				$\alpha = 0.75$ and $\beta = 0.75$			
		u_{ADM} [103]	u_{VIM} [103]	u_{OTM} [104]	u_{Haar}	u_{ADM} [103]	u_{VIM} [103]	u_{OTM} [104]	u_{Haar}
0.2	0.25	0.060440	0.06111	0.061929	0.0601168	0.063002	0.062922	0.062920	0.0633685
	0.5	0.244329	0.24618	0.248365	0.244247	0.258161	0.256856	0.256782	0.256326
	0.75	0.559866	0.56056	0.562348	0.559936	0.592855	0.587790	0.588104	0.595415
0.4	0.25	0.059620	0.05996	0.061392	0.0591215	0.063371	0.063291	0.063305	0.063968
	0.5	0.242066	0.24303	0.246833	0.241821	0.264157	0.262868	0.262916	0.260722
	0.75	0.558992	0.55902	0.562276	0.558771	0.615589	0.610213	0.611786	0.618446
0.6	0.25	0.059004	0.05898	0.060883	0.0583544	0.063713	0.063642	0.063669	0.0644986
	0.5	0.240363	0.24033	0.245395	0.239941	0.269702	0.268564	0.268707	0.264632
	0.75	0.558407	0.55777	0.562273	0.557834	0.636878	0.631709	0.634637	0.639038

4.10 Convergence Analysis of Two-dimensional Haar Wavelet Method

In this section, we have introduced the error analysis for the two-dimensional Haar wavelet method.

We assume that, $f(x, y) \in C^2([a,b] \times [a,b])$ and there exist $M > 0$; for which

$$\left| \frac{\partial^2 f(x, y)}{\partial x \partial y} \right| \le M \text{ , for all } x, y \in [a,b] \times [a,b].$$

Next, we may proceed as follows, suppose $f_{nm}(x, y) = \sum_{i=0}^{n-1} \sum_{j=0}^{m-1} c_{ij} h_i(x) h_j(y)$,

where, $n = 2^{\alpha+1}$, $\alpha = 0,1,2,...$ and $m = 2^{\beta+1}$, $\beta = 0,1,2,...$.

Then,

$$f(x, y) - f_{nm}(x, y) = \sum_{i=n}^{\infty} \sum_{j=m}^{\infty} c_{ij} h_i(x) h_j(y) + \sum_{i=n}^{\infty} \sum_{j=0}^{m-1} c_{ij} h_i(x) h_j(y) + \sum_{i=0}^{n-1} \sum_{j=m}^{\infty} c_{ij} h_i(x) h_j(y).$$

From Parseval's formula, we have

$$\|f(x,y) - f_{nm}(x,y)\|^2 = \int_a^b \int_a^b (f(x,y) - f_{nm}(x,y))^2 \, dx \, dy$$

$$= \sum_{p=n}^{\infty} \sum_{s=m}^{\infty} \sum_{i=n}^{\infty} \sum_{j=m}^{\infty} c'_{ij} c'_{ps} \int_a^b h_i(x) h_p(x) dx \int_a^b h_j(y) h_s(y) dy$$

$$+ \sum_{p=n}^{\infty} \sum_{s=0}^{m-1} \sum_{i=n}^{\infty} \sum_{j=0}^{m-1} c'_{ij} c'_{ps} \int_a^b h_i(x) h_p(x) dx \int_a^b h_j(y) h_s(y) dy$$

$$+ \sum_{p=0}^{n-1} \sum_{s=m}^{\infty} \sum_{i=0}^{n-1} \sum_{j=m}^{\infty} c'_{ij} c'_{ps} \int_a^b h_i(x) h_p(x) dx \int_a^b h_j(y) h_s(y) dy$$

$$= \sum_{i=n}^{\infty} \sum_{j=m}^{\infty} c'^2_{ij} + \sum_{i=n}^{\infty} \sum_{j=0}^{m-1} c'^2_{ij} + \sum_{i=0}^{n-1} \sum_{j=m}^{\infty} c'^2_{ij} \,,$$

where, $c'^2_{ij} = \dfrac{c_{ij}(b-a)^2}{2^{i+j}}$ and

$$c_{ij} = \int_a^b \left(\int_a^b f(x,y) h_i(y) dy \right) h_j(x) dx$$

$$= \int_a^b \left(\int_{a+k\left(\frac{b-a}{2^i}\right)}^{a+\left(k+\frac{1}{2}\right)\left(\frac{b-a}{2^i}\right)} f(x,y) dy \quad - \int_{a+\left(k+\frac{1}{2}\right)\left(\frac{b-a}{2^i}\right)}^{a+(k+1)\left(\frac{b-a}{2^i}\right)} f(x,y) dy \right) h_j(x) dx.$$

Using the Mean value theorem of Integral calculus, we have

$$a + k\frac{(b-a)}{2^i} \le y_1 \le a + \left(k + \frac{1}{2}\right)\frac{(b-a)}{2^i}, \quad a + \left(k + \frac{1}{2}\right)\frac{(b-a)}{2^i} \le y_2 \le a + (k+1)\frac{(b-a)}{2^i}.$$

Hence, we obtain

$$c_{ij} = (b-a)\int_a^b \left(f(x,y_1)2^{-i-1} - f(x,y_2)2^{-k-1} \right) h_j(x) dx .$$

Again by using the Mean value theorem,

$$c_{ij} = 2^{-i-1}(b-a)\int_a^b (f(x,y_1) - f(x,y_2)) h_j(x) dx$$

Using Lagrange's Mean value theorem,

$$c_{ij} = 2^{-i-1}(b-a)\int_a^b\left((y_1-y_2)\frac{\partial f(x,y^*)}{\partial y}\right)h_j(x)dx \quad \text{where} \quad y_1 \le y^* \le y_2$$

$$= 2^{-i-1}(b-a)(y_1-y_2)\left(\int_{a+k\left(\frac{b-a}{2^j}\right)}^{a+\left(k+\frac{1}{2}\right)\left(\frac{b-a}{2^j}\right)}\frac{\partial f(x,y^*)}{\partial y}dx - \int_{a+\left(k+\frac{1}{2}\right)\left(\frac{b-a}{2^j}\right)}^{a+(k+1)\left(\frac{b-a}{2^j}\right)}\frac{\partial f(x,y^*)}{\partial y}dx\right)$$

$$= 2^{-i-1}(b-a)(y_1-y_2)\left(2^{-j-1}(b-a)\frac{\partial f}{\partial y}(x_1,y^*) - 2^{-j-1}(b-a)\frac{\partial f}{\partial y}(x_2,y^*)\right).$$

Now, we use the mean value theorem of Integral calculus

$$a+k\frac{(b-a)}{2^j} \le x_1 \le a+\left(k+\frac{1}{2}\right)\frac{(b-a)}{2^j}, \quad a+\left(k+\frac{1}{2}\right)\frac{(b-a)}{2^j} \le x_2 \le a+(k+1)\frac{(b-a)}{2^j}$$

$$c_{ij} \le 2^{-i-j-2}(b-a)^2(y_1-y_2)(x_1-x_2)\frac{\partial^2 f(x^*,y^*)}{\partial x\partial y}.$$

But for $x_1 \le x^* \le x_2$, $(y_1-y_2) \le (b-a)$ and $(x_1-x_2) \le (b-a)$,

We obtain,

$$c_{ij} \le \frac{(b-a)^4}{2^{i+j+2}}M, \quad \text{if} \quad \left|\frac{\partial^2 f(x^*,y^*)}{\partial x\partial y}\right| \le M.$$

Therefore, $c_{ij}'^2 = c_{ij}^2\frac{(b-a)^2}{2^{i+j}} \le \frac{(b-a)^{10}}{2^{3i+3j+4}}M^2$

$$\sum_{n=k}^{\infty}\sum_{m=l}^{\infty}c_{nm}'^2 \le \sum_{n=2^{\alpha+1}}^{\infty}\sum_{m=2^{\beta+1}}^{\infty}\frac{(b-a)^{10}}{2^{3i+3j+4}}M^2, \quad \alpha,\beta = 0,1,2,\ldots$$

$$\le (b-a)^{10}M^2\sum_{n=2^{\alpha+1}}^{\infty}\sum_{i=\beta+1}^{\infty}\sum_{m=2^i}^{2^{i+1}-1}2^{-3i-3j-4}$$

$$\le (b-a)^{10}M^2\sum_{n=2^{\alpha+1}}^{\infty}2^{-3j-4}\sum_{i=\beta+1}^{\infty}(2^{i+1}-1-2^i+1)2^{-3i}$$

$$\le (b-a)^{10}M^2\sum_{n=2^{\alpha+1}}^{\infty}2^{-3j-4}\sum_{i=\beta+1}^{\infty}2^{-2i}$$

$$\le (b-a)^{10}M^2\sum_{n=2^{\alpha+1}}^{\infty}2^{-3j-4}2^{-2(\beta+1)}\frac{1}{\left(1-\frac{1}{2^2}\right)}$$

$$\leq \frac{4(b-a)^{10}}{3l^2} M^2 2^{-4} \sum_{j=\alpha+1}^{\infty} \sum_{n=2^j}^{2^{j+1}-1} 2^{-3j}$$

$$\leq \frac{4(b-a)^{10}}{3l^2} M^2 2^{-4} \sum_{j=\alpha+1}^{\infty} 2^{-2j}$$

$$\leq \frac{4(b-a)^{10}}{3l^2} M^2 2^{-4} \left(\frac{4}{3}\right) 2^{-2(\alpha+1)}$$

$$\leq \left(\frac{16}{9}\right) \frac{(b-a)^{10}}{l^2 k^2} M^2 2^{-4}$$

$$= \left(\frac{16}{144}\right) \frac{(b-a)^{10}}{l^2 k^2} M^2 \quad .65$$

Next, $\displaystyle\sum_{n=k}^{\infty} \sum_{m=0}^{l-1} c_{nm}'^2 \leq \sum_{n=k}^{\infty} \sum_{m=0}^{l-1} \frac{(b-a)^{10} M^2}{2^{3i+3j+4}} \leq \sum_{n=2^{\alpha+1}}^{\infty} \frac{(b-a)^{10} M^2}{2^{3j+4}} \sum_{i=0}^{\beta} \sum_{m=2^i-1}^{2^{i+1}-1} 2^{-3i}$

$$\leq \sum_{n=2^{\alpha+1}}^{\infty} \frac{(b-a)^{10} M^2}{2^{3j+4}} \sum_{i=0}^{\beta} (2^{-2i} + 2^{-3i})$$

$$\leq \left(\frac{52}{21}\right) 2^{-4} (b-a)^{10} M^2 \sum_{j=\alpha+1}^{\infty} \sum_{n=2^j}^{2^{j+1}-1} 2^{-3j}$$

$$\leq \left(\frac{52}{336}\right) (b-a)^{10} M^2 \sum_{j=\alpha+1}^{\infty} 2^{-2j}$$

$$\leq \left(\frac{52}{336}\right) (b-a)^{10} M^2 \left(\frac{2^{-2(\alpha+1)}}{(1-\frac{1}{2^2})}\right)$$

$$= \frac{52(b-a)^{10} M^2}{252 k^2} .$$

Similarly, we have $\displaystyle\sum_{n=0}^{k-1} \sum_{m=l}^{\infty} c_{nm}'^2 \leq \frac{52(b-a)^{10} M^2}{252 l^2} .$

Then

$$\sum_{n=k}^{\infty} \sum_{m=l}^{\infty} c_{nm}'^2 + \sum_{n=k}^{\infty} \sum_{m=0}^{l-1} c_{nm}'^2 + \sum_{n=0}^{k-1} \sum_{m=l}^{\infty} c_{nm}'^2 \leq \left(\frac{16}{144}\right) \frac{(b-a)^{10}}{l^2 k^2} M^2 + \frac{52(b-a)^{10} M^2}{252 k^2} + \frac{52(b-a)^{10} M^2}{252 l^2}.$$

Hence, we obtain $\|f(x,y) - f_{kl}(x,y)\| \leq \frac{(b-a)^{10} M^2}{3} \left(\frac{1}{3l^2 k^2} + \frac{13}{21 k^2} + \frac{13}{21 l^2}\right).$

131

As $l \to \infty$ and $k \to \infty$, we can get $\left\| f(x,y) - f_{kl}(x,y) \right\| \to 0$.

4.11 Conclusion

The numerical solutions of fractional order Burgers-Fisher equation, generalized Fisher's type equation and the time- and space-fractional Fokker-Planck equations have been analyzed in this chapter by utilizing two-dimensional Haar wavelet method. The obtained results are then compared with optimal homotopy asymptotic method (OHAM) solutions, exact solutions and with results available in literature. The Haar wavelet technique provides quite satisfactory results for the fractional order Burgers-Fisher (4.27) and generalized Fisher equations (4.52). The main advantage of this Haar wavelet method is that they transfer the whole scheme into a system of algebraic equations for which the computation is easy and simple. OHAM allows fine tuning of convergence region and rate of convergence by suitably identifying convergence control parameters $C_1, C_2, C_3, \ldots$. It has been observed that for Burgers-Fisher equation OHAM provides more accurate results than the Haar wavelet method as presented in Tables. But in case of generalized Fisher's equation both the methods are competitive. The results obtained by OHAM are slightly more accurate than the results obtained by Haar wavelet method.

The solutions of time- and space-fractional Fokker-Planck equations have been compared with exact solutions as well as results obtained by Adomian decomposition method (ADM), Variational iteration method (VIM) and Operational Tau method (OTM) which are available in open literature. These results have been cited in the tables in order to justify the accuracy and efficiency of the proposed scheme based on two-dimensional Haar wavelet method. It can be noticed that the Haar wavelet technique provides quite satisfactory results in comparison to results obtained by ADM, VIM and OTM [103-105] for the fractional order Fokker-Planck equations as demonstrated in Tables.

CHAPTER 5

5 Application of Legendre Wavelet Methods for Numerical Solution of Fractional Differential Equations

5.1 Introduction

In contemporary years, fractional calculus has become the focus of curiosity for many researchers in exclusive disciplines of applied science and engineering because of the fact that a realistic modelling of a physical phenomenon can be efficiently executed by way of utilizing fractional calculus. For the intent of this chapter, the Caputo's definition of fractional derivative will be used. The advantage of Caputo's approach is that the initial conditions for fractional differential equations with Caputo's derivatives tackle the normal kind as for integer-order differential equations.

The investigation of traveling wave solutions for nonlinear fractional order partial differential equations plays an important role in the study of nonlinear physical phenomena. It is significant to find new solutions, since either new exact solutions or numerical approximate solutions may provide more information for understanding the physical phenomena. In this chapter, the numerical solutions of fractional order partial differential equations comprising Caputo fractional derivative are discussed. The fractional differential equations such as KdV-Burger-Kuramoto (KBK) equation, seventh order KdV (sKdV) equation and Kaup-Kupershmidt (KK) equation have been solved using two-dimensional Legendre wavelet and Legendre multi-wavelet methods.

The main focus of the present chapter is the application of two-dimensional Legendre wavelet technique for solving nonlinear fractional differential equations like time-fractional KBK equation, time-fractional sKdV equation in order to demonstrate the efficiency and accuracy of the proposed wavelet method. Also, the time-fractional Kaup-

Kupershmidt equation has been solved by using two-dimensional Legendre multi-wavelet method. The obtained numerical approximate results of the proposed Legendre wavelet methods are then compared with the exact solutions and those available in literature.

5.2 Outline of Present Study

Consider a nonlinear time-fractional parabolic partial differential equation of the form

$$\frac{\partial^\alpha u}{\partial t^\alpha} = -u \frac{\partial}{\partial x}\left(\frac{2u}{x} - x\right) + u \frac{\partial^2 u}{\partial x^2}, \qquad t > 0, \ x > 0 \tag{5.1}$$

with Dirichlet boundary conditions

$$u(0,t) = 0 \ \text{ and } \ u(1,t) = E_\alpha(t^\alpha),$$

where α is the parameter describing the order of the fractional time derivative and E_α is the Mittag-Leffler function. Fractional diffusion equations like eq. (5.1) arise in continuous time random walks, modelling of anomalous diffusive and sub-diffusive systems, unification of diffusion and wave propagation phenomenon etc. The motivation of the present work is the application of two dimensional Legendre wavelets technique for solving the problem of fractional partial differential equations with Dirichlet boundary conditions. To exhibit the effectiveness, the obtained numerical approximate results of 2D Legendre wavelet technique are compared with that of Haar wavelet method as well as with the exact solution derived by using HPM.

Next, we consider the following time-fractional KdV-Burgers-Kuramoto (KBK) equation [109]

$$\frac{\partial^\alpha u}{\partial t^\alpha} + u \frac{\partial u}{\partial x} - \lambda_1 \frac{\partial^2 u}{\partial x^2} + \lambda_2 \frac{\partial^3 u}{\partial x^3} + \lambda_3 \frac{\partial^4 u}{\partial x^4} = f(x,t), \qquad t > 0, \ x > 0 \tag{5.2}$$

where α is the order of the fractional time derivative and $\lambda_1, \lambda_2, \lambda_3 \geq 0$ are parameters characterizing instability, dispersion and dissipation respectively [110]. The classical KBK equation is an important mathematical model arising in many different physical contexts to describe some physical processes in motion of turbulence and other unstable process systems. It can be also used to describe long waves on a viscous fluid flowing down along an inclined plane [111], unstable drift waves in plasma [112] and turbulent cascade model in a barotropic atmosphere [113].

There are a lot of studies available for the classical KBK equation and some profound results have been established. But according to the best possible information of the authors, the detailed study of the nonlinear fractional order KBK equation is only beginning. Very few mathematical methods such as homotopy analysis method [114], He's variational iteration method and Adomian's decomposition method [115] are available open in literature for the numerical solution of fractional KBK equation.

The KdV type of equations, which were first derived by Korteweg and de Vries (1895) and used to describe weakly nonlinear shallow water waves, have emerged as an important class of nonlinear evolution equation and are often used in practical applications. In reality, the next state of a physical phenomenon might depend not only on its current state but also on its historical states (non-local property), which can be successfully modeled by using the theory of derivatives and integrals of fractional order. The seventh-order KdV (sKdV) equation was first introduced by Pomeau et al. [116] in order to discuss the structural stability of the KdV equation under singular perturbation.

The time-fractional generalized sKdV equation is given by [117]

$$\frac{\partial^\alpha u}{\partial t^\alpha} + \frac{\partial}{\partial x}(g(u)) + \frac{\partial^3 u}{\partial x^3} - \frac{\partial^5 u}{\partial x^5} + \sigma \frac{\partial^7 u}{\partial x^7} = f(x,t), \quad t > 0, \ x > 0 \qquad (5.3)$$

where σ is a constant, α $(0 < \alpha \leq 1)$ is the parameter describing the order of the fractional time derivative and $f(x,t)$ is the forcing term. The sKdV equation arises in fluid flow through porous media, fluid dynamics, plasma physics, optical fibers, elasticity, economics, optimization, hydrodynamic, hydro-magnetic stability, structural, medical imaging, pure and applied sciences [118-120].

Next we consider fractional order Kaup-Kupershmidt equation. Here we compare two different methods, one numerical technique viz. Legendre multiwavelet method and the other analytical technique viz. optimal homotopy asymptotic method (OHAM) for solving fractional order Kaup-Kupershmidt (KK) equation. Two-dimensional Legendre multiwavelet expansion together with operational matrices of fractional integration and derivative of wavelet functions is used to compute the numerical solution of nonlinear time-fractional Kaup-Kupershmidt (KK) equation. The approximate solutions of time fractional Kaup-Kupershmidt equation thus obtained by Legendre multiwavelet method are compared with the exact solutions as well as with optimal homotopy asymptotic method (OHAM).

Consider the following time-fractional Kaup-Kupershmidt equation [121]

$$\frac{\partial^\alpha u}{\partial t^\alpha} + 45u^2 \frac{\partial u}{\partial x} - 15p \frac{\partial u}{\partial x} \frac{\partial^2 u}{\partial x^2} - 15u \frac{\partial^3 u}{\partial x^3} + \frac{\partial^5 u}{\partial x^5} = 0, \qquad t > 0, \ x > 0 \qquad (5.4)$$

Eq. (5.4) is a variation of the following Kaup-Kupershmidt equation [122-125]:

$$u_t + 45u^2 u_x - 15p u_x u_{xx} - 15u u_{xxx} + u_{xxxxx} = 0,$$

Here $0 < \alpha \leq 1$, is the parameter describing the order of the fractional time derivative. The classical Kaup-Kupershmidt equation is an important dispersive equation proposed first by Kaup in 1980 [122] and is developed by Kupershmidt in 1994 [123]. This equation arises in the study of capillary gravity waves. The classical Kaup-Kupershmidt equation is known to be integrable [124] for $p = \frac{5}{2}$ and to have bilinear representations [125], but the explicit form of its *N*-soliton solution is apparently not known. A great deal of research work has been invested in recent years for the study of classical Kaup-Kupershmidt equations. Various methods have been developed independently by which soliton and solitary wave solutions may be obtained for nonlinear evolution equations. Our aim in the present work is to implement two-dimensional Legendre multiwavelet and optimal homotopy asymptotic method in order to exhibit the capabilities of these methods in handling nonlinear equation like fractional order Kaup-Kupershmidt equation.

5.3 Solution of Time-Fractional Parabolic Partial Differential Equation

5.3.1 Application of HPM to Find the Exact Solution of Fractional order Parabolic PDE

Consider a nonlinear time-fractional partial differential equation of the form

$$\frac{\partial^\alpha u}{\partial t^\alpha} = -u \frac{\partial}{\partial x}\left(\frac{2u}{x} - x\right) + u \frac{\partial^2 u}{\partial x^2}, \qquad t > 0, \ x > 0.$$

This implies $\quad \dfrac{\partial^\alpha u}{\partial t^\alpha} = \dfrac{2u^2}{x^2} - \dfrac{2u}{x}\dfrac{\partial u}{\partial x} + u + u \dfrac{\partial^2 u}{\partial x^2}, \quad t > 0, \ x > 0,$ \qquad (5.5)

where $0 < \alpha \leq 1$, subject to the initial condition

$$u(x,0) = x^2 \,. \tag{5.6}$$

To solve eq. (5.5) by homotopy perturbation method [25, 26], we construct the following homotopy:

$$(1-p)\,\frac{\partial^\alpha u}{\partial t^\alpha} + p\left(\frac{\partial^\alpha u}{\partial t^\alpha} - \frac{2u^2}{x^2} + \frac{2u}{x}\frac{\partial u}{\partial x} - u - u\frac{\partial^2 u}{\partial x^2}\right) = 0\,. \tag{5.7}$$

This implies

$$\frac{\partial^\alpha u}{\partial t^\alpha} = p\left(\frac{2u^2}{x^2} - \frac{2u}{x}\frac{\partial u}{\partial x} + u + u\frac{\partial^2 u}{\partial x^2}\right). \tag{5.8}$$

By substituting $u(x,t) = \sum\limits_{n=0}^{\infty} p^n u_n(x,t)$ in eq. (5.8), we get

$$\frac{\partial^\alpha}{\partial t^\alpha}\left(\sum_{n=0}^{\infty} p^n u_n(x,t)\right) = p\left[\frac{2}{x^2}\left(\sum_{n=0}^{\infty} p^n u_n(x,t)\right)^2 - \frac{2}{x}\left(\sum_{n=0}^{\infty} p^n u_n(x,t)\right)\frac{\partial}{\partial x}\left(\sum_{n=0}^{\infty} p^n u_n(x,t)\right)\right.$$
$$\left. + \sum_{n=0}^{\infty} p^n u_n(x,t) + \left(\sum_{n=0}^{\infty} p^n u_n(x,t)\right)\frac{\partial^2}{\partial x^2}\left(\sum_{n=0}^{\infty} p^n u_n(x,t)\right)\right]. \tag{5.9}$$

Collecting the coefficients of different powers of p for eq. (5.9), we have the following equations.

Coefficients of p^0 : $\dfrac{\partial^\alpha u_0}{\partial t^\alpha} = 0\,.$ $\tag{5.10}$

Coefficients of p^1 : $\dfrac{\partial^\alpha u_1}{\partial t^\alpha} = \dfrac{2}{x^2}u_0^2 - \dfrac{2}{x}u_0\dfrac{\partial u_0}{\partial x} + u_0 + u_0\dfrac{\partial^2 u_0}{\partial x^2}\,.$ $\tag{5.11}$

Coefficients of p^2 :

$$\frac{\partial^\alpha u_2}{\partial t^\alpha} = \frac{2}{x^2}(2u_0 u_1) - \frac{2}{x}\left(u_0\frac{\partial u_1}{\partial x} + u_1\frac{\partial u_0}{\partial x}\right) + u_1 + \left(\frac{\partial^2 u_0}{\partial x^2}u_1 + u_0\frac{\partial^2 u_1}{\partial x^2}\right). \tag{5.12}$$

and so on.

By putting $u(x,0) = u_0$ in eqs. (5.10) to (5.12) and solving them, we obtain

$$u_1(x,t) = \frac{x^2 t^\alpha}{\Gamma(1+\alpha)}\,, \tag{5.13}$$

$$u_2(x,t) = \frac{x^2 t^{2\alpha}}{\Gamma(1+2\alpha)}\,, \tag{5.14}$$

and so on.

Finally, the approximate solution for eq. (5.5) is given by

$$u = u_0(x,t) + u_1(x,t) + u_2(x,t) + \dots \tag{5.15}$$

Thus, we have

$$u(x,t) = x^2 + \frac{x^2 t^\alpha}{\Gamma(1+\alpha)} + \frac{x^2 t^{2\alpha}}{\Gamma(1+2\alpha)} + \dots$$

$$= x^2 E_\alpha(t^\alpha), \tag{5.16}$$

where E_α is the Mittag-Leffler function.

Taking $\alpha = 1$ in eq. (5.16), we reproduce the solution of the problem as follows

$$u(x,t) = x^2 \left[1 + \frac{t}{\Gamma(2)} + \frac{t^2}{\Gamma(3)} + \frac{t^3}{\Gamma(4)} + \dots \right].$$

The solution is equivalent to the exact solution in a closed form

$$u(x,t) = x^2 e^t.$$

It is clear that a closed form of solution is obtainable by adding more terms to the homotopy perturbation series.

5.3.2 Application of two-dimensional Haar Wavelet for Numerical Solution of Fractional PDE

To solve the nonlinear fractional PDE considered in eqs. (5.5) and (5.6). Let us divide both

space and time interval [0, 1] into m equal subintervals; each of width $\Delta = \dfrac{1}{m}$.

Haar wavelet solution of $u(x,t)$ is sought by assuming that $\dfrac{\partial^2 u(x,t)}{\partial x^2}$ can be expanded in

terms of Haar wavelets as

$$\frac{\partial^2 u(x,t)}{\partial x^2} = \sum_{i=1}^{m} \sum_{j=1}^{m} c_{ij} h_i(x) h_j(t). \tag{5.17}$$

Integrating eq. (5.17) with respect to x from 0 to x, we get

$$\frac{\partial u(x,t)}{\partial x} - p(t) = \sum_{i=1}^{m} \sum_{j=1}^{m} c_{ij} Q h_i(x) h_j(t). \tag{5.18}$$

Again, integrating eq. (5.18) with respect to x from 0 to x, we get

$$u(x,t) = \sum_{i=1}^{m} \sum_{j=1}^{m} c_{ij} Q^2 h_i(x) h_j(t) + q(t) + x p(t). \tag{5.19}$$

Putting $x = 0$, in eq. (5.19), we get

$$q(t) = u(0,t) = 0 .$$ (5.20)

Putting $x = 1$, in eq. (5.19), we get

$$p(t) = u(1,t) - u(0,t) - \sum_{i=1}^{m}\sum_{j=1}^{m} c_{ij}\left[Q^2 h_i(x)\right]_{x=1} h_j(t)$$

$$= u(1,t) - \sum_{i=1}^{m}\sum_{j=1}^{m} c_{ij}\left[Q^2 h_i(x)\right]_{x=1} h_j(t) .$$ (5.21)

Putting eq. (5.21) in eqs. (5.18) and (5.19), we have

$$\frac{\partial u(x,t)}{\partial x} = \sum_{i=1}^{m}\sum_{j=1}^{m} c_{ij} Q h_i(x)h_j(t) + u(1,t) - \sum_{i=1}^{m}\sum_{j=1}^{m} c_{ij}\left[Q^2 h_i(x)\right]_{x=1} h_j(t) .$$ (5.22)

$$u(x,t) = \sum_{i=1}^{m}\sum_{j=1}^{m} c_{ij} Q^2 h_i(x)h_j(t) + x\left[u(1,t) - \sum_{i=1}^{m}\sum_{j=1}^{m} c_{ij}\left[Q^2 h_i(x)\right]_{x=1} h_j(t)\right] .$$ (5.23)

The nonlinear term presented in eq. (5.5) can be approximated using Haar wavelet function as

$$u\frac{\partial^2 u}{\partial x^2} - u\frac{\partial}{\partial x}\left(\frac{2u}{x}\right) = \sum_{i=1}^{m}\sum_{j=1}^{m} d_{ij} h_i(x)h_j(t) ,$$

which yields

$$u\frac{\partial^2 u}{\partial x^2} + \frac{2u}{x}\left(\frac{u}{x} - \frac{\partial u}{\partial x}\right) = \sum_{i=1}^{m}\sum_{j=1}^{m} d_{ij} h_i(x)h_j(t) .$$ (5.24)

Therefore substituting eqs. (5.17), (5.22) and (5.23) in eq. (5.24), we have

$$\left(\sum_{i=1}^{m}\sum_{j=1}^{m} c_{ij} Q^2 h_i(x)h_j(t) + x\left[u(1,t) - \sum_{i=1}^{m}\sum_{j=1}^{m} c_{ij}\left[Q^2 h_i(x)\right]_{x=1} h_j(t)\right]\right)\left(\sum_{i=1}^{m}\sum_{j=1}^{m} c_{ij} h_i(x)h_j(t)\right)$$

$$+ \frac{2}{x}\left(\sum_{i=1}^{m}\sum_{j=1}^{m} c_{ij} Q^2 h_i(x)h_j(t) + x\left[u(1,t) - \sum_{i=1}^{m}\sum_{j=1}^{m} c_{ij}\left[Q^2 h_i(x)\right]_{x=1} h_j(t)\right]\right) \times$$

$$\left[\frac{1}{x}\left(\sum_{i=1}^{m}\sum_{j=1}^{m} c_{ij} Q^2 h_i(x)h_j(t) + x\left[u(1,t) - \sum_{i=1}^{m}\sum_{j=1}^{m} c_{ij}\left[Q^2 h_i(x)\right]_{x=1} h_j(t)\right]\right) - \right.$$ (5.25)

$$\left.\left(\sum_{i=1}^{m}\sum_{j=1}^{m} c_{ij} Q h_i(x)h_j(t) + u(1,t) - \sum_{i=1}^{m}\sum_{j=1}^{m} c_{ij}\left[Q^2 h_i(x)\right]_{x=1} h_j(t)\right)\right] = \sum_{i=1}^{m}\sum_{j=1}^{m} d_{ij} h_i(x)h_j(t) .$$

Substituting eq. (5.24) in eq. (5.5), we will have

$$\frac{\partial^{\alpha} u}{\partial t^{\alpha}} = \sum_{i=1}^{m}\sum_{j=1}^{m} d_{ij} h_i(x) h_j(t) + u. \tag{5.26}$$

Now applying J^{α} to both sides of eq. (5.26) yields

$$u(x,t) - u(x,0) = J^{\alpha}\left(\sum_{i=1}^{m}\sum_{j=1}^{m} d_{ij} h_i(x) h_j(t) + u\right). \tag{5.27}$$

Substituting eqs. (5.6) and (5.23) in eq. (5.27), we get

$$\sum_{i=1}^{m}\sum_{j=1}^{m} c_{ij} Q^2 h_i(x) h_j(t) + x\left[u(1,t) - \sum_{i=1}^{m}\sum_{j=1}^{m} c_{ij}\left[Q^2 h_i(x)\right]_{x=1} h_j(t)\right] - x^2 =$$

$$\sum_{i=1}^{m}\sum_{j=1}^{m} d_{ij} h_i(x) Q_t^{\alpha} h_j(t) + \left(\sum_{i=1}^{m}\sum_{j=1}^{m} c_{ij} Q^2 h_i(x) Q_t^{\alpha} h_j(t)\right. \tag{5.28}$$

$$\left. + x\left[J^{\alpha} u(1,t) - \sum_{i=1}^{m}\sum_{j=1}^{m} c_{ij}\left[Q^2 h_i(x)\right]_{x=1} Q_t^{\alpha} h_j(t)\right]\right).$$

Now substituting the collocation points $x_l = \dfrac{l-0.5}{m}$ and $t_k = \dfrac{k-0.5}{m}$ for $l,k = 1,2,\ldots,m$ in

eqs. (5.25) and (5.28), we have $2m^2$ equations in $2m^2$ unknowns in c_{ij} and d_{ij}. By solving these system of equations using mathematical software, the Haar wavelet coefficients c_{ij} and d_{ij} can be obtained.

5.3.3 Application of two-dimensional Legendre Wavelet for Solving Fractional PDE

The Legendre wavelet solution of $u(x,t)$ for the nonlinear fractional PDE considered in eqs. (5.5) and (5.6) is sought by assuming that $u(x,t)$ can be expanded in terms of Legendre wavelets as

$$u(x,t) = \sum_{n=1}^{2^{k_1-1}M_1-1}\sum_{i=0}^{2^{k_2-1}}\sum_{l=1}^{M_2-1}\sum_{j=0}^{} c_{n,i,l,j}\, \psi_{n,i,l,j}(x,t), \tag{5.29}$$

where $n = 1,\ldots,2^{k_1-1}, i = 0,\ldots,M_1-1, l = 1,\ldots,2^{k_2-1}, j = 0,\ldots,M_2-1$.

Applying J_t^{α} on both sides of eq. (5.5), we have

$$u(x,t) - u(x,0) = J_t^{\alpha}\left[-u\frac{\partial}{\partial x}\left(\frac{2u}{x} - x\right) + u\frac{\partial^2 u}{\partial x^2}\right].$$

This implies

140

$$u(x,t) - u(x,0) = J_t^\alpha \left[-\left(\sum_{n=1}^{2^{k_1-1}M_1-1} \sum_{i=0}^{2^{k_2-1}M_2-1} \sum_{l=1}^{M_2-1} \sum_{j=0} c_{n,i,l,j} \psi_{n,i,l,j}(x,t) \right) \times \right.$$

$$\frac{\partial}{\partial x} \left(\frac{2}{x} \left(\sum_{n=1}^{2^{k_1-1}M_1-1} \sum_{i=0}^{2^{k_2-1}M_2-1} \sum_{l=1}^{} \sum_{j=0} c_{n,i,l,j} \psi_{n,i,l,j}(x,t) \right) - x \right) + \qquad (5.30)$$

$$\left. \left(\sum_{n=1}^{2^{k_1-1}M_1-1} \sum_{i=0}^{2^{k_2-1}M_2-1} \sum_{l=1}^{} \sum_{j=0} c_{n,i,l,j} \psi_{n,i,l,j}(x,t) \right) \times \frac{\partial^2}{\partial x^2} \left(\sum_{n=1}^{2^{k_1-1}M_1-1} \sum_{i=0}^{2^{k_2-1}M_2-1} \sum_{l=1}^{} \sum_{j=0} c_{n,i,l,j} \psi_{n,i,l,j}(x,t) \right) \right].$$

Now substituting the collocation points $x_l = \dfrac{l-0.5}{2^{k_1-1}M_1}$ and $t_r = \dfrac{r-0.5}{2^{k_2-1}M_2}$ for

$l = 1, 2, ..., 2^{k_1-1}M_1$ and $r = 1, 2, ..., 2^{k_2-1}M_2$ in eq. (5.30), we have $\left(2^{k_1-1}M_1\right)\left(2^{k_2-1}M_2\right)$ equations in $\left(2^{k_1-1}M_1\right)\left(2^{k_2-1}M_2\right)$ unknowns involving $c_{n,i,l,j}$. By solving this system of equations using mathematical software, the Legendre wavelet coefficients $c_{n,i,l,j}$ can be obtained.

5.4   Numerical Results of Fractional Order PDE

The following Tables 5.1-5.3 show the comparison of the absolute errors for fractional order partial differential equation obtained by using Haar wavelet method and Legendre wavelet method at different values of x, t and α. Tables 5.4 and 5.5 respectively show the approximate solutions of fractional order partial differential equation (5.5) obtained by using Haar wavelet method, Legendre wavelet method and Homotopy perturbation method at various points of x and t taking $\alpha = 0.5$ and 0.75. The results thus obtained have been cited in the Tables in order to justify the accuracy and efficiency of the proposed schemes.

Table 5.1   Comparison of absolute errors obtained by Haar wavelet method and Legendre wavelet method for classical order partial differential equation (5.5) at various points of x and t for $\alpha = 1$.

x	$t = 0.2$		$t = 0.4$		$t = 0.6$		$t = 0.8$	
	$\|u_{Exact} - u_{Haar}\|$	$\|u_{Exact} - u_{LW}\|$	$\|u_{Exact} - u_{Haar}\|$	$\|u_{Exact} - u_{LW}\|$	$\|u_{Exact} - u_{Haar}\|$	$\|u_{Exact} - u_{LW}\|$	$\|u_{Exact} - u_{Haar}\|$	$\|u_{Exact} - u_{LW}\|$
0	0	0	0	0	0	0	0	0
0.1	2.14328E-3	3.92494E-8	9.25684E-4	1.09313E-7	9.10577E-4	1.33628E-7	3.57450E-3	1.27536E-7
0.2	3.81027E-3	1.56998E-7	1.64566E-3	4.37251E-7	1.61880E-3	5.34510E-7	6.35467E-3	5.10146E-7
0.3	5.00098E-3	3.53244E-7	2.15993E-3	9.83815E-7	2.12468E-3	1.20265E-6	8.34051E-3	1.14783E-6
0.4	5.71541E-3	6.27990E-7	2.46849E-3	1.74900E-6	2.42821E-3	2.13804E-6	9.53201E-3	2.04058E-6
0.5	5.95355E-3	9.81235E-7	2.57135E-3	2.73282E-6	2.52938E-3	3.34069E-6	9.92917E-3	3.18841E-6
0.6	5.71541E-3	1.41298E-6	2.46849E-3	3.93526E-6	2.42821E-3	4.81059E-6	9.53201E-3	4.59131E-6
0.7	5.00098E-3	1.92322E-6	2.15993E-3	5.35632E-6	2.12468E-3	6.54775E-6	8.34051E-3	6.24929E-6

x								
0.8	3.81027E-3	2.51196E-6	1.64566E-3	6.99601E-6	1.61880E-3	8.55216E-6	6.35467E-3	8.16234E-6
0.9	2.14328E-3	3.17920E-6	9.25684E-4	8.85433E-6	9.10577E-4	1.08238E-5	3.57450E-3	1.03305E-5
1.0	0	6.16414E-6	0	2.46565E-5	0	5.54772E-5	0	9.86262E-5

Table 5.2 Comparison of absolute errors obtained by Haar wavelet method and Legendre wavelet method for fractional order partial differential equation (5.5) at various points of x and t for $\alpha = 0.75$.

x	$t = 0.2$		$t = 0.4$		$t = 0.6$		$t = 0.8$	
	$\lvert u_{Exact} - u_{Haar} \rvert$	$\lvert u_{Exact} - u_{LW} \rvert$	$\lvert u_{Exact} - u_{Haar} \rvert$	$\lvert u_{Exact} - u_{LW} \rvert$	$\lvert u_{Exact} - u_{Haar} \rvert$	$\lvert u_{Exact} - u_{LW} \rvert$	$\lvert u_{Exact} - u_{Haar} \rvert$	$\lvert u_{Exact} - u_{LW} \rvert$
0	0	0	0	0	0	0	0	0
0.1	3.24200E-4	8.05544E-6	1.64793E-3	4.26508E-6	3.90569E-3	1.02880E-5	6.80080E-3	1.20536E-5
0.2	2.90100E-3	3.22218E-5	6.85948E-3	1.70603E-5	1.06992E-2	4.11520E-5	1.53909E-2	4.82144E-5
0.3	8.26860E-3	7.24990E-5	1.34063E-2	3.83857E-5	1.79335E-2	9.25921E-5	2.34600E-2	1.08482E-4
0.4	1.43532E-2	1.28887E-4	1.97217E-2	6.82413E-5	2.41796E-2	1.64608E-4	2.97960E-2	1.92858E-4
0.5	1.97971E-2	2.01386E-4	2.45854E-2	1.06627E-4	2.84360E-2	2.57200E-4	3.36037E-2	3.01340E-4
0.6	2.34026E-2	2.89996E-4	2.70595E-2	1.53543E-4	2.99891E-2	3.70368E-4	3.43426E-2	4.33929E-4
0.7	2.41057E-2	3.94717E-4	2.63927E-2	2.08989E-4	2.82977E-2	5.04113E-4	3.16167E-2	5.90626E-4
0.8	2.09565E-2	5.15548E-4	2.19721E-2	2.72965E-4	2.29403E-2	6.58433E-4	2.51261E-2	7.71430E-4
0.9	1.31498E-2	6.52491E-4	1.33111E-2	3.45472E-4	1.35947E-2	8.33329E-4	1.46467E-2	9.76341E-4
1.0	0	8.05544E-4	0	4.26508E-4	0	0.00102880	0	0.00120536

Table 5.3 Comparison of absolute errors obtained by Haar wavelet method and Legendre wavelet method for fractional order partial differential equation (5.5) at various points of x and t for $\alpha = 0.5$.

x	$t = 0.2$		$t = 0.4$		$t = 0.6$		$t = 0.8$	
	$\lvert u_{Exact} - u_{Haar} \rvert$	$\lvert u_{Exact} - u_{LW} \rvert$	$\lvert u_{Exact} - u_{Haar} \rvert$	$\lvert u_{Exact} - u_{LW} \rvert$	$\lvert u_{Exact} - u_{Haar} \rvert$	$\lvert u_{Exact} - u_{LW} \rvert$	$\lvert u_{Exact} - u_{Haar} \rvert$	$\lvert u_{Exact} - u_{LW} \rvert$
0	0	0	0	0	0	0	0	0
0.1	2.50310E-3	4.50884E-5	4.78710E-3	3.56336E-5	7.30539E-3	5.72330E-5	1.05971E-2	6.74305E-5
0.2	1.15518E-2	1.80354E-4	1.55024E-2	1.42534E-4	1.92456E-2	2.28932E-4	2.41756E-2	2.69722E-4
0.3	2.34904E-2	4.05796E-4	2.80273E-2	3.20702E-4	3.18941E-2	5.15097E-4	3.72663E-2	6.06875E-4
0.4	3.55962E-2	7.21415E-4	3.97116E-2	5.70137E-4	4.29010E-2	9.15729E-4	4.78790E-2	1.07889E-3
0.5	4.55434E-2	1.12721E-3	4.85005E-2	8.90839E-4	5.05414E-2	1.43083E-3	5.46027E-2	1.68576E-3
0.6	5.13466E-2	1.62318E-3	5.27682E-2	1.28281E-3	5.35106E-2	2.06039E-3	5.64007E-2	2.42750E-3
0.7	5.12355E-2	2.20933E-3	5.11514E-2	1.74604E-3	5.07538E-2	2.80442E-3	5.24535E-2	3.30410E-3
0.8	4.35902E-2	2.88566E-3	4.24697E-2	2.28055E-3	4.13874E-2	3.66291E-3	4.20889E-2	4.31555E-3
0.9	2.69659E-2	3.65216E-3	2.57206E-2	2.88632E-3	2.46829E-2	4.63588E-3	2.47617E-2	5.46187E-3
1.0	0	4.50884E-3	0	3.56336E-3	0	5.72330E-3	0	6.74305E-3

Table 5.4 The approximate solutions of fractional order partial differential equation (5.5) using Haar wavelet method, homotopy perturbation method (HPM) and Legendre wavelet method at various points of x and t for $\alpha = 0.5$.

142

x	$t=0.2$			$t=0.4$			$t=0.6$			$t=0.8$		
	u_{Haar}	$u_{Legendre}$	u_{HPM}	u_{Haar}	$u_{Legendre}$	u_{HPM}	u_{Haar}	$u_{Legendre}$	u_{HPM}	u_{Haar}	$u_{Legendre}$	u_{HPM}
0	0	0	0	0	0	0	0	0	0	0	0	0
0.1	0.014717	0.018035	0.017990	0.019705	0.024336	0.024300	0.025527	0.031519	0.03146	0.032853	0.039996	0.03992
0.2	0.060408	0.072141	0.071961	0.075175	0.097344	0.097202	0.092130	0.126077	0.12585	0.113197	0.159983	0.15971
0.3	0.133417	0.162317	0.16191	0.162291	0.219025	0.21870	0.195885	0.283674	0.28316	0.237565	0.359962	0.35935
0.4	0.231021	0.288564	0.28784	0.278404	0.389377	0.38881	0.334440	0.504310	0.50339	0.403966	0.639933	0.63885
0.5	0.350894	0.450882	0.44975	0.421457	0.608402	0.60751	0.506071	0.787984	0.78655	0.610988	0.999895	0.99821
0.6	0.491052	0.649269	0.64765	0.589825	0.876098	0.87482	0.709473	1.134700	1.13264	0.857595	1.439850	1.43742
0.7	0.649723	0.883728	0.88152	0.782146	1.192470	1.19072	0.943592	1.544450	1.54164	1.142970	1.959790	1.95649
0.8	0.825288	1.154260	1.15137	0.997238	1.557510	1.55523	1.207540	2.017240	2.01358	1.466440	2.559730	2.55541
0.9	1.016300	1.460860	1.45720	1.234100	1.971220	1.96833	1.500600	2.553070	2.54843	1.827450	3.239660	3.23420
1.0	1.22140	1.803530	1.79902	1.49182	2.433610	2.43004	1.82212	3.151940	3.14621	2.22554	3.999580	3.99284

Table 5.5 The approximate solutions of fractional order partial differential equation (5.5) using Haar wavelet method, homotopy perturbation method (HPM) and Legendre wavelet method at various points of x and t for $\alpha = 0.75$.

x	$t=0.2$			$t=0.4$			$t=0.6$			$t=0.8$		
	u_{Haar}	$u_{Legendre}$	u_{HPM}	u_{Haar}	$u_{Legendre}$	u_{HPM}	u_{Haar}	$u_{Legendre}$	u_{HPM}	u_{Haar}	$u_{Legendre}$	u_{HPM}
0	0	0	0	0	0	0	0	0	0	0	0	0
0.1	0.01189	0.01406	0.01405	0.01656 6	0.018009	0.018004	0.022127	0.022639	0.022629	0.029096	0.028179	0.028166
0.2	0.05176	0.05622	0.05619	0.066533	0.072035	0.072018	0.083584	0.090558	0.090516	0.104411	0.112715	0.112667
0.3	0.11819	0.12649	0.126422	0.147670	0.162079	0.162041	0.181924	0.203755	0.203662	0.223726	0.253608	0.253500
0.4	0.20978	0.22488	0.22475	0.258414	0.288141	0.288073	0.315719	0.362231	0.362066	0.385888	0.450859	0.450666
0.5	0.32515	0.35137	0.35117	0.397542	0.450221	0.450114	0.483966	0.565986	0.565729	0.589999	0.704468	0.704166
0.6	0.46311	0.50597	0.50568	0.564116	0.648318	0.648164	0.685952	0.815020	0.814649	0.835554	1.014430	1.014000
0.7	0.62259	0.68869	0.68829	0.757387	0.882432	0.882223	0.921136	1.109330	1.108830	1.122 13	1.380760	1.380170
0.8	0.80265	0.89951	0.89899	0.976740	1.152560	1.152290	1.189100	1.448920	1.448270	1.449 47	1.803440	1.802670
0.9	1.00249	1.13844	1.13779	1.221690	1.458710	1.458370	1.489510	1.833790	1.832960	1.817 33	2.282470	2.281500
1.0	1.22140	1.40548	1.40468	1.491820	1.800880	1.800460	1.822120	2.263940	2.262910	2.22554	2.817870	2.816660

5.5 Implementation of Legendre Wavelets for Solving Fractional KBK Equation

Consider the nonlinear time-fractional KBK equation [107]

$$\frac{\partial^{\alpha} u}{\partial t^{\alpha}} + u \frac{\partial u}{\partial x} - \lambda_1 \frac{\partial^2 u}{\partial x^2} + \lambda_2 \frac{\partial^3 u}{\partial x^3} + \lambda_3 \frac{\partial^4 u}{\partial x^4} = f(x,t), \qquad t > 0, \ x > 0 \qquad (5.31)$$

where $0 < \alpha \le 1$, subject to the initial condition $u(x,0) = 0$ and $f(x,t)$ is the forcing term. To show the effectiveness and accuracy of proposed scheme, two test examples have been considered. The numerical solutions thus obtained are compared with the exact solutions.

The Legendre wavelet solution of $u(x,t)$ is sought by assuming that $u(x,t)$ can be expanded in terms of Legendre wavelets as

$$u(x,t) = \sum_{n=1}^{2^{k_1-1}} \sum_{i=0}^{M_1-1} \sum_{l=1}^{2^{k_2-1}} \sum_{j=0}^{M_2-1} c_{n,i,l,j} \, \psi_{n,i,l,j}(x,t), \qquad (5.32)$$

where $n = 1,...,2^{k_1-1}, i = 0,...,M_1-1, \ l = 1,...,2^{k_2-1}, \ j = 0,...,M_2-1$.

The nonlinear term presented in eq. (5.31) can be approximated using Legendre wavelet function as

$$u \frac{\partial u}{\partial x} = \sum_{n=1}^{2^{k_1-1}} \sum_{i=0}^{M_1-1} \sum_{l=1}^{2^{k_2-1}} \sum_{j=0}^{M_2-1} a_{n,i,l,j} \, \psi_{n,i,l,j}(x,t). \qquad (5.33)$$

This implies

$$\left(\sum_{n=1}^{2^{k_1-1}} \sum_{i=0}^{M_1-1} \sum_{l=1}^{2^{k_2-1}} \sum_{j=0}^{M_2-1} c_{n,i,l,j} \, \psi_{n,i,l,j}(x,t) \right) \left[\sum_{n=1}^{2^{k_1-1}} \sum_{i=0}^{M_1-1} \sum_{l=1}^{2^{k_2-1}} \sum_{j=0}^{M_2-1} c_{n,i,l,j} \frac{\partial \psi_{n,i,l,j}(x,t)}{\partial x} \right]$$
$$= \sum_{n=1}^{2^{k_1-1}} \sum_{i=0}^{M_1-1} \sum_{l=1}^{2^{k_2-1}} \sum_{j=0}^{M_2-1} a_{n,i,l,j} \, \psi_{n,i,l,j}(x,t). \qquad (5.34)$$

Again applying J_t^{α} on both sides of eq. (5.31) we have

$$u(x,t) - u(x,0) = J_t^{\alpha} \left[f(x,t) - u \frac{\partial u}{\partial x} + \lambda_1 \frac{\partial^2 u}{\partial x^2} - \lambda_2 \frac{\partial^3 u}{\partial x^3} - \lambda_3 \frac{\partial^4 u}{\partial x^4} \right]. \qquad (5.35)$$

Putting eq. (5.32) and (5.33) in eq. (5.35), we have

$$u(x,t)-u(x,0)= J_t^{\alpha}\left[f(x,t)- \sum_{n=1}^{2^{k_1-1}M_1-1}\sum_{i=0}^{2^{k_2-1}M_2-1}\sum_{l=1}^{2^{k_2-1}M_2-1}\sum_{j=0}^{M_2-1} a_{n,i,l,j}\,\psi_{n,i,l,j}(x,t)\right.$$

$$+\lambda_1\left(\sum_{n=1}^{2^{k_1-1}M_1-1}\sum_{i=0}^{2^{k_2-1}M_2-1}\sum_{l=1}^{2^{k_2-1}M_2-1}\sum_{j=0}^{M_2-1} c_{n,i,l,j}\,\frac{\partial^2\psi_{n,i,l,j}(x,t)}{\partial x^2}\right)$$

$$-\lambda_2\left(\sum_{n=1}^{2^{k_1-1}M_1-1}\sum_{i=0}^{2^{k_2-1}M_2-1}\sum_{l=1}^{2^{k_2-1}M_2-1}\sum_{j=0}^{M_2-1} c_{n,i,l,j}\,\frac{\partial^3\psi_{n,i,l,j}(x,t)}{\partial x^3}\right) \tag{5.36}$$

$$\left.-\lambda_3\left(\sum_{n=1}^{2^{k_1-1}M_1-1}\sum_{i=0}^{2^{k_2-1}M_2-1}\sum_{l=1}^{2^{k_2-1}M_2-1}\sum_{j=0}^{M_2-1} c_{n,i,l,j}\,\frac{\partial^4\psi_{n,i,l,j}(x,t)}{\partial x^4}\right)\right].$$

Now substituting the collocation points $x_l = \dfrac{l-0.5}{2^{k_1-1}M_1}$ and $t_r = \dfrac{r-0.5}{2^{k_2-1}M_2}$ for

$l=1,2,\dots,2^{k_1-1}M_1$ and $r=1,2,\dots,2^{k_2-1}M_2$ in eqs. (5.34) and (5.36), we have

$2\left(2^{k_1-1}M_1\right)\left(2^{k_2-1}M_2\right)$ equations in $2\left(2^{k_1-1}M_1\right)\left(2^{k_2-1}M_2\right)$ unknowns in $a_{n,i,l,j}$ and $c_{n,i,l,j}$.

By solving this system of equations using mathematical software, the Legendre wavelet coefficients $a_{n,i,l,j}$ and $c_{n,i,l,j}$ can be obtained.

Example 5.1 Consider the time-fractional KBK equation (5.31) with the following forcing term

$$f(x,t)=\frac{t^{\alpha}\cos x}{\Gamma(1+\alpha)}-\frac{t^{4\alpha}\cos(x)\sin(x)}{\left(\Gamma(1+2\alpha)\right)^2}+\lambda_1\frac{t^{2\alpha}\cos(x)}{\Gamma(1+2\alpha)}+\lambda_2\frac{t^{2\alpha}\sin(x)}{\Gamma(1+2\alpha)}+\lambda_3\frac{t^{2\alpha}\cos(x)}{\Gamma(1+2\alpha)}. \tag{5.37}$$

The exact solution of eq. (5.31) is given by

$$u(x,t)=\frac{t^{2\alpha}\cos(x)}{\Gamma(1+2\alpha)}. \tag{5.38}$$

In case of example 5.1, Table 5.6 shows the comparison of absolute errors obtained by Legendre wavelet method for eq. (5.31) taking $\lambda_1=\lambda_2=\lambda_3=1$ and $\alpha=1$. Similarly Table 5.7 shows the comparison of absolute errors for eq. (5.31) taking $\alpha=0.75$. Table 5.8 shows the L_2 and L_{∞} errors at different values of α and x. Consequently, it is observed from Tables 5.6-5.8 that the solutions obtained by the present method are in good agreement with the exact results.

Example 5.2 Consider the time-fractional KBK equation (5.31) with the following forcing term

$$f(x,t) = \frac{t^\alpha \sin(x)}{\Gamma(1+\alpha)} + \frac{t^{4\alpha} \cos(x) \sin(x)}{(\Gamma(1+2\alpha))^2} + \lambda_1 \frac{t^{2\alpha} \sin(x)}{\Gamma(1+2\alpha)} - \lambda_2 \frac{t^{2\alpha} \cos(x)}{\Gamma(1+2\alpha)} + \lambda_3 \frac{t^{2\alpha} \sin(x)}{\Gamma(1+2\alpha)}. \quad (5.39)$$

The exact solution of eq. (5.31) is given by

$$u(x,t) = \frac{t^{2\alpha} \sin(x)}{\Gamma(1+2\alpha)}. \quad (5.40)$$

In case of example 5.2, Table 5.9 shows the comparison of absolute errors obtained by Legendre wavelet method for eq. (5.31) taking $\lambda_1 = \lambda_2 = \lambda_3 = 1$ and $\alpha = 1$. Similarly Table 5.10 shows the comparison of absolute errors for eq. (5.31) taking $\alpha = 0.75$. Consequently, it is observed from Tables 5.9 and 5.10 that the solutions obtained by the present method are in good agreement with the exact results.

5.6 Numerical Results and Discussion of Time-Fractional KBK Equation

In order to measure the accuracy of the numerical scheme, L_2 and L_∞ error norms are calculated using the following formulae

$$L_2 = R.M.S.Error = \frac{1}{\sqrt{N}} \sqrt{\sum_{k=1}^{N} \left(\left| u_{approx}(x,t_k) - u_{exact}(x,t_k) \right| \right)^2}, \quad (5.41)$$

$$L_\infty = \max \left| u_{approx}(x,t_k) - u_{exact}(x,t_k) \right|. \quad (5.42)$$

The comparison of absolute errors for time-fractional KBK equation (5.31) given in example 5.1 have been exhibited in Tables 5.6 and 5.7 which are constructed using the results obtained by Legendre wavelet method at different values of x and t taking $\alpha = 1$ and 0.75 respectively. Similarly Tables 5.9 and 5.10 show absolute errors of fractional order KBK equation (5.31) for example 5.2, at various points of x and t taking $\alpha = 1$ and 0.75 respectively. To show the accuracy of proposed method, L_2 and L_∞ error norms for fractional order nonlinear KBK equation given in example 5.1 has been presented in Table 5.8. From Tables 5.6-5.10, one can see a pretty good agreement between the exact solutions and the solutions acquired by two-dimensional Legendre wavelet method.

Table 5.6   Comparison of absolute errors obtained by Legendre wavelet method for KBK equation (5.31) given in example 5.1 at various points of x and t taking $\alpha = 1$.

x	$\left|u_{Exact} - u_{Legendre}\right|$					
	$t = 0$	$t = 0.1$	$t = 0.2$	$t = 0.3$	$t = 0.4$	$t = 0.5$
0.1	6.95349E-6	1.84959E-4	2.90830E-4	9.67277E-5	7.19605E-4	2.50855E-3
0.2	3.73063E-4	2.97674E-4	4.23930E-4	2.76159E-4	5.99905E-4	2.64995E-3
0.3	8.23433E-4	4.25867E-4	5.67587E-4	4.61419E-4	4.94075E-4	2.83828E-3
0.4	1.34267E-3	5.68389E-4	7.19135E-4	6.46241E-4	4.14924E-4	3.09695E-3
0.5	1.92911E-3	7.24113E-4	8.76214E-4	8.25379E-4	3.72850E-4	3.44474E-3
0.6	2.58055E-3	8.91885E-4	1.03672E-3	9.94495E-4	3.75989E-4	3.89591E-3
0.7	3.29387E-3	1.07048E-3	1.19879E-3	1.15008E-3	4.30298E-4	4.46022E-3
0.8	4.06469E-3	1.25857E-3	1.36074E-3	1.28944E-3	5.39558E-4	5.14289E-3
0.9	4.88696E-3	1.45468E-3	1.52113E-3	1.41067E-3	7.05318E-4	5.94439E-3
1.0	5.75262E-3	1.65715E-3	1.67872E-3	1.5127E-3	9.26776E-4	6.86019E-3

Table 5.7   Comparison of absolute errors obtained by Legendre wavelet method for fractional order KBK equation (5.31) given in example 5.1 at various points of x and t taking $\alpha = 0.75$.

x	$\left|u_{Exact} - u_{Legendre}\right|$							
	$t = 0$	$t = 0.1$	$t = 0.2$	$t = 0.3$	$t = 0.4$	$t = 0.5$	$t = 0.6$	$t = 0.7$
0.1	9.99667E-4	2.12737E-4	2.28422E-4	7.56638E-3	1.76708E-2	9.57606E-2	2.20683E-2	1.05767E-2
0.2	9.08162E-4	2.41145E-4	2.65580E-3	9.06168E-3	2.18543E-2	5.85324E-2	2.74249E-2	1.98501E-2
0.3	7.96724E-4	2.86820E-4	3.10412E-3	1.07513E-2	2.64650E-2	1.30486E-2	3.19023E-2	2.75266E-2
0.4	6.65884E-4	3.51375E-4	3.63645E-3	1.26528E-2	3.15340E-2	4.06402E-2	3.56728E-2	3.38164E-2
0.5	8.39996E-4	3.19966E-4	2.78217E-3	8.89023E-3	2.04192E-2	3.80953E-2	7.45291E-3	8.48950E-3
0.6	7.41453E-4	3.22493E-4	2.93705E-3	9.67846E-3	2.29045E-2	6.76929E-2	8.91490E-3	4.26215E-3
0.7	6.31244E-4	3.35989E-4	3.12840E-3	1.05325E-2	2.54926E-2	1.00724E-1	9.53959E-3	1.40098E-3
0.8	5.10374E-4	3.61167E-4	3.36005E-3	1.14623E-2	2.82012E-2	1.36832E-1	9.45691E-3	2.80664E-4
0.9	3.80015E-4	3.98257E-4	3.63348E-3	1.24718E-2	3.10362E-2	1.75597E-1	8.77358E-3	9.43238E-4
1.0	2.41511E-4	4.47018E-4	3.94789E-3	1.35589E-2	3.39907E-2	2.16518E-1	7.57357E-3	7.23009E-4

Table 5.8 L_2 and L_∞ error norms for nonlinear time-fractional KBK equation (5.31) given in example 5.1 using two-dimensional Legendre wavelet method at various points of x.

x	$\alpha = 1$		$\alpha = 0.75$	
	L_2	L_∞	L_2	L_∞
0.1	1.07540E-3	2.50855E-3	3.56012E-2	9.57606E-2
0.2	1.14498E-3	2.64995E-3	2.53472E-2	5.85324E-2
0.3	1.27112E-3	2.83828E-3	1.86148E-2	3.19023E-2
0.4	1.46195E-3	3.09695E-3	2.55832E-2	4.06402E-2
0.5	1.71756E-3	3.44474E-3	1.61377E-2	3.80953E-2
0.6	2.03462E-3	3.89591E-3	2.75358E-2	6.76929E-2
0.7	2.40950E-3	4.46022E-3	3.70968E-2	1.00724E-1
0.8	2.83903E-3	5.14289E-3	4.96876E-2	1.36832E-1
0.9	3.32003E-3	5.94439E-3	6.32895E-2	1.75597E-1
1.0	3.84851E-3	6.86019E-3	7.76957E-2	2.16518E-1

Table 5.9   Comparison of absolute errors obtained by Legendre wavelet method for fractional order KBK equation (5.31) given in example 5.2 at various points of *x* and *t* taking $\alpha = 1$.

x	$\left|u_{Exact} - u_{Legendre}\right|$						
	$t = 0$	$t = 0.1$	$t = 0.2$	$t = 0.3$	$t = 0.4$	$t = 0.5$	$t = 0.6$
0.1	4.98657E-5	5.68684E-5	1.28221E-4	4.93990E-4	1.48989E-3	3.49306E-3	6.95761E-3
0.2	1.04370E-4	5.39855E-5	1.19191E-4	4.39997E-4	1.31699E-3	3.07391E-3	6.12894E-3
0.3	1.69932E-4	4.85989E-5	1.04660E-4	3.69101E-4	1.10257E-3	2.56670E-3	5.13534E-3
0.4	2.46500E-4	4.05274E-5	8.31235E-5	2.76311E-4	8.35246E-4	1.95025E-3	3.94182E-3
0.5	3.34173E-4	2.95642E-5	5.30284E-5	1.56464E-4	5.03251E-4	1.20250E-3	2.51167E-3
0.6	4.33146E-4	1.54809E-5	1.27887E-5	4.30468E-6	9.45733E-5	3.00882E-4	8.06986E-4
0.7	5.43658E-4	1.96621E-6	3.91878E-5	1.85428E-4	4.02820E-4	7.77358E-4	1.21073E-3
0.8	6.65935E-4	2.30271E-5	1.04464E-4	4.17885E-4	1.00074E-3	2.05467E-3	3.57988E-3
0.9	8.00141E-4	4.79469E-5	1.84526E-4	6.97968E-4	1.71050E-3	3.55273E-3	6.33795E-3
1.0	9.46323E-4	7.69510E-5	2.80724E-4	1.03017E-3	2.54254E-3	5.29182E-3	9.52067E-3

Table 5.10   Comparison of absolute errors obtained by Legendre wavelet method for fractional order KBK equation (5.31) given in example 5.2 at various points of *x* and *t* taking $\alpha = 0.75$.

x	$\left|u_{Exact} - u_{Legendre}\right|$							
	$t = 0.05$	$t = 0.1$	$t = 0.15$	$t = 0.2$	$t = 0.25$	$t = 0.3$	$t = 0.35$	$t = 0.4$
0.1	2.27075E-5	2.46815E-4	7.82738E-4	1.72484E-3	3.10534E-3	4.90591E-3	7.05637E-3	9.42941E-3
0.2	2.61128E-5	2.14264E-4	6.52493E-4	1.40683E-3	2.46587E-3	3.76612E-3	5.19167E-3	6.56591E-3
0.3	2.80289E-5	1.72666E-4	4.94899E-4	1.02750E-3	1.71007E-3	2.42812E-3	3.01363E-3	3.23418E-3
0.4	2.78829E-5	1.19612E-4	3.04250E-4	5.76276E-4	8.21037E-4	8.67143E-4	4.88257E-4	6.10355E-4
0.5	3.15224E-5	1.14364E-4	3.08178E-4	6.41627E-4	1.04190E-3	1.40877E-3	1.62634E-3	1.55604E-3
0.6	3.54238E-5	8.08914E-5	1.61045E-4	2.66399E-4	2.74380E-4	3.61691E-4	6.09843E-4	1.84669E-3
0.7	3.64308E-5	3.35835E-5	2.33063E-5	1.85579E-4	6.28651E-4	1.55294E-3	3.16851E-3	5.70490E-3
0.8	3.38764E-5	3.04752E-5	2.51819E-4	7.27157E-4	1.68784E-3	3.38895E-3	6.09183E-3	1.00748E-2
0.9	2.71227E-5	1.14065E-4	5.31069E-4	1.37042E-3	2.92247E-3	5.49997E-3	9.41849E-3	1.50075E-2
1.0	1.55712E-5	2.19782E-4	8.67153E-4	2.12648E-3	4.35005E-3	7.91130E-3	1.31829E-2	2.05479E-2

5.7 Application of Analytical and Numerical Methods for Solving Time-Fractional sKdV Equation

5.7.1 Implementation of Legendre Wavelet Method for Numerical Solution of Fractional sKdV Equation

To show the effectiveness and accuracy of proposed scheme, we consider two test examples. The numerical solutions thus obtained are compared with the exact solutions and solutions obtained by HAM.

Consider the nonlinear time-fractional generalized sKdV equation [117]

$$\frac{\partial^{\alpha} u}{\partial t^{\alpha}} + u\frac{\partial u}{\partial x} + \frac{\partial^3 u}{\partial x^3} - \frac{\partial^5 u}{\partial x^5} + \sigma\frac{\partial^7 u}{\partial x^7} = f(x,t), \qquad 0 < \alpha \le 1 \tag{5.43}$$

with initial condition $u(x,t_0) = g(x)$.

The Legendre wavelet solution of $u(x,t)$ is sought by assuming that $u(x,t)$ can be expanded in terms of Legendre wavelet as

$$u(x,t) = \sum_{n=1}^{2^{k_1-1}} \sum_{i=0}^{M_1-1} \sum_{l=1}^{2^{k_2-1}} \sum_{j=0}^{M_2-1} c_{n,i,l,j}\, \psi_{n,i,l,j}(x,t), \tag{5.44}$$

where $n = 1,...,2^{k_1-1}, i = 0,...,M_1-1, l = 1,...,2^{k_2-1}, j = 0,...,M_2-1$.

The nonlinear term presented in eq. (5.43) can be approximated using Legendre wavelet function as

$$u\frac{\partial u}{\partial x} = \sum_{n=1}^{2^{k_1-1}} \sum_{i=0}^{M_1-1} \sum_{l=1}^{2^{k_2-1}} \sum_{j=0}^{M_2-1} a_{n,i,l,j}\, \psi_{n,i,l,j}(x,t). \tag{5.45}$$

This implies

$$\left(\sum_{n=1}^{2^{k_1-1}} \sum_{i=0}^{M_1-1} \sum_{l=1}^{2^{k_2-1}} \sum_{j=0}^{M_2-1} c_{n,i,l,j}\, \psi_{n,i,l,j}(x,t)\right)\left[\sum_{n=1}^{2^{k_1-1}} \sum_{i=0}^{M_1-1} \sum_{l=1}^{2^{k_2-1}} \sum_{j=0}^{M_2-1} c_{n,i,l,j}\, \frac{\partial \psi_{n,i,l,j}(x,t)}{\partial x}\right]$$
$$= \sum_{n=1}^{2^{k_1-1}} \sum_{i=0}^{M_1-1} \sum_{l=1}^{2^{k_2-1}} \sum_{j=0}^{M_2-1} a_{n,i,l,j}\, \psi_{n,i,l,j}(x,t). \tag{5.46}$$

Again applying J_t^{α} on both sides of eq. (5.43) we have

$$u(x,t) - u(x,0) = J_t^\alpha \left[f(x,t) - u\frac{\partial u}{\partial x} - \frac{\partial^3 u}{\partial x^3} + \frac{\partial^5 u}{\partial x^5} - \sigma\frac{\partial^7 u}{\partial x^7} \right]. \tag{5.47}$$

Putting eqs. (5.44) and (5.45) in eq. (5.47), we have

$$\sum_{n=1}^{2^{k_1-1}M_1-1} \sum_{i=0}^{2^{k_2-1}} \sum_{l=1}^{M_2-1} \sum_{j=0} c_{n,i,l,j}\,\psi_{n,i,l,j}(x,t) - u(x,0) = J_t^\alpha \Big[f(x,t) -$$

$$\sum_{n=1}^{2^{k_1-1}M_1-1} \sum_{i=0}^{2^{k_2-1}} \sum_{l=1}^{M_2-1} \sum_{j=0} a_{n,i,l,j}\psi_{n,i,l,j}(x,t) - \sum_{n=1}^{2^{k_1-1}M_1-1} \sum_{i=0}^{2^{k_2-1}} \sum_{l=1}^{M_2-1} \sum_{j=0} c_{n,i,l,j} \frac{\partial^3}{\partial x^3}\psi_{n,i,l,j}(x,t) + \tag{5.48}$$

$$\sum_{n=1}^{2^{k_1-1}M_1-1} \sum_{i=0}^{2^{k_2-1}} \sum_{l=1}^{M_2-1} \sum_{j=0} c_{n,i,l,j} \frac{\partial^5}{\partial x^5}\psi_{n,i,l,j}(x,t) - \sigma\sum_{n=1}^{2^{k_1-1}M_1-1} \sum_{i=0}^{2^{k_2-1}} \sum_{l=1}^{M_2-1} \sum_{j=0} c_{n,i,l,j} \frac{\partial^7}{\partial x^7}\psi_{n,i,l,j}(x,t) \Big]$$

Now substituting the collocation points $x_l = \dfrac{l-0.5}{2^{k_1-1}M_1}$ and $t_r = \dfrac{r-0.5}{2^{k_2-1}M_2}$ for

$l = 1,2,\dots,2^{k_1-1}M_1$ and $r = 1,2,\dots,2^{k_2-1}M_2$ in eqs. (5.46) and (5.48), we have $2\big(2^{k_1-1}M_1\big)\big(2^{k_2-1}M_2\big)$ equations in $2\big(2^{k_1-1}M_1\big)\big(2^{k_2-1}M_2\big)$ unknowns in $a_{n,i,l,j}$ and $c_{n,i,l,j}$. By solving this system of equations using mathematical software, the Legendre wavelet coefficients $a_{n,i,l,j}$ and $c_{n,i,l,j}$ can be obtained.

5.7.2 Comparison with HAM for Solution of Time Fractional sKdV Equation

Consider the nonlinear time-fractional generalized sKdV equation [117]

$$\frac{\partial^\alpha u}{\partial t^\alpha} + u\frac{\partial u}{\partial x} + \frac{\partial^3 u}{\partial x^3} - \frac{\partial^5 u}{\partial x^5} + \sigma\frac{\partial^7 u}{\partial x^7} = 0,\ 0 < \alpha \le 1, \tag{5.49}$$

subject to the initial condition [120]

$$u(x,0) = a_0 + a_6 \sec h^6(kx),$$

where $k = \dfrac{5}{\sqrt{1538}}$, $a_0 = c - \dfrac{18000}{769^2}$, $a_6 = \dfrac{519750}{769^2}$ and c is an arbitrary parameter.

To obtain the approximate solution of the time-fractional sKdV equation (5.49), we choose the linear operator

$$\mathscr{L}[\phi(x,t;p)] = D_t^\alpha \phi(x,t;p). \tag{5.50}$$

Let us construct the m- th order deformation equation for eq. (5.49) as follows

$$\mathscr{L}\left[u_m(x,t) - \chi_m u_{m-1}(x,t)\right] = \hbar \mathfrak{R}_m\left(u_0, u_1, \ldots, u_{m-1}\right), \tag{5.51}$$

where $\mathfrak{R}_m\left(u_0, u_1, \ldots, u_{m-1}\right) = \dfrac{1}{(m-1)!} \dfrac{\partial^{m-1} \mathscr{N}\left[\phi(x,t;p)\right]}{\partial p^{m-1}}\Bigg|_{p=0}$, \tag{5.52}

$$\mathscr{N}\left[\phi(x,t;p)\right] = D_t^\alpha \phi(x,t;p) + \phi(x,t;p)\frac{\partial \phi(x,t;p)}{\partial x} + \frac{\partial^3 \phi(x,t;p)}{\partial x^3} - \frac{\partial^5 \phi(x,t;p)}{\partial x^5} + \sigma \frac{\partial^7 \phi(x,t;p)}{\partial x^7},$$

auxiliary function $H(x,t) = 1$,

and $\phi(x,t;p) = u_0(x,t) + \sum\limits_{m=1}^{\infty} p^m u_m(x,t)$,

$$u_m(x,t) = \frac{1}{m!} \frac{\partial^m \phi(x,t;p)}{\partial p^m}\Bigg|_{p=0}.$$

Now, the solution of the first deformation equation of eq. (5.51) is given by

$$u_1(x,t) = \hbar J_t^\alpha \left[\frac{\partial^\alpha u_0}{\partial t^\alpha} + u_0 \frac{\partial u_0}{\partial x} + \frac{\partial^3 u_0}{\partial x^3} - \frac{\partial^5 u_0}{\partial x^5} + \sigma \frac{\partial^7 u_0}{\partial x^7}\right]. \tag{5.53}$$

Similarly, the solutions of second and third order deformation equations are

$$u_2(x,t) = u_1(x,t) + \hbar J_t^\alpha \left[\frac{\partial^\alpha u_1}{\partial t^\alpha} + u_0 \frac{\partial u_1}{\partial x} + u_1 \frac{\partial u_0}{\partial x} + \frac{\partial^3 u_1}{\partial x^3} - \frac{\partial^5 u_1}{\partial x^5} + \sigma \frac{\partial^7 u_1}{\partial x^7}\right], \tag{5.54}$$

$$u_3(x,t) = u_2(x,t) + \hbar J_t^\alpha \left[\frac{\partial^\alpha u_2}{\partial t^\alpha} + u_0 \frac{\partial u_2}{\partial x} + u_1 \frac{\partial u_1}{\partial x} + u_2 \frac{\partial u_0}{\partial x} + \frac{\partial^3 u_2}{\partial x^3} - \frac{\partial^5 u_2}{\partial x^5} + \sigma \frac{\partial^7 u_2}{\partial x^7}\right]. \tag{5.55}$$

By putting the initial condition $u_0 = u(x,0)$ in eqs. (5.53)- (5.55) and solving them, we obtain the expressions for u_1, u_2, u_3.

Finally, the approximate solution for time fractional seventh order KdV equation is given by

$$u = u_1(x,t) + u_2(x,t) + u_3(x,t) + \ldots \tag{5.56}$$

Example 5.3 Consider nonlinear time-fractional generalized sKdV equation (5.49) subject to the following initial condition $u(x,0) = 0$ and the forcing term

$$f(x,t) = \frac{t^\alpha \cos(x)}{\Gamma(1+\alpha)} - \frac{t^{4\alpha} \sin(x)\cos(x)}{\left(\Gamma(1+2\alpha)\right)^2} + \frac{3t^{2\alpha} \sin(x)}{\Gamma(1+2\alpha)}, \tag{5.57}$$

The exact solution of eq. (5.49) is given by

$$u(x,t) = \frac{t^{2\alpha} \cos(x)}{\Gamma(1+2\alpha)}.$$

The numerical solutions of the example 5.3 are presented for $\sigma = 1$ in Tables 5.11 and 5.12. The results are compared with the exact solutions. It has been observed from Tables 5.11 and 5.12 that the solutions obtained by present method are in good agreement with that of exact solutions.

Example 5.4 Consider nonlinear homogeneous time-fractional sKdV equation (5.49) subject to the following initial condition [120]

$$u(x,0) = a_0 + a_6 \sec h^6(kx), \qquad (5.58)$$

where $k = \dfrac{5}{\sqrt{1538}}$, $a_0 = c - \dfrac{18000}{769^2}$, $a_6 = \dfrac{519750}{769^2}$ and c is an arbitrary parameter.

The numerical solutions of the example 5.4 are presented for $\sigma = 0.01$ in Table 5.13 and 5.14. The results are compared with the exact solutions as well as solutions obtained by HAM. It has been observed from Tables 5.13 and 5.14 that the solutions obtained by present method are in good agreement with the exact solutions and the solutions obtained by HAM.

5.8 Numerical Results and Discussion of Time-Fractional sKdV Equation

The comparison of the L_2 and L_∞ error norms for time-fractional sKdV equation (5.49) given in example 5.3 and 5.4 have been exhibited in Tables 5.11 and 5.14 which are constructed using the results obtained by Legendre wavelet method at different values of t taking $M = 6, 8$ and 4 when $\alpha = 1$. Tables 5.12 and 5.13 show the absolute errors of time-fractional sKdV equation (5.49) for example 5.3 at various points of x and t taking $\alpha = 0.75, 0.9$ and 0.85 respectively. Similarly Tables 5.15 illustrates the absolute errors of fractional order sKdV equation (5.49) for example 5.4, at various points of x and t taking $\alpha = 0.75$. Agreement between present numerical results and exact solutions appears very satisfactory through illustration in Tables 5.11 to 5.15. To show the accuracy of proposed method, L_2 and L_∞ error norms for classical order nonlinear sKdV equation given in examples 5.3 and 5.4, have been presented in Tables 5.16. Again to examine the accuracy and reliability of the Legendre wavelets for solving fractional order sKdV equation, we compare the approximate solution of Legendre wavelet with the 4th order approximate solution obtained by HAM taking $\hbar = -1.45$. As pointed out by Liao [33] in general, by

means of the so-called $\hbar$-curve, it is straight forward to choose a proper value of $\hbar$ which ensures the convergence of series solution. To investigate the influence of $\hbar$ on the solution series, we plot $\hbar$-curve of partial derivatives of $u(x,t)$ obtained from the 4$^{\text{th}}$ order HAM solution as shown in Figure 5.1.
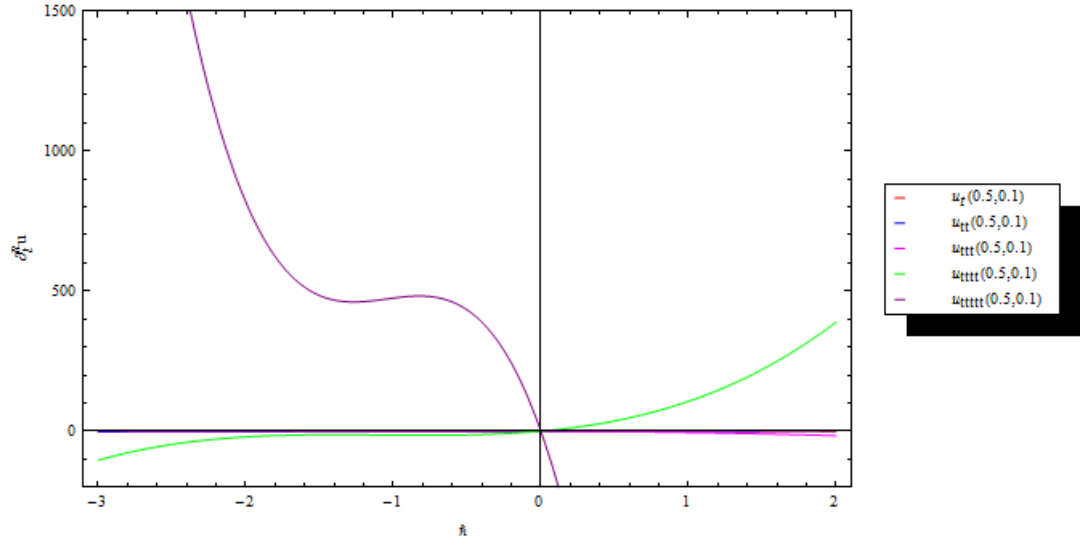
Figure 5.1   The $\hbar$-curve for partial derivatives of $u(x,t)$ for the 4$^{\text{th}}$ order HAM solution taking $x = 0.5, t = 0.1$ and $\alpha = 0.75.$

Table 5.11   Comparison of L_2 and L_∞ error norms obtained by two-dimensional Legendre wavelet method for nonlinear sKdV equation (5.49) given in example 5.3 at various points t taking $M = 6$ and 8 when $\alpha = 1$.

t	$M = 8, k = 2$		$M = 6, k = 2$	
	L_2	L_∞	L_2	L_∞
0.05	9.16437E-6	5.3919E-6	4.18475E-5	2.13437E-5
0.10	1.01505E-4	5.5779E-5	3.62294E-4	1.82466E-4
0.15	4.68588E-4	2.3893E-4	1.31216E-3	6.41485E-4
0.20	1.43992E-3	6.9125E-4	3.34637E-3	1.58899E-3
0.25	3.50308E-3	1.6015E-3	7.00733E-3	3.23727E-3
0.30	7.34409E-3	3.2189E-3	1.29496E-2	5.83178E-3
0.35	1.39175E-2	5.8669E-3	2.19626E-2	9.66262E-3
0.40	2.45602E-2	9.9599E-3	3.49928E-2	1.50760E-2
0.45	4.11652E-2	1.6021E-2	5.31644E-2	2.24858E-2

0.50	4.86290E-2	2.6175E-2	8.00433E-2	3.34444E-2

Table 5.12   Comparison of approximate solutions obtained by two-dimensional Legendre wavelet method for fractional order nonlinear sKdV equation (5.49) given in example 5.3 at various points of x and t taking $\alpha = 0.75$.

x	$|u_{Exact} - u_{LW}|$					
	$t = 0.05$	$t = 0.1$	$t = 0.15$	$t = 0.2$	$t = 0.25$	$t = 0.3$
0.1	1.48844E-3	1.02439E-3	1.34522E-3	6.84404E-3	1.65336E-2	3.16301E-2
0.2	1.44428E-3	8.04932E-4	1.87684E-3	7.87671E-3	1.83517E-2	3.47030E-2
0.3	1.38657E-3	5.78750E-4	2.38982E-3	8.83756E-3	2.00105E-2	0.37488E-2
0.4	1.31595E-3	3.49808E-4	2.87396E-3	9.70634E-3	2.14745E-2	3.99294E-2
0.5	3.14870E-3	5.32314E-3	8.43096E-3	1.46331E-2	2.77386E-2	5.23307E-2
0.6	3.56192E-3	5.91560E-3	9.27444E-3	1.57778E-2	2.93468E-2	5.46608E-2
0.7	3.94745E-3	6.45309E-3	1.00217E-2	1.67499E-2	3.06354E-2	5.64109E-2
0.8	4.30041E-3	6.92704E-3	1.06584E-2	1.75272E-2	3.15695E-2	5.75265E-2
0.9	4.61606E-3	7.32937E-3	1.11714E-2	1.80894E-2	3.21175E-2	5.79590E-2
1	4.88988E-3	7.65262E-3	1.15487E-2	1.84184E-2	3.22520E-2	5.76668E-2

Table 5.13   Absolute errors obtained by two-dimensional Legendre wavelet method for fractional order nonlinear sKdV equation (5.49) given in example 5.3 at various points of x and t taking $\alpha = 0.9$ and 0.85.

x	$|u_{Exact} - u_{LW}|$									
	$\alpha = 0.9$					$\alpha = 0.85$				
	$t = 0.05$	$t = 0.1$	$t = 0.15$	$t = 0.2$	$t = 0.25$	$t = 0.05$	$t = 0.1$	$t = 0.15$	$t = 0.2$	$t = 0.25$
0.1	1.9246E-2	1.3604E-2	4.4142E-3	3.8954E-2	7.4497E-2	6.9542E-4	7.6950E-3	1.5974E-2	2.5318E-2	3.8521E-2
0.2	1.7746E-2	1.2199E-2	5.2290E-3	3.9733E-2	7.7033E-2	7.1046E-5	1.0510E-2	1.8741E-2	2.8015E-2	4.4560E-2
0.3	1.6012E-2	1.0617E-2	6.0247E-3	4.0160E-2	7.8958E-2	5.7288E-4	1.3190E-2	2.1255E-2	3.0330E-2	5.0048E-2
0.4	1.4047E-2	8.8587E-3	6.7945E-3	4.0212E-2	8.0217E-2	1.2304E-3	1.5746E-2	2.3537E-2	3.2285E-2	5.5001E-2
0.5	1.1856E-2	6.9277E-3	7.5331E-3	3.9867E-2	8.0759E-2	2.1161E-3	6.6038E-3	2.9885E-3	2.1245E-2	3.8269E-2
0.6	9.4467E-3	4.8277E-3	8.2358E-3	3.9110E-2	8.0539E-2	3.1420E-4	6.6306E-5	1.1018E-2	2.9948E-2	5.0558E-2
0.7	6.8278E-3	2.5638E-3	8.8993E-3	3.7927E-2	7.9514E-2	1.4167E-3	6.3441E-3	1.8809E-2	3.8240E-2	6.2237E-2
0.8	4.0113E-3	1.4338E-4	9.5203E-3	3.6306E-2	7.7648E-2	3.1190E-3	1.2661E-2	2.6382E-2	4.6132E-2	7.3303E-2
0.9	1.0121E-3	2.4241E-3	1.0096E-2	3.4243E-2	7.4911E-2	4.7975E-3	1.8884E-2	3.3728E-2	5.3601E-2	8.3721E-2
1	2.1510E-3	5.1261E-3	1.0624E-2	3.1738E-2	7.1281E-2	6.4193E-3	2.4976E-2	4.0805E-2	6.0597E-2	9.3426E-2

Table 5.14 Comparison of L_2 and L_∞ error norms obtained by two-dimensional Legendre wavelet method for nonlinear sKdV equation (5.49) given in example 5.4 at various points t taking $M = 4$ and 8 when $\alpha = 1$.

t	$M = 8, k = 1$		$M = 4, k = 1$	
	L_2	L_∞	L_2	L_∞
0	1.13870E-5	4.68205E-6	6.44281E-5	3.33213E-5
0.1	5.72636E-3	2.66655E-3	9.28479E-3	5.07039E-3
0.2	1.27713E-2	5.63322E-3	1.78148E-2	9.90263E-3
0.3	2.15239E-2	9.08072E-3	2.55958E-2	1.44389E-2
0.4	3.23356E-2	1.32161E-2	3.26941E-2	1.86549E-2
0.5	4.55238E-2	1.82721E-2	3.91898E-2	2.25262E-2
0.6	6.13666E-2	2.45038E-2	4.51782E-2	2.60282E-2
0.7	8.35997E-2	3.85932E-2	5.07729E-2	2.91367E-2

Table 5.15 Comparison of approximate solutions obtained by two-dimensional Legendre wavelet method and homotopy analysis method for fractional order nonlinear sKdV equation (5.49) given in example 5.4 at various points of x and t taking $\hbar = -1.45$ and $\alpha = 0.75$.

x	$t = 0.1$		$t = 0.2$		$t = 0.3$		$t = 0.4$		$t = 0.5$	
	$u_{Legendre}$	u_{HAM}	$u_{Legendre}$	u_{HAM}	$u_{Legendre}$	u_{HAM}	$u_{Legendre}$	u_{HAM}	$u_{Legendre}$	u_{HAM}
0.1	0.875221	0.878962	0.877833	0.878771	0.880844	0.877951	0.884388	0.876460	0.888389	0.874258
0.2	0.872626	0.878151	0.874683	0.877764	0.877135	0.876133	0.880292	0.873178	0.884275	0.868821
0.3	0.869184	0.876495	0.870688	0.875954	0.872539	0.873596	0.875166	0.869306	0.878919	0.862975
0.4	0.864923	0.874003	0.865885	0.873369	0.867102	0.870405	0.869065	0.864971	0.872379	0.856928
0.5	0.859870	0.870687	0.860309	0.870036	0.860870	0.866623	0.862047	0.860286	0.864719	0.850864
0.6	0.854057	0.866560	0.854000	0.865984	0.853892	0.862302	0.854172	0.855343	0.856005	0.844932
0.7	0.847514	0.861637	0.846994	0.861234	0.846217	0.857483	0.845500	0.850213	0.846308	0.839240
0.8	0.840276	0.855935	0.839334	0.855810	0.837896	0.852198	0.836095	0.844940	0.835701	0.833856
0.9	0.832376	0.849472	0.831059	0.849727	0.828980	0.846463	0.826023	0.839545	0.824260	0.828801
1.0	0.823849	0.842268	0.822212	0.842999	0.819522	0.840286	0.815349	0.834021	0.812067	0.824053

Table 5.16 L_2 and L_∞ error norm for nonlinear time-fractional sKdV equation using two-dimensional Legendre wavelet methods at various points t taking $\alpha = 1$.

t	Example 5.3		Example 5.4	
	L_2	L_∞	L_2	L_∞
0.1	3.20987E-5	5.5779E-5	1.81083E-3	2.66655E-3
0.2	4.55341E-4	6.9125E-4	4.03863E-3	5.63322E-3
0.3	2.32241E-3	3.2189E-3	6.80646E-3	9.08072E-3
0.4	7.76660E-3	9.1236E-3	1.02254E-2	1.32161E-2
0.5	1.53778E-2	2.6175E-2	1.43959E-2	1.82721E-2

The percentage errors of sKdV equation (5.49) for example 5.4 has been shown in Table 5.17 at various points of x and t. Comparison of approximate solutions obtained by two-dimensional Legendre wavelet method, homotopy analysis method and optimal homotopy analysis method for fractional order nonlinear sKdV equation (5.49) have been demonstrated in Table 5.18 taking $\alpha = 0.75$. Agreement between present numerical results and exact solutions appears very satisfactory through illustration in Tables 5.11-5.18.

Table 5.17   Percentage errors obtained by two-dimensional Legendre wavelet method for classical nonlinear sKdV equation (5.49) given in example 5.4 at various points of x and t for $\alpha = 1$.

x	$\left| u_{Exact} - u_{LW} \right|$			
	$t = 0$	$t = 0.1$	$t = 0.2$	$t = 0.3$
0.1	3.60870E-4	6.36455E-2	1.88943E-1	3.73007E-1
0.2	4.48452E-4	9.41269E-2	2.50788E-1	4.70472E-1
0.3	5.07751E-4	1.24566E-1	3.11652E-1	5.64999E-1
0.4	5.36868E-4	1.54740E-1	3.71078E-1	6.55872E-1
0.5	5.33951E-4	1.84430E-1	4.28610E-1	7.42358E-1
0.6	4.97215E-4	2.13419E-1	4.83794E-1	8.23722E-1
0.7	4.24966E-4	2.41502E-1	5.36188E-1	8.99238E-1
0.8	3.15643E-4	2.68483E-1	5.85363E-1	9.68192E-1
0.9	1.67864E-4	2.94177E-1	6.30919E-1	1.02990
1.0	1.94903E-4	3.18421E-1	6.72482E-1	1.08372

Table 5.18   Comparison of approximate solutions obtained by two-dimensional Legendre wavelet method, homotopy analysis method and optimal homotopy analysis method for fractional order nonlinear sKdV equation (5.49) given in example 5.4 at various points of x and t taking $\alpha = 0.75$.

x	$t=0.1$			$t=0.2$			$t=0.3$			$t=0.4$			$t=0.5$		
	$u_{Legendre}$	u_{HAM}	$u_{OptimalHAM}$	$u_{Legendre}$	u_{HAM}	$u_{Optimal}$	$u_{Legendre}$	u_{HAM}	$u_{Optimal}$	$u_{Legendre}$	u_{HAM}	$u_{Optimal}$	$u_{Legendre}$	u_{HAM}	$u_{Optimal}$
0.1	0.875221	0.878962	0.879025	0.877833	0.878771	0.8794	0.880844	0.877951	0.879728	0.884388	0.876460	0.880029	0.888389	0.874258	0.880313
0.2	0.872626	0.878151	0.878288	0.874683	0.877764	0.879035	0.877135	0.876133	0.879689	0.880292	0.873178	0.880291	0.884275	0.868821	0.880855
0.3	0.869184	0.876495	0.876693	0.870688	0.875954	0.877809	0.872539	0.873596	0.878788	0.875166	0.869306	0.879686	0.878919	0.862975	0.88053
0.4	0.864923	0.874003	0.874247	0.865885	0.873369	0.875727	0.867102	0.870405	0.877024	0.869065	0.864971	0.878216	0.872379	0.856928	0.879334
0.5	0.859870	0.870687	0.870956	0.860309	0.870036	0.872793	0.860870	0.866623	0.874403	0.862047	0.860286	0.875882	0.864719	0.850864	0.87727
0.6	0.854057	0.866560	0.86683	0.854000	0.865984	0.869015	0.853892	0.862302	0.870931	0.854172	0.855343	0.872691	0.856005	0.844932	0.874342
0.7	0.847514	0.861637	0.861882	0.846994	0.861234	0.864406	0.846217	0.857483	0.866619	0.845500	0.850213	0.868651	0.846308	0.839240	0.870558
0.8	0.840276	0.855935	0.856127	0.839334	0.855810	0.858978	0.837896	0.852198	0.861478	0.836095	0.844940	0.863774	0.835701	0.833856	0.865929
0.9	0.832376	0.849472	0.849583	0.831059	0.849727	0.852749	0.828980	0.846463	0.855525	0.826023	0.839545	0.858074	0.824260	0.828801	0.860467
1.0	0.823849	0.842268	0.84227	0.822212	0.842999	0.845738	0.819522	0.840286	0.848778	0.815349	0.834021	0.85157	0.812067	0.824053	0.85419

5.9 Convergence of Legendre wavelet

Theorem 5.1 (Convergence Theorem)

If a continuous function $u(x,t) \in L^2(\Re \times \Re)$ defined on $[0,1) \times [0,1)$ has bounded mixed fourth partial derivative $\left| \dfrac{\partial^4 u(x,t)}{\partial x^2 \partial t^2} \right| \leq K$, then the Legendre wavelets expansion of $u(x,t)$ converges uniformly to it.

Proof:

Let $u(x,t)$ be a function defined on $[0,1) \times [0,1)$ and $\left| \dfrac{\partial^4 u(x,t)}{\partial x^2 \partial t^2} \right| \leq K$, K is a positive constant.

The Legendre wavelet coefficients of continuous functions $u(x,t)$ are defined as

$$c_{n_1,m_1,n_2,m_2} = \int_0^1 \int_0^1 u(x,t)\psi_{n_1,m_1}(x)\,\psi_{n_2,m_2}(t)\,dxdt$$

$$= \int_{I_2} \int_{I_1} u(x,t)\sqrt{\left(m_1 + \frac{1}{2}\right)\left(m_2 + \frac{1}{2}\right)}\, 2^{\frac{k_1+k_2}{2}} P_{m_1}\!\left(2^{k_1} x - \hat{n}_1\right) P_{m_2}\!\left(2^{k_2} t - \hat{n}_2\right) dxdt$$

157

where $I_1 = \left[\dfrac{\hat{n}_1 - 1}{2^{k_1 - 1}}, \dfrac{\hat{n}_1 + 1}{2^{k_1 - 1}}\right)$ and $I_2 = \left[\dfrac{\hat{n}_2 - 1}{2^{k_2 - 1}}, \dfrac{\hat{n}_2 + 1}{2^{k_2 - 1}}\right)$.

Now by change of variable $2^{k_1} x - \hat{n}_1 = y$, we obtain

$$c_{n_1, m_1, n_2, m_2} = \sqrt{\left(m_1 + \frac{1}{2}\right)\left(m_2 + \frac{1}{2}\right)} \frac{2^{\frac{k_1 + k_2}{2}}}{2^{k_1}}$$

$$\int_{\frac{\hat{n}_2 - 1}{2^{k_2 - 1}}}^{\frac{\hat{n}_2 + 1}{2^{k_2 - 1}}} \left(\int_{-1}^{1} u\left(\frac{\hat{n}_1 + y}{2^{k_1}}, t\right) P_{m_1}(y) dy\right) P_{m_2}\left(2^{k_2} t - \hat{n}_2\right) dt. \tag{5.59}$$

Now

$$\int_{-1}^{1} u\left(\frac{\hat{n}_1 + y}{2^{k_1}}, t\right) P_{m_1}(y) dy = \frac{1}{(2m_1 + 1)} \int_{-1}^{1} u\left(\frac{\hat{n}_1 + y}{2^{k_1}}, t\right) \left(P'_{m_1 + 1}(y) - P'_{m_1 - 1}(y)\right) dy,$$

$$\text{since } (2m_1 + 1) P_{m_1}(y) = P'_{m_1 + 1}(y) - P'_{m_1 - 1}(y)$$

$$= \frac{1}{(2m_1 + 1)} \left[u\left(\frac{\hat{n}_1 + y}{2^{k_1}}, t\right)\left(P_{m_1 + 1}(y) - P_{m_1 - 1}(y)\right)\Big|_{-1}^{1} - \int_{-1}^{1} \frac{\partial u}{\partial y}\left(P_{m_1 + 1}(y) - P_{m_1 - 1}(y)\right) dy \right]$$

$$= \frac{-1}{(2m_1 + 1)} \left[\int_{-1}^{1} \frac{\partial u}{\partial y}\left(P_{m_1 + 1}(y) - P_{m_1 - 1}(y)\right) dy \right]$$

$$= \frac{1}{(2m_1 + 1)} \int_{-1}^{1} \frac{\partial^2 u}{\partial y^2} \left[\frac{P_{m_1 + 2}(y) - P_{m_1}(y)}{(2m_1 + 3)} - \frac{P_{m_1}(y) - P_{m_1 - 2}(y)}{(2m_1 - 1)} \right] dy \tag{5.60}$$

Substituting eq. (5.60) in eq. (5.59), we have

$$c_{n_1, m_1, n_2, m_2} = \sqrt{\left(m_1 + \frac{1}{2}\right)\left(m_2 + \frac{1}{2}\right)} \frac{2^{\frac{k_1 + k_2}{2}}}{2^{k_1}} \frac{1}{(2m_1 + 1)} \int_{-1}^{1} \left(\int_{\frac{\hat{n}_2 - 1}{2^{k_2 - 1}}}^{\frac{\hat{n}_2 + 1}{2^{k_2 - 1}}} \frac{\partial^2 u}{\partial y^2} P_{m_2}\left(2^{k_2} t - \hat{n}_2\right) dt \right)$$

$$\times \left[\frac{P_{m_1 + 2}(y) - P_{m_1}(y)}{(2m_1 + 3)} - \frac{P_{m_1}(y) - P_{m_1 - 2}(y)}{(2m_1 - 1)} \right] dy. \tag{5.61}$$

Similarly,

$$\int_{\frac{\hat{n}_2-1}{2^{k_2-1}}}^{\frac{\hat{n}_2+1}{2^{k_2-1}}} \frac{\partial^2 u}{\partial y^2} P_{m_2}\left(2^{k_2}t-\hat{n}_2\right)dt$$

$$= \frac{1}{2^{k_2}(2m_2+1)}\int_{-1}^{1}\frac{\partial^4 u}{\partial w^2 \partial y^2}\left[\frac{P_{m_2+2}(w)-P_{m_2}(w)}{(2m_2+3)}-\frac{P_{m_2}(w)-P_{m_2-2}(w)}{(2m_2-1)}\right]dw, \qquad (5.62)$$

where $w = 2^{k_2}\,t-\hat{n}_2$.

Substituting eq. (5.62) in eq. (5.61), we have

$$c_{n_1,m_1,n_2,m_2} = \sqrt{\left(m_1+\frac{1}{2}\right)\left(m_2+\frac{1}{2}\right)}\,\frac{1}{2^{\frac{k_1+k_2}{2}}(2m_1+1)(2m_2+1)}\int_{-1}^{1}\int_{-1}^{1}\frac{\partial^4 u}{\partial w^2 \partial y^2}$$

$$\left[\left(\frac{P_{m_2+2}(w)-P_{m_2}(w)}{(2m_2+3)}-\frac{P_{m_2}(w)-P_{m_2-2}(w)}{(2m_2-1)}\right)\left(\frac{P_{m_1+2}(y)-P_{m_1}(y)}{(2m_1+3)}-\frac{P_{m_1}(y)-P_{m_1-2}(y)}{(2m_1-1)}\right)\right]dwdy.$$

Now suppose

$$R_1(y)=(2m_1-1)P_{m_1+2}(y)-(2m_1-1)P_{m_1}(y)-(2m_1+3)P_{m_1}(y)+(2m_1+3)P_{m_1-2}(y)$$

$$= (2m_1-1)P_{m_1+2}(y)-2(2m_1+1)P_{m_1}(y)+(2m_1+3)P_{m_1-2}(y),$$

and

$$R_2(w)=(2m_2-1)P_{m_2+2}(w)-(2m_2-1)P_{m_2}(w)-(2m_2+3)P_{m_2}(w)+(2m_2+3)P_{m_2-2}(w)$$

$$= (2m_2-1)P_{m_2+2}(w)-2(2m_2+1)P_{m_2}(w)+(2m_2+3)P_{m_2-2}(w).$$

Therefore, $\left|c_{n_1,m_1,n_2,m_2}\right|\le \lambda_{m_1,m_2}^{k_1,k_2}\int_{-1}^{1}\int_{-1}^{1}\left|\frac{\partial^4 u}{\partial w^2 \partial y^2}\right|\left|R_1(y)\right|\left|R_2(w)\right|dwdy$

$$\le \lambda_{m_1,m_2}^{k_1,k_2}K\int_{-1}^{1}\int_{-1}^{1}\left|R_1(y)\right|\left|R_2(w)\right|dwdy \qquad (5.63)$$

where $\lambda_{m_1,m_2}^{k_1,k_2} = \sqrt{\left(m_1+\frac{1}{2}\right)\left(m_2+\frac{1}{2}\right)}\,\dfrac{1}{2^{\frac{k_1+k_2}{2}}(2m_1+1)^2(2m_1-3)(2m_2+1)^2(2m_2-3)}.$

Now using Cauchy-Schwarz inequality

$$\left(\int_{-1}^{1}|R_1(y)|dy\right)^2 \le \left(\int_{-1}^{1}1^2 dy\right)\int_{-1}^{1}\left[(2m_1-1)^2+(4m_1+2)^2+(2m_1+3)^2\right]$$

$$\times \left[P_{m_1+2}^2(y)+P_{m_1}^2(y)+P_{m_1-2}^2(y)\right]dy$$

$$\le 2\left[(2m_1-1)^2+(4m_1+2)^2+(2m_1+3)^2\right]\left[\frac{2}{(2m_1+5)}+\frac{2}{(2m_1+1)}+\frac{2}{(2m_1-3)}\right]$$

$$\int_{-1}^{1}|R_1(y)|dy \le 2\sqrt{\left[(2m_1-1)^2+(4m_1+2)^2+(2m_1+3)^2\right]\left[\frac{1}{(2m_1+5)}+\frac{1}{(2m_1+1)}+\frac{1}{(2m_1-3)}\right]}$$

$$(5.64)$$

Similarly,

$$\int_{-1}^{1}|R_2(w)|dw \le 2\sqrt{\left[(2m_2-1)^2+(4m_2+2)^2+(2m_2+3)^2\right]\left[\frac{1}{(2m_2+5)}+\frac{1}{(2m_2+1)}+\frac{1}{(2m_2-3)}\right]}$$

$$(5.65)$$

Putting eqs. (5.64) and (5.65) in eq. (5.63), we have

$$\left|c_{n_1,m_1,n_2,m_2}\right| \le 4K\lambda_{m_1,m_2}^{k_1,k_2}\eta_{m_1,m_2}, \tag{5.66}$$

where

$$\eta_{m_1,m_2} = \sqrt{\left[(2m_1-1)^2+(4m_1+2)^2+(2m_1+3)^2\right]\left[\frac{1}{(2m_1+5)}+\frac{1}{(2m_1+1)}+\frac{1}{(2m_1-3)}\right]}$$

$$\times \sqrt{\left[(2m_2-1)^2+(4m_2+2)^2+(2m_2+3)^2\right]\left[\frac{1}{(2m_2+5)}+\frac{1}{(2m_2+1)}+\frac{1}{(2m_2-3)}\right]}$$

Therefore $\sum_{n_1=0}^{\infty}\sum_{m_1=0}^{\infty}\sum_{n_2=0}^{\infty}\sum_{m_2=0}^{\infty}c_{n_1,m_1,n_2,m_2}$ is absolutely convergent.

Hence according to Ref. [44], the Legendre series expansion of $u(x,t)$ converges uniformly. □

Theorem 5.2 (Error Estimate)

If a continuous function $u(x,t) \in L^2(\Re \times \Re)$ defined on $[0,1)\times[0,1)$ be bounded viz. $|u(x,t)| \le K$, then

160

$$\left\| \varepsilon_{u,k_1,M_1,k_2,M_2} \right\|_{L^2_\omega[[0,1)\times[0,1)]} \leq 4K \left[\sum_{n_1=2^{k_1-1}+1}^{\infty} \sum_{m_1=M_1}^{\infty} \sum_{n_2=2^{k_2-1}+1}^{\infty} \sum_{m_2=M_2}^{\infty} \left(\lambda_{m_1,m_2}^{k_1,k_2} \eta_{m_1,m_2} \right)^2 \right]^{\frac{1}{2}}.$$

where $\lambda_{m_1,m_2}^{k_1,k_2} = \sqrt{\left(m_1 + \dfrac{1}{2} \right)\left(m_2 + \dfrac{1}{2} \right)} \dfrac{1}{2^{\frac{k_1+k_2}{2}} (2m_1+1)^2 (2m_1-3)(2m_2+1)^2 (2m_2-3)}$,

and $\eta_{m_1,m_2} = \sqrt{\left[(2m_1-1)^2 + (4m_1+2)^2 + (2m_1+3)^2 \right] \left[\dfrac{1}{(2m_1+5)} + \dfrac{1}{(2m_1+1)} + \dfrac{1}{(2m_1-3)} \right]}$

$\times \sqrt{\left[(2m_2-1)^2 + (4m_2+2)^2 + (2m_2+3)^2 \right] \left[\dfrac{1}{(2m_2+5)} + \dfrac{1}{(2m_2+1)} + \dfrac{1}{(2m_2-3)} \right]}$

Proof:

$$\left\| \varepsilon_{u,k_1,M_1,k_2,M_2} \right\|_{L^2_\omega[[0,1)\times[0,1)]}^2$$

$$= \int_0^1 \int_0^1 \left| u(x,t) - \sum_{n_1=1}^{2^{k_1-1}} \sum_{m_1=0}^{M_1-1} \sum_{n_2=1}^{2^{k_2-1}} \sum_{m_2=0}^{M_2-1} c_{n_1,m_1,n_2,m_2} \, \psi_{n_1,m_1}(x) \, \psi_{n_2,m_2}(t) \right|^2 \omega(x)\omega(t) dx dt$$

$$= \int_0^1 \int_0^1 \left| \sum_{n_1=2^{k_1-1}+1}^{\infty} \sum_{m_1=M_1}^{\infty} \sum_{n_2=2^{k_2-1}+1}^{\infty} \sum_{m_2=M_2}^{\infty} c_{n_1,m_1,n_2,m_2} \, \psi_{n_1,m_1}(x)\psi_{n_2,m_2}(t) \right|^2 dx dt$$

$$= \sum_{n_1=2^{k_1-1}+1}^{\infty} \sum_{m_1=M_1}^{\infty} \sum_{n_2=2^{k_2-1}+1}^{\infty} \sum_{m_2=M_2}^{\infty} \left| c_{n_1,m_1,n_2,m_2} \right|^2 \tag{5.67}$$

Substituting eq. (5.66) of theorem 5.1, in eq. (5.67) we obtain

$$\left\| \varepsilon_{u,k_1,M_1,k_2,M_2} \right\|_{L^2_\omega[[0,1)\times[0,1)]}^2 \leq \sum_{n_1=2^{k_1-1}+1}^{\infty} \sum_{m_1=M_1}^{\infty} \sum_{n_2=2^{k_2-1}+1}^{\infty} \sum_{m_2=M_2}^{\infty} \left(4K\lambda_{m_1,m_2}^{k_1,k_2} \eta_{m_1,m_2} \right)^2 \tag{5.68}$$

where $\lambda_{m_1,m_2}^{k_1,k_2} = \sqrt{\left(m_1 + \dfrac{1}{2} \right)\left(m_2 + \dfrac{1}{2} \right)} \dfrac{1}{2^{\frac{k_1+k_2}{2}} (2m_1+1)^2 (2m_1-3)(2m_2+1)^2 (2m_2-3)}$,

and $\eta_{m_1,m_2} = \sqrt{\left[(2m_1-1)^2 + (4m_1+2)^2 + (2m_1+3)^2 \right] \left[\dfrac{1}{(2m_1+5)} + \dfrac{1}{(2m_1+1)} + \dfrac{1}{(2m_1-3)} \right]}$

$$\times \sqrt{\left[(2m_2 - 1)^2 + (4m_2 + 2)^2 + (2m_2 + 3)^2\right]\left[\frac{1}{(2m_2 + 5)} + \frac{1}{(2m_2 + 1)} + \frac{1}{(2m_2 - 3)}\right]}$$

Eq. (5.68) implies

$$\left\|\varepsilon_{u,k_1,M_1,k_2,M_2}\right\|_{L^2_\omega[[0,1)\times[0,1)]} \leq \left[\sum_{n_1=2^{k_1-1}+1}^{\infty} \sum_{m_1=M_1}^{\infty} \sum_{n_2=2^{k_2-1}+1}^{\infty} \sum_{m_2=M_2}^{\infty} \left(4K\lambda_{m_1,m_2}^{k_1,k_2} \eta_{m_1,m_2}\right)^2\right]^{\frac{1}{2}} \qquad \square$$

5.10 Solution of Fractional Kaup-Kupershmidt Equation Using Legendre Multiwavelets

5.10.1 Introduction of Legendre Multiwavelets

Legendre multiwavelets $\psi_{n,m}(x) = \psi(k,n,m,x)$ have four arguments; $n = 0,1,2,...,2^k - 1$, $k \in \mathbb{Z}^+$, m is the order of Legendre polynomials and x is normalized time. They are defined on the interval $[0,1)$ as [126]

$$\psi_{n,m}(x) = \begin{cases} \sqrt{2m+1}\, 2^{\frac{k}{2}} L_m\left(2^k x - n\right), & \dfrac{n}{2^k} \leq x < \dfrac{n+1}{2^k}, \\ 0, & \text{elsewhere} \end{cases}$$

where $m = 0,1,...,M-1$, $n = 0,1,2,...,2^k - 1$.

Here, $L_m(x)$ are the well-known shifted Legendre polynomials of order m, which are defined on the interval $[0,1]$, and can be determined with the aid of the following recurrence formulae:

$$L_0(x) = 1,$$

$$L_1(x) = 2x - 1,$$

$$L_{m+1}(x) = \left(\frac{2m+1}{m+1}\right)(2x-1)L_m(x) - \left(\frac{m}{m+1}\right)L_{m-1}(x), \quad m = 1,2,3,.... \quad .$$

The two-dimensional Legendre multiwavelets are defined as

$$\psi_{n_1,m_1,n_2,m_2}(x,t) = \begin{cases} AL_{m_1}\left(2^{k_1} x - n_1\right)L_{m_2}\left(2^{k_2} t - n_2\right), & \dfrac{n_1}{2^{k_1}} \leq x < \dfrac{n_1+1}{2^{k_1}}, \dfrac{n_2}{2^{k_2}} \leq t < \dfrac{n_2+1}{2^{k_2}} \\ \\ 0, & \text{elsewhere} \end{cases}$$

162

where $A = \sqrt{(2m_1 + 1)(2m_2 + 1)}\ 2^{\frac{k_1 + k_2}{2}}$, n_1 and n_2 are defined similarly to n; k_1 and k_2 are any positive integers, m_1 and m_2 are the orders for shifted Legendre polynomials and $\psi_{n_1, m_1, n_2, m_2}(x, t)$ forms a basis for $L^2([0, 1) \times [0, 1))$.

5.10.2 Function Approximation

A function $f(x, t)$ defined over $[0,1) \times [0,1)$ can be expanded in terms of Legendre multiwavelet as [126]

$$f(x, t) = \sum_{n=0}^{\infty} \sum_{i=0}^{\infty} \sum_{l=0}^{\infty} \sum_{j=0}^{\infty} c_{n,i,l,j} \psi_{n,i,l,j}(x, t). \tag{5.69}$$

If the infinite series in eq. (5.69) is truncated, then it can be written as

$$f(x, t) \cong \sum_{n=0}^{2^{k_1}-1} \sum_{i=0}^{M_1} \sum_{l=0}^{2^{k_2}-1} \sum_{j=0}^{M_2} c_{n,i,l,j} \psi_{n,i,l,j}(x, t) = \Psi^T(x) C \Psi(t), \tag{5.70}$$

where $\Psi(x)$ and $\Psi(t)$ are $2^{k_1}(M_1 + 1) \times 1$ and $2^{k_2}(M_2 + 1) \times 1$ matrices, respectively.

$$\Psi(x) \equiv \left[\psi_{0,0}(x), \psi_{0,1}(x), \ldots, \psi_{0,M_1}(x), \psi_{1,0}(x), \ldots, \psi_{1,M_1}(x), \ldots, \psi_{(2^{k_1}-1),0}(x), \ldots, \psi_{(2^{k_1}-1),M_1}(x) \right]^T,$$

$$\Psi(t) \equiv \left[\psi_{0,0}(t), \psi_{0,1}(t), \ldots, \psi_{0,M_2}(t), \psi_{1,0}(t), \ldots, \psi_{1,M_2}(t), \ldots, \psi_{(2^{k_2}-1),0}(t), \ldots, \psi_{(2^{k_2}-1),M_2}(t) \right]^T.$$

Also, C is a $2^{k_1}(M_1 + 1) \times 2^{k_2}(M_2 + 1)$ matrix whose elements can be calculated from the formula

$$c_{n,i,l,j} = \int_0^1 \int_0^1 \psi_{n,i}(x) \psi_{l,j}(t) f(x, t) dt dx, \tag{5.71}$$

with $n = 0, 1, \ldots, 2^{k_1} - 1, i = 0, \ldots, M_1, l = 0, 1, \ldots, 2^{k_2} - 1, j = 0, \ldots, M_2$.

5.10.3 Operational Matrix of the General Order Integration [127]

The integration of

$$\Psi(t) \equiv [\psi_{0,0}(t), \ldots, \psi_{0,M}(t), \psi_{1,0}(t), \ldots, \psi_{1,M}(t), \ldots, \psi_{(2^k-1),0}(t), \ldots, \psi_{(2^k-1),M}(t)]^T \qquad \text{can} \qquad \text{be}$$

approximated by

$$\int_0^t \Psi(\tau) d\tau \cong Q \Psi(t), \tag{5.72}$$

where Q is called the Legendre multiwavelet operational matrix of integration. To derive the Legendre multiwavelet operational matrix of the general order of integration, let us recall the fractional integral of order $\alpha(>0)$, defined by Podlubny [41]

$$J^{\alpha}f(t) = \frac{1}{\Gamma(\alpha)}\int_0^t (t-\tau)^{\alpha-1}f(\tau)d\tau, \quad \alpha > 0, \ \alpha \in \Re^+ \tag{5.73}$$

where $\Re^+$ is the set of positive real numbers.

The Legendre multiwavelet operational matrix Q^{α} for integration of the general order α is given by

$$Q^{\alpha}\Psi(t) = J^{\alpha}\Psi(t)$$
$$= \left[J^{\alpha}\psi_{0,0}(t),...,J^{\alpha}\psi_{0,M}(t), J^{\alpha}\psi_{1,0}(t),...,J^{\alpha}\psi_{1,M}(t), J^{\alpha}\psi_{(2^k-1),0}(t),...,J^{\alpha}\psi_{(2^k-1),M}(t) \right]^T,$$

where

$$J^{\alpha}\psi_{n,m}(t) = \begin{cases} (2m+1)^{1/2}2^{k/2}J^{\alpha}L_m(2^kt-n), & \dfrac{n}{2^k} \le t < \dfrac{n+1}{2^k}, \\ 0, & \text{elsewhere} \end{cases}$$

for $n = 0,1,2,...,2^k-1$, $m = 0,1,2,...,M$ is the order of the Legendre polynomials and M is a fixed positive integer.

5.11 Application of Analytical and Numerical Methods for Solving Time-Fractional Kaup-Kupershmidt Equation

5.11.1 Solution of Fractional Kaup-Kupershmidt Equation Using Legendre Multiwavelets

To exhibit the effectiveness and accuracy of proposed numerical scheme, we consider the time-fractional Kaup-Kupershmidt equation. The numerical solutions thus obtained are compared with the exact solutions as well as with the solutions obtained by OHAM.

Consider the nonlinear time-fractional generalized Kaup-Kupershmidt equation [121]

$$\frac{\partial^{\alpha}u}{\partial t^{\alpha}} + 45u^2\frac{\partial u}{\partial x} - 15p\frac{\partial u}{\partial x}\frac{\partial^2 u}{\partial x^2} - 15u\frac{\partial^3 u}{\partial x^3} + \frac{\partial^5 u}{\partial x^5} = 0, \tag{5.74}$$

with initial condition

$$u(x,0) = \frac{1}{4} w^2 \lambda^2 \sec h^2\left(\frac{\lambda w x}{2}\right) + \frac{w^2 \lambda^2}{12}. \tag{5.75}$$

The exact solution of eq. (5.74) is given by [121]

$$u(x,t) = \frac{1}{4} w^2 \lambda^2 \sec h^2\left\{\frac{\lambda}{2}\left(\frac{-w^5(-8\lambda^2\mu + 16\mu^2 + \lambda^4)}{16\,\Gamma(1+\alpha)} t^\alpha + wx\right)\right\} + \frac{w^2\lambda^2}{12}, \tag{5.76}$$

where λ, μ and w are constant with $w \neq 0$.

The Legendre multiwavelet solution of $u(x,t)$ is sought by assuming that $u(x,t)$ can be expanded in terms of Legendre multiwavelet as

$$u(x,t) = \sum_{n=0}^{2^{k_1}-1}\sum_{i=0}^{M_1}\sum_{l=0}^{2^{k_2}-1}\sum_{j=0}^{M_2} d_{n,i,l,j}\,\psi_{n,i,l,j}(x,t), \tag{5.77}$$

where $n = 0,...,2^{k_1}-1, i = 0,...,M_1, l = 0,...,2^{k_2}-1, j = 0,...,M_2$.

The nonlinear terms presented in eq. (5.74) can be approximated using Legendre multiwavelet function as

$$u^2\frac{\partial u}{\partial x} = \sum_{n=0}^{2^{k_1}-1}\sum_{i=0}^{M_1}\sum_{l=0}^{2^{k_2}-1}\sum_{j=0}^{M_2} a_{n,i,l,j}\,\psi_{n,i,l,j}(x,t), \tag{5.78}$$

$$\frac{\partial u}{\partial x}\frac{\partial^2 u}{\partial x^2} = \sum_{n=0}^{2^{k_1}-1}\sum_{i=0}^{M_1}\sum_{l=0}^{2^{k_2}-1}\sum_{j=0}^{M_2} b_{n,i,l,j}\,\psi_{n,i,l,j}(x,t), \tag{5.79}$$

and
$$u\frac{\partial^3 u}{\partial x^3} = \sum_{n=0}^{2^{k_1}-1}\sum_{i=0}^{M_1}\sum_{l=0}^{2^{k_2}-1}\sum_{j=0}^{M_2} c_{n,i,l,j}\,\psi_{n,i,l,j}(x,t). \tag{5.80}$$

This implies

$$\left(\sum_{n=0}^{2^{k_1}-1}\sum_{i=0}^{M_1}\sum_{l=0}^{2^{k_2}-1}\sum_{j=0}^{M_2} d_{n,i,l,j}\,\psi_{n,i,l,j}(x,t)\right)^2\left[\sum_{n=0}^{2^{k_1}-1}\sum_{i=0}^{M_1}\sum_{l=0}^{2^{k_2}-1}\sum_{j=0}^{M_2} d_{n,i,l,j}\,\frac{\partial\psi_{n,i,l,j}(x,t)}{\partial x}\right] =$$
$$\sum_{n=0}^{2^{k_1}-1}\sum_{i=0}^{M_1}\sum_{l=0}^{2^{k_2}-1}\sum_{j=0}^{M_2} a_{n,i,l,j}\,\psi_{n,i,l,j}(x,t). \tag{5.81}$$

$$\left(\sum_{n=0}^{2^{k_1}-1}\sum_{i=0}^{M_1}\sum_{l=0}^{2^{k_2}-1}\sum_{j=0}^{M_2} d_{n,i,l,j}\,\frac{\partial\psi_{n,i,l,j}(x,t)}{\partial x}\right)\left[\sum_{n=0}^{2^{k_1}-1}\sum_{i=0}^{M_1}\sum_{l=0}^{2^{k_2}-1}\sum_{j=0}^{M_2} d_{n,i,l,j}\,\frac{\partial^2\psi_{n,i,l,j}(x,t)}{\partial x^2}\right]$$
$$= \sum_{n=0}^{2^{k_1}-1}\sum_{i=0}^{M_1}\sum_{l=0}^{2^{k_2}-1}\sum_{j=0}^{M_2} b_{n,i,l,j}\,\psi_{n,i,l,j}(x,t), \tag{5.82}$$

and

$$\left(\sum_{n=0}^{2^{k_1}-1} \sum_{i=0}^{M_1} \sum_{l=0}^{2^{k_2}-1} \sum_{j=0}^{M_2} d_{n,i,l,j}\, \psi_{n,i,l,j}(x,t) \right)\left[\sum_{n=0}^{2^{k_1}-1} \sum_{i=0}^{M_1} \sum_{l=0}^{2^{k_2}-1} \sum_{j=0}^{M_2} d_{n,i,l,j}\, \frac{\partial^3 \psi_{n,i,l,j}(x,t)}{\partial x^3} \right]$$

$$= \sum_{n=0}^{2^{k_1}-1} \sum_{i=0}^{M_1} \sum_{l=0}^{2^{k_2}-1} \sum_{j=0}^{M_2} c_{n,i,l,j}\, \psi_{n,i,l,j}(x,t). \tag{5.83}$$

Again applying J_t^{α} on both sides of eq. (5.74) we have

$$u(x,t)-u(x,0) = J_t^{\alpha}\left[-45u^2 \frac{\partial u}{\partial x} +15p\frac{\partial u}{\partial x}\frac{\partial^2 u}{\partial x^2} +15u\frac{\partial^3 u}{\partial x^3} - \frac{\partial^5 u}{\partial x^5} \right]. \tag{5.84}$$

Putting eqs. (5.77), (5.78), (5.79) and (5.80) in eq. (5.84), we have

$$\sum_{n=0}^{2^{k_1}-1} \sum_{i=0}^{M_1} \sum_{l=0}^{2^{k_2}-1} \sum_{j=0}^{M_2} d_{n,i,l,j}\psi_{n,i,l,j}(x,t)-u(x,0) = J_t^{\alpha}\left[-45\left(\sum_{n=0}^{2^{k_1}-1} \sum_{i=0}^{M_1} \sum_{l=0}^{2^{k_2}-1} \sum_{j=0}^{M_2} a_{n,i,l,j}\psi_{n,i,l,j}(x,t) \right) \right.$$

$$+15p\left(\sum_{n=0}^{2^{k_1}-1} \sum_{i=0}^{M_1} \sum_{l=0}^{2^{k_2}-1} \sum_{j=0}^{M_2} b_{n,i,l,j}\psi_{n,i,l,j}(x,t) \right) +15\left(\sum_{n=0}^{2^{k_1}-1} \sum_{i=0}^{M_1} \sum_{l=0}^{2^{k_2}-1} \sum_{j=0}^{M_2} c_{n,i,l,j}\psi_{n,i,l,j}(x,t) \right) \tag{5.85}$$

$$\left. - \sum_{n=1}^{2^{k_1}-1} \sum_{i=0}^{M_1-1} \sum_{l=1}^{2^{k_2}-1} \sum_{j=0}^{M_2-1} d_{n,i,l,j}\, \frac{\partial^5 \psi_{n,i,l,j}(x,t)}{\partial x^5} \right].$$

Now substituting the collocation points $x_l = \dfrac{l-0.5}{2^{k_1}(M_1+1)}$ and $t_r = \dfrac{r-0.5}{2^{k_2}(M_2+1)}$ for

$l = 1,2,\ldots,2^{k_1}(M_1+1)$ and $r = 1,2,\ldots,2^{k_2}(M_2+1)$ in eqs. (5.81), (5.82), (5.83) and (5.85),

we have $4\big(2^{k_1}(M_1+1)\big)\big(2^{k_2}(M_2+1)\big)$ equations in $4\big(2^{k_1}(M_1+1)\big)\big(2^{k_2}(M_2+1)\big)$ unknowns in

$a_{n,i,l,j}$, $b_{n,i,l,j}$, $c_{n,i,l,j}$ and $d_{n,i,l,j}$. By solving this system of equations using mathematical

software, the Legendre multiwavelet coefficients $a_{n,i,l,j}$, $b_{n,i,l,j}$, $c_{n,i,l,j}$ and $d_{n,i,l,j}$ can be

obtained.

5.11.2 Comparison with OHAM for Solution of Time-Fractional Kaup-Kupershmidt Equation

Using optimal homotopy asymptotic method [128], the homotopy for eq. (5.74) can be written as

$$(1-p)L(\varphi(x,t\,;p)) = H(p)\left[\frac{\partial^{\alpha}\varphi(x,t\,;p)}{\partial t^{\alpha}} + 45\varphi(x,t\,;p)^{2}\frac{\partial\varphi(x,t\,;p)}{\partial x}\right.$$
$$\left.-15p\frac{\partial\varphi(x,t;p)}{\partial x}\frac{\partial^{2}\varphi(x,t;p)}{\partial x^{2}} - 15\varphi(x,t;p)\frac{\partial^{3}\varphi(x,t;p)}{\partial x^{3}} + \frac{\partial^{5}\varphi(x,t;p)}{\partial x^{5}}\right], \qquad (5.86)$$

where $\quad \varphi(x,t\,;p) = u_{0}(x,t) + \sum\limits_{i=1}^{\infty}u_{i}(x,t)p^{i}\,,$ (5.87)

$$H(p) = C_{1}p + C_{2}p^{2} + C_{3}p^{3} + \ldots, \qquad (5.88)$$

$$N(\varphi(x,t\,;p)) = N_{0}(u_{0}(x,t)) + \sum\limits_{k=1}^{\infty}N_{k}(u_{0},u_{1},\ldots,u_{k})p^{k}\,. \qquad (5.89)$$

Substituting eqs. (5.87) to (5.89) in eq. (5.86) and equating the coefficients of different powers in p, we have the following system of partial differential equations.

Coefficients of $p^{0}:\dfrac{\partial^{\alpha}u_{0}(x,t)}{\partial t^{\alpha}} = 0\,.$ (5.90)

Coefficients of $p^{1}:\dfrac{\partial^{\alpha}u_{1}(x,t)}{\partial t^{\alpha}} - \dfrac{\partial^{\alpha}u_{0}(x,t)}{\partial t^{\alpha}} = C_{1}\left[\dfrac{\partial^{\alpha}u_{0}(x,t)}{\partial t^{\alpha}} + 45(u_{0}(x,t))^{2}\dfrac{\partial u_{0}(x,t)}{\partial x}\right.$

$$\left.-15p\frac{\partial u_{0}(x,t)}{\partial x}\frac{\partial^{2}u_{0}(x,t)}{\partial x^{2}} - 15u_{0}(x,t)\frac{\partial^{3}u_{0}(x,t)}{\partial x^{3}} + \frac{\partial^{5}u_{0}(x,t)}{\partial x^{5}}\right]. \qquad (5.91)$$

Coefficients of $p^{2}:$

$$\frac{\partial^{\alpha}u_{2}(x,t)}{\partial t^{\alpha}} - \frac{\partial^{\alpha}u_{1}(x,t)}{\partial t^{\alpha}} = C_{1}\left[\frac{\partial^{\alpha}u_{1}(x,t)}{\partial t^{\alpha}} + 45\left(2u_{0}(x,t)u_{1}(x,t)\frac{\partial u_{0}(x,t)}{\partial x} + \right.\right.$$
$$\left.(u_{0}(x,t))^{2}\frac{\partial u_{1}(x,t)}{\partial x}\right) - 15p\left(\frac{\partial u_{0}(x,t)}{\partial x}\frac{\partial^{2}u_{1}(x,t)}{\partial x^{2}} + \frac{\partial u_{1}(x,t)}{\partial x}\frac{\partial^{2}u_{0}(x,t)}{\partial x^{2}}\right)$$
$$\left.-15\left(u_{0}(x,t)\frac{\partial^{3}u_{1}(x,t)}{\partial x^{3}} + u_{1}(x,t)\frac{\partial^{3}u_{0}(x,t)}{\partial x^{3}}\right) + \frac{\partial^{5}u_{1}(x,t)}{\partial x^{5}}\right] \qquad (5.92)$$
$$+ C_{2}\left[\frac{\partial^{\alpha}u_{0}(x,t)}{\partial t^{\alpha}} + 45(u_{0}(x,t))^{2}\frac{\partial u_{0}(x,t)}{\partial x} - 15p\frac{\partial u_{0}(x,t)}{\partial x}\frac{\partial^{2}u_{0}(x,t)}{\partial x^{2}}\right.$$
$$\left.-15u_{0}(x,t)\frac{\partial^{3}u_{0}(x,t)}{\partial x^{3}} + \frac{\partial^{5}u_{0}(x,t)}{\partial x^{5}}\right],$$

and so on.

For solving fractional Kaup-Kupershmidt equation using OHAM, we consider the following initial condition for equation (5.74)

$$u(x,0) = \frac{1}{4} w^2 \lambda^2 \sec h^2\left(\frac{\lambda w x}{2}\right) + \frac{w^2 \lambda^2}{12}.$$

Using the initial condition $u_0 = u(x,0)$ and solving eq. (5.90) to eq. (5.92), we obtain the expressions for u_0, u_1 and u_2.

Finally, the second order approximate solution for time-fractional Kaup-Kupershmidt equation is given by

$$u = u_0(x,t) + u_1(x,t) + u_2(x,t). \tag{5.93}$$

The optimal values of the convergence control parameters C_1 and C_2 can be obtained using collocation method given in eq. (1.33) of chapter 1.

5.12 Numerical Results of Fractional Kaup-Kupershmidt Equation

The comparison of the absolute errors for time-fractional Kaup-Kupershmidt equation (5.74) has been exhibited in Tables 5.19 and 5.22 which are constructed using the results obtained by two-dimensional Legendre multiwavelet method and OHAM at different values of x and t taking $\alpha = 1$. In the present analysis, to examine the accuracy and reliability of the Legendre multi-wavelets for solving fractional order Kaup-Kupershmidt equation, we compare the approximate solution of Legendre multiwavelets with the exact solution as well as with second order approximate solution obtained by OHAM. Tables 5.20, 5.21 and 5.23, 5.24 show the comparison of absolute errors of fractional order Kaup-Kupershmidt equation (5.74) at various points of x and t taking $\alpha = 0.5$ and 0.75. Agreement between present numerical results obtained by Legendre multiwavelets and exact solutions appears very satisfactory through illustrations in Tables 5.19, 5.20 and 5.21.

Table 5.19 Comparison of absolute errors obtained by two-dimensional Legendre multiwavelet method for nonlinear Kaup-Kupershmidt equation given in eq. (5.74) at various points of x and t taking $\lambda = 0.1, \mu = 0, w = 1$ and $\alpha = 1$.

x	$\left\|u_{Exact} - u_{LegendreMultiwavelet}\right\|$								
	$t=0.1$	$t=0.2$	$t=0.3$	$t=0.4$	$t=0.5$	$t=0.6$	$t=0.7$	$t=0.8$	$t=0.9$
0.1	3.5268E-10	7.0333E-10	1.0519E-9	1.3985E-9	1.7430E-9	2.0855E-9	2.4259E-9	2.7643E-9	3.1007E-9
0.2	7.0308E-10	1.4041E-9	2.1031E-9	2.8001E-9	3.4950E-9	4.1879E-9	4.8788E-9	5.5676E-9	6.2544E-9
0.3	1.0532E-9	2.1043E-9	3.1535E-9	4.2006E-9	5.2456E-9	6.2887E-9	7.3297E-9	8.3687E-9	9.4057E-9

x									
0.4	1.4028E-9	2.8037E-9	4.2025E-9	5.5994E-9	6.9942E-9	8.3869E-9	9.7777E-9	1.1166E-8	1.2553E-8
0.5	1.7520E-9	3.5020E-9	5.2500E-9	6.9959E-9	8.7399E-9	1.0482E-8	1.2222E-8	1.3959E-8	1.5695E-8
0.6	2.1004E-9	4.1988E-9	6.2953E-9	8.3897E-9	1.0482E-8	1.2572E-8	1.4661E-8	1.6747E-8	1.8832E-8
0.7	2.4480E-9	4.8941E-9	7.3381E-9	9.7802E-9	1.2220E-8	1.4658E-8	1.7094E-8	1.9528E-8	2.1960E-8
0.8	2.7946E-9	5.5873E-9	8.3780E-9	1.1166E-8	1.3953E-8	1.6738E-8	1.9521E-8	2.2302E-8	2.5081E-8
0.9	3.1402E-9	6.2783E-9	9.4146E-9	1.2548E-8	1.5881E-8	1.8811E-8	2.1939E-8	2.5066E-8	2.8191E-8

Table 5.20   Comparison of absolute errors obtained by two-dimensional Legendre multiwavelet method for fractional order nonlinear Kaup-Kupershmidt equation given in eq. (5.74) at various points of x and t taking $\lambda = 0.1, \mu = 0, w = 1$ and $\alpha = 0.75$.

x	$\left\|u_{Exact} - u_{LegendreMultiwavelet}\right\|$								
	$t = 0.1$	$t = 0.2$	$t = 0.3$	$t = 0.4$	$t = 0.5$	$t = 0.6$	$t = 0.7$	$t = 0.8$	$t = 0.9$
0.1	6.7734E-10	1.1369E-9	1.5349E-9	1.8967E-9	2.2340E-9	2.5523E-9	2.8551E-9	3.1456E-9	3.4253E-9
0.2	1.3533E-9	2.2769E-9	3.0806E-9	3.8142E-9	4.5010E-9	5.1516E-9	5.7729E-9	6.3709E-9	6.9489E-9
0.3	2.0287E-9	3.4161E-9	4.6251E-9	5.7303E-9	6.7663E-9	7.7489E-9	8.6884E-9	9.5937E-9	1.0469E-8
0.4	2.7033E-9	4.5538E-9	6.1677E-9	7.6441E-9	9.0289E-9	1.0343E-8	1.1600E-8	1.2812E-8	1.3986E-8
0.5	3.3768E-9	5.6898E-9	7.7079E-9	9.5548E-9	1.1287E-8	1.2933E-8	1.4507E-8	1.6026E-8	1.7497E-8
0.6	4.0490E-9	6.8234E-9	9.2450E-9	1.1462E-8	1.3542E-8	1.5518E-8	1.7409E-8	1.9234E-8	2.1001E-8
0.7	4.7196E-9	7.9544E-9	1.0778E-8	1.3364E-8	1.5791E-8	1.8096E-8	2.0304E-8	2.2434E-8	2.4497E-8
0.8	5.3883E-9	9.0822E-9	1.2307E-8	1.5261E-8	1.8034E-8	2.0668E-8	2.3191E-8	2.5624E-8	2.7983E-8
0.9	6.0548E-9	1.0206E-8	1.3832E-8	1.7152E-8	2.0269E-8	2.3232E-8	2.6068E-8	2.8805E-8	3.1458E-8

Table 5.21   Comparison of absolute errors obtained by two-dimensional Legendre multiwavelet method for fractional order nonlinear Kaup-Kupershmidt equation given in eq. (5.74) at various points of x and t taking $\lambda = 0.1, \mu = 0, w = 1$ and $\alpha = 0.5$.

x	$\left\|u_{Exact} - u_{LegendreMultiwavelet}\right\|$								
	$t = 0.1$	$t = 0.2$	$t = 0.3$	$t = 0.4$	$t = 0.5$	$t = 0.6$	$t = 0.7$	$t = 0.8$	$t = 0.9$
0.1	1.2348E-9	1.7431E-9	2.1251E-9	2.4420E-9	2.7198E-9	2.9690E-9	3.1958E-9	3.4065E-9	3.6035E-9
0.2	2.4789E-9	3.5107E-9	4.2915E-9	4.9425E-9	5.5158E-9	6.0321E-9	6.5038E-9	6.9435E-9	7.3559E-9
0.3	3.7221E-9	5.2770E-9	6.4561E-9	7.4411E-9	8.3096E-9	9.0928E-9	9.8093E-9	1.0477E-8	1.1105E-8
0.4	4.9638E-9	7.0412E-9	8.6182E-9	9.9366E-9	1.1100E-8	1.2149E-8	1.3111E-8	1.4007E-8	1.4850E-8
0.5	6.2035E-9	8.8026E-9	1.0776E-8	1.2428E-8	1.3886E-8	1.5202E-8	1.6407E-8	1.7532E-8	1.8589E-8
0.6	7.4407E-9	1.0560E-8	1.2931E-8	1.4915E-8	1.6667E-8	1.8248E-8	1.9697E-8	2.1049E-8	2.2321E-8
0.7	8.6750E-9	1.2314E-8	1.5080E-8	1.7395E-8	1.9440E-8	2.1287E-8	2.2979E-8	2.4558E-8	2.6044E-8
0.8	9.9058E-9	1.4063E-8	1.7223E-8	1.9869E-8	2.2209E-8	2.4317E-8	2.6251E-8	2.8058E-8	2.9756E-8
0.9	1.1132E-8	1.5806E-8	1.9359E-8	2.2335E-8	2.4964E-8	2.7338E-8	2.9514E-8	3.1546E-8	3.3457E-8

Table 5.22   Comparison of absolute errors obtained by optimal homotopy asymptotic method (OHAM) for nonlinear Kaup-Kupershmidt equation given in eq. (5.74) at various points of x and t taking $\lambda = 0.1, \mu = 0, w = 1$ and $\alpha = 1$.

x	$\left\|u_{Exact} - u_{OHAM}\right\|$								
	$t = 0.1$	$t = 0.2$	$t = 0.3$	$t = 0.4$	$t = 0.5$	$t = 0.6$	$t = 0.7$	$t = 0.8$	$t = 0.9$
0.1	3.4968E-10	3.6511E-9	6.5846E-9	9.1501E-9	1.1377E-8	1.3177E-8	1.4638E-8	1.5732E-8	1.6457E-8
0.2	7.2934E-6	7.2553E-6	7.2176E-6	7.1802E-6	7.1432E-6	7.1065E-6	7.0701E-6	7.0341E-6	6.9983E-6
0.3	2.6793E-5	2.6721E-5	2.6651E-5	2.6581E-5	2.6511E-5	2.6442E-5	2.6372E-5	2.6303E-5	2.6235E-5

0.4	5.8103E-5	5.8005E-5	5.7906E-5	5.7807E-5	5.7709E-5	5.7611E-5	5.7513E-5	5.7426E-5	5.7330E-5
0.5	1.0061E-4	1.0049E-4	1.0037E-4	1.0024E-4	1.0013E-4	1.0001E-4	9.9885E-5	9.9976E-5	9.9643E-5
0.6	1.5350E-4	1.5336E-4	1.5323E-4	1.5309E-4	1.5295E-4	1.5281E-4	1.5268E-4	1.5254E-4	1.5240E-4
0.7	2.1579E-4	2.1564E-4	2.1549E-4	2.1535E-4	2.1520E-4	2.1506E-4	2.1491E-4	2.1476E-4	2.1461E-4
0.8	2.8635E-4	2.8621E-4	2.8606E-4	2.8591E-4	2.8576E-4	2.8561E-4	2.8546E-4	2.8531E-4	2.8516E-4
0.9	3.6399E-4	3.6384E-4	3.6370E-4	3.6355E-4	3.6341E-4	3.6326E-4	3.6312E-4	3.6297E-4	3.6282E-4

Table 5.23   Comparison of absolute errors obtained by optimal homotopy asymptotic method (OHAM) for fractional order nonlinear Kaup-Kupershmidt equation given in eq. (5.74) at various points of x and t taking $\lambda = 0.1, \mu = 0, w = 1$ and $\alpha = 0.75$.

x	$|u_{Exact} - u_{OHAM}|$								
	$t = 0.1$	$t = 0.2$	$t = 0.3$	$t = 0.4$	$t = 0.5$	$t = 0.6$	$t = 0.7$	$t = 0.8$	$t = 0.9$
0.1	6.7141E-10	3.7954E-9	5.8412E-9	7.4404E-9	8.7416E-9	9.8151E-9	1.0702E-8	1.1428E-8	1.2015E-8
0.2	7.2899E-6	7.2528E-6	7.2254E-6	7.2014E-6	7.1794E-6	7.1589E-6	7.1395E-6	7.1209E-6	7.1032E-6
0.3	2.6785E-5	2.6716E-5	2.6665E-5	2.6620E-5	2.6578E-5	2.6540E-5	2.6503E-5	2.6467E-5	2.6434E-5
0.4	5.8094E-5	5.7998E-5	5.7926E-5	5.7862E-5	5.7804E-5	5.7749E-5	5.7697E-5	5.7647E-5	5.7599E-5
0.5	1.0060E-4	1.0048E-4	1.0039E-4	1.0031E-4	1.0024E-4	1.0017E-4	1.0011E-4	1.0005E-4	9.9992E-5
0.6	1.5349E-4	1.5335E-4	1.5326E-4	1.5317E-4	1.5308E-4	1.5301E-4	1.5293E-4	1.5286E-4	1.5279E-4
0.7	2.1577E-4	2.1563E-4	2.1552E-4	2.1543E-4	2.1534E-4	2.1526E-4	2.1518E-4	2.1511E-4	2.1503E-4
0.8	2.8634E-4	2.8619E-4	2.8608E-4	2.8599E-4	2.8590E-4	2.8582E-4	2.8574E-4	2.8566E-4	2.8559E-4
0.9	3.6397E-4	3.6384E-4	3.6373E-4	3.6364E-4	3.6355E-4	3.6347E-4	3.6339E-4	3.6331E-4	3.6324E-4

Table 5.24   Comparison of absolute errors obtained by optimal homotopy asymptotic method (OHAM) for fractional order nonlinear Kaup-Kupershmidt equation given in eq. (5.74) at various points of x and t taking $\lambda = 0.1, \mu = 0, w = 1$ and $\alpha = 0.5$.

x	$|u_{Exact} - u_{OHAM}|$								
	$t = 0.1$	$t = 0.2$	$t = 0.3$	$t = 0.4$	$t = 0.5$	$t = 0.6$	$t = 0.7$	$t = 0.8$	$t = 0.9$
0.1	1.2175E-9	3.7606E-9	4.9831E-9	5.8529E-9	6.5343E-9	7.0939E-9	7.5661E-8	7.9718E-9	8.3247E-9
0.2	7.2836E-6	7.2523E-6	7.2354E-6	7.2223E-6	7.2112E-6	7.2015E-6	7.1927E-6	7.1846E-6	7.1771E-6
0.3	2.6773E-5	2.6715E-5	2.6683E-5	2.6659E-5	2.6638E-5	2.6620E-5	2.6603E-5	2.6588E-5	2.6573E-5
0.4	5.8078E-5	5.7996E-5	5.7952E-5	5.7917E-5	5.7888E-5	5.7862E-5	5.7839E-5	5.7817E-5	5.7797E-5
0.5	1.0058E-4	1.0048E-4	1.0042E-4	1.0038E-4	1.0034E-4	1.0031E-4	1.0028E-4	1.0026E-4	1.0023E-4
0.6	1.5346E-4	1.5335E-4	1.5329E-4	1.5324E-4	1.5320E-4	1.5316E-4	1.5313E-4	1.5310E-4	1.5307E-4
0.7	2.1575E-4	2.1563E-4	2.1556E-4	2.1551E-4	2.1547E-4	2.1543E-4	2.1539E-4	2.1536E-4	2.1533E-4
0.8	2.8631E-4	2.8619E-4	2.8612E-4	2.8607E-4	2.8603E-4	2.8599E-4	2.8595E-4	2.8592E-4	2.8589E-4
0.9	3.6395E-4	3.6383E-4	3.6376E-4	3.6371E-4	3.6367E-4	3.6363E-4	3.6360E-4	3.6356E-4	3.6354E-4

Table 5.25 L_2 and L_∞ error norms for nonlinear time-fractional Kaup-Kupershmidt equation using two-dimensional Legendre multiwavelet methods and OHAM at various points x taking $\alpha = 0.5, 0.75$ and 1.

x	Error analysis with regard to Legendre multiwavelet						Error analysis with regard to OHAM					
	$\alpha = 1$		$\alpha = 0.75$		$\alpha = 0.5$		$\alpha = 1$		$\alpha = 0.75$		$\alpha = 0.5$	
	L_2	L_∞	L_2	L_∞	L_2	L_∞	L_2	L_∞	L_2	L_∞	L_2	L_∞
0.1	5.8488 E-9	3.1007 E-9	6.9992 E-9	3.4253 E-9	8.1275 E-9	3.6035 E-9	3.4295 E-8	1.6457 E-8	2.5818 E-8	7.2899 E-6	7.7622 E-8	8.3247 E-9
0.2	1.1764	6.2544	1.4079	6.9489	1.6515	7.3559	2.1434	7.2934	2.1557	1.2015	2.1653	7.2836

	E-8	E-9	E-8	E-9	E-8	E-9	E-5	E-6	E-5	E-8	E-5	E-6
0.3	1.7675 E-8	9.4057 E-9	2.1283 E-8	1.0469 E-8	2.4895 E-8	1.1105 E-8	7.9538 E-5	2.6793 E-5	7.9770 E-5	2.6785 E-5	7.9951 E-5	2.6773 E-5
0.4	2.3578 E-8	1.2553 E-8	2.8413 E-8	1.3986 E-8	3.3266 E-8	1.4850 E-8	1.7313 E-4	5.8103 E-5	1.7345 E-4	5.8094 E-5	1.7372 E-4	5.8078 E-5
0.5	2.9473 E-8	1.5695 E-8	3.5532 E-8	1.7497 E-8	4.1624 E-8	1.8589 E-8	3.0045 E-4	1.0061 E-4	3.0045 E-4	1.0060 E-4	3.0109 E-4	1.0058 E-4
0.6	3.2498 E-8	1.8832 E-8	4.2638 E-8	2.1001 E-8	4.9965 E-8	2.2321 E-8	4.5885 E-4	1.5350 E-4	4.5931 E-4	1.5349 E-4	4.5967 E-4	1.5346 E-4
0.7	4.1224 E-8	2.1960 E-8	4.9727 E-8	2.4497 E-8	5.8286 E-8	2.6044 E-8	6.4560 E-4	2.1579 E-4	6.4609 E-4	2.1577 E-4	6.4647 E-4	2.1575 E-4
0.8	4.7077 E-8	2.5081 E-8	5.6795 E-8	2.7983 E-8	6.6585 E-8	2.9756 E-8	8.5727 E-4	2.8635 E-4	8.5777 E-4	2.8634 E-4	8.5815 E-4	2.8631 E-4
0.9	5.2969 E-8	2.8191 E-8	6.3842 E-8	3.1458 E-8	7.6494 E-8	3.3457 E-8	1.0902 E-3	3.6399 E-4	1.0907 E-3	3.6397 E-4	1.0911 E-3	3.6395 E-4

It may be observed from Tables 5.19-5.24, absolute errors for Legendre multiwavelet method are lesser than that of OHAM. Moreover, L_2 and L_∞ error norms confirm that Legendre multiwavelet method provides more accurate and better solution than OHAM.

5.13 Conclusion

In this chapter, two dimensional Legendre wavelet method has been successfully implemented to obtain the numerical solution of fractional order parabolic partial differential equation subject to Dirichlet boundary conditions, fractional KBK equation and fractional sKdV equation. In case of fractional order PDE with Dirichlet boundary conditions, the acquired numerical results of Legendre wavelet methods are compared with exact solutions obtained by HPM as well as with numerical solution of Haar wavelet method. These results have been cited in the Tables in order to justify the accuracy and efficiency of the proposed schemes. For fractional order parabolic partial differential equation, Legendre wavelet method provides more accurate results than the Haar wavelet method as shown in Tables 5.1-5.5. In case of fractional KBK equation, the obtained results are compared with exact solutions. Agreement between present numerical results and exact solutions appear very satisfactory through illustrations in Tables 5.6-5.10. The obtained results demonstrate the efficiency, accuracy and reliability of the proposed algorithm based on two-dimensional Legendre wavelet method and its applicability to nonlinear time fractional KBK equation.

The fractional order sKdV equation has been solved by using two-dimensional Legendre wavelet method. The results are compared with exact solutions and also with homotopy

analysis method (HAM) and optimal HAM solutions. Tables 5.11-5.18 illustrate a pretty good agreement between present numerical results obtained by Legendre wavelet method with homotopy analysis method and exact solutions. The present scheme is very simple, effective and convenient for obtaining numerical solutions of nonlinear time-fractional seventh order KdV equation.

Next, the fractional Kaup-Kupershmidt equation has been solved numerically by using two-dimensional Legendre multiwavelet method and optimal homotopy asymptotic method (OHAM). The results obtained by Legendre multiwavelet method are then compared with exact solutions as well as with optimal homotopy asymptotic method (OHAM). One can observe a pretty good agreement between present numerical results obtained by Legendre multiwavelet method with optimal homotopy asymptotic method and exact solutions through illustrated results in Tables 5.19-5.25. The obtained results demonstrate the accuracy, efficiency and reliability of the proposed algorithm based on two-dimensional Legendre multiwavelet method and its applicability to nonlinear time-fractional Kaup-Kupershmidt equation. It may be observed from Tables 5.19-5.25, absolute errors for Legendre multiwavelet method are lesser than that of OHAM. Moreover, L_2 and L_∞ error norms confirm that Legendre multiwavelet method provides more accurate and better solution than OHAM. Thus, Legendre multiwavelet method provides more accurate and better solution in comparison to OHAM. The application of the proposed numerical method based on two-dimensional Legendre multiwavelet method for the solutions of time-fractional Kaup-Kupershmidt equation satisfactorily justifies its simplicity, efficiency and applicability. The present numerical scheme is quite simple, effective and expedient for obtaining numerical solution of fractional Kaup-Kupershmidt (KK) equation in comparison to analytical approach of OHAM.

6 Application of Chebyshev Wavelet Methods for Numerical Simulation of Fractional Differential Equations

6.1 Introduction

Nowadays, Chebyshev polynomials have become more significant in numerical evaluation. Among the four forms of Chebyshev polynomials, the first and second kinds are certain cases of the symmetric Jacobi polynomials, whereas the third and fourth kinds are unique instances of the non-symmetric Jacobi polynomials. Great attention has been focused on first and second kinds of Chebyshev polynomials $T_n(x)$ and $U_n(x)$ and their various uses in numerous applications. Nevertheless, there are very few articles that concentrate on the wavelets shaped through these two types of Chebyshev polynomials for application in fractional partial differential equations. This motivates our curiosity in such wavelets. In this chapter our aim is to study application of Chebyshev wavelets for the solution of fractional order differential equations. Moreover, the Chebyshev wavelets are competent for solving some fractional and integral equations [45, 46].

There are several advantages of using Chebyshev wavelets approximations based on collocation spectral method. First, unlike most numerical methods, it is now conventional that they are characterized by the use of exponentially decaying errors. Second, various numerical methods do not perform well near singularities, whereas approximations through wavelets effectively handle singularities in the problem. Also, due to their fast convergence, Chebyshev wavelets method does not undergo from the instability problems related with other numerical methods.

In this chapter, fractional order partial differential equations comprising Caputo fractional derivative and Riesz fractional derivative are considered. This chapter is devoted to study the application of Chebyshev wavelets for numerical solution of fractional differential equations involving Caputo and Riesz fractional derivative. The prime focus of the present chapter is to implement two-dimensional Chebyshev wavelet technique for solving nonlinear fractional differential equations like time-fractional Sawada-Kotera (SK) equation, Riesz fractional Camassa-Holm (CH) equation and Riesz fractional Sine-Gordon (SG) equation in order to demonstrate the efficiency and accuracy of the proposed method.

6.2 Outline of Present Study

Consider the following time-fractional generalized fifth-order Sawada-Kotera equation [129]

$$\frac{\partial^\alpha u}{\partial t^\alpha} + 45u^2 \frac{\partial u}{\partial x} + 15\frac{\partial u}{\partial x}\frac{\partial^2 u}{\partial x^2} + 15\frac{\partial^3 u}{\partial x^3}u + \frac{\partial^5 u}{\partial x^5} = 0, \qquad t > 0, \ x > 0 \tag{6.1}$$

which is the variation of the fifth-order Sawada-Kotera equation [49, 130-132]. Here $0 < \alpha \le 1$, is the parameter describing the order of the fractional time derivative. The fractional derivative is considered in the Caputo sense.

The classical Sawada-Kotera equation is an important mathematical model arising in many different physical contexts to describe motion of long waves in shallow water under gravity and in a one dimensional nonlinear lattice and has wide applications in quantum mechanics and nonlinear optics. It is well known that wave phenomena of plasma media and fluid dynamics are modelled by kink shaped tanh solution or by bell shaped sech solutions. This equation also used in modeling waves that propagate in opposite directions. There are a lot of studies for the classical Sawada-Kotera equation and some profound results have been established. But according to the best possible information of the authors, the detailed study of the nonlinear fractional order Sawada-Kotera equation is only beginning.

Consider the following Camassa-Holm equation with Riesz time-fractional derivative [133]

$$\begin{aligned}{}^R_0 D^\alpha_t u(x,t) + 2ku_x(x,t) - u_{xxt}(x,t) + 3u(x,t)u_x(x,t) - 2u_x(x,t)u_{xx}(x,t) - \\ u(x,t)u_{xxx}(x,t) = 0\end{aligned} \tag{6.2}$$

where $k \neq 0$ is a constant, and $u(x,t)$ is the unknown function depending on temporal variable t and spatial variable x. $_0^R D_t^\alpha$ is the Riesz fractional derivative.

The Camassa-Holm equation is used to describe physical model for the unidirectional propagation of waves in shallow water [134, 135]. This equation is widely used in fluid dynamics, continuum mechanics, aerodynamics, and models for shock wave formation, solitons, turbulence, mass transport, and the solution representing the water's free surface above a flat bottom [136, 137]. The Camassa–Holm equation has been obtained by Fokas and Fuchssteiner [138] and Lenells [139]. Camassa and Holm [140] put forward the derivation of the solution as a model for dispersive shallow water waves and revealed that it is formally integrable finite dimensional Hamiltonian system and its solitary waves are solitons. The classical Camassa-Holm equation has attracted much research interest in recent years both from analytical and numerical point of view and some exhaustive results have been established. The intension of the present work is to perform two-dimensional Chebyshev wavelet technique in order to exhibit the competency of this method for the numerical solution of nonlinear Camassa-Holm equations with the Riesz time-fractional derivative.

Next, a numerical process involving Chebyshev wavelet method has been implemented for computing the approximate solution of Riesz space fractional sine-Gordon equation (SGE). The fractional sine-Gordon equation is considered as an interpolation between the classical Sine-Gordon equation equation (corresponding to $\alpha = 2$) and nonlocal sine-Gordon equation (corresponding to $\alpha = 1$).

Consider the Riesz space fractional sine-Gordon equation proposed in [141, 142] as follows:

$$u_{tt} - {}^R D_x^\alpha u + \sin u = 0, \quad 1 < \alpha \leq 2, \tag{6.3}$$

where ${}^R D_x^\alpha$ denotes the Riesz fractional derivative. Eq. (6.3) is the variation of the sine-Gordon equation. The classical sine-Gordon equation, an elementary equation of modern nonlinear wave theory has accomplished great repute primarily due to its substantiated applications in diverse fields of science and engineering. It arises in various disciplines of physics, such as propagation of magnetic flux on Josephson junctions, propagation of optical pulses in resonant laser media, field theory, sound propagation in a crystal lattice, in ferromagnetism and ferroelectric substances and in nonlinear optics etc. [132, 143]. In

these applications, the sine-Gordon equation provides the simplest nonlinear description of physical phenomena in different configurations. The more adequate modelling can be prevailed corresponding to generalization of classical sine-Gordon equation. In particular, taking into account of nonlinear effects, corresponding to long-rang interactions of particles, complex law of medium dispersion or curvilinear geometry of the initial boundary problem, classical sine-Gordon equation results in nonlocal generalization of SGE.

Various methods such as the homotopy analysis method [144], modified decomposition method [145], variational iteration method [146], and tanh method [147] have been implemented to evaluate approximate analytical solution of the classical sine-Gordon equation. Using numerical experiments, Ablowitz et al. [148] examined the numerical behaviour of a double-discrete, completely integrable discretization of the sine-Gordon equation. Herbst and Ablowitz [149] provided the numerical results of the sine-Gordon equation acquired by use of the explicit symplectic method. However the comprehensive study of the fractional sine-Gordon equation is only the beginning. In this work, we will consider fractional sine-Gordon equation with a number of initial values. The motivation of the present work is to establish that the Chebyshev wavelet method as a powerful tool for solving the Riesz factional sine-Gordon equation.

6.3 Formulation of Time-Fractional Sawada-Kotera Equation

Consider the following generalized Sawada-Kotera equation

$$\frac{\partial u}{\partial t} + au^2 \frac{\partial u}{\partial x} + b\frac{\partial u}{\partial x}\frac{\partial^2 u}{\partial x^2} + c\frac{\partial^3 u}{\partial x^3}u + d\frac{\partial^5 u}{\partial x^5} = 0, \tag{6.4}$$

where a, b, c and d are constants, $u(x,t)$ is a field variable, $x \in \Omega$ is a space coordinate in the propagation direction of the field, and $t \in \Gamma$ is the time. Employing a potential function $v(x,t)$ on the field variable and setting $u(x,t) = v_x(x,t)$ yields the potential equation of the Sawada-Kotera equation (6.4) in the form

$$v_{xt}(x,t) + av_x^2(x,t)v_{xx}(x,t) + bv_{xx}(x,t)v_{xxx}(x,t) + cv_{xxxx}(x,t)v_x(x,t) + dv_{6x}(x,t) = 0 .\tag{6.5}$$

The functional of the potential equation (6.5) can be represented as

$$J(v) = \int_\Omega dx \int_\Gamma \left[v(x,t) \left[c_1 v_{xt}(x,t) + c_2 a v_x^2(x,t) v_{xx}(x,t) + c_3 b v_{xx}(x,t) v_{xxx}(x,t) \right. \right.$$

$$\left. \left. + c_4 c v_{xxxx}(x,t) v_x(x,t) + c_5 d v_{6x}(x,t) \right] \right] dt \qquad (6.6)$$

where c_1, c_2, c_3, c_4 and c_5 are unknown constants to be determined. Integrating eq. (6.6) by parts and taking $v_t|_\Omega = v_x|_\Omega = v_{xx}|_\Omega = v_{xxx}|_\Omega = v_{5x}|_\Omega = 0$ yield

$$J(v) = \int_\Omega dx \int_\Gamma \left[-c_1 v_t(x,t) v_x(x,t) - \frac{c_2 a}{3} v_x^4(x,t) + \left(\frac{c_4 c}{2} - \frac{b c_3}{2} \right) v_x(x,t) v_{xx}^2(x,t) - \right.$$

$$\left. c_4 c v_x^2(x,t) v_{xxx}(x,t) + c_5 d v_x(x,t) v_{5x}(x,t) \right] dt. \qquad (6.7)$$

The constants $c_1, c_2, c_3, c_4,$ and c_5 can be determined taking the variation of the functional (6.7) to make it optimal. Integrating each term by parts and using the variation optimum condition of the functional $J(v)$, the following expression can be obtained:

$$2c_1 v_{xt}(x,t) + 4c_2 a v_x^2(x,t) v_{xx}(x,t) + c_3 b v_{xx}(x,t) v_{xxx}(x,t)$$

$$- 2c_4 c v_{xxxx}(x,t) v_x(x,t) - 2c_5 d v_{6x}(x,t) = 0 . \qquad (6.8)$$

Comparing the obtained result in eq. (6.8) with the equivalent eq. (6.5), we get

$$c_1 = \frac{1}{2}, \quad c_2 = \frac{1}{4}, \quad c_3 = 1, \quad c_4 = -\frac{1}{2}, \quad \text{and} \quad c_5 = -\frac{1}{2}.$$

The functional expression given by eq. (6.7) obtains directly the Lagrangian form of the Sawada-Kotera equation:

$$L(v_t, v_x, v_{xx}, v_{xxx}, v_{5x}) = -\frac{1}{2} v_t(x,t) v_x(x,t) - \frac{a}{12} v_x^4(x,t) - \left(\frac{2b+c}{4} \right) v_x(x,t) v_{xx}^2(x,t)$$

$$+ \frac{c}{2} v_x^2(x,t) v_{xxx}(x,t) - \frac{d}{2} v_x(x,t) v_{5x}(x,t). \qquad (6.9)$$

Similarly, the Lagrangian of the time-fractional Sawada-Kotera equation can be written as

$$F\left({}_0 D_t^\alpha v, v_x, v_{xx}, v_{xxx}, v_{5x} \right) = -\frac{1}{2} \, {}_0 D_t^\alpha v(x,t) v_x(x,t) - \frac{a}{12} v_x^4(x,t)$$

$$- \left(\frac{2b+c}{4} \right) v_x(x,t) v_{xx}^2(x,t) + \frac{c}{2} v_x^2(x,t) v_{xxx}(x,t) - \frac{d}{2} v_x(x,t) v_{5x}(x,t). \qquad (6.10)$$

Then the functional of the time-fractional Sawada-Kotera equation will be

$$J(v) = \int_\Omega dx \int_\Gamma F\left({}_0 D_t^\alpha v, v_x, v_{xx}, v_{xxx}, v_{5x} \right) dt .$$

The variation of above functional w.r.t $v(x,t)$ leads to

$$\delta J(v) = \int_\Omega dx \int_\Gamma \left[\frac{\partial F}{\partial\, _0D_t^\alpha v}\, \delta\left(_0D_t^\alpha v(x,t)\right) + \frac{\partial F}{\partial v_x}\, \delta v_x(x,t) + \frac{\partial F}{\partial v_{xx}}\, \delta v_{xx}(x,t) + \right.$$

$$\left. \frac{\partial F}{\partial v_{xxx}}\, \delta v_{xxx}(x,t) + \frac{\partial F}{\partial v_{5x}}\, \delta v_{5x}(x,t) \right] dt. \tag{6.11}$$

By Lemma 4.1, upon integrating the right-hand side of eq. (6.11), we have

$$\delta J(v) = \int_\Omega dx \int_\Gamma \left[_tD_T^\alpha \left(\frac{\partial F}{\partial\, _0D_t^\alpha v} \right) - \frac{\partial}{\partial x} \left(\frac{\partial F}{\partial v_x} \right) + \frac{\partial^2}{\partial x^2} \left(\frac{\partial F}{\partial v_{xx}} \right) \right.$$

$$\left. - \frac{\partial^3}{\partial x^3} \left(\frac{\partial F}{\partial v_{xxx}} \right) - \frac{\partial^5}{\partial x^5} \left(\frac{\partial F}{\partial v_{5x}} \right) \right] \delta v(x,t) dt. \tag{6.12}$$

Optimizing the variation of the functional $J(v)$, i.e. $\delta J(v) = 0$, yields the Euler–Lagrange equation for the time-fractional Sawada-Kotera equation in the following expression:

$$_tD_T^\alpha \left(\frac{\partial F}{\partial\, _0D_t^\alpha v} \right) - \frac{\partial}{\partial x} \left(\frac{\partial F}{\partial v_x} \right) + \frac{\partial^2}{\partial x^2} \left(\frac{\partial F}{\partial v_{xx}} \right) - \frac{\partial^3}{\partial x^3} \left(\frac{\partial F}{\partial v_{xxx}} \right) - \frac{\partial^5}{\partial x^5} \left(\frac{\partial F}{\partial v_{5x}} \right) = 0 \tag{6.13}$$

Substituting the Lagrangian of the time-fractional Sawada-Kotera equation (6.10) into Euler–Lagrange formula (6.13) yields

$$-_tD_T^\alpha v_x(x,t) + _0D_t^\alpha v_x(x,t) + 2av_x^2(x,t)v_{xx}(x,t) - (4b+10c)v_{xx}(x,t)v_{xxx}(x,t) -$$

$$(2b+3c)v_{xxxx}(x,t)v_x(x,t) + 2dv_{6x}(x,t) = 0.$$

Substituting the potential function $v_x(x,t) = u(x,t)$ and taking $a = \dfrac{45}{2}, b = \dfrac{-105}{8}, c = \dfrac{15}{4},$

and $d = \dfrac{1}{2}$ yields

$$-_tD_T^\alpha u(x,t) + _0D_t^\alpha u(x,t) + 45u^2(x,t)u_x(x,t) + 15u_x(x,t)u_{xx}(x,t)$$

$$+ 15u_{xxx}(x,t)u(x,t) + u_{5x}(x,t) = 0. \tag{6.14}$$

The right-hand side Riemann–Liouville fractional derivative is interpreted as a future state of the process in physics. So the right-derivative is generally neglected in applications, when the present state of the process does not depend on the results of the future development, and so the right-derivative in eq. (6.14) can be neglected. Hence the time-fractional Sawada-Kotera equation can be represented by

$$_0D_t^\alpha u(x,t) + 45u^2(x,t)u_x(x,t) + 15u_x(x,t)u_{xx}(x,t) + 15u_{xxx}(x,t)u(x,t) + u_{5x}(x,t) = 0. \tag{6.15}$$

6.4 Application of Analytical and Numerical Methods for Solving Fractional Sawada-Kotera Equation

6.4.1 Implementation of Chebyshev Wavelet on Time-Fractional Sawada-Kotera Equation

To show the effectiveness and accuracy of proposed scheme, we consider the time-fractional Sawada-Kotera equation. The numerical solutions thus obtained are compared with the exact solutions for classical case and also solutions obtained by HAM in fractional order case.

Consider the nonlinear time-fractional generalized Sawada-Kotera equation [150]

$$\frac{\partial^\alpha u}{\partial t^\alpha} + 45u^2 \frac{\partial u}{\partial x} + 15\frac{\partial u}{\partial x}\frac{\partial^2 u}{\partial x^2} + 15\frac{\partial^3 u}{\partial x^3}u + \frac{\partial^5 u}{\partial x^5} = 0, \qquad (6.16)$$

with initial condition $u(x,t_0) = g(x)$.

The Chebyshev wavelet solution of $u(x,t)$ is sought by assuming that $u(x,t)$ can be expanded in terms of Chebyshev wavelet as

$$u(x,t) = \sum_{n=1}^{2^{k_1-1}} \sum_{i=0}^{M_1-1} \sum_{l=1}^{2^{k_2-1}} \sum_{j=0}^{M_2-1} c_{n,i,l,j}\, \psi_{n,i,l,j}(x,t), \qquad (6.17)$$

where $n = 1,...,2^{k_1-1}, i = 0,...,M_1-1, l = 1,...,2^{k_2-1}, j = 0,...,M_2-1.$

The nonlinear terms presented in eq. (6.16) can be approximated using Chebyshev wavelet function as

$$u^2 \frac{\partial u}{\partial x} = \sum_{n=1}^{2^{k_1-1}} \sum_{i=0}^{M_1-1} \sum_{l=1}^{2^{k_2-1}} \sum_{j=0}^{M_2-1} a_{n,i,l,j}\, \psi_{n,i,l,j}(x,t), \qquad (6.18)$$

and

$$\frac{\partial u}{\partial x}\frac{\partial^2 u}{\partial x^2} + \frac{\partial^3 u}{\partial x^3}u = \sum_{n=1}^{2^{k_1-1}} \sum_{i=0}^{M_1-1} \sum_{l=1}^{2^{k_2-1}} \sum_{j=0}^{M_2-1} b_{n,i,l,j}\, \psi_{n,i,l,j}(x,t). \qquad (6.19)$$

This implies

$$\left(\sum_{n=1}^{2^{k_1-1}} \sum_{i=0}^{M_1-1} \sum_{l=1}^{2^{k_2-1}} \sum_{j=0}^{M_2-1} c_{n,i,l,j}\psi_{n,i,l,j}(x,t)\right)^2 \left[\sum_{n=1}^{2^{k_1-1}} \sum_{i=0}^{M_1-1} \sum_{l=1}^{2^{k_2-1}} \sum_{j=0}^{M_2-1} c_{n,i,l,j} \frac{\partial \psi_{n,i,l,j}(x,t)}{\partial x}\right] =$$
$$\sum_{n=1}^{2^{k_1-1}} \sum_{i=0}^{M_1-1} \sum_{l=1}^{2^{k_2-1}} \sum_{j=0}^{M_2-1} a_{n,i,l,j}\, \psi_{n,i,l,j}(x,t), \qquad (6.20)$$

and

$$\left(\sum_{n=1}^{2^{k_1-1}}\sum_{i=0}^{M_1-1}\sum_{l=1}^{2^{k_2-1}}\sum_{j=0}^{M_2-1}c_{n,i,l,j}\frac{\partial\psi_{n,i,l,j}(x,t)}{\partial x}\right)\left[\sum_{n=1}^{2^{k_1-1}}\sum_{i=0}^{M_1-1}\sum_{l=1}^{2^{k_2-1}}\sum_{j=0}^{M_2-1}c_{n,i,l,j}\frac{\partial^2\psi_{n,i,l,j}(x,t)}{\partial x^2}\right]+$$

$$\left(\sum_{n=1}^{2^{k_1-1}}\sum_{i=0}^{M_1-1}\sum_{l=1}^{2^{k_2-1}}\sum_{j=0}^{M_2-1}c_{n,i,l,j}\frac{\partial^3\psi_{n,i,l,j}(x,t)}{\partial x^3}\right)\left[\sum_{n=1}^{2^{k_1-1}}\sum_{i=0}^{M_1-1}\sum_{l=1}^{2^{k_2-1}}\sum_{j=0}^{M_2-1}c_{n,i,l,j}\psi_{n,i,l,j}(x,t)\right] \qquad (6.21)$$

$$=\sum_{n=1}^{2^{k_1-1}}\sum_{i=0}^{M_1-1}\sum_{l=1}^{2^{k_2-1}}\sum_{j=0}^{M_2-1}b_{n,i,l,j}\,\psi_{n,i,l,j}(x,t).$$

Again applying J_t^α on both sides of eq. (6.16), we have

$$u(x,t)-u(x,0)=J_t^\alpha\left[-45u^2\frac{\partial u}{\partial x}-15\left(\frac{\partial u}{\partial x}\frac{\partial^2 u}{\partial x^2}+\frac{\partial^3 u}{\partial x^3}u\right)-\frac{\partial^5 u}{\partial x^5}\right]. \qquad (6.22)$$

Putting eqs. (6.17), (6.18) and (6.19) in eq. (6.22), we have

$$\sum_{n=1}^{2^{k_1-1}}\sum_{i=0}^{M_1-1}\sum_{l=1}^{2^{k_2-1}}\sum_{j=0}^{M_2-1}c_{n,i,l,j}\psi_{n,i,l,j}(x,t)-u(x,0)$$

$$=J_t^\alpha\left[-45\left(\sum_{n=1}^{2^{k_1-1}}\sum_{i=0}^{M_1-1}\sum_{l=1}^{2^{k_2-1}}\sum_{j=0}^{M_2-1}a_{n,i,l,j}\psi_{n,i,l,j}(x,t)\right)\right.$$

$$-15\left(\sum_{n=1}^{2^{k_1-1}}\sum_{i=0}^{M_1-1}\sum_{l=1}^{2^{k_2-1}}\sum_{j=0}^{M_2-1}b_{n,i,l,j}\psi_{n,i,l,j}(x,t)\right) \qquad (6.23)$$

$$\left.-\sum_{n=1}^{2^{k_1-1}}\sum_{i=0}^{M_1-1}\sum_{l=1}^{2^{k_2-1}}\sum_{j=0}^{M_2-1}c_{n,i,l,j}\frac{\partial^5\psi_{n,i,l,j}(x,t)}{\partial x^5}\right].$$

Now substituting the collocation points $x_l=\dfrac{l-0.5}{2^{k_1-1}M_1}$ and $t_r=\dfrac{r-0.5}{2^{k_2-1}M_2}$ for

$l=1,2,\ldots,2^{k_1-1}M_1$ and $r=1,2,\ldots,2^{k_2-1}M_2$ in eqs. (6.20), (6.21) and (6.23), we have $3\left(2^{k_1-1}M_1\right)\left(2^{k_2-1}M_2\right)$ equations in $3\left(2^{k_1-1}M_1\right)\left(2^{k_2-1}M_2\right)$ unknowns in $a_{n,i,l,j}$, $b_{n,i,l,j}$ and $c_{n,i,l,j}$. By solving this system of equations using mathematical software, the Chebyshev wavelet coefficients $a_{n,i,l,j}$, $b_{n,i,l,j}$ and $c_{n,i,l,j}$ can be obtained.

6.4.2 Comparison with HAM for Solution of Time-Fractional Sawada-Kotera Equation

Consider the nonlinear time-fractional generalized Sawada-Kotera equation [150]

$$\frac{\partial^\alpha u}{\partial t^\alpha} + 45u^2 \frac{\partial u}{\partial x} + 15u \frac{\partial^2 u}{\partial x^2} + 15 \frac{\partial^3 u}{\partial x^3} u + \frac{\partial^5 u}{\partial x^5} = 0, \tag{6.24}$$

subject to the initial condition [131]

$$u(x,0) = 2k^2 \sec h^2(k(x-\lambda)),$$

where $k\ (\neq 0)$ and λ are arbitrary constants and $0 < \alpha \leq 1$.

To obtain the approximate solution of the time-fractional Sawada-Kotera equation (6.24), we choose the linear operator

$$L[\phi(x,t;p)] = D_t^\alpha \phi(x,t;p). \tag{6.25}$$

Now, we construct the m th order deformation equation for eq. (6.24) as follows [34 ,151-153]

$$L[u_m(x,t) - \chi_m u_{m-1}(x,t)] = \hbar \Re_m(u_0, u_1, ..., u_{m-1}), \tag{6.26}$$

where $\Re_m(u_0, u_1, ..., u_{m-1}) = \dfrac{1}{(m-1)!} \dfrac{\partial^{m-1} N[\phi(x,t;p)]}{\partial p^{m-1}} \Bigg|_{p=0}. \tag{6.27}$

$$N[\phi(x,t;p)] = D_t^\alpha \phi(x,t;p) + 45(\phi(x,t;p))^2 \frac{\partial \phi(x,t;p)}{\partial x} + 15 \frac{\partial \phi(x,t;p)}{\partial x} \frac{\partial^2 \phi(x,t;p)}{\partial x^2}$$
$$+ 15 \frac{\partial^3 \phi(x,t;p)}{\partial x^3} \phi(x,t;p) + \frac{\partial^5 \phi(x,t;p)}{\partial x^5},$$

and $\phi(x,t;p) = u_0(x,t) + \displaystyle\sum_{m=1}^{\infty} p^m u_m(x,t),$

$$u_m(x,t) = \frac{1}{m!} \frac{\partial^m \phi(x,t;p)}{\partial p^m} \Bigg|_{p=0}.$$

Now the solution of the first deformation equation in eq. (6.26) is given by

$$u_1(x,t) = \hbar J_t^\alpha \left[\frac{\partial^\alpha u_0}{\partial t^\alpha} + 45u_0^2 \frac{\partial u_0}{\partial x} + 15 \frac{\partial u_0}{\partial x} \frac{\partial^2 u_0}{\partial x^2} + 15 \frac{\partial^3 u_0}{\partial x^3} u_0 + \frac{\partial^5 u_0}{\partial x^5} \right]. \tag{6.28}$$

Similarly, the solutions of second, third and fourth order deformation equations are

$$u_2(x,t) = u_1(x,t) + \hbar J_t^\alpha \left[\frac{\partial^\alpha u_1}{\partial t^\alpha} + 90u_0 u_1 \frac{\partial u_0}{\partial x} + 45u_0^2 \frac{\partial u_1}{\partial x} + 15\left(\frac{\partial u_0}{\partial x} \frac{\partial^2 u_1}{\partial x^2} + \frac{\partial u_1}{\partial x} \frac{\partial^2 u_0}{\partial x^2} \right) \right.$$
$$\left. + 15\left(\frac{\partial^3 u_1}{\partial x^3} u_0 + \frac{\partial^3 u_0}{\partial x^3} u_1 \right) + \frac{\partial^5 u_1}{\partial x^5} \right], \tag{6.29}$$

$$u_3(x,t) = u_2(x,t) + \hbar\, J_t^\alpha \left[\frac{\partial^\alpha u_2}{\partial t^\alpha} + 45\left(u_1^{\,2}\frac{\partial u_0}{\partial x} + 2u_0 u_2\frac{\partial u_0}{\partial x} + 2u_0 u_1\frac{\partial u_1}{\partial x} + u_0^{\,2}\frac{\partial u_2}{\partial x} \right) + \right.$$

$$\left. 15\left(\frac{\partial u_0}{\partial x}\frac{\partial^2 u_2}{\partial x^2} + \frac{\partial u_1}{\partial x}\frac{\partial^2 u_1}{\partial x^2} + \frac{\partial u_2}{\partial x}\frac{\partial^2 u_0}{\partial x^2} \right) + 15\left(\frac{\partial^3 u_2}{\partial x^3}u_0 + \frac{\partial^3 u_1}{\partial x^3}u_1 + \frac{\partial^3 u_0}{\partial x^3}u_2 \right) + \frac{\partial^5 u_2}{\partial x^5} \right], \quad (6.30)$$

$$u_4(x,t) = u_3(x,t) + \hbar\, J_t^\alpha \left[\frac{\partial^\alpha u_3}{\partial t^\alpha} + 45\left(2u_1 u_2\frac{\partial u_0}{\partial x} + 2u_0 u_3\frac{\partial u_0}{\partial x} + u_1^{\,2}\frac{\partial u_1}{\partial x} + 2u_0 u_2\frac{\partial u_1}{\partial x} + \right.\right.$$

$$\left. 2u_0 u_1\frac{\partial u_2}{\partial x} + u_0^{\,2}\frac{\partial u_3}{\partial x} \right) + 15\left(\frac{\partial u_0}{\partial x}\frac{\partial^2 u_3}{\partial x^2} + \frac{\partial u_1}{\partial x}\frac{\partial^2 u_2}{\partial x^2} + \frac{\partial u_2}{\partial x}\frac{\partial^2 u_1}{\partial x^2} + \frac{\partial u_3}{\partial x}\frac{\partial^2 u_0}{\partial x^2} \right) + \quad (6.31)$$

$$\left. 15\left(\frac{\partial^3 u_3}{\partial x^3}u_0 + \frac{\partial^3 u_2}{\partial x^3}u_1 + \frac{\partial^3 u_1}{\partial x^3}u_2 + \frac{\partial^3 u_0}{\partial x^3}u_3 \right) + \frac{\partial^5 u_3}{\partial x^5} \right],$$

and so on.

By putting the initial condition $u_0 = u(x,0)$ in eqs. (6.28)-(6.31) and solving them, we obtain the expressions for u_1, u_2, u_3, u_4 and so on.

Finally, the approximate solution for time fractional fifth-order Sawada-Kotera equation is given by

$$u = u_1(x,t) + u_2(x,t) + u_3(x,t) + u_4(x,t) + \dots \quad (6.32)$$

6.5 Numerical Results of Fractional Sawada-Kotera Equation

The comparison of the absolute errors for time-fractional fifth-order Sawada-Kotera equation (6.16) has been exhibited in Table 6.1 which is constructed using the results obtained by Chebyshev wavelet method at different values of x and t taking $\alpha = 1$. Similarly Table 6.2 shows the comparison of approximate solutions of fractional order Sawada-Kotera equation (6.16) at various points of x and t taking $\alpha = 0.5$. Agreement between present numerical results and exact solutions appears very satisfactory through illustrations in Tables 6.1 and 6.2. To show the accuracy of proposed method L_2 and L_∞ error norms for classical order nonlinear Sawada-Kotera equation have been presented in Table 6.3. In the present analysis, to examine the accuracy and reliability of the Chebyshev wavelets for solving fractional order Sawada-Kotera equation, we compare the approximate solution of Chebyshev wavelet with the fifth-order approximate solution

obtained by HAM taking $\hbar = -1$. As pointed out by Liao [33], in general, by means of the so-called $\hbar$-curve, it is straight forward to choose a proper value of $\hbar$ which ensures the convergence of series solution. To investigate the influence of $\hbar$ on the solution series, we plot $\hbar$-curve of partial derivatives of $u(x,t)$ obtained from the fifth order HAM solution as shown in Figure 6.1.
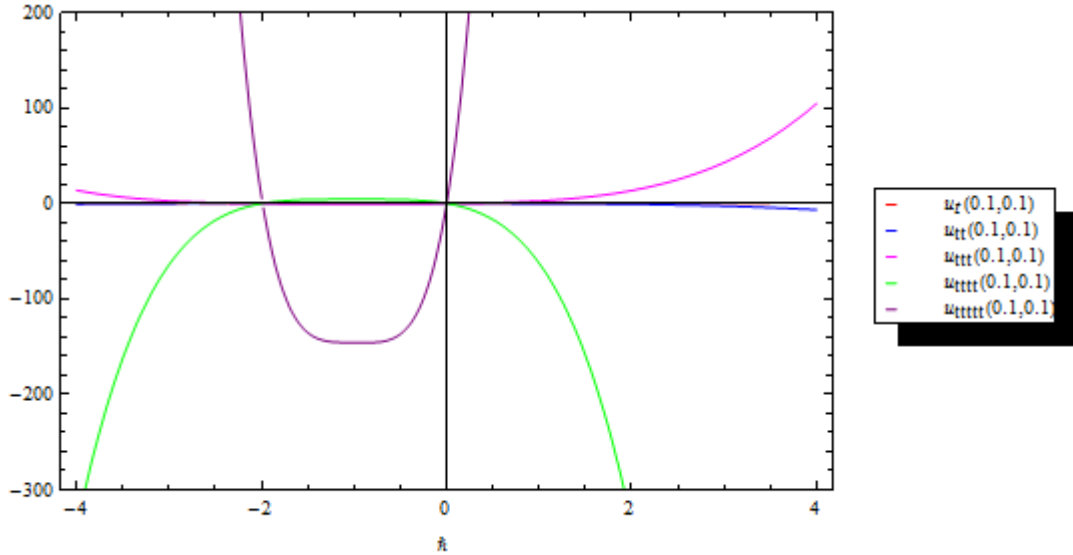
Figure 6.1 The $\hbar$-curve for partial derivatives of $u(x,t)$ for the 5th order HAM solution taking $x = 0.1, t = 0.1$ and $\alpha = 0.5$.

Table 6.1 Comparison of absolute errors obtained by two-dimensional Chebyshev wavelet method for classical nonlinear Sawada-Kotera equation given in eq. (6.16) at various points of x and t taking $\alpha = 1$.

x	$\|u_{Exact} - u_{CWM}\|$									
	$t = 0$	$t = 0.1$	$t = 0.2$	$t = 0.3$	$t = 0.4$	$t = 0.5$	$t = 0.6$	$t = 0.7$	$t = 0.8$	$t = 0.9$
0.1	2.3394E-3	1.3646E-3	2.3696E-3	2.9815E-3	3.8367E-3	4.6925E-3	5.2186E-3	5.7875E-3	8.2658E-3	1.6805E-2
0.2	2.6097E-3	1.0767E-3	1.9063E-3	2.3403E-3	3.0586E-3	3.7661E-3	3.9981E-3	3.9267E-3	5.1666E-3	1.1581E-3
0.3	2.8468E-3	8.7155E-4	1.5326E-3	1.7868E-3	2.3576E-3	2.8825E-3	2.7549E-3	1.9657E-3	1.9447E-3	6.4023E-3
0.4	3.0282E-3	7.5225E-4	1.2490E-3	1.3226E-3	1.7342E-3	2.0403E-3	1.4875E-3	9.2722E-5	1.3891E-3	1.2842E-3
0.5	3.1322E-3	7.2105E-4	1.0555E-3	9.4823E-4	1.1879E-3	1.2373E-3	1.9461E-4	2.2433E-3	4.8194E-3	3.7539E-3
0.6	3.1383E-3	7.7914E-4	9.5098E-4	6.6340E-4	7.1781E-4	4.7117E-4	1.1238E-3	4.4781E-3	8.3267E-3	8.6876E-3
0.7	3.0277E-3	9.2665E-4	9.3356E-4	4.6693E-4	3.2177E-4	2.6046E-4	2.4666E-3	6.7864E-3	1.1887E-2	1.3488E-2
0.8	2.7843E-3	1.1626E-3	1.0005E-3	3.5681E-4	2.6502E-6	9.5989E-4	3.8313E-3	9.1541E-3	1.5473E-2	1.8125E-2
0.9	2.3953E-3	1.4847E-3	1.1484E-3	3.3029E-4	2.5848E-4	1.6291E-3	5.2136E-3	1.1564E-2	1.9051E-2	2.2563E-2

Table 6.2 Comparison of approximate solutions obtained by two-dimensional Chebyshev wavelet method and homotopy analysis method for fractional order nonlinear Sawada-Kotera equation given in eq. (6.16) at various points of x and t taking $\hbar = -1$ and $\alpha = 0.5$.

x	$t=0.05$		$t=0.1$		$t=0.15$		$t=0.2$		$t=0.25$		$t=0.3$		$t=0.35$		$t=0.4$	
	u_{CWM}	u_{HAM}	u_{CWM}	u_{HAM}	u_{CWM}	u_{HAM}	u_{CWM}	u_{HAM}	u_{CWM}	u_{HAM}	u_{CWM}	u_{HAM}	u_{CWM}	u_{HAM}	u_{CWM}	u_{HAM}
0.1	0.166651	0.17821	0.171782	0.178058	0.174807	0.177938	0.17661	0.177836	0.177852	0.177748	0.178998	0.177669	0.180348	0.177598	0.182066	0.177734
0.2	0.169437	0.179118	0.173314	0.179009	0.175723	0.178924	0.177294	0.178853	0.178503	0.178792	0.179687	0.17874	0.18107	0.178696	0.182778	0.178657
0.3	0.172229	0.179707	0.174756	0.179643	0.176499	0.179592	0.177818	0.179552	0.17899	0.179518	0.180218	0.179492	0.181640	0.179471	0.183341	0.179457
0.4	0.175030	0.179975	0.176107	0.179954	0.177132	0.179938	0.178179	0.179927	0.179311	0.17992	0.180586	0.179917	0.182052	0.179919	0.183749	0.179925
0.5	0.177842	0.179919	0.177367	0.179942	0.177622	0.179959	0.178374	0.179976	0.179461	0.179993	0.180786	0.180012	0.182301	0.180034	0.183996	0.180058
0.6	0.180668	0.17954	0.178538	0.179606	0.177968	0.179655	0.178402	0.179698	0.179439	0.179738	0.180816	0.179777	0.182382	0.179816	0.184077	0.179855
0.7	0.183505	0.178839	0.17962	0.178948	0.178172	0.179029	0.178264	0.179097	0.179244	0.179158	0.180673	0.179214	0.182292	0.179268	0.183986	0.17932
0.8	0.186351	0.177824	0.180614	0.177973	0.178235	0.178084	0.177961	0.178176	0.178875	0.178256	0.180356	0.178329	0.182029	0.178396	0.183721	0.17846
0.9	0.189198	0.17650	0.18152	0.176689	0.178161	0.176629	0.177496	0.176944	0.178335	0.177043	0.179865	0.17713	0.181591	0.17721	0.183278	0.177283

Table 6.3 L_2 and L_∞ error norms for nonlinear time-fractional Sawada-Kotera equation using two-dimensional Chebyshev wavelet method at various points of t taking $\alpha = 1$.

t	L_2	L_∞
0	2.82595E-3	3.1383E-3
0.1	1.04820E-3	1.4847E-3
0.2	1.42858E-3	2.3696E-3
0.3	1.53123E-3	2.9815E-3
0.4	1.96462E-3	3.8367E-3
0.5	2.45110E-3	4.6925E-3
0.6	3.37089E-3	5.2186E-3
0.7	6.15247E-3	1.1564E-2
0.8	1.02032E-2	1.9051E-2
0.9	1.26293E-2	2.2563E-2

6.6   Application of Two-Dimensional Chebyshev Wavelet Method on Time-Fractional Camassa-Holm Equation

Consider the nonlinear Camassa-Holm equations with the Riesz time-fractional derivative [133]

$$
{}_0^R D_t^\alpha u(x,t) + 2k u_x(x,t) - \frac{2}{3} u_{xxt}(x,t) + 3u(x,t)u_x(x,t) + u_x(x,t)u_{xx}(x,t)
$$
$$
+ \frac{1}{2} u(x,t)u_{xxx}(x,t) = 0, \tag{6.33}
$$

with initial condition [133]

$$
u(x,0) = -k + k\sinh(x) . \tag{6.34}
$$

184

The Chebyshev wavelet solution of $u(x,t)$ is sought by assuming that $u(x,t)$ can be expanded in terms of Chebyshev wavelet as

$$u(x,t) = \sum_{n=1}^{2^{k_1-1}} \sum_{i=0}^{M_1-1} \sum_{l=1}^{2^{k_2-1}} \sum_{j=0}^{M_2-1} c_{n,i,l,j}\, \psi_{n,i,l,j}(x,t),$$ (6.35)

where $n = 1,...,2^{k_1-1}, i = 0,...,M_1 - 1,\ l = 1,...,2^{k_2-1},\ j = 0,...,M_2 - 1$.

Substituting eq. (6.35) in eq. (6.33), we will have

$$\left(\sum_{n=1}^{2^{k_1-1}} \sum_{i=0}^{M_1-1} \sum_{l=1}^{2^{k_2-1}} \sum_{j=0}^{M_2-1} c_{n,i,l,j}\, {}_{0}^{R}D_t^{\alpha}\left(\psi_{n,i,l,j}(x,t)\right) \right) + 2k \left[\sum_{n=1}^{2^{k_1-1}} \sum_{i=0}^{M_1-1} \sum_{l=1}^{2^{k_2-1}} \sum_{j=0}^{M_2-1} c_{n,i,l,j}\, \frac{\partial \psi_{n,i,l,j}(x,t)}{\partial x} \right]$$

$$- \frac{2}{3}\left(\sum_{n=1}^{2^{k_1-1}} \sum_{i=0}^{M_1-1} \sum_{l=1}^{2^{k_2-1}} \sum_{j=0}^{M_2-1} c_{n,i,l,j}\, \frac{\partial^3 \psi_{n,i,l,j}(x,t)}{\partial x^2 \partial t} \right) + 3\left[\left(\sum_{n=1}^{2^{k_1-1}} \sum_{i=0}^{M_1-1} \sum_{l=1}^{2^{k_2-1}} \sum_{j=0}^{M_2-1} c_{n,i,l,j} \psi_{n,i,l,j}(x,t) \right) \right.$$

$$\times \left. \left(\sum_{n=1}^{2^{k_1-1}} \sum_{i=0}^{M_1-1} \sum_{l=1}^{2^{k_2-1}} \sum_{j=0}^{M_2-1} c_{n,i,l,j}\, \frac{\partial \psi_{n,i,l,j}(x,t)}{\partial x} \right) \right] + \left[\left(\sum_{n=1}^{2^{k_1-1}} \sum_{i=0}^{M_1-1} \sum_{l=1}^{2^{k_2-1}} \sum_{j=0}^{M_2-1} c_{n,i,l,j}\, \frac{\partial \psi_{n,i,l,j}(x,t)}{\partial x} \right) \right.$$

$$\times \left(\sum_{n=1}^{2^{k_1-1}} \sum_{i=0}^{M_1-1} \sum_{l=1}^{2^{k_2-1}} \sum_{j=0}^{M_2-1} c_{n,i,l,j}\, \frac{\partial^2 \psi_{n,i,l,j}(x,t)}{\partial x^2} \right) \right] + \frac{1}{2}\left[\left(\sum_{n=1}^{2^{k_1-1}} \sum_{i=0}^{M_1-1} \sum_{l=1}^{2^{k_2-1}} \sum_{j=0}^{M_2-1} c_{n,i,l,j} \psi_{n,i,l,j}(x,t) \right) \right.$$

(6.36)

$$\left. \times \left(\sum_{n=1}^{2^{k_1-1}} \sum_{i=0}^{M_1-1} \sum_{l=1}^{2^{k_2-1}} \sum_{j=0}^{M_2-1} c_{n,i,l,j}\, \frac{\partial^3 \psi_{n,i,l,j}(x,t)}{\partial x^3} \right) \right] = 0 \ .$$

Now substituting the collocation points $x_l = \dfrac{l-0.5}{2^{k_1-1}M_1}$ and $t_r = \dfrac{r-0.5}{2^{k_2-1}M_2}$ for

$l = 1, 2,...,2^{k_1-1}M_1$ and $r = 1, 2,...,2^{k_2-1}M_2$ in eq. (6.34) and (6.36), we have $\left(2^{k_1-1}M_1\right)\left(2^{k_2-1}M_2\right)$ equations in $\left(2^{k_1-1}M_1\right)\left(2^{k_2-1}M_2\right)$ unknowns in $c_{n,i,l,j}$. By solving this system of equations using mathematical software, the Chebyshev wavelet coefficients $c_{n,i,l,j}$ can be obtained.

6.7 Numerical Results and Discussion

The comparison of the absolute errors for Riesz time-fractional Camassa-Holm equation (6.33) has been exhibited in Table 6.4 which is constructed using the results obtained by Chebyshev wavelet method at different values of x and t taking $\alpha = 0.5$. Similarly Table 6.5 shows the comparison of the absolute errors for time-fractional Camassa-Holm equation (6.33) at various points of x and t taking $\alpha = 0.75$. Again in order to examine the accuracy and reliability of the Chebyshev wavelets for solving fractional order Camassa-

Holm equation, we compare the approximate numerical solutions of Chebyshev wavelet with the approximate solutions obtained by HAM and VIM. Agreement between present numerical solutions with analytical solutions like VIM and HAM appear very satisfactory through the illustration in Tables 6.4 and 6.5. To show the accuracy of proposed method L_2 and L_∞ error norms for fractional order nonlinear Camassa-Holm equation have been presented in Table 6.6.

Table 6.4   Comparison of absolute errors obtained by two-dimensional Chebyshev wavelet method for fractional nonlinear Camassa-Holm equation given in eq. (6.33) at various points of x and t taking $\alpha = 0.5$.

x	Comparison with different Analytical methods									
	$t = 0.1$		$t = 0.2$		$t = 0.3$		$t = 0.4$		$t = 0.5$	
	$\lvert u_{CWM} - u_{VIM}\rvert$	$\lvert u_{CWM} - u_{HAM}\rvert$	$\lvert u_{CWM} - u_{VIM}\rvert$	$\lvert u_{CWM} - u_{HAM}\rvert$	$\lvert u_{CWM} - u_{VIM}\rvert$	$\lvert u_{CWM} - u_{HAM}\rvert$	$\lvert u_{CWM} - u_{VIM}\rvert$	$\lvert u_{CWM} - u_{HAM}\rvert$	$\lvert u_{CWM} - u_{VIM}\rvert$	$\lvert u_{CWM} - u_{HAM}\rvert$
0.1	2.1329E-3	2.1361E-3	7.8868E-4	7.8402E-4	5.4917E-3	5.4858E-3	8.4921E-3	8.4852E-3	9.3582E-3	9.3504E-3
0.2	4.0685E-4	4.0868E-4	1.5069E-3	1.5042E-3	4.8677E-3	4.8643E-3	7.0508E-3	7.0468E-3	7.7726E-3	7.7680E-3
0.3	1.3197E-3	1.3192E-3	2.2497E-3	2.2491E-3	4.2747E-3	4.2739E-3	5.6335E-3	5.6326E-3	6.1955E-3	6.1945E-3
0.4	3.0276E-3	3.0287E-3	2.9895E-3	2.9912E-3	3.6831E-3	3.6852E-3	4.2131E-3	4.2155E-3	4.6052E-3	4.6080E-3
0.5	4.6974E-3	4.7003E-3	3.6982E-3	3.7024E-3	3.0627E-3	3.0681E-3	2.7621E-3	2.7684E-3	2.9790E-3	2.9862E-3
0.6	6.3093E-3	6.3142E-3	4.3472E-3	4.3545E-3	2.3829E-3	2.3921E-3	1.2524E-3	1.2634E-3	1.2937E-3	1.3062E-3
0.7	7.8429E-3	7.8503E-3	4.9074E-3	4.9184E-3	1.6122E-3	1.6261E-3	3.4466E-4	3.2816E-4	4.7449E-4	4.5561E-4
0.8	9.2769E-3	9.2874E-3	5.3489E-3	5.3644E-3	7.1856E-4	7.3824E-4	2.0588E-3	2.0354E-3	2.3504E-3	2.3236E-3
0.9	1.0589E-2	1.0603E-2	5.6408E-3	5.6619E-3	3.3100E-4	3.0414E-4	3.9205E-3	3.8884E-3	4.3597E-3	4.3229E-3

Table 6.5   Comparison of absolute errors obtained by two-dimensional Chebyshev wavelet method for fractional nonlinear Camassa-Holm equation given in eq. (6.33) at various points of x and t taking $\alpha = 0.75$.

x	Comparison with different Analytical methods											
	$t = 0.1$		$t = 0.2$		$t = 0.3$		$t = 0.4$		$t = 0.5$		$t = 0.6$	
	$\lvert u_{CWM} - u_{VIM}\rvert$	$\lvert u_{CWM} - u_{HAM}\rvert$	$\lvert u_{CWM} - u_{VIM}\rvert$	$\lvert u_{CWM} - u_{HAM}\rvert$	$\lvert u_{CWM} - u_{VIM}\rvert$	$\lvert u_{CWM} - u_{HAM}\rvert$	$\lvert u_{CWM} - u_{VIM}\rvert$	$\lvert u_{CWM} - u_{HAM}\rvert$	$\lvert u_{CWM} - u_{VIM}\rvert$	$\lvert u_{CWM} - u_{HAM}\rvert$	$\lvert u_{CWM} - u_{VIM}\rvert$	$\lvert u_{CWM} - u_{HAM}\rvert$
0.1	6.3182 E-3	6.3150 E-3	6.4241 E-3	6.4194 E-3	7.3466 E-3	7.3408 E-3	9.1567 E-3	9.1498 E-3	1.0373 E-2	1.0365 E-2	9.1687 E-3	9.1599 E-3
0.2	6.2304 E-3	6.2285 E-3	6.4316 E-3	6.4290 E-3	6.9095 E-3	6.9062 E-3	7.9849 E-3	7.9809 E-3	8.7183 E-3	8.7137 E-3	7.8194 E-3	7.8144 E-3
0.3	6.1456 E-3	6.1451 E-3	6.4473 E-3	6.4466 E-3	6.4856 E-3	6.4848 E-3	6.8251 E-3	6.8242 E-3	7.0637 E-3	7.0627 E-3	6.4553 E-3	6.4542 E-3
0.4	6.0535 E-3	6.0547 E-3	6.4548 E-3	6.4565 E-3	6.0540 E-3	6.0561 E-3	5.6571 E-3	5.6596 E-3	5.3955 E-3	5.3983 E-3	5.0703 E-3	5.0735 E-3
0.5	5.9436 E-3	5.9465 E-3	6.4379 E-3	6.4421 E-3	5.5938 E-3	5.5991 E-3	4.4598 E-3	4.4661 E-3	3.6984 E-3	3.7056 E-3	3.6578 E-3	3.6659 E-3

186

0.6	5.8047 E-3	5.8097 E-3	6.3792 E-3	6.3865 E-3	5.0829 E-3	5.0922 E-3	3.2114 E-3	3.2223 E-3	1.9567 E-3	1.9692 E-3	2.2104 E-3	2.2243 E-3
0.7	5.6251 E-3	5.6325 E-3	6.2610 E-3	6.2720 E-3	4.4990 E-3	4.5130 E-3	1.8896 E-3	1.9061 E-3	1.5382 E-4	1.7269 E-4	7.1993 E-4	7.4103 E-4
0.8	5.3923 E-3	5.4028 E-3	6.0645 E-3	6.0800 E-3	3.8186 E-3	3.8383 E-3	4.7116 E-4	4.9455 E-4	1.7276 E-3	1.7008 E-3	8.2260 E-4	7.9259 E-4
0.9	5.0929 E-3	5.1071 E-3	5.7699 E-3	5.7910 E-3	3.0173 E-3	3.0441 E-3	1.0680 E-3	1.0360 E-3	3.7057 E-3	3.6689 E-3	2.4271 E-3	2.3859 E-3

Table 6.6 L_2 and L_∞ error norms for nonlinear time-fractional Camassa-Holm equation using two-dimensional Chebyshev wavelet methods at various points x taking $\alpha = 0.5$ and 0.75.

x	Error analysis with regard to VIM				Error analysis with regard to HAM			
	$\alpha = 0.5$		$\alpha = 0.75$		$\alpha = 0.5$		$\alpha = 0.75$	
	L_2	L_∞	L_2	L_∞	L_2	L_∞	L_2	L_∞
0.1	6.38694E-3	9.3582E-3	7.11978E-3	1.0373E-2	6.38112E-3	9.3504E-3	7.11421E-3	1.0365E-2
0.2	5.40607E-3	7.7726E-3	7.40310E-3	8.7183E-3	5.39997E-3	7.7680E-3	7.39944E-3	8.7137E-3
0.3	4.55570E-3	6.1955E-3	6.57708E-3	7.0637E-3	4.55487E-3	6.1945E-3	6.57624E-3	7.0627E-3
0.4	3.90422E-3	4.6052E-3	5.79917E-3	6.4548E-3	3.90650E-3	4.6080E-3	5.80137E-3	6.4565E-3
0.5	3.53718E-3	4.6974E-3	5.08283E-3	6.4379E-3	3.54257E-3	4.7003E-3	5.08802E-3	6.4421E-3
0.6	3.53417E-3	6.3093E-3	4.45818E-3	6.3792E-3	3.54135E-3	6.3142E-3	4.46615E-3	6.3865E-3
0.7	3.90066E-3	7.8429E-3	3.98320E-3	6.2610E-3	3.90730E-3	7.8503E-3	3.99254E-3	6.2720E-3
0.8	4.56822E-3	9.2769E-3	3.74878E-3	6.0645E-3	4.57187E-3	9.2874E-3	3.75621E-3	6.0800E-3
0.9	5.46221E-3	1.0589E-2	3.85351E-3	5.7699E-3	5.46048E-3	1.0603E-2	3.85381E-3	5.7910E-3

The following Figures 6.2-6.4 demonstrate the graphical comparison of the numerical solutions obtained by two-dimensional Chebyshev wavelet approximation with regard to VIM and HAM taking $\alpha = 0.75$ and $\alpha = 0.5$ respectively.
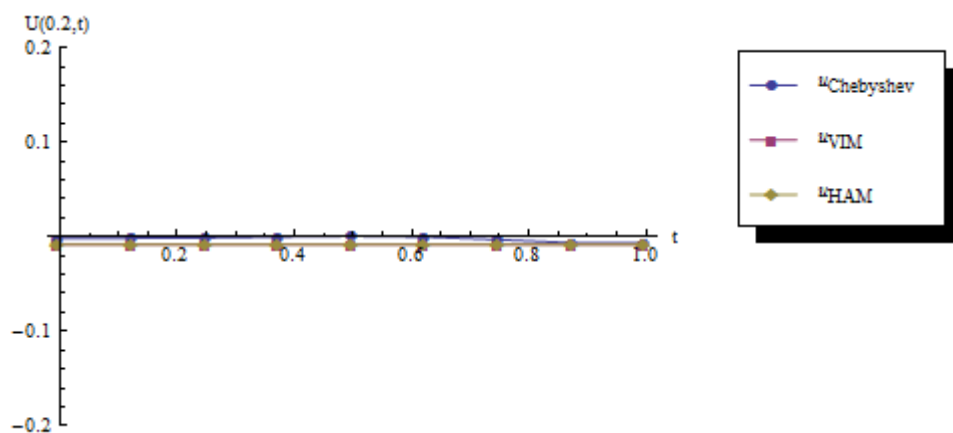
Figure 6.2   Comparison of numerical solutions of $u(0.2, t)$ obtained by two-dimensional Chebyshev wavelet method with regard to VIM and HAM for $\alpha = 0.75$.
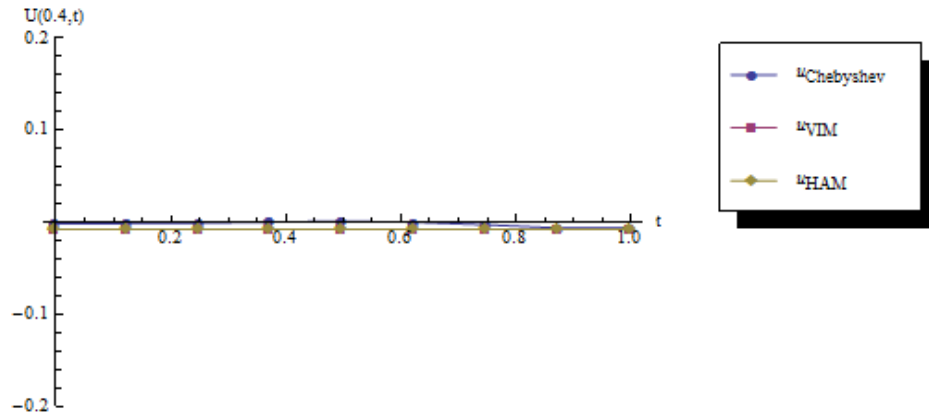
Figure 6.3 Comparison of numerical solutions of $u(0.4, t)$ obtained by two-dimensional Chebyshev wavelet method with regard to VIM and HAM for $\alpha = 0.75$.
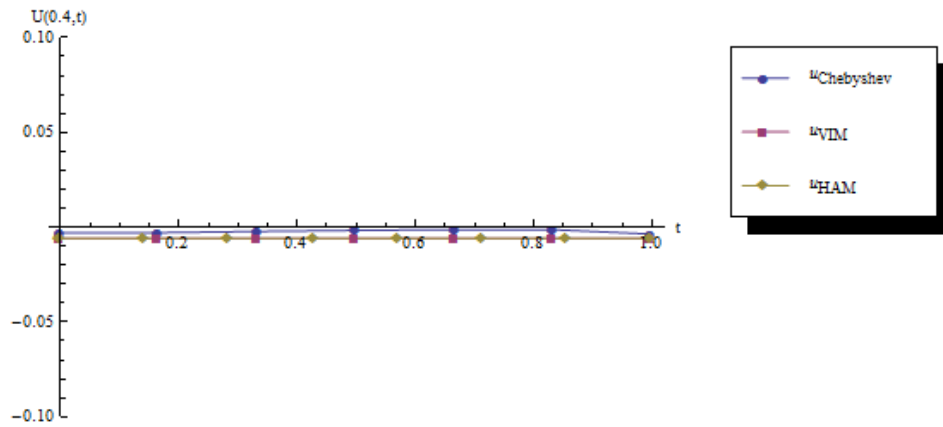
Figure 6.4 Comparison of numerical solutions of $u(0.4, t)$ obtained by two-dimensional Chebyshev wavelet method with regard to VIM and HAM for $\alpha = 0.5$.

6.8 Implementation of Two-Dimensional Chebyshev Wavelet Method for Approximate Solution of Riesz Space Fractional Sine-Gordon Equation

In this section, two test examples have been considered with a purpose to exhibit the effectiveness and accuracy of proposed Chebyshev wavelet method for numerical solution of Riesz fractional sine-Gordon equation given in eq. (6.3). The numerical solutions acquired are compared with the exact solutions for classical case and also solutions obtained by modified homotopy analysis method with Fourier transform (MHAM-FT) in fractional order case [141].

Consider the nonlinear Riesz space fractional sine-Gordon equation [141, 142]

$$u_{tt} - {}^{R}D_x^{\alpha}u + \sin u = 0, \qquad 1 < \alpha \leq 2 \qquad (6.37)$$

with initial conditions $u(x,0) = f(x)$ and $u_t(x,0) = g(x)$. $\qquad (6.38)$

The Chebyshev wavelet solution of $u(x,t)$ is sought through assuming that $u(x,t)$ can be expanded in terms of Chebyshev wavelet as

$$u(x,t) = \sum_{n=1}^{2^{k_1-1}} \sum_{i=0}^{M_1-1} \sum_{l=1}^{2^{k_2-1}} \sum_{j=0}^{M_2-1} c_{n,i,l,j} \, \psi_{n,i,l,j}(x,t), \qquad (6.39)$$

where $n = 1,...,2^{k_1-1}, i = 0,..., M_1 - 1, l = 1,...,2^{k_2-1}, j = 0,..., M_2 - 1$.

Now applying eq. (6.39) in eq. (6.37), we have

$$\frac{\partial^2}{\partial t^2}\left(\sum_{n=1}^{2^{k_1-1}} \sum_{i=0}^{M_1-1} \sum_{l=1}^{2^{k_2-1}} \sum_{j=0}^{M_2-1} c_{n,i,l,j}\psi_{n,i,l,j}(x,t)\right) - {}^{R}D_x^{\alpha}\left(\sum_{n=1}^{2^{k_1-1}} \sum_{i=0}^{M_1-1} \sum_{l=1}^{2^{k_2-1}} \sum_{j=0}^{M_2-1} c_{n,i,l,j}\psi_{n,i,l,j}(x,t)\right)$$
$$+ \sin\left(\sum_{n=1}^{2^{k_1-1}} \sum_{i=0}^{M_1-1} \sum_{l=1}^{2^{k_2-1}} \sum_{j=0}^{M_2-1} c_{n,i,l,j}\psi_{n,i,l,j}(x,t)\right) = 0. \qquad (6.40)$$

Now substituting the collocation points $x_l = \dfrac{l - 0.5}{2^{k_1-1}M_1}$ and $t_r = \dfrac{r - 0.5}{2^{k_2-1}M_2}$ for

$l = 1, 2, ..., 2^{k_1-1}M_1$ and $r = 1, 2, ..., 2^{k_2-1}M_2$ in eq. (6.40), we have $\left(2^{k_1-1}M_1\right)\left(2^{k_2-1}M_2\right)$ equations in $\left(2^{k_1-1}M_1\right)\left(2^{k_2-1}M_2\right)$ unknowns in $c_{n,i,l,j}$. By solving this system of equations using mathematical software, the Chebyshev wavelet coefficients $c_{n,i,l,j}$ can be obtained.

Example 6.1 Consider nonlinear Riesz fractional SGE equation (6.37) subject to the following initial conditions [145, 146]

$$u(x,0) = 0, \qquad u_t(x,0) = 4\sec h(x). \qquad (6.41)$$

The numerical solutions of example 6.1 are presented in Tables 6.7-6.9. The results are compared with the exact solutions and also with solutions obtained by MHAM-FT [141]. It has been noticed from Tables 6.7-6.9 that the solutions obtained by present method are in good agreement with the exact solutions and those with MHAM-FT [141].

Example 6.2 In this case, we shall find approximate solution of the nonlinear Riesz fractional SGE equation (6.37) with given initial conditions [145, 146]

$$u(x,0) = \pi + \varepsilon \cos(\mu x), \qquad u_t(x,0) = 0. \qquad (6.42)$$

189

where ε and μ are parameters. The numerical solutions of the example 6.2 are presented

for $\mu = \dfrac{\sqrt{2}}{2}, \varepsilon = 0.001$ in Tables 6.10-6.12. The results are compared with the exact

solutions as well as solutions obtained by MHAM-FT, which is discussed in following

section. It has been observed from Tables 6.10-6.12 that the solutions attained by present

method are in pretty good agreement with the exact solutions and those obtained by

MHAM-FT [141].

6.9 Numerical Results and Discussion

In the present numerical investigation, in order to examine the accuracy and reliability of

the proposed Chebyshev wavelet technique for solving fractional order sine-Gordon

equation, the absolute errors have been compared with the exact solutions and those

obtained by MHAM-FT for different values of x and t taking $\hbar = -1$. In case of $\alpha = 2$,

using the results of Chebyshev wavelet method, the numerical solutions of classical SGE

equation (6.37) given in examples 6.1 and 6.2 have been exhibited in Tables 6.7 and 6.10.

Similarly the absolute errors for fractional SGE eq. (6.37) given in examples 6.1 and 6.2

have been demonstrated in Tables 6.9-6.12 which are devised using the results attained by

Chebyshev wavelet method and MHAM-FT at different values of x and t taking $\alpha = 1.75$

and 1.5 respectively. We observe that the proposed numerical simulation results are in

good agreement with the exact solutions and those obtained by MHAM-FT [141] through

illustrations in Tables 6.7-6.12.

Table 6.7   The absolute errors obtained by two-dimensional Chebyshev wavelet method with
regard to exact solutions for classical SGE eq. (6.37) given in example 6.1 at various points of x
and t taking $\alpha = 2$.

x	$\lvert u_{CWM} - u_{Exact} \rvert$									
	$t = 0.01$	$t = 0.02$	$t = 0.03$	$t = 0.04$	$t = 0.05$	$t = 0.06$	$t = 0.07$	$t = 0.08$	$t = 0.09$	$t = 0.10$
0.01	6.7054E-6	2.5570E-5	5.5014E-5	9.3603E-5	1.4004E-4	1.9318E-4	2.5198E-4	3.1551E-4	3.8298E-4	4.5367E-4
0.02	6.6806E-6	2.5524E-5	5.4947E-5	9.3514E-5	1.3992E-4	1.9303E-4	2.5177E-4	3.1524E-4	3.8263E-4	4.5321E-4
0.03	6.6617E-6	2.5485E-5	5.4885E-5	9.3423E-5	1.3980E-4	1.9285E-4	2.5154E-4	3.1494E-4	3.8224E-4	4.5271E-4
0.04	6.6468E-6	2.5449E-5	5.4820E-5	9.3322E-5	1.3965E-4	1.9265E-4	2.5127E-4	3.1459E-4	3.8179E-4	4.5214E-4
0.05	6.6341E-6	2.5412E-5	5.4749E-5	9.3205E-5	1.3948E-4	1.9241E-4	2.5095E-4	3.1417E-4	3.8126E-4	4.5149E-4
0.06	6.6222E-6	2.5372E-5	5.4666E-5	9.3066E-5	1.3927E-4	1.9212E-4	2.5056E-4	3.1367E-4	3.8063E-4	4.5072E-4
0.07	6.6101E-6	2.5327E-5	5.4569E-5	9.2900E-5	1.3902E-4	1.9177E-4	2.5010E-4	3.1308E-4	3.7990E-4	4.4984E-4
0.08	6.5969E-6	2.5275E-5	5.4455E-5	9.2703E-5	1.3872E-4	1.9135E-4	2.4955E-4	3.1240E-4	3.7906E-4	4.4882E-4
0.09	6.5819E-6	2.5214E-5	5.4322E-5	9.2474E-5	1.3838E-4	1.9087E-4	2.4892E-4	3.1160E-4	3.7808E-4	4.4765E-4
0.10	6.5642E-6	2.5144E-5	5.4168E-5	9.2210E-5	1.3798E-4	1.9032E-4	2.4820E-4	3.1069E-4	3.7698E-4	4.4633E-4

Table 6.8   The absolute errors obtained by two-dimensional Chebyshev wavelet method with regard to MHAM solutions for fractional SGE eq. (6.37) given in example 6.1 at various points of x and t taking $\alpha = 1.75$.

x	$|u_{CWM} - u_{MHAM}|$									
	$t=0.01$	$t=0.02$	$t=0.03$	$t=0.04$	$t=0.05$	$t=0.06$	$t=0.07$	$t=0.08$	$t=0.09$	$t=0.10$
0.01	8.9761E-4	3.5234E-3	7.7847E-3	1.3593E-2	2.0864E-2	2.9519E-2	3.9482E-2	5.0680E-2	6.3047E-2	7.6517E-2
0.02	8.7243E-4	3.4244E-3	7.5651E-3	1.3207E-2	2.0270E-2	2.8673E-2	3.8343E-2	4.9210E-2	6.1206E-2	7.4270E-2
0.03	8.4432E-4	3.3142E-3	7.3209E-3	1.2780E-2	1.9611E-2	2.7738E-2	3.7088E-2	4.7592E-2	5.9187E-2	7.1809E-2
0.04	8.1361E-4	3.1937E-3	7.0545E-3	1.2314E-2	1.8895E-2	2.6722E-2	3.5727E-2	4.5843E-2	5.7006E-2	6.9159E-2
0.05	7.8057E-4	3.0642E-3	6.7684E-3	1.1814E-2	1.8127E-2	2.5636E-2	3.4274E-2	4.3977E-2	5.4684E-2	6.6339E-2
0.06	7.4549E-4	2.9268E-3	6.4651E-3	1.1285E-2	1.7315E-2	2.4489E-2	3.2740E-2	4.2009E-2	5.2238E-2	6.3373E-2
0.07	7.0863E-4	2.7825E-3	6.1467E-3	1.0730E-2	1.6465E-2	2.3287E-2	3.1136E-2	3.9953E-2	4.9685E-2	6.0281E-2
0.08	6.7026E-4	2.6322E-3	5.8156E-3	1.0153E-2	1.5581E-2	2.2040E-2	2.9472E-2	3.7822E-2	4.7042E-2	5.7081E-2
0.09	6.3062E-4	2.4771E-3	5.4737E-3	9.5579E-2	1.4670E-2	2.0755E-2	2.7758E-2	3.5630E-2	4.4323E-2	5.3793E-2
0.10	5.8994E-4	2.3179E-3	5.1231E-3	8.9478E-2	1.3737E-2	1.9439E-2	2.6004E-2	3.3388E-2	4.1545E-2	5.0435E-2

Table 6.9   The absolute errors obtained by two-dimensional Chebyshev wavelet method with regard to MHAM solutions for fractional SGE eq. (6.37) given in example 6.1 at various points of x and t taking $\alpha = 1.5$.

x	$|u_{CWM} - u_{MHAM}|$									
	$t=0.01$	$t=0.02$	$t=0.03$	$t=0.04$	$t=0.05$	$t=0.06$	$t=0.07$	$t=0.08$	$t=0.09$	$t=0.10$
0.01	4.1180E-4	1.6331E-3	3.6485E-3	6.4435E-3	1.0005E-2	1.4321E-2	1.9381E-2	2.5175E-2	3.1695E-2	3.8932E-2
0.02	4.5144E-4	1.7862E-3	3.9798E-3	7.0093E-3	1.0853E-2	1.5491E-2	2.0905E-2	2.7077E-2	3.3992E-2	4.1636E-2
0.03	4.8403E-4	1.9118E-3	4.2512E-3	7.4718E-3	1.1544E-2	1.6443E-2	2.2142E-2	2.8617E-2	3.5847E-2	4.3810E-2
0.04	5.1000E-4	2.0117E-3	4.4665E-3	7.8376E-3	1.2090E-2	1.7191E-2	2.3110E-2	2.9818E-2	3.7286E-2	4.5490E-2
0.05	5.2980E-4	2.0877E-3	4.6295E-3	8.1133E-3	1.2499E-2	1.7749E-2	2.3828E-2	3.0702E-2	3.8339E-2	4.6708E-2
0.06	5.4386E-4	2.1413E-3	4.7438E-3	8.3051E-3	1.2781E-2	1.8130E-2	2.4313E-2	3.1292E-2	3.9031E-2	4.7498E-2
0.07	5.5260E-4	2.1742E-3	4.8128E-3	8.4189E-3	1.2945E-2	1.8347E-2	2.4582E-2	3.1609E-2	3.9390E-2	4.7890E-2
0.08	5.5640E-4	2.1879E-3	4.8400E-3	8.4608E-3	1.3000E-2	1.8412E-2	2.4651E-2	3.1674E-2	3.9441E-2	4.7915E-2
0.09	5.5565E-4	2.1839E-3	4.8287E-3	8.4363E-3	1.2955E-2	1.8337E-2	2.4536E-2	3.1507E-2	3.9208E-2	4.7601E-2
0.10	5.5073E-4	2.1638E-3	4.7821E-3	8.3510E-3	1.2818E-2	1.8134E-2	2.4252E-2	3.1127E-2	3.8715E-2	4.6978E-2

Table 6.10   Comparison of absolute errors obtained by two-dimensional Chebyshev wavelet method with regard to exact solutions and MHAM for classical SGE eq. (6.37) given in example 6.2 at various points of x and t taking $\alpha = 2$.

x	$|u_{CWM} - u_{MHAM}|$									
	$t=0.01$	$t=0.02$	$t=0.03$	$t=0.04$	$t=0.05$	$t=0.06$	$t=0.07$	$t=0.08$	$t=0.09$	$t=0.10$
0.01	3.359E-10	9.694E-12	5.667E-10	1.320E-9	2.255E-9	3.360E-9	4.619E-9	6.021E-9	7.553E-9	9.204E-9
0.02	2.329E-10	1.131E-10	6.708E-10	1.425E-9	2.363E-9	3.469E-9	4.732E-9	6.139E-9	7.676E-9	9.334E-9
0.03	1.456E-10	2.005E-10	7.588E-10	1.514E-9	2.453E-9	3.562E-9	4.827E-9	6.237E-9	7.779E-9	9.442E-9
0.04	7.237E-11	2.738E-10	8.323E-10	1.588E-9	2.528E-9	3.638E-9	4.905E-9	6.318E-9	7.863E-9	9.531E-9
0.05	1.161E-11	3.345E-10	8.930E-10	1.649E-9	2.589E-9	3.700E-9	4.969E-9	6.383E-9	7.931E-9	9.602E-9
0.06	3.809E-11	3.840E-10	9.423E-10	1.698E-9	2.638E-9	3.749E-9	5.019E-9	6.434E-9	7.984E-9	9.658E-9
0.07	7.807E-11	4.237E-10	9.814E-10	1.737E-9	2.677E-9	3.788E-9	5.057E-9	6.473E-9	8.025E-9	9.699E-9
0.08	1.095E-10	4.547E-10	1.012E-9	1.767E-9	2.706E-9	3.816E-9	5.085E-9	6.501E-9	8.053E-9	9.728E-9

| 0.09 | 1.336E-10 | 4.782E-10 | 1.034E-9 | 1.788E-9 | 2.726E-9 | 3.836E-9 | 5.104E-9 | 6.519E-9 | 8.071E-9 | 9.746E-9 |
| 0.10 | 1.514E-10 | 4.953E-10 | 1.051E-9 | 1.803E-9 | 2.740E-9 | 3.848E-9 | 5.114E-9 | 6.529E-9 | 8.079E-9 | 9.754E-9 |

Table 6.11 The absolute errors obtained by two-dimensional Chebyshev wavelet method with regard to MHAM solutions for fractional SGE eq. (6.37) given in example 6.2 at various points of x and t taking $\alpha = 1.75$.

x	$\lvert u_{CWM} - u_{MHAM} \rvert$							
	$t=0.01$	$t=0.02$	$t=0.03$	$t=0.04$	$t=0.05$	$t=0.06$	$t=0.07$	$t=0.08$
0.01	7.80306E-4	3.12057E-3	7.02163E-3	1.24867E-2	1.95210E-2	2.81321E-2	3.83293E-2	5.01238E-2
0.02	9.25929E-4	3.67903E-3	8.22523E-3	1.45343E-2	2.25797E-2	3.23383E-2	4.37906E-2	5.69199E-2
0.03	1.05489E-3	4.17342E-3	9.29032E-3	1.63455E-2	2.52839E-2	3.60551E-2	4.86136E-2	6.29182E-2
0.04	1.16806E-3	4.60703E-3	1.02240E-2	1.79324E-2	2.76518E-2	3.93077E-2	5.28314E-2	6.81597E-2
0.05	1.26625E-3	4.98308E-3	1.10333E-2	1.93069E-2	2.97013E-2	4.21207E-2	5.64760E-2	7.26847E-2
0.06	1.35029E-3	5.30471E-3	1.17249E-2	2.04806E-2	3.14498E-2	4.45181E-2	5.95788E-2	7.65325E-2
0.07	1.42099E-3	5.57500E-3	1.23055E-2	2.14649E-2	3.29144E-2	4.65237E-2	6.21708E-2	7.97417E-2
0.08	1.47911E-3	5.79696E-3	1.27817E-2	2.22709E-2	3.41118E-2	4.81604E-2	6.42819E-2	8.23499E-2
0.09	1.52543E-3	5.97352E-3	1.31597E-2	2.29095E-2	3.50582E-2	4.94507E-2	6.59415E-2	8.43939E-2
0.10	1.56068E-3	6.10756E-3	1.34458E-2	2.33912E-2	3.57696E-2	5.04168E-2	6.71784E-2	8.59096E-2

Table 6.12 The absolute errors obtained by two-dimensional Chebyshev wavelet method with regard to MHAM solutions for fractional SGE eq. (6.37) given in example 2 at various points of x and t taking $\alpha = 1.5$.

x	$\lvert u_{CWM} - u_{MHAM} \rvert$									
	$t=0.01$	$t=0.02$	$t=0.03$	$t=0.04$	$t=0.05$	$t=0.06$	$t=0.07$	$t=0.08$	$t=0.09$	$t=0.10$
0.01	1.0416E-3	3.9097E-3	8.2311E-3	1.3648E-2	1.9820E-2	2.6420E-2	3.3137E-2	3.9675E-2	4.5752E-2	5.1101E-2
0.02	8.0050E-4	2.9839E-3	6.2331E-3	1.0244E-2	1.4727E-2	1.9403E-2	2.4008E-2	2.8289E-2	3.2006E-2	3.4932E-2
0.03	5.7955E-4	2.1356E-3	4.4026E-3	7.1261E-2	1.0062E-2	1.2977E-2	1.5650E-2	1.7867E-2	1.9427E-2	2.0138E-2
0.04	3.7779E-4	1.3611E-3	2.7317E-3	4.2801E-3	5.8053E-3	7.1154E-3	8.0265E-3	8.3635E-3	7.9594E-3	6.6553E-3
0.05	1.9432E-4	6.5698E-4	1.2127E-3	1.6933E-3	1.9371E-3	1.7893E-3	1.1019E-3	2.6672E-4	2.4516E-3	5.5813E-3
0.06	2.8208E-5	1.9564E-5	1.6195E-4	6.4725E-4	1.5621E-3	3.0273E-3	5.1587E-3	8.0671E-3	1.1858E-2	1.6634E-2
0.07	1.2142E-4	5.5452E-4	1.3997E-3	2.7541E-3	4.7112E-3	7.3608E-3	1.0789E-2	1.5080E-2	2.0312E-2	2.6563E-2
0.08	2.5546E-4	1.0685E-3	2.5078E-3	4.6397E-3	7.5286E-3	1.1236E-2	1.5823E-2	2.1348E-2	2.7865E-2	3.5429E-2
0.09	3.7472E-4	1.5258E-3	3.4933E-3	6.3162E-3	1.0032E-2	1.4679E-2	2.0294E-2	2.6911E-2	3.4565E-2	4.3289E-2
0.10	4.8006E-4	1.9296E-3	4.3631E-3	7.7951E-3	1.2240E-2	1.7714E-2	2.4232E-2	3.1808E-2	4.0460E-2	5.0202E-2

6.10 Convergence Analysis of Chebyshev Wavelet

Theorem 6.1 (Convergence Theorem)

If a continuous function $u(x,t) \in L^2(\Re \times \Re)$ defined on $[0,1) \times [0,1)$ be bounded viz. $\lvert u(x,t) \rvert \leq K$, then the Chebyshev wavelets expansion of $u(x,t)$ converges uniformly to it.

Proof:

Let $u(x,t)$ be a function defined on $[0,1) \times [0,1)$ and $|u(x,t)| \leq K$, K is a positive constant.

The Chebyshev wavelet coefficients of continuous functions $u(x,t)$ are defined as

$$c_{n_1,m_1,n_2,m_2} = \int_0^1 \int_0^1 u(x,t) \psi_{n_1,m_1}(x) \psi_{n_2,m_2}(t) dx dt$$

$$= \int_0^1 \int_{I_1} u(x,t) 2^{\frac{k_1}{2}} \bar{U}_{m_1}\left(2^{k_1}x - 2n_1 + 1\right) \psi_{n_2,m_2}(t) dx\, dt, \quad \text{where } I_1 = \left[\frac{n_1-1}{2^{k_1-1}}, \frac{n_1}{2^{k_1-1}}\right)$$

$$= 2^{\frac{k_1}{2}} \sqrt{\frac{2}{\pi}} \int_0^1 \int_{I_1} u(x,t) U_{m_1}\left(2^{k_1}x - 2n_1 + 1\right) \psi_{n_2,m_2}(t) dx\, dt.$$

Now by change of variable $2^{k_1}x - 2n_1 + 1 = y$, we obtain

$$c_{n_1,m_1,n_2,m_2} = \frac{2^{\frac{k_1}{2}}}{2^{k_1}} \sqrt{\frac{2}{\pi}} \int_0^1 \psi_{n_2,m_2}(t) \left(\int_{-1}^1 u\left(\frac{y + 2n_1 - 1}{2^{k_1}}, t\right) U_{m_1}(y) dy\right) dt.$$

Applying mean value theorem of integral calculus, we have

$$c_{n_1,m_1,n_2,m_2} = \frac{1}{2^{\frac{k_1}{2}}} \sqrt{\frac{2}{\pi}} \int_0^1 \psi_{n_2,m_2}(t) u\left(\frac{\xi + 2n_1 - 1}{2^{k_1}}, t\right) \left(\int_{-1}^1 U_{m_1}(y) dy\right) dt, \quad \text{where } \xi \in (-1,1)$$

$$= \frac{1}{2^{\frac{k_1}{2}}} \sqrt{\frac{2}{\pi}} \int_0^1 \psi_{n_2,m_2}(t) u\left(\frac{\xi + 2n_1 - 1}{2^{k_1}}, t\right) \left(\frac{T_{m_1+1}(y)}{m_1 + 1}\right)_{-1}^1 dt$$

$$= \frac{1}{2^{\frac{k_1}{2}}} \sqrt{\frac{2}{\pi}} \left(\frac{1 - (-1)^{m_1+1}}{m_1 + 1}\right) \int_0^1 \psi_{n_2,m_2}(t) u\left(\frac{\xi + 2n_1 - 1}{2^{k_1}}, t\right) dt$$

$$= \frac{1}{2^{\frac{k_1}{2}}} \sqrt{\frac{2}{\pi}} \left(\frac{1 - (-1)^{m_1+1}}{m_1 + 1}\right) \int_{I_2} u\left(\frac{\xi + 2n_1 - 1}{2^{k_1}}, t\right) 2^{\frac{k_2}{2}} \bar{U}_{m_2}\left(2^{k_2}t - 2n_2 + 1\right) dt,$$

where $I_2 = \left[\frac{n_2-1}{2^{k_2-1}}, \frac{n_2}{2^{k_2-1}}\right)$

$$= \frac{1}{2^{\frac{k_1}{2}}} \frac{2}{\pi} 2^{\frac{k_2}{2}} \left(\frac{1-(-1)^{m_1+1}}{m_1+1} \right) \int_{I_2} u\left(\frac{\xi+2n_1-1}{2^{k_1}}, t \right) U_{m_2}\left(2^{k_2}t - 2n_2 + 1 \right) dt .$$

Again by change of variable $2^{k_2}t - 2n_2 + 1 = w,$ we get

$$c_{n_1,m_1,n_2,m_2} = \frac{1}{2^{\frac{k_1}{2}}} \frac{2}{\pi} 2^{\frac{k_2}{2}} \frac{1}{2^{k_2}} \left(\frac{1-(-1)^{m_1+1}}{m_1+1} \right) \int_{-1}^{1} u\left(\frac{\xi+2n_1-1}{2^{k_1}}, \frac{w+2n_2-1}{2^{k_2}} \right) U_{m_2}(w)dw$$

$$= \frac{1}{2^{\frac{k_1+k_2}{2}}} \frac{2}{\pi} \left(\frac{1-(-1)^{m_1+1}}{m_1+1} \right) \int_{-1}^{1} u\left(\frac{\xi+2n_1-1}{2^{k_1}}, \frac{w+2n_2-1}{2^{k_2}} \right) U_{m_2}(w)dw .$$

Applying mean value theorem of integral calculus, we have

$$c_{n_1,m_1,n_2,m_2} = \frac{1}{2^{\frac{k_1+k_2}{2}}} \frac{2}{\pi} \left(\frac{1-(-1)^{m_1+1}}{m_1+1} \right) u\left(\frac{\xi+2n_1-1}{2^{k_1}}, \frac{\eta+2n_2-1}{2^{k_2}} \right) \int_{-1}^{1} U_{m_2}(w)dw ,$$

where $\eta \in (-1,1)$

$$= \frac{1}{2^{\frac{k_1+k_2}{2}}} \frac{2}{\pi} \left(\frac{1-(-1)^{m_1+1}}{m_1+1} \right) u\left(\frac{\xi+2n_1-1}{2^{k_1}}, \frac{\eta+2n_2-1}{2^{k_2}} \right) \left(\frac{T_{m_2+1}(w)}{m_2+1} \right)_{-1}^{1}$$

$$= \frac{1}{2^{\frac{k_1+k_2}{2}}} \frac{2}{\pi} \left(\frac{1-(-1)^{m_1+1}}{m_1+1} \right)\left(\frac{1-(-1)^{m_2+1}}{m_2+1} \right) u\left(\frac{\xi+2n_1-1}{2^{k_1}}, \frac{\eta+2n_2-1}{2^{k_2}} \right) .$$

Therefore,

$$\left| c_{n_1,m_1,n_2,m_2} \right| = \frac{1}{2^{\frac{k_1+k_2}{2}}} \frac{2}{\pi} \left(\frac{1-(-1)^{m_1+1}}{m_1+1} \right)\left(\frac{1-(-1)^{m_2+1}}{m_2+1} \right) \left| u\left(\frac{\xi+2n_1-1}{2^{k_1}}, \frac{\eta+2n_2-1}{2^{k_2}} \right) \right|$$

$$\leq \frac{1}{2^{\frac{k_1+k_2}{2}}} \frac{2}{\pi} \left(\frac{1-(-1)^{m_1+1}}{m_1+1} \right)\left(\frac{1-(-1)^{m_2+1}}{m_2+1} \right) K \qquad (6.43)$$

Therefore $\displaystyle\sum_{n_1=0}^{\infty}\sum_{m_1=0}^{\infty}\sum_{n_2=0}^{\infty}\sum_{m_2=0}^{\infty} c_{n_1,m_1,n_2,m_2}$ is absolutely convergent.

Hence the Chebyshev series expansion of $u(x,t)$ converges uniformly. $\qquad\square$

Theorem 6.2 (Error Estimate)

If a continuous function $u(x,t) \in L^2(\Re \times \Re)$ defined on $[0,1) \times [0,1)$ be bounded viz. $|u(x,t)| \leq K$, then

$$\left\| \varepsilon_{u,k_1,M_1,k_2,M_2} \right\|_{L^2_\omega[(0,1)\times[0,1)]} \leq \left[\sum_{n_1=2^{k_1-1}+1}^{\infty} \sum_{m_1=M_1}^{\infty} \sum_{n_2=2^{k_2-1}+1}^{\infty} \sum_{m_2=M_2}^{\infty} \left\{ \frac{1}{2^{\frac{k_1+k_2}{2}}} \frac{2}{\pi} \left(\frac{1-(-1)^{m_1+1}}{m_1+1} \right) \left(\frac{1-(-1)^{m_2+1}}{m_2+1} \right) K \right\}^2 \right]^{\frac{1}{2}}$$

.

Proof:

$$\left\| \varepsilon_{u,k_1,M_1,k_2,M_2} \right\|^2_{L^2_\omega[(0,1)\times[0,1)]}$$

$$= \int_0^1 \int_0^1 \left| u(x,t) - \sum_{n_1=1}^{2^{k_1-1}} \sum_{m_1=0}^{M_1-1} \sum_{n_2=1}^{2^{k_2-1}} \sum_{m_2=0}^{M_2-1} c_{n_1,m_1,n_2,m_2} \psi_{n_1,m_1}(x) \psi_{n_2,m_2}(t) \right|^2 \omega_{n_1}(x)\omega_{n_2}(t)dxdt$$

$$= \int_0^1 \int_0^1 \left| \sum_{n_1=2^{k_1-1}+1}^{\infty} \sum_{m_1=M_1}^{\infty} \sum_{n_2=2^{k_2-1}+1}^{\infty} \sum_{m_2=M_2}^{\infty} c_{n_1,m_1,n_2,m_2} \psi_{n_1,m_1}(x) \psi_{n_2,m_2}(t) \right|^2 \omega_{n_1}(x)\omega_{n_2}(t)dxdt$$

$$= \sum_{n_1=2^{k_1-1}+1}^{\infty} \sum_{m_1=M_1}^{\infty} \sum_{n_2=2^{k_2-1}+1}^{\infty} \sum_{m_2=M_2}^{\infty} \left| c_{n_1,m_1,n_2,m_2} \right|^2 \int_0^1 \int_0^1 \left| \psi_{n_1,m_1}(x) \psi_{n_2,m_2}(t) \right|^2 \omega_{n_1}(x)\omega_{n_2}(t)dxdt$$

$$= \sum_{n_1=2^{k_1-1}+1}^{\infty} \sum_{m_1=M_1}^{\infty} \sum_{n_2=2^{k_2-1}+1}^{\infty} \sum_{m_2=M_2}^{\infty} \left| c_{n_1,m_1,n_2,m_2} \right|^2 . \qquad (6.44)$$

Substituting eq. (6.43) of theorem 6.1, in eq. (6.44) we obtain

$$\left\| \varepsilon_{u,k_1,M_1,k_2,M_2} \right\|^2_{L^2_\omega[(0,1)\times[0,1)]} \leq \sum_{n_1=2^{k_1-1}+1}^{\infty} \sum_{m_1=M_1}^{\infty} \sum_{n_2=2^{k_2-1}+1}^{\infty} \sum_{m_2=M_2}^{\infty} \left(\frac{1}{2^{\frac{k_1+k_2}{2}}} \frac{2}{\pi} \left(\frac{1-(-1)^{m_1+1}}{m_1+1} \right) \left(\frac{1-(-1)^{m_2+1}}{m_2+1} \right) K \right)^2$$

This implies

$$\left\| \varepsilon_{u,k_1,M_1,k_2,M_2} \right\|_{L^2_\omega[(0,1)\times[0,1)]} \leq \left[\sum_{n_1=2^{k_1-1}+1}^{\infty} \sum_{m_1=M_1}^{\infty} \sum_{n_2=2^{k_2-1}+1}^{\infty} \sum_{m_2=M_2}^{\infty} \left(\frac{1}{2^{\frac{k_1+k_2}{2}}} \frac{2}{\pi} \left(\frac{1-(-1)^{m_1+1}}{m_1+1} \right) \left(\frac{1-(-1)^{m_2+1}}{m_2+1} \right) K \right)^2 \right]^{\frac{1}{2}} \qquad \square$$

6.11 Conclusion

The time fractional fifth-order Sawada-Kotera equation has been solved by using two-dimensional Chebyshev wavelet method. The obtained results are then compared with exact solutions as well as with homotopy analysis method in fractional order case. The obtained results demonstrate the accuracy, efficiency and reliability of the proposed algorithm based on two-dimensional Chebyshev wavelet method and its applicability to nonlinear time fractional Sawada-Kotera equation. Agreement between present numerical results obtained by Chebyshev wavelet method with homotopy analysis method and exact solutions appear very satisfactory through illustrative results in Tables 6.1-6.3.

In case of nonlinear Camassa-Holm equation with Riesz time-fractional derivative, the results obtained by two-dimensional Chebyshev wavelet method are compared with the solutions obtained by homotopy analysis method and variational iteration method. The results demonstrated in Tables 6.4-6.6 show the accuracy, efficiency and plausibility of the proposed algorithm based on two-dimensional Chebyshev wavelet method and its applicability to nonlinear Camassa-Holm equation with Riesz time-fractional derivative. One can observe a pretty good agreement between the present numerical results obtained by Chebyshev wavelet method with homotopy analysis method and variational iteration method solutions through illustrations in Tables 6.4-6.6.

Next, the Chebyshev wavelet method (CWM) has been successfully employed to demonstrate the approximate numerical solutions of the Riesz fractional sine-Gordon equation. The proposed wavelet method has been implemented for the first time to solve the fractional sine-Gordon equation numerically. Two test examples are given in order to show the validity and accuracy of this procedure. Also, the acquired results are compared with the exact solutions as well as with MHAM-FT [141], which reveals the efficiency and plausibility of the proposed Chebyshev wavelet method. The results exhibited in Tables 6.7-6.12 illustrate a pretty good agreement between the present numerical method with MHAM-FT and exact solution.

In this work, we consider fractional order Sawada-Kotera equation, fractional Camassa-Holm equation and fractional sine-Gordon equations. The motivation of the present work is to illustrate that the two-dimensional Chebyshev wavelet method as a powerful tool for solving the fractional Sawada-Kotera equation, Riesz fractional Camassa-Holm equation

and Riesz fractional sine-Gordon equation. Finally, it is worthwhile to mention that the proposed method is a promising and powerful method for solving fractional differential equations in mathematical physics. Also, the present scheme is very simple, effective and appropriate for obtaining numerical solutions of fractional differential equations. Analyzing the numerical results, it can be concluded that the two-dimensional Chebyshev wavelet method provides accurate numerical solutions for fractional differential equations.

CHAPTER 7

7 Application of Hermite Wavelet Method for Numerical Simulation of Fractional Differential Equations

7.1 Introduction

In this chapter, a new wavelet method based on the Hermite wavelet expansion together with operational matrices of fractional integration and derivative of wavelet functions is proposed to solve time-fractional modified Fornberg-Whitham (mFW) equation. The technique is also implemented for finding the numerical solution to a coupled system of nonlinear time-fractional Jaulent-Miodek (JM) equations. Consequently, the approximate solutions of time-fractional modified Fornberg-Whitham equation and fractional Jaulent-Miodek equations acquired by using Hermite wavelet technique were compared with those derived by using optimal homotopy asymptotic method (OHAM) and exact solutions.

Again as the exact solution of fractional Fornberg-Whitham equation is unknown, we employ first integral method to determine exact solutions. The solitary wave solution of fractional modified Fornberg-Whitham equation has been attained by using first integral method. Analytical techniques such as First Integral Method (FIM) and OHAM are applied in order to determine the exact solutions of fractional order modified Fornberg-Whitham equation.

The Fornberg-Whitham equation is given by [154]

$$\frac{\partial u}{\partial t} - \frac{\partial^3 u}{\partial x^2 \partial t} + \frac{\partial u}{\partial x} + u\frac{\partial u}{\partial x} = 3\frac{\partial u}{\partial x}\frac{\partial^2 u}{\partial x^2} + u\frac{\partial^3 u}{\partial x^3}, \tag{7.1}$$

which was first proposed by Whitham in 1967 for studying the qualitative behavior of wave breaking [155]. In 1978, Fornberg and Whitham [156] obtained a peaked solution

consisting of an arbitrary constant. Modifying the nonlinear term $u\dfrac{\partial u}{\partial x}$ in (7.1) to $u^2\dfrac{\partial u}{\partial x}$, He et al. proposed in [154] the modified Fornberg-Whitham equation as follows

$$\frac{\partial u}{\partial t} - \frac{\partial^3 u}{\partial x^2 \partial t} + \frac{\partial u}{\partial x} + u^2 \frac{\partial u}{\partial x} = 3\frac{\partial u}{\partial x}\frac{\partial^2 u}{\partial x^2} + u\frac{\partial^3 u}{\partial x^3}, \qquad t>0,\ x>0 \tag{7.2}$$

Consider the following time-fractional modified Fornberg-Whitham equation

$$\frac{\partial^\alpha u}{\partial t^\alpha} - \frac{\partial^3 u}{\partial x^2 \partial t} + \frac{\partial u}{\partial x} + u^2 \frac{\partial u}{\partial x} = 3\frac{\partial u}{\partial x}\frac{\partial^2 u}{\partial x^2} + u\frac{\partial^3 u}{\partial x^3}. \tag{7.3}$$

Here $0<\alpha\le1$, is the parameter representing the order of the fractional time derivative. The fractional derivative is considered in the Caputo sense. A great deal of research work has been invested in recent years for the study of classical order modified Fornberg-Whitham equations. Various methods such as the bifurcation theory and the method of phase portraits analysis [154], reduced differential transform method [157], and variational iteration method [158] have been developed independently for the solution of modified Fornberg-Whitham equation. But according to the best possible information of the authors, the detailed study of the nonlinear fractional order modified Fornberg-Whitham equation is only beginning.

In contemporary years, significant research has been done to study the classical Jaulent-Miodek equations. Various methods such as unified algebraic method [124], Adomian decomposition method [159], tanh-sech method [160], homotopy perturbation method [161], exp-function method [162], and homotopy analysis method [163] had been implemented for solving of coupled Jaulent-Miodek equations. But in keeping with the available information, the comprehensive analysis of the nonlinear fractional order coupled Jaulent-Miodek equation is only an initiation.

Consider the following time-fractional coupled Jaulent-Miodek (JM) equations

$$\frac{\partial^\alpha u}{\partial t^\alpha} + \frac{\partial^3 u}{\partial x^3} + \frac{3}{2}v\frac{\partial^3 v}{\partial x^3} + \frac{9}{2}\frac{\partial v}{\partial x}\frac{\partial^2 v}{\partial x^2} - 6u\frac{\partial u}{\partial x} - 6uv\frac{\partial v}{\partial x} - \frac{3}{2}\frac{\partial u}{\partial x}v^2 = 0, \tag{7.4}$$

$$\frac{\partial^\alpha v}{\partial t^\alpha} + \frac{\partial^3 v}{\partial x^3} - 6\frac{\partial u}{\partial x}v - 6u\frac{\partial v}{\partial x} - \frac{15}{2}\frac{\partial v}{\partial x}v^2 = 0, \tag{7.5}$$

which is associated with energy-dependent Schrödinger potential [164-166]. Here $0<\alpha\le1$, is the parameter representing the order of the fractional derivative, deemed in the Caputo sense. This present chapter emphasizes on the implementation of two-

dimensional Hermite wavelet method to solve the problem of fractional differential equations. With a view to exhibit the capabilities of the proposed wavelet method, we employ the method to deal with fractional modified Fornberg-Whitham equation and fractional order coupled Jaulent-Miodek equations. The approximate solutions attained via Hermite wavelet technique were compared with exact solutions and those derived by using OHAM in case of fractional order.

7.2 Algorithm of Hermite Wavelet Method

The proposed numerical algorithm implemented in our numerical experiment is simple, very easy to implement and it does not depend upon mesh of discretized time and space. Furthermore, it is also efficient in computation.

Input: Consider the following general differential equation of the form

$$\mathscr{A}\, u(x,t) = 0, \tag{7.6}$$

which can be written as $\mathscr{L}\, u(x,t) + \mathscr{N}\, u(x,t) = g(x,t),$ (7.7)

where $\mathscr{L}$ is the linear operator,

$\mathscr{N}$ is the nonlinear operator,

$g(x,t)$ is the known function.

Output: The approximate solution of $u(x,t)$.

Initial Step: Enter the values of M (order of Hermite polynomial) and k (level of resolution).

Step I: Construct the Hermite wavelet using the following formula

$$\psi_{n_1,m_1,n_2,m_2}(x,t) = \begin{cases} AH_{m_1}\!\left(2^{k_1}x - \hat{n}_1\right)H_{m_2}\!\left(2^{k_2}t - \hat{n}_2\right), & \dfrac{\hat{n}_1 - 1}{2^{k_1}} \le x < \dfrac{\hat{n}_1 + 1}{2^{k_1}}, \\[2mm] & \dfrac{\hat{n}_2 - 1}{2^{k_2}} \le t < \dfrac{\hat{n}_2 + 1}{2^{k_2}} \\[2mm] 0, & \text{elsewhere} \end{cases} \tag{7.8}$$

where $A = \sqrt{\dfrac{1}{n_1!\,2^{n_1}\sqrt{\pi}}}\sqrt{\dfrac{1}{n_2!\,2^{n_2}\sqrt{\pi}}}\; 2^{\frac{k_1+k_2}{2}},$

m_1 and m_2 are order of Hermite polynomials,

n_1 and n_2 are translation parameters,

k_1 and k_2 are positive integers specifying level of resolution.

Step II: Set $u(x,t) = \sum\limits_{n_1=1}^{2^{k_1-1}} \sum\limits_{m_1=0}^{M_1-1} \sum\limits_{n_2=1}^{2^{k_2-1}} \sum\limits_{m_2=0}^{M_2-1} a_{n_1,m_1,n_2,m_2}\, \psi_{n_1,m_1,n_2,m_2}(x,t),$ (7.9)

and nonlinear term $\mathcal{N} u(x,t) = \sum\limits_{n_1=1}^{2^{k_1-1}} \sum\limits_{m_1=0}^{M_1-1} \sum\limits_{n_2=1}^{2^{k_2-1}} \sum\limits_{m_2=0}^{M_2-1} b_{n_1,m_1,n_2,m_2}\, \psi_{n_1,m_1,n_2,m_2}(x,t).$ (7.10)

Step III: Compute $\mathcal{L}^{-1}[\mathcal{L}\, u(x,t) + \mathcal{N}\, u(x,t)] = \mathcal{L}^{-1}[g(x,t)]$ (7.11)

Step IV: For $i = 1(1)M_1 2^{k_1-1}$ do

         compute $x_i = \dfrac{2i-1}{2M_1 2^{k_1-1}}$ (collocation points for spatial variable)

         end

         For $j = 1(1)M_2 2^{k_2-1}$ do

         calculate $t_j = \dfrac{2j-1}{2M_2 2^{k_2-1}}$ (collocation points for temporal variable)

         end

Step V: Substituting the collocation points x_i and t_j obtained in Step IV in eq. (7.11) and obtain the system of algebraic equations in a_{n_1,m_1,n_2,m_2} and b_{n_1,m_1,n_2,m_2}.

Step VI: By solving the system of equations obtained in Step V using Newton's method, the Hermite wavelet coefficients a_{n_1,m_1,n_2,m_2} and b_{n_1,m_1,n_2,m_2} can be obtained.

Step VII: Substituting the value of a_{n_1,m_1,n_2,m_2} in eq. (7.9), obtain the approximate solution for $u(x,t)$.

Step VIII: Stop.

7.3 Application of Analytical and Numerical Methods for Solving Time-Fractional Modified Fornberg-Whitham Equation

7.3.1 Two-Dimensional Hermite Wavelet Method for Solving Nonlinear Time-Fractional Modified Fornberg-Whitham Equation

To exhibit the effectiveness and accuracy of proposed numerical scheme, we consider the time-fractional modified Fornberg-Whitham equation. The numerical solutions thus obtained are compared with the exact solutions in case of classical order and with the solutions obtained by OHAM in case of fractional order respectively.

Consider the nonlinear time-fractional modified Fornberg-Whitham equation

$$\frac{\partial^\alpha u}{\partial t^\alpha} - \frac{\partial^3 u}{\partial x^2 \partial t} + \frac{\partial u}{\partial x} + u^2 \frac{\partial u}{\partial x} = 3 \frac{\partial u}{\partial x} \frac{\partial^2 u}{\partial x^2} + u \frac{\partial^3 u}{\partial x^3}, \qquad t > 0, \; x > 0, \tag{7.12}$$

with initial condition

$$u(x,0) = \frac{3}{4}\left(\sqrt{15} - 5\right)\sec h^2\left(\frac{1}{20}\sqrt{10\left(5 - \sqrt{15}\right)}\right)x. \tag{7.13}$$

The exact solution of eq. (7.12) is given by [154]

$$u(x,t) = \frac{3}{4}\left(\sqrt{15} - 5\right)\sec h^2\left[\frac{1}{20}\sqrt{10\left(5 - \sqrt{15}\right)}\left(x - (5 - \sqrt{15})t\right)\right]. \tag{7.14}$$

The Hermite wavelet solution of $u(x,t)$ is sought by assuming that $u(x,t)$ can be expanded in terms of Hermite wavelet as

$$u(x,t) = \sum_{n=1}^{2^{k_1-1}} \sum_{i=0}^{M_1-1} \sum_{l=1}^{2^{k_2-1}} \sum_{j=0}^{M_2-1} d_{n,i,l,j}\, \psi_{n,i,l,j}(x,t), \tag{7.15}$$

where $n = 1,...,2^{k_1-1}, i = 0,...,M_1 - 1, l = 1,...,2^{k_2-1}, j = 0,...,M_2 - 1.$

The nonlinear terms presented in eq. (7.12) can be approximated using Hermite wavelet function as

$$u^2 \frac{\partial u}{\partial x} = \sum_{n=1}^{2^{k_1-1}} \sum_{i=0}^{M_1-1} \sum_{l=1}^{2^{k_2-1}} \sum_{j=0}^{M_2-1} a_{n,i,l,j}\, \psi_{n,i,l,j}(x,t), \tag{7.16}$$

$$\frac{\partial u}{\partial x}\frac{\partial^2 u}{\partial x^2} = \sum_{n=1}^{2^{k_1-1}}\sum_{i=0}^{M_1-1}\sum_{l=1}^{2^{k_2-1}}\sum_{j=0}^{M_2-1} b_{n,i,l,j}\,\psi_{n,i,l,j}(x,t),\qquad(7.17)$$

and
$$u\frac{\partial^3 u}{\partial x^3} = \sum_{n=1}^{2^{k_1-1}}\sum_{i=0}^{M_1-1}\sum_{l=1}^{2^{k_2-1}}\sum_{j=0}^{M_2-1} c_{n,i,l,j}\,\psi_{n,i,l,j}(x,t).\qquad(7.18)$$

This implies

$$\left(\sum_{n=1}^{2^{k_1-1}}\sum_{i=0}^{M_1-1}\sum_{l=1}^{2^{k_2-1}}\sum_{j=0}^{M_2-1} d_{n,i,l,j}\psi_{n,i,l,j}(x,t)\right)^2 \times \left[\sum_{n=1}^{2^{k_1-1}}\sum_{i=0}^{M_1-1}\sum_{l=1}^{2^{k_2-1}}\sum_{j=0}^{M_2-1} d_{n,i,l,j}\frac{\partial\psi_{n,i,l,j}(x,t)}{\partial x}\right]$$
$$= \sum_{n=1}^{2^{k_1-1}}\sum_{i=0}^{M_1-1}\sum_{l=1}^{2^{k_2-1}}\sum_{j=0}^{M_2-1} a_{n,i,l,j}\,\psi_{n,i,l,j}(x,t).\qquad(7.19)$$

$$\left(\sum_{n=1}^{2^{k_1-1}}\sum_{i=0}^{M_1-1}\sum_{l=1}^{2^{k_2-1}}\sum_{j=0}^{M_2-1} d_{n,i,l,j}\frac{\partial\psi_{n,i,l,j}(x,t)}{\partial x}\right)\times\left[\sum_{n=1}^{2^{k_1-1}}\sum_{i=0}^{M_1-1}\sum_{l=1}^{2^{k_2-1}}\sum_{j=0}^{M_2-1} d_{n,i,l,j}\frac{\partial^2\psi_{n,i,l,j}(x,t)}{\partial x^2}\right]$$
$$= \sum_{n=1}^{2^{k_1-1}}\sum_{i=0}^{M_1-1}\sum_{l=1}^{2^{k_2-1}}\sum_{j=0}^{M_2-1} b_{n,i,l,j}\,\psi_{n,i,l,j}(x,t),\qquad(7.20)$$

and

$$\left[\sum_{n=1}^{2^{k_1-1}}\sum_{i=0}^{M_1-1}\sum_{l=1}^{2^{k_2-1}}\sum_{j=0}^{M_2-1} d_{n,i,l,j}\psi_{n,i,l,j}(x,t)\right]\left(\sum_{n=1}^{2^{k_1-1}}\sum_{i=0}^{M_1-1}\sum_{l=1}^{2^{k_2-1}}\sum_{j=0}^{M_2-1} d_{n,i,l,j}\frac{\partial^3\psi_{n,i,l,j}(x,t)}{\partial x^3}\right)$$
$$= \sum_{n=1}^{2^{k_1-1}}\sum_{i=0}^{M_1-1}\sum_{l=1}^{2^{k_2-1}}\sum_{j=0}^{M_2-1} c_{n,i,l,j}\psi_{n,i,l,j}(x,t).\qquad(7.21)$$

Again applying J_t^α on both sides of eq. (7.12) we have

$$u(x,t)-u(x,0) = J_t^\alpha\left[\frac{\partial^3 u}{\partial x^2\partial t} - \frac{\partial u}{\partial x} - u^2\frac{\partial u}{\partial x} + 3\frac{\partial u}{\partial x}\frac{\partial^2 u}{\partial x^2} + u\frac{\partial^3 u}{\partial x^3}\right].\qquad(7.22)$$

Putting eqs. (7.15), (7.16), (7.17) and (7.18) in eq. (7.22), we have

$$\sum_{n=1}^{2^{k_1-1}} \sum_{i=0}^{M_1-1} \sum_{l=1}^{2^{k_2-1}} \sum_{j=0}^{M_2-1} d_{n,i,l,j} \psi_{n,i,l,j}(x,t) - u(x,0) =$$

$$J_t^{\alpha} \left[\frac{\partial^3}{\partial x^2 \partial t} \left(\sum_{n=1}^{2^{k_1-1}} \sum_{i=0}^{M_1-1} \sum_{l=1}^{2^{k_2-1}} \sum_{j=0}^{M_2-1} d_{n,i,l,j} \psi_{n,i,l,j}(x,t) \right) - \right.$$

$$\frac{\partial}{\partial x} \left(\sum_{n=1}^{2^{k_1-1}} \sum_{i=0}^{M_1-1} \sum_{l=1}^{2^{k_2-1}} \sum_{j=0}^{M_2-1} d_{n,i,l,j} \psi_{n,i,l,j}(x,t) \right) - \sum_{n=1}^{2^{k_1-1}} \sum_{i=0}^{M_1-1} \sum_{l=1}^{2^{k_2-1}} \sum_{j=0}^{M_2-1} a_{n,i,l,j} \psi_{n,i,l,j}(x,t) +$$

$$\left. 3 \left(\sum_{n=1}^{2^{k_1-1}} \sum_{i=0}^{M_1-1} \sum_{l=1}^{2^{k_2-1}} \sum_{j=0}^{M_2-1} b_{n,i,l,j} \psi_{n,i,l,j}(x,t) \right) + \sum_{n=1}^{2^{k_1-1}} \sum_{i=0}^{M_1-1} \sum_{l=1}^{2^{k_2-1}} \sum_{j=0}^{M_2-1} c_{n,i,l,j} \psi_{n,i,l,j}(x,t) \right].$$

(7. 23)

Now substituting the collocation points $x_l = \dfrac{l - 0.5}{2^{k_1-1} M_1}$ and $t_r = \dfrac{r - 0.5}{2^{k_2-1} M_2}$ for

$l = 1, 2, \ldots, 2^{k_1-1} M_1$ and $r = 1, 2, \ldots, 2^{k_2-1} M_2$ in eqs. (7.19), (7.20), (7.21) and (7.23), we

have $4\left(2^{k_1-1} M_1\right)\left(2^{k_2-1} M_2\right)$ equations in $4\left(2^{k_1-1} M_1\right)\left(2^{k_2-1} M_2\right)$ unknowns in $a_{n,i,l,j}$, $b_{n,i,l,j}$,

$c_{n,i,l,j}$ and $d_{n,i,l,j}$. By solving this system of equations using Newton's method, the

Hermite wavelet coefficients $a_{n,i,l,j}$, $b_{n,i,l,j}$, $c_{n,i,l,j}$ and $d_{n,i,l,j}$ can be obtained.

7.3.2 To Compare with OHAM for Solution of Time-Fractional Modified Fornberg-Whitham Equation

Using optimal homotopy asymptotic method [30-32], the homotopy for eqs. (7.12) can be

written as

$$(1 - p)L(\varphi(x,t\,;p)) = H(p)\left[\frac{\partial^\alpha \varphi(x,t\,;p)}{\partial t^\alpha} - \frac{\partial^3}{\partial x^2 \partial t} \varphi(x,t\,;p) + \frac{\partial}{\partial x} \varphi(x,t\,;p) \right.$$

$$\left. + \varphi(x,t\,;p)^2 \frac{\partial \varphi(x,t\,;p)}{\partial x} - 3\frac{\partial \varphi(x,t\,;p)}{\partial x}\frac{\partial^2 \varphi(x,t\,;p)}{\partial x^2} - \varphi(x,t\,;p)\frac{\partial^3 \varphi(x,t\,;p)}{\partial x^3} \right],$$

(7.24)

where $\varphi(x,t\,;p) = u_0(x,t) + \displaystyle\sum_{i=1}^{\infty} u_i(x,t)p^i$, (7.25)

$$H(p) = C_1 p + C_2 p^2 + C_3 p^3 + \ldots .$$

(7.26)

Substituting eqs. (7.25) and (7.26) in eq. (7.24) and equating the coefficients of different

powers in p, we have the following system of partial differential equations.

Coefficients of $p^0 : \dfrac{\partial^\alpha u_0(x,t)}{\partial t^\alpha} = 0$. (7.27)

Coefficients of p^1 : $\dfrac{\partial^\alpha u_1(x,t)}{\partial t^\alpha} - \dfrac{\partial^\alpha u_0(x,t)}{\partial t^\alpha} = C_1\left[\dfrac{\partial^\alpha u_0(x,t)}{\partial t^\alpha} - \dfrac{\partial^3 u_0(x,t)}{\partial x^2 \partial t} + \dfrac{\partial u_0(x,t)}{\partial x}\right.$

$$\left. + (u_0(x,t))^2 \dfrac{\partial u_0(x,t)}{\partial x} - 3\dfrac{\partial u_0(x,t)}{\partial x}\dfrac{\partial^2 u_0(x,t)}{\partial x^2} - u_0(x,t)\dfrac{\partial^3 u_0(x,t)}{\partial x^3}\right]. \qquad (7.28)$$

Coefficients of p^2 :

$$\dfrac{\partial^\alpha u_2(x,t)}{\partial t^\alpha} - \dfrac{\partial^\alpha u_1(x,t)}{\partial t^\alpha} = C_1\left[\dfrac{\partial^\alpha u_1(x,t)}{\partial t^\alpha} - \dfrac{\partial^3 u_1(x,t)}{\partial x^2 \partial t} + \dfrac{\partial u_1(x,t)}{\partial x} + \right.$$

$$\left(2u_0(x,t)u_1(x,t)\dfrac{\partial u_0(x,t)}{\partial x} + (u_0(x,t))^2 \dfrac{\partial u_1(x,t)}{\partial x}\right)$$

$$-3\left(\dfrac{\partial u_0(x,t)}{\partial x}\dfrac{\partial^2 u_1(x,t)}{\partial x^2} + \dfrac{\partial u_1(x,t)}{\partial x}\dfrac{\partial^2 u_0(x,t)}{\partial x^2}\right)$$

$$-\left(u_0(x,t)\dfrac{\partial^3 u_1(x,t)}{\partial x^3} + u_1(x,t)\dfrac{\partial^3 u_0(x,t)}{\partial x^3}\right)\right] + C_2\left[\dfrac{\partial^\alpha u_0(x,t)}{\partial t^\alpha} - \dfrac{\partial^3 u_0(x,t)}{\partial x^2 \partial t}\right.$$

$$\left. + \dfrac{\partial u_0(x,t)}{\partial x} + (u_0(x,t))^2 \dfrac{\partial u_0(x,t)}{\partial x} - 3\dfrac{\partial u_0(x,t)}{\partial x}\dfrac{\partial^2 u_0(x,t)}{\partial x^2} - u_0(x,t)\dfrac{\partial^3 u_0(x,t)}{\partial x^3}\right].$$

$$(7.29)$$

Coefficients of p^3 :

$$\dfrac{\partial^\alpha u_3(x,t)}{\partial t^\alpha} - \dfrac{\partial^\alpha u_2(x,t)}{\partial t^\alpha} = C_1\left[\dfrac{\partial^\alpha u_2(x,t)}{\partial t^\alpha} - \dfrac{\partial^3 u_2(x,t)}{\partial x^2 \partial t} + \dfrac{\partial u_2(x,t)}{\partial x} + \left((u_1(x,t))^2 \dfrac{\partial u_0(x,t)}{\partial x} + \right.\right.$$

$$\left. + 2u_0(x,t)u_2(x,t)\dfrac{\partial u_0(x,t)}{\partial x} + 2u_0(x,t)u_1(x,t)\dfrac{\partial u_1(x,t)}{\partial x} + (u_0(x,t))^2 \dfrac{\partial u_2(x,t)}{\partial x}\right) -$$

$$3\left(\dfrac{\partial u_0(x,t)}{\partial x}\dfrac{\partial^2 u_2(x,t)}{\partial x^2} + \dfrac{\partial u_1(x,t)}{\partial x}\dfrac{\partial^2 u_1(x,t)}{\partial x^2} + \dfrac{\partial u_2(x,t)}{\partial x}\dfrac{\partial^2 u_0(x,t)}{\partial x^2}\right)$$

$$-\left(u_0(x,t)\dfrac{\partial^3 u_2(x,t)}{\partial x^3} + u_1(x,t)\dfrac{\partial^3 u_1(x,t)}{\partial x^3} + u_2(x,t)\dfrac{\partial^3 u_0(x,t)}{\partial x^3}\right)\right] + C_2\left[\dfrac{\partial^\alpha u_1(x,t)}{\partial t^\alpha}\right.$$

$$- \dfrac{\partial^3 u_1(x,t)}{\partial x^2 \partial t} + \dfrac{\partial u_1(x,t)}{\partial x} + \left(2u_0(x,t)u_1(x,t)\dfrac{\partial u_0(x,t)}{\partial x} + (u_0(x,t))^2 \dfrac{\partial u_1(x,t)}{\partial x}\right)$$

$$-3\left(\dfrac{\partial u_0(x,t)}{\partial x}\dfrac{\partial^2 u_1(x,t)}{\partial x^2} + \dfrac{\partial u_1(x,t)}{\partial x}\dfrac{\partial^2 u_0(x,t)}{\partial x^2}\right) - \left(u_0(x,t)\dfrac{\partial^3 u_1(x,t)}{\partial x^3} + u_1(x,t)\dfrac{\partial^3 u_0(x,t)}{\partial x^3}\right)\right]$$

$$+ C_3\left[\dfrac{\partial^\alpha u_0(x,t)}{\partial t^\alpha} - \dfrac{\partial^3 u_0(x,t)}{\partial x^2 \partial t} + \dfrac{\partial u_0(x,t)}{\partial x} + (u_0(x,t))^2 \dfrac{\partial u_0(x,t)}{\partial x}\right.$$

$$\left. - 3\dfrac{\partial u_0(x,t)}{\partial x}\dfrac{\partial^2 u_0(x,t)}{\partial x^2} - u_0(x,t)\dfrac{\partial^3 u_0(x,t)}{\partial x^3}\right],$$

$$(7.30)$$

and so on.

For solving fractional order modified Fornberg-Whitham equation using OHAM, we consider the following initial condition for equation (7.12)

$$u(x,0) = \frac{3}{4}\left(\sqrt{15} - 5\right)\sec h^2\left(\frac{1}{20}\sqrt{10\left(5 - \sqrt{15}\right)}\right)x.$$

Using the initial condition $u_0 = u(x,0)$ and solving eq. (7.27) to eq. (7.30), we obtain the expressions for u_0, u_1, u_2, u_3 and so on.

Finally, the third order approximate solution for time-fractional modified Fornberg-Whitham equation is given by

$$u = u_0(x,t) + u_1(x,t) + u_2(x,t) + u_3(x,t). \tag{7.31}$$

The optimal values of the convergence control constants C_1, C_2 and C_3 can be obtained using weighted residual least square method given in eqs. (1.34) and (1.35) of chapter 1.

7.4 Numerical Results and Discussion

The comparison of the absolute errors for time-fractional modified Fornberg-Whitham equation (7.12) have been exhibited in Tables 7.1 and 7.2 which are generated using the results obtained by two-dimensional Hermite wavelet method and OHAM at different values of x and t taking $\alpha = 1$. In the present analysis, to examine the accuracy and reliability of the Hermite wavelets for solving fractional order modified Fornberg-Whitham equation, we compare the approximate solution of Hermite wavelets with the third order approximate solution obtained by OHAM. Tables 7.3 and 7.4 show the absolute errors of fractional order modified Fornberg-Whitham equation (7.12) at various points of x and t taking $\alpha = 0.75$ and 0.5 respectively. Agreement between present numerical results for time-fractional modified Fornberg-Whitham equation obtained by Hermite wavelets and OHAM appears very satisfactory through illustrations in Tables 7.5 and 7.6. Table 7.7 shows the L_2 and L_∞ error norms for fractional modified Fornberg-Whitham equation using two-dimensional Hermite wavelet methods and OHAM at various points of t taking $\alpha = 0.75$ and 0.5.

Table 7.1 The absolute errors obtained by two-dimensional Hermite wavelet method for nonlinear modified Fornberg-Whitham equation given in eq. (7.12) at various points of x and t taking $\alpha = 1$.

x	$\lvert u_{Exact} - u_{Hermite\,wavelet} \rvert$								
	$t = 0.1$	$t = 0.2$	$t = 0.3$	$t = 0.4$	$t = 0.5$	$t = 0.6$	$t = 0.7$	$t = 0.8$	$t = 0.9$
0.1	3.7564E-4	5.5722E-4	5.1447E-4	2.1718E-4	3.6388E-4	1.2543E-3	2.4734E-3	4.0313E-3	5.9263E-3
0.2	3.6817E-4	5.4379E-4	5.0090E-4	2.1372E-4	3.4281E-4	1.1905E-3	2.3457E-3	3.8163E-3	5.6007E-3
0.3	3.6433E-4	5.3561E-4	4.9206E-4	2.1218E-4	3.2489E-4	1.1373E-3	2.2382E-3	3.6336E-3	5.3201E-3
0.4	3.6412E-4	5.3275E-4	4.8812E-4	2.1292E-4	3.0961E-4	1.0938E-3	2.1497E-3	3.4808E-3	5.0827E-3
0.5	3.6757E-4	5.3531E-4	4.8929E-4	2.1630E-4	2.9639E-4	1.0593E-3	2.0792E-3	3.3572E-3	4.8871E-3
0.6	3.7478E-4	5.4349E-4	4.9589E-4	2.2274E-4	2.8468E-4	1.0331E-3	2.0259E-3	3.2615E-3	4.7320E-3
0.7	3.8584E-4	5.5751E-4	5.0827E-4	2.3274E-4	2.7383E-4	1.0144E-3	1.9888E-3	3.1928E-3	4.6163E-3
0.8	4.0091E-4	5.7767E-4	5.2688E-4	2.4690E-4	2.6312E-4	1.0023E-3	1.9670E-3	3.1500E-3	4.5391E-3
0.9	4.2025E-4	6.0441E-4	5.5231E-4	2.6594E-4	2.5171E-4	9.9595E-4	1.9595E-3	3.1322E-3	4.4992E-3

Table 7.2 The absolute errors obtained by optimal homotopy asymptotic method (OHAM) for modified Fornberg-Whitham equation given in eq. (7.12) at various points of x and t taking $\alpha = 1$.

x	$\lvert u_{Exact} - u_{OHAM} \rvert$								
	$t = 0.1$	$t = 0.2$	$t = 0.3$	$t = 0.4$	$t = 0.5$	$t = 0.6$	$t = 0.7$	$t = 0.8$	$t = 0.9$
0.1	6.4610E-6	1.2928E-5	5.7106E-5	1.2329E-4	2.0699E-4	3.0203E-4	4.0061E-4	4.9330E-4	5.6917E-4
0.2	2.5099E-5	2.2342E-5	8.7492E-6	6.6918E-5	1.4918E-4	2.5087E-4	3.6563E-4	4.8544E-4	6.0074E-4
0.3	4.3236E-5	5.6305E-5	3.7197E-5	1.4365E-5	9.6935E-5	2.0734E-4	3.4071E-4	4.9050E-4	6.4853E-4
0.4	6.0707E-5	8.8650E-5	8.0295E-5	3.3830E-5	5.0831E-5	1.7204E-4	3.2644E-4	5.0897E-4	7.1289E-4
0.5	7.7360E-5	1.1908E-4	1.2014E-4	7.7185E-5	1.1402E-5	1.4551E-4	3.2329E-4	5.4121E-4	7.9400E-4
0.6	9.3052E-5	1.4735E-4	1.5637E-4	1.1527E-4	2.0905E-5	1.2816E-4	3.3161E-4	5.8741E-4	8.9183E-4
0.7	1.0765E-4	1.7320E-4	1.8867E-4	1.4773E-4	4.5730E-5	1.2029E-4	3.5157E-4	6.4760E-4	1.0061E-3
0.8	1.2105E-4	1.9644E-4	2.1678E-4	1.7429E-4	6.2814E-5	1.2211E-4	3.8324E-4	7.2163E-4	1.1365E-3
0.9	1.3314E-4	2.1689E-4	2.4049E-4	1.9473E-4	7.1997E-5	1.3366E-4	4.2653E-4	8.0916E-4	1.2824E-3

Table 7.3 The absolute errors obtained by two-dimensional Hermite wavelet method and third order OHAM solution for fractional order nonlinear modified Fornberg-Whitham equation given in eq. (7.12) at various points of x and t taking $\alpha = 0.75$.

x	$\lvert u_{Exact} - u_{OHAM} \rvert$								
	$t = 0.1$	$t = 0.2$	$t = 0.3$	$t = 0.4$	$t = 0.5$	$t = 0.6$	$t = 0.7$	$t = 0.8$	$t = 0.9$
0.1	4.7565E-4	3.5641E-3	8.0016E-3	1.3396E-2	1.9495E-2	2.6133E-2	3.3182E-2	4.0509E-2	4.7923E-2
0.2	8.8635E-4	1.2693E-3	4.8602E-3	9.4511E-3	1.4770E-2	2.0648E-2	2.6963E-2	3.3585E-2	4.0320E-2
0.3	2.2468E-3	1.0167E-3	1.7374E-3	5.5349E-3	1.0084E-2	1.5214E-2	2.0804E-2	2.6727E-2	3.2788E-2
0.4	3.6037E-3	3.2904E-3	1.3619E-3	1.6542E-3	5.4468E-3	9.8382E-3	1.4712E-2	1.9946E-2	2.5339E-2
0.5	4.9553E-3	5.5482E-3	4.4327E-3	2.1843E-3	8.6443E-4	4.5308E-3	8.7013E-3	1.3255E-2	1.7987E-2
0.6	6.2997E-3	7.7868E-3	7.4700E-3	5.9744E-3	3.6545E-3	6.9903E-4	2.7806E-3	6.6656E-3	1.0747E-2
0.7	7.6352E-3	1.0003E-2	1.0469E-2	9.7098E-3	8.1023E-3	5.8419E-3	3.0385E-3	1.9102E-4	3.6320E-3
0.8	8.9603E-3	1.2193E-2	1.3425E-2	1.3384E-2	1.2471E-2	1.0888E-2	8.7451E-3	6.1561E-3	3.3425E-3

| 0.9 | 1.0273E-2 | 1.4356E-2 | 1.6335E-2 | 1.6992E-2 | 1.6754E-2 | 1.5830E-2 | 1.4328E-2 | 1.2363E-2 | 1.0162E-2 |

Table 7.4 The absolute errors obtained by two-dimensional Hermite wavelet method and third order OHAM solution for fractional order nonlinear modified Fornberg-Whitham equation given in eq. (7.12) at various points of x and t taking $\alpha = 0.5$.

x	$\left|u_{OHAM} - u_{Hermite\,wavelet}\right|$								
	$t=0.1$	$t=0.2$	$t=0.3$	$t=0.4$	$t=0.5$	$t=0.6$	$t=0.7$	$t=0.8$	$t=0.9$
0.1	1.2334E-2	4.0688E-3	1.4027E-2	1.6573E-2	1.5687E-2	1.5562E-2	1.5805E-2	6.6256E-3	3.5980E-2
0.2	1.5565E-2	3.8814E-4	1.0784E-2	1.3953E-2	1.3347E-2	1.3079E-2	1.3374E-2	6.0014E-3	3.0299E-2
0.3	1.8769E-2	3.2892E-3	7.5422E-3	1.1332E-2	1.0998E-2	1.0573E-2	1.0901E-2	5.3094E-3	2.4724E-2
0.4	2.1934E-2	6.9543E-3	4.3072E-3	8.7171E-3	8.6477E-3	8.0497E-3	8.3899E-3	4.5590E-3	1.9229E-2
0.5	2.5043E-2	1.0597E-2	1.0867E-3	6.1147E-3	6.3028E-3	5.5169E-3	5.8492E-3	3.7602E-3	1.3790E-2
0.6	2.8082E-2	1.4209E-2	2.1116E-3	3.5329E-3	3.9725E-3	2.9834E-3	3.2865E-3	2.9235E-3	8.3783E-3
0.7	3.1037E-2	1.7780E-2	5.2800E-3	9.8022E-4	1.6663E-3	4.5848E-4	7.1012E-4	2.0604E-3	2.9665E-3
0.8	3.3892E-2	2.1298E-2	8.4099E-3	1.5347E-3	6.0631E-4	2.0482E-3	1.8707E-3	1.1828E-3	2.4738E-3
0.9	3.6632E-2	2.4754E-2	1.1492E-2	4.0027E-3	2.8348E-3	4.5263E-3	4.4464E-3	3.0333E-4	7.9720E-3

Table 7.5 Comparison of approximate solutions obtained by two-dimensional Hermite wavelet method and optimal homotopy asymptotic method for fractional order nonlinear modified Fornberg-Whitham equation given in eq. (7.12) at various points of x and t taking $\alpha = 0.75$.

x	$t=0.1$		$t=0.2$		$t=0.3$		$t=0.4$		$t=0.5$		$t=0.6$		$t=0.7$		$t=0.8$		$t=0.9$	
	u_{HW}	u_{OHAM}	u_{HW}	u_{OHAM}	u_{HW}	u_{OHAM}	u_{HW}	u_{OHAM}	u_{HW}	u_{OHAM}	u_{HW}	u_{OHAM}	u_{HW}	u_{OHAM}	u_{HW}	u_{OHAM}	u_{HW}	u_{OHAM}
0.1	-0.84414	-0.84495	-0.84068	-0.84367	-0.83584	-0.84165	-0.83002	-0.83905	-0.82346	-0.83594	-0.81635	-0.83238	-0.80879	-0.82840	-0.80095	-0.82404	-0.79298	-0.81933
0.2	-0.84449	-0.84509	-0.84175	-0.84444	-0.83759	-0.84298	-0.83241	-0.84090	-0.82649	-0.83828	-0.81999	-0.83518	-0.81304	-0.83164	-0.80576	-0.82770	-0.79836	-0.82338
0.3	-0.84435	-0.84476	-0.84235	-0.84473	-0.83885	-0.84385	-0.83431	-0.84229	-0.82901	-0.84016	-0.82312	-0.83753	-0.81677	-0.83444	-0.81006	-0.83093	-0.80321	-0.82703
0.4	-0.84375	-0.84395	-0.84247	-0.84455	-0.83963	-0.84423	-0.83571	-0.84320	-0.83103	-0.84157	-0.82574	-0.83942	-0.81997	-0.83679	-0.81383	-0.83372	-0.80752	-0.83024
0.5	-0.84268	-0.84266	-0.84211	-0.84389	-0.83991	-0.84415	-0.83661	-0.84365	-0.83253	-0.84253	-0.82783	-0.84085	-0.82264	-0.83869	-0.81705	-0.83606	-0.81129	-0.83302
0.6	-0.84115	-0.84091	-0.84128	-0.84277	-0.83971	-0.84358	-0.83702	-0.84362	-0.83352	-0.84301	-0.82941	-0.84182	-0.82478	-0.84013	-0.81975	-0.83796	-0.81452	-0.83535
0.7	-0.83915	-0.83868	-0.83998	-0.84117	-0.83903	-0.84255	-0.83693	-0.84312	-0.83401	-0.84302	-0.83046	-0.84233	-0.82639	-0.84110	-0.82189	-0.83939	-0.81719	-0.83724
0.8	-0.83669	-0.83600	-0.83821	-0.83910	-0.83787	-0.84105	-0.83634	-0.84215	-0.83399	-0.84256	-0.83099	-0.84236	-0.82746	-0.84162	-0.82349	-0.84038	-0.81932	-0.83867
0.9	-0.83379	-0.83286	-0.83598	-0.83657	-0.83624	-0.83908	-0.83527	-0.84072	-0.83346	-0.84163	-0.83101	-0.84193	-0.82800	-0.84167	-0.82455	-0.84090	-0.82088	-0.83966

Table 7.6 Comparison of approximate solutions obtained by two-dimensional Hermite wavelet method and optimal homotopy asymptotic method for fractional order nonlinear modified Fornberg-Whitham equation given in eq. (7.12) at various points of x and t taking $\alpha = 0.5$.

x	$t=0.1$		$t=0.2$		$t=0.3$		$t=0.4$		$t=0.5$		$t=0.6$		$t=0.7$		$t=0.8$		$t=0.9$	
	u_{HW}	u_{OHAM}	u_{HW}	u_{OHAM}	u_{HW}	u_{OHAM}	u_{HW}	u_{OHAM}	u_{HW}	u_{OHAM}	u_{HW}	u_{OHAM}	u_{HW}	u_{OHAM}	u_{HW}	u_{OHAM}	u_{HW}	u_{OHAM}
0.1	-0.85594	-0.84360	-0.83668	-0.84073	-0.82344	-0.83747	-0.81743	-0.83401	-0.81471	-0.83040	-0.81114	-0.82671	-0.80713	-0.82294	-0.81248	-0.81911	-0.85122	-0.81524
0.2	-0.85	-0.84	-0.84	-0.84	-0.82	-0.83	-0.82	-0.83	-0.81	-0.83	-0.8	-0.82	-0.8	-0.82	-0.81	-0.82	-0.8	-0.8

t																		
	929	372	118	157	807	885	188	584	928	263	1620	928	1246	583	629	230	4899	1869
0.3	-0.86214	-0.84337	-0.84523	-0.84195	-0.83223	-0.83977	-0.82589	-0.83722	-0.82342	-0.83442	-0.82086	-0.83143	-0.81740	-0.82831	-0.81976	-0.82507	-0.84646	-0.82174
0.4	-0.86449	-0.84256	-0.84881	-0.84185	-0.83593	-0.84024	-0.82944	-0.83815	-0.82711	-0.83576	-0.82509	-0.83314	-0.82196	-0.83035	-0.82286	-0.82742	-0.84361	-0.82438
0.5	-0.86632	-0.84127	-0.85189	-0.84130	-0.83916	-0.84025	-0.83252	-0.83863	-0.83035	-0.83665	-0.82889	-0.83441	-0.82611	-0.83196	-0.82559	-0.82935	-0.84039	-0.82660
0.6	-0.86762	-0.83954	-0.85449	-0.84028	-0.84191	-0.83979	-0.83513	-0.83866	-0.83313	-0.83710	-0.83225	-0.83523	-0.82985	-0.83314	-0.82793	-0.83085	-0.83678	-0.82841
0.7	-0.86838	-0.83735	-0.85659	-0.83882	-0.84417	-0.83889	-0.83725	-0.83823	-0.83543	-0.83710	-0.83516	-0.83562	-0.83317	-0.83388	-0.82986	-0.83192	-0.83276	-0.82979
0.8	-0.86860	-0.83471	-0.85819	-0.83689	-0.84594	-0.83753	-0.83889	-0.83736	-0.83726	-0.83665	-0.83761	-0.83556	-0.83605	-0.83418	-0.83138	-0.83256	-0.82827	-0.83075
0.9	-0.86826	-0.83163	-0.85929	-0.83453	-0.84722	-0.83573	-0.84004	-0.83604	-0.83859	-0.83576	-0.83959	-0.83506	-0.83849	-0.83405	-0.83246	-0.83277	-0.82330	-0.83127

Table 7.7 L_2 and L_∞ error norms for fractional order nonlinear modified Fornberg-Whitham equation using two-dimensional Hermite wavelet methods at various points of t taking $\alpha = 0.75$ and 0.5.

t	$\alpha = 0.75$		$\alpha = 0.5$	
	L_2	L_∞	L_2	L_∞
0.1	1.80944E-2	3.6632E-2	7.80858E-2	1.0273E-2
0.2	2.39252E-2	2.4754E-2	4.21019E-2	1.4356E-2
0.3	2.69190E-2	1.4027E-2	2.49960E-2	1.6335E-2
0.4	3.00791E-2	1.6573E-2	2.72568E-2	1.6992E-2
0.5	3.52921E-2	1.5687E-2	2.62040E-2	1.9495E-2
0.6	4.31487E-2	1.5562E-2	2.55744E-2	2.6133E-2
0.7	5.34017E-2	1.5805E-2	2.62044E-2	3.3182E-2
0.8	6.55134E-2	6.6256E-3	1.29004E-2	4.0509E-2
0.9	7.87788E-2	3.5980E-2	5.94344E-2	4.7923E-2

The following Figures 7.1 and 7.2 demonstrate the graphical comparison of the numerical solutions obtained by two-dimensional Hermite wavelet approximation with regard to OHAM for $\alpha = 0.75$ and 0.5 respectively.
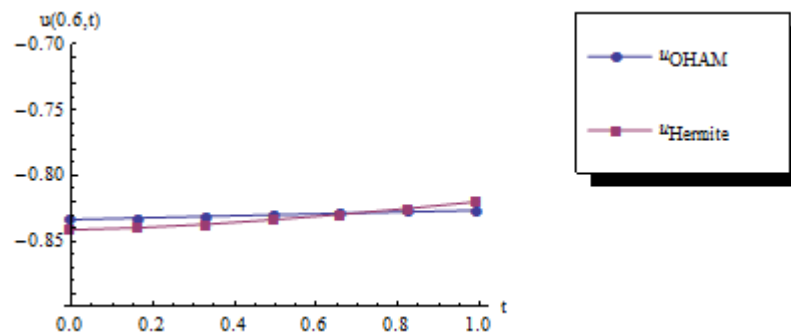
Figure 7.1 Comparison of the numerical solutions of $u(0.6,t)$ obtained by OHAM with regard to two-dimensional Hermite wavelet approximation for $\alpha = 0.75$.
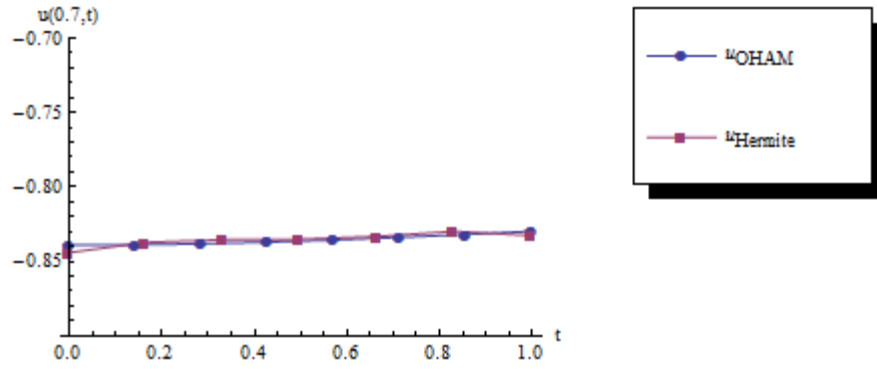
Figure 7.2   Comparison of the numerical solutions of $u(0.7,t)$ obtained by OHAM with regard to two-dimensional Hermite wavelet approximation for $\alpha = 0.5$.

7.5   Application of Analytical Methods to Determine the Exact Solutions of Time-Fractional Modified Fornberg-Whitham Equation

7.5.1 Implementation of the First Integral Method for Solving Fractional Modified Fornberg-Whitham Equation

Let us consider the following time-fractional modified Fornberg-Whitham equation

$$\frac{\partial^{\alpha} u}{\partial t^{\alpha}} - \frac{\partial^{\alpha}}{\partial t^{\alpha}}\left(\frac{\partial^2 u}{\partial x^2}\right) + \frac{\partial u}{\partial x} + u^2\frac{\partial u}{\partial x} = 3\frac{\partial u}{\partial x}\frac{\partial^2 u}{\partial x^2} + u\frac{\partial^3 u}{\partial x^3}, \tag{7.32}$$

Here $0 < \alpha \leq 1$, is the parameter representing the order of the fractional time derivative. In this present section, new exact solution of fractional modified Fornberg-Whitham equation has been derived using the first integral method. The first integral method has been implemented for finding exact solution of fractional modified Fornberg-Whitham equation given in eq. (7.32) with an intention to demonstrate the efficacy and accuracy of the proposed method. The exact solutions devised are compared with the numerical solution obtained by OHAM.

Let us introduce the following fractional complex transform in eq. (7.32):

$$u(x,t) = \Psi(\xi), \quad \xi = kx - \frac{\lambda t^{\alpha}}{\Gamma(\alpha+1)}, \tag{7.33}$$

where k and λ are constants.

By applying the fractional complex transform (7.33), eq. (7.32) can be transformed to the following nonlinear ordinary differential equation

$$-\lambda \Psi_\xi(\xi) + \lambda k^2 \Psi_{\xi\xi\xi}(\xi) + k\Psi_\xi(\xi) + k\left(\Psi(\xi)\right)^2 \Psi_\xi(\xi) = 3k^3 \Psi_\xi(\xi)\Psi_{\xi\xi}(\xi)$$
$$+ k^3 \Psi(\xi)\Psi_{\xi\xi\xi}(\xi). \tag{7.34}$$

Integrating eq. (7.34) once with respect to ξ, we obtain

$$\tilde{\xi}_0 - \lambda \Psi(\xi) + \lambda k^2 \Psi_{\xi\xi}(\xi) + k\Psi(\xi) + \frac{k}{3}\left(\Psi(\xi)\right)^3 = \frac{3}{2}k^3\left(\Psi_\xi(\xi)\right)^2$$
$$+ k^3\left(\Psi(\xi)\Psi_{\xi\xi}(\xi) - \frac{\left(\Psi_\xi(\xi)\right)^2}{2}\right), \tag{7.35}$$

where $\tilde{\xi}_0$ is an integration constant.

Using eqs. (1.6) and (1.7) of chapter 1, eq. (7.35) can be written as the following two-dimensional autonomous system

$$\frac{dX(\xi)}{d\xi} = Y(\xi),$$

$$\left(\lambda k^2 - k^3 X\right)\frac{dY(\xi)}{d\xi} = \lambda X(\xi) - \frac{k}{3}\left(X(\xi)\right)^3 - kX(\xi) + k^3\left(Y(\xi)\right)^2 - \xi_0. \tag{7.36}$$

According to the first integral method, we suppose that $X(\xi)$ and $Y(\xi)$ are the nontrivial solutions of eq. (7.36) and

$$Q(X,Y) = \sum_{i=0}^{m} a_i(X)Y^i$$

is an irreducible polynomial in the complex domain $\mathbb{C}\,[X, Y]$ such that

$$Q[X(\xi),Y(\xi)] = \sum_{i=0}^{m} a_i(X(\xi))Y^i(\xi) = 0, \tag{7.37}$$

where $a_i(X(\xi))$, $i = 0,1,2,...,m$ are polynomials in X and $a_m(X) \neq 0$. Eq. (7.37) is called the first integral to eq. (7.36). Applying the division theorem 1.1 of chapter 1, there exists a polynomial $g(X) + h(X)Y$ in the complex domain $\mathbb{C}\,[X, Y]$ such that

$$\frac{dQ}{d\xi} = (g(X) + h(X)Y)\sum_{i=0}^{m} a_i(X)Y^i. \tag{7.38}$$

Considering $m = 1$ in eq. (7.38), we obtain

$$\frac{\partial Q}{\partial X}\frac{dX}{d\xi} + \frac{\partial Q}{\partial Y}\frac{dY}{d\xi} = (g(X) + h(X)Y)(a_0(X) + a_1(X)Y). \tag{7.39}$$

Equating the coefficients of Y^i, $i = 0,1$ on both sides of eq. (7.39), we have

$$Y^0: \quad a_1(X)\left(\lambda X(\xi) - \frac{k}{3}(X(\xi))^3 - kX(\xi) - \xi_0\right) = a_0(X)g(X)\left(\lambda k^2 - k^3 X\right). \tag{7.40}$$

$$Y^1: \quad \dot{a}_0(X)\left(\lambda k^2 - k^3 X\right) = \left(a_0(X)h(X) + a_1(X)g(X)\right)\left(\lambda k^2 - k^3 X\right). \tag{7.41}$$

$$Y^2: \quad \dot{a}_1(X)\left(\lambda k^2 - k^3 X\right) = a_1(X)h(X)\left(\lambda k^2 - k^3 X\right) - a_1(X)k^3. \tag{7.42}$$

Since $a_i(X)$, $i = 0,1$ are polynomials in X, from eq. (7.42) we infer that $a_1(X)$ is a

constant and $h(X) = \dfrac{k}{\lambda - kX}$. For simplicity, we take $a_1(X) = 1$. Then balancing the

degrees of $a_0(X)$ and $g(X)$, eq. (7.41) indicates that $\deg(g(X)) \le \deg(a_0(X))$, thus

from eq. (7.41), we conclude that $\deg(g(X)) = 1$.

Now suppose that

$$g(X) = b_1 X + b_0, \quad a_0(X) = \frac{A_2}{2}X^2 + A_1 X + A_0, \quad (b_1 \ne 0, A_2 \ne 0), \tag{7.43}$$

where b_1, b_0, A_2, A_1 and A_0 are all constants to be determined later. Using eq. (7.41), we

find that

$$b_0 = A_1 - \frac{kA_0}{\lambda}, \tag{7.44}$$

$$b_1 = A_2 - \frac{A_1 k}{\lambda} - \frac{k^2 A_0}{\lambda^2}. \tag{7.45}$$

Next, substituting $a_0(X)$ and $g(X)$ in eq. (7.40) and consequently equating the

coefficients of X^i, $i = 0,1,2,3,4$ to zero, we obtain the following system of nonlinear

algebraic equations:

$$X^0: \quad b_0 A_0 \lambda k^2 + \xi_0 = 0. \tag{7.46}$$

$$X^1: \quad b_0 A_1 \lambda k^2 + b_1 A_0 \lambda k^2 - b_0 A_0 k^3 = \lambda - k. \tag{7.47}$$

$$X^2: \quad \frac{b_0 A_2 \lambda k^2}{2} + b_1 A_1 \lambda k^2 - b_0 A_1 k^3 - A_0 b_1 k^3 = 0. \tag{7.48}$$

$$X^3: \quad \frac{b_1 A_2 \lambda k^2}{2} - \frac{b_0 A_2 k^3}{2} - b_1 A_1 k^3 = \frac{-k}{3}. \tag{7.49}$$

$$X^4: \quad -\frac{b_1 A_2 k^3}{2} = 0. \tag{7.50}$$

Solving the above system of eqs. (7.46)-(7.50) simultaneously, we get the following family of nontrivial solutions

$$A_0 = \frac{-i\sqrt{\lambda}(\lambda^2 - 3\lambda k + 3k^2)}{3k\sqrt{k^4(k-\lambda)}}, A_1 = \frac{-i\lambda^{\frac{3}{2}}}{3\sqrt{k^4(k-\lambda)}}, A_2 = \frac{-2i\sqrt{\lambda}k}{3\sqrt{k^4(k-\lambda)}}. \tag{7.51}$$

and $A_0 = \dfrac{i\sqrt{\lambda}(\lambda^2 - 3\lambda k + 3k^2)}{3k\sqrt{k^4(k-\lambda)}}, A_1 = \dfrac{i\lambda^{\frac{3}{2}}}{3\sqrt{k^4(k-\lambda)}}, A_2 = \dfrac{2i\sqrt{\lambda}k}{3\sqrt{k^4(k-\lambda)}}.$ $\qquad$ (7.52)

Case I: Substituting the values of A_0, A_1 and A_2, obtained in eq. (7.51) into eq. (7.37), we get

$$Y(\xi) = \frac{2i\sqrt{\lambda}k}{3\sqrt{k^4(k-\lambda)}} X^2 + \frac{i\lambda^{\frac{3}{2}}}{3\sqrt{k^4(k-\lambda)}} X + \frac{i\sqrt{\lambda}(\lambda^2 - 3\lambda k + 3k^2)}{3k\sqrt{k^4(k-\lambda)}},$$

or $\qquad \dfrac{dX(\xi)}{d\xi} = \dfrac{2i\sqrt{\lambda}k}{3\sqrt{k^4(k-\lambda)}} X^2 + \dfrac{i\lambda^{\frac{3}{2}}}{3\sqrt{k^4(k-\lambda)}} X + \dfrac{i\sqrt{\lambda}(\lambda^2 - 3\lambda k + 3k^2)}{3k\sqrt{k^4(k-\lambda)}}.$ $\qquad$ (7.53)

Solving eq. (7.53), we obtain the exact solution to eq. (7.32) as

$u(x,t) = \Psi(\xi)$

$$= X(\xi) = \frac{-1}{2k}\left[\lambda + i\sqrt{3}(\lambda - 2k)\tanh\left(\frac{(\lambda - 2k)\left(\sqrt{\lambda}\sqrt{k^4(k-\lambda)}\xi + 3i\lambda k^5\eta_1 - 3ik^6\eta_1\right)}{2\sqrt{3}(\lambda - k)k^4}\right)\right], \tag{7.54}$$

where η_1 is an arbitrary constant.

Case II: Substituting the values of A_0, A_1 and A_2 from eq. (7.52) into eq. (7.37), we get

$$Y(\xi) = -\frac{2i\sqrt{\lambda}k}{3\sqrt{k^4(k-\lambda)}} X^2 - \frac{i\lambda^{\frac{3}{2}}}{3\sqrt{k^4(k-\lambda)}} X - \frac{i\sqrt{\lambda}(\lambda^2 - 3\lambda k + 3k^2)}{3k\sqrt{k^4(k-\lambda)}}$$

or $\qquad \dfrac{dX(\xi)}{d\xi} = -\dfrac{2i\sqrt{\lambda}k}{3\sqrt{k^4(k-\lambda)}} X^2 - \dfrac{i\lambda^{\frac{3}{2}}}{3\sqrt{k^4(k-\lambda)}} X - \dfrac{i\sqrt{\lambda}(\lambda^2 - 3\lambda k + 3k^2)}{3k\sqrt{k^4(k-\lambda)}}$ $\qquad$ (7.55)

Solving eq. (7.55), we obtain the exact solution to eq. (7.32) as

$u(x,t) = \Psi(\xi)$

$$= X(\xi) = \frac{i}{2k}\left[i\lambda + \sqrt{3}(\lambda - 2k)\tanh\left(\frac{(\lambda - 2k)\left(\sqrt{\lambda}\sqrt{k^4(k-\lambda)}\xi + 3i\lambda k^5\eta_2 - 3ik^6\eta_2\right)}{2\sqrt{3}(\lambda - k)k^4}\right)\right] \tag{7.56}$$

where η_2 is an arbitrary constant.

The established solutions in eqs. (7.54) and (7.56) have been checked by putting them into the eq. (7.34). Thus the new exact solutions given in eqs. (7.54) and (7.56) for time-

fractional modified Fornberg-Whitham equation have been first time obtained in this present section.

7.5.2 Implementation of OHAM for Approximate Solution of Fractional Modified Fornberg-Whitham Equation

To exhibit the effectiveness and accuracy of proposed scheme, we consider the fractional modified Fornberg-Whitham equation with an initial condition. The solutions thus obtained are compared with the exact solutions obtained by first integral method.

Using optimal homotopy asymptotic method [30-32], the homotopy for eq. (7.32) can be written as

$$(1-p)L(\varphi(x,t\,;p)) = H(p)\left[\frac{\partial^\alpha \varphi(x,t\,;p)}{\partial t^\alpha} - \frac{\partial^\alpha}{\partial t^\alpha}\left(\frac{\partial^2 \varphi(x,t\,;p)}{\partial x^2}\right) + \frac{\partial \varphi(x,t\,;p)}{\partial x}\right.$$

$$\left. + \varphi(x,t\,;p)^2 \frac{\partial \varphi(x,t\,;p)}{\partial x} - 3\frac{\partial \varphi(x,t\,;p)}{\partial x}\frac{\partial^2 \varphi(x,t\,;p)}{\partial x^2} - \varphi(x,t\,;p)\frac{\partial^3 \varphi(x,t\,;p)}{\partial x^3}\right], \quad (7.57)$$

where $\varphi(x,t;p) = u_0(x,t) + \sum_{i=1}^{\infty} u_i(x,t)p^i$, $\qquad (7.58)$

$$H(p) = C_1 p + C_2 p^2 + C_3 p^3 + \dots. \qquad (7.59)$$

Substituting eqs. (7.58) and (7.59) in eq. (7.57) and equating the coefficients of different powers in p, we have the following system of partial differential equations.

Coefficients of $p^0 : \dfrac{\partial^\alpha u_0(x,t)}{\partial t^\alpha} = 0$. $\qquad\qquad (7.60)$

Coefficients of $p^1 : \dfrac{\partial^\alpha u_1(x,t)}{\partial t^\alpha} - \dfrac{\partial^\alpha u_0(x,t)}{\partial t^\alpha} = C_1\left[\dfrac{\partial^\alpha u_0(x,t)}{\partial t^\alpha} - \dfrac{\partial^\alpha}{\partial t^\alpha}\left(\dfrac{\partial^2 u_0(x,t)}{\partial x^2}\right)\right.$

$$\left. + \frac{\partial u_0(x,t)}{\partial x} + (u_0(x,t))^2\frac{\partial u_0(x,t)}{\partial x} - 3\frac{\partial u_0(x,t)}{\partial x}\frac{\partial^2 u_0(x,t)}{\partial x^2} - u_0(x,t)\frac{\partial^3 u_0(x,t)}{\partial x^3}\right]. \qquad (7.61)$$

Coefficients of $p^2 :$

$$\frac{\partial^\alpha u_2(x,t)}{\partial t^\alpha} - \frac{\partial^\alpha u_1(x,t)}{\partial t^\alpha} = C_1 \left[\frac{\partial^\alpha u_1(x,t)}{\partial t^\alpha} - \frac{\partial^\alpha}{\partial t^\alpha}\left(\frac{\partial^2 u_1(x,t)}{\partial x^2}\right) + \frac{\partial u_1(x,t)}{\partial x} \right.$$

$$+ \left(2u_0(x,t)u_1(x,t)\frac{\partial u_0(x,t)}{\partial x} + (u_0(x,t))^2\frac{\partial u_1(x,t)}{\partial x}\right) - 3\left(\frac{\partial u_0(x,t)}{\partial x}\frac{\partial^2 u_1(x,t)}{\partial x^2} + \right.$$

$$\left. \frac{\partial u_1(x,t)}{\partial x}\frac{\partial^2 u_0(x,t)}{\partial x^2}\right) - \left(u_0(x,t)\frac{\partial^3 u_1(x,t)}{\partial x^3} + u_1(x,t)\frac{\partial^3 u_0(x,t)}{\partial x^3}\right)\right]$$

$$+ C_2\left[\frac{\partial^\alpha u_0(x,t)}{\partial t^\alpha} - \frac{\partial^\alpha}{\partial t^\alpha}\left(\frac{\partial^2 u_0(x,t)}{\partial x^2}\right) + \frac{\partial u_0(x,t)}{\partial x} + (u_0(x,t))^2\frac{\partial u_0(x,t)}{\partial x}\right.$$

$$\left. - 3\frac{\partial u_0(x,t)}{\partial x}\frac{\partial^2 u_0(x,t)}{\partial x^2} - u_0(x,t)\frac{\partial^3 u_0(x,t)}{\partial x^3}\right], \qquad (7.62)$$

and so on.

For solving fractional order modified Fornberg-Whitham equation using OHAM, we consider the following initial condition for equation (7.32)

$$u(x,0) = \frac{-1}{2k}\left[\lambda + i\sqrt{3}(\lambda - 2k)\tanh\left\{\frac{(\lambda - 2k)\left(\sqrt{\lambda}\sqrt{k^4(k-\lambda)}(kx) + 3i\lambda k^5\eta_1 - 3ik^6\eta_1\right)}{2\sqrt{3}(\lambda - k)k^4}\right\}\right]. \quad (7.63)$$

Using the initial condition $u_0 = u(x,0)$ and solving eq. (7.60) to eq. (7.62), we obtain the expressions for u_0, u_1, u_2 and so on.

Finally, the third order approximate solution for fractional modified Fornberg-Whitham equation is given by

$$u = u_0(x,t) + u_1(x,t) + u_2(x,t). \qquad (7.64)$$

The optimal values of the convergence control parameters C_1 and C_2 can be obtained using weighted residual least square method given in eqs. (1.34) and (1.35) of chapter 1.

7.6   Numerical Results and Discussion

The comparison of the absolute errors for fractional modified Fornberg-Whitham equation (7.32) have been exhibited in Tables 7.8-7.10 which are generated by using the results obtained by first integral method and OHAM at different values of α. In order to examine the accuracy and reliability of first integral method for solving fractional order nonlinear modified Fornberg-Whitham equation, we compare the exact solution obtained by using first integral method with the third order approximate OHAM solutions. Table 7.11 illustrates the L_2 and L_∞ error norms for fractional modified Fornberg-Whitham equation given in eq. (7.32) at various points of t taking $\alpha = 0.5$ and 0.75. Figures 7.3-7.6

demonstrate the comparison of approximate solutions obtained by OHAM with first integral method for modified Fornberg-Whitham equation. It can be observed that the derived numerical simulation results are in good agreement with the exact solutions obtained by first integral method through illustrations in Tables and figures.

Table 7.8 The absolute errors obtained by OHAM for nonlinear modified Fornberg-Whitham equation given in eq. (7.32) at various points of x and t taking $k = 1$, $\lambda = 2.5$, $\eta_1 = 1$, and $\alpha = 1$.

x	$|u_{Exact} - u_{OHAM}|$									
	$t = 0.1$	$t = 0.2$	$t = 0.3$	$t = 0.4$	$t = 0.5$	$t = 0.6$	$t = 0.7$	$t = 0.8$	$t = 0.9$	$t = 1.0$
0.1	9.3908E-4	8.9819E-4	2.8677E-5	1.5351E-3	3.6724E-3	6.2730E-3	9.2349E-3	1.2462E-2	1.5864E-2	1.9351E-2
0.2	1.1574E-3	1.2728E-3	5.0544E-4	1.0041E-3	3.1298E-3	5.7577E-3	8.7828E-3	1.2107E-2	1.5637E-2	1.9284E-2
0.3	1.3864E-3	1.6646E-3	1.0025E-3	4.5210E-4	2.5680E-3	5.2267E-3	8.3199E-3	1.1746E-2	1.5413E-2	1.9227E-2
0.4	16274E-3	2.0759E-3	1.5231E-3	1.2413E-4	1.9834E-3	4.6765E-3	7.8428E-3	1.1379E-2	1.5188E-2	1.9178E-2
0.5	1.8818E-3	2.5092E-3	2.0703E-3	7.2846E-4	1.3721E-3	4.1029E-3	7.3478E-3	1.1000E-2	1.4960E-2	1.9135E-2
0.6	2.1514E-3	2.9676E-3	2.6480E-3	1.3652E-3	7.2944E-4	3.5016E-3	6.8304E-3	1.0605E-2	1.4725E-2	1.9094E-2
0.7	2.4381E-3	3.4543E-3	3.2605E-3	2.0392E-3	5.0184E-5	2.8671E-3	6.2856E-3	1.0191E-2	1.4480E-2	1.9053E-2
0.8	2.7441E-3	3.9732E-3	3.9127E-3	2.7562E-3	6.7161E-4	2.1934E-3	5.7074E-3	9.7520E-3	1.4218E-2	1.9007E-2
0.9	3.0720E-3	4.5286E-3	4.6103E-3	3.5225E-3	1.4428E-3	1.4734E-3	5.0890E-3	9.2805E-3	1.3936E-2	1.8951E-2
1.0	3.4245E-3	5.1254E-3	5.3596E-3	4.3457E-3	2.2716E-3	6.9904E-4	4.4222E-3	8.7694E-3	1.3624E-2	1.8880E-2

Table 7.9 The absolute errors obtained by third order OHAM for nonlinear modified Fornberg-Whitham equation given in eq. (7.32) at various points of x and t taking $k = 1$, $\lambda = 2.5$, $\eta_1 = 1$, and $\alpha = 0.75$.

x	$|u_{Exact} - u_{OHAM}|$									
	$t = 0.1$	$t = 0.2$	$t = 0.3$	$t = 0.4$	$t = 0.5$	$t = 0.6$	$t = 0.7$	$t = 0.8$	$t = 0.9$	$t = 1.0$
0.1	1.5780E-3	8.3963E-4	7.3067E-4	2.7686E-3	5.0835E-3	7.5542E-3	1.0094E-2	1.2641E-2	1.5139E-2	1.7548E-2
0.2	1.9515E-3	1.3377E-3	1.9635E-4	2.2546E-3	4.6313E-3	7.1966E-3	9.8595E-3	1.2551E-2	1.5217E-2	1.7813E-2
0.3	2.3436E-3	1.8601E-3	3.6403E-4	1.1749E-3	4.1550E-3	6.8173E-3	9.6052E-3	1.2446E-2	1.5283E-2	1.8069E-2
0.4	2.7562E-3	2.4098E-3	9.5402E-4	1.1456E-3	3.6507E-3	6.4126E-3	9.3285E-3	1.2321E-2	1.5333E-2	1.8312E-2
0.5	3.1920E-3	2.9902E-3	1.5775E-3	5.4267E-4	3.1141E-3	5.9781E-3	9.0252E-3	1.2174E-2	1.5363E-2	1.8541E-2
0.6	3.6537E-3	3.6052E-3	2.2390E-3	9.8730E-5	2.5405E-3	5.5091E-3	8.6907E-3	1.2000E-2	1.5370E-2	1.8749E-2
0.7	4.1442E-3	4.2590E-3	2.9435E-3	7.8394E-4	1.9243E-3	5.0001E-3	8.3195E-3	1.1792E-2	1.5349E-2	1.8934E-2
0.8	4.6671E-3	4.9566E-3	3.6966E-3	1.5190E-3	1.2590E-3	4.4443E-3	7.9051E-3	1.1546E-2	1.5293E-2	1.9089E-2
0.9	5.2262E-3	5.7034E-3	4.5047E-3	2.3111E-3	5.3754E-4	3.8345E-3	7.4401E-3	1.1252E-2	1.5195E-2	1.9207E-2
1.0	5.8260E-3	6.5056E-3	5.3752E-3	3.1681E-3	2.4874E-3	3.1621E-3	6.9156E-3	1.0904E-2	1.5047E-2	1.9279E-2

Table 7.10 The absolute errors obtained by third order OHAM for nonlinear modified Fornberg-Whitham equation given in eq. (7.32) at various points of x and t taking $k = 1$, $\lambda = 2.5$, $\eta_1 = 1$, and $\alpha = 0.5$.

x	$\lvert u_{Exact} - u_{OHAM}\rvert$									
	$t=0.1$	$t=0.2$	$t=0.3$	$t=0.4$	$t=0.5$	$t=0.6$	$t=0.7$	$t=0.8$	$t=0.9$	$t=1.0$
0.1	2.2513E-3	7.4423E-4	1.0160E-3	2.7858E-3	4.4912E-3	6.1032E-3	7.6093E-3	9.0044E-3	1.0286E-2	1.1455E-2
0.2	2.7556E-3	1.2335E-3	6.1201E-4	2.5001E-3	4.3430E-3	6.1056E-3	7.7717E-3	9.3342E-3	1.0789E-2	1.2136E-2
0.3	3.2903E-3	1.7588E-3	1.6932E-4	2.1737E-3	4.1529E-3	6.0647E-3	7.8897E-3	9.6181E-3	1.1245E-2	1.2769E-2
0.4	3.8590E-3	2.3241E-3	3.1646E-4	1.8023E-3	3.9160E-3	5.9757E-3	7.9580E-3	9.8510E-3	1.1648E-2	1.3347E-2
0.5	4.4652E-3	2.9338E-3	8.5036E-4	1.3803E-3	3.6268E-3	5.8327E-3	7.9708E-3	1.0026E-2	1.1993E-2	1.3865E-2
0.6	5.1131E-3	3.5931E-3	1.4381E-3	9.0172E-4	3.2786E-3	5.6289E-3	7.9209E-3	1.0138E-2	1.2271E-2	1.4314E-2
0.7	5.8072E-3	4.3078E-3	2.0862E-3	3.5928E-4	2.8640E-3	5.3561E-3	7.7998E-3	1.0175E-2	1.2473E-2	1.4685E-2
0.8	6.5529E-3	5.0845E-3	2.8021E-3	2.5513E-4	2.3740E-3	5.0051E-3	7.5977E-3	1.0129E-2	1.2588E-2	1.4967E-2
0.9	7.3558E-3	5.9304E-3	3.5944E-3	9.5096E-4	1.7984E-3	4.5648E-3	7.3028E-3	9.9877E-3	1.2604E-2	1.5145E-2
1.0	8.2226E-3	6.8540E-3	4.4727E-3	1.7391E-3	1.1254E-3	4.0224E-3	6.9015E-3	9.7347E-3	1.2506E-2	1.5205E-2

Table 7.11 L_2 and L_∞ error norms for time-fractional nonlinear modified Fornberg-Whitham equation given in eq. (7.32) at various points of t taking $\alpha = 0.75$ and 0.5.

t	$\alpha = 0.75$		$\alpha = 0.5$	
	L_2	L_∞	L_2	L_∞
0.1	1.19640E-2	5.8260E-3	1.68180E-2	8.2226E-3
0.2	1.22987E-2	6.5056E-3	1.46109E-2	6.8540E-3
0.3	8.97947E-3	5.3752E-3	7.03247E-3	4.4727E-3
0.4	5.83484E-3	3.1681E-3	5.36896E-3	2.7858E-3
0.5	1.02858E-2	5.0835E-3	1.06703E-2	4.4912E-3
0.6	1.82208E-2	7.5542E-3	1.74206E-2	6.1056E-3
0.7	2.77533E-2	1.0094E-2	2.42832E-2	7.9708E-3
0.8	3.78696E-2	1.2641E-2	3.10113E-2	1.0175E-2
0.9	4.82540E-2	1.5370E-2	3.75238E-2	1.2604E-2
1.0	5.87011E-2	1.9279E-2	4.37840E-2	1.5205E-2
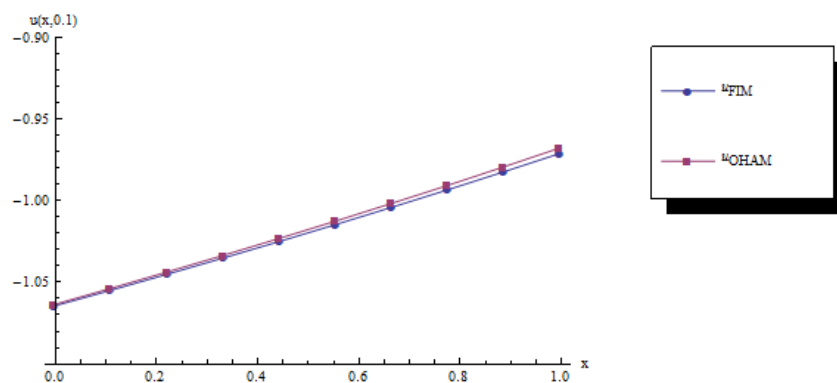
Figure 7.3   Comparison of approximate solution obtained by OHAM with the exact solution obtained by FIM for fractional modified Fornberg-Whitham equation at $t = 0.1$ taking $\alpha = 1$.
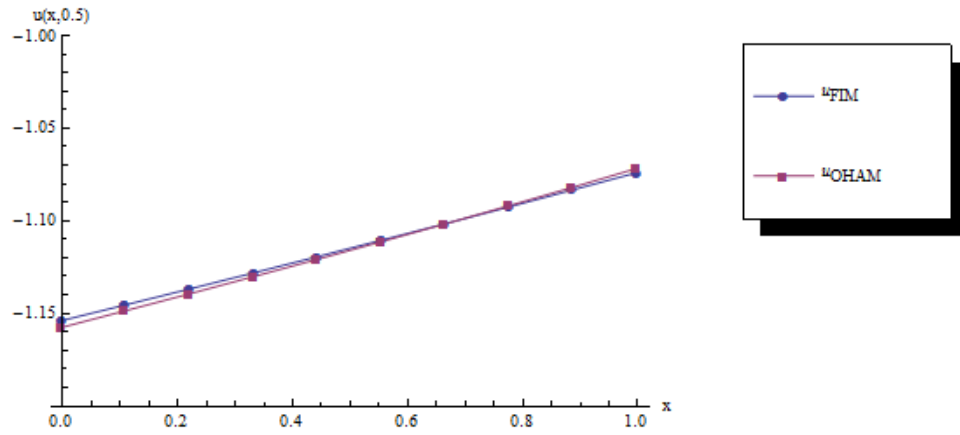
Figure 7.4   Comparison of approximate solution obtained by OHAM with the exact solution obtained by FIM for fractional modified Fornberg-Whitham equation at $t = 0.5$ taking $\alpha = 1$.
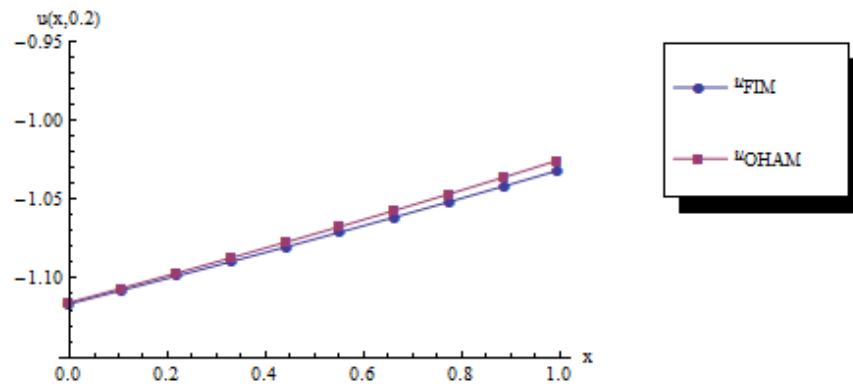
Figure 7.5   Comparison of approximate solution obtained by OHAM with the exact solution obtained by FIM for fractional modified Fornberg-Whitham equation at $t = 0.2$ taking $\alpha = 0.75$.
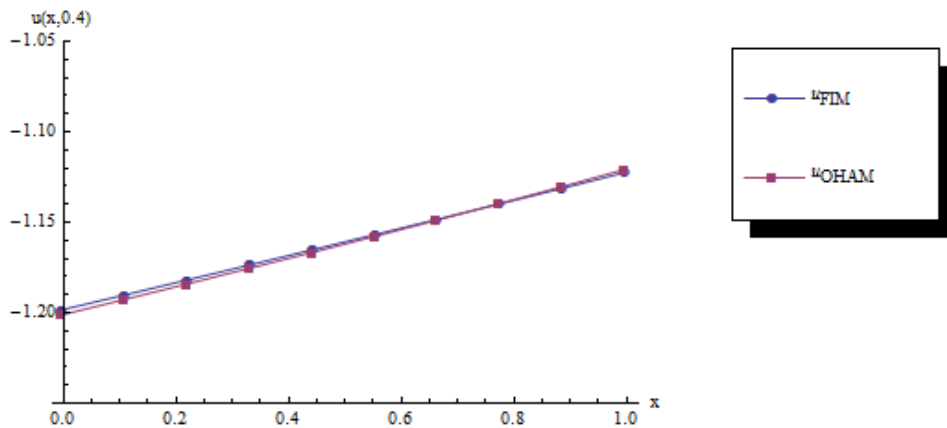
Figure 7.6   Comparison of approximate solution obtained by OHAM with the exact solution obtained by FIM for fractional modified Fornberg-Whitham equation $t = 0.4$ taking $\alpha = 0.5$.

7.7 Application of Analytical and Numerical Methods for Solving Time-Fractional Coupled Jaulent-Miodek Equation

7.7.1 Two-Dimensional Hermite Wavelet Method for Solving Nonlinear Time-Fractional Coupled Jaulent-Miodek Equations

To demonstrate the accuracy and efficiency of the proposed numerical technique, we consider time-fractional coupled Jaulent-Miodek equation. The numerical approximate solutions thus achieved are compared with the exact solutions in case of classical order and with the solutions obtained by OHAM in case of fractional order respectively.

Consider the nonlinear time-fractional coupled Jaulent-Miodek equations

$$\frac{\partial^{\alpha} u}{\partial t^{\alpha}} + \frac{\partial^3 u}{\partial x^3} + \frac{3}{2} v \frac{\partial^3 v}{\partial x^3} + \frac{9}{2} \frac{\partial v}{\partial x} \frac{\partial^2 v}{\partial x^2} - 6u \frac{\partial u}{\partial x} - 6uv \frac{\partial v}{\partial x} - \frac{3}{2} \frac{\partial u}{\partial x} v^2 = 0, \tag{7.65}$$

$$\frac{\partial^{\alpha} v}{\partial t^{\alpha}} + \frac{\partial^3 v}{\partial x^3} - 6 \frac{\partial u}{\partial x} v - 6u \frac{\partial v}{\partial x} - \frac{15}{2} \frac{\partial v}{\partial x} v^2 = 0, \tag{7.66}$$

with initial conditions [163]

$$u(x,0) = \frac{1}{8} \lambda^2 \left[1 - 4 \sec h^2 \left(\frac{\lambda x}{2} \right) \right], \tag{7.67}$$

$$v(x,0) = \lambda \sec h \left(\frac{\lambda x}{2} \right), \tag{7.68}$$

where λ is an arbitrary constant.

For $\alpha = 1$, the exact solutions of eqs. (7.65) and (7.66) are given by [163]

$$u(x,t) = \frac{1}{8} \lambda^2 \left[1 - 4 \sec h^2 \left[\frac{1}{2} \lambda \left(x + \frac{1}{2} \lambda^2 t \right) \right] \right], \tag{7.69}$$

$$v(x,t) = \lambda \sec h \left[\frac{1}{2} \lambda \left(x + \frac{1}{2} \lambda^2 t \right) \right]. \tag{7.70}$$

The Hermite wavelet solutions of $u(x,t)$ and $v(x,t)$ are sought by assuming that $u(x,t)$ and $v(x,t)$ can be expanded in terms of Hermite wavelets as

$$u(x,t)=\sum_{n=1}^{2^{k_1-1}}\sum_{i=0}^{M_1-1}\sum_{l=1}^{2^{k_2-1}}\sum_{j=0}^{M_2-1}a_{n,i,l,j}\,\psi_{n,i,l,j}(x,t),\tag{7.71}$$

$$v(x,t)=\sum_{n=1}^{2^{k_1-1}}\sum_{i=0}^{M_1-1}\sum_{l=1}^{2^{k_2-1}}\sum_{j=0}^{M_2-1}b_{n,i,l,j}\,\psi_{n,i,l,j}(x,t),\tag{7.72}$$

where $n=1,\ldots,2^{k_1-1}, i=0,\ldots,M_1-1, l=1,\ldots,2^{k_2-1}, j=0,\ldots,M_2-1$.

The nonlinear terms appeared in eqs. (7.65) and (7.66) can be approximated using Hermite wavelet function as

$$v\frac{\partial^3 v}{\partial x^3}=\sum_{n=1}^{2^{k_1-1}}\sum_{i=0}^{M_1-1}\sum_{l=1}^{2^{k_2-1}}\sum_{j=0}^{M_2-1}c_{n,i,l,j}\,\psi_{n,i,l,j}(x,t),\tag{7.73}$$

$$\frac{\partial v}{\partial x}\frac{\partial^2 v}{\partial x^2}=\sum_{n=1}^{2^{k_1-1}}\sum_{i=0}^{M_1-1}\sum_{l=1}^{2^{k_2-1}}\sum_{j=0}^{M_2-1}d_{n,i,l,j}\,\psi_{n,i,l,j}(x,t),\tag{7.74}$$

$$u\frac{\partial u}{\partial x}=\sum_{n=1}^{2^{k_1-1}}\sum_{i=0}^{M_1-1}\sum_{l=1}^{2^{k_2-1}}\sum_{j=0}^{M_2-1}e_{n,i,l,j}\,\psi_{n,i,l,j}(x,t),\tag{7.75}$$

$$uv\frac{\partial v}{\partial x}=\sum_{n=1}^{2^{k_1-1}}\sum_{i=0}^{M_1-1}\sum_{l=1}^{2^{k_2-1}}\sum_{j=0}^{M_2-1}f_{n,i,l,j}\,\psi_{n,i,l,j}(x,t),\tag{7.76}$$

$$\frac{\partial u}{\partial x}v^2=\sum_{n=1}^{2^{k_1-1}}\sum_{i=0}^{M_1-1}\sum_{l=1}^{2^{k_2-1}}\sum_{j=0}^{M_2-1}g_{n,i,l,j}\,\psi_{n,i,l,j}(x,t),\tag{7.77}$$

$$\frac{\partial u}{\partial x}v=\sum_{n=1}^{2^{k_1-1}}\sum_{i=0}^{M_1-1}\sum_{l=1}^{2^{k_2-1}}\sum_{j=0}^{M_2-1}h_{n,i,l,j}\,\psi_{n,i,l,j}(x,t),\tag{7.78}$$

$$u\frac{\partial v}{\partial x}=\sum_{n=1}^{2^{k_1-1}}\sum_{i=0}^{M_1-1}\sum_{l=1}^{2^{k_2-1}}\sum_{j=0}^{M_2-1}p_{n,i,l,j}\,\psi_{n,i,l,j}(x,t),\tag{7.79}$$

$$\frac{\partial v}{\partial x}v^2=\sum_{n=1}^{2^{k_1-1}}\sum_{i=0}^{M_1-1}\sum_{l=1}^{2^{k_2-1}}\sum_{j=0}^{M_2-1}q_{n,i,l,j}\,\psi_{n,i,l,j}(x,t),\tag{7.80}$$

This implies

$$\left(\sum_{n=1}^{2^{k_1-1}}\sum_{i=0}^{M_1-1}\sum_{l=1}^{2^{k_2-1}}\sum_{j=0}^{M_2-1}b_{n,i,l,j}\psi_{n,i,l,j}(x,t)\right)\times\left[\sum_{n=1}^{2^{k_1-1}}\sum_{i=0}^{M_1-1}\sum_{l=1}^{2^{k_2-1}}\sum_{j=0}^{M_2-1}b_{n,i,l,j}\frac{\partial^3\psi_{n,i,l,j}(x,t)}{\partial x^3}\right]=$$
$$\sum_{n=1}^{2^{k_1-1}}\sum_{i=0}^{M_1-1}\sum_{l=1}^{2^{k_2-1}}\sum_{j=0}^{M_2-1}c_{n,i,l,j}\psi_{n,i,l,j}(x,t),\tag{7.81}$$

$$\left(\sum_{n=1}^{2^{k_1-1}} \sum_{i=0}^{M_1-1} \sum_{l=1}^{2^{k_2-1}} \sum_{j=0}^{M_2-1} b_{n,i,l,j} \frac{\partial \psi_{n,i,l,j}(x,t)}{\partial x} \right) \times \left[\sum_{n=1}^{2^{k_1-1}} \sum_{i=0}^{M_1-1} \sum_{l=1}^{2^{k_2-1}} \sum_{j=0}^{M_2-1} b_{n,i,l,j} \frac{\partial^2 \psi_{n,i,l,j}(x,t)}{\partial x^2} \right]$$

$$= \sum_{n=1}^{2^{k_1-1}} \sum_{i=0}^{M_1-1} \sum_{l=1}^{2^{k_2-1}} \sum_{j=0}^{M_2-1} d_{n,i,l,j} \, \psi_{n,i,l,j}(x,t), \tag{7.82}$$

$$\left(\sum_{n=1}^{2^{k_1-1}} \sum_{i=0}^{M_1-1} \sum_{l=1}^{2^{k_2-1}} \sum_{j=0}^{M_2-1} a_{n,i,l,j} \psi_{n,i,l,j}(x,t) \right) \times \left[\sum_{n=1}^{2^{k_1-1}} \sum_{i=0}^{M_1-1} \sum_{l=1}^{2^{k_2-1}} \sum_{j=0}^{M_2-1} a_{n,i,l,j} \frac{\partial \psi_{n,i,l,j}(x,t)}{\partial x} \right]$$

$$= \sum_{n=1}^{2^{k_1-1}} \sum_{i=0}^{M_1-1} \sum_{l=1}^{2^{k_2-1}} \sum_{j=0}^{M_2-1} e_{n,i,l,j} \, \psi_{n,i,l,j}(x,t), \tag{7.83}$$

$$\left(\sum_{n=1}^{2^{k_1-1}} \sum_{i=0}^{M_1-1} \sum_{l=1}^{2^{k_2-1}} \sum_{j=0}^{M_2-1} a_{n,i,l,j} \psi_{n,i,l,j}(x,t) \right) \times \left(\sum_{n=1}^{2^{k_1-1}} \sum_{i=0}^{M_1-1} \sum_{l=1}^{2^{k_2-1}} \sum_{j=0}^{M_2-1} b_{n,i,l,j} \psi_{n,i,l,j}(x,t) \right)$$

$$\times \left(\sum_{n=1}^{2^{k_1-1}} \sum_{i=0}^{M_1-1} \sum_{l=1}^{2^{k_2-1}} \sum_{j=0}^{M_2-1} b_{n,i,l,j} \frac{\partial \psi_{n,i,l,j}(x,t)}{\partial x} \right) = \sum_{n=1}^{2^{k_1-1}} \sum_{i=0}^{M_1-1} \sum_{l=1}^{2^{k_2-1}} \sum_{j=0}^{M_2-1} f_{n,i,l,j} \psi_{n,i,l,j}(x,t), \tag{7.84}$$

$$\left(\sum_{n=1}^{2^{k_1-1}} \sum_{i=0}^{M_1-1} \sum_{l=1}^{2^{k_2-1}} \sum_{j=0}^{M_2-1} a_{n,i,l,j} \frac{\partial \psi_{n,i,l,j}(x,t)}{\partial x} \right) \times \left[\sum_{n=1}^{2^{k_1-1}} \sum_{i=0}^{M_1-1} \sum_{l=1}^{2^{k_2-1}} \sum_{j=0}^{M_2-1} b_{n,i,l,j} \psi_{n,i,l,j}(x,t) \right]^2$$

$$= \sum_{n=1}^{2^{k_1-1}} \sum_{i=0}^{M_1-1} \sum_{l=1}^{2^{k_2-1}} \sum_{j=0}^{M_2-1} g_{n,i,l,j} \psi_{n,i,l,j}(x,t), \tag{7.85}$$

$$\left(\sum_{n=1}^{2^{k_1-1}} \sum_{i=0}^{M_1-1} \sum_{l=1}^{2^{k_2-1}} \sum_{j=0}^{M_2-1} a_{n,i,l,j} \frac{\partial \psi_{n,i,l,j}(x,t)}{\partial x} \right) \times \left[\sum_{n=1}^{2^{k_1-1}} \sum_{i=0}^{M_1-1} \sum_{l=1}^{2^{k_2-1}} \sum_{j=0}^{M_2-1} b_{n,i,l,j} \psi_{n,i,l,j}(x,t) \right]$$

$$= \sum_{n=1}^{2^{k_1-1}} \sum_{i=0}^{M_1-1} \sum_{l=1}^{2^{k_2-1}} \sum_{j=0}^{M_2-1} h_{n,i,l,j} \psi_{n,i,l,j}(x,t), \tag{7.86}$$

$$\left(\sum_{n=1}^{2^{k_1-1}} \sum_{i=0}^{M_1-1} \sum_{l=1}^{2^{k_2-1}} \sum_{j=0}^{M_2-1} a_{n,i,l,j} \psi_{n,i,l,j}(x,t) \right) \times \left(\sum_{n=1}^{2^{k_1-1}} \sum_{i=0}^{M_1-1} \sum_{l=1}^{2^{k_2-1}} \sum_{j=0}^{M_2-1} b_{n,i,l,j} \frac{\partial \psi_{n,i,l,j}(x,t)}{\partial x} \right)$$

$$= \sum_{n=1}^{2^{k_1-1}} \sum_{i=0}^{M_1-1} \sum_{l=1}^{2^{k_2-1}} \sum_{j=0}^{M_2-1} p_{n,i,l,j} \psi_{n,i,l,j}(x,t), \tag{7.87}$$

and

$$\left(\sum_{n=1}^{2^{k_1-1}M_1-1}\sum_{i=0}^{2^{k_2-1}}\sum_{l=1}^{M_2-1}\sum_{j=0}b_{n,i,l,j}\frac{\partial\psi_{n,i,l,j}(x,t)}{\partial x}\right)\times\left[\sum_{n=1}^{2^{k_1-1}M_1-1}\sum_{i=0}^{2^{k_2-1}}\sum_{l=1}^{M_2-1}\sum_{j=0}b_{n,i,l,j}\psi_{n,i,l,j}(x,t)\right]^2$$

$$=\sum_{n=1}^{2^{k_1-1}M_1-1}\sum_{i=0}^{2^{k_2-1}}\sum_{l=1}^{M_2-1}\sum_{j=0}q_{n,i,l,j}\psi_{n,i,l,j}(x,t).$$

(7.88)

Again employing J_t^α on both sides of eqs. (7.65) and (7.66) we have

$$u(x,t)-u(x,0)=J_t^\alpha\left[-\frac{\partial^3 u}{\partial x^3}-\frac{3}{2}v\frac{\partial^3 v}{\partial x^3}-\frac{9}{2}\frac{\partial v}{\partial x}\frac{\partial^2 v}{\partial x^2}+6u\frac{\partial u}{\partial x}+6uv\frac{\partial v}{\partial x}+\frac{3}{2}\frac{\partial u}{\partial x}v^2\right],$$

(7.89)

$$v(x,t)-v(x,0)=J_t^\alpha\left[-\frac{\partial^3 v}{\partial x^3}+6\frac{\partial u}{\partial x}v+6u\frac{\partial v}{\partial x}+\frac{15}{2}\frac{\partial v}{\partial x}v^2\right].$$

(7.90)

Putting eqs. (7.73)- (7.80) in eqs. (7.89) and (7.90), we have

$$\sum_{n=1}^{2^{k_1-1}M_1-1}\sum_{i=0}^{2^{k_2-1}}\sum_{l=1}^{M_2-1}\sum_{j=0}a_{n,i,l,j}\psi_{n,i,l,j}(x,t)-u(x,0)=$$

$$J_t^\alpha\left[-\left(\sum_{n=1}^{2^{k_1-1}M_1-1}\sum_{i=0}^{2^{k_2-1}}\sum_{l=1}^{M_2-1}\sum_{j=0}a_{n,i,l,j}\frac{\partial^3\psi_{n,i,l,j}(x,t)}{\partial x^3}\right)\right.$$

$$-\frac{3}{2}\left(\sum_{n=1}^{2^{k_1-1}M_1-1}\sum_{i=0}^{2^{k_2-1}}\sum_{l=1}^{M_2-1}\sum_{j=0}c_{n,i,l,j}\psi_{n,i,l,j}(x,t)\right)-\frac{9}{2}\left(\sum_{n=1}^{2^{k_1-1}M_1-1}\sum_{i=0}^{2^{k_2-1}}\sum_{l=1}^{M_2-1}\sum_{j=0}d_{n,i,l,j}\psi_{n,i,l,j}(x,t)\right)$$

(7.91)

$$+6\left(\sum_{n=1}^{2^{k_1-1}M_1-1}\sum_{i=0}^{2^{k_2-1}}\sum_{l=1}^{M_2-1}\sum_{j=0}e_{n,i,l,j}\psi_{n,i,l,j}(x,t)\right)+6\left(\sum_{n=1}^{2^{k_1-1}M_1-1}\sum_{i=0}^{2^{k_2-1}}\sum_{l=1}^{M_2-1}\sum_{j=0}f_{n,i,l,j}\psi_{n,i,l,j}(x,t)\right)$$

$$\left.+\frac{3}{2}\left(\sum_{n=1}^{2^{k_1-1}M_1-1}\sum_{i=0}^{2^{k_2-1}}\sum_{l=1}^{M_2-1}\sum_{j=0}g_{n,i,l,j}\psi_{n,i,l,j}(x,t)\right)\right],$$

$$\sum_{n=1}^{2^{k_1-1}M_1-1}\sum_{i=0}^{2^{k_2-1}}\sum_{l=1}^{M_2-1}\sum_{j=0}b_{n,i,l,j}\psi_{n,i,l,j}(x,t)-v(x,0)=$$

$$J_t^\alpha\left[-\left(\sum_{n=1}^{2^{k_1-1}M_1-1}\sum_{i=0}^{2^{k_2-1}}\sum_{l=1}^{M_2-1}\sum_{j=0}b_{n,i,l,j}\frac{\partial^3\psi_{n,i,l,j}(x,t)}{\partial x^3}\right)\right.$$

(7.92)

$$+6\left(\sum_{n=1}^{2^{k_1-1}M_1-1}\sum_{i=0}^{2^{k_2-1}}\sum_{l=1}^{M_2-1}\sum_{j=0}h_{n,i,l,j}\psi_{n,i,l,j}(x,t)\right)+6\left(\sum_{n=1}^{2^{k_1-1}M_1-1}\sum_{i=0}^{2^{k_2-1}}\sum_{l=1}^{M_2-1}\sum_{j=0}p_{n,i,l,j}\psi_{n,i,l,j}(x,t)\right)$$

$$\left.+\frac{15}{2}\left(\sum_{n=1}^{2^{k_1-1}M_1-1}\sum_{i=0}^{2^{k_2-1}}\sum_{l=1}^{M_2-1}\sum_{j=0}q_{n,i,l,j}\psi_{n,i,l,j}(x,t)\right)\right].$$

Now substituting the collocation points $x_l = \dfrac{l-0.5}{2^{k_1-1}M_1}$ and $t_r = \dfrac{r-0.5}{2^{k_2-1}M_2}$ for

$l = 1, 2, \ldots, 2^{k_1-1}M_1$ and $r = 1, 2, \ldots, 2^{k_2-1}M_2$ in eqs. (7.81)-(7.88), and in (7.91), (7.92), we have $10\left(2^{k_1-1}M_1\right)\left(2^{k_2-1}M_2\right)$ equations in $10\left(2^{k_1-1}M_1\right)\left(2^{k_2-1}M_2\right)$ unknowns. By solving these systems of equations using Newton's method, the Hermite wavelet coefficients can be acquired.

7.7.2 To Compare with OHAM for Solution of Nonlinear Time-Fractional Coupled Jaulent-Miodek Equation

Implementing optimal homotopy asymptotic method [30], the homotopy for eqs. (7.65) and (7.66) can be written as

$$
\begin{aligned}
(1-p)L(\varphi(x,t\,;p)) = H(p)\Bigg[&\frac{\partial^\alpha \varphi(x,t\,;p)}{\partial t^\alpha} + \frac{\partial^3}{\partial x^3}\varphi(x,t\,;p) + \frac{3}{2}\psi(x,t\,;p)\frac{\partial^3\psi(x,t\,;p)}{\partial x^3} \\
&+ \frac{9}{2}\frac{\partial\psi(x,t\,;p)}{\partial x}\frac{\partial^2\psi(x,t\,;p)}{\partial x^2} - 6\varphi(x,t\,;p)\frac{\partial\varphi(x,t\,;p)}{\partial x} \\
&- 6\varphi(x,t\,;p)\psi(x,t\,;p)\frac{\partial\psi(x,t\,;p)}{\partial x} - \frac{3}{2}\frac{\partial\varphi(x,t\,;p)}{\partial x}(\psi(x,t\,;p))^2 \Bigg],
\end{aligned} \tag{7.93}
$$

$$
\begin{aligned}
(1-p)L(\psi(x,t\,;p)) = \tilde{H}(p)\Bigg[&\frac{\partial^\alpha \psi(x,t\,;p)}{\partial t^\alpha} + \frac{\partial^3}{\partial x^3}\psi(x,t\,;p) - 6\frac{\partial\varphi(x,t\,;p)}{\partial x}\psi(x,t\,;p) \\
&- 6\varphi(x,t\,;p)\frac{\partial\psi(x,t\,;p)}{\partial x} - \frac{15}{2}\frac{\partial\psi(x,t\,;p)}{\partial x}(\psi(x,t\,;p))^2 \Bigg],
\end{aligned} \tag{7.94}
$$

where $\varphi(x,t\,;p) = u_0(x,t) + \sum_{i=1}^{\infty} u_i(x,t)p^i$, $\qquad\qquad$ (7.95)

$\psi(x,t\,;p) = v_0(x,t) + \sum_{i=1}^{\infty} v_i(x,t)p^i$, $\qquad\qquad$ (7.96)

$H(p) = C_1 p + C_2 p^2 + C_3 p^3 + \ldots,$ $\qquad\qquad$ (7.97)

$\tilde{H}(p) = \tilde{C}_1 p + \tilde{C}_2 p^2 + \tilde{C}_3 p^3 + \ldots.$ $\qquad\qquad$ (7.98)

Substituting eqs. (7.95)-(7.98) in eqs. (7.93) and (7.94) and then comparing the coefficients of identical powers in p, we have the following system of equations.

Coefficients of p^0: $\dfrac{\partial^\alpha u_0(x,t)}{\partial t^\alpha} = 0$, $\qquad$ (7.99)

$$\frac{\partial^\alpha v_0(x,t)}{\partial t^\alpha} = 0. \qquad (7.100)$$

Coefficients of p^1:

$$\frac{\partial^\alpha u_1(x,t)}{\partial t^\alpha} - \frac{\partial^\alpha u_0(x,t)}{\partial t^\alpha} = C_1\left[\frac{\partial^\alpha u_0(x,t)}{\partial t^\alpha} + \frac{\partial^3 u_0(x,t)}{\partial x^3} + \frac{3}{2}v_0(x,t)\frac{\partial^3 v_0(x,t)}{\partial x^3}\right.$$

$$+ \frac{9}{2}\frac{\partial v_0(x,t)}{\partial x}\frac{\partial^2 v_0(x,t)}{\partial x^2} - 6u_0(x,t)\frac{\partial u_0(x,t)}{\partial x}$$

$$\left. - 6u_0(x,t)v_0(x,t)\frac{\partial v_0(x,t)}{\partial x} - \frac{3}{2}\frac{\partial u_0(x,t)}{\partial x}(v_0(x,t))^2\right], \qquad (7.101)$$

$$\frac{\partial^\alpha v_1(x,t)}{\partial t^\alpha} - \frac{\partial^\alpha v_0(x,t)}{\partial t^\alpha} = \tilde{C}_1\left[\frac{\partial^\alpha v_0(x,t)}{\partial t^\alpha} + \frac{\partial^3}{\partial x^3}v_0(x,t) - 6\frac{\partial u_0(x,t)}{\partial x}v_0(x,t)\right.$$

$$\left. - 6u_0(x,t)\frac{\partial v_0(x,t)}{\partial x} - \frac{15}{2}\frac{\partial v_0(x,t)}{\partial x}(v_0(x,t))^2\right]. \qquad (7.102)$$

Coefficients of p^2:

$$\frac{\partial^\alpha u_2(x,t)}{\partial t^\alpha} - \frac{\partial^\alpha u_1(x,t)}{\partial t^\alpha} = C_1\left[\frac{\partial^\alpha u_1(x,t)}{\partial t^\alpha} + \frac{\partial^3 u_1(x,t)}{\partial x^3} + \frac{3}{2}\left(v_0(x,t)\frac{\partial^3 v_1(x,t)}{\partial x^3}\right.\right.$$

$$\left. + v_1(x,t)\frac{\partial^3 v_0(x,t)}{\partial x^3}\right) + \frac{9}{2}\left(\frac{\partial v_0(x,t)}{\partial x}\frac{\partial^2 v_1(x,t)}{\partial x^2} + \frac{\partial v_1(x,t)}{\partial x}\frac{\partial^2 v_0(x,t)}{\partial x^2}\right)$$

$$- 6\left(u_0(x,t)\frac{\partial u_1(x,t)}{\partial x} + u_1(x,t)\frac{\partial u_0(x,t)}{\partial x}\right) - 6\left(u_1(x,t)v_0(x,t)\frac{\partial v_0(x,t)}{\partial x}\right.$$

$$\left. + u_0(x,t)v_1(x,t)\frac{\partial v_0(x,t)}{\partial x} + u_0(x,t)v_0(x,t)\frac{\partial v_1(x,t)}{\partial x}\right) \qquad (7.103)$$

$$\left.\left. - \frac{3}{2}\left(2v_0(x,t)v_1(x,t)\frac{\partial u_0(x,t)}{\partial x} + (v_0(x,t))^2\frac{\partial u_1(x,t)}{\partial x}\right)\right]\right| +$$

$$C_2\left[\frac{\partial^\alpha u_0(x,t)}{\partial t^\alpha} + \frac{\partial^3 u_0(x,t)}{\partial x^3} + \frac{3}{2}v_0(x,t)\frac{\partial^3 v_0(x,t)}{\partial x^3} + \frac{9}{2}\frac{\partial v_0(x,t)}{\partial x}\frac{\partial^2 v_0(x,t)}{\partial x^2}\right.$$

$$\left. - 6u_0(x,t)\frac{\partial u_0(x,t)}{\partial x} - 6u_0(x,t)v_0(x,t)\frac{\partial v_0(x,t)}{\partial x} - \frac{3}{2}\frac{\partial u_0(x,t)}{\partial x}(v_0(x,t))^2\right],$$

$$\frac{\partial^{\alpha} v_2(x,t)}{\partial t^{\alpha}} - \frac{\partial^{\alpha} v_1(x,t)}{\partial t^{\alpha}} = \tilde{C}_1 \left[\frac{\partial^{\alpha} v_1(x,t)}{\partial t^{\alpha}} + \frac{\partial^3 v_1(x,t)}{\partial x^3} - 6\left(\frac{\partial u_0(x,t)}{\partial x} v_1(x,t) + \right. \right.$$

$$\frac{\partial u_1(x,t)}{\partial x} v_0(x,t) \Bigg) - 6\left(u_1(x,t)\frac{\partial v_0(x,t)}{\partial x} + u_0(x,t)\frac{\partial v_1(x,t)}{\partial x} \right) \qquad (7.104)$$

$$\left. -\frac{15}{2}\left(2v_0(x,t)v_1(x,t)\frac{\partial v_0(x,t)}{\partial x} + (v_0(x,t))^2 \frac{\partial v_1(x,t)}{\partial x} \right) \right]$$

$$+ \tilde{C}_2 \left[\frac{\partial^{\alpha} v_0(x,t)}{\partial t^{\alpha}} + \frac{\partial^3}{\partial x^3} v_0(x,t) - 6\frac{\partial u_0(x,t)}{\partial x} v_0(x,t) \right.$$

$$\left. - 6u_0(x,t)\frac{\partial v_0(x,t)}{\partial x} - \frac{15}{2}\frac{\partial v_0(x,t)}{\partial x}(v_0(x,t))^2 \right],$$

and so on.

For solving fractional order coupled Jaulent-Miodek equations using OHAM, the following initial conditions for equations (7.65) and (7.66) are considered

$$u(x,0) = \frac{1}{8}\lambda^2 \left[1 - 4\sec h^2\left(\frac{\lambda x}{2} \right) \right],$$

$$v(x,0) = \lambda \sec h\left(\frac{\lambda x}{2} \right).$$

Using the initial conditions $u_0 = u(x,0)$ and $v_0 = v(x,0)$ and solving eqs. (7.99) to (7.104), we obtain the expressions for $u_0, v_0; u_1, v_1; u_2, v_2$ and so on.

Finally, the third order approximate solutions for time-fractional nonlinear coupled Jaulent-Miodek equations are given by

$$u = u_0(x,t) + u_1(x,t) + u_2(x,t), \qquad (7.105)$$

$$v = v_0(x,t) + v_1(x,t) + v_2(x,t). \qquad (7.106)$$

The optimal values of the convergence control parameters C_1, C_2 and $\tilde{C}_1$, $\tilde{C}_2$ can be obtained using weighted residual least square method given in eqs. (1.34) and (1.35) of chapter 1.

7.8 Numerical Results and Discussion

The comparison of the absolute errors for nonlinear time-fractional coupled Jaulent-Miodek equations (7.65) and (7.66) have been illustrated in Tables 7.12 and 7.13 that are generated through the results attained by two-dimensional Hermite wavelet method and OHAM at various points of x and t taking $\alpha = 1$. In the present study, in order to inspect

the accuracy and reliability of Hermite wavelets for solving fractional order nonlinear coupled system of Jaulent-Miodek equations, we compare the numerical approximate solutions obtained by using Hermite wavelets with the third order approximate OHAM solutions. Tables 7.14-7.17 illustrate the comparison of absolute errors of fractional order Jaulent-Miodek equations (7.65) and (7.66) at various points of x and t taking $\alpha = 0.75$ and 0.5 respectively. Agreements between present numerical results for time-fractional Jaulent-Miodek (JM) equation obtained by Hermite wavelets and OHAM appear very satisfactory through illustrations in Tables 7.12-7.18, which also confirm the validity of the accurate solution by Hermite wavelets.

Table 7.12   The absolute errors with regard to $u(x,t)$ obtained by Hermite wavelet method for nonlinear system of coupled Jaulent-Miodek equations given in eqs. (7.65) and (7.66) at various points of x and t taking $\alpha = 1$ and $\lambda = 0.5$.

x	$\left| u_{Exact} - u_{Hermite\,wavelet} \right|$								
	$t=0.1$	$t=0.2$	$t=0.3$	$t=0.4$	$t=0.5$	$t=0.6$	$t=0.7$	$t=0.8$	$t=0.9$
0.1	2.0553E-6	4.6970E-6	2.0543E-5	4.5657E-5	9.0317E-5	1.3421E-4	1.8769E-4	2.5054E-4	3.2257E-4
0.2	2.2375E-6	1.3360E-5	3.3614E-5	6.3236E-5	1.1255E-4	1.6141E-4	2.2021E-4	2.8892E-4	3.6751E-4
0.3	6.2475E-6	2.1113E-5	4.4884E-5	7.7842E-5	1.3034E-4	1.8239E-4	2.4438E-4	3.1645E-4	3.9868E-4
0.4	1.0252E-5	2.8524E-5	5.5227E-5	9.0679E-5	1.4527E-5	1.9909E-4	2.6257E-4	3.3593E-4	4.1938E-4
0.5	6.7072E-6	2.7007E-5	6.1236E-5	1.1011E-4	1.8039E-4	2.6055E-4	3.5746E-4	4.7156E-4	6.0328E-4
0.6	7.1378E-6	2.7087E-5	6.0652E-5	1.0857E-4	1.7763E-4	2.5639E-4	3.5173E-4	4.6421E-4	5.9434E-4
0.7	6.3626E-6	2.5083E-5	5.6901E-5	1.0257E-4	1.6888E-4	2.4445E-4	3.3619E-4	4.4468E-4	5.7054E-4
0.8	5.1634E-6	2.1991E-5	5.1218E-5	9.3599E-5	1.5592E-4	2.2684E-4	3.1326E-4	4.1581E-4	5.3510E-4
0.9	3.7368E-6	1.8227E-5	4.4262E-5	8.2587E-5	1.3998E-4	2.0510E-4	2.8485E-4	3.7985E-4	4.9074E-4

Table 7.13   The absolute errors with regard to $v(x,t)$ obtained by Hermite wavelet method for nonlinear system of coupled Jaulent-Miodek equations given in eqs. (7.65) and (7.66) at various points of x and t taking $\alpha = 1$ and $\lambda = 0.5$.

x	$\left| v_{Exact} - v_{Hermite\,wavelet} \right|$								
	$t=0.1$	$t=0.2$	$t=0.3$	$t=0.4$	$t=0.5$	$t=0.6$	$t=0.7$	$t=0.8$	$t=0.9$
0.1	1.0266E-4	1.2531E-4	7.4403E-5	4.2725E-5	2.2305E-4	4.4542E-4	7.0631E-4	9.9217E-4	1.2894E-3
0.2	6.8598E-6	6.3948E-5	2.0545E-4	4.0998E-4	6.7411E-4	9.7665E-4	1.3136E-3	1.6714E-3	2.0365E-3
0.3	8.6641E-5	2.4761E-4	4.7556E-4	7.6247E-4	1.1045E-3	1.4804E-3	1.8858E-3	2.3069E-3	2.7302E-3
0.4	1.7814E-4	4.2632E-4	7.3694E-4	1.1016E-3	1.5161E-3	1.9591E-3	2.4257E-3	2.9022E-3	3.3748E-3
0.5	1.6264E-4	2.3867E-4	2.4153E-4	1.8420E-4	8.2495E-5	5.6018E-5	2.1508E-4	3.8165E-4	5.4268E-4
0.6	7.7242E-5	7.4979E-5	6.0988E-6	1.1639E-4	2.7664E-4	4.6748E-4	6.7260E-4	8.7936E-4	1.0751E-3
0.7	1.9921E-6	7.6519E-5	2.1056E-4	3.9113E-4	6.0232E-4	8.3738E-4	1.0799E-3	1.3178E-3	1.5387E-3
0.8	7.6073E-5	2.1710E-4	4.1005E-4	6.4194E-4	8.9692E-4	1.1685E-3	1.4405E-3	1.7010E-3	1.9382E-3
0.9	1.4522E-4	3.4725E-4	5.9317E-4	8.7004E-4	1.1620E-3	1.4631E-3	1.7569E-3	2.0321E-3	2.2773E-3

Table 7.14 The absolute errors with regard to $u(x,t)$ obtained by two-dimensional Hermite wavelet method and third order OHAM solution for fractional order nonlinear coupled Jaulent-Miodek equations given in eqs. (7.65) and (7.66) at various points of x and t taking $\alpha = 0.75$ and $\lambda = 0.5$.

x	$\left|u_{OHAM} - u_{Hermite\,wavelet}\right|$								
	$t=0.1$	$t=0.2$	$t=0.3$	$t=0.4$	$t=0.5$	$t=0.6$	$t=0.7$	$t=0.8$	$t=0.9$
0.1	7.4968E-6	3.0040E-5	6.3702E-5	1.0598E-4	1.5534E-4	2.0969E-4	2.6883E-4	3.3038E-4	3.9195E-4
0.2	1.9727E-5	5.0514E-5	9.1979E-5	1.4208E-4	1.9931E-4	2.6235E-4	3.3101E-4	4.0334E-4	4.7734E-4
0.3	3.0934E-5	6.8532E-5	1.1601E-4	1.7181E-4	2.3442E-4	3.0327E-4	3.7815E-4	4.5748E-4	5.3958E-4
0.4	4.1653E-5	8.5048E-5	1.3716E-4	1.9693E-4	2.6291E-4	3.3516E-4	4.1348E-4	4.9660E-4	5.8308E-4
0.5	4.7032E-5	1.0898E-4	1.8956E-4	2.8591E-4	3.9484E-4	5.1702E-4	6.5070E-4	7.9455E-4	9.4703E-4
0.6	5.0687E-5	1.1373E-4	1.9513E-4	2.9216E-4	4.0149E-4	5.2437E-4	6.5901E-4	8.0432E-4	9.5894E-4
0.7	5.2128E-5	1.1459E-4	1.9494E-4	2.9053E-4	3.9790E-4	5.1884E-4	6.5148E-4	7.9493E-4	9.4801E-4
0.8	5.2327E-5	1.1287E-4	1.9061E-4	2.8301E-4	3.8642E-4	5.0316E-4	6.3127E-4	7.7000E-4	9.1831E-4
0.9	5.1682E-5	1.0929E-4	1.8321E-4	2.7101E-4	3.6885E-4	4.7954E-4	6.0099E-4	7.3260E-4	8.7341E-4

Table 7.15 The absolute errors with regard to $v(x,t)$ obtained by two-dimensional Hermite wavelet method and third order OHAM solution for fractional order nonlinear coupled Jaulent-Miodek equations given in eqs. (7.65) and (7.66) at various points of x and t taking $\alpha = 0.75$ and $\lambda = 0.5$.

x	$\left|v_{OHAM} - v_{Hermite\,wavelet}\right|$								
	$t=0.1$	$t=0.2$	$t=0.3$	$t=0.4$	$t=0.5$	$t=0.6$	$t=0.7$	$t=0.8$	$t=0.9$
0.1	8.9842E-5	1.1334E-5	1.9121E-4	4.0028E-4	6.0268E-4	7.8294E-4	9.1713E-4	9.8878E-4	9.8134E-4
0.2	9.1969E-5	3.1053E-4	5.8586E-4	8.7629E-4	1.1504E-3	1.3940E-3	1.5852E-3	1.7089E-3	1.7502E-3
0.3	2.6796E-4	5.9763E-4	9.6132E-4	1.3253E-3	1.6626E-3	1.9604E-3	2.1985E-3	2.3636E-3	2.4420E-3
0.4	4.3878E-4	8.7377E-4	1.3192E-3	1.7495E-3	2.1422E-3	2.4855E-3	2.7614E-3	2.9580E-3	3.0627E-3
0.5	1.9169E-4	1.7339E-4	8.2319E-5	2.5428E-5	1.1164E-4	1.7211E-4	1.8761E-4	1.5108E-4	5.5148E-5
0.6	3.6408E-4	7.1595E-4	2.2882E-4	3.8801E-4	5.1629E-4	6.1082E-4	6.5499E-4	6.4337E-4	5.7004E-4
0.7	1.0684E-4	2.9537E-4	5.0987E-4	7.1171E-4	8.7304E-4	9.9249E-4	1.0560E-3	1.0596E-3	9.9889E-4
0.8	2.3933E-4	4.9968E-4	7.6306E-4	9.9920E-4	1.1852E-3	1.3211E-3	1.3953E-3	1.4052E-3	1.3476E-3
0.9	3.6156E-4	6.8549E-4	9.8986E-4	1.2525E-3	1.4554E-3	1.5998E-3	1.6766E-3	1.6845E-3	1.6216E-3

Table 7.16 The absolute errors with regard to $u(x,t)$ obtained by two-dimensional Hermite wavelet method and third order OHAM solution for fractional order nonlinear coupled Jaulent-Miodek equations given in eqs. (7.65) and (7.66) at various points of x and t taking $\alpha = 0.5$ and $\lambda = 0.5$.

x	$\left|u_{OHAM} - u_{Hermite\,wavelet}\right|$								
	$t=0.1$	$t=0.2$	$t=0.3$	$t=0.4$	$t=0.5$	$t=0.6$	$t=0.7$	$t=0.8$	$t=0.9$
0.1	2.1552E-5	8.1878E-5	1.4911E-4	2.1501E-4	2.7542E-4	3.2160E-4	3.5273E-4	3.6046E-4	3.3639E-4

0.2	1.0292E-5	7.7946E-5	1.5643E-4	2.3633E-4	3.1247E-4	3.7782E-4	4.3104E-4	4.6468E-4	4.7123E-4
0.3	4.1238E-6	6.7652E-5	1.5385E-4	2.4384E-4	3.3140E-4	4.1103E-4	4.8085E-4	5.3418E-4	5.6425E-4
0.4	2.0429E-5	5.2912E-5	1.4387E-4	2.4062E-4	3.3588E-4	4.2555E-4	5.0718E-4	5.7474E-4	6.2205E-4
0.5	8.1331E-6	1.1511E-4	2.6479E-4	4.2458E-4	5.8491E-4	7.4584E-4	9.0415E-4	1.0570E-3	1.2014E-3
0.6	3.5413E-5	8.4721E-5	2.3575E-4	3.9943E-4	5.6478E-4	7.3306E-4	9.0046E-4	1.0645E-3	1.2226E-3
0.7	6.6534E-5	4.7447E-5	1.9658E-4	3.6070E-4	5.2736E-4	6.9890E-4	8.7092E-4	1.0413E-3	1.2076E-3
0.8	9.9929E-5	5.3824E-6	1.4987E-4	3.1142E-4	4.7612E-4	6.4732E-4	8.1999E-4	9.9225E-4	1.1618E-3
0.9	1.3460E-4	3.9949E-5	9.7606E-5	2.5404E-4	4.1400E-4	5.8175E-4	7.5163E-4	9.2194E-4	1.0905E-3

Table 7.17 The absolute errors with regard to $v(x,t)$ obtained by two-dimensional Hermite wavelet method and third order OHAM solution for fractional order nonlinear coupled Jaulent-Miodek equations given in eqs. (7.65) and (7.66) at various points of x and t taking $\alpha = 0.5$ and $\lambda = 0.5$.

x	$\lvert v_{OHAM} - v_{Hermite\,wavelet} \rvert$								
	$t=0.1$	$t=0.2$	$t=0.3$	$t=0.4$	$t=0.5$	$t=0.6$	$t=0.7$	$t=0.8$	$t=0.9$
0.1	8.3521E-5	2.9312E-4	4.2261E-4	4.3707E-4	3.3456E-4	1.0091E-4	2.5336E-4	7.3818E-4	1.3635E-3
0.2	3.3416E-4	6.5094E-4	8.5761E-4	9.3554E-4	8.9197E-4	7.1374E-4	4.1479E-4	1.2595E-5	5.7631E-4
0.3	5.6957E-4	9.8211E-4	1.2548E-3	1.3850E-3	1.3888E-3	1.2538E-3	9.9728E-4	6.1325E-4	9.5719E-5
0.4	7.9133E-4	1.2891E-3	1.6175E-3	1.7897E-3	1.8301E-3	1.7270E-3	1.5006E-3	1.1468E-3	6.6099E-4
0.5	3.9482E-4	3.6236E-4	3.4634E-4	3.9120E-4	5.0371E-4	6.8476E-4	9.2508E-4	1.2283E-3	1.5984E-3
0.6	2.0871E-4	1.0875E-4	4.8599E-5	5.8024E-5	1.3694E-4	2.8552E-4	4.9242E-4	7.5994E-4	1.0908E-3
0.7	4.4730E-5	1.0899E-4	2.0229E-4	2.1800E-4	1.6237E-4	3.5946E-5	1.4821E-4	3.9122E-4	6.9475E-4
0.8	9.7652E-5	2.9380E-4	4.0997E-4	4.4120E-4	3.9923E-4	2.8531E-4	1.1391E-4	1.1510E-4	4.0251E-4
0.9	2.2031E-4	4.4782E-4	5.7730E-4	6.1511E-4	5.7787E-4	4.6746E-4	2.9953E-4	7.4704E-5	2.0705E-4

Table 7.18 L_2 and L_∞ error norms for fractional order nonlinear coupled Jaulent-Miodek equation using two-dimensional Hermite wavelet method and OHAM at various points t taking $\alpha = 0.5, 0.75$ and 1.

t	Error analysis of $u(x,t)$ with regard to Hermite wavelet						Error analysis of $v(x,t)$ with regard to Hermite wavelet					
	$\alpha=1$		$\alpha=0.75$		$\alpha=0.5$		$\alpha=1$		$\alpha=0.75$		$\alpha=0.5$	
	L_2	L_∞	L_2	L_∞	L_2	L_∞	L_2	L_∞	L_2	L_∞	L_2	L_∞
0.1	1.8177 E-5	2.8524 E-5	1.2666 E-4	5.2327 E-5	1.8669 E-4	4.387 8E-4	3.3034 E-4	1.7814 E-4	1.2194 E-3	4.387 8E-4	1.152 7E-3	7.913 3E-4
0.2	6.4740 E-5	1.0252 E-5	2.7930 E-4	1.1459 E-4	2.1085 E-4	8.737 7E-4	7.0640 E-4	4.2632 E-4	1.6021 E-3	8.737 7E-4	1.891 5E-3	1.289 1E-3
0.3	1.4786 E-4	6.1236 E-5	4.7612 E-4	1.9513 E-4	5.3609 E-4	1.319 2E-3	1.1998 E-3	7.3694 E-4	2.2193 E-3	1.319 2E-3	2.401 9E-3	1.617 5E-3
0.4	2.6529 E-4	1.1011 E-4	7.1047 E-4	2.9216 E-4	9.2243 E-4	1.749 5E-3	1.8260 E-3	1.1016 E-3	2.9950 E-3	1.749 5E-3	2.639 0E-3	1.789 7E-3
0.5	4.1778 E-4	1.8039 E-4	9.7402 E-4	4.0149 E-4	1.3166 E-3	2.142 2E-3	2.5736 E-3	1.5161 E-3	3.6883 E-3	2.142 2E-3	3.688 3E-3	1.830 1E-3
0.6	6.3551 E-4	2.6055 E-4	1.2522 E-3	5.2437 E-4	1.7134 E-3	2.485 5E-3	3.4075 E-3	1.9591 E-3	4.2743 E-3	2.485 5E-3	2.434 3E-3	1.727 0E-3
0.7	8.6958 E-4	3.5746 E-4	1.5929 E-3	6.5901 E-4	2.1030 E-3	2.761 4E-3	4.3001 E-3	2.4257 E-3	4.7064 E-3	2.761 4E-3	2.169 2E-3	1.500 6E-3

0.8	1.1454 E-3	4.7156 E-4	1.9410 E-3	8.0432 E-4	2.4760 E-3	2.958 0E-3	5.1364 E-3	2.9022 E-3	4.9604 E-3	2.958 0E-3	2.120 0E-3	1.228 3E-3
0.9	1.4642 E-3	6.0328 E-4	2.3095 E-3	9.5894 E-4	2.8242 E-3	3.062 7E-3	6.1166 E-3	3.3748 E-3	5.0141 E-3	3.062 7E-3	2.658 8E-3	1.598 4E-3

7.9 Convergence of Hermite wavelet

Theorem 7.1 (Convergence Theorem)

If a continuous function $u(x,t) \in L^2(\Re \times \Re)$ defined on $[0,1) \times [0,1)$ be bounded, i.e., $|u(x,t)| \le K$, then the Hermite wavelets expansion of $u(x,t)$ converges uniformly to it.

Proof:

Let $u(x,t)$ be a function defined on $[0,1) \times [0,1)$ and $|u(x,t)| \le K$, where K is a positive constant.

The Hermite wavelet coefficients of continuous functions $u(x,t)$ are defined as

$$c_{ij} = \int_0^1 \int_0^1 u(x,t)\,\psi_i(x)\,\psi_j(t)\,dx\,dt$$

$$= 2^{\frac{k_1}{2}} \sqrt{\frac{1}{n_1!\,2^{n_1}\sqrt{\pi}}} \int_0^1 \int_{I_1} u(x,t)\,H_{m_1}\!\left(2^{k_1} x - \hat{n}_1\right) \psi_j(t)\,dx\,dt, \quad \text{where } I_1 = \left[\frac{\hat{n}_1 - 1}{2^{k_1}}, \frac{\hat{n}_1 + 1}{2^{k_1}}\right).$$

Now by change of variable $2^{k_1} x - \hat{n}_1 = y$, we get

$$c_{ij} = \frac{2^{\frac{k_1}{2}}}{2^{k_1}} \sqrt{\frac{1}{n_1!\,2^{n_1}\sqrt{\pi}}} \int_0^1 \psi_j(t)\left(\int_{-1}^1 u\!\left(\frac{y + 2n_1 - 1}{2^{k_1}}, t\right) H_{m_1}(y)\,dy\right) dt.$$

Using the mean value theorem of integral calculus, we will have

$$c_{ij} = \frac{1}{2^{\frac{k_1}{2}}} \sqrt{\frac{1}{n_1!\,2^{n_1}\sqrt{\pi}}} \int_0^1 \psi_j(t)\,u\!\left(\frac{\xi + 2n_1 - 1}{2^{k_1}}, t\right)\left(\int_{-1}^1 H_{m_1}(y)\,dy\right) dt, \quad \text{where } \xi \in (-1,1)$$

$$= \frac{1}{2^{\frac{k_1}{2}}} \sqrt{\frac{1}{n_1!\,2^{n_1}\sqrt{\pi}}} \int_0^1 \psi_j(t)\,u\!\left(\frac{\xi + 2n_1 - 1}{2^{k_1}}, t\right)\left(\int_{-1}^1 \frac{H'_{m_1+1}(y)}{2(m_1+1)}\,dy\right) dt,$$

$$\text{since } H'_{m_1+1}(y) = 2(m_1+1)H_{m_1}(y)$$

$$= \frac{1}{2^{\frac{k_1}{2}}} \sqrt{\frac{1}{n_1! 2^{n_1} \sqrt{\pi}}} \int_0^1 \psi_j(t) u\left(\frac{\xi + 2n_1 - 1}{2^{k_1}}, t\right) \left(\frac{H_{m_1+1}(y)}{2(m_1+1)}\right)\bigg|_{-1}^1 dt$$

$$= \frac{1}{2^{\frac{k_1}{2}}} \sqrt{\frac{1}{n_1! 2^{n_1} \sqrt{\pi}}} \left(\frac{H_{m_1+1}(1) - H_{m_1+1}(-1)}{2(m_1+1)}\right) \int_0^1 \psi_j(t) u\left(\frac{\xi + 2n_1 - 1}{2^{k_1}}, t\right) dt$$

$$= \frac{1}{2^{\frac{k_1}{2}}} \sqrt{\frac{1}{n_1! 2^{n_1} \sqrt{\pi}}} \left(\frac{H_{m_1+1}(1) - H_{m_1+1}(-1)}{2(m_1+1)}\right)$$

$$\int_{I_2} u\left(\frac{\xi + 2n_1 - 1}{2^{k_1}}, t\right) 2^{\frac{k_2}{2}} \sqrt{\frac{1}{n_2! 2^{n_2} \sqrt{\pi}}} H_{m_2}\left(2^{k_2} t - \hat{n}_2\right) dt,$$

where $I_2 = \left[\dfrac{\hat{n}_2 - 1}{2^{k_2}}, \dfrac{\hat{n}_2 + 1}{2^{k_2}}\right)$.

$$c_{ij} = \frac{1}{2^{\frac{k_1}{2}}} 2^{\frac{k_2}{2}} \sqrt{\frac{1}{n_1! 2^{n_1} \sqrt{\pi}}} \sqrt{\frac{1}{n_2! 2^{n_2} \sqrt{\pi}}} \left(\frac{H_{m_1+1}(1) - H_{m_1+1}(-1)}{2(m_1+1)}\right)$$

$$\times \int_{I_2} u\left(\frac{\xi + 2n_1 - 1}{2^{k_1}}, t\right) H_{m_2}\left(2^{k_2} t - \hat{n}_2\right) dt.$$

Again by change of variable $2^{k_2} t - \hat{n}_2 = w,$ we get

$$c_{ij} = \frac{1}{2^{\frac{k_1}{2}}} \frac{2^{\frac{k_2}{2}}}{2^{k_2}} \sqrt{\frac{1}{n_1! 2^{n_1} \sqrt{\pi}}} \sqrt{\frac{1}{n_2! 2^{n_2} \sqrt{\pi}}} \left(\frac{H_{m_1+1}(1) - H_{m_1+1}(-1)}{2(m_1+1)}\right)$$

$$\times \int_{-1}^1 u\left(\frac{\xi + 2n_1 - 1}{2^{k_1}}, \frac{w + 2n_2 - 1}{2^{k_2}}\right) H_{m_2}(w) dw.$$

Using the mean value theorem of integral calculus, we have

$$c_{ij} = \frac{1}{2^{\frac{k_1+k_2}{2}}} \sqrt{\frac{1}{n_1! 2^{n_1} \sqrt{\pi}}} \sqrt{\frac{1}{n_2! 2^{n_2} \sqrt{\pi}}} \left(\frac{H_{m_1+1}(1) - H_{m_1+1}(-1)}{2(m_1+1)}\right)$$

$$\times u\left(\frac{\xi + 2n_1 - 1}{2^{k_1}}, \frac{\eta + 2n_2 - 1}{2^{k_2}}\right) \int_{-1}^1 H_{m_2}(w) dw,$$

231

where $\eta \in (-1,1)$

$$= \frac{1}{2^{\frac{k_1+k_2}{2}}} \sqrt{\frac{1}{n_1! 2^{n_1} \sqrt{\pi}}} \sqrt{\frac{1}{n_2! 2^{n_2} \sqrt{\pi}}} \left(\frac{H_{m_1+1}(1) - H_{m_1+1}(-1)}{2(m_1+1)} \right)$$

$$\times u\left(\frac{\xi + 2n_1 - 1}{2^{k_1}}, \frac{\eta + 2n_2 - 1}{2^{k_2}} \right) \int_{-1}^{1} \frac{H'_{m_2}(w)}{2(m_2+1)} dw$$

since $H'_{m_2+1}(w) = 2(m_2+1)H_{m_2}(w)$

$$= \frac{1}{2^{\frac{k_1+k_2}{2}}} \sqrt{\frac{1}{n_1! 2^{n_1} \sqrt{\pi}}} \sqrt{\frac{1}{n_2! 2^{n_2} \sqrt{\pi}}} \left(\frac{H_{m_1+1}(1) - H_{m_1+1}(-1)}{2(m_1+1)} \right)$$

$$\times u\left(\frac{\xi + 2n_1 - 1}{2^{k_1}}, \frac{\eta + 2n_2 - 1}{2^{k_2}} \right) \left(\frac{H_{m_2+1}(w)}{2(m_2+1)} \right)_{-1}^{1}$$

$$= \frac{1}{2^{\frac{k_1+k_2}{2}}} \sqrt{\frac{1}{n_1! 2^{n_1} \sqrt{\pi}}} \sqrt{\frac{1}{n_2! 2^{n_2} \sqrt{\pi}}} \left(\frac{H_{m_1+1}(1) - H_{m_1+1}(-1)}{2(m_1+1)} \right) \times$$

$$\left(\frac{H_{m_2+1}(1) - H_{m_2+1}(-1)}{2(m_2+1)} \right) \times u\left(\frac{\xi + 2n_1 - 1}{2^{k_1}}, \frac{\eta + 2n_2 - 1}{2^{k_2}} \right).$$

Therefore,

$$|c_{ij}| = \left| \frac{1}{2^{\frac{k_1+k_2}{2}}} \sqrt{\frac{1}{n_1! 2^{n_1} \sqrt{\pi}}} \sqrt{\frac{1}{n_2! 2^{n_2} \sqrt{\pi}}} \left(\frac{H_{m_1+1}(1) - H_{m_1+1}(-1)}{2(m_1+1)} \right) \right.$$

$$\left. \times \left(\frac{H_{m_2+1}(1) - H_{m_2+1}(-1)}{2(m_2+1)} \right) u\left(\frac{\xi + 2n_1 - 1}{2^{k_1}}, \frac{\eta + 2n_2 - 1}{2^{k_2}} \right) \right|$$

$$\leq \frac{1}{2^{\frac{k_1+k_2}{2}}} \sqrt{\frac{1}{n_1! 2^{n_1} \sqrt{\pi}}} \sqrt{\frac{1}{n_2! 2^{n_2} \sqrt{\pi}}} \left(\frac{H_{m_1+1}(1) - H_{m_1+1}(-1)}{2(m_1+1)} \right) \left(\frac{H_{m_2+1}(1) - H_{m_2+1}(-1)}{2(m_2+1)} \right) K,$$

since $u(x,t)$ is bounded.

Therefore $\sum_{i=0}^{\infty} \sum_{j=0}^{\infty} c_{ij}$ is absolutely convergent.

Hence from [44], the Hermite series expansion of $u(x,t)$ converges uniformly. $\quad\square$

7.10 Conclusion

In this chapter, the numerical solution of time-fractional modified Fornberg-Whitham equation has been determined by using two-dimensional Hermite wavelet method. The results thus obtained are then compared with exact solutions as well as with optimal homotopy asymptotic method (OHAM). The obtained results demonstrate the accuracy, efficiency and reliability of the proposed algorithm based on two-dimensional Hermite wavelet method and its applicability to nonlinear time-fractional modified Fornberg-Whitham equation. Agreement between present numerical results obtained by Hermite wavelet method with optimal homotopy asymptotic method and exact solutions appear very satisfactory through illustrative results in Tables 7.1-7.7.

The solitary wave solution of fractional modified Fornberg-Whitham equation has been obtained for the first time by using first integral method. The fractional order modified Fornberg-Whitham equation has also been solved by using the optimal homotopy asymptotic method. The acquired numerical approximate results are compared with the exact solutions obtained through first integral method, which reveals that the efficiency and plausibility of the proposed OHAM technique. The results exhibited in Tables 7.8-7.10 demonstrate a pretty good agreement between the present numerical methods with the exact solution. Finally, it is worthwhile to mention that the first integral method is promising and powerful for solving nonlinear fractional differential equations in mathematical physics.

Next, the two-dimensional Hermite wavelet method has been implemented to coupled fractional differential equation viz. fractional Jaulent-Miodek equation. The results thus obtained are then compared with exact solutions as well as with optimal homotopy asymptotic method (OHAM). The evaluated outcomes demonstrate the efficiency, accuracy and reliability of the proposed algorithm based on two-dimensional Hermite wavelet approach and its applicability to nonlinear time-fractional coupled Jaulent-Miodek equations. It can be observed that the agreement between proposed numerical results attained by Hermite wavelet technique with optimal homotopy asymptotic method and exact solutions appear very satisfactory by means of illustrative results in Tables 7.12-7.18. The present scheme is easy to implement, effective and suitable for acquiring numerical solutions of nonlinear time-fractional coupled Jaulent-Miodek equations.

The application of the proposed numerical approach based on two-dimensional Hermite wavelet method for the solutions of time-fractional modified Fornberg-Whitham equation and fractional coupled Jaulent-Miodek equations quite satisfactorily justifies its simplicity, effectivity and applicability.

CHAPTER 8

8 Implementation of Petrov-Galerkin Method for Solving FPDEs

8.1 Introduction

In the present chapter, Petrov-Galerkin method has been utilized for the numerical solution of fractional KdV–Burgers (KdVB) equation and fractional Sharma-Tasso-Olver (STO) equation. In past few years, tremendous effort has been anticipated by the researchers on the study of nonlinear evolution equations appeared in mathematical physics. The nonlinear fractional differential equations have been solved numerically through the Petrov-Galerkin approach by utilizing a linear hat function as the trial function and a quintic B-spline function as the test function.

In the present study, we consider one of the well-known equations namely the Korteweg-de Vries–Burgers (KdVB) which play an essential role in both applied mathematics and physics. Especially Korteweg–de Vries (KdV) type equations had been paid of more attention due to its various applications in plasma physics, solid-state physics and quantum field theory.

The Korteweg-de Vries-Burgers equation is a nonlinear partial differential equation of the form

$$u_t + \varepsilon u u_x - v u_{xx} + \mu u_{xxx} = 0,\tag{8.1}$$

which was first derived by Su and Gardner [167]. It arises in quite a lot of contexts as a model equation incorporating a few foremost physical phenomena viz. dispersion, viscosity and nonlinear advection. This equation arises within the description of long wave propagation in shallow water [168], propagation of waves in elastic tube stuffed with a viscous fluid [169] and weakly nonlinear plasma waves with certain dissipative effects [170]. It additionally represents long wavelength approximations where the effect of the nonlinear advection $u u_x$ is counterbalanced by means of the dispersion u_{xxx}.

235

The KdVB equation given in eq. (8.1) is a combination of the Burgers' (when $\mu = 0$) and the KdV equations (when $\nu = 0$). In the year 1939, Burger proposed an equation (known as Burgers' equation) for the study of turbulence and approximate theory of flow through a shock wave traveling in a viscous fluid [49, 171]. The KdV equation was first suggested by Korteweg and de Vries [172]. This equation was used to study the change in shape of long waves moving in a rectangular channel [132, 172]. When diffusion dominates dispersion, the numerical solutions of eq. (8.1) tend to behave like Burgers' equation solutions and hence the steady-state solutions of the KdVB equation are monotonic shocks. However, when dispersion dominates, the KdV behavior is observed and the shocks are oscillatory.

A number of theoretical issues associated to the KdVB equation have received substantial attention. Many analytical and numerical methods have been proposed in recent past for the study of classical KdV-Burgers equation. Various methods such as the decomposition method [173], tanh method [174], hyperbolic tangent method and exponential rational function approach [175], Septic B-spline method [176], Radial basis functions [177], Quartic B-spline Galerkin approach [178] and quintic B-spline finite elements [179] had been developed independently and had been used to acquire exact as well as numerical solutions of KdVB equation. However so far as we know that no numerical works has been reported to solve the fractional KdVB equation. Methods such as Adomian decomposition method [180], and homotopy perturbation method [181] were used to obtain the approximate solution of fractional KdVB equation.

Let us consider the time-fractional KdV-Burgers equation [181-183] as follows

$$D_t^\alpha u + \varepsilon u u_x - \nu u_{xx} + \mu u_{xxx} = 0,\tag{8.2}$$

where ε, ν and μ are constants and α denotes the order of fractional derivative whose range is $0 < \alpha \leq 1$.

In the present numerical scheme, fractional derivative has been discretized by Grünwald-Letnikov derivative and the fractional KdVB equation has been converted directly into finite difference equation. Then it has been adjusted in the form of implicit finite difference scheme.

Next, the Sharma-Tasso-Olver equation has been considered, which plays an essential role both in physics and applied mathematics. Remarkable effort has been anticipated by the

researchers for studying nonlinear equations arising in mathematical physics. In recent years, Sharma-Tasso-Olver equations [184, 185] had been paid of more attention due to its numerous implementations in mathematical physics.

Let us consider the time-fractional Sharma-Tasso-Olver equation [186] as follows

$$D_t^\alpha u + 3au_x^2 + 3au^2 u_x + 3auu_{xx} + au_{xxx} = 0, \tag{8.3}$$

where $u(x,t)$ is the unknown function depending on the spatial variable x and the temporal variable t and a is a real parameter. Here α denotes the order of fractional derivative whose range is $0 < \alpha \le 1$.

Eq. (8.3) can also be written as [185]

$$D_t^\alpha u + \frac{3}{2}a(u^2)_{xx} + a(u^3)_x + au_{xxx} = 0. \tag{8.4}$$

This equation contains both linear dispersive term au_{xxx} and the double nonlinear terms $(u^2)_{xx}$ and $(u^3)_x$. The equation was first derived by Tasso [187] in 1976 as an example of odd members of the Burgers hierarchy by extending the linearization achieved through the Cole-Hopf ansatz to equations containing as highest derivatives odd space derivatives. In a subsequent report [188], the properties of the wave envelope solutions of this equation are investigated.

The Sharma–Tasso–Olver equation appears in many scientific applications such as quantum field theory, plasma physics, dispersive wave phenomena, relativistic physics, nonlinear optics and physical sciences [184]. It also arises as an evolution equation that possesses an infinitely many symmetries [189]. Many analytical and numerical methods have been proposed in recent past for the study of classical Sharma-Tasso-Olver equation. Various methods such as the Cole–Hopf transformations method [190], the Adomian decomposition method [186], the variational iteration method (VIM) [186], the homotopy perturbation method [186], Bäcklund transform method [185], Exp-solution method [191], improved G'/G-expansion method [192], tanh and extended tanh method [193] had been used to acquire exact as well as numerical solutions of Sharma-Tasso-Olver equation.

According to the best possible information of the authors, so far no numerical works has been reported to solve the fractional Sharma-Tasso-Olver equation. The approximate analytical solution of fractional Sharma–Tasso–Olver equation has been obtained by using the homotopy analysis method [194], improved generalized tanh-coth method [195], the

Adomian decomposition method [186], the variational iteration method (VIM) [186], and homotopy perturbation method [186]. In the present numerical scheme fractional derivative has been discretized by Grünwald-Letnikov derivative and the fractional Sharma-Tasso-Olver equation has been converted directly into finite difference equation. Then it has been adjusted in the form of implicit finite difference scheme.

The present chapter emphasizes on the application of Petrov-Galerkin method for solving the fractional differential equations such as the fractional KdVB equation and the fractional Sharma-Tasso-Olver equation with a view to exhibit the capabilities of this method in handling nonlinear equation. The main objective of this chapter is to establish the efficiency and accuracy of Petrov-Galerkin method in solving fractional differential equtaions numerically by implementing a linear hat function as the trial function and a quintic B-spline function as the test function.

8.2 Implementation of Petrov-Galerkin Method for Numerical Solution of Time-Fractional Kdv-Burgers Equation

Let us consider the time-fractional KdV-Burgers equation [181-183] as

$$D_t^\alpha u + \varepsilon u u_x - v u_{xx} + \mu u_{xxx} = 0,$$ (8.5)

with initial condition [196]

$$u(x,0) = \frac{-1}{50\varepsilon v\mu}\left[250\lambda\mu^2 + 6v^3 \sec h^2\left(\frac{vx}{10\mu}\right)\left(-1+\sinh\left(\frac{vx}{5\mu}\right)\right)\right].$$ (8.6)

Eq. (8.5) implies

$$D_t^\alpha u + \frac{\varepsilon}{2}(u^2)_x - v u_{xx} + \mu u_{xxx} = 0,$$

where ε, v and η are constants, α denotes the order of fractional derivative whose range is $0 < \alpha \leq 1$.

The exact solution of eq. (8.5) is given by [196]

$$u(x,t) = \frac{-1}{50\varepsilon v\mu}\left[250\lambda\mu^2 + 6v^3 \sec h^2\left(\frac{1}{2}\left(\frac{vx}{5\mu} + \frac{\lambda t^\alpha}{\Gamma(\alpha+1)}\right)\right)\left(-1+\sinh\left(\frac{vx}{5\mu} + \frac{\lambda t^\alpha}{\Gamma(\alpha+1)}\right)\right)\right].$$

(8.7)

The space interval $a_1 \leq x \leq b_1$ is discretized with $(N+1)$ uniform grid points $x_j = a_1 + jh$, $j = 0,1,2,...,N$ and the grid spacing is given by $h = \dfrac{b_1 - a_1}{N}$. Let $U_j(t)$ denotes the approximation to the exact solution $u(x_j, t)$. We sought the approximate solution of eq. (8.5) as

$$u(x,t) = \sum_{j=0}^{N} U_j(t)\varphi_j(x), \qquad (8.8)$$

where $\varphi_j(x)$, $j = 0,1,2,...,N$ are trial functions.

In order to deal with the nonlinear term uu_x, the product approximation technique [191] is utilised as follows:

$$u^2(x,t) = \sum_{j=0}^{N} U_j^2(t)\varphi_j(x), \qquad (8.9)$$

where $\varphi_j(x)$; $j = 0,1,2,...,N$ are the usual piecewise linear hat functions given by

$$\varphi_j(x) = \begin{cases} 1 + \dfrac{x - jh}{j}, & x \in [x_{j-1}, x_j) \\ 1 - \dfrac{x - jh}{j}, & x \in [x_j, x_{j+1}) \\ 0, & \text{elsewhere.} \end{cases} \qquad (8.10)$$

The unknown functions $U_j(t)$ are determined from the variational formulation

$$\left\langle D_t^\alpha u, \psi_j \right\rangle + \frac{\varepsilon}{2}\left\langle (u^2)_x, \psi_j \right\rangle - v\left\langle u_{xx}, \psi_j \right\rangle + \mu\left\langle u_{xxx}, \psi_j \right\rangle = 0, \qquad (8.11)$$

where $\psi_j(x)$, $j = 0,1,2,...,N$ are quintic B-spline functions taken as the test functions and are given by

$$\psi_j(x) = \frac{1}{h^5} \begin{cases} (x - x_{j-3})^5; & x \in [x_{j-3}, x_{j-2}) \\ (x - x_{j-3})^5 - 6(x - x_{j-2})^5; & x \in [x_{j-2}, x_{j-1}) \\ (x - x_{j-3})^5 - 6(x - x_{j-2})^5 + 15(x - x_{j-1})^5; & x \in [x_{j-1}, x_j) \\ (x - x_{j-3})^5 - 6(x - x_{j-2})^5 + 15(x - x_{j-1})^5 - 20(x - x_j)^5; & x \in [x_j, x_{j+1}) \\ (x - x_{j-3})^5 - 6(x - x_{j-2})^5 + 15(x - x_{j-1})^5 - 20(x - x_j)^5 + 15(x - x_{j+1})^5; & x \in [x_{j+1}, x_{j+2}) \\ \begin{aligned} &(x - x_{j-3})^5 - 6(x - x_{j-2})^5 + 15(x - x_{j-1})^5 - 20(x - x_j)^5 \\ &\quad + 15(x - x_{j+1})^5 - 6(x - x_{j+2})^5; \end{aligned} & x \in [x_{j+2}, x_{j+3}) \\ 0 & \text{elsewhere} \end{cases}$$

Integrating by parts the above eq. (8.11), we obtain

$$\left\langle D_t^\alpha u, \psi_j \right\rangle + \frac{\varepsilon}{2}\left\langle (u^2)_x, \psi_j \right\rangle - v\left\langle u_x, (\psi_j)_x \right\rangle + \mu\left\langle u_x, (\psi_j)_{xx} \right\rangle = 0. \tag{8.12}$$

Each linear hat function covers two elements so that each subinterval $[x_j, x_{j+1}]$ is covered by two linear hat functions. On the other hand each quantic B-spline covers six elements so that each subinterval $[x_j, x_{j+1}]$ is covered by six splines. In terms of local co-ordinate system given by

$$\xi = x - x_j, \ 0 < \xi \le h.$$

Both the linear hat functions, φ_j and the quantic B-spline functions, ψ_j over the element $[x_j, x_{j+1}]$ can be defined as follows:

$$\varphi_j = \frac{\xi}{h},$$

$$\varphi_{j+1} = 1 - \frac{\xi}{h},$$

and $\quad \psi_{j-2} = 1 - 5\left(\frac{\xi}{h}\right) + 10\left(\frac{\xi}{h}\right)^2 - 10\left(\frac{\xi}{h}\right)^3 + 5\left(\frac{\xi}{h}\right)^4 - \left(\frac{\xi}{h}\right)^5,$

$$\psi_{j-1} = 26 - 50\left(\frac{\xi}{h}\right) + 20\left(\frac{\xi}{h}\right)^2 + 20\left(\frac{\xi}{h}\right)^3 - 20\left(\frac{\xi}{h}\right)^4 + 5\left(\frac{\xi}{h}\right)^5,$$

$$\psi_j = 66 - 60\left(\frac{\xi}{h}\right)^2 + 30\left(\frac{\xi}{h}\right)^4 - 10\left(\frac{\xi}{h}\right)^5,$$

$$\psi_{j+1} = 26 + 50\left(\frac{\xi}{h}\right) + 20\left(\frac{\xi}{h}\right)^2 - 20\left(\frac{\xi}{h}\right)^3 - 20\left(\frac{\xi}{h}\right)^4 + 10\left(\frac{\xi}{h}\right)^5,$$

$$\psi_{j+2} = 1 + 5\left(\frac{\xi}{h}\right) + 10\left(\frac{\xi}{h}\right)^2 + 10\left(\frac{\xi}{h}\right)^3 + 5\left(\frac{\xi}{h}\right)^4 - 5\left(\frac{\xi}{h}\right)^5,$$

$$\psi_{j+3} = \left(\frac{\xi}{h}\right)^5.$$

From eq. (8.12), we have

$$\int_{x_0}^{x_N} \sum_{j=0}^{N} D_t^\alpha U_j(t)\varphi_j(x)\psi_j(x)dx + \frac{\varepsilon}{2}\int_{x_0}^{x_N} \sum_{j=0}^{N} U_j^2(t)\varphi_j'(x)\psi_j(x)dx -$$

$$v\int_{x_0}^{x_N} \sum_{j=0}^{N} U_j(t)\varphi_j'(x)\psi_j'(x)dx + \mu\int_{x_0}^{x_N} \sum_{j=0}^{N} U_j(t)\varphi_j'(x)\psi_j''(x)dx = 0. \tag{8.13}$$

Next we set $I_1 = \int_{x_0}^{x_N} \sum_{j=0}^{N} D_t^\alpha U_j(t) \varphi_j(x) \psi_j(x) dx$,

$$I_2 = \int_{x_0}^{x_N} \sum_{j=0}^{N} U_j^2(t) \varphi_j'(x) \psi_j(x) dx,$$

$$I_3 = \int_{x_0}^{x_N} \sum_{j=0}^{N} U_j(t) \varphi_j'(x) \psi_j'(x) dx,$$

$$I_4 = \int_{x_0}^{x_N} \sum_{j=0}^{N} U_j(t) \varphi_j'(x) \psi_j''(x) dx,$$

where $D_t^\alpha U_j(t)$ is defined by

$$D_t^\alpha U_j(t) = \lim_{\substack{\Delta t \to 0 \\ \Delta tn = t-a}} (\Delta t)^{-\alpha} \sum_{r=0}^{n} \omega_r^\alpha U_j(t - \Delta tr).$$

Now $I_1 = \int_{x_0}^{x_N} \sum_{j=0}^{N} D_t^\alpha U_j(t) \varphi_j(x) \psi_j(x) dx$

$$= \int_{x_{j-3}}^{x_{j-2}} (\Delta t)^{-\alpha} \sum_{r=0}^{n} \omega_r^\alpha U_{j-3}^{n-r} \varphi_{j-3}(x) \psi_{j-3}(x) dx + \int_{x_{j-3}}^{x_{j-2}} (\Delta t)^{-\alpha} \sum_{r=0}^{n} \omega_r^\alpha U_{j-2}^{n-r} \varphi_{j-2}(x) \psi_{j-3}(x) dx +$$

$$+ \int_{x_{j-2}}^{x_{j-1}} (\Delta t)^{-\alpha} \sum_{r=0}^{n} \omega_r^\alpha U_{j-2}^{n-r} \varphi_{j-2}(x) \psi_{j-2}(x) dx + \int_{x_{j-2}}^{x_{j-1}} (\Delta t)^{-\alpha} \sum_{r=0}^{n} \omega_r^\alpha U_{j-1}^{n-r} \varphi_{j-1}(x) \psi_{j-2}(x) dx$$

$$+ \int_{x_{j-1}}^{x_j} (\Delta t)^{-\alpha} \sum_{r=0}^{n} \omega_r^\alpha U_{j-1}^{n-r} \varphi_{j-1}(x) \psi_{j-1}(x) dx + \int_{x_{j-1}}^{x_j} (\Delta t)^{-\alpha} \sum_{r=0}^{n} \omega_r^\alpha U_j^{n-r} \varphi_j(x) \psi_{j-1}(x) dx$$

$$+ \int_{x_j}^{x_{j+1}} (\Delta t)^{-\alpha} \sum_{r=0}^{n} \omega_r^\alpha U_j^{n-r} \varphi_j(x) \psi_j(x) dx + \int_{x_j}^{x_{j+1}} (\Delta t)^{-\alpha} \sum_{r=0}^{n} \omega_r^\alpha U_{j+1}^{n-r} \varphi_{j+1}(x) \psi_j(x) dx$$

$$+ \int_{x_{j+1}}^{x_{j+2}} (\Delta t)^{-\alpha} \sum_{r=0}^{n} \omega_r^\alpha U_{j+1}^{n-r} \varphi_{j+1}(x) \psi_{j+1}(x) dx + \int_{x_{j+1}}^{x_{j+2}} (\Delta t)^{-\alpha} \sum_{r=0}^{n} \omega_r^\alpha U_{j+2}^{n-r} \varphi_{j+2}(x) \psi_{j+1}(x) dx$$

$$+ \int_{x_{j+2}}^{x_{j+3}} (\Delta t)^{-\alpha} \sum_{r=0}^{n} \omega_r^\alpha U_{j+2}^{n-r} \varphi_{j+2}(x) \psi_{j+2}(x) dx + \int_{x_{j+2}}^{x_{j+3}} (\Delta t)^{-\alpha} \sum_{r=0}^{n} \omega_r^\alpha U_{j+3}^{n-r} \varphi_{j+3}(x) \psi_{j+3}(x) dx$$

$$= (\Delta t)^{-\alpha} \sum_{r=0}^{n} \omega_r^\alpha \left[\frac{h}{42} \left(U_{j-3}^{n-r} + 120 U_{j-2}^{n-r} + 1191 U_{j-1}^{n-r} + 2416 U_j^{n-r} + 1191 U_{j+1}^{n-r} \right. \right. \tag{8.14}$$
$$\left. \left. + 120 U_{j+2}^{n-r} + U_{j+3}^{n-r} \right) \right].$$

Similarly,

$$I_2 = \frac{1}{6} \left[-(U_{j-3}^n)^2 - 56(U_{j-2}^n)^2 - 245(U_{j-1}^n)^2 + 245(U_{j+1}^n)^2 + 56(U_{j+2}^n)^2 + (U_{j+3}^n)^2 \right], \tag{8.15}$$

$$I_3 = \frac{-1}{h}\left[U_{j-3}^n + 24U_{j-2}^n + 15U_{j-1}^n - 80U_j^n + 15U_{j+1}^n + 24U_{j+2}^n + U_{j+3}^n\right], \tag{8.16}$$

$$I_4 = \frac{1}{h^2}\left[-5U_{j-3}^n - 40U_{j-2}^n + 95U_{j-1}^n - 95U_{j+1}^n + 40U_{j+2}^n + 5U_{j+3}^n\right]. \tag{8.17}$$

Substituting eqs. (8.14)-(8.17) in eq. (8.13), we have

$$(\Delta t)^{-\alpha}\sum_{r=0}^n \omega_r^\alpha\left[\frac{h}{42}\left(U_{j-3}^{n-r} + 120U_{j-2}^{n-r} + 1191U_{j-1}^{n-r} + 2416U_j^{n-r} + 1191U_{j+1}^{n-r} + 120U_{j+2}^{n-r} + U_{j+3}^{n-r}\right)\right]$$

$$+ \frac{\varepsilon}{12}\left[-(U_{j-3}^n)^2 - 56(U_{j-2}^n)^2 - 245(U_{j-1}^n)^2 + 245(U_{j+1}^n)^2 + 56(U_{j+2}^n)^2 + (U_{j+3}^n)^2\right]$$

$$+ \frac{\nu}{h}\left[U_{j-3}^n + 24U_{j-2}^n + 15U_{j-1}^n - 80U_j^n + 15U_{j+1}^n + 24U_{j+2}^n + U_{j+3}^n\right]$$

$$+ \frac{\mu}{h^2}\left[-5U_{j-3}^n - 40U_{j-2}^n + 95U_{j-1}^n - 95U_{j+1}^n + 40U_{j+2}^n + 5U_{j+3}^n\right] = 0, \tag{8.18}$$

where $j = 1,2,...,N$. Now to solve the above system, we assume U_j^n to be a discrete approximation to the exact solution $u(x_j, t_n)$. $U_j^n = 0$ for $j = -2, -1, 0, N+1, N+2$ and $N+3$. The system (8.18) is three time level scheme, so we require two initial time levels and for the computation, the exact value at time equals zero and time equals Δt are used for the required initial conditions. This nonlinear system (8.18) can be solved by Newton's method in order to compute the unknown approximate solutions U_j^n. Hence the required solution of the time-fractional KdVB equation can be found.

8.3   Numerical Results and Discussion

The comparison of the absolute errors for time-fractional KdVB equation (8.5) have been exhibited in Tables 8.1 and 8.2 which are generated using the results acquired by means of Petrov-Galerkin method and the new method proposed in Ref. [196] at different values of x and t taking $\alpha = 0.75$ and 0.5 respectively. In this present analysis, in order to evaluate the accuracy and reliability of the Petrov-Galerkin for solving fractional order KdVB equation, we compare L_2 and L_∞ error norms at various points of t taking $\alpha = 1, 0.75$ and 0.5 as illustrated in Tables 8.3-8.6. Agreement between present numerical results for time-fractional KdVB equation obtained by Petrov-Galerkin method appears very satisfactory through illustrations in Tables 8.1-8.6. The computed outcomes exhibit

that this proposed procedure can also be comfortably applied to such variety of nonlinear equations and good accuracy can also be also attained. With the aid of conducting a comparison between the absolute error for the obtained numerical results and the analytic solution of the KdVB equation we will test the accuracy of the proposed procedure.

Table 8.1   The absolute errors obtained by Petrov-Galerkin method with regard to solution obtained by new method in ref [196] for time-fractional KdV-Burgers equation given in (8.5) at various points of x and t taking $\alpha = 0.75, \lambda = 1, \varepsilon = 6, \nu = 1$ and $\mu = 2$.

x	$|u_{PGM} - u_{Exact}|$							
	$t=0.2$	$t=0.3$	$t=0.4$	$t=0.5$	$t=0.6$	$t=0.7$	$t=0.8$	$t=0.9$
0.1	1.46833E-3	2.79680E-3	4.03999E-3	5.21834E-3	6.34158E-3	7.41499E-3	8.44173E-3	9.42393E-3
0.2	1.47268E-3	2.80387E-3	4.04863E-3	5.22763E-3	6.35075E-3	7.42339E-3	8.44882E-3	9.42925E-3
0.3	1.47692E-3	2.81075E-3	4.0570E-3	5.23656E-3	6.35949E-3	7.43129E-3	8.45536E-3	9.43397E-3
0.4	1.48107E-3	2.81745E-3	4.06509E-3	5.24514E-3	6.36780E-3	7.43871E-3	8.46143E-3	9.43807E-3
0.5	1.48512E-3	2.82396E-3	4.07291E-3	5.25337E-3	6.37568E-3	7.44562E-3	8.46676E-3	9.44157E-3
0.6	1.48908E-3	2.83028E-3	4.08045E-3	5.26124E-3	6.38314E-3	7.45204E-3	8.47164E-3	9.44446E-3
0.7	1.49293E-3	2.83640E-3	4.08772E-3	5.26875E-3	6.39017E-3	7.45797E-3	8.47595E-3	9.44674E-3
0.8	1.49669E-3	2.84234E-3	4.09472E-3	5.27591E-3	6.39676E-3	7.46341E-3	8.47972E-3	9.44842E-3
0.9	1.50034E-3	2.84809E-3	4.10143E-3	5.28272E-3	6.40293E-3	7.46834E-3	8.48293E-3	9.44949E-3
1.0	1.50390E-3	2.85364E-3	4.10787E-3	5.28916E-3	6.40867E-3	7.47279E-3	8.48559E-3	9.44996E-3

Table 8.2   The absolute errors obtained by Petrov-Galerkin method with regard to solution obtained by new method in ref [196] for time-fractional KdV-Burgers equation given in (8.5) at various points of x and t taking $\alpha = 0.5, \lambda = 10, \varepsilon = 6, \nu = 0.05$ and $\mu = 0.1$.

x	$|u_{PGM} - u_{Exact}|$								
	$t=0.1$	$t=0.2$	$t=0.3$	$t=0.4$	$t=0.5$	$t=0.6$	$t=0.7$	$t=0.8$	$t=0.9$
0.1	1.7701E-4	2.5821E-4	2.7527E-4	2.8030E-4	2.8209E-4	2.8281E-4	2.8313E-4	2.8328E-4	2.8335E-4
0.2	1.7476E-4	2.5594E-4	2.7284E-4	2.7781E-4	2.7958E-4	2.8030E-4	2.8062E-4	2.8076E-4	2.8084E-4
0.3	1.7328E-4	2.5369E-4	2.7042E-4	2.7535E-4	2.7710E-4	2.7781E-4	2.7812E-4	2.7827E-4	2.7834E-4
0.4	1.7181E-4	2.5146E-4	2.6802E-4	2.7290E-4	2.7464E-4	2.7534E-4	2.7565E-4	2.7579E-4	2.7587E-4
0.5	1.7035E-4	2.4924E-4	2.6565E-4	2.7047E-4	2.7219E-4	2.7289E-4	2.7319E-4	2.7334E-4	2.7341E-4
0.6	1.6890E-4	2.4704E-4	2.6329E-4	2.6806E-4	2.6977E-4	2.7046E-4	2.7076E-4	2.7090E-4	2.7097E-4
0.7	1.6746E-4	2.4486E-4	2.6094E-4	2.6568E-4	2.6736E-4	2.6804E-4	2.6834E-4	2.6848E-4	2.6856E-4
0.8	1.6603E-4	2.4269E-4	2.5862E-4	2.6331E-4	2.6497E-4	2.6565E-4	2.6595E-4	2.6609E-4	2.6616E-4
0.9	1.6460E-4	2.4055E-4	2.5632E-4	2.6096E-4	2.6261E-4	2.6327E-4	2.6357E-4	2.6371E-4	2.6378E-4
1.0	1.6319E-4	2.3842E-4	2.5403E-4	2.5862E-4	2.6026E-4	2.6092E-4	2.6121E-4	2.6135E-4	2.6142E-4

Table 8.3 L_2 and L_∞ error norms for nonlinear KdV-Burgers equation using Petrov-Galerkin method at various points of t taking $\alpha = 1, \varepsilon = 6, \nu = 0.0005$ and $\mu = 0.1$.

t	L_2	L_∞
0.1	1.29814E-10	8.90530E-11

0.2	3.24729E-10	2.22708E-10
0.3	4.55738E-10	3.12239E-10
0.4	6.51429E-10	4.46194E-10
0.5	7.83639E-10	5.36188E-10
0.6	9.80090E-10	6.70419E-10
0.7	1.11351E-9	7.60861E-10
0.8	1.31070E-9	8.95346E-10
0.9	1.44534E-9	9.86221E-10
1.0	1.61436E-9	9.16034E-10

Table 8.4 L_2 and L_∞ error norms for nonlinear fractional KdV-Burgers equation using Petrov-Galerkin method at various points of t taking $\lambda = 1, \varepsilon = 6, \nu = 1$ and $\mu = 2$.

t	$\alpha = 1$		$\alpha = 0.75$		$\alpha = 0.5$	
	L_2	L_∞	L_2	L_∞	L_2	L_∞
0.1	9.40227E-5	6.92880E-5	2.70831E-3	8.69312E-4	3.76753E-3	1.20338E-3
0.2	2.33997E-4	1.72421E-4	7.40982E-3	2.37321E-3	9.22147E-3	2.93842E-3
0.3	3.21139E-4	2.36466E-4	1.16462E-2	3.72295E-3	1.34609E-2	4.28162E-3
0.4	4.56772E-4	3.36334E-4	1.55966E-2	4.97718E-3	1.70414E-2	5.41254E-3
0.5	5.37234E-4	3.95255E-4	1.93290E-2	6.15847E-3	2.01827E-2	6.40209E-3
0.6	6.68680E-4	4.92039E-4	2.28764E-2	7.27798E-3	2.29996E-2	7.28747E-3
0.7	7.42556E-4	5.45962E-4	2.62573E-2	8.34210E-3	2.55619E-2	8.09123E-3
0.8	8.70077E-4	6.39846E-4	2.94832E-2	9.35489E-3	2.79162E-2	8.83089E-3
0.9	9.37568E-4	6.88894E-4	3.25620E-2	1.03192E-2	3.00956E-2	9.51990E-3

Table 8.5 L_2 and L_∞ error norms for nonlinear fractional KdV-Burgers equation using Petrov-Galerkin method at various points of t taking $\lambda = 0.5, \varepsilon = 6, \nu = 0.05$ and $\mu = 0.1$.

t	$\alpha = 1$		$\alpha = 0.75$		$\alpha = 0.5$	
	L_2	L_∞	L_2	L_∞	L_2	L_∞
0.1	1.47277E-6	1.08060E-6	6.58012E-5	2.11747E-5	9.01591E-5	2.89412E-5
0.2	3.67927E-6	2.69904E-6	1.78696E-4	5.74413E-5	2.20265E-4	7.06189E-5
0.3	5.13661E-6	3.76477E-6	2.79767E-4	8.98432E-5	3.21907E-4	1.03109E-4
0.4	7.33184E-6	5.37326E-6	3.74120E-4	1.20036E-4	4.08641E-4	1.30788E-4
0.5	8.77274E-6	6.42404E-6	4.63866E-4	1.48708E-4	4.85733E-4	1.55354E-4
0.6	1.09575E-5	8.02246E-6	5.50119E-4	1.76221E-4	5.55895E-4	1.77683E-4
0.7	1.23825E-5	9.05825E-6	6.33550E-4	2.02793E-4	6.20744E-4	1.98298E-4
0.8	1.45561E-5	1.06465E-6	7.14595E-4	2.28570E-4	6.81337E-4	2.17540E-4
0.9	1.59651E-5	1.16672E-5	7.93554E-4	2.53649E-4	7.38412E-4	2.35646E-4

Table 8.6 L_2 and L_∞ error norms for nonlinear fractional KdV-Burgers equation using Petrov-Galerkin method at various points of t taking $\lambda = 0.1, \varepsilon = 6, \nu = 5$ and $\mu = 6$.

t	$\alpha = 1$		$\alpha = 0.75$		$\alpha = 0.5$	
	L_2	L_∞	L_2	L_∞	L_2	L_∞
0.1	3.47775E-3	2.43860E-3	2.17042E-3	7.07133E-4	2.90983E-3	9.47258E-3
0.2	8.56125E-3	6.00577E-3	5.83656E-3	1.90089E-3	7.04589E-3	2.29277E-3
0.3	1.08264E-2	7.56579E-3	9.06678E-3	2.95199E-3	1.02359E-2	3.32980E-3
0.4	1.53527E-2	1.07535E-2	1.20464E-2	3.92097E-3	1.29361E-2	4.20707E-3
0.5	1.65410E-2	1.15427E-2	1.48546E-2	4.83370E-3	1.53231E-2	4.98221E-3

0.6	2.07597E-2	1.45268E-2	1.75348E-2	5.70435E-3	1.74875E-2	5.68476E-3
0.7	2.09164E-2	1.46238E-2	2.01140E-2	6.54177E-3	1.94832E-2	6.33230E-3
0.8	2.52064E-2	1.75783E-2	2.26106E-2	7.35196E-3	2.13452E-2	6.93626E-3
0.9	2.41525E-2	1.69991E-2	2.50377E-2	8.13924E-3	2.30980E-2	7.50459E-3

8.4 Implementation of Petrov-Galerkin Method for Numerical Solution of Time-Fractional Sharma-Tasso-Olver Equation

This section involves the numerical simulations by means of proposed Petrov-Galerkin method for time-fractional Sharma-Tasso-Olver equation.

Let us consider the time-fractional Sharma-Tasso-Olver equation [186] as

$$D_t^\alpha u + 3au_x^2 + 3au^2u_x + 3auu_{xx} + au_{xxx} = 0, \qquad (8.19)$$

with initial condition [186]

$$u(x,0) = \frac{2\lambda[w + \tanh(\lambda x)]}{1 + w\tanh(\lambda x)}, \qquad (8.20)$$

where λ and w are constants.

Eq. (8.19) implies

$$D_t^\alpha u + \frac{3a}{2}(u^2)_{xx} + a(u^3)_x + au_{xxx} = 0,$$

where α denotes the order of fractional derivative whose range is $0 < \alpha \leq 1$.

For $\alpha = 1$, the exact solution of eq. (8.19) is given by [186]

$$u(x,t) = \frac{2\lambda[w + \tanh(\lambda(x - 4a\lambda^2 t))]}{1 + w\tanh(\lambda(x - 4a\lambda^2 t))}. \qquad (8.21)$$

The space interval $a_1 \leq x \leq b_1$ is discretized with (N+1) uniform grid points $x_j = a_1 + jh$, $j = 0,1,2,...,N$ and the grid spacing is given by $h = \frac{b_1 - a_1}{N}$. Let $U_j(t)$ denotes the approximation to the exact solution $u(x_j,t)$. We sought the approximate solution of eq. (8.19) as

$$u(x,t) = \sum_{j=0}^{N} U_j(t)\varphi_j(x), \qquad (8.22)$$

where $\varphi_j(x)$, $j = 0,1,2,...,N$ are trial functions.

In order to deal with the nonlinear terms u^2 and u^3, the product approximation technique [197] is utilised as follows:

$$u^2(x,t) = \sum_{j=0}^{N} U_j^2(t)\varphi_j(x),$$

$$u^3(x,t) = \sum_{j=0}^{N} U_j^3(t)\varphi_j(x), \tag{8.23}$$

where $\varphi_j(x)$, $j = 0,1,2,...,N$ are the usual piecewise linear hat functions given by

$$\varphi_j(x) = \begin{cases} 1 + \dfrac{x - jh}{j}, & x \in [x_{j-1}, x_j) \\ 1 - \dfrac{x - jh}{j}, & x \in [x_j, x_{j+1}) \\ 0, & \text{elsewhere.} \end{cases} \tag{8.24}$$

The unknown functions $U_j(t)$ are determined from the variational formulation

$$\left\langle D_t^\alpha u, \psi_j \right\rangle + \frac{3a}{2}\left\langle (u^2)_{xx}, \psi_j \right\rangle + a\left\langle (u^3)_x, \psi_j \right\rangle + a\left\langle u_{xxx}, \psi_j \right\rangle = 0, \tag{8.25}$$

where $\psi_j(x)$; $j = 0,1,2,...,N$ are quintic B-spline functions taken as the test functions and are given by

$$\psi_j(x) = \frac{1}{h^5} \begin{cases} (x - x_{j-3})^5; & x \in [x_{j-3}, x_{j-2}) \\ (x - x_{j-3})^5 - 6(x - x_{j-2})^5; & x \in [x_{j-2}, x_{j-1}) \\ (x - x_{j-3})^5 - 6(x - x_{j-2})^5 + 15(x - x_{j-1})^5; & x \in [x_{j-1}, x_j) \\ (x - x_{j-3})^5 - 6(x - x_{j-2})^5 + 15(x - x_{j-1})^5 - 20(x - x_j)^5; & x \in [x_j, x_{j+1}) \\ (x - x_{j-3})^5 - 6(x - x_{j-2})^5 + 15(x - x_{j-1})^5 - 20(x - x_j)^5 + 15(x - x_{j+1})^5; & x \in [x_{j+1}, x_{j+2}) \\ (x - x_{j-3})^5 - 6(x - x_{j-2})^5 + 15(x - x_{j-1})^5 - 20(x - x_j)^5 \\ \qquad + 15(x - x_{j+1})^5 - 6(x - x_{j+2})^5; & x \in [x_{j+2}, x_{j+3}) \\ 0 & \text{elsewhere.} \end{cases}$$

Integrating by parts the above eq. (8.25), we obtain

$$\left\langle D_t^\alpha u, \psi_j \right\rangle - \frac{3a}{2}\left\langle (u^2)_x, (\psi_j)_x \right\rangle + a\left\langle (u^3)_x, \psi_j \right\rangle + a\left\langle u_x, (\psi_j)_{xx} \right\rangle = 0. \tag{8.26}$$

Each linear hat function covers two elements so that each subinterval $[x_j, x_{j+1}]$ is covered by two linear hat functions. On the other hand each quantic B-spline covers six elements

so that each subinterval $[x_j, x_{j+1}]$ is covered by six splines. In terms of local co-ordinate system given by

$$\xi = x - x_j, \ 0 < \xi \leq h.$$

Both the linear hat functions, φ_j and the quantic B-spline functions, ψ_j over the element $[x_j, x_{j+1}]$ can be defined as follows:

$$\varphi_j = \frac{\xi}{h},$$

$$\varphi_{j+1} = 1 - \frac{\xi}{h},$$

and $\quad \psi_{j-2} = 1 - 5\left(\frac{\xi}{h}\right) + 10\left(\frac{\xi}{h}\right)^2 - 10\left(\frac{\xi}{h}\right)^3 + 5\left(\frac{\xi}{h}\right)^4 - \left(\frac{\xi}{h}\right)^5,$

$$\psi_{j-1} = 26 - 50\left(\frac{\xi}{h}\right) + 20\left(\frac{\xi}{h}\right)^2 + 20\left(\frac{\xi}{h}\right)^3 - 20\left(\frac{\xi}{h}\right)^4 + 5\left(\frac{\xi}{h}\right)^5,$$

$$\psi_j = 66 - 60\left(\frac{\xi}{h}\right)^2 + 30\left(\frac{\xi}{h}\right)^4 - 10\left(\frac{\xi}{h}\right)^5,$$

$$\psi_{j+1} = 26 + 50\left(\frac{\xi}{h}\right) + 20\left(\frac{\xi}{h}\right)^2 - 20\left(\frac{\xi}{h}\right)^3 - 20\left(\frac{\xi}{h}\right)^4 + 10\left(\frac{\xi}{h}\right)^5,$$

$$\psi_{j+2} = 1 + 5\left(\frac{\xi}{h}\right) + 10\left(\frac{\xi}{h}\right)^2 + 10\left(\frac{\xi}{h}\right)^3 + 5\left(\frac{\xi}{h}\right)^4 - 5\left(\frac{\xi}{h}\right)^5,$$

$$\psi_{j+3} = \left(\frac{\xi}{h}\right)^5.$$

From eq. (8.26), we have

$$\int_{x_0}^{x_N} \sum_{j=0}^{N} D_t^{\alpha} U_j(t) \varphi_j(x) \psi_j(x) dx - \frac{3a}{2} \int_{x_0}^{x_N} \sum_{j=0}^{N} U_j^2(t) \varphi_j(x) \psi'_j(x) dx$$

$$+ a \int_{x_0}^{x_N} \sum_{j=0}^{N} U_j^3(t) \varphi'_j(x) \psi_j(x) dx + a \int_{x_0}^{x_N} \sum_{j=0}^{N} U_j(t) \varphi'_j(x) \psi''_j(x) dx = 0. \tag{8.27}$$

Next we set $I_1 = \int_{x_0}^{x_N} \sum_{j=0}^{N} D_t^{\alpha} U_j(t) \varphi_j(x) \psi_j(x) dx,$

$$I_2 = \int_{x_0}^{x_N} \sum_{j=0}^{N} U_j^2(t) \varphi'_j(x) \psi'_j(x) dx,$$

$$I_3 = \int_{x_0}^{x_N} \sum_{j=0}^{N} U_j^3(t) \varphi_j'(x) \psi_j(x) dx,$$

$$I_4 = \int_{x_0}^{x_N} \sum_{j=0}^{N} U_j(t) \varphi_j'(x) \psi_j''(x) dx,$$

where $D_t^\alpha U_j(t)$ is defined by

$$D_t^\alpha U_j(t) = \lim_{\substack{\Delta t \to 0 \\ \Delta t n = t - a}} (\Delta t)^{-\alpha} \sum_{r=0}^{n} \omega_r^\alpha U_j(t - \Delta t r).$$

Now $I_1 = \int_{x_0}^{x_N} \sum_{j=0}^{N} D_t^\alpha U_j(t) \varphi_j(x) \psi_j(x) dx$

$$= \int_{x_{j-3}}^{x_{j-2}} (\Delta t)^{-\alpha} \sum_{r=0}^{n} \omega_r^\alpha U_{j-3}^{n-r} \varphi_{j-3}(x) \psi_{j-3}(x) dx + \int_{x_{j-3}}^{x_{j-2}} (\Delta t)^{-\alpha} \sum_{r=0}^{n} \omega_r^\alpha U_{j-2}^{n-r} \varphi_{j-2}(x) \psi_{j-3}(x) dx +$$

$$+ \int_{x_{j-2}}^{x_{j-1}} (\Delta t)^{-\alpha} \sum_{r=0}^{n} \omega_r^\alpha U_{j-2}^{n-r} \varphi_{j-2}(x) \psi_{j-2}(x) dx + \int_{x_{j-2}}^{x_{j-1}} (\Delta t)^{-\alpha} \sum_{r=0}^{n} \omega_r^\alpha U_{j-1}^{n-r} \varphi_{j-1}(x) \psi_{j-2}(x) dx$$

$$+ \int_{x_{j-1}}^{x_j} (\Delta t)^{-\alpha} \sum_{r=0}^{n} \omega_r^\alpha U_{j-1}^{n-r} \varphi_{j-1}(x) \psi_{j-1}(x) dx + \int_{x_{j-1}}^{x_j} (\Delta t)^{-\alpha} \sum_{r=0}^{n} \omega_r^\alpha U_j^{n-r} \varphi_j(x) \psi_{j-1}(x) dx$$

$$+ \int_{x_j}^{x_{j+1}} (\Delta t)^{-\alpha} \sum_{r=0}^{n} \omega_r^\alpha U_j^{n-r} \varphi_j(x) \psi_j(x) dx + \int_{x_j}^{x_{j+1}} (\Delta t)^{-\alpha} \sum_{r=0}^{n} \omega_r^\alpha U_{j+1}^{n-r} \varphi_{j+1}(x) \psi_j(x) dx$$

$$+ \int_{x_{j+1}}^{x_{j+2}} (\Delta t)^{-\alpha} \sum_{r=0}^{n} \omega_r^\alpha U_{j+1}^{n-r} \varphi_{j+1}(x) \psi_{j+1}(x) dx + \int_{x_{j+1}}^{x_{j+2}} (\Delta t)^{-\alpha} \sum_{r=0}^{n} \omega_r^\alpha U_{j+2}^{n-r} \varphi_{j+2}(x) \psi_{j+1}(x) dx$$

$$+ \int_{x_{j+2}}^{x_{j+3}} (\Delta t)^{-\alpha} \sum_{r=0}^{n} \omega_r^\alpha U_{j+2}^{n-r} \varphi_{j+2}(x) \psi_{j+2}(x) dx + \int_{x_{j+2}}^{x_{j+3}} (\Delta t)^{-\alpha} \sum_{r=0}^{n} \omega_r^\alpha U_{j+3}^{n-r} \varphi_{j+3}(x) \psi_{j+3}(x) dx$$

$$= (\Delta t)^{-\alpha} \sum_{r=0}^{n} \omega_r^\alpha \left[\frac{h}{42} \left(U_{j-3}^{n-r} + 120 U_{j-2}^{n-r} + 1191 U_{j-1}^{n-r} + 2416 U_j^{n-r} + 1191 U_{j+1}^{n-r} + 120 U_{j+2}^{n-r} + U_{j+3}^{n-r} \right) \right].$$

(8.28)

Similarly,

$$I_2 = \frac{-1}{h} \left[(U_{j-3}^n)^2 + 24(U_{j-2}^n)^2 + 15(U_{j-1}^n)^2 - 80(U_j^n)^2 + 15(U_{j+1}^n)^2 + 24(U_{j+2}^n)^2 + (U_{j+3}^n)^2 \right],$$

(8.29)

$$I_3 = \frac{1}{6} \left[-(U_{j-3}^n)^3 - 56(U_{j-2}^n)^3 - 245(U_{j-1}^n)^3 + 245(U_{j+1}^n)^3 + 56(U_{j+2}^n)^3 + (U_{j+3}^n)^3 \right], \qquad (8.30)$$

$$I_4 = \frac{1}{h^2} \left[-5 U_{j-3}^n - 40 U_{j-2}^n + 95 U_{j-1}^n - 95 U_{j+1}^n + 40 U_{j+2}^n + 5 U_{j+3}^n \right]. \qquad (8.31)$$

Substituting eqs. (8.28)-(8.31) in eq. (8.27), we have

248

$$(\Delta t)^{-\alpha} \sum_{r=0}^{n} \omega_r^{\alpha} \left[\frac{h}{42} \left(U_{j-3}^{n-r} + 120 U_{j-2}^{n-r} + 1191 U_{j-1}^{n-r} + 2416 U_j^{n-r} + 1191 U_{j+1}^{n-r} + 120 U_{j+2}^{n-r} + U_{j+3}^{n-r} \right) \right]$$

$$+ \frac{3a}{2h} \left[(U_{j-3}^n)^2 + 24(U_{j-2}^n)^2 + 15(U_{j-1}^n)^2 - 80(U_j^n)^2 + 15(U_{j+1}^n)^2 + 24(U_{j+2}^n)^2 + (U_{j+3}^n)^2 \right]$$

$$+ \frac{a}{6} \left[-(U_{j-3}^n)^3 - 56(U_{j-2}^n)^3 - 245(U_{j-1}^n)^3 + 245(U_{j+1}^n)^3 + 56(U_{j+2}^n)^3 + (U_{j+3}^n)^3 \right]$$

$$+ \frac{a}{h^2} \left[-5U_{j-3}^n - 40U_{j-2}^n + 95U_{j-1}^n - 95U_{j+1}^n + 40U_{j+2}^n + 5U_{j+3}^n \right] = 0,$$

(8.32)

where $j = 1, 2, 3, 4, ..., N$. Now to solve the above system, we assume U_j^n to be a discrete approximation to the exact solution $u(x_j, t_n)$. $U_j^n = 0$ for $j = -2, -1, 0, N+1, N+2$ and $N+3$. The system (8.32) is three time level scheme, so we require two initial time levels and for the computation, the exact value at time equals zero and time equals Δt are used for the required initial conditions. This nonlinear system (8.32) can be solved by Newton's method in order to compute the unknown approximate solutions U_j^n. Hence the required solution of the time-fractional Sharma-Tasso-Olver equation can be found.

8.5   Numerical Results and Discussion

In this present analysis, the absolute errors for Sharma-Tasso-Olver equation (8.19) have been exhibited in Table 8.7 in case of integer order $\alpha = 1$. In order to evaluate the accuracy and reliability of the Petrov-Galerkin for solving fractional order Sharma-Tasso-Olver equation, the absolute errors obtained by Petrov-Galerkin and VIM have been presented in Tables 8.8 and 8.9 for various points of x and t taking $\alpha = 0.75$ and 0.5 respectively. The comparison of L_2 and L_∞ error norms at various points of t taking $\alpha = 0.75$ and 0.5 has been illustrated in Table 8.10. Agreement between present numerical results for time-fractional Sharma-Tasso-Olver equation obtained by Petrov-Galerkin method appears very satisfactory through illustrations in Tables 8.7-8.10. The computed outcomes exhibit that this proposed procedure can also be comfortably applied to such variety of nonlinear equations and good accuracy can also be attained. The accuracy of the proposed procedure can be examined with the aid of conducting a comparison between the absolute errors obtained by proposed numerical results and the VIM solutions of the fractional Sharma-Tasso-Olver equation. A comprehensible inference can be drawn from

the numerical results that the proposed Petrov-Galerkin method imparts highly accurate numerical solutions for nonlinear fractional differential equations.

Table 8.7 The absolute errors obtained by Petrov-Galerkin method with regard to exact solution for time-fractional Sharma-Tasso-Olver equation given in (8.19) at various points of x and t taking $\alpha = 1$, $\lambda = 0.01$, $w = 0.05$, and $a = 1$.

x	$\|u_{PGM} - u_{Exact}\|$									
	$t=0.01$	$t=0.02$	$t=0.03$	$t=0.04$	$t=0.05$	$t=0.06$	$t=0.07$	$t=0.08$	$t=0.09$	$t=0.1$
1	2.23959E-5	4.42244E-5	6.54935E-5	8.62037E-5	1.06349E-4	1.25918E-4	1.44892E-4	1.63248E-4	1.80957E-4	1.9799E-4
2	2.58227E-5	5.16002E-5	7.73625E-5	1.03126E-4	1.28891E-4	1.54645E-4	1.80359E-4	2.05993E-4	2.31490E-4	2.5678E-4
3	1.55609E-5	3.15260E-5	4.80049E-5	6.50892E-5	8.28516E-5	1.01344E-4	1.20597E-4	1.40617E-4	1.61390E-4	1.8287E-4
4	1.07875E-5	2.15582E-5	3.25306E-5	4.39120E-5	5.58949E-5	6.86546E-5	8.23457E-5	9.71000E-5	1.13024E-4	1.3019E-4
5	1.02889E-5	1.94437E-5	2.77437E-5	3.54742E-5	4.29222E-5	5.03723E-5	5.81029E-5	6.63819E-5	7.54633E-5	8.5583E-5
6	1.39288E-5	2.52770E-5	3.42716E-5	4.11663E-5	4.62383E-5	4.97847E-5	5.21189E-5	5.35662E-5	5.44601E-5	5.5137E-5
7	2.31580E-5	4.24684E-5	5.79771E-5	6.97697E-5	7.79699E-5	8.27384E-5	8.42708E-5	8.27945E-5	7.85668E-5	7.1871E-5
8	4.14883E-5	7.91986E-5	1.12952E-4	1.42603E-4	1.68044E-4	1.89204E-4	2.06047E-4	2.18575E-4	2.26826E-4	2.3087E-4
9	7.40691E-5	1.46667E-4	2.17516E-4	2.86355E-4	3.52940E-4	4.17049E-4	4.78481E-4	5.37061E-4	5.92634E-4	6.4507E-4

Table 8.8 The absolute errors obtained by Petrov-Galerkin method with regard to solution obtained by VIM for time-fractional Sharma-Tasso-Olver equation given in (8.19) at various points of x and t taking $a = 1, \lambda = 0.01, w = 0.05$ and $\alpha = 0.75$.

x	$\|u_{PGM} - u_{VIM}\|$								
	$t=0.1$	$t=0.2$	$t=0.3$	$t=0.4$	$t=0.5$	$t=0.6$	$t=0.7$	$t=0.8$	$t=0.9$
1	1.0614E-8	2.1103E-8	3.0835E-8	4.0017E-8	4.8760E-8	5.7131E-8	6.5178E-8	7.2937E-8	8.0437E-8
2	1.0601E-8	2.1075E-8	3.0795E-8	3.9965E-8	4.8696E-8	5.7056E-8	6.5093E-8	7.2843E-8	8.0332E-8
3	1.0584E-8	2.1044E-8	3.0749E-8	3.9905E-8	4.8623E-8	5.6971E-8	6.4996E-8	7.2734E-8	8.0212E-8
4	1.0566E-8	2.1008E-8	3.0696E-8	3.9838E-8	4.8541E-8	5.6874E-8	6.4886E-8	7.2610E-8	8.0076E-8
5	1.0546E-8	2.0968E-8	3.0638E-8	3.9762E-8	4.8449E-8	5.6767E-8	6.4763E-8	7.2473E-8	7.9924E-8
6	1.0524E-8	2.0925E-8	3.0574E-8	3.9679E-8	4.8348E-8	5.6648E-8	6.4627E-8	7.2321E-8	7.9757E-8
7	1.0501E-8	2.0877E-8	3.0504E-8	3.9588E-8	4.8237E-8	5.6518E-8	6.4480E-8	7.2156E-8	7.9575E-8
8	1.0474E-8	2.0825E-8	3.0428E-8	3.9490E-8	4.8117E-8	5.6378E-8	6.4319E-8	7.1977E-8	7.9377E-8
9	1.0446E-8	2.0769E-8	3.0347E-8	3.9384E-8	4.7988E-8	5.6227E-8	6.4147E-8	7.1784E-8	7.9164E-8
10	1.0416E-8	2.0709E-8	3.0260E-8	3.9271E-8	4.7850E-8	5.6065E-8	6.3962E-8	7.1577E-8	7.8937E-8

Table 8.9 The absolute errors obtained by Petrov-Galerkin method with regard to solution obtained by VIM for time-fractional Sharma-Tasso-Olver equation given in (8.19) at various points of x and t taking $a = 1, \lambda = 0.01, w = 0.05$ and $\alpha = 0.5$.

x	$\|u_{PGM} - u_{VIM}\|$								
	$t=0.1$	$t=0.2$	$t=0.3$	$t=0.4$	$t=0.5$	$t=0.6$	$t=0.7$	$t=0.8$	$t=0.9$
1	1.2512E-8	2.4987E-8	3.6440E-8	4.7065E-8	5.6977E-8	6.6251E-8	7.4944E-8	8.3098E-8	9.0749E-8
2	1.2495E-8	2.4954E-8	3.6392E-8	4.7004E-8	5.6903E-8	6.6165E-8	7.4847E-8	8.2990E-8	9.0632E-8
3	1.2477E-8	2.4917E-8	3.6338E-8	4.6934E-8	5.6818E-8	6.6066E-8	7.4735E-8	8.2866E-8	9.0496E-8
4	1.2456E-8	2.4875E-8	3.6276E-8	4.6854E-8	5.6722E-8	6.5954E-8	7.4608E-8	8.2726E-8	9.0343E-8
5	1.2432E-8	2.4828E-8	3.6208E-8	4.6766E-8	5.6614E-8	6.5829E-8	7.4467E-8	7.2569E-8	9.0171E-8

6	1.2406E-8	2.4776E-8	3.6132E-8	4.6668E-8	5.6496E-8	6.5692E-8	7.4311E-8	7.2396E-8	8.9983E-8
7	1.2378E-8	2.4719E-8	3.6049E-8	4.6561E-8	5.6367E-8	6.5541E-8	7.4141E-8	7.2208E-8	8.9777E-8
8	1.2347E-8	2.4658E-8	3.5960E-8	4.6445E-8	5.6227E-8	6.5379E-8	7.3957E-8	7.2004E-8	8.9554E-8
9	1.2314E-8	2.4592E-8	3.5863E-8	4.6321E-8	5.6076E-8	6.5204E-8	7.3758E-8	7.1784E-8	8.9314E-8
10	1.2278E-8	2.4521E-8	3.5760E-8	4.6188E-8	5.5915E-8	6.5016E-8	7.3546E-8	7.1549E-8	8.9057E-8

Table 8.10 L_2 and L_∞ error norms for time-fractional Sharma-Tasso-Olver equation using Petrov-Galerkin method at various points of t taking $\lambda = a = 1$, and $w = 0.5$.

t	$\alpha = 0.75$		$\alpha = 0.5$	
	L_2	L_∞	L_2	L_∞
0.1	3.32917E-8	1.06143E-8	3.92436E-8	1.25119E-8
0.2	6.61903E-8	2.11033E-8	7.83723E-8	2.49873E-8
0.3	9.67138E-8	3.08351E-8	1.14294E-7	3.64403E-8
0.4	1.25515E-7	4.00176E-8	1.47621E-7	4.70657E-8
0.5	1.52935E-7	4.87599E-8	1.78709E-7	5.69776E-8
0.6	1.79190E-7	5.71309E-8	2.07798E-7	6.62518E-8
0.7	2.04431E-7	6.51783E-8	2.23007E-7	7.49444E-8
0.8	2.28769E-7	7.29378E-8	2.60638E-7	8.30987E-8
0.9	2.52290E-7	8.04370E-8	2.84636E-7	9.07498E-8

8.6   Conclusion

In the present chapter, we have presented the Petrov-Galerkin method for solving time-fractional KdV-Burgers equation and time-fractional Sharma-Tasso-Olver equation numerically by implementing a linear hat function as the trial function and a quintic B-spline function as the test function. This numerical method seems to be competent of producing numerical solutions of high accuracy for the fractional differential equations. A comparison between the numerical results is carried out to illustrate the pertinent feature of the proposed algorithm. The acquired numerical approximate solutions preserve good accuracy when compared with the exact solutions. The accuracy of the method is assessed in terms of L_2 and L_∞ error norms. A comprehensible inference can be drawn from the numerical results that the proposed Petrov-Galerkin method imparts highly accurate numerical solutions for nonlinear fractional differential equations.

References

[1]   L. Debnath, *Wavelet transforms and their applications.* Birkhäuser, Boston, 2002.

[2]   J. Morlet, G. Arens, I. Fourgeau, and D. Giard, "Wave propagation and sampling theory," *Geophysics*, vol. 47, pp. 203-236, 1982.

[3]   A. Grossmann, and J. Morlet, "Decomposition of Hardy functions into square integrable wavelets of constant shape," *SIAM Journal of Mathematical Analysis*, vol. 15, pp. 723-736, 1984.

[4]   J. Stromberg, "A modified Franklin system and higher order systems of *Rn* as unconditional bases for Hardy spaces," *Conference in Harmonic Analysis in Honor of A. Zygmund*, vol. 2, pp. 475-493. edit. W. Beckner et al., Wadsworth Mathematics Series, 1982.

[5]   Y. Meyer, "Principe d'incertitude, bases hilbertiennes et alg´ebres d'operateurs," *Seminaire Bourbaki*, vol. 28, pp. 209-223, 1986.

[6]   S. G. Mallat, "Multiresolution approximations and wavelet orthonormal bases of $L^2(\Re)$," *Transactions of the American Mathematical Society*, vol. 315, no. 1, pp. 69-87, 1989.

[7]   I. Daubechies, *Ten lectures on wavelets.* Philadelphia: Society for Industrial and Applied Mathematics, 1992.

[8]   C. K. Chui, *An Introduction to Wavelets*, Academic Press, London, UK, 1992.

[9]   G. Beylkin, R. Coifman, and V. Rokhlin, "Fast wavelet transforms and numerical algorithms," *Communications on Pure and Applied Mathematics*, vol. 44, no. 2, pp. 141-183, 1991.

[10]   J. H. He, "A new approach to nonlinear partial differential equations," *Communications in Nonlinear Science and Numerical Simulation*, vol. 2, no. 4, pp. 230-235, 1997.

[11]   J. H. He, "Variational Iteration Method-a kind of non-linear analytical technique; some examples," *International Journal of Nonlinear Mechanics*, vol. 34, pp. 699-708, 1999.

[12] J. H. He, "A review on some new recently developed nonlinear analytical techniques," *International Journal of Nonlinear Sciences and Numerical Simulation*, vol. 1, pp. 51-70, 2000.

[13] M. Tatari, and M. Dehghan, "On the convergence of He's variational iteration method," *Journal of Computational and Applied Mathematics*, vol. 207, pp. 121-128, 2007.

[14] Z. Feng, "On explicit exact solutions to the compound Burgers–KdV equation," *Physics Letter A*, vol. 293, pp. 57-66, 2002.

[15] Z. Feng, and X. Wang, "The first integral method to the two-dimensional Burgers–Korteweg–de Vries equation," *Physics Letter A*, vol. 308, pp. 173-178, 2003.

[16] Z. Feng, and G. Chenb, "Solitary wave solutions of the compound Burgers–Korteweg–de Vries equation," *Physica A*, vol. 352, pp. 419-435, 2005.

[17] K. R. Raslan, "The first integral method for solving some important nonlinear partial differential equations," *Nonlinear Dynamics*, vol. 53, pp. 281-286, 2008.

[18] Z. Feng, "Traveling wave behavior for a generalized Fisher equation," *Chaos, Solitons and Fractals*, vol. 38, pp. 481-488, 2008.

[19] Z. Feng, and R. Knobel, "Traveling waves to a Burgers–Korteweg–de Vries-type equation with higher-order nonlinearities," *Journal of Mathematical Analysis and Applications*, vol. 328, pp. 1435-1450, 2007.

[20] W. H. Su, X. J. Yang, H. Jafari, and D. Baleanu, "Fractional complex transform method for wave equations on Cantor sets within local fractional differential operator," *Advances in Difference Equations*, vol. 2013, no. 97, pp. 1-8, 2013.

[21] X. J. Yang, D. Baleanu, and H. M. Srivastava, *Local Fractional Integral Transforms and Their* Applications. Academic Press, Elsevier, London, 2015 (ISBN 978-0-12-804002-7).

[22] T. R. Ding, and C. Z. Li, *Ordinary Differential Equations*. Peking University Press, Peking, 1996.

[23] N. Bourbaki, *Commutative Algebra*. Addison-Wesley, Paris, 1972.

[24] Z. Feng, and X. Wang, "Explicit exact solitary wave solutions for the Kundu equation and the derivative Schrödinger equation," *Physica Scripta*, vol. 64, no. 1, pp. 7-14, 2001.

[25] J. H. He, "Homotopy perturbation method: a new nonlinear analytical technique," *Applied Mathematics and Computation*, vol. 135, pp. 73-79, 2003.

[26] J. H. He, "Homotopy perturbation technique," *Computer Methods in Applied Mechanics and Engineering*, vol. 178, pp. 257-262, 1999.

[27] A. Ghorbani, "Beyond Adomian polynomials: He polynomials," *Chaos, solitons and Fractals*, vol. 39, pp. 1486-1492, 2009.

[28] V. Marinca, N. Herisanu, and I. Nemes, "Optimal homotopy asymptotic method with application to thin film flow," *Central European Journal of Physics*, vol. 6, no. 3, pp. 648-653, 2008.

[29] V. Marinca, N. Herisanu, C. Bota, and B. Marinca, "An optimal homotopy asymptotic method applied to the steady flow of fourth-grade fluid past a porous plate," *Applied Mathematics Letters*, vol. 22, no. 2, pp. 245-251, 2009.

[30] V. Marinca, and N. Herisanu, "An optimal homotopy asymptotic method for solving nonlinear equations arising in heat transfer," *International Communications in Heat and Mass Transfer*, vol. 35, pp. 710-715, 2008.

[31] R. A. Shah, S. Islam, A. M. Siddiqui, and A. Haroon, "Optimal homotopy asymptotic method solution of unsteady second grade fluid in wire coating analysis," *Journal of the Korea Society for Industrial and Applied Mathematics*, vol. 15, no. 3, pp. 201-222, 2011.

[32] M. Ghoreishi, A. I. B. Md. Ismail, A. K. Alomari, and A. S. Bataineh, The comparison between homotopy analysis method and optimal homotopy asymptotic method for nonlinear age-structured population models," *Communications in Nonlinear Science and Numerical Simulation*, vol. 17, pp. 1163-1177, 2012.

[33] S. Liao, "On the homotopy analysis method for nonlinear problems," *Applied Mathematics and Computation*, vol. 147, pp. 499-513, 2004.

[34] S. Saha Ray, and A. Patra, "Application of homotopy analysis method and Adomian Decomposition Method for the Solution of Neutron Diffusion Equation in the Hemisphere and Cylindrical Reactors," *Journal of Nuclear Engineering & Technology*, vol. 1, no. 2-3, pp. 1-12, 2011.

[35] S. Liao, "An optimal homotopy analysis approach for strongly nonlinear differential equations," *Communications in Nonlinear Science and Numerical Simulation*, vol. 15, pp. 2003-2016, 2010.

[36] A. Haar, "Zur theorie der orthogonalen Funktionsysteme," *Mathematical Annalysis*, vol. 69, pp. 331-371, 1910.

[37] Ü. Lepik, "Numerical solution of evolution equations by the Haar Wavelet method," *Applied Mathematics and Computation*, vol. 185, pp. 695-704, 2007.

[38] S. Saha Ray, "On Haar wavelet operational matrix of general order and its application for the numerical solution of fractional Bagley Torvik equation," *Applied Mathematics and Computation*, vol. 218, pp. 5239-5248, 2012.

[39] C. F. Chen, and C. H. Hsiao, "Haar wavelet method for solving lumped and distributed parameter-systems," *IEE Proc-Control Theory Appication*, vol. 144, no. 1, pp. 87-94, 1997.

[40] S. Saha Ray, and A. Patra, "Haar wavelet operational methods for the numerical solutions of Fractional order nonlinear oscillatory Van der Pol system," *Applied Mathematics and Computation*, vol. 220, pp. 659-667, 2013.

[41] I. Podlubny, *Fractional Differential Equations.* Academic press, New work, 1999.

[42] M. Rehman, and R. A. Khan, "The Legendre wavelet method for solving fractional differential equations," *Communications in Nonlinear Science and Numerical Simulation*, vol. 16, pp. 4163-4173, 2011.

[43] M. Razzaghi, and S. Yousefi, "The Legendre wavelets operational matrix of integration," *International Journal of Systems Science*, vol. 32, pp. 495-502, 2001.

[44] N. Liu, and E. B. Lin, "Legendre wavelet method for numerical solutions of partial differential equations," *Numerical Methods for Partial Differential Equations*, vol. 26, no. 1, pp. 81-94, 2010.

[45] L. Zhu, and Q. Fan, "Solving fractional nonlinear Fredholm integro-differential equations by the second kind Chebyshev wavelet," *Communications in Nonlinear Science and Numerical Simulation*, vol. 17, pp. 2333-2341, 2012.

[46] Y. Wang, and Q. Fan, "The second kind Chebyshev wavelet method for solving fractional differential equations," *Applied Mathematics and Computation*, vol. 218, pp. 8592-8601, 2012.

[47] U. Saeed, and M. Rehman, "Hermite Wavelet Method for Fractional Delay Differential Equations," *Journal of Difference Equations*, vol. 2014, pp. 1-8, Article ID 359093, 2014.

[48] A. Ali, M. A. Iqbal, and S. T. Mohyud-Din, "Hermite wavelets method for boundary value problems," *International Journal of Modern Applied Physics*, vol. 3, no. 1, pp. 38-47, 2013.

[49] A. M. Wazwaz, *Partial Differential equations and Solitary Waves Theory*, Springer/HEP, Berlin, 2009.

[50] A. Dogan, "A Galerkin finite element approach to Burger's equation," *Applied Mathematics and Computation*, vol. 157, pp. 331-346, 2004.

[51] A. H. Khater, R. S. Temsah, and M. M. Hassan, "A Chebyshev spectral collocation method for solving Burgers' type equations," *Journal of Computational and Applied Mathematics*, vol. 222, pp. 333-350, 2008.

[52] A. Korkmaz, A. M. Aksoy, and I. Dag, "Quartic B-spline differential quadrature method," *International Journal Nonlinear Science*, vol. 11, no. 4, pp. 403-411, 2011.

[53] B. Saka, and I. Dag, "Quartic B-spline collocation method to the numerical solutions of the Burgers' equation," *Chaos Solitons Fractals*, vol. 32, pp. 1125-1137, 2007.

[54] T. Ozis, E. N. Aksan, and A. Ozdes, "A finite element approach for solution of Burgers' equation," *Applied Mathematics and Computation*, vol. 139, pp. 417-428, 2003.

[55] L. A. Hassanien, A. A. Salama, and H. A. Hosham, "Fourth-order finite difference method for solving Burgers' equation," *Applied Mathematics and Computation*, vol. 170, pp. 781-800, 2005.

[56] S. Kutulay, A. R. Bahadir, and A. Odes, "Numerical solution of the one-dimensional Burgers' equation: explicit and exact-explicit finite difference methods," *Journal of Computational and Applied Mathematics*, vol. 103, pp. 251-261, 1999.

[57] S. Kutulay, A. Esen, and I. Dag, "Numerical solutions of the Burgers' equation by the least-squares quadratic B-spline finite element method," *Journal of Computational and Applied Mathematics*, vol. 167, pp. 21-33, 2004.

[58] D. Irk, "Sextic B-spline collocation method for the Modified Burgers' equation," *Kybernetes*, vol. 38, no. 9, pp. 1599-1620, 2009.

[59] A. G. Bratsos, and L. A. Petrakis, "An implicit numerical scheme for the modified Burgers' equation," *International Journal for Numerical Methods in Biomedical Engineering*, vol. 27, no. 2, pp. 232-237, 2011.

[60] T. Roshan, and K. S. Bhamra, "Numerical solution of the modified Burgers' equation by Petrov-Galerkin method," *Applied Mathematics and Computation*, vol. 218, pp. 3673-3679, 2011.

[61] M. A. Ramadan, and T. S. El-Danaf, "Numerical treatment for the modified Burgers' equation," *Mathematics and Computers in Simulation*, vol. 70, pp. 90-98, 2005.

[62] R. P. Zhang, X. J. Yu, and G. Z. Zhao, "Modified Burgers' equation by the local discontinuous Galerkin method," *Chinese Physics B*, vol. 22, no. 3, pp. 030210 (1-5), 2013.

[63] Y. Duan, R. Liu, and Y. Jiang, "Lattice Boltzmann model for the modified Burgers' equation," *Applied Mathematics and Computation*, vol. 202, pp. 489-497, 2008.

[64] H. N. A. Ismail, K. Raslan, and A. A. Abd Rabboh, "Adomian decomposition method for Burger's-Huxley and Burger's-Fisher equations," *Applied Mathematics and Computation*, vol. 159, pp. 291-301, 2004.

[65] M. Javidi, "A numerical solution of the generalized Burgers-Huxley equation by spectral collocation method," *Applied Mathematics and Computation*, vol. 172, no. 2, pp. 338-344, 2006.

[66] A. M. Wazwaz, "Analytic study on Burgers, Fisher, Huxley equations and combined forms of these equations," *Applied Mathematics and Computation*, vol. 195, pp. 754-761, 2008.

[67] S. H. Hashemi, H. R. M. Daniali, and D. D. Ganji, "Numerical simulation of the generalized Huxley equation by He's homotopy perturbation method," *Applied Mathematics and Computation*, vol. 192, no. 1, pp. 157-161, 2007.

[68] X. W. Zhou, "Exp-Function method for solving Huxley equation," *Mathematical Problems in Engineering*, vol. 2008, pp. 1-7, Article ID 538489, 2008.

[69] I. Hashim, M. S. M. Noorani, and B. Batiha, "A note on the Adomian decomposition method for the generalized Huxley equation," *Applied Mathematics and Computation*, vol. 181, no. 2, pp. 1439-1445, 2006.

[70] B. Batiha, M. S. M. Noorani, and I. Hashim, "Numerical simulation of the generalized Huxley equation by He's variational iteration method," *Applied Mathematics and Computation*, vol. 186, no. 2, pp. 1322-1325, 2007.

[71] M. Sari, and G. Gürarslan, "Numerical solutions of the generalized Burgers-Huxley equation by a Differential Quadrature method," *Mathematical Problems in Engineering*, vol. 2009, pp. 1-11, Article ID 370765, 2009.

[72] X. Y. Wang, Z. S. Zhu, and Y. K. Lu, "Solitary wave solutions of the generalized Burgers-Huxley equation," *Journal of Physics A: Mathematical and General*, vol. 23, pp. 271-274, 1990.

[73] T. S. El-Danaf, "Solitary wave solutions for the generalized Burgers-Huxley equation," *International Journal of Nonlinear Sciences and Numerical Simulation*, vol. 8, no. 3, pp. 315-318, 2007.

[74] Z. Yan, "The modified KdV equation with variable coefficients: Exact uni/bi-variable travelling wave-like solutions," *Applied Mathematics and Computation*, vol. 203, pp. 106-112, 2008.

[75] M. K. Kadalbajoo, and A. Awasthi, "A numerical method based on Crank-Nicolson scheme for Burgers' equation," *Applied Mathematics and Computation*, vol. 182, pp. 1430-1442, 2006.

[76] R. Jiwari, "A Haar wavelet quasilinearization approach for numerical simulation of Burgers' equation," *Computer Physics Communications*, vol. 183, pp. 2413-2423, 2012.

[77] W. L. Wood, "An exact solution for Burger's equation," *Communications in Numerical Methods in Engineering*, vol. 22, no. 7, pp. 797-798, 2006.

[78] K. Rahman, N. Helil, and R. Yimin, "Some new semi-implicit finite difference schemes for numerical solution of Burgers equation," *International conference on Computer Application and System Modeling*, Proceedings 14, art. no. 5622119, V14-(451-455), DOI. 10.1109/ICCASM.2010.5622119, 2010.

[79] R. C. Mittal, and R. K. Jain, "Numerical solutions of nonlinear Burgers' equation with modified cubic B-splines collocation method," *Applied Mathematics and Computation*, vol. 218, pp. 7839-7855, 2012.

[80] A. Bekir, "On travelling wave solutions to combined KdV-mKdV equation and modified Burgers-KdV equation," *Communications in Nonlinear Science and Numerical Simulation*, vol. 14, pp. 1038-1042, 2009.

[81] A. M. Wazwaz, "A Study on compacton-like solutions for the modified KdV and fifth order KdV-like equations," *Applied Mathematics and Computation*, vol. 147, pp. 439-447, 2004.

[82] D. Kaya, "An application for the higher order modified KdV equation by decomposition method," *Communications in Nonlinear Science and Numerical Simulation*, vol. 10, pp. 693-702, 2005.

[83] J. Zhang, Y. Wu, and X. Li, "Quasi-periodic solution of the (2+1)-dimensional Boussinesq-Burgers soliton equation," *Physica A: Statistical Mechanics and Its Applications*, vol. 319, no. 1, pp. 213-232, 2003.

[84] L. Zhang, L. F. Zhang, and C. Li, "Some new exact solutions of Jacobian elliptic function about the generalized Boussinesq equation and Boussinesq-Burgers equation," *Chinese Physics B.*, vol. 17, no. 2, pp. 403-410, 2008.

[85] A. S. A. Rady, and M. Khalfallah, "On soliton solutions for Boussinesq-Burgers equations," *Communications in Nonlinear Science and Numerical Simulation*, vol. 15, pp. 886-894, 2010.

[86] P. Wang, B. Tian, W. Liu, X. Lü, and Y. Jiang, "Lax pair, Bäcklund transformation and multi-soliton solutions for the Boussinesq–Burgers equations from shallow

water waves," *Applied Mathematics and Computation*, vol. 218, pp. 1726-1734, 2011.

[87]   A. Chen, and X. Li, "Darboux transformation and soliton solutions for Boussinesq–Burgers equation," *Chaos, Solitons and Fractals*, vol. 27, no. 1, pp. 43-49, 2006.

[88]   M. Ghoreishi, A. I. B. Md. Ismail, A. K. Alomari, and A. S. Bataineh, "The comparison between homotopy analysis method and optimal homotopy asymptotic method for nonlinear age-structured population models," *Communications in Nonlinear Science and Numerical Simulation*, vol. 17, pp. 1163-1177, 2012.

[89]   J. Biazar, and H. Aminikhan, "Study of convergence of homotopy perturbation method for systems of partial differential equations," *Computers and Mathematics with Applications*, vol. 58, pp. 2221-2230, 2009.

[90]   S. G. Samko, A. A. Kilbas, and O. I. Marichev, *Fractional Integrals and derivatives: Theory and Applications*, Taylor and Francis, London, 1993.

[91]   A. A. Kilbas, H. M. Srivastava, and J. J. Trujillo, *Theory and Applications of Fractional Differential Equations*, *North-Holland Mathematical Studies*, 204, Elsevier (North-Holland) Science Publishers, Amsterdam, the Netherlands, 2006.

[92]   K. S. Miller, and B. Ross, *An Introduction to the Fractional Calculus and Fractional Differential Equations*, Wiley, New York, 1993.

[93]   M. Caputo. Linear models of dissipation whose Q is almost frequency independent. Part II *Geophys. J. R. Astron. Soc.*, 13, pp. 529-539, 1967. [Reprinted in *Fractional Calculus and Applied Analysis* 11, pp. 4-14 (2008)]

[94]   H. J. Holmgren, *Om differentialkalkylen med indices af hvad natur som helst*, Kungliga Svenska Vetenskaps-Akademins Handlingar, vol. 5, No. 11, 1-83, Stockholm (in Swedish), 1865.

[95]   B. Riemann, *Versuch einer allgemeinen Auffassung der Integration und Differentiation*, In: Gesammelte Werke und Wissenschaftlicher Nachlass. Teubner, Leipzig, Germany, 331-344, 1876.

[96]   H. Risken, *The Fokker-Planck Equation: Methods of solution and Applications*, Springer, Berlin, 1989.

[97]   J. Biazar, P. Gholamin, and K. Hosseini, "Variational iteration method for solving Fokker-Planck equation," *Journal of the Franklin Institute*, vol. 347, pp. 1137-1147, 2010.

[98]   A. Yildirm, "Application of the homotopy perturbation method for the Fokker-Planck equation," *International Journal for Numerical Methods in Biomedical Engineering*, vol. 26, pp. 1144-1154, 2010.

[99]   R. Metzler, and J. Klafter, "The random walk's guide to anomalous diffusion: A fractional dynamics approach," *Physics Reports*, vol. 339, pp. 1-77, 2000.

[100]   T. D. Frank, *Nonlinear Fokker-Planck equations: Fundamentals and Applications*, Springer, Berlin, 2005.

[101]   S. Saha Ray, "Exact solutions for time-fractional diffusion-wave equations by decomposition method," *Physica Scripta*, vol. 75, pp. 53-61, 2007.

[102]   L. Yan, "Numerical solutions of Fractional Fokker-Planck equations using Iterative Laplace transform method," *Abstract and Applied Analysis*, vol. 2013, pp. 1-7, Article ID 465160, 2013.

[103]   Z. Odibat, and S. Momani, "Numerical solution of Fokker-Planck equation with space- and time-fractional derivatives," *Physics Letter A*, vol. 369, pp. 349-358, 2007.

[104]   S. K. Vanani, and A. Aminataei, "A numerical algorithm for the space and time fractional Fokker-Planck equation," *International Journal of Numerical methods for Heat & Fluid Flow*, vol. 22, no. 8, 1037-1052, 2012.

[105]   A. Yildirm, "Analytical approach to Fokker-Planck equation with space- and time-fractional derivatives by means of the homotopy perturbation method," *Journal of King Saud University* (*Science*), vol. 22, pp. 257-264, 2010.

[106]   J. Zhang, and G. Yan, "A lattice Boltzmann model for the Burgers-Fisher equation," *Chaos*, vol. 20, pp. 023129(1-12), 2010.

[107]   Y. Liu, "General solution of space fractional Fisher's nonlinear diffusion equation," *Journal of Fractional Calculus and Applications*, vol. 1, no. 2, pp. 1-8, 2011.

[108]   A. M. Wazwaz, and A. Gorguis, "An analytic study of Fisher's equation by using Adomian decomposition method," *Applied Mathematics and Computation*, vol. 154, pp. 609-620, 2004.

[109]   L. Wei, and Y. He, "Numerical algorithm based on an implicit fully discrete local discontinuous Galerkin method for the time-fractional KdV-Burgers-Kuramoto equation," *Cornell University Library. arXiv:1201.1156v2*, 2012.

[110]   T. Kawahara, "Formation of saturated solitons in a nonlinear dispersive system with instability and dissipation," *Physical Review Letters*, vol. 51, pp. 381–383, 1983.

[111] J. Topper, and T. Kawahara, "Approximate equations for long nonlinear waves on a viscous fluid," *Journal of the Physical Society of Japan*, vol. 44, pp. 663-666, 1978.

[112] B. Cohen, J. Krommes, W. Tang, and M. Rosenbluth, "Non-linear saturation of the dissipative trapped-ion mode by mode coupling," *Nuclear Fusion*, vol. 16, pp. 971–992, 1976.

[113] F. Huang, and S. Liu, "Physical mechanism and model of turbulent cascades in a barotropic atmosphere," *Advances in Atmospheric Sciences*, vol. 21, pp. 34-40, 2004.

[114] L. Song, and H. Zhang, "Application of homotopy analysis method to fractional KdV–Burgers–Kuramoto equation," *Physics Letter A*, vol. 367, pp. 88-94, 2007.

[115] M. Safari, D. D. Ganji, and M. Moslemi, "Application of He's variational iteration method and Adomian's decomposition method to the fractional KdV–Burgers–Kuramoto equation," *Computers and Mathematics with Applications*, vol. 58, pp. 2091-2097, 2009.

[116] Y. Pomeau, A. Ramani, and B. Grammaticos, "Structural stability of the Korteweg-de Vries solitons under a singular perturbation," *Physica D: Nonlinear Phenomena*, vol. 31, no. 1, pp. 127-134, 1988.

[117] L. Wei, Y. He, and Y. Zhang, "Numerical analysis of the fractional seventh-order KDV equation using an Implicit Fully Discrete Local Discontinuous Galerkin method," *International Journal of Numerical Analysis and Modeling*, vol. 10, no. 2, pp. 430-444, 2013.

[118] S. T. Mohyud-Din, M. A. Noor, and K. I. Noor, "Travelling wave solutions of seventh-order generalized KdV equations by variational iteration method using Adomian's polynomial," *International Journal of Modern Physics B*, vol. 23, no. 15, pp. 3265-3277, 2009.

[119] S. T. Mohyud-Din, M. A. Noor, and K. I. Noor, "Traveling wave solutions of seventh-order generalized KdV equations using He's polynomials," *International Journal of Nonlinear Sceinces and Numerical Simulation*, vol. 10, no. 2, pp. 227-233, 2009.

[120] S. T. Mohyud-Din, M. A. Noor, and F. Jabeen, "Modified variational iteration method for traveling wave solutions of seventh-order generalized KdV equations," *International Journal for Computational Methods in Engineering Science and Mechanics*, vol. 12, pp. 107-113, 2011.

[121] N. Shang, and B. Zheng, "Exact solutions for three fractional partial differential equations by the (G'/G) method," *International Journal of Applied Mathematics*, vol. 43, no. 3, 1-6, 2013.

[122] D. J. Kaup, "On the inverse scattering for cubic eigenvalue problems of the class equations," *Studies in Applied Mathematics*, vol. 62, pp. 189-195, 1980.

[123] B. A. Kupershmidt, "A super Korteweg-de-Vries equatons: an integrable system," *Physics Letters A*, vol. 102, pp. 213-218, 1994.

[124] E. Fan, "Uniformly constructing a series of explicit exact solutions to nonlinear equations in mathematical physics," *Chaos, Solitons and Fractals*, vol. 16, pp. 819-839, 2003.

[125] M. Inc, "On numerical soliton solution of the Kaup–Kupershmidt equation and convergence analysis of the decomposition method," *Applied Mathematics and Computation*, vol. 172, no. 1, pp. 72-85, 2006.

[126] S. A. Yousefi, "Numerical solution of a model describing biological species living together by using Legendre Multiwavelet method," *International Journal of Nonlinear Science*, vol. 11, no. 1, pp. 109-113, 2011.

[127] A. K. Gupta, and S. Saha Ray, "Travelling Wave Solution of Fractional KdV-Burger-Kuramoto Equation Describing Nonlinear Physical Phenomena," *AIP Advances*, vol. 4, pp. 097120-(1-11), DOI: 10.1063/1.4895910, 2014.

[128] A. K. Gupta, and S. Saha Ray, "Comparison between Homotopy Perturbation method and Optimal Homotopy Asymptotic method for the Soliton solution of Boussinesq-Burgers equation," *Computers and Fluids*, vol. 103, pp. 34-41, 2014.

[129] B. Zheng, "Exact solutions for some fractional partial differential equations by the (G'/G) method," *Mathematical Problems in Engineering*, vol. 2013, pp. 1-13, Article ID 826369, 2013.

[130] H. Naher, F. A. Abdullah, and S. T. Mohyud-Din, "Extended generalized Riccati equation mapping method for the fifth-order Sawada-Kotera equation," *AIP Advances*, vol. 3, 052104-(1-14), 2013.

[131] S. Dinarvand, S. Khosravi, A. Doosthoseini, and M. M. Rashidi, "The homotopy analysis method for solving the Sawada-Kotera and Lax's fifth-order KdV equations," *Advances in Theoretical and Applied Mechanics*, vol. 1, no. 7, pp. 327-335, 2008.

[132] L. Debnath, *Nonlinear Partial Differential Equations for Scientists and Engineers*, Birkhauser, Springer, New York, 2012.

[133] Y. Zhang, "Time-fractional Camassa-Holm equation: Formulation and solution using Variational methods," *Journal of Computational and Nonlinear Dynamics*, vol. 8, pp. 041020-(1-7), 2013.

[134] F. Guo, and W. Peng, "Blowup solutions for the generalized two-component Camassa-Holm system on the circle," *Nonlinear Analysis*, vol. 105, pp. 120-133, 2014.

[135] T. Rehman, G. Gambino, and S. Roy Choudhury, "Smooth and non-smooth travelling wave solutions of some generalized Camassa-Holm equations," *Communications in Nonlinear Science and Numerical Simulation*, vol. 19, pp. 1746-1769, 2014.

[136] R. Camassa, D. Holm, and J. Hyman, "A new integrable shallow water equation," *Advances in Applied Mechanics*, vol. 31, pp. 1-33, 1994.

[137] R. S. Johnson, "Camassa–Holm, Korteweg-de Vries and related models for water waves," *Journal of Fluid Mechanics*, vol. 455, pp. 63-82, 2002.

[138] A. Fokas, and B. Fuchssteiner, "Symplectic structures, their Backlund transformation and hereditary symmetries," *Physica D: Nonlinear Phenomena*, vol. 4, no. 1, pp. 47-66, 1981.

[139] J. Lenells, "Conservation laws of the Camassa–Holm equation," *Journal of Physics A: Mathematical and General*, vol. 38, no. 4, pp. 869-880, 2005.

[140] R. Camassa, and D. Holm, "An integrable shallow water equation with peaked solutions," *Physical Review Letters*, vol. 71, pp. 1661-1664, 1993.

[141] S. Saha Ray, "Soliton Solutions of Nonlinear and Nonlocal Sine-Gordon Equation involving Riesz space fractional derivative," *Zeitschrift für Naturforschung A*, vol. 70, no. 8, pp. 659–667, 2015.

[142] G. Alfimov, T. Pierantozzi, and L. Vázquez, "Numerical study of a fractional sine-Gordon equation," *Fractional differentiation and its applications, FDA*, vol. 4, pp. 644-649, 2004.

[143] R. K. Dodd, J. C. Eilbeck, J. D. Gibbon, and H. C. Morris, *Solitons and nonlinear wave solutions*, Academic, London, 1982.

[144] U. Yücel, "Homotopy analysis method for the sine-Gordon equation with initial conditions," *Applied Mathematics and Computation*, vol. 203, pp. 387-395, 2008.

[145] D. Kaya, "A numerical solution of the sine-Gordon equation using the modified decomposition method," *Applied Mathematics and Computation*, vol. 143, pp. 309-317, 2003.

[146] B. Batiha, M. S. M. Noorani, and I. Hashim, "Numerical solution of sine-Gordon equation by variational iteration method," *Physics Letters A*, vol. 370, pp. 437-440, 2007.

[147] A. M. Wazwaz, "The tanh method: exact solutions of the sine-Gordon and the sinh-Gordon equations," *Applied Mathematics and Computation*, vol. 167, pp. 1196-1210, 2005.

[148] M. J. Ablowitz, B. M. Herbst, and C. Schober, "On the numerical solution of the sine-Gordon equation. I: Integrable discretizations and homoclinic manifolds," *Journal of Computational Physics*, vol. 126, pp. 299-314, 1996.

[149] B. M. Herbst, and M. J. Ablowitz, "Numerical homoclinic instabilities in the sine-Gordon equation," *Quaestiones Mathematicae*, vol. 15, no. 3, pp. 345-363, 1992.

[150] O. S. Iyiola, "A numerical study of Ito equation and Sawada-Kotera equation both of time-fractional type," *Advances in Mathematics: Scientific Journal*, vol. 2, no. 2, pp. 71-79, 2013.

[151] A. Saadatmandi, and M. Dehghan, "A new operational matrix for solving fractional-order differential equations," *Computers and Mathematics with Applications*, vol. 59, pp. 1326-1336, 2010.

[152] M. Dehghan, J. Manafian, and A. Saadatmandi, "Solving nonlinear fractional partial differential equations using the homotopy analysis method," *Numerical Methods for Partial Differential Equations*, vol. 26, pp. 448-479, 2009.

[153] M. Dehghan, J. Manafian, and A. Saadatmandi, "The solution of the linear fractional partial differential equations using the homotopy analysis method," *Zeitschrift für Naturforschung A*, vol. 65a, no. 11, pp. 935-949, 2010.

[154] B. He, Q. Meng, and S. Li, "Explicit peakon and solitary wave solutions for the modified Fornberg-Whitham equation," *Applied Mathematics and Computation*, vol. 217, pp. 1976-1982, 2010.

[155] G. B. Whitham, "Variational methods and applications to water wave," *Proceedings of the Royal Society of London A: Mathematical, Physical and Engineering Sciences*, vol. 299, pp. 6-25, 1967.

[156] B. Fornberg, and G. B. Whitham, "A numerical and theoretical study of certain nonlinear wave phenomena," *Philosophical Transactions of the Royal Society of London A: Mathematical, Physical and Engineering Sciences*, vol. 289, pp. 373-404, 1978.

[157] S. Hesam, A. Nazemi, and A. Haghbin, "Reduced differential transform method for solving the Fornberg-Whitham type equation," *International Journal of Nonlinear Science*, vol. 13, no. 2, pp. 158-162, 2012.

[158] J. Lu, "An analytical approach to the Fornberg–Whitham type equations by using the variational iteration method," *Computers and Mathematics with Applications*, vol. 61, no. 8, pp. 2010-2013, 2011.

[159] D. Kaya, and S. M. El-Sayed, "A numerical method for solving Jaulent–Miodek equation," *Physics Letter A*, vol. 318, pp. 345–353, 2003.

[160] A. M. Wazwaz, "The tanh-coth and the sech methods for exact solutions of the Jaulent–Miodek equation," *Physics Letter A*, vol. 366, pp. 85–90, 2007.

[161] A. Yildirim, and A. Kelleci, "Numerical Simulation of the Jaulent-miodek Equation by He's Homotopy Perturbation Method," *World Applied Sciences Journal*, vol. 7, pp. 84-89, 2009.

[162] J. H. He, and L. N. Zhang, "Generalized solitary solution and compacton-like solution of the Jaulent-Miodek equations using the Exp-function method," *Physics Letters A*, vol. 372, no. 7, pp. 1044-1047, 2008.

[163] M. M. Rashidi, G. Domairry, and S. Dinarvand, "The Homotopy analysis method for explicit analytical solutions of Jaulent–Miodek equations," *Numerical Methods for Partial Differential Equations*, vol. 25, no. 2, pp. 430-439, 2009.

[164] H. T. Ozer, and S. Salihoglu, "Nonlinear Schrödinger equations and $N=1$ super-conformal algebra," *Chaos Solitons Fractals*, vol. 33, pp. 1417-1423, 2007.

[165] S. Y. Lou, "A direct perturbation method: nonlinear Schrodinger equation with loss," *Chinese Physics Letters*, vol. 16, pp. 659-661, 1999.

[166] A. Atangana, and D. Baleanu, "Nonlinear fractional Jaulent-Miodek and Whitham-Broer-Kaup equations within Sumudu transform," *Abstract and Applied Analysis*, vol. 2013, Article ID 160681, pp. 1-8, 2013.

[167] C. H. Su, and C. S. Gardner, "Korteweg-de Vries Equation and Generalizations. III. Derivation of the Korteweg-de-Vries and Burgers' equation," *Journal of Mathematical Physics*, *vol*. 10, no. 3, pp. 536-539, 1969.

[168] R. S. Jonson, "A nonlinear equation incorporating damping and dispersion," *Journal of Fluid Mechanics*, vol. 42, no. 1, pp. 49-60, 1970.

[169] R. S. Jonson, "Shallow water waves in a viscous fluid – the undular bore," *Physics of Fluids*, vol. 15, no. 10, pp. 1693-1699, 1972.

[170] H. Grad, and P. N. Hu, "Unified shock profile in a plasma," *Physics of Fluids*, vol. 10, no. 12, pp. 2596-2602, 1967.

[171] S. Saha Ray and A. K. Gupta, "Numerical simulation for Burger and Boussinesq-Burger Equatios using Novel schemes based on Haar wavelet collocation method," *Applied Mathematics and Information Sciences* (Accepted).

[172] D. J. Korteweg, and G. de Vries, "On the change of form of long waves advancing in a rectangular Canal and on a new type of long stationary waves," *Philosophical Magazine series* 5, vol. 39, no. 240, pp. 422-443, 1895.

[173] D. Kaya, "An application of the decomposition method for the KdVB equation," *Applied Mathematics and Computation*, vol. 152, pp. 279-288, 2004.

[174] B. Sahu, and R. Roychoudhury, "Travelling wave solution of Korteweg-de Vries–Burger's equation," *Czechoslovak Journal of Physics*, vol. 53, no. 6, pp. 517-527, 2003.

[175] M. A. Helal, and M. S. Mehanna, "A comparison between two different methods for solving KdV-Burgers equation," *Chaos, Solitons and Fractals*, vol. 28, pp. 320-326, 2006.

[176] T. S. A. El-Danaf, "Septic B-spline method of the Korteweg-de Vries-Burger's equation," *Communication of Nonlinear Science and Numerical Simulation*, vol. 13, pp. 554-566, 2008.

[177] S. Haq, S. U. Islam, and M. Uddin, "A mesh-free method for the numerical solution of the KdV-Burgers equation," *Applied Mathematical Modelling*, vol. 33, pp. 3442-3449, 2009.

[178] B. Saka, and I. Dag, "Quartic B-spline Galerkin approach to the numerical solutions of the KdVB equation," *Applied Mathematics and Computation*, vol. 215, pp. 746-758, 2009.

[179] S. I. Zaki, "A quintic B-spline finite elements scheme for the KdVB equation," *Computer Methods in Applied Mechanics and Engineering*, vol. 188, pp. 121-134, 2000.

[180] Q. Wang, "Numerical solution for fractional KdV-Burgers equation by Adomian decomposition method," *Applied Mathematics and Computation*, vol. 182, pp. 1048-1055, 2006.

[181] Q. Wang, "Homotopy perturbation method for fractional KdV-Burgers equation," *Chaos, Solitons and Fractals*, vol. 35, pp. 843-850, 2008.

[182] S. T. Demiray, Y. Pandir, and H. Bulut, "Generalized Kudryashov method for time-fractional differential equations," *Abstract and Applied Analysis*, vol. 2014, Article ID 901540, pp. 1-13, 2014.

[183] A. El-Ajou, O. A. Arqub, and S. Momani, "Approximate analytical solution of the nonlinear fractional KdV–Burgers equation: A new iterative algorithm," *Journal of Computational Physics*, vol. 293, pp. 81-95, 2015.

[184] A. G. Johnpillai, and C. M. Khalique, "On the solutions and conservation laws for the Sharma-Tasso-Olver equation," *ScienceAsia*, vol. 40, no. 6, pp. 451-455, 2014.

[185] Y. Shang, Y. Huang, and W. Yuan, "Bäcklund transformations and abundant exact and explicit solutions of the Sharma-Tasso-Olver equation," *Applied Mathematics and Computation*, vol. 217, pp. 7172-7183, 2011.

[186] L. Song, Q. Wang, and H. Zhang, "Rational approximation solution of the fractional Sharma–Tasso–Olever equation," *Journal of Computational and Applied Mathematics*, vol. 224, pp. 210-218, 2009.

[187] H. Tasso, "Cole's ansatz and extensions of Burgers' equation," *Max Planck Institute für Plasmaphysik*, Report number IPP-6-142, Garching, 1976.

[188] A. S. Sharma, and H. Tasso, "Connection between wave envelope and explicit solution of a nonlinear dispersive equation," *Max Planck Institute für Plasmaphysik*, Report number IPP-6-158, Garching, 1977.

[189] P. J. Olver, "Evolution equation possessing infinite many symmetries," *Journal of Mathematical Physics*, vol. 18, no. 6, pp. 1212–1215, 1977.

[190] Z. Yan, "Integrability of two types of the (2+1)-dimensional generalized Sharma–Tasso–Olver integro-differential equations," *MM. Res.*, vol. 22, pp. 302-324, 2003.

[191] B. Erbas, and E. Yusufoglu, "Exp-function method for constructing exact solutions of Sharma-Tasso-Olver equation," *Chaos, Solitons and Fractals*, vol. 41, pp. 2326-2330, 2009.

[192] Y. He, S. Li, and Y. Long, "Exact Solutions to the Sharma-Tasso-Olver equation by using Improved G'/G – Expansion method," *Journal of Applied Mathematics*, vol. 2013, Article ID 247234, pp. 1-6, 2013.

[193] A. M. Wazwaz, "New solitons and kinks solutions to the Sharma-Tasso-Olver equation," *Applied Mathematics and Computation*, vol. 188, no. 2, pp. 1205-1213, 2007.

[194] A. Esen, O. Tasbozan, and N. M. Yagmurlu, "Approximate Analytical Solutions of the Fractional Sharma-Tasso-Olver equation using Homotopy Analysis Method and a comparison with other methods," *Cankaya University Journal of Science and Engineering*, vol. 9, no. 2, pp. 139-147, 2012.

[195] A. Cesar, and S. Gómez, "A nonlinear fractional Sharma–Tasso–Olver equation: New exact solutions," *Applied Mathematics and Computation*, vol. 266, pp. 385-389, 2015.

[196] S. Sahoo, and S. Saha Ray, "A new method for exact solutions of variant types of time fractional Korteweg–de Vries equations in shallow water waves," *Mathematical Methods in Applied Sciences*, DOI. 10.1002/mma.3970. 2016.

[197] I. Christie, D. F. Griffths, A. R. Mitchell, and J. M. Sanz-Serna, "Product approximation for nonlinear problems in finite element methods," *IMA Journal of Numerical Analysis*, vol. 1, pp. 253-266, 1981.

Dissemination

Internationally indexed journals (*Web of Science, SCI, Scopus, etc.*)

1. S. Saha Ray and A. K. Gupta, 2013, "On the solution of Burgers-Huxley and Huxley equation using Wavelet collocation method", *Computer Modeling in Engineering and Sciences*, Vol. 91, No. 6, pp. 409-424.

2. A. K. Gupta and S. Saha Ray, 2014, "Comparison between Homotopy Perturbation method and Optimal Homotopy Asymptotic method for the Soliton solution of Boussinesq-Burgers equation", *Computers and Fluids*, Vol. 103, pp. 34-41.

3. S. Saha Ray and A. K. Gupta, 2014, "Comparative Analysis of Variational iteration method and Haar wavelet method for the numerical solutions of Burgers-Huxley and Huxley Equations", *Journal of Mathematical Chemistry*, Vol. 52, No. 4, pp. 1066-1080.

4. A. K. Gupta and S. Saha Ray, 2014, "Wavelet methods for Solving Fractional order Differential equations", *Mathematical Problems in Engineering*, Vol. 2014, Article ID 140453, 11 pages.

5. S. Saha Ray and A. K. Gupta, 2014, "An approach with Haar wavelet collocation method for Numerical Simulation of Modified KdV and Modified Burgers Equations", *Computer Modeling in Engineering and Sciences*, Vol. 103, No. 5, pp. 315-341.

6. A. K. Gupta and S. Saha Ray, 2014, "Travelling Wave Solution of Fractional KdV-Burger-Kuramoto Equation Describing Nonlinear Physical Phenomena", *AIP Advances*, Vol. 4, pp. 097120(1-11).

7. S. Saha Ray and A. K. Gupta, 2014, "A two-dimensional Haar wavelet approach for the numerical simulations of time and space fractional Fokker-Planck equations in modelling of anomalous diffusion systems", *Journal of Mathematical Chemistry*, Vol. 52, pp. 2277-2293.

8. A. K. Gupta and S. Saha Ray, 2014. "Numerical treatment for investigation of squeezing unsteady nanofluid flow between two parallel plates", *Powder Technology*, Vol. 279, pp. 282-289.

9. A. K. Gupta and S. Saha Ray, 2014, "On the Solutions of Fractional Burgers-Fisher and Generalized Fisher's Equations Using Two Reliable Methods", *International Journal of Mathematics and Mathematical Sciences*, Vol. 2014, Article ID 682910. 16 pages.

10. A. K. Gupta and S. Saha Ray, 2015. "An investigation with Hermite Wavelets for accurate solution of Fractional Jaulent-Miodek Equation associated with energy-dependent Schrödinger potential", *Applied Mathematics and Computation*, Vol. 270, pp. 458-471.

11. A. K. Gupta and S. Saha Ray, 2015, "Numerical treatment for the solution of Fractional Fifth Order Sawada-Kotera Equation using Second Kind Chebyshev Wavelet Method", *Applied Mathematical Modelling*, Vol. 39, pp. 5121–5130.

12. S. Saha Ray and A. K. Gupta, 2015, "A Numerical Investigation of time-Fractional modified Fornberg-Whitham Equation for analyzing the behavior of water waves", *Applied Mathematics and Computation*, Vol. 266, pp. 135-148.

13. A. K. Gupta and S. Saha Ray, 2016, "The Comparison of two reliable methods for accurate solution of time-Fractional Kaup-Kupershmidt Equation arising in Capillary Gravity Waves", *Mathematical Methods in the Applied Sciences*, Vol. 39, No. 3, pp. 583-592.

14. S. Saha Ray and A. K. Gupta, 2016. "Numerical solution of Fractional Partial differential equation of parabolic type with Dirichlet boundary conditions using Two-dimensional Legendre wavelets method", *Journal of Computational and Nonlinear Dynamics*, Vol. 11, No. 1, pp. 011012(1-9).

15. A. K. Gupta and S. Saha Ray, 2016. "A novel attempt for finding comparatively accurate solution for sine-Gordon equation comprising Riesz space fractional derivative", *Mathematical Methods in the Applied Sciences*, Vol. 39, No. 11, pp. 2871-2882.

16. S. Saha Ray and A. K. Gupta, 2016. "Application of Novel Schemes Based on Haar Wavelet Collocation Method for Burger and Boussinesq-Burger Equations", *Applied Mathematics and Information Sciences*, Vol. 10, No. 4, pp. 1513-1524.

17. A. K. Gupta and S. Saha Ray, 2016, "Two-Dimensional Chebyshev Wavelet Method for Camassa-Holm Equation with Riesz Fractional Derivative Describing Propagation of Shallow Water Waves", *Fundamenta Informaticae*. (Article in Press)

18. A. K. Gupta and S. Saha Ray, 2016, "Two-dimensional Legendre Wavelet Method for Travelling Wave Solutions of Time-Fractional Generalized Seventh order KdV Equation", Accepted (*Computers and Mathematics with Applications*)

Conferences

1. A. K. Gupta and S. Saha Ray, 2016, "Numerical Solution of time-Fractional Sharma-Tasso-Olver Equation using Petrov-Galerkin Method," *Proceeding of International Workshop and Conference on Analysis and Applied Mathematics (IWCAAM2016)*, p. 127.

Communicated Papers

1. A. K. Gupta and S. Saha Ray, "Comparison between Two Reliable Methods for Accurate Solution of Fractional Modified Fornberg-Whitham Equation Arising in Water Waves".

2. A. K. Gupta and S. Saha Ray, "On the solution of time-fractional KdV-Burgers equation using Petrov-Galerkin method for propagation of long wave in shallow water".